

DOCTORAL THESIS

---

# Trophic cascade modelling in bathyal ecosystems

---

*Author:*

Valeria MAMOURIDIS

*Supervisor:*

Dr. Francesc MAYNOU

*Thesis submitted in partial fulfilment of the requirements  
for the degree of Doctor of Philosophy in Marine Sciences*

*in the*

Bio-Economic Modelling Research Group

Dept. de Recursos Marins Renovables (ICM-CSIC)

*and the*

Dept. de Ingeniería Hidráulica, Marítima y Ambiental

(EHMA-UPC)

March 2015

*“I am tempted to give one more instance showing how plants and animals, most remote in the scale of nature, are bound together by a web of complex relations”*

Charles Darwin

*To Virginia, Dimitri, Eleonora and Vittorio  
and all children of my cousins and dear friends.  
Look forward bringing the awareness of the past.*



## *Abstract*

Dept. de Ingenieria Hidráulica, Marítima y Ambiental (EHMA-UPC)

Dept. de Recursos Marins Renovables (ICM-CSIC)

Thesis submitted for the Ph.D. degree in Marine Sciences

### **Trophic Cascade Modelling in Bathyal Ecosystems**

Valeria MAMOURIDIS

Different aspects of the bathyal ecosystem have been treated with the final aim to investigate trophic cascade mechanisms driven by fishery (top-down control), a phenomenon that in bathyal systems has never been studied. This was exemplified by the in-depth study of the exploited soft-bottom continental slope off Catalonia (NW Mediterranean), where the important fishery of the highly priced red shrimp, *Aristeus antennatus*, is carried out and the structure of mayor pathways of the trophic web is known. However due to the (almost complete) lack of information about the fauna in the sediment, this thesis presents a first quantitative seasonal study on the macrobenthos (infauna) in the studied habitat. Also an analysis on the landings per unit effort (LPUE) of the red shrimp fleet has been developed to define the principal influential variables that determine fisheries production. All these studies have in common the investigation of the dynamics of the bathyal system at different levels of organization (population, assemblage and ecosystem) in relation to environmental and fisheries drivers.

In Part I (Chapter 2) the infaunal assemblage in two main habitats, inside the canyon and on the adjacent slope, has been described and has been related to environmental and trophic variables. Important seasonal changes have been detected mainly inside the canyon along over the year. This seasonal variability is associated to the primary production, to river efflux (the Besós river near the study

area) and to the seasonal occurrence of the Levantine Intermediate Waters (LIW) that affect to the chemical and nutritional value of sediment and near bottom waters. All variables, used as proxy for these three environmental causes, explain the seasonal variability in biomass/abundance and changes in taxonomic composition, that reflects, when it occurs, the seasonal turnover of trophic types. With respect to the environmental analysis, the canyon was more influenced by seasonal variations and the terrigenous provision than the open slope, that conversely was more related to primary production and in general showed less evidence of seasonality. The taxonomic/trophic composition of the infauna was explained with these environmental conditions. In fact the canyon showed high variability in trophic types for the most abundant taxa, whereas the adjacent slope was dominated by sub-surface deposit feeders. Moreover, inside the canyon a temporal turnover of major taxa and trophic habits was observed, whereas the adjacent slope showed the seasonal occurrence in February of the genus *Prochaetoderma* spp. that eats on foraminifera especially linked to primary production. The advection processes also explain the higher biomass and abundance in our study than in nearby areas (e.g. the Toulon canyon, that is not an extension of any river. This study was mandatory in order to reconstruct the food web, because it is an important link component between organic matter and the megafauna.

Part II (Chapter 3 and 4) concerns to a long term study of *A. antennatus* landings per unit effort (LPUE) performed through regression analysis using both frequentist and Bayesian additive models. With the frequentist approach the variability explained by the final model (using a total of six predictors) captured the 43% of the total LPUE variability. The set of fishery-related variables (the daily trips performed by vessels, the gross registered tonnage and the factor vessel) was the most important source, with an explained deviance (DE) of 20.58%, followed by temporal (inter and intra-annual variability, DE = 13.12%) and finally economic variables (the ex-vessel shrimp price, DE = 9.30%). We found that data derived from fishery, as well as independent data came from scientific surveys, provide similar indices of the exploited species. The study also showed that the number of trips per month is the most influential variable and that after a certain value

---

it does not correspond to an effective increment in landings per unit effort while high LPUE corresponds to low values of shrimp price. We argued that probably the price drops due to the high availability of the product. Thus it may be appropriate to reduce the limit of the number of trips per month for a reasonable management. Finally if boats hold a random effect, their average effect on the response returns irrelevant, so their use is needless for standardization purposes. For a methodological point of view, in Chapter 4 where the bayesian approach has been used (distributional structured additive regression models, DSTAR), has been shown that a mixed effect model allows to account for correlated data in repeated measurement of catching units.

Part III covers the ecosystem approach of this thesis and is divided into Chapter 5 where we built a steady-state model of the bathyal food web (soft bottom community on the continental slope at 600–800 m depths) and Chapter 6 where the occurrence of trophic cascade was investigated. A total of 40 carbon flows among 7 internal and 6 external compartments, were reconstructed using linear inverse modelling (LIM) by merging site-specific biomass data, on-board oxygen consumption measurements and published parameters to create population and physiological constraints. The total carbon flux to the community was  $2.62 \text{ mmol C m}^{-2} \text{ d}^{-1}$ , entering as vertical ( $5.2\text{E-}03 \text{ mmol C m}^{-2} \text{ d}^{-1}$ ) and advective organic matter ( $2.6\text{E-}00 \text{ mmol C m}^{-2} \text{ d}^{-1}$ ). The influx was then partitioned between the total organic matter in sediment, 87.05%) and suspension and filter feeding (12.95%), among zooplankton (1.08%), suprabenthos (3.07%) and macrobenthos (95.74%). The fate of carbon deposited in sediments was its burial, its degradation by prokaryotes or the ingestion by metazoan deposit feeders. The total ingestion of C in sediments by the metazoan community (excluding the meiofauna) was  $0.83 \text{ mmol C m}^{-2} \text{ d}^{-1}$ , corresponding to the 31.68% of the total C entering the food web and to the 36.34% of the C in sediments, so we deduced that the rest was used by the prokaryote and nematod community ( $1.58 \text{ mmol C m}^{-2} \text{ d}^{-1}$ , 69.28%) or trapped in the sediment ( $0.73 \text{ mmol C m}^{-2} \text{ d}^{-1}$ , 32.19%). The respiration of the whole community (including the total organic matter, TOM) was  $1.89 \text{ mmol C m}^{-2} \text{ d}^{-1}$ : 83.75% for sediments, including prokaryotes and meiofauna, 13.34% for

macrofauna, 2.86% for megafauna, including the red shrimp *A. antennatus*. The dynamic simulation was based on a system of ordinary differential equations to predict biomass trends during 5 years after perturbations induced by red shrimp fishery (top-down driver) and by food supply limitations (bottom-up driver). Our simulation demonstrated that trophic cascades induced by fishery cannot occur through major components of the bathyal food web. We searched for the incidence of trophic cascade through one, two and three interactions also including the organic matter in sediment for the most complex trophic cascade hypothesis, but we only found very ephemeral indirect effects persisting less than 10 days, that we considered not enough to demonstrate the occurrence of this mechanism in the system. On the contrary we found indirect effects persisting more than one month driven by the source limitation. Our results are in agreement with previous studies in which trophic cascades have not been detected in benthic/detritic food webs, with some similarities to the bathyal food web, which depends on allochthonous detritus. We explain the lack of trophic cascade with the important role of detritus in the bathyal ecosystems. The dead organic matter or detritus, whereas it is frequently overlooked, is a common feature of most ecosystems mainly in benthic ecosystems sustained by allochthonous sources. So, we hypothesised that it is the component controlling the food web dynamics, a mechanism known as donor-control.



## *Resumen*

Dept. de Ingeniería Hidráulica, Marítima y Ambiental (EHMA-UPC)

Dept. de Recursos Marinos Renovables (ICM-CSIC)

Memoria presentada para optar al grado de Doctor en Ciencias del Mar

### **Modelado de Cascada Trófica en Ecosistemas Batiales**

Valeria MAMOURIDIS

Diferentes aspectos del ecosistema batial han sido tratados con el objetivo final de investigar mecanismos de cascada trófica impulsados por la pesca (tipo de control top-down), un fenómeno que nunca había sido estudiado en sistemas batiales. Para ello, en esta tesis nos hemos centrado en el estudio del talud continental de fondo suave frente Cataluña (Mediterráneo noroccidental), donde se lleva a cabo la pesquería de la gamba roja *Aristeus antennatus* y la estructura de la red trófica es relativamente conocida. Sin embargo, para poder conseguir ese objetivo y por la falta de información sobre la fauna en el sedimento, esta tesis presenta un primer estudio cuantitativo del macrobentos (infauna) en el hábitat estudiado. También un análisis sobre los desembarques por unidad de esfuerzo (LPUE) de la pesquería de gamba ha sido desarrollado para definir las principales variables que influyen en las variaciones de captura de esa especie. Todos estos estudios tienen en común la investigación de las dinámicas del sistema batial en diferentes niveles de organización (población, comunidad y ecosistema) en relación con variables ambientales y pesqueras.

En la Parte I (Capítulo 2) se ha desarrollado el estudio de la composición de la infauna en dos hábitats principales, dentro del cañón y en el talud abierto, y se ha relacionado con variables ambientales y tróficas. Se han detectado cambios estacionales importantes de biomasa, composición taxonómica y tipos de alimentación,

principalmente en el interior del cañón a lo largo de todo el año. Esta variabilidad estacional se asocia con la producción primaria, el flujo de río (e.g. el Besós cerca de la zona de estudio) y a la aparición estacional de las Aguas Intermedias de Levante (LIW) que afectan a la química y al valor nutritivo de los sedimentos y de las aguas cerca del fondo. Las diferentes variables que se utilizaron, se pueden reconducir a estas tres causas ambientales, explicando la variabilidad estacional en la biomasa/abundancia y en la composición taxonómica, que se reflejan en la variabilidad de las tipologías de alimentación. El cañón está más influenciado por las variaciones estacionales y la provisión terrígena que el talud abierto, que contrariamente resultó ser más relacionado con la producción primaria y en general mostró menor evidencia de estacionalidad. Estas condiciones ambientales pueden explicar la composición taxonómica/trófico de la infauna. De hecho en el cañón mostró se encontró una alta variabilidad en los tipos tróficos para los taxones más abundantes, mientras que el talud abierto estaba dominado por taxones que se alimentan de detrito refractario. Por otra parte, en el interior del cañón se observó una rotación temporal de las principales taxones y hábitos tróficos, mientras que el talud adyacente mostró una diferencia evidente sólo en febrero por la dominancia del género *Prochaetoderma* spp. que se alimenta de foraminíferos. Los procesos de advección también explican la mayor biomasa y abundancia en el área de estudio que en otras zonas cercanas (por ejemplo, el cañón de Toulon, que no es extensión de ningún río). Este estudio fue necesario para estimar los flujos de la red trófica relacionados a la infauna.

La Parte II (capítulos 3 y 4) se refiere a un estudio a largo plazo de los desembarques por unidad de esfuerzo (LPUE) de *A. antennatus* realizado a través de un análisis de regresión y utilizando modelos aditivos generalizados (GAM) con el enfoque frecuentista y sus extensiones como los modelos de regresión aditivos distribucionales estructurados, DSTAR de enfoque bayesiano. Con el enfoque frecuentista la variabilidad explicada por el modelo final (con un total de seis predictores) capturó el 43 % de la variabilidad total del LPUE. El conjunto de variables relacionadas con la pesca (los viajes diarios realizados por los barcos el tonelaje de registro bruto y los barcos mismos) fue la fuente más importante, con

una devianza explicada (DE) de 20.58 %, seguido de variables temporales (inter e intra-anual, DE = 13.12%) y finalmente de variables económicas (el precio de la gamba, DE = 9.30%). Encontramos que los datos derivados de la pesca, así como los datos independientes de ella proporcionados por estudios científicos, devuelven índices similares para la especie explotada. El estudio también mostró que el número de viajes por mes es la variable más influyente. Esa variable después de un cierto valor no se corresponde con un incremento efectivo de los desembarques por unidad de esfuerzo, mientras que al crecer de ese mismo los precios de la gamba bajan, probablemente por la alta disponibilidad del producto. Por lo tanto, puede ser apropiado reducir el límite de la cantidad de viajes al mes a ese umbral encontrado para una gestión razonable del recurso. Por último, si los barcos tienen un efecto aleatorio su efecto sobre la respuesta promedio resulta nulo, por lo que no hay necesidad de utilizar ese factor para fines de normalización. Desde la perspectiva metodológica en el capítulo 4 se demostró (mediante el enfoque bayesiano) que los modelos de efectos mixtos permiten evitar dificultades en la estimación cuando los datos temporales están correlados.

La parte III cubre el enfoque ecosistémico de esta tesis y se divide en el Capítulo 5, donde se construyó un modelo estacionario de la red trófica batial (comunidad de fondo blando en el talud continental entre 600 y 800 m de profundidad) y el Capítulo 6, donde se investigó la ocurrencia de cascadas tróficas. Un total de 40 flujos de carbono entre 7 compartimentos internos y 6 externos, fueron reconstruidos utilizando modelación lineal inversa (LIM) mediante la fusión de datos de biomasa específicos del lugar, las tasas de consumo de oxígeno del sedimento (SOC) y otros parámetros publicados para crear limitaciones poblacionales y fisiológicos. El flujo total de carbono a la comunidad fue  $2.62 \text{ mmol C m}^{-2} \text{ d}^{-1}$ , entrando como materia orgánica por caída vertical ( $5.2\text{E-}03 \text{ mmol C m}^{-2} \text{ d}^{-1}$ ) o por transporte advectivo ( $2.6\text{E-}00 \text{ mmol C m}^{-2} \text{ d}^{-1}$ ). Después, ese flujo se repartió entre la materia orgánica en el sedimento (87.05 %) y alimentación de materia orgánica en suspensión (12.95 %), repartido entre zooplancton (1.08 %), suprabentos (3.07 %) y macrobentos (95.74 %). El destino del carbono depositado en los sedimentos es su enterramiento, su degradación por parte de los procariotas o la ingestión por los

---

metazoos que se alimentan de materia orgánica depositada. La entrada de C total en la comunidad de metazoos (excluyendo la meiofauna) fue de  $0.83 \text{ mmol C m}^{-2} \text{ d}^{-1}$ , correspondiente al 31.68 % del carbono total que entra en la red trófica y al 36.34 % del C en los sedimentos, por lo que se dedujo por esa forma indirecta que el resto fue utilizado por los procariotas y la meiofauna ( $1.58 \text{ mmol C m}^{-2} \text{ d}^{-1}$ , 69.28 %) o atrapado en el sedimento ( $0.73 \text{ mmol C m}^{-2} \text{ d}^{-1}$ , 32.19 %). La respiración de toda la comunidad (incluyendo la materia orgánica total del sedimento, TOM) fue de  $1.89 \text{ mmol C m}^{-2} \text{ d}^{-1}$ : 83.75 % de los sedimentos, incluyendo procariotas y meiofauna, 13.34 % de macrofauna, 2.86 % para megafauna, incluyendo la gamba *A. antennatus*.

La simulación dinámica se basó en un sistema de ecuaciones diferenciales ordinarias para predecir las tendencias de biomasa durante 5 años después de las perturbaciones inducidas por la pesca de la gamba (proceso top-down) y por las limitaciones de alimento primario, representado por el detrito de origen alóctono (proceso bottom-up). La simulación demostró que las cascadas tróficas inducidas por la pesca no pueden ocurrir a través de los principales componentes de la red trófica batial. Se buscó su incidencia a través de dos y tres interacciones incluyendo también la materia orgánica en los sedimentos en la hipótesis más complicada, pero sólo encontramos efectos indirectos muy efímeros que persistieron menos de 10 días, y que no se consideraron suficientes para demostrar la ocurrencia de este mecanismo en el sistema. Por el contrario hemos encontrado efectos indirectos que persisten más de un mes impulsados por la limitación de fuente de energía en la red. Nuestros resultados están de acuerdo con estudios previos en los que no se han detectado las cascadas tróficas en las redes tróficas bentónicas/detríticas, que tienen algunas similitudes con la red trófica batial, en cuanto dependen de detrito alóctono. Explicamos esta falta de cascada trófica con la importante función del detrito en los ecosistemas batiales. La materia orgánica muerta o detrito es una característica común de la mayoría de los ecosistemas, principalmente en los ecosistemas bentónicos que reciben energía de origen alóctono. Valoramos la hipótesis de que el detrito es el componente que controla la dinámica de la red trófica, un mecanismo conocido como controlados por los donantes.

# *Acknowledgements*

First I would like to express my deepest gratitude to my supervisor Dr. Francesc Maynou, for guiding me along this long path; a scientist with ample knowledge in both statistics and marine sciences and also with appreciable inner calm. I thank you because finally in this occasion, I could combine two passions, ecology and statistics.

To Dr. Joan Cartes especially for the years before the Ph.D. when I worked under his supervision. Thanks for teaching me deep-sea peracarids during preparation of samples for SIA. I have always been and I continue to be interested in the macrofauna that marked my first steps in research.

To Dr. Germán Aneiros, a real teacher and to Pr. Carmen Cadarso and Pr. Thomas Kneib, to share with me their ample knowledge on statistics.

To Pr. Karline Soetaert and Dr. Dick van Oevelen, to help me in food web modelling and share their vision of doing science. Thank you very much for allowing me to start the theoretical study of food webs, that I loved so much and I hope to continue with this theme.

I am also deeply grateful to Dr. Santiago Parra for transmitting its knowledge in polychetes' taxonomy.

Then, I would like to thank all participants of the projects and other not directly involved, but whom I worked with: Pr. L. Salvini-Plawen, Dr. Ignacio Salinas, Dr. C. Salas and Dr. S. Gofas for their help in taxonomic identifications of caudofoveates, sipunculans, bivalves and gasteropods respectively, Dr. E. Fanelli especially for her help in the preparation of the published version of the first chapter, Dr. C. Lo Iacono and Pr. M. Carrassón.

In this context I want to thank also Ph.D. students I worked with more or less closely: especially Dorina Seitaj for her help in SOC experiments and Leda Zucca (I will remember all hours we spent in the lab between the freezer, the microscope, the muffle and the balance), Nadja Klein for her important help to understand distributional regression, and also of course Cristina Lopez, V. Papiol and Laurine Burdorf.

---

I also want to show a deep gratitude to all researchers of the ICM. Especially I would like to thank Dr. Antoni Lombarte, Dr. Domingo Lloris, Dr. Eva Galimany, Dr. Teresa Madurell, Dr. Erica Vidal, Dr. Pilar Olivar for their words and support. And also thanks to Dr. Marta Coll and Dr. Isabel Palomera for giving me the opportunity to take part in their Congress as volunteer with the other mates.

During these years, mainly during the master, I also appreciated the passion in teaching of many professors, especially I would remember Pr. Alberto Rodríguez-Casal, Pr. Juan Carlos Pardo Fernández, Pr. José Antonio Vilar Fernández, Pr. Juan Vilar Fernández and Pr. Salvador Naya Fernández.

The professional but also very funny crew of “Garcia del Cid”. Thanks for the kitchen apron “Ada carbonara”, that I use so often! and also to the crew of the “Sarmiento del Gamboa”.

Special thanks to all the administrative staff of the ICM for all the work they have done and do and their availability and courtesy.

Many thanks to my friend Juan Pablo Sáez for his drawings that helped to illustrate this thesis: Figures [1.1](#), [1.8](#), [1.9](#), [1.11](#), [G.3](#), [G.4](#), [H.7](#). I wish that you can continue with your project in scientific illustration.

Then, can not miss many many many thanks to all the mates of “el pasillo de recursos”, many along the entire stay at the ICM. Gracias Ainhoa mi compañera de despacho desde el cominzo aunque luchamos un poco por el aire acondicionado (;P), el gatofilo (como yo) nemertinofilo (yo paso lo siento!!!) Fernando, Marta la mascota del pasillo, las bailarinas Dafni y Raquel de muy buen corazón, Giuliano el fotógrafo del despacho, Lucie y su “que dura es la vida” (te echo de menos darling), Albert, Silvia y Andres los trotamundos, Ángel de principios sólidos, la sonriente Daniela, Ulla el clown, Sam siempre muy tranquilo, Federico que no quiere ganar (a quien lo cuentas?) y Claudio que no sabe perder partidos de volley (prrr ☺), Anabel gran organizadora, Marc el único andorrano biólogo marino, Sonia el vulcano de fiesta, John el pragmático, Noelia que se fue en un plis, Valerio il pescatore sportivo, Teresa, Alba otra que se ensució las manos de barro buscando poliquetos, Costantinos, Ariadna que le gustan los gatos también, Vanesa, Laura, Rigoberto, Dani, Giulia and Carol the rec-rollers, Samuele, David . . . and I do not forget Anamari and el niño de Isabela (jeje) y Amalia, Natalia, Sara and tooooooodos los demás compañeros del ICM. Aaaaaaaaand, let me say:

“GRANDES CHANCLAS!!!” and also: GRANDES son los de EL GRUPO ANTI-VOLLEY (q realmente no existe pero me entraron muchas risas cuando lo escuché decir) and LOS DEL INSTITUTO DE AL LADO . . . ;P. Si no podrá ser con todos, espero, por lo menos con algunos, seguir manteniendo el contacto. 🏹

AAAAll the folks of the de keete (the big brother), especially Silvia, Michele, Vanessa, Misha, Dorina, Tadao, Diana, Francesc and little c. Thanks to you I lived a special and intense experience of life in that big house where all cultures meet. But it was very difficult to keep the kitchen clean . . .

Thanks of course to the powerful network of all my friends, however many are far, you are always present: Camilla and Cecilia, Annalisa, Monica e Sandra le mie amiche superchicche adesso tutto mamme e avete dovuto necessariamente cambiare i vostri poteri . . . , Pierpaolo (aó quando ci ributtiamo in mare?), Federica my favorite classmate (anche altri lo erano ma . . . tu sei rimasta!!!). Per quanto vi riguarda, cari miei, non saprei proprio sintetizzare le troppe cose che mi uniscono a voi e per cui vi adoro . . . Non pensavo mi sareste mancati tanto ma per fortuna c'è Skype per i momenti critici! :). All of you are important to me, as well as Alessandra, Alma que expresa todos sentimientos y Mike que tiene la razón lógica, Germana mio mito femminile in apnea (dopo William Trubridge però ;D), Simone che non dorme mai, Donatella il mio sopraaaaaaano preferiiiiiiiito (♩) e Alberto ovviamente che a ragione é il mio pianista preferito (♩), Emma e Giovanna (vivono, fanno e sono cultura e non solo), Renza che ha sempre un pensiero per tutti ed io per lei, Mitzi la scultura greca, Fina y Vicente que me ayudaron tanto durante mi estancia en Coruña. Y luego Chiara (🍷) ovviamente, presente da prima di arrivare a Barcellona (carrer Fonollar 20), y todas sus amigas super divertidas, Cecilia la loca, Nick uno sprint di energia, la romántica Carol, la pequeña Sushianti, Angela the surfer, chérie Virginie, Rosa aunque no te gusta el swing. Sois una diferente de la otra y tal vez bastante de mí, pero cada una con sus características y calidades que aprecio mucho, sois excepcionales! E poi Rospa e Rospi alias Federica e Fabrizio, ottima famiglia di ceta di 🍃 e la positiva Enrica. Y también quiero agradecer a Javier el poeta estadístico que vive por su “mar atlántico”, Diana y Juan Carlos compañeros de piso excelentes, Héctor el mejor escritor contemporáneo, Natalia and Venere du' caratteri forti molto forti, Patri la campeona del cubiletras (niña te echo de menos, bueno tu también compites por el puesto de excelencia de flatmate), Elena bio-energetic-bailarina, Pina che non auguro a nessuno di conoscere in aereo . . . (ahahah), Alí e la ricciuta Amal, la justa Coté y Montse gran

pintora. E poi non posso dimenticare Livia, non conosco persona più risolutiva!! (Cami, per il momento lasciamo a tua madre il podio, ok?) e neanche Lello, voi siete parte della mia famiglia. E non posso dimenticare la dolce Mahbubeh che lotta per le cause giuste. Thanks to those who listened to me, understanding what it means to be there hours and weeks and I do not say how much more, to find at least one answer to thousand questions. All of you have won a big part in my big heart (:D) and I simply cannot imagine my life without you.

E poi, sebbene non siate stati presenti durante questi anni, non per vostra colpa ovviamente, voglio ringraziare tutti voi amici del circolo di subacquea “CantoDeLAgua”, perché con voi ho imparato il significato di credere l’uno nell’altro e la responsabilità di avere sempre l’occhio attento per l’altro. Ho imparato molto da voi e mi mancano le alzatacce alle 6 di domenica mattina. quindi, oltre Pier e Germana, ricordo ad Andrea, Daniela, Claudio, Marina, Emiliano e tutti tutti gli altri amici.

Thanks also to Santi and all the nice people of the Absenta and to the new cute folks I met thanks to the Lindy hop, especially Serena, Gunter and Martina. I’ve danced and smiled a lot with you! Thanks thanks thanks. Thanks to all “las kukas”, fantastic people of the association Tota Cuca Viu , please, excuse me for leaving you during these last months. 🌸

I am also grateful to the Spanish, Catalan, Galician and Dutch people, because they hosted me during these years and that will remain in my heart even when finished this cycle and I will land elsewhere to start another. Thank You.

Finally thanks to all my family, especially Michela, my “super-sister” e miglior cuoca del mondo, Luciano and my uncles Soulis, Nikos (I8ela na eimai kontá sas perisótero chróno, zitw signwmi) and Takis (sýntoma 8a paízoyme mazi chartiá ;D), my aunts Daniela (e pure con te giocherò a ...burraco!! che non ci giochiamo da tanto :D), Evi and Giorgia, and Stratos, and my cousins Alberto il sognatore ed il suo 🌸 Genziana, Despo and Ioannis (♪♪♪) and Solidea e Giovanni and all all other components of the family.

To my parents, doubtless; and to Vittorio and Lola. Thank you a lot for what you have done for me.

Of course unquestionable thanks to my laptop ♀ and to my fantastic cat 🐱.



Considering that I extended a lot, I think it is appropriate to close, so, if I did not mention someone, please, understand that acknowledgements have a limit ... as well as the thesis does...

Never stop, only reflect enough but not too much, so ... Let's go discover new worlds and enjoy the life!

# *Contributions to Chapters*

## **Chapter 2: A temporal analysis on the dynamics of deep-sea macrofauna: influence of environmental variability in the Catalan Sea (western Mediterranean)**

Published in modified form in Deep Sea Research I, 58: 323–337 (2011) doi: [10.1016/j.dsr.2011.01.005](https://doi.org/10.1016/j.dsr.2011.01.005)

Valeria Mamouridis<sup>1</sup>, Joan E Cartes<sup>1</sup>, Santiago Parra<sup>2</sup>, Emanuela Fanelli<sup>3</sup>, José Ignacio Saiz Salinas<sup>4</sup>

VM SP and JISS made the taxonomic identification, VM and JEC made the statistical analysis, JEC and EF made the sampling design, VM JEC EF the field work, VM JEC wrote the paper

## **Chapter 3: Analysis and standardization of landings per unit effort of red shrimp from the trawl fleet of Barcelona (NW Mediterranean)**

Published in modified form in: Scientia Marina, 78(1) (2014) doi: <http://dx.doi.org/10.3989/scimar.03926.14A>

Valeria Mamouridis<sup>1</sup>, Francesc Maynou<sup>1</sup>, Germán Aneiros Pérez<sup>5</sup>

VM FM and GAP designed the analysis, VM made the statistical analysis, VM and FM wrote the paper

## **Chapter 4: Extended Additive Regression for Analysing LPUE Indices in Fishery Research**

Published in modified form in Reports in Statistics and Operations Research. Universidade de Santiago de Compostela. Departamento de Estadística e Investigación Operativa. Vol. 29/10/2013 (2013-01). <http://eio.usc.es/index.php/es/reports->.

Valeria Mamouridis<sup>1</sup>, Nadja Klein<sup>6</sup>, Thomas Kneib<sup>6</sup>, Carmen Cadarso Suárez<sup>7</sup>, Francesc Maynou<sup>1</sup>

VM, TK and NK designed the study, VM made the statistical analysis, VM NK TK CCS FM wrote the paper

### **Chapter 5: Food web modelling in a soft-bottom continental slope ecosystem (NW Mediterranean)**

Valeria Mamouridis<sup>1</sup>, Karline Soetaert<sup>8</sup>, Dick van Oevelen<sup>8</sup>, Francesc Maynou<sup>1</sup>, Emanuela Fanelli<sup>3</sup>, Joan E Cartes<sup>1</sup>

VM, DVO, KS and FM designed the study, VM and DVO made the model, VM the analysis, VM, FM, EF, JEC collected data, VM and FM wrote the chapter

### **Chapter 6: Simulation of trophic cascade in the bathyal ecosystem**

Valeria Mamouridis<sup>1</sup>, Francesc Maynou<sup>1</sup>, Karline Soetaert<sup>8</sup>, Dick van Oevelen<sup>8</sup>

VM, KS, DVO and FM designed the study, VM made the model and the statistical analysis, VM wrote the chapter

#### **Affiliations:**

- 1) Institut de Ciències del Mar (ICM-CSIC), Passeig Marítim de la Barceloneta 37–49, 08003 Barcelona, Spain.
- 2) Instituto Español de Oceanografía, P.O. BOX 130, 15080 A Coruña, Spain.
- 3) Marine Environmental Research Centre - ENEA Santa Teresa, Pozzuolo di Lerici, 19032 (SP), Italy.
- 4) Dpto de Biología Animal y Genética, Fac. de Ciencias, Universidad del País Vasco, E-48080 Bilbao, Vizcaya, Spain.
- 5) Facultade de Informática, Campus de Elviña s/n, Universidade da Coruña, 15071 A Coruña, Spain.
- 6) Georg-August-University, Centre for Statistics , Platz der Göttinger Sieben, 37073 Göttingen, Germany.
- 7) Unidade de Bioestadística, Facultad de Medicina e Odontolox´a, Rúa San Francisco s/n, 15782 Santiago de Compostela, Spain.

8) NIOZ (Royal Netherlands Institute for Sea Research) Yerseke, Korringaweg 7,  
P.O. Box 140, 4400 AC Yerseke, The Netherlands.

---

## Contents

---

<b>Abstract</b>	<b>v</b>
<b>Resumen</b>	<b>ix</b>
<b>Acknowledgements</b>	<b>xiii</b>
<b>Contributions to chapters</b>	<b>xviii</b>
<b>Contents</b>	<b>xxi</b>
<b>List of Figures</b>	<b>xxv</b>
<b>List of Tables</b>	<b>xxxix</b>
<b>INTRODUCTION</b>	<b>1</b>
<b>1 General introduction</b>	<b>3</b>
1.1 Justification of the study . . . . .	5
1.2 Food webs and trophic cascades . . . . .	8
1.2.1 Food webs: concepts and models . . . . .	8
1.2.2 Trophic cascades and other mechanisms . . . . .	17
1.3 The bathyal domain in the NW Mediterranean sea: energy transfer and faunal composition . . . . .	25
1.4 Deep-sea fisheries, management and models . . . . .	32
1.4.1 The red shrimp fishery in Catalonia . . . . .	32
1.4.2 Monospecific and ecosystem approaches to fisheries and ex- isting models . . . . .	33
1.4.3 The complexity of a model and the bias-variance problem . .	36
1.5 Generalized linear and additive models . . . . .	39
1.6 The study area . . . . .	42
1.7 Purposes of the study . . . . .	46

---

<b>PART I</b>	<b>49</b>
<b>2 A temporal analysis on the dynamics of deep-sea macrofauna: influence of environmental variability in the Catalan Sea (western Mediterranean)</b>	<b>51</b>
2.1 Introduction . . . . .	53
2.2 Materials and Methods . . . . .	55
2.2.1 The Study area and sampling design . . . . .	55
2.2.2 Environmental data collection . . . . .	56
2.2.2.1 Diversity and biomass trends by season . . . . .	57
2.2.3 Statistical analysis . . . . .	58
2.3 Results . . . . .	60
2.3.1 Taxonomic composition . . . . .	60
2.3.2 Diversity and biomass trends by habitat and season . . . . .	60
2.3.3 Assemblage structure: composition by habitat (canyon and adjacent slope) . . . . .	64
2.3.4 Environmental variables . . . . .	65
2.3.5 Influence of environmental variables . . . . .	67
2.3.6 Regression models . . . . .	71
2.4 Discussion . . . . .	72
2.4.1 Comparison with other quantitative studies . . . . .	74
2.4.2 Dynamics of infauna assemblages . . . . .	75
<b>PART II</b>	<b>81</b>
<b>3 Analysis and standardization of landings per unit effort of red shrimp from the trawl fleet of Barcelona (NW Mediterranean)</b>	<b>83</b>
3.1 Introduction . . . . .	85
3.2 Materials and Methods . . . . .	87
3.2.1 Data source . . . . .	87
3.2.2 Model construction . . . . .	89
3.2.3 Theoretical response probability function . . . . .	90
3.2.4 Selection criteria and explained deviance . . . . .	91
3.2.5 LPUE standardization . . . . .	91
3.3 Results . . . . .	92
3.3.1 Overview of data and response distribution . . . . .	92
3.3.2 Model building and comparison . . . . .	95
3.3.3 The descriptive model . . . . .	95
3.3.4 LPUE standardization . . . . .	100
3.4 Discussion . . . . .	101
3.4.1 The role of explanatory variables . . . . .	101
3.4.2 Implications for management . . . . .	103
<b>4 Extended Additive Regression for Analysing LPUE Indices in Fishery Research</b>	<b>105</b>

4.1	Introduction . . . . .	107
4.2	Materials and Methods . . . . .	111
4.2.1	Data description . . . . .	111
4.2.2	Methodology . . . . .	112
4.3	Results . . . . .	117
4.3.1	Model selection, diagnostics and comparison . . . . .	117
4.3.2	Description of partial effects . . . . .	122
4.4	Discussion . . . . .	126
<b>PART III</b>		<b>131</b>
<b>5</b>	<b>Food web modelling in a soft-bottom continental slope ecosystem (NW Mediterranean)</b>	<b>133</b>
5.1	Introduction . . . . .	135
5.2	Materials and Methods . . . . .	137
5.2.1	The study area . . . . .	137
5.2.2	Biomass data . . . . .	139
5.2.3	Other data . . . . .	141
5.2.4	Literature data . . . . .	142
5.2.5	Linear inverse modelling . . . . .	144
5.2.6	Food web structure . . . . .	147
5.2.7	Network indices . . . . .	149
5.2.8	Software . . . . .	153
5.3	Results . . . . .	153
5.3.1	The food web . . . . .	153
5.3.2	The network indices . . . . .	158
5.3.3	Oxygen consumption results . . . . .	159
5.4	Discussion . . . . .	159
5.4.1	Inputs and resource partitioning . . . . .	160
5.4.2	Community respiration . . . . .	164
5.4.3	Network analysis . . . . .	165
<b>6</b>	<b>Simulation of trophic cascade in the bathyal ecosystem</b>	<b>167</b>
6.1	Introduction . . . . .	169
6.2	Materials and Methods . . . . .	172
6.2.1	The dynamic model . . . . .	173
6.2.2	Local stability of the food web . . . . .	175
6.2.3	The simulation . . . . .	176
6.2.3.1	Couples of species . . . . .	178
6.2.4	Software . . . . .	178
6.3	Results . . . . .	179
6.3.1	Interactions effected . . . . .	179
6.3.2	The total biomass . . . . .	180
6.3.3	Relative biomasses . . . . .	181
6.4	Discussion . . . . .	182

---

<b>PART IV</b>	<b>187</b>
<b>7 General discussion</b>	<b>189</b>
7.1 General discussion . . . . .	191
7.2 PART I The infauna in the continental slope . . . . .	191
7.3 PART II Landings per unit effort LPUE . . . . .	193
7.4 PART III The bathyal food web . . . . .	196
7.5 PART III Trophic cascades and drivers in the bathyal ecosystem. . .	201
<b>8 Conclusions</b>	<b>205</b>
8.1 Conclusions . . . . .	206
<b>APPENDICES</b>	<b>209</b>
<b>A EAF models</b>	<b>211</b>
<b>B Complementary material – Chapter 2</b>	<b>215</b>
<b>C Complementary material – Chapter 3</b>	<b>219</b>
C.1 Exploratory study on the response variable LPUE and diagnostic plots of the final model . . . . .	220
<b>D Complementary material – Chapter 4</b>	<b>223</b>
D.1 Model selection . . . . .	224
D.2 Comparison of partial effects among models . . . . .	226
<b>E Complementary material – Chapter 5</b>	<b>233</b>
E.1 Sediment Oxygen Consumption . . . . .	234
E.2 LIM equations . . . . .	235
E.3 Results of the food web model . . . . .	238
E.4 Network indices equations and results . . . . .	241
<b>F Complementary material – Chapter 6</b>	<b>247</b>
<b>G Species Pictures</b>	<b>251</b>
<b>H Field and Laboratory material</b>	<b>259</b>
H.1 SOC experiment and Winkler titration . . . . .	266
<b>I Offprint</b>	<b>269</b>
I.1 Publications . . . . .	270
I.2 Congress proceedings . . . . .	353
<b>References</b>	<b>367</b>



---

## List of Figures

---

1.1	The red shrimp <i>Aristeus antennatus</i> (Risso, 1816). . . . .	5
1.2	Three examples of theoretical food webs. In columns: (A) binary and (B) quantified food webs. In rows: (1) Random model, (2) Cascade model and (3) Niche model with $N = 9$ compartments $S$ and $L = 30$ number of links. . . . .	11
1.3	The fate of consumed energy for a given component (or an individual). Symbols represent: $C$ = energy consumed, $A$ = energy assimilated, $E$ = the egested energy, $P$ = the produced energy, $M$ = the energy used for maintenance. Idea of the figures taken from A) Moore and de Ruiter (2012) and B) Brey (2001). . . . .	13
1.4	Output of the dynamic simulation for the niche food web in Figure 1.2, 3-B. The time span is 20 years and plot, headed by a number from 1 to 9, corresponds to each species of the food web. On the $y$ axis are shown the biomasses. Dark: unperturbed biomass; red: biomasses perturbed by 1/2 of the original value; green: biomass perturbed by 2 of the original value. . . . .	15
1.5	Functional response types described by Holling (1959). A) Type I and B) Corresponding relative mortality. C) Type II and D) Corresponding relative mortality. E) Type III and F) Corresponding relative mortality. . . . .	18
1.6	Example of the trophic cascade between otter, sea urchin and kelp (then also extended to killer whale) in the ecosystem of the Aleutian Islands (Alaska, USA) (Estes et al., 1998). . . . .	19
1.7	Description of the hypothesis of two alternative states in the ecosystem nearby the Medes Reserve (western Mediterranean) explainable by mechanisms of trophic cascade. From Pinnegar et al. (2000). . . . .	21
1.8	Principal domains of benthic and pelagic regions. Depths are not to scale. . . . .	26
1.9	Principal pathways in the bathyal domain. BBL = Benthic Boundary Layer, modified from WWF/IUCN (2004), pg. 28. . . . .	27
1.10	Global distribution of cold-water corals. From Roberts et al. (2006). . . . .	29

1.11	Fishing grounds of the red shrimp fishery at the continental slope off Catalonia. Modified from Sardà et al. (1997). . . . .	33
1.12	The bias-variance trade-off in model fitting with increasing complexity (the more parametrization, the higher complexity). Increasing the model complexity also the variance increases, while the bias decreases. The best fit occurs when both are minimized (vertical dashed line). Here error defines whatever measure used to summarise the error of the model, being the integrated or the average mean square error or the predictive risk. See the text for more details.	37
1.13	The Balearic basin and study area inside the red polygon. . . . .	43
2.1	Map of the study area off the Catalan coast, showing the positions of samples inside canyons Besòs and Berenguera (C1, C2) and on the adjacent slopes (S1, S2) stations. . . . .	55
2.2	Diversity parameters: $S$ represents the total number of species, $H'$ is the Shannon index in S1 (white dots) and C1 (black dots). . . . .	61
2.3	(a) Annual mean biomass (WWmg/m <sup>2</sup> ) profiles of total infauna and major taxa, (b) Annual mean density (ind/m <sup>2</sup> ) of total infauna, polychaetes and crustaceans, (c) individual mean weight (WWmg/ind) of polychaetes, crustaceans and molluscs. Dark gray bars indicate C1 samples and light gray bars indicate S1 samples. . . . .	62
2.4	nMDS ordination of samples from a full year (B1, B2, B3 and B4). Labels indicated: <i>hom</i> = water column homogenization and <i>str</i> = water column stratification for the factor WATER CONDITIONS. Symbols indicate: full cycles = canyon; empty cycles = adjacent slope for the factor HABITAT. . . . .	64
2.5	Environmental variables as a function of season. Temperature above the bottom ( $T_{5mab}$ ); salinity ( $S_{5mab}$ ); fluorescence ( $f_{0-500m}$ ); water turbidity close to the bottom ( $turb_{5mab}$ ); potential redox of sediments (at a depth of 1 cm: $Eh$ ); $tom$ in sediments. (dark dots): canyon; (white dots): adjacent slope. . . . .	66
2.6	Environmental variables. a) <i>Chla</i> in surface by satellite imagery (dark dots: canyon; white dots: adjacent slope); b) river flow (m <sup>3</sup> s <sup>-1</sup> ) of the two most important rivers in central Catalan coasts.	67
2.7	PCAs of environmental variables collected in (a) canyon stations and (b) adjacent slope. . . . .	68
2.8	CCA of broad taxa, considering both canyon and adjacent slope samples, with selected environmental variables. . . . .	69
2.9	CCA of dominant species (a) inside the canyon and (b) on the adjacent slope and the environmental variables. For the full name of species' acronyms see Table 2.1. . . . .	70
3.1	Time series from 1994 to 2008 of LPUE data and spline estimation (upper panel) and mean annual North Atlantic Oscillation (NAO) (lower panel). . . . .	93

3.2	From top to bottom: spline estimation of the fuel price, monthly total number of trips performed by the fleet from year 1996 to 2008, and relationship between the fuel price and the total monthly number of trips. . . . .	94
3.3	Partial effects of model 7. Bayesian credible intervals (95%). . . . .	99
3.4	Comparison between the fishery-derived (standardized LPUE) and the SGMED index. Variables have been normalized for comparison. . . . .	100
4.1	Boxplots for MSEP calculated for all models. See Table 4.2 and Equations in the text for model specifications. . . . .	119
4.2	QQplots of the normalized residuals calculated as described in the methodology section for all models. . . . .	121
4.3	QQplots for normality of catching units parameters as random effects in the mixed model M8. $\alpha_\mu$ refer to random effects in the predictor for location, while $\alpha_\sigma$ refers to the predictor for the shape. . . . .	122
4.4	Interval plots of estimated random effects in the predictor for location ( $\alpha_\mu$ ) and shape ( $\alpha_\sigma$ ) on the upper and lower plots respectively. Bars indicates 95% CI. . . . .	123
4.5	Nonparametric effects for the model M8. Effects on predictors for $\mu$ (left side) and for $\sigma$ (right side). Grey shapes represent 95% credible intervals. . . . .	124
5.1	The food web study area comprises the soft-bottom slope in front of the Catalonia at 600-800 m. . . . .	138
5.2	A) Binary food web, B) quantified food web by the model, C) legend of the flows ( $\text{mmol C m}^{-2} \text{ d}^{-1}$ ). . . . .	153
5.3	Food web carbon flows ( $\text{mmol C m}^{-2} \text{ d}^{-1}$ ). See Table 5.2 for abbreviations of food web compartments and Tables E.4 and E.4 for the values of the flows. The legend shows maximum and minimum flow values estimated through the parsimonium solution. . . . .	154
5.4	Barplot of the food web flows (mean $\pm$ sd, $\text{mmol C m}^{-2} \text{ d}^{-1}$ ) estimated using the MCMC method in descending order from the left to the right. . . . .	155
5.5	Sediment Community Oxygen Consumption ( $\text{mmol O}_2 \text{ m}^{-2} \text{ d}^{-1}$ ) as a function of depth (m). The grey points are observations, the continuous line represents the mean fitted value, the dashed lines corresponds to the average SCOC value (also in the Figure) at comparable depths (here we set 700 m the interpolations between 600-800 m depths, the range of our food web) and the estimation by our food web model is represented in red, the average is the red dot (with the corresponding number) and the segment represents the range. The function is the model in Equation E.2, Appendix E. Also the $r^2$ is reported. . . . .	159

5.6	Food web carbon flows ( $\text{mmol C m}^{-2} \text{ d}^{-1}$ ) as in Figure 5.3 but divided in A) input (green), B) output (red) and C) internal (black) flows. See Table 5.2 for abbreviations of food web compartments and Tables E.4 and E.4 for flows' estimations. The legend shows maximum and minimum flows estimated through the parsimonium solution. . . . .	160
6.1	(A) Food web net flows and (B) trophic position of components. Colours correspond to compartments: orange = zooplankton (ZPL); red = suprabenthos (SBN); green = macrobenthos (MABN); blue = invertebrates from megafauna (MEBN); light blue = fish from megafauna (ICT); violet = red shrimp <i>Aristeus antennatus</i> (AANT).	172
6.2	A) Changes of relative biomasses during the 5 years using $p=(0,5,-5)$ .	181
6.3	B) Changes of relative biomasses during the 5 years using $p=(0,20,-20)$ . . . . .	182
6.4	C) Changes of relative biomasses during the 5 years using $p=(0,50,-50)$ . . . . .	183
C.1	From left to right, upper panels, histogram and kernel density estimations of $\text{lpue}$ ; middle panels, box-plot and cumulative distribution function of data and of the gamma distribution; lower panels, QQ-plots of sample quantiles versus gamma and normal distribution quantiles. . . . .	221
C.2	Residual diagnostics for model 7. (A) Histogram of deviance residuals; (B) QQ-plot of deviance residuals; (C) deviance residuals against linear predictor; (D) response against fitted values. . . . .	222
D.1	Nonparametric effects on the predictor for $\mu$ for the LN fixed effect model M1 and the mixed effects model M2 with best DIC score. Grey shapes represent 95% credible intervals. . . . .	227
D.2	Nonparametric effects for the LN fixed effect model M3 with best DIC score. Effects on predictor for $\mu$ (left side) and for $\sigma^2$ (right side). Grey shapes represent 95% credible intervals. . . . .	228
D.3	Nonparametric effects for the LN mixed effect model M4 with best DIC score. Effects on predictor for $\mu$ (left side) and for $\sigma^2$ (right side). Grey shapes represent 95% credible intervals. . . . .	229
D.4	Nonparametric effects on the predictor for $\mu$ for the GA fixed effect model M5 and the mixed effects model M6 with best DIC score. Grey shapes represent 95% credible intervals. . . . .	230
D.5	Nonparametric effects for the GA fixed effect model M7 with best DIC score. Effects on predictor for $\mu$ (left side) and for $\sigma$ (right side). Grey shapes represent 95% credible intervals. . . . .	231
D.6	Nonparametric effects for the GA mixed effect model M8 with best DIC score. Effects on predictor for $\mu$ (left side) and for $\sigma$ (right side). Grey shapes represent 95% credible intervals. . . . .	232

E.1	Range estimation of food web flows. The dark point represents the parsimonious solution, the segments minimum to maximum ranges.	238
F.1	A) Changes of total biomass during the 5 years using $p=(0,5,-5)$ .	248
F.2	B) Changes of total biomass during the 5 years using $p=(0,5,-5)$ .	249
F.3	C) Changes of total biomass during the 5 years using $p=(0,50,-50)$ .	250
G.1	A) The Shortfin spiny eel <i>Notacanthus bonaparte</i> Risso, 1840. Latium, MEDITS-IT, 2004; B) The macrurid Roughtip grenadier <i>Nezumia sclerorhynchus</i> (Valenciennes, 1838). Latium, MEDITS-IT, 2004; C) The Jewel lanternfish <i>Lampanyctus crocodilus</i> (Risso, 1810). Latium, MEDITS-IT, 2004; D) <i>Cyclothone braueri</i> , Jespersen & Tåning, 1926. Antromare survey, 2010.	252
G.2	A) The Rabbit fish <i>Chimaera monstrosa</i> , Linnaeus, 1758. Latium, MEDITS-IT, 2003; B) <i>Alepocephalus rostratus</i> Risso, 1820. Catalan Sea, Biomare 2007; C) The deep-water coral <i>Isidella elongata</i> . Catalan Sea, Antromare July 2011.	253
G.3	A) The Blackmouth catshark <i>Galeus melastomus</i> , Rafinesque, 1810; B) The Common Atlantic grenadier <i>Nezumia aequalis</i> (Günther, 1878); C) The European hake <i>Merluccius merluccius</i> (Linnaeus, 1758). January 2015. ©Juan Pablo Sáez.	254
G.4	A) The Jewel lanternfish <i>Lampanyctus crocodilus</i> (Risso, 1810); B) The half-naked hatchetfish <i>Argyropelecus hemigymnus</i> , Cocco, 1829. January 2015. ©Juan Pablo Sáez.	255
G.5	A) The bivalve <i>Kelliella miliaris</i> (Philippi, 1844) B) The cumacean <i>Leucon (Epileucon) longirostris</i> Sars, 1871, ♂; C) A caudofoveat belonging to the genus <i>Falcidens</i> Salvini-Plawen, 1968; D) The bivalve <i>Ennucula aegeensis</i> (Forbes, 1844); E) The amphipod <i>Carangoliopsis spinulosa</i> Ledoyer, 1970; F) The ophiurid <i>Amphiura chiajei</i> Forbes, 1843 (oral view); G) <i>Campilaspis glabra</i> G. O. Sars, 1879; H) The ophiurid <i>Amphipholis squamata</i> (Delle Chiaje, 1828) (dorsal view). Specimens from boxcorer and suprabenthic sledge. Biomare 2007, Antromare 2010-2011.	256
G.6	A) <i>Leucon (Macrauloleucon) siphonatus</i> Calman, 1905; B) <i>Campylaspis squamifera</i> Fage, 1929; C) The amphipod <i>Stegocephaloides christianiensis</i> (Boeck, 1871); D) <i>Leucon (Crymoleucon) macrorhinus</i> Fage, 1951; E) The amphipod <i>Idunella nana</i> (Schiecke, 1973); F) <i>Diastylodes serrata</i> (Sars G.O., 1865); G) <i>Eudorella truncatula</i> (Bate, 1856); H) Postnauplius of a cumacean (probably <i>L. longirostris</i> ). Specimens from boxcorer and suprabenthic sledge. Biomare 2007, Antromare 2010-2011.	257
H.1	Boxcorer. B/O García del Cid, Catalan Sea, BIOMARE October, 2007.	260
H.2	Multicorer. B/O García del Cid, Catalan Sea, BIOMARE October, 2007.	261

---

H.3	(A) WP2 used to sample zooplankton and micronekton. (B) Suprabenthic sledge used to sample suprabenthos. B/O García del Cid, Catalan Sea, BIOMARE October, 2007. . . . .	262
H.4	A) A lid with different holes used to introduce the stirrer, sensors for digital records or pipettes for the Winkler titration; B) The perspex chambers ( $d = 30$ cm). All material provided by the Ecosystem studies department of the NIOZ-Yerseke. . . . .	263
H.5	A lip containing a Teflon-coated magnetic stirrer. All material provided by the Ecosystem studies department of the NIOZ-Yerseke. . . . .	264
H.6	An incubation with water. Preparing experiments at the NIOZ-Yerseke, 2011. . . . .	265
H.7	Scheme for soc experiments and Winkler titration. . . . .	267

---

## List of Tables

---

1.1	Size-based classification of benthos with size range and main groups in each size class. . . . .	9
1.2	Soft-bottom trophic cascades recompiled from literature. Cascades in parenthesis are based on circumstantial evidence. Ref: (1) Pipitone et al. (2000) ; (2) Pauly (1985); (3) Christensen (1998); (4) Caddy (1983); (5) Aronson (1990); (6) Virnstein (1977). . . . .	22
2.1	One way SIMPER analysis (factor used: habitat) based on Bray-Curtis similarity (cut-off: 80%). Percentage contribution and cumulative percentage of taxa are reported for each level of the factor, as well as the acronyms of taxa used as labels in CCAs. AM: amphipoda, PO: polychaeta, IS: isopoda, SI: sipuncala, EC: echinodermata, BI: bivalvia, CA: caudofoveata, CU: cumacea. . . . .	63
2.2	A) Permanova based on Sperman rank correlation distance matrix of whole dataset and B) pairwise tests (Only significant tests are reported; Monte Carlo significance within brackets if differs from permanova's). (ns: not significant; *: < 0.05, **: < 0.01, ***: < 0.001). Factors: habitat (levels: <i>can</i> , <i>slo</i> ) and water column condition (levels: homogenized, <i>hom</i> , and stratified, <i>str</i> ) . . . . .	65
2.3	GAMs for A) the total biomass of the macrofauna, B) Polychaetes' biomass C) Crustaceans' biomass and D) Molluscs' biomass. For each response, the right side of the model, the significance of the effect, the GCV, the AIC, the adjusted r-squared (R2) and the deviance explained (DE) are given. . . . .	72
3.1	List of variables. Differences between pairs of categories of the variable <i>month</i> were checked through Tukey HSD test. Non-significantly different categories were grouped to create the new variable <i>period</i> , to which the same test was applied. The same procedure was applied for the variable <i>code</i> , to create the variable <i>group</i> (all significant tests with $p \leq 0.001$ ). . . . .	89

3.2	Model construction. N, number associated with each model; model, models right part of the formula; df, models degree of freedom; RD, residual deviance, DE, percentage of deviance explained by each model; AIC, Akaike Information Criterion; term(ns), insignificant terms in a model; term (+), terms not incorporated in next steps (i.e. models with the incorporation of <i>hp</i> or <i>fprice</i> gave a lower DE than the incorporation of <i>grt</i> and <i>time</i> , respectively). Model 12 is the model used for standardization. . . . .	96
3.3	Results of the final model (Equation 3.3). Results associated with (a) linear terms, (b) smooth terms and (c) global estimations. $\mu$ : estimation of the mean; $\sigma$ : standard deviation; $t$ : value of $t$ -statistic; $F$ : the $F$ -statistic value; $p$ : $p$ -value associated to the $t$ or the $F$ statistic; DE: deviance explained by each term in percentage; $edf$ : effective degrees of freedom; $\lambda$ : estimated smoothing parameter; $df$ : total degree of freedom; $scale$ : estimation of the scale parameter; $R^2(\text{adj})$ : adjusted R-squared; AIC: Akaike Information Criterion; GCV, generalized cross validation; $DE_{tot}$ (%): percentage of total deviance explained by the model. . . . .	97
4.1	List of variables. . . . .	112
4.2	Global scores of selected models. M: model coding; A: the assumed distribution is log-normal (LG) or gamma (GA); B: (LO) the location varies w.r.t. explanatory variables while the second parameter is constant or (LS) both vary; C: if the unit-specific effect is considered as fixed, thus the model has only fixed effects (FI) or random and the model is a mixed effects model (MI); DEV, the residual deviance; EP: Effective total number of Parameters, DIC: Deviance Information Criterion, MSEP, mean and sd of the mean square error of predictions calculated through 10-fold validation. . . . .	118
4.3	Estimations of linear fixed effects for the model M8, Eq. (4.3) associated to A) $\mu$ and B) $\sigma$ respectively. . . . .	122
5.1	Main information about sampling stacios: CODE: code of each station; POS: the corresponding positions; DEPTH: the corresponding depths; YEAR: the years when samples were performed; HAB: specific habitat, MUD: mud habitat on the open slope, and MD: mud coral habitat (with <i>Isidella elongata</i> ) on the open slope. . . . .	137
5.2	Standing stocks of the food web compartments for the soft bottom slope food web. The binary structure is defined in Section 5.2.6 and quantified by data available in Section 5.2.2. A) Compartments' name, B) Abbreviation used through the text, C) Stock values (mean, $\text{mmol C m}^{-2}$ ), D) Origin of data: A=ANTROMARE B=BIOMARE, E) Number of samples. (*) Excluding megaichthyofauna and <i>A. antennatus</i> . (**) % $C_{org}$ in sediment (gDW). . . . .	143
5.3	Derived global estimations, [ $min, max$ ], ( $\text{mmol C m}^{-2} \text{ d}^{-1}$ ) of important processes in the food web. . . . .	156



5.4	Derived estimations of flows related to the red shrimp fishery, $[min, max]$ . (A) expressed in $mmol\ C\ m^{-2}\ d^{-1}$ ; (B) expressed in $Kg\ km^{-2}\ y^{-1}$ ; (C) expressed in $Kg\ boat^{-1}\ d^{-1}$ , here d is “working day” and has the same units of LPUE in Chapters 3 and 4. $F_t$ is the total fishing rate; $F_a$ is the portion of fishing pressure on red shrimp; $F_i$ is the portion of fishing pressure on the fish stock; $F_b$ is the portion of fishing pressure on invertebrates. . . . .	157
5.5	The trophic level and omnivory index (mean $\pm$ sd) for all living components. . . . .	158
6.1	Possible pathways of trophic cascade. MLT = mid trophic levels, AANT, ICT and MEBN, LTL = lower trophic levels, MABN, SBN and ZPL. * Jointly. ** Jointly or all subsets. *** Jointly or MEBN. . . . .	172
6.2	Relationship investigated. . . . .	177
6.3	List of indicators (response variables) and their description. . . . .	179
6.4	Couples of components between which the <i>shift</i> occurs. . . . .	180
A.1	Alphabetical list of models used in the ecosystem approach of fisheries (PART 1/2). Revised from (Plagányi, 2007). References are: 1. Fulton, Smith and Johnson, 2004, 2. Fulton et al., 2005, 3. Yodzis and Innes, 1992, 4. Yodzis, 1998, 5. Koen-Alonso and Yodzis, 2005, 6. Bogstad et al., 1997, 7. Stefánsson and Palsson, 1998, 8. Butterworth and Thomson, 1995, 9. Mori and Butterworth, 2004, 10. Mori and Butterworth, 2005, 11. Mori and Butterworth, 2006, 12. Thomson et al., 2000, 13. Constable, 2006, 14. Baretta-Bekker et al., 1997, 15. Livingston and Methot, 1998, 16. Hollowed et al., 2000, 17. Tjelmeland and Lindstrøm, 2005, 18. Christensen and Pauly, 1992, 19. Christensen and Walters, 2004, 20. Polovina, 1984, 21. Walters et al., 1997, 22. (Walters et al., 2000), 23. Begley and Howell, 2004, 24. Trenkel et al., 2004, 25. Taylor and Stefánsson, 2004, 26. Taylor and Taeknigardur, 2011, 27. Finnoff and Tschirhart, 2003, 28. Finnoff and Tschirhart, 2008, 29. Alonzo et al., 2003, 30. DeAngelis and Gross, 1992, 31. Purcell and Kirby, 2006, 32. Shin and Cury, 2004, 33. Fulton, Smith and Johnson, 2004, 34. Fulton, Parslow, Smith and Johnson, 2004, 35. McDonald et al., 2006, 36. Watters et al., 2005, 37. Watters et al., 2006, 38. Punt and Butterworth, 1995, 39. Jurado-Molina et al., 2005, 40. Garrison et al., 2010, 41. Sparholt, 1995, 42. Sparre, 1991, 43. Tjelmeland and Bogstad, 1998, 44. Colomb et al., 2004, 45. Shin and Cury, 2001, 46. Bertignac et al., 1998, 47. Lehodey et al., 2003, 48. Lehodey et al., 2008, 49. Tjelmeland and Lindstrøm, 2005, 50. Bax, 1985, 51. Plagányi and Butterworth, 2006, 52. Sekine et al., 1991, 53. Hamre and Hatlebakk, 1998. . . . .	212
A.2	Alphabetical list of models used in the ecosystem approach of fisheries (PART 2/2). Revised from (Plagányi, 2007). References in A.1. . . . .	213

B.1	List of species (PART 1/3). Mean number of specimens (ind/m <sup>2</sup> ) collected from canyon adjacent slope. . . . .	216
B.2	List of species (PART 2/3). Mean number of specimens (ind/m <sup>2</sup> ) collected from canyon adjacent slope. . . . .	217
B.3	List of species (PART 3/3). Mean number of specimens (ind/m <sup>2</sup> ) collected from canyon adjacent slope. . . . .	218
D.1	Global scores for LN models. 1a) fixed effects models with predictor $\eta_\mu$ , 1b) fixed effects models with predictors $\eta_\mu$ and $\eta_{\sigma^2}$ , 2a) mixed effects models with predictor $\eta_\mu$ , 2b) mixed effects models with predictors $\eta_\mu$ and $\eta_{\sigma^2}$ . PRED: specifies the predictor, and VAR: defines the variables in the corresponding predictor. DEV: residual deviance; EP: Effective total number of Parameters, DIC: Deviance Information Criterion. Models without global scores could not be estimated (see the corresponding Chapter). . . . .	224
D.2	Global scores for GA models. 1a) fixed effects models with predictor $\eta_\mu$ , 1b) fixed effects models with predictors $\eta_\mu$ and $\eta_\sigma$ , 2a) mixed effects models with predictor $\eta_\mu$ , 2b) mixed effects models with predictors $\eta_\mu$ and $\eta_\sigma$ . PRED: specifies the predictor, and VAR: defines the variables in the corresponding predictor. DEV: residual deviance; EP: Effective total number of Parameters, DIC: Deviance Information Criterion. Models without global scores could not be estimated (see text). . . . .	225
E.1	Constraints imposed to the model. (A) TOM compartment, (B) Faunal compartments, (C) Diet constraint (only for the red shrimp). A: assimilation, R: respiration, U: Uptake. SOC = sediment oxygen consumption; BE = burial efficiency; RR = respiration rate; NGE = net growth efficiency; AE = assimilation efficiency; MR = maintenance respiration; PR = production rate; DP = proportion of source $j$ in the diet of predator $j$ . . . . .	235
E.2	Equations of the binary food web and steady-state assumption incorporated in the food web model. . . . .	236

E.3	Parameters and constrains for the food web model. In brackets minimum and maximum values of parameters are reported, while single values correspond to the mean of parameters. <i>Tlim</i> = temperature limitation; SOC = sediment oxygen consumption; BE = burial efficiency; RR = respiration rate; NGE = net growth efficiency; AE = assimilation efficiency; MR = maintenance respiration; PR = production rate; DP = proportion of source <i>j</i> in the diet of predator <i>j</i> ; FR = fishing rate; CR = catch rate. References: (1) Epping et al., 2002, (2) Own data from ANTROMARE survey, (3) Burdige et al., 1999, (4) van Oevelen, Soetaert, Middelburg, Herman, Moodley, Hamels, Moens and Heip, 2006 and references therein, (5) Mahaut et al., 1995, (6) Company and Sardà, 1998, (7) van Oevelen, Soetaert, García, de Stigter, Cunha, Pusceddu and Danovaro, 2011, (8) Cartes, Brey, Sorbe and Maynou, 2002, (9) Own data from BIOMARE survey, (10) Fauchald and Jumars, 1979, (11) Cartes, Papiol and Guijarro, 2008, (12) From longitudinal data of the Catalan government. . . . .	237
E.4	Food web flows' estimations: range (minimum and maximum), least distance and least square (mean) solutions. Flows in $\text{mmol C m}^{-2} \text{d}^{-1}$ . . . . .	239
E.5	MCMC (mean and standard deviation) solution and Coefficient of Variation (CoV) for the food web flows. . . . .	240
E.6	Nomenclature of symbols used in calculation of network index equations (Table E.7). Revised from Kones et al. (2009). . . . .	241
E.7	Network Index formulas (PART 1/2). See Table E.6 for the definition of terms. References: (1) Hirata and Ulanowicz, 1984, (2) Latham II, 2006, (3) Kones et al., 2009, (4) Pimm and Lawton, 1980, (5) Finn, 1976, (6) Finn, 1980, (7) Patten and Higashi, 1984, (8) Allesina and Ulanowicz, 2004, (9) Ulanowicz, 1986, (10) Ulanowicz and Norden, 1990, (11) Ulanowicz, 2004, (12) Ulanowicz, 2000, (13) Christensen and Pauly, 1992, (14) Lindeman, 1942. Revisited from ref. 3. . . . .	242
E.8	Network Index formulas (PART 2/2). See Table E.6 for the definition of terms. References: (1) Hirata and Ulanowicz, 1984, (2) Latham II, 2006, (3) Kones et al., 2009, (4) Pimm and Lawton, 1980, (5) Finn, 1976, (6) Finn, 1980, (7) Patten and Higashi, 1984, (8) Allesina and Ulanowicz, 2004, (9) Ulanowicz, 1986, (10) Ulanowicz and Norden, 1990, (11) Ulanowicz, 2004, (12) Ulanowicz, 2000, (13) Christensen and Pauly, 1992, (14) Lindeman, 1942. Revisited from ref. 3. . . . .	243
E.9	Estimations of network indices. A) Basic properties and Pathway analysis; B) Network uncertainty and constraint efficiencies; C) Environmental analysis. . . . .	244
E.10	Indices of system growth and development. . . . .	245
H.1	Reagents for one sample of water (10ml). . . . .	266



---

## INTRODUCTION

---



# CHAPTER 1

---

General introduction

---





## 1.1 Justification of the study

Deep sea occupies more than two-thirds of the Earth's surface of which a very small fraction has been investigated. Deep sea remains still largely unexplored in terms of biota and their spatial and temporal dynamics. Studies have been directed toward interesting habitats such as the canyons crossing the slope (Vetter and Dayton, 1998), the seamounts (de Forges et al., 2000), the mid-ocean ridges and the hydrothermal vents (Van Dover, 1995; Van Dover et al., 2002).

In recent decades the interest towards deep-sea ecosystems increased due to warnings about fisheries impacts. Researchers realised that fishing in the deep sea might affect or already has affected these widely considered fragile ecosystems (in the North Atlantic: Gordon, 2001; Koslow et al., 2000; in the Mediterranean: Moranta et al., 2000; Politou et al., 2003). Many deep-sea species show k-selection (and so fragile) characteristics: longevity, late age at maturity, slow growth and low fecundity, leading to an exceptionally low productivity (Devine et al., 2006). The consequences are high vulnerability to overfishing and potentially little resilience to overexploitation (Koslow et al., 2000). Examples of fragile species are

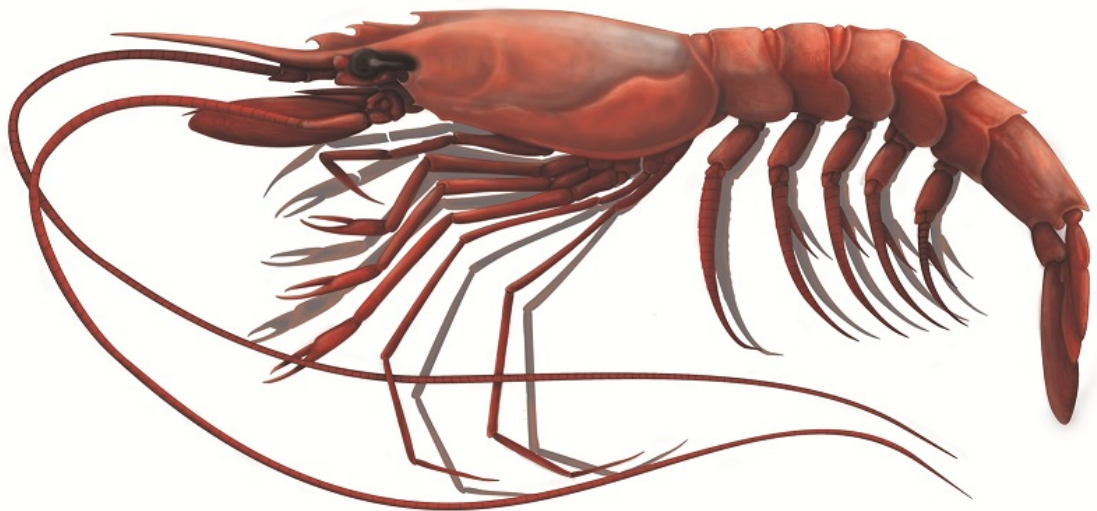


FIGURE 1.1: The red shrimp *Aristeus antennatus* (Risso, 1816).

the Blue ling (*Molva dypterygia*) and the roundnose grenadier (*Coryphaenoides rupestris*) harvested in the Atlantic and Norwegian Sea. Another example is the orange roughy (*Hoplostethus atlanticus*) usually fished in Australian waters (Gordon, 2001; Koslow et al., 2000), whose vulnerability depends on its practice to concentrate in restricted areas, i.e. the high aggregation on seamounts (Gordon, 2001).

In the Mediterranean, harvested deep-sea species are mainly represented by crustaceans decapoda, such as the deep-water shrimps *Aristeus antennatus* (Figure 1.1) and *Aristeomorpha foliacea*, while among fishes and cephalopods there are *Lophius* spp., *Phycis* spp., *Merluccius merluccius* (Figure G.3, C) and *Illex coindetii* (Politou et al., 2003). They represent a moderate part of the deep-sea landings. By-catch examples without any economic interest are macrourids, e.g. *Nezumia* spp. (Figure G.1, B) and *Hymenocephalus italicus*, and sharks, such as the lantern shark *Etmopterus spinax* and *Galeus melastomus* (Figure G.3, A). Sharks are top predators and more likely present k-selectivity behaviour and their decline in abundance has been demonstrated in the Mediterranean by Cartes, Fanelli, Lloris and Matallanas (2013); Ferretti et al. (2008); Maynou et al. (2011). The causes probably rely on a combination of direct human impacts that have grown in intensity in the 20th century and the intrinsic characteristics of this fauna, as mentioned above, such as slow growth rates, high longevity (e.g. 20 years in *E. spinax*: Coelho and Erzini, 2008), low fecundity and high trophic position (Dulvy et al., 2003; Ferretti et al., 2008; Myers and Worm, 2005). Recently the same k-characteristics have been proved in the production of macrourid fishes (Fernandez-Arcaya et al., 2013). On the contrary we should be aware that not all declines are due to overfishing. For example has been argued that the local extinction of the deep-water shrimp *A. foliacea* is probably due to the warming and salinization of Mediterranean deep waters as a consequence of the decreased freshwater flow from the Nile since the completion of the High Aswan Dam in 1964 (Cartes, Maynou and Fanelli, 2011).

In any case, threats of fishing in deep-sea environments engrave on the target and by-catch species and probably on other components of the system and its dynamics through indirect mechanisms. One of the clearest impacts of deep water fisheries has been demonstrated on benthic habitats, because these fisheries are almost represented by large trawling boats, notoriously destructive of the seabed,

influencing the biomass and the structure of communities (see e.g. [Cartes et al., 2009](#)).

An holistic approach to investigate possible damages on ecosystem functioning is to analyse the energy flows and their changes after external perturbations. Changes in flows are strictly related to changes in biomasses. For example, the impact of excessive fishing effort on predators jointly with unfavourable state of the environment, can cascade down to lower trophic levels of the food web, affecting such populations and/or the whole ecosystem, with the selective reduction or expansion of some trophic guilds (e.g. [Casini et al., 2008](#); [Reid and Croxall, 2001](#)). This top-down control has been documented in many near-shore ecosystems as well as other types of control.

In bathyal systems these phenomena have not been documented yet for the paucity of data. The identification and quantification of functional interactions between biological components are the basis to eventually predict the response of the system to fisheries. This goal is strongly hampered by the lack of high-quality empirical data in deep-sea ecosystems (e.g. [Brown and Gillooly, 2003](#)), being direct measurements or experimentations notoriously difficult even for comparatively well studied shallow water ecosystems ([van Oevelen, Soetaert, Middelburg, Herman, Moodley, Hamels, Moens and Heip, 2006](#)). Nevertheless, an ecosystemic approach is urgently needed because human pressures are increasing more rapidly than our understanding of the systems being exploited ([Glover and Smith, 2003](#)), in line with the ecosystem approach to fisheries (EAF) framework. Traditional marine research investigates isolated parts of the ecosystem, while mathematical models can merge this fragmentary information into an integrative framework. Food web modelling developed in last decades (e.g. [Angelini and Agostinho, 2005](#); [Coll, Lotze and Romanuk, 2008](#); [van Oevelen et al., 2009](#); [Vézina and Savenkoff, 1999](#); [Woodward et al., 2005](#)) can identify the missing information to improve research in this direction.

The final objective of this Ph.D. thesis is to quantify the effects of fishing activity (usually referred to as a top-down control) in the food web of the bathyal ecosystem (NW Mediterranean) accounting also for bottom-up processes such as the entry of energy to the system. The top-down control usually might evolve into trophic cascade i.e. alteration of the relative abundances between adjacent trophic cascades ([Estes et al., 1998](#); [Paine, 1980](#)). This has been exemplified by the in-depth study of the exploited continental slope ecosystem in the Catalan sea,

where the important fishery of the highly priced red shrimp (*Aristeus antennatus*) is carried out and the trophic web structure is relatively well documented (e.g., Carrassón and Cartes, 2002; Cartes et al., 2009; Fanelli, Cartes and Papiol, 2011).

Concrete objectives are:

1. Identify and fill important lacks to built up the food web. No quantitative data of deep-sea infauna (macrobenthos) were collected in the study area before this thesis, however the infauna is a key component of benthic pathways. Similarly any knowledge about oxygen consumption of sediment (SOC) was available.
2. Describe the red shrimp fishery, in terms of landings per unit effort (LPUE), to understand which are the influential factors affecting this fishery index and so the abundance variability of the species.
3. Describe the bathyal food web and dynamically simulate top-down and bottom-up effects, considering the red shrimp as the key species of the model. The simulation study is mandatory being time series unavailable.

## 1.2 Food webs and trophic cascades

### 1.2.1 Food webs: concepts and models

Since 70s when networks were imported from physic and social sciences into ecology biologists have become increasingly interested in describing and analysing the trophic dynamics of ecosystems (Lindeman, 1942; Odum, 1957). In 2010 the 5% of scientific production in ecology included the word “network” in title, abstract or keywords (Heleno et al., 2014). These studies have shown a promising approach for deepening our understanding of ecological processes in ecosystems (O’Neill, 1969). Now significant progresses are making in e.g. moving from static to temporal dynamic networks and using network analysis as a practical conservation tool (Heleno et al., 2014).

Food webs (who eats whom) describe the exchange of matter among different compartments within a community or more generally within an ecosystem when also abiotic components are included. The exchange (or transfer) is represented

by a flow from a component to another and it can be measured as organic matter (wet or dry weight), energy (joule) or as an element, C, N, P (mole) transferred in a given unit of time. For instance, the latter is used to draw the elements' cycles.

A common categorization of food webs is through the origin of energy they belong to. Usually they are divided into two categories: 1) based on primary production or 2) based on detritus. Another possibility is the combination of both. This is a convention used in understanding pathways and define different modes of organisation as well as different dynamics. Primary producer based webs start with one or more primary producers that take energy incorporated in inorganic compounds and make it available for all other consumers as organic matter. Detritus based webs start with one or more forms of nonliving organic matter that originates outside the system (allochthonous source) or produced by system's components e.g. faeces (autochthonous source).

In theoretical ecology food webs can be described qualitatively, quantitatively and through the function of its components. The (basic) qualitative description is through the "binary" food web, that defines the structure of the interacting components, i.e., if a flow exists or not between two components of the web. In practise applied researchers have been classified the components (single species or functional groups) through the size (e.g. for the benthos components see Table 1.1), because roughly the bigger eats the smaller. It is also a good practical method because abundance data are typically collected in distinct size classes (however megafauna comprises too many size classes and may be divided more accurately) and weight-specific physiological processes scale with body size.

The literature is full of theoretical studies on binary food web models. For a given number  $N$  of species  $s_i$ , with  $i = 1, \dots, N$  and a given number  $L$  of links, a binary food web can be represented as a  $N \times N$  matrix  $\mathbf{S}$ , where if the species  $s_i$  (in rows) is a prey of species  $s_j$  (in columns), then element  $s_{i,j} = 1$  otherwise  $s_{i,j} = 0$ . The

Size class	Size ranges	typifying groups
Bacteria	0.5 – 4 $\mu$ m	aerobic, anaerobic, chemo-autotrophs, fermenters
Microbenthos	< 63 $\mu$ m	agellates, ciliates
Meiobenthos	63 – 500 $\mu$ m	nematodes, foraminifera, ostracods
Macrobenthos	0.5 – 20mm	polychaetes, bivalves, peracarids, echinoderms
Megabenthos	> 2cm	crustacean decapods, fish, cephalopods

TABLE 1.1: Size-based classification of benthos with size range and main groups in each size class.

set of nonzero matrix elements can be defined as  $s_{i,j}^1, \dots, s_{i,j}^L$  where the superindex is introduced to recognize the existence of some link  $l$ , with  $l = 1, \dots, L$ . Theoretical ecologists have suggested simple rules to generate binary food webs, based on theoretical distributions for the links  $l$ , or some other parameter in more complex models, e.g. assuming  $l \in U(0, 1)$ , the uniform distribution, in the simplest case of a random food web. Currently existing models are: the random, the cascade, the niche and the nested-hierarchy models (Cattin et al., 2004; Cohen and Newman, 1985; Williams and Martinez, 2000). The two latter models may describe more realistic food webs. Examples of binary food webs are visualised in Figure 1.2, column (A). But, species interactions  $s_{i,j}$  are only feasible (can exist) if enough energy is transferred to the predator. To assess the “energetic feasibility”, a food web needs to be quantified. Also the qualitative feasibility of a food web can be assessed, however it needs and gives less information (Moore and de Ruiter, 2012). The quantification generates a  $N \times N$  flow matrix  $\mathbf{X}$ , whose elements  $x_{i,j}$  are estimates of the magnitudes of the feeding flows. The corresponding quantified food webs of the examples given in column (A) are shown in column (B) of the same Figure 1.2. It can be observed that not all binary models return quantitative solutions, so they are not feasible, such as the case of the random model example in (1). All such theoretical models have a probability to be feasible, however it is different between each other.

These “quantified food webs” represent a gateway to achieve a quantitative understanding of the functional interactions between biological (and when possible abiotic) components, in order to eventually predict the response of the system to anthropogenic and environmental forces. It can be argued that quantification of flows should need a good knowledge of the structure of the food web under study, however in most cases it is impossible. In fact, the quantification of biological interactions is strongly hampered by the lack of sufficient high-quality empirical data, because the elucidation of food web flows from direct measurement or experimentation is notoriously difficult (e.g., Brown and Gillooly, 2003; van Oevelen, Soetaert, Middelburg, Herman, Moodley, Hamels, Moens and Heip, 2006). For example, deep-water data sets are emblematic of under-sampled food webs. To overcome these data limitations and extract as much information as possible from them, modelling of real food webs have been developed, e.g. through linear inverse techniques (e.g., Angelini and Agostinho, 2005; van Oevelen et al., 2009; Woodward et al., 2005).

Mathematical models used for quantification are based on the first and second laws of thermodynamics, possible through the so called mass balance equations (O'Neill, 1969). The main concept is that all energy must be taken into account and all the energy loss from a component must flow to other components. The assumption of steady state is essential for the basic design of the model. However the equilibrium in real systems is seldom fulfilled, it is reasonable considering the

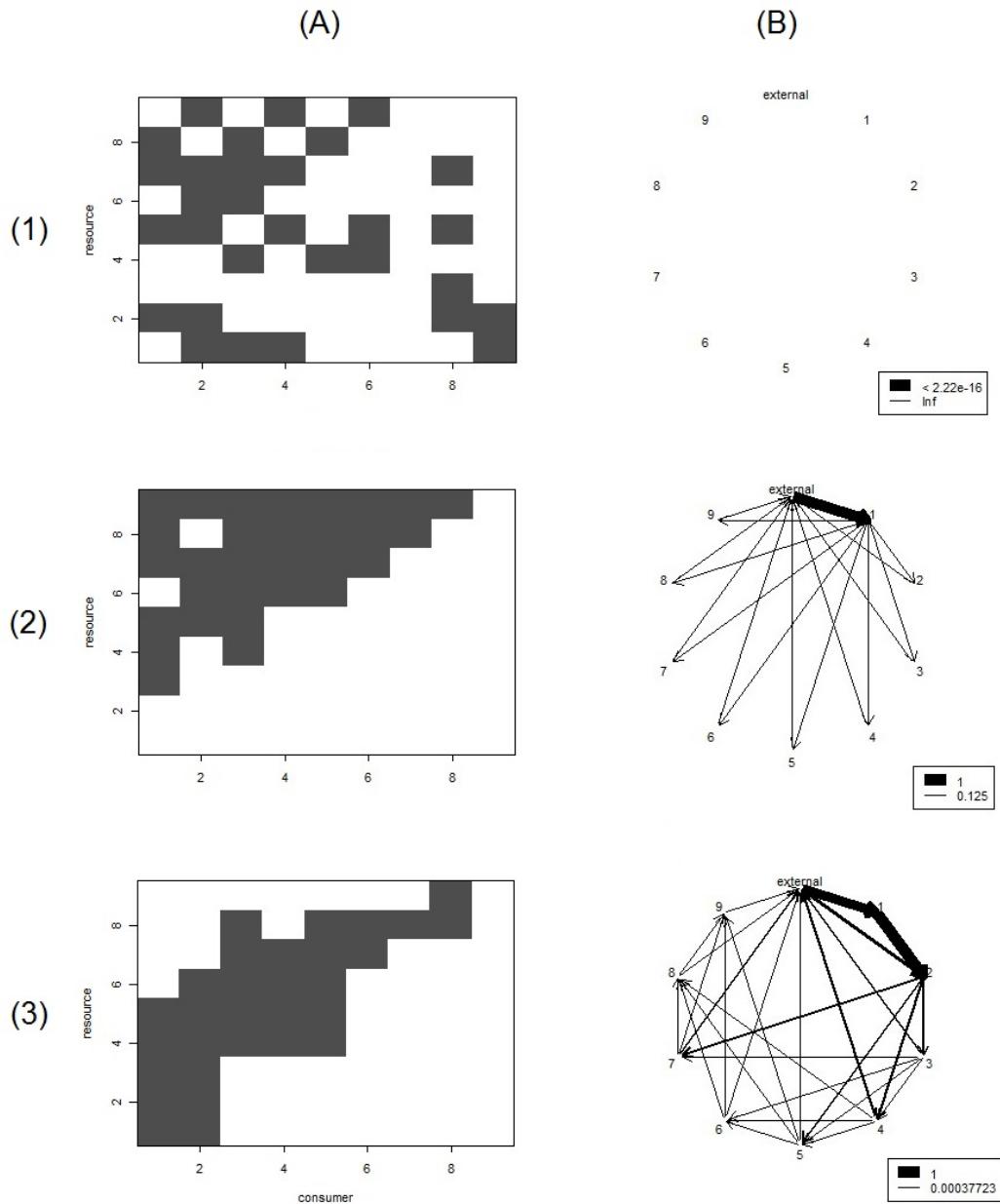


FIGURE 1.2: Three examples of theoretical food webs. In columns: (A) binary and (B) quantified food webs. In rows: (1) Random model, (2) Cascade model and (3) Niche model with  $N = 9$  compartments  $S$  and  $L = 30$  number of links.

average compartment size as constant when the interval of time is properly chosen (O'Neill, 1969).

Here we use the notation  $s$  to define the quantity of a species (biomass or density is irrelevant in this chapter). Each mass balance describes the rate of change of a compartment  $s_i$  in terms of differences between inputs and outputs. For a living compartment  $s_i$ , it could look like

$$\frac{ds_i}{dt} = G_{ci} - (L_{ei} + L_{mi} + L_{pi}), \quad (1.1)$$

where  $G_{ci}$  is the gain of mass by consumed (ingested) energy,  $L_{ei}$  is the loss through egestion (or unassimilated energy),  $L_{mi}$  is the loss due to metabolic activity and  $L_{pi}$  is the loss due to predation by other compartments. In a steady-state model the derivative of  $s_i$  with respect to the time  $t$  is  $ds_i/dt = 0$ . Usually models consider the energetic efficiency,  $e$ , of trophic interactions as the product of the assimilation efficiency,  $a$ , and the production efficiency,  $p$  or also expressed by the ratio of the new energy produced,  $P$  (in form of individual growth and/or reproduction) to the energy consumed,  $C$ ,

$$e = a \times p = \frac{P}{C}. \quad (1.2)$$

Equation 1.2 implies that  $0 \leq e \leq 1$ , otherwise the population dies. The portion of energy of a prey consumed by a predator that is not assimilated (e.g. faeces) and the assimilated portion that is mineralized (i.e. maintenance respiration) is

$$1 - e = \frac{E + M}{C} \quad (1.3)$$

where  $E$  represents the egested (unassimilated) energy and  $M$  is the energy used for maintenance (maintenance respiration).

Figure 1.3 shows the fate of consumed energy for a given component and can be divided into three main processes: assimilation, production and mineralization that occur in two steps. The first considers that the consumed biomass ( $C$ ) is divided into assimilated ( $A$ ) and unassimilated ( $E$ ) biomass. So, the assimilation efficiency is



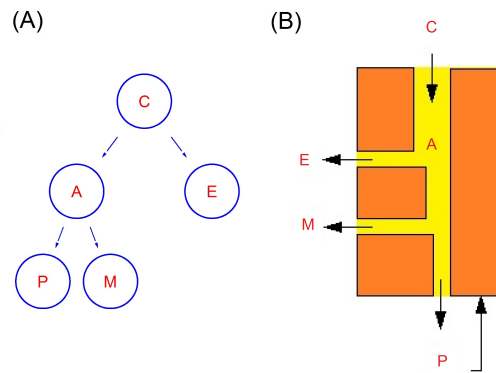


FIGURE 1.3: The fate of consumed energy for a given component (or an individual). Symbols represent:  $C$  = energy consumed,  $A$  = energy assimilated,  $E$  = the egested energy,  $P$  = the produced energy,  $M$  = the energy used for maintenance. Idea of the figures taken from A) Moore and de Ruiter (2012) and B) Brey (2001).

$$a = \frac{A}{C}. \quad (1.4)$$

The proportion of the unassimilated portion,  $1 - a$ , is

$$1 - a = \frac{E}{C}. \quad (1.5)$$

The portion  $E$  returns to the surrounding through different processes, and refers only to organic material, it is not lost to the environment and serves to other livings as energy source. This different forms of unassimilated organic compounds are autochthonous inputs to detritus and return to the labile or refractory detritus depending on their respective C:N ratios. They also can leave the system if they are allochthonous source for other systems. So, the assimilation efficiency can vary depending on the quality of the source.

The second step refers to the assimilated portion, that is transformed into new energy, i.e. production, or it is mineralized in e.g.  $\text{CO}_2$ . Thus,

$$p = G + \frac{R}{A} \quad (1.6)$$

and

$$1 - p = \frac{M}{A}. \quad (1.7)$$

For example, the organic carbon is mineralized in different forms of dissolved CO<sub>2</sub>, e.g. carbonate or bicarbonate, and the organic nitrogen in ammonium which represent the corresponding “waste”. Taking into account both  $a$  and  $p$  the energy efficiency in Equation 1.2 can be then fully defined. The energy budget scheme described in Figure 1.3 and Equations from 1.2 to 1.7 can be further partitioned, for example  $P$  into production for growth and production for reproduction, that are respectively associated to the respiration for maintenance and respiration during reproductive period. Thus, the scheme is a simplification, but to date the assessment through sensitivity analyses leads to believe that the impact is relatively small (Moore and de Ruiter, 2012). All modelling approaches consider these basic assumptions or some reasonable modification. Very common is the use of matrix calculation, such as in the linear inverse modelling (LIM), used in the present thesis. For each component  $s_i$  the main equation in a LIM is

$$\frac{ds_i}{dt} = \sum_{j=1}^J x_{j,i} - \sum_{k=1}^K x_{i,k} \quad (1.8)$$

where  $x_{.,}$  defines the quantified connection between each component the species  $s_i$  and its sources  $s_j$  or its consumer  $s_k$ , such that  $x_{j,i}$  with  $j = 1, \dots, J$ , defines incoming flows and  $x_{i,k}$ , with  $k = 1, \dots, K$  outgoing flows to and from component  $s_i$ , and such relationships are fixed. When the model describes the variation of the biomasses in time, the system shifts to a dynamic problem, such that,  $ds_i/dt \neq 0$ . In this case, the relationships  $x_{.,}$  in Equation 1.8 are not fixed and are functions of e.g. the state variables,  $s_i$ , different parameters to be defined ( $p_n^1, p_m^2$ , with  $n = 1, \dots, N$  and  $m = 1, \dots, M$ ) and the time ( $t$ ), such that

$$\sum_{j=1}^J x_{j,i} = \sum f(s_i, s_j, p_n^1, t) \quad \sum_{k=1}^K x_{i,k} = \sum f(s_i, s_k, p_m^2, t), \quad (1.9)$$

as has been described by van Oevelen, Middelburg, Soetaert and Moodley (2006).

Figure 1.4 represents the dynamic output of the simulation made for all species of the niche food web (row (3), Figure 1.2). The black line represents the stable

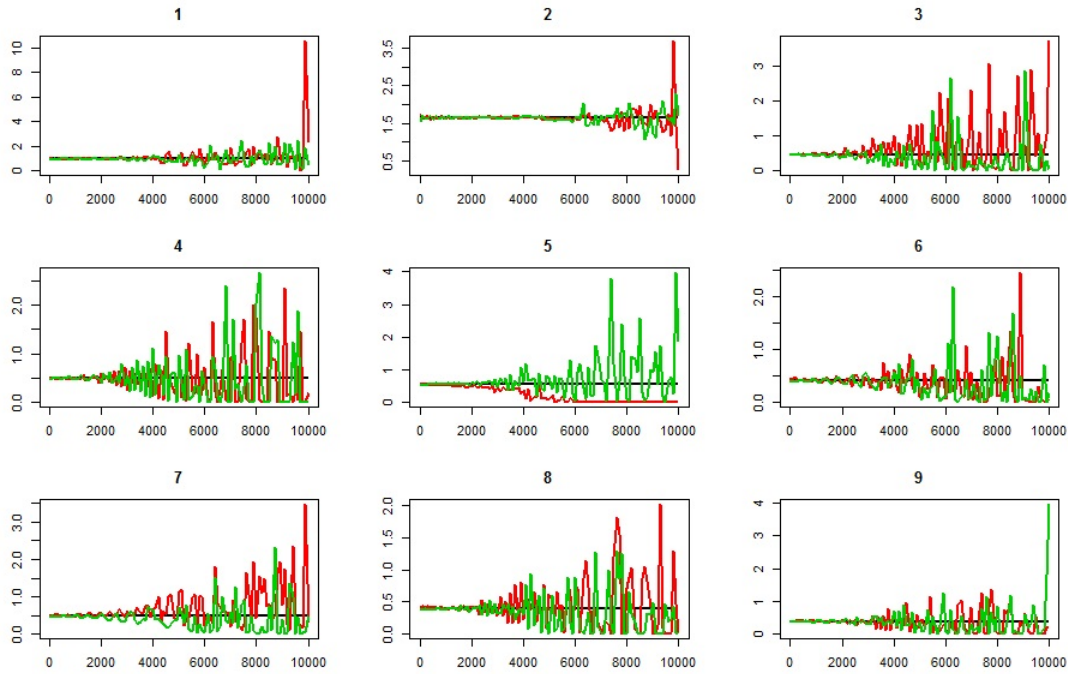


FIGURE 1.4: Output of the dynamic simulation for the niche food web in Figure 1.2, 3-B. The time span is 20 years and plot, headed by a number from 1 to 9, corresponds to each species of the food web. On the  $y$  axis are shown the biomasses. Dark: unperturbed biomass; red: biomasses perturbed by  $1/2$  of the original value; green: biomass perturbed by 2 of the original value.

unperturbated biomass, while red and green lines show negatively and positively perturbed biomasses respectively (the half or the double of the original biomasses).

In the following two main dynamic models are introduced and that originate from the assumption of two main classes of food web (Moore et al., 2004, 1993): 1) based on primary production and 2) based on detritus. These models are based on variations of the Lotka-Volterra equation and they account for the conservation of energy assumption. In the primary producer-based models for producer  $s_i$ , the equation is

$$\frac{ds_i}{dt} = r_i s_i - \sum_{j=1}^N f(s_i) s_j \quad (1.10)$$

where  $s_i$  is the producer,  $s_j$ , the consumer,  $r_i$  is the growth rate of the producer and  $f(s_i)$  is the functional relationship between  $s_i$  and  $s_j$ , with  $i \neq j$  if the model refers to competing species or  $i = j$  in the case of intraspecific competition, which depends on the biomass of the producer  $s_i$ .

The detritus-based model includes as extra-component the detritus,  $s_d$ , such that,

$$\frac{ds_d}{dt} = r_d + \sum_{i=1}^N \sum_{j=1}^N (1 - a_j) f(s_i) s_j + \sum_{i=1}^N d_i s_i - \sum_{j=1}^N f(s_d) s_j \quad (1.11)$$

where the subscript  $d$  defines all parameters and biomass of the detritus, that is a nonliving component, while  $s_i$  and  $s_j$  are all living components. The detritus may have an allochthonous origin, represented by  $r_d$ , or autochthonous origin such as the production of detritus as mortality from predation  $\sum_{i=1}^N \sum_{j=1}^N (1 - a_j) f(s_i) s_j$  or as mortality for physiological reasons  $\sum_{i=1}^N d_i s_i$ . The functional response between prey and predator is represented by  $f(s_i)$  and must be defined. Finally, the direct consumption of detritus is described by  $-\sum_{j=1}^N f(s_d) s_j$ .

Then, for both classes of food web the equation for a consumer  $s_i$  (Moore et al., 1993) is

$$\frac{ds_i}{dt} = -d_i s_i + \sum_{j=1}^N a_i p_i f(s_j) s_j - \sum_{j=1}^N f(s_j) s_i \quad (1.12)$$

where  $d_i$  is the dead rate of the consumer (natural mortality other than predation), while  $-\sum_{j=1}^N f(s_j) s_i$  represents the death for predation (or intraspecific competition when  $i = j$ ) and finally  $\sum_{j=1}^N a_i p_i f(s_j) s_j$  describes the growth of the consumer that involves the functional response to be defined and accounts for the assimilation efficiency  $a_i$  and the consumption efficiency  $p_i$  of the consumer.

The function describing the prey-consumer relationship has been widely discussed and different functions have been proposed and can be summarised in three main types (Holling, 1959). The type I function,  $f^1(s_i)$ , depends on prey density and depicts a linear relationship, such that,

$$f^1(s_i) = c_{ij} s_i, \quad (1.13)$$

where  $c_{ij}$  is the consumption coefficient. The predation by predator  $s_j$  on prey  $s_i$  increases with the density of the prey.

The type II,  $f^2(s_i)$ , is defined as

$$f^2(s_i) = \frac{cs_i}{1 + chs_i}. \quad (1.14)$$

Here the parameter  $h$  represents the handling time. The attack rate increases with prey density approaching a constant when the predator becomes satisfied.

Finally the type III,  $f^3(s_i)$  (Real, 1977), takes the form

$$f^3(s_i) = \frac{\alpha s_i^x}{\beta + s_i^x}, \quad (1.15)$$

where  $x$  is the encounter rate of the predator,  $\alpha$  is the maximum feeding rate and  $\beta$  is the density of the prey generating the half of  $\alpha$ . When  $x = 1$  the response coincides with the Holling type II, while when  $x > 1$  the functional response becomes a sigmoid.

As introduced at the beginning of the chapter different types of perturbation can influence the system, such as fishery and environmental factors among others. The impact may engrave the component directly involved in the perturbation (i.e. the harvested species) and/or indirectly other components positioned more or less away from the origin of the disturbance in the network (e.g. distant one or more trophic levels from the affected species). The change in relative biomass can be used as a measure of the effect of the perturbation and may be associated to mechanisms such as trophic cascades and phase shifts.

## 1.2.2 Trophic cascades and other mechanisms

The term trophic cascade was coined by Paine (1980) to describe the alteration in abundances of lower trophic levels after the loss of apex predators. It has been then applied to the three-trophic levels, (the Green World Hypothesis, GWH, proposed by Hairston et al., 1960 in terrestrial ecosystems) and then generalized to systems of one to five trophic levels, as in the Exploitative Ecosystem Hypothesis (EEH) of (Fretwell, 1987). Strictly defined (Menge, 1995; Strauss, 1991), trophic cascades are predatory interactions involving three trophic levels, e.g. primary carnivores, by suppressing herbivores, increase plant abundance. Although cascade-type effects have been reported to extend through four or more trophic levels (e.g. Carpenter and Kitchell, 1988). Over the past 50 years the debate on

the existence and importance of trophic cascades has produced numerous analyses. Experimental studies have addressed this subject in a variety of habitats, in terrestrial (e.g. [Spiller and Schoener, 1994](#)) and aquatic ecosystems, such as lakes and streams ([Carpenter et al., 1985, 2001](#); [Scheffer et al., 1993](#)), near-shore systems ([Estes et al., 1998](#)) and open ocean ([Casini et al., 2008](#); [Jackson et al., 2001](#); [Scheffer et al., 2001](#); [Shiomoto et al., 1997](#)).

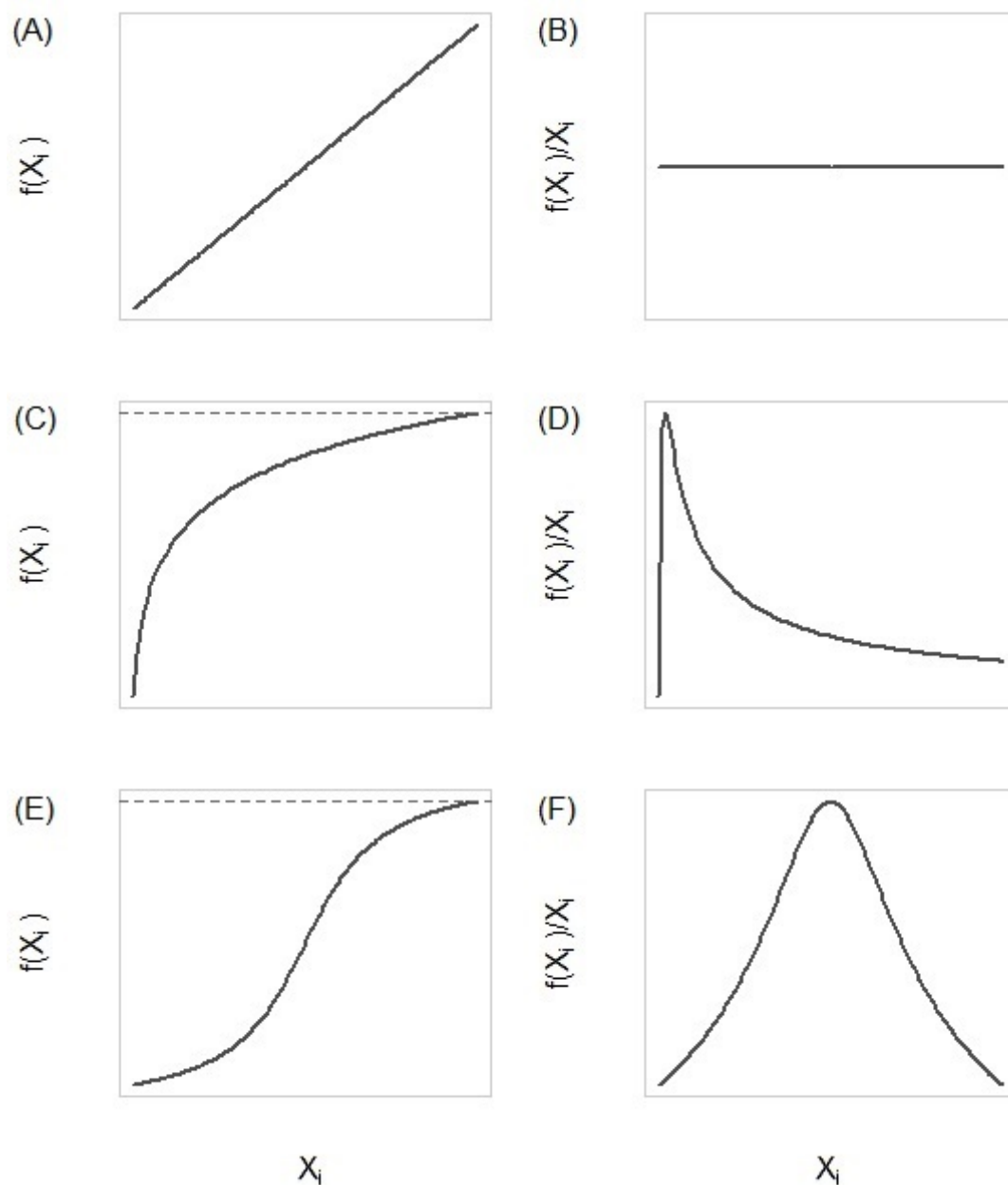


FIGURE 1.5: Functional response types described by [Holling \(1959\)](#). A) Type I and B) Corresponding relative mortality. C) Type II and D) Corresponding relative mortality. E) Type III and F) Corresponding relative mortality.

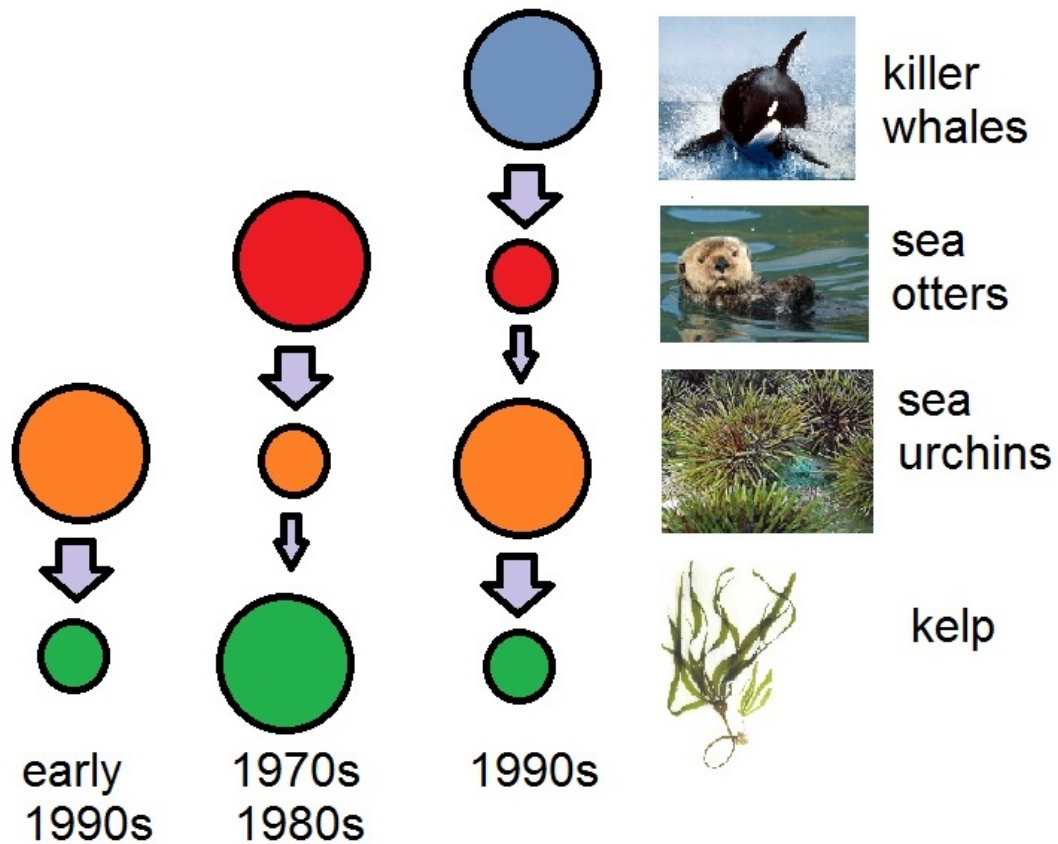


FIGURE 1.6: Example of the trophic cascade between otter, sea urchin and kelp (then also extended to killer whale) in the ecosystem of the Aleutian Islands (Alaska, USA) (Estes et al., 1998).

In the literature there is a predominance of aquatic cases of trophic cascades, something that led Strong (1992) to assert “trophic cascades are all wet” and the mechanism is prominent in simple food chains. In more diverse ecosystems with spatial heterogeneity and trophic specialisation, trophic cascades were hypothesised to be less evident because buffered by complex interactions (Strong, 1992). Nowadays, conscious of the complexity held by ecosystems, we do not even refer to simplified trophic chains (although in some cases it is still a good approximation, e.g. in some pelagic ecosystems) but to trophic networks, hence trophic cascading refers to the effects of one component on another component  $n$ -trophic levels far, that may trickle across the entire web till its basis.

A famous example of trophic cascade is the interactions between otter, sea urchin and kelp (then also extended to killer whale) in the ecosystem of the Aleutian Islands (Alaska, USA) described by Estes et al. (1998) (Figure 1.6). The sea otter (*Enhydra lutris*) was abundant before the unregulated exploitation performed

across the North Pacific (Kenyon, 1969). Then, after protection in early 1990s, was able to recover reaching in 1970s maxima abundances in few areas but was completely absent in others (Rotterman and Jackson, 1988). In the areas without *E. lutris* (also in early 1900s), the populations of sea urchin *Strongylocentrotus polyacanthus* grew and kelp forest declined. Conversely, zones with sea otter populations, showed low sea urchin populations and high production of kelps (Estes and Palmisano, 1974). Has been hypothesised that suppressing the carnivorous, herbivorous expands its population till algae decline and vice versa. So, the predator acts in a top-down control. Then, during 1990s, another unexpected synchronous decline was observed in otter populations. That synchronism avoids the hypothesis of populations redistribution, on the contrary lines of evidence pointed to increased predation by killer whale (*Orcinus orca*). The most likely explanation is the shift of prey source base for killer whale, that feeds on marine mammals (Felleman et al., 1991), such as Steller sea lions and harbor seals. Both populations collapsed few years before sea otter decline, inducing the feeding shift of the killer whale to sea otter populations, reducing its abundance and in turn restoring sea urchin populations with the consequent depletion of kelp (Figure 1.6).

In the Mediterranean, works concerning possible trophic cascades have a limited history, however they comprise some of the most comprehensive data of any littoral system (Pinnegar et al., 2000). One example is the system sparid, sea urchin and fleshy algae (Sala et al., 1998). The sparid fish eats on sea urchin, that in turn grazes on fleshy algae. In the rocky littoral of the Medes protected areas invertebrate-feeding fish are more abundant compared to sites outside (e.g. Bell, 1983). The sparids (*Diplodus sargus* and *D. vulgaris*) and the wrasse *Coris julis* are the major predators of adults and juveniles respectively of sea urchins, mainly *Paracentrotus lividus* (Sala, 1997a). At adjacent non-protected sites with a low density of predatory fish, *P. lividus* populations were shown to be 3-4 times higher (Sala and Zabala, 1996). At these sites, the sea urchins remove large erect algae and induce the formation of coralline barrens. Sala et al. (1998) suggested that the increment of coralline algae may be one symptom of intensive human exploitation. Transition from coralline barrens back to erect algal assemblages is possible when sea urchins are eliminated as has been observed by experimental removal (Nédélec, 1982). Parallel studies found that also epifaunal groups (e.g. amphipods, gastropods, decapods and ophiuroids) became more abundant when fish were excluded, probably as a consequence of reduced predation and of the increment of fleshy erect algae that provide a structural habitat and food for many



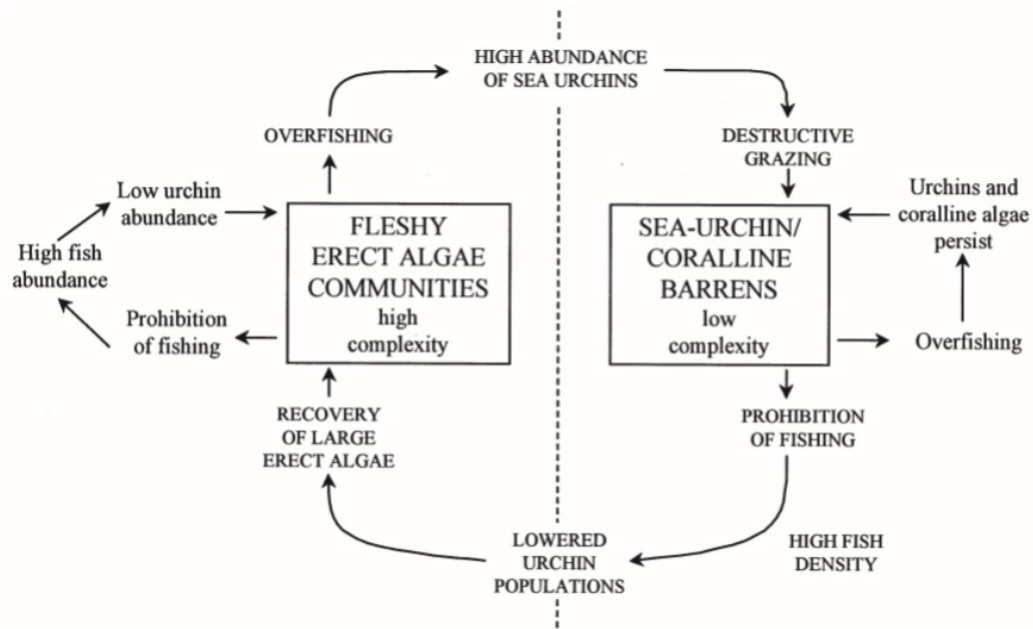


FIGURE 1.7: Description of the hypothesis of two alternative states in the ecosystem nearby the Medes Reserve (western Mediterranean) explainable by mechanisms of trophic cascade. From [Pinnegar et al. \(2000\)](#).

of the invertebrates ([Sala, 1997b](#)).

An energy-based simulation of the Mediterranean rocky-sublittoral system predicted how depletion of invertebrate-consuming fish such as *Diplodus* spp. might result in the dominance of sea urchins, that would dramatically reduce algae, epifauna and gross and net primary production ([McClanahan and Sala, 1997](#)). The indication is that once a high population of sea urchins has developed, recovery of those fish that eat algae and epifauna might be slowed or even made impossible because their food resources drop below the minimum threshold necessary for in situ population development ([McClanahan and Sala, 1997](#)). In conclusion, two alternative states were described for this ecosystem (Figure 1.7): (1) an overgrazed community with high abundance of sea urchins and low algal biomass with coralline barrens and (2) a “developed” community with an abundance of fish and dominance of fleshy algae ([McClanahan and Sala, 1997](#)).

A more recent study ([Cardona et al., 2007](#)), performed off northern Minorca (Balearic Islands), found no evidence of trophic cascade for the same ecosystem explained by the limited recruitment of both fish and sea urchins due to the extreme oligotrophy of the area.

Among benthic marine systems, there is comparatively little evidence for trophic cascade in soft bottom communities in shallow waters and are summarised in Table 1.2.

Fishery-target populations may recover after a cessation of fishing activities (Pipitone et al., 2000), but there has been little regard for potential indirect effects on prey species. Caging experiments in shallow soft bottom communities have showed that the exclusion of predators generally results in large increases in density and diversity of infaunal species (Virnstein, 1977). However, because trawls and dredges may inflict considerable physical damage on infauna populations (Kaiser and Spencer, 1996; Prena et al., 1999), the effects of predation and thus observation of any potential trophic cascades may be obscured (see review by Jennings and Kaiser, 1998); populations may even show increases after cessation of trawling, despite increases in their predators. Pipitone et al. (2000) reported an eight-fold increase in fish biomass over the four years following a trawling ban in the Gulf of Castellammare (Sicily, Italy). Biomasses of certain target species such as *Mullus barbatus* increased 33-fold with respect to data collected prior to the closure, however the biomass of cephalopods (excluding *Octopus vulgaris*) declined. This was in agreement with the findings by Pauly (1985) for the Gulf of Thailand. Where predators of squid pre-recruits were common, squid was less common, but as fishing intensified and indeed rays and sawfish virtually disappeared, cephalopods became more important. Similar trends were predicted by Christensen (1998) using a simulation model, where increased fishing pressure resulted in declines of most demersal groups like rays, crabs, lobsters and large piscivorous fish, and, indirectly, increases in some of their potential prey such as cephalopods, scads and shrimp. These “prey-release” predictions also agreed with an observed increase in

	Components	Location	ref
1	Humans-fish-cephalopod	Gulf of Castellammare (Italy)	1
2	Humans-large fish-scad/ shrimp/cephalopod	Gulf of Thailand	2, 3
3	(Humans-fish-cephalopod)	NW Africa	4
4	(Humans-fish-ophiuroid)	Irish Sea & English Channel	5
5	(Humans-fish-infauna)	Chesapeake Bay (USA)	6

TABLE 1.2: Soft-bottom trophic cascades recompiled from literature. Cascades in parenthesis are based on circumstantial evidence. Ref: (1) Pipitone et al. (2000); (2) Pauly (1985); (3) Christensen (1998); (4) Caddy (1983); (5) Aronson (1990); (6) Virnstein (1977).

shrimp recruitment in the Gulf of Thailand by Pauly (1982) following the increase in fishing pressure and an observed decrease in total shrimp production following a trawl ban in Indonesia (Garcia, 1986).

Another example comes from the coasts of west Africa, where Caddy (1983) argued that the occasional domination by cephalopods (particularly squid) may be a general feature of intensively fished soft-bottom demersal systems. Between 1960-1970 has been observed a relevant increment of cephalopods in catches, simultaneously with a dramatic decline in sparid fishery. Indirect effects through trophic relationships have been hypothesised without suggesting any clear mechanism such as trophic cascade (Caddy, 1983).

On the south-west coast of Great Britain an example involves ophiuroids, that have experienced considerable changes in abundance over the past century (Holme, 1984). Also Aronson (1989) demonstrated that predation pressure on ophiuroids was significantly lower where fishes and portunid crabs were rare amongst soft bottoms, in comparison with adjacent sites on rocky reefs where potential predators (e.g. fish, crabs and starfish) were relatively abundant. Overfishing along UK and Irish coasts has severely depleted teleost predators, and it has been suggested that this has resulted in a system dominated by echinoderms and crustaceans (Aronson, 1989, 1990, 1992).

Trophic cascades have been found also in a temperate seagrass (*Zostera marina*) community in Sweden through cage experiment coupled with nutrient enrichment (Moksnes et al., 2008). In this work cascades results in high diversified system in contrast with the suggestion that community-wide trophic cascades are unusual and restricted to low-diversity systems with simple trophic interactions (Strong, 1992). They suggest that the interaction strength in the community was strongly skewed towards two functionally dominant components, the algae *Ulva* sp. and amphipod *Gammarus locusta*, consistent. So, it is the number and complexity of only strong interactions that determines whether trophic cascades can develop (Duffy, 2003).

Trophic cascade is a consequence of top-down controls, but more hypotheses of control exist in food web dynamics, such that by the lower reaches of the web and by intermediate species. The first consists of changes in basal species mediated by resource limitations at the basis of the food web, such as plants and phytoplankton (their abundances are driven by physical and chemical forces, e.g. nutrient

limitations) and are subjected to a bottom-up control. The trophic cascades *sensu stricto* are top-down controlled, however [Strong \(1992\)](#) states that in real trophic cascades top-down influence combines with the always strong bottom-up influence through a food chain ([Carpenter and Kitchell, 1988](#); [Oksanen, 1990](#); [Power, 1992](#)). So, it seems that top-down dominance is not the norm and not necessarily all trophic interactions cascade. [Strong \(1992\)](#) argued that among all ecological communities, cascades are restricted to fairly low-diversity areas as mentioned above. Contrariwise, where consumption is highly differentiated the overall effect of trophic cascades is buffered.

[DeAngelis \(1980\)](#) discussed the presence of a particular type of bottom-up control, existing in detritus based food webs, called donor-control. [Moore and de Ruiter \(2012\)](#) explained that when a system is controlled by a donor-control process, the population density and rate of input of the donor has an effect on the consumer population density, whereas the population density and dynamics of the consumer has no direct effect on the dynamics of the donor population or resource.

Finally the last control type consists of population changes in intermediate trophic levels and has been called wasp-waist control ([Cury et al., 2000](#)). This kind of control has been found in upwelling ecosystems, where the intermediate trophic level is occupied by small planktivorous fish, usually represented by one or few schooling species, such as sardine and anchovy, that influence the dynamics of predators, such as piscivorous fish, seabirds and mammals, in order of importance ([Cury et al., 2000](#)).

It has been suggested that large-scale oceanographic factors may influence the susceptibility of the system to show a trophic cascade. Studies suggest a high spatial variation in trophic forces, as documented comparing different regions of the North Atlantic. At the northern areas top-down control dominates, where species diversity and ocean temperatures are lower, whereas bottom-up control dominates southern areas in warmer waters and biological diversity ([Frank et al., 2007, 2006](#)). Southern ecosystems may be more resilient to overfishing because high species diversity facilitates replacement of the overfished species and warmer temperatures support higher demographic rates.

Other examples of all types of mediation have been described and are supported by literature. For example the control of the nutrient P inputs was shown to be effective in mitigating cultural eutrophication working as a bottom-up control

(Schindler, 2006). Contrariwise the meta-analysis by Worm and Myers (2003) in the North Atlantic sea tested the consistency of either the “top-down” or the “bottom-up” hypothesis for a well-documented predator-prey couple represented by the atlantic cod, *Gadus morhua* (an overfished stock) and northern shrimp (*Pandalus borealis*). Their result strongly supported the “top-down” hypothesis. Notwithstanding these results proceeding from a relatively simplified system, in real systems it is difficult to separate the two forces that probably act synergistically or antagonistically. Möllmann et al. (2008) found a species-level trophic cascade involving three trophic levels (copepods-sprat-cod). The decreasing biomass of *G. morhua* is significantly and negatively correlated with the sprat (*Sprattus sprattus*) biomass, indicating top-down control. Trophic cascading proceeded down to the copepod *Pseudocalanus acuspes*, whose biomass time-series is negatively related to the increased sprat stock. The cascading effect over two trophic levels is further demonstrated by the significantly positive relationship between cod and *P. acuspes*. The same authors investigated climate-induced changes at all trophic levels, discovering that the most pronounced changes occurred at the zooplankton and fish trophic levels. In the zooplankton, dominance changed between the copepods *P. acuspes* and *Acartia* spp. as a result of reduced salinities and increased temperatures. The change in hydrography also affected the reproductive success of the major fish species, resulting in a change in dominance from the piscivorous cod to the planktivorous sprat. Thus, both causes probably act together and also induce a “regime shift” of the ecosystem.

### **1.3 The bathyal domain in the NW Mediterranean sea: energy transfer and faunal composition**

Conventionally, the bathyal domain corresponds to the continental slope and the corresponding water masses (Figure 1.8) at the same depths. Some authors refer to the deep sea for waters below the 1000 m, but for others it begins at 200 m depth. Once deep sea (and the bathyal domain) was considered lifeless and without alterations, albeit this viewpoint has been changing throughout last decades. In the Mediterranean sea the bathyal domain matches depths between 200 m where the continental shelf ends, and 3000 m where the abyssal zone starts. The water

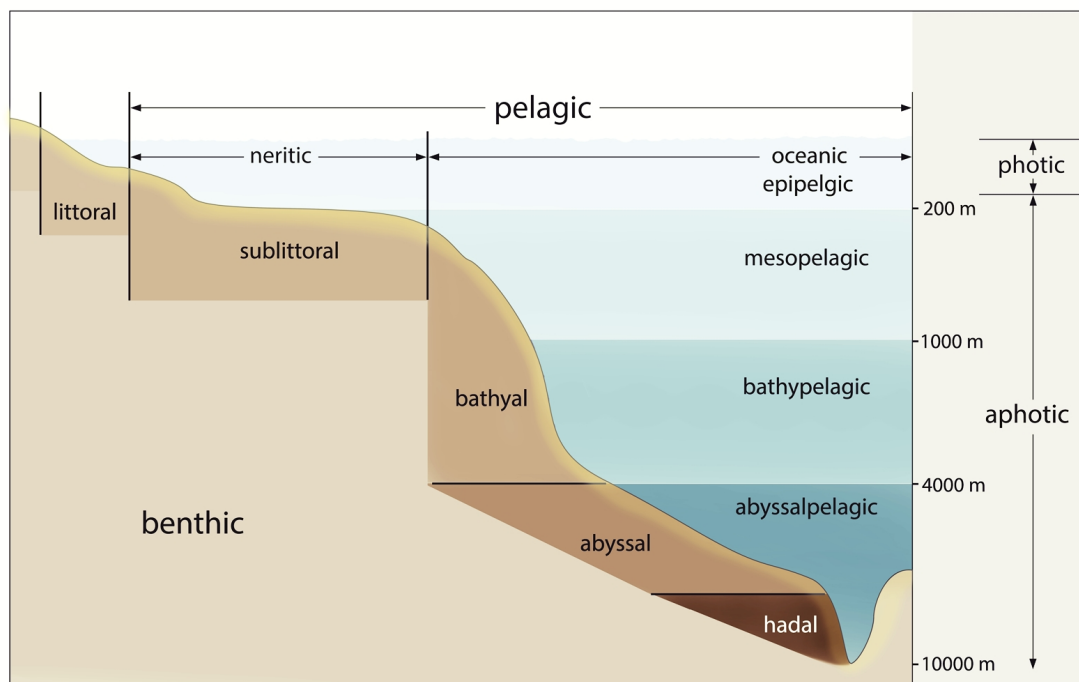


FIGURE 1.8: Principal domains of benthic and pelagic regions. Depths are not to scale.

masses corresponding to the (benthic) bathyal domain are subdivided into meso- and bathypelagic (Figure 1.8).

The deep sea mostly belongs to allochthonous energy sources deriving from the photic zone, where the sun's rays and nutrients allow the primary production (Broecker, 1991). The main pathways are the vertical flux of organic matter from the photic zone, which origin is usually called pelagic, and the advective flux through the slopes (and even more through canyons), of which the origin is partially or mainly terrigenous, and also a vertical active migration of zooplankton, micronekton and bigger meso- and bathypelagic fish (Figure 1.9).

Early investigations pointed to a high stability of deep sea ecosystems, regarding both their structure and dynamics (Grassle and Sanders, 1973), also assumed at seasonal and inter-annual time scales (Sanders, 1968). This point of view, however, has progressively changed in recent decades with the increasing evidence of aspects such as the seasonal influx of the phytodetritus to deep sea environments (Billett et al., 1983; Deuser et al., 1981; Hecker, 1990) and the non-continuous reproduction or peaks in the recruitment reported for deep sea species. In the north Pacific the primary production, the particulate organic matter produced in the surface and reaching bathyal depths (around 500 m) has been estimated to range from 20%

to 50%, while does not reach the 5% at abyssal depths (Buesseler et al., 2007). In the Mediterranean the percentage at same depth could be less due to the constant high temperature of water column, that should permits a rapid degradation of particles by bacteria (Goutx et al., 2007).

Population densities are lower in the Mediterranean then in the Atlantic, a feature related to the much lower availability of organic matter on the Mediterranean seabed, due to the oligotrophic characteristics of the Mediterranean sea. Globally, the Mediterranean sea is an oligotrophic sea. The flux of particles along the water column (total particle flux has been estimated 32.9 and 8.1 g m<sup>-2</sup> y<sup>-1</sup> at 80 and 1000 m respectively: Miquel et al., 1994 in the Ligurian Sea) and the concentration of (total or labile) organic matter on deep-sea bottoms follow a seasonal pattern with peaks coupled with the spring peak of primary production (Cartes, Grémare, Maynou, Villora-Moreno and Dinet, 2002).

Continental margins are important areas in terms of energy transfer, biogeochemical cycles and biological production (Levin and Sibuet, 2012; Valiela, 1995; Walsh, 1991). The physical processes, that transfer water and particulate matter from the continental shelf to the deep sea (Nittrouer and Wright, 1994) mainly through

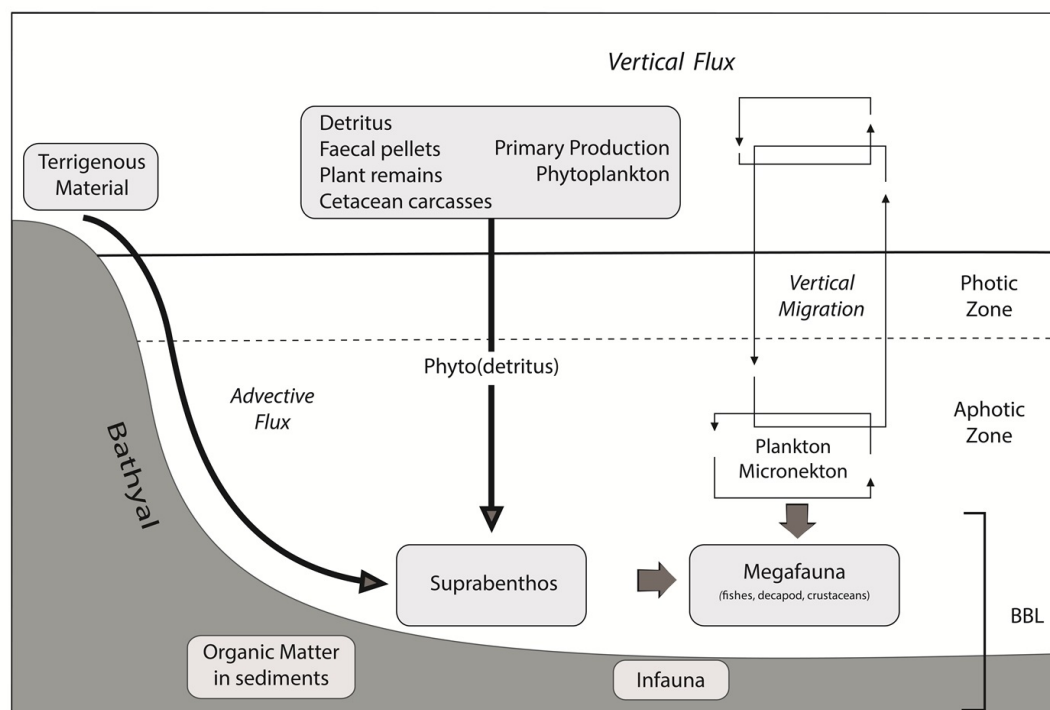


FIGURE 1.9: Principal pathways in the bathyal domain. BBL = Benthic Boundary Layer, modified from WWF/IUCN (2004), pg. 28.

submarine canyons (northern California: [Puig et al., 2003](#); north-western Mediterranean: [Puig et al., 2008](#)), provide favourable environments to sustain highly diversified communities, such as the cold water communities (CWC habitats: [Huvenne et al., 2011](#)).

Time-series studies have shown that deep sea can experience rapid inputs of food supplies from overlying surface waters ([Billett et al., 1983](#)), as well as rapid responses by micro-, meio- and macrofaunal taxa (e.g. foraminifera [Gooday, 1988](#)). In the Pacific Ocean a coupling between the particulate organic carbon (POC) production at the surface and the seafloor (~ 4000 m) communities has been observed with a time lag of 40 to 60 days ([Baldwin et al., 1998](#); [Ruhl and Smith, 2004](#)). Also in the Mediterranean coupling between phytoplankton production and deep-sea organisms responses as been proved ([Fanelli et al., 2009](#)). However here, the high temperatures of water column make that organic matter undergoes a rapid degradation while falling to the deep, and mitigate the response of benthic fauna to the phytoplankton blooms. Energy in the deep sea is only produced by chemosynthesis e.g. in hydrothermal vents ([Corliss, 1979](#)), but its quantification is still scant; in fact, it is likely that the majority of these structures have been not yet discovered. In the oceanic abyssal floor, such structures and seamounts are not dominant, occupying less than 1% ([Smith et al., 2009](#)). Conversely soft-sediments constitute the most characteristic biotope of deep sea bottoms and energy flow and carbon cycling in these environments more realistically could describe the “usual” dynamics of a deep sea ecosystem. Soft bottom are also much more accessible and thus influenced by anthropogenic processes such as mineral extraction and fishing activity ([Smith et al., 2009](#)).

The deep Mediterranean fauna displays a high degree of eurybathic species along the slope and the abyssal domains. Certain areas of the Mediterranean deep sea are benthic diversity hotspots, harbouring high densities of endemic taxa, e.g. submarine canyons ([Gili et al., 1999](#)), cold seeps associated to mud volcanoes (hosting the chemosynthetic communities), cold water coral reefs (CWC) ([Roberts et al., 2006](#)), seamounts and brine pools. Among bathyal amphipods, a high percentage (49.2%) is endemic ([Bellan-Santini, 1990](#)), even higher than in coastal zones, probably due to the absence of pelagic free larvae ([Cartes et al., 2004](#)). Canyons present unique characteristics with large differences in the sediment fluxes and hydrodynamic features ([Canals et al., 2009](#); [Palanques et al., 2006](#)), affecting the abundance and species composition of the fauna ([Gili et al., 2000](#)). Cold water



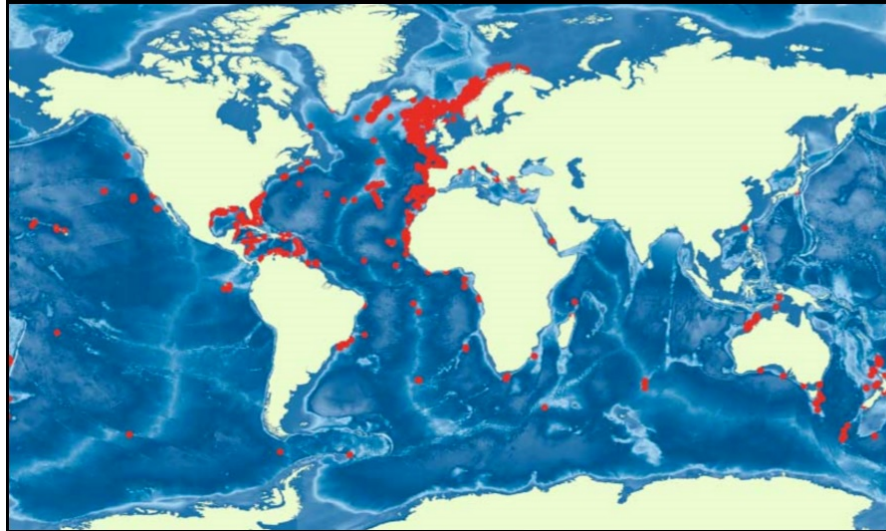


FIGURE 1.10: Global distribution of cold-water corals. From [Roberts et al. \(2006\)](#).

corals are cnidarians encompassing stony corals (Scleractinia), such as *Madrepora oculata* and *Lophelia pertusa*, and soft corals (Octocorallia, including bamboo corals, i.e. *Isidella elongata*, Figure G.2, C), black corals (Antipatharia), and hydrocorals (Stylasteridae). They are azooxanthellate (i.e., lacking symbiotic dinoflagellates) and often form colonies supported by a common skeleton, providing structural habitat for other species. CWC colonies have been observed mainly in oceanic waters at high latitudes (Figure 1.10).

Although this distribution is skewed due to the intensive research activity performed almost by the developed world ([Roberts et al., 2006](#)). CWC communities in the Mediterranean, dominated by *M. oculata* and with less abundance by *L. pertusa*, have been observed at the heads of some canyons within the Gulf of Lions, one of the areas of the world's oceans with the highest canyon density ([Harris and Whiteway, 2011](#)). CWC promotes the presence of a highly diverse associated fauna ([Buhl-Mortensen et al., 2010](#)) acting as potential areas of refuge, breeding and feeding for many deep-sea species, including commercially important fish ([D'Onghia et al., 2010](#); [Gori et al., 2013](#); [Ross and Quattrini, 2007](#)). Higher biomass and diversity of mega and macrofauna has been found also in habitats with the soft-bottom *Isidella elongata* ([Cartes, LoIacono, Mamouridis, López-Pérez and Rodríguez, 2013](#); [Mamouridis, Cartes and Fanelli, 2014a,b](#)) (Figure G.2).

In the continental slope the fish assemblage from 200 to 2250 m ([Moranta et al.,](#)

1998; Stefanescu et al., 1994) comprises ca. 90 species in the western Mediterranean (some species in Figures G.1, G.2, G.3, G.4). The biomass strongly decreases from 200 m to 800 m (the odd is around 10:1). About decapod crustaceans, the number of species reported from 200 to 4000 m is ca. 60. Regarding to the macrofauna, Fredj and Laubier (1985) reported ca. 2100 benthic species deeper than 200 m in the Mediterranean. However the densities in the Mediterranean are reported to be about 1/10 of the Atlantic at comparable depths (Flach and Heip, 1996). In contrast the swimming macrofauna (suprabenthos or hyperbenthos) showed diversity peaks at mid-bathyal depths in the Balearic and in the Algerian Basin, with some variation depending on the taxon considered (around 600 m for amphipods; around 1200 m for cumaceans) (Cartes et al., 2003; Cartes and Sorbe, 1996, 1999; Cartes, Mamouridis and Fanelli, 2011) (see Figures G.5 and G.5).

Pérès and Picard (1964) established the transition between the circalittoral and bathyal domains in the Mediterranean at around 180-200 m depth. Two main broad biocenoses (“facies”) in the bathyal Mediterranean have been defined (Pérès, 1985; Pérès and Picard, 1964): (1) soft-bottom communities and (2) hard-bottom communities. Depending on the nature of the sediment, the hydrodynamism and mainland influence, the broad soft-bottom biocenosis has been further divided into three horizons: the (1) upper, (2) middle and (3) lower slope horizons (Pérès, 1985). This community zonation related to the depth has been adopted also for benthopelagic megafaunal species, belonging to invertebrates and ichthyofauna and another division has been then proposed in the middle slope, between upper and lower mid-slopes (e.g. Cartes, 1998; Cartes and Sardà, 1993; Colloca et al., 2003).

The upper slope horizon holds characters of a transitional zone between the continental shelf and the bathyal domain, comprising a large share of eurybathic forms and extending to 400-500 m deep. Within megafauna, the crustaceans *Parapaneus longirostris* and *Nephrops norvegicus* are characteristic species of this horizon. The middle slope horizon, characterized by firmer and more compact muds, is the zone where most taxonomic groups achieve maximum diversity, mainly Peracarida. Within megabenthos, the *Aristeus antennatus* is a characteristic species of this zone. The lower horizon of the slope is characterised by the decapods *Stereomastis sculpta*, *Acanthephyra eximia* and *Nematocarcinus exilis* (Abelló and Valladares, 1988), and the fishes *Bathypterois mediterraneus*, *Alepocephalus rostratus* (Figure G.2, B), *Lepidion lepidion* and *Coryphaenoides guentheri*. Then,

benthopelagic communities incorporate also bathypelagic species, although they live mostly in open waters (e.g. the *Argyropelecus hemigymnus*, Figure G.4, B, and the *Lampanyctus crocodilus* Figures G.1, C and G.4, A).

Common chondrichthyans are *Galeus melastomus* (Figure G.3, A) and *Etmopterus spinax*. New research suggested a direct relationship between environmental changes (increases in temperature and salinity in intermediate waters) and the decline of this deep-water sharks (Cartes, Fanelli, Lloris and Matallanas, 2013), confirming a trend that has been seen in many regions of the world. These authors also suggest that the increased fishery effort is another factor explaining the drop in shark abundance in the Catalan slope while in other regions of the western Mediterranean, also subjected to fishery pressure, *E. spinax* is still dominant (e.g. in the Sicily Channel: Fiorentino, 2009) and in the Eastern Mediterranean, where deep-sea sharks (*Centrophorus* spp., *Hexanchus griseus* and *E. spinax*) and represent the most abundant fish species in Levantine bathyal communities.

With respect to bacteria and meiofauna, there is high variability in their contribution to the community. For example, below 500 m depth in the western Mediterranean the contribution of bacteria to organic matter degradation is low (2.5 times of the total). Contrariwise in the eastern Mediterranean bacteria represent 35.8% of the living biomass and the bacteria-meiofauna biomass ratio is very high (20 times) (Western Mediterranean: Danovaro et al., 1999; Eastern Mediterranean: Danovaro and Serresi, 2000; Danovaro et al., 1995).

The food web is likely a “coupled benthopelagic trophic system”, mainly composed by the “pelagic” zooplankton feeding on particulate organic matter in the water column (e.g. the gastropod *Cymbulia peroni*, with  $\delta^{15}\text{N}=2.6\text{‰}$  corresponding to TL=2 in pelagic food webs) and “benthic” deposit feeders *Leucon longirostris* and *Amphipholis squamata* (Figure G.5, B and H) with mean  $\delta^{15}\text{N}$  of 4.6‰ and 4.6‰ respectively also corresponding to TL=2 in benthic food webs (Fanelli, Cartes and Papiol, 2011; Fanelli, Papiol, Cartes, Rumolo, Brunet and Sprovieri, 2011). Has been found that predators with higher trophic levels in the bathyal network are *Alepocephalus rostratus* (Figure G.2, B) and *Nezumia aequalis* (Figure G.3, B), that tend to be more planktivorous and benthivorous respectively. Suspension feeders have relatively little importance in the Mediterranean, due to its oligotrophic waters, so they are important only locally. “Intermediate” species between TL=1 and 2 are common and benthopelagic megafauna show overlapped trophic position, however fish TLs are higher in average than decapod crustaceans

( $\delta^{15}\text{N}$  ranges for fishes: 7.27–11.31‰;  $\delta^{15}\text{N}$  ranges for decapods: 6.36–9.72‰) (Papiol et al., 2013). The red shrimp is predator of a wide range of sources and shows a relatively high trophic level, however it is not the highest found in this community. It shows  $\delta^{15}\text{N}$  values of  $9.50 \pm 0.64$ ‰ in the mainland slope and eats preferentially on benthic dwellers (Papiol et al., 2013).

## 1.4 Deep-sea fisheries, management and models

Recently, there has been an increase in public awareness, leading to a demand for better management of marine resources in the Mediterranean area (e.g. WWF/IUCN, 2004). It has been suggested that during the past decade in EU waters, the 88% of monitored marine fish stocks have been overfished (Thurstan et al., 2010). In this context, other authors have predicted a global collapse of fisheries within the next few decades (Worm et al., 2006, 2009). International treaties have been already signed by Mediterranean countries, such as the Convention on Biological Diversity (CBD) or the UN Framework Convention on Climate Change (UNFCCC) (Coll and Libralato, 2012).

During the last 50 years the ultimate target of industrial fisheries worldwide is the deep sea (Glover and Smith, 2003), following the relentless depletion of fish communities on the continental shelves (Christensen et al., 2003, e.g.), in a sort of “(over)fishing down the bathymetric range effect” (Haedrich et al., 2001; Morato et al., 2006, e.g.). This trend can have dangerous effects when considering that deep-sea species are highly vulnerable (k-selection characteristics) and with little resilience to over exploitation (Haedrich et al., 2001). Deep-water fisheries are documented since the early 1930s targeting especially the highly prized decapod crustaceans Norway lobster and red shrimps (Oliver, 1993). Fisheries production of deep-living decapods are actually increasing in the last years (Politou et al., 2003) and do not show symptoms of decline yet.

### 1.4.1 The red shrimp fishery in Catalonia

In the western Mediterranean deep water fisheries are limited to the continental slope shallower than 900 m, corresponding to the upper and middle zones (Carbonell et al., 1999; Righini and Abella, 1994; Sardà et al., 1994), while the eastern

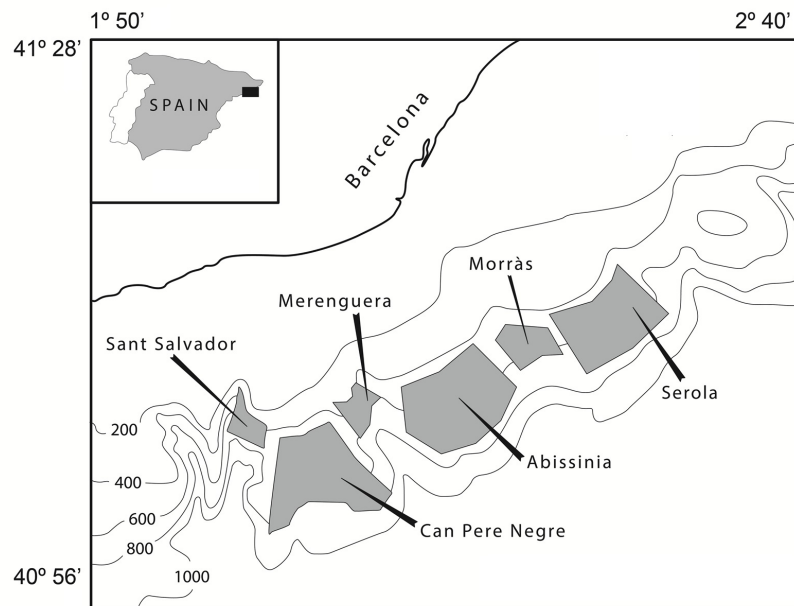


FIGURE 1.11: Fishing grounds of the red shrimp fishery at the continental slope off Catalonia. Modified from [Sardà et al. \(1997\)](#).

deep sea began to be exploited in 2000s ([Politou et al., 2003](#)). The fishery of the highly priced red shrimp *Aristeus antennatus* is the main fishing activity performed in the NW Mediterranean deep sea. Off Catalonia there is a total of 7 fishing grounds (Figure 1.11). Also by-catch species, such as *Merluccius merluccius* (Figure G.3, C), *Micromesistius poutassou*, *Phycis blennoides* and deep-sea sharks are fished and some of them sold.

#### 1.4.2 Monospecific and ecosystem approaches to fisheries and existing models

Since ancient times fishing has been a major source of food and has provided employment and economic benefits for humanity. Besides, with increasing knowledge and development of fishing technologies and effort, it was realised (middle of the 20th century) that aquatic resources are not unlimited. Proper management systems must be set up to sustain fisheries because they largely contribute to feeding the human population and at the same time the best way to respect the environment and ecosystems be found. Fisheries usually target from one to several species, depending on the fishing method. Until early the 1990s fisheries management focused on regulating the fishing activity of only target species (“Target

Resource Oriented Management” or TROM paradigm). However fisheries often affect other components of the ecosystem: the fishing of by-catch non-target species is very common and such species can be either commercialised or discarded at sea. Moreover the removal of some species and the destruction of the environment due to invasive gears may affect other species or the habitat.

In addition is reasonable to consider that human activities interact with natural changes, so, when analysing and managing marine resources, is straightforward the need to adopt an integrated view of such complex systems (Botsford et al., 1997; Cury et al., 2003; Duda and Sherman, 2002). This implies a progress towards the so-called ecosystem approach to fisheries (EAF) (e.g. Botsford et al., 1997; Coll and Libralato, 2012; FAO, 2003).

Fisheries management in Europe is still largely based on single-species assessments and does not fully incorporate the wider ecosystem context and impacts in fisheries policy. The reason is yet the lack of a coherent strategy (Möllmann et al., 2013), although policy principles are in place (e.g. the Marine Strategy Framework Directive; the Good Environmental Status indicators). The scientific community has shown a growing interest on ecosystem-based studies, with an increasing application of ecological and bio-economic models such as ECOPATH with ECOSIM (Coll, Lotze and Romanuk, 2008; Coll and Libralato, 2012) or the MEFISTO (Merino et al., 2007) and several other models. All such mathematical models deal with the ecosystem approach: as “simple” as studying predator-prey interactions or more complex models studying the impact on the whole ecosystem. Some examples will be given later.

The different types of models can be summarized into three categories:

1. Extensions of single-species assessment models.
2. Multi-species models, that allows few interactions (see Punt and Butterworth, 1995).
3. Ecosystem models (Christensen and Pauly, 1992; Pauly et al., 2000; Polovina, 1984; Walters et al., 1997).

All models are listed in tables A.1 and A.2 (revised from Plagányi, 2007). Give a description of all existing models is not the purpose of this thesis, for which, if the reader has the interest may consult the extensive review for multi-species

and ecosystem approaches applied to fisheries by [Hollowed et al. \(2000\)](#) and its revision by [Plagányi \(2007\)](#). Plagányi highlighted the different characteristics and data requirements for each of these models inasmuch as the importance to select the best model that fits with the real situation. The issue is complex, also due to the high number of processes involved and difficulties in the selection of parameters. It is therefore a very difficult selection, as well as the proper use of this wide range of models.

The ECOPATH software, the most widely used in the scientific community, offers a systematic approach to ecosystem modelling dealing with the massbalancing problem ([Christensen and Walters, 2004](#); [Christensen and Pauly, 1992](#)). A clear benefit is that data input and massbalancing are performed in a standardized and user-friendly way ([van Oevelen et al., 2010](#)). The model was originally formulated by [Polovina \(1984\)](#) as an ensemble of linear equations and has been development during 90's ([Christensen and Pauly, 1992](#)), with Ecosim ([Walters et al., 2000, 1997](#)), allowing for dynamic modelling, and Ecospace ([Walters et al., 1999](#)) for spatial modelling. The linear system is solved using standard matrix algebra. To solve the system a generalized inverse is used if the determinant is zero or the matrix is not square (that works in most cases, [Mackay, 1981](#)). If the set of equations (see [Christensen and Pauly, 1992](#)) is over-determined (more equations than unknowns), and the equations are not mutually consistent the generalized inverse method provides least squares estimates, which minimize discrepancies ([Christensen and Pauly, 1992](#)). Thus, the ECOPATH is able to solve even- or over-determined problems, but it is also able to estimate a posteriori “missing” stocks (an under-determined situation). An algorithms tries to estimate iteratively as many “missing” stocks as possible before setting up the set of linear equations becoming then an even- or over-determined system, that can be solved by the generalized inverse method. Thus, ECOPATH circumvents the problem of mathematical indeterminacy artificially upgrading the number of equations until the matrix equation is completely determined by imposing fixed values for, e.g., physiological parameters.

When the algebraic system become even- or over-determined, then the energy balance is ensured within each group using an equation pretty similar to the following:

$$C = P + R + U$$

where  $C$  is consumption,  $P$  production,  $R$  respiration and  $U$  unassimilated food, in line with energy conservation assumptions for biological units [Winberg \(1956\)](#) and pretty similar to the set of equations discussed in [Section 1.2.1](#). However the energy equation in ECOPATH does not account for gonadal production and is defined a priori such that it is impossible to change its energetic assumptions, an opportunity that would be very useful when dealing with real data. Moreover the ECOPATH remains restricted to singlecurrency data ( $t\ km^{-2}$ ), as it does not allow the simultaneous solution of mass balances for multiple elements.

In conclusion, the major problems arise from the under-determined solution method and rigidity of model settings in ECOPATH. These problems are differently approached in the so-called Linear Inverse Modelling (LIM) ([Soetaert and Petzoldt, 2010](#); [van Oevelen, Soetaert, Middelburg, Herman, Moodley, Hamels, Moens and Heip, 2006](#); [van Oevelen et al., 2010](#)) originally proposed by [Vézina and Platt \(1988\)](#). In this thesis there is no intention to criticise the ECOPATH approach, that is to date the most used by the scientific community and the most productive, although we are interested in using other promising methods in ecological modelling that could support and improved ecosystem approach to fisheries management.

### **1.4.3 The complexity of a model and the bias-variance problem**

An important issue to account for when modelling is the compromise between simplicity and complexity of the model on order to represent the reality in the “best form”. That is related to the trade-off between variance and bias of a model or estimator. An estimator is any quantity calculated from the sample data which is used to give information about an unknown variable in the population. For example, the linear regression of variable  $Y$  with respect to some covariates  $X$  is an estimator. The LIM model that provides estimations of unknown flows between the component of the system is also an estimator. So, the number of examples is huge. When modelling we try to reduce the error of the estimator (that cannot be completely eliminated) to augment its “quality”. Solving the variance-bias trade-off is meant to choose a model that accurately captures the regularities in the sample (reducing the bias), but also generalizes well to unseen data (reducing the variance). So, there are two sources of error, the bias and the



variance, that the bias-variance trade-off problem tries to minimize. Figure 1.12 is a graphical explanation of such a problem. The bias refers to the portion of error from erroneous assumptions and is the difference between the estimator's expected value and the true value of the unknown variable being estimated. Contrariwise, the variance refers to the portion of error derived from sensitivity to fluctuations in the sample. It measures how far samples are from the real variable. As a consequence, a variance of zero indicates that all the values are identical.

Formally, if we want to estimate the real function  $f(x)$  using a sample of the random variable  $X$  with observations  $x_1, \dots, x_n$ , through  $\hat{f}_n(x)$ , as estimator of the function, then the squared error loss function is

$$L(f(x), \hat{f}_n(x)) = (f(x) - \hat{f}_n(x))^2. \quad (1.16)$$

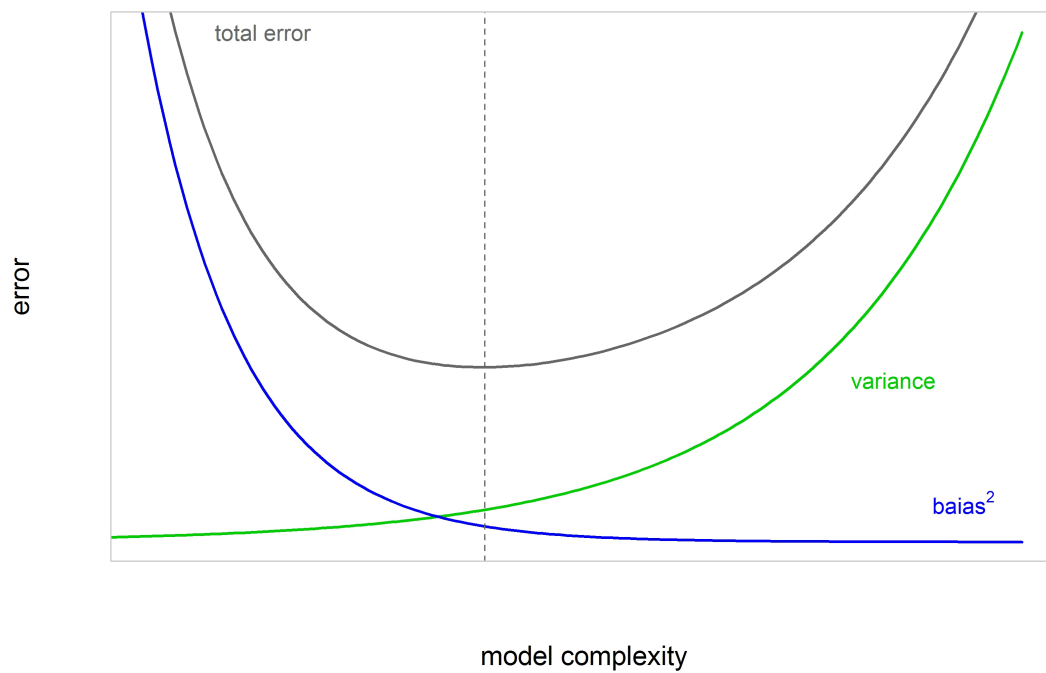


FIGURE 1.12: The bias-variance trade-off in model fitting with increasing complexity (the more parametrization, the higher complexity). Increasing the model complexity also the variance increases, while the bias decreases. The best fit occurs when both are minimized (vertical dashed line). Here error defines whatever measure used to summarise the error of the model, being the integrated or the average mean square error or the predictive risk. See the text for more details.

The expectation of this loss is called risk or mean squared error (MSE)

$$\text{MSE} = R(f(x), \hat{f}_n(x)) = E[L(f(x), \hat{f}_n(x))]. \quad (1.17)$$

The mean squared error can be decomposed into bias and variance of the estimator

$$\text{MSE} = \text{Bias}[\hat{f}_n(x)]^2 + \text{Var}[\hat{f}_n(x)]. \quad (1.18)$$

The bias is the difference between the real function  $f(x)$  and the expectation (or mean) of the estimator  $E[\hat{f}_n(x)]$ ,

$$\text{Bias}[\hat{f}_n(x)] = E[\hat{f}_n(x)] - f(x). \quad (1.19)$$

The variance is the expectation (mean) of the squared distance between the estimator and the real function,

$$\text{Var}[\hat{f}_n(x)] = E[(\hat{f}_n(x) - E[\hat{f}_n(x)])^2]. \quad (1.20)$$

The above definitions refer to the MSE (or risk) at a point  $x$ . To summarise the risk over different values of  $x$  we use the integrated mean squared error for density estimations, i.e.

$$R(f, \hat{f}_n) = \int R(f(x), \hat{f}_n(x)) dx. \quad (1.21)$$

For regression problems, where the response random variable  $Y$  with observations  $y_1, \dots, y_n$  and covariate  $X$  with observations  $x_1, \dots, x_n$ , and regression function,  $r(x)$ , such that

$$y_i = r(x_i) + \epsilon,$$

can also be used the average mean squared error

$$R(r, \hat{r}_n) = \frac{1}{n} \sum_{x=1}^n R(r(x_i), \hat{r}_n(x_i)). \quad (1.22)$$

In the practise we do not calculate the average mean squared error using the true function, that remains unknown, instead simulations are required and in applications is common practice estimate it through sub sets or equally simulations and it is of common use for quantifying the goodness of fit of a model without a real need to distinguish between bias and variance, because the MSE must be minimized. In conclusion, a statistical model could not be nether too simple nor to complex to perform well.

In ecosystem modelling, the problem is somehow different and still unsolved for many aspects or should be better described. In any case, one important observation is that, if limited and/or noisy data, then model results are uncertain even in complex models (Plagányi, 2007).

## 1.5 Generalized linear and additive models

Regression models have been used throughout the thesis, in particular in Chapter 2 where the biomass of macrofauna has been analysed in dependence of many environmental covariates, and in Chapters 3 and 4 where the index LPUE (landings per unit effort) was modelled as a combination of functions of environmental, fishery and economic covariates.

In generalized linear models (GLM, McCullagh and Nelder, 1989), for a given random response  $Y$  with observations  $y_1, \dots, y_I$  and a set of covariates  $x_1, \dots, x_P$ , the impact of the covariates on the conditional expectation of the response,  $E[y_i|x_p]$ , is modelled as a linear combination of the covariate effects, such that

$$\eta_i = \beta_0 + \beta_1 x_{i1} + \dots + \beta_P x_{iP}, \quad (1.23)$$

where  $\beta_0, \beta_1, \dots, \beta_P$  are the regression coefficients associated to each covariate  $x_p$  and  $\eta_i$  is the linear predictor, linked to the conditional expectation  $E[y_i|x_p]$  with a suitable transformation function  $G$ ,

$$\eta_i = G(E[y_i|x_p]) \quad (1.24)$$

to be defined accordingly to the distribution function assumed for the response.

Similarly the generalized additive models (GAM, [Hastie and Tibshirani, 1990](#)), the most commonly used models within the generalized regression approach, has the following linear predictor,

$$\eta_i = \beta_0 + s_1(x_{i1}) + \dots + s_P(x_{iP}), \quad (1.25)$$

where regression coefficients  $\beta_0, \beta_1, \dots, \beta_P$  for covariates are replaced by nonlinear functions  $s_1, \dots, s_P$ . The GAM model is preferred when the assumption of a simple linear impact is unrealistic for some of the covariates and a more flexible semiparametric approach is required. Nonlinear functions are estimated from the data, using for example penalized spline approaches (see [Ruppert et al., 2003](#); [Wood, 2006](#)).

Both GLM and GAM allows for interactions between covariates. The GLM formulation for the interaction is pretty similar to the simple linear regression with interaction,

$$\eta_i = \beta_0 + \beta_1 x_{i1} + \dots + \beta_P x_{iP} + \gamma_1 x_{i1} x_{i2} + \dots + \gamma_D x_{iP-1} x_{iP}, \quad (1.26)$$

where regression coefficients  $\gamma_1, \dots, \gamma_D$  account for  $D$  interactions between two covariates (or more).

Also in a GAM, nonlinear functions can represent the interaction between two covariates (or more), such that

$$\eta_i = \beta_0 + s_1(x_{i1}) + \dots + s_P(x_{iP}) + t_1(x_{i1} x_{i2}) + \dots + t_D(x_{iP-1} x_{iP}). \quad (1.27)$$

Here are defined both main effects  $s_1, \dots, s_P$  of covariates  $x_1, \dots, x_P$  and interaction effects,  $t_1, \dots, t_D$ , between two different covariates.

The GAM is not a strictly smooth effects model, allowing for both linear relationships and smooth functions. In this case the effects of part of covariates can be modelled as coefficients  $\beta_p$  (or  $\gamma_d$ ) and the rest as smooth functions  $s_p$  (or  $t_d$ ). So, if main effects are modelled, an even more generic formulation of the GAM is

$$\eta_i = z_i' \delta + \sum_{p=1}^P s_p(x_{ip}). \quad (1.28)$$

Here,  $z_i$  is a vector containing binary, categorical or continuous linearly related variables and  $\delta$  the corresponding vector of parameters.

Other extensions are generalized linear mixed models (GLMMs, [Pinheiro and Bates, 2000](#)) and generalized additive mixed models (GAMMs, [Wood, 2006](#)). These models should be used when data are collected repeatedly over time for the same individual (for example the same boat of a fleet as discussed in [Chapter 4](#)) to account for some of its unobserved characteristics. So, if the individuals are indexed as  $i = 1, \dots, n$  and the repeated measurements for each individual are indexed as  $j = 1, \dots, n_i$ , the GLMM takes the form

$$\eta_{ij} = \beta_0 + \beta_1 x_{ij1} + \dots + \beta_P x_{ijP} + \alpha_i, \quad (1.29)$$

and the GAMM

$$\eta_{ij} = \beta_0 + s_1(x_{ij1}) + \dots + s_P(x_{ijP}) + \alpha_i. \quad (1.30)$$

In both cases, the additional parameter  $\alpha_i$  describes any effect specific to the individuals that is not represented in the effects of covariates  $x_1, \dots, x_P$  and should be specified as random effects, i.e.  $\alpha_i$  i.i.d.  $N(0, \tau^2)$ , as usual in the statistical community, to acknowledge the fact that individuals represent a sample from the population. In applied science they are usually specified as fixed effect.

GLM, GAM, GLMM and GAMM allow the modelling of the conditional expectation of the mean (or location) of the response. So, all these classes are defined by only one predictor  $\eta$ , that refers to  $E[y]$  or  $\mu$ . In many cases, could be of interest also the modelling not only of the location but also of higher order parameters of the distribution assumed, such as the scale and the shape. This extension leads to the class of generalized additive models for location scale and shape (GAMLSS [Stasinopoulos and Rigby, 2007](#)), of which the Bayesian counterpart is the extended or distributional structured additive regression model (DSTAR [Klein et al., 2013](#)), applied in [Chapter 4](#). These models are defined by as many predictors as the parameters of the response distribution to be estimated. So, if the distribution of the response  $Y$  with observations  $y_1, \dots, y_I$  has the probability density function

$f(y_i|\theta_k)$  conditional on  $\theta_1, \dots, \theta_K$  parameters of the distribution, each of the parameters can be modelled in dependence of covariates  $x_1 \dots, x_P$ , through a linear

predictor  $\eta_{\theta_k}$  and the appropriate monotonic transformation function  $G_k$  between  $\theta_k$  and  $\eta_{\theta_k}$ , that may differ for each  $\theta_k$ . Here the subindex  $k$  is introduced to account also for higher order parameters of the distribution, that are not considered in previous models. Briefly, the first two parameters  $\mu_i$  and  $\sigma_i$  are usually characterized as location and scale parameters, while the remaining parameter(s), if any, are characterized as shape parameters.

Now, the model is defined by  $k$  equations, one for each parameter  $\theta_k$ . The predictor  $\eta_{\theta_k}$  can be defined similarly to the models above as an additive combination of covariates effects, as linear coefficient or unknown function to be flexibly estimated by data. So, accordingly to the GLM model, the GAMLSS accounting only for linear effects is

$$\eta_{i\theta_k} = \beta_0 + \beta_1 x_{i1} + \dots + \beta_P x_{iP}, \quad (1.31)$$

while according to the GAM, it is

$$\eta_{i\theta_k} = \beta_0 + s_1(x_{i1}) + \dots + s_P(x_{iP}), \quad (1.32)$$

and so on for all other models specified up to Equation 1.30. The formulation of a predictor in GAMLSS can be then generalised as

$$\eta_{ij,\theta_k} = z'_{ij}\delta + \sum_{p=1}^P s_p(x_{ijp}) + \alpha_i, \quad (1.33)$$

where linearly related covariates, binary or categorical variables effects, included in  $z_{ij}$ , smooth function, defined by  $s_1, \dots, s_P$ , and random effects,  $\alpha_i$ , are jointly incorporated into the same predictor  $\eta_{ij,\theta_k}$  specified for the parameter  $\theta_k$ .

## 1.6 The study area

This study was carried out on mainland slope of the Balearic basin located in the NW Mediterranean (Figure 1.13). The sampling was performed along the mid-slope off the Catalanian coast (between 40°48'9" N and 41°09'3" N - 2°04'0" E

and  $2^{\circ}35'4''$  E) near Barcelona within projects BIOMARE (ref. CTM2006-13508-C02-02/MAR) and ANTROMARE (ref. CTM2009-12214-C02-01-MAR).

The Balearic Basin is located in the western Mediterranean and represents a transitional region between the Liguro-Provençal and Algerian basins 1.13. It includes the Catalan Sea, located between the Balearic Islands and the Iberian peninsula, and the wide Gulf of Valencia in the south of this sea. With the exception of the Gulf of Lions, the continental shelves of the NW Mediterranean are narrow.

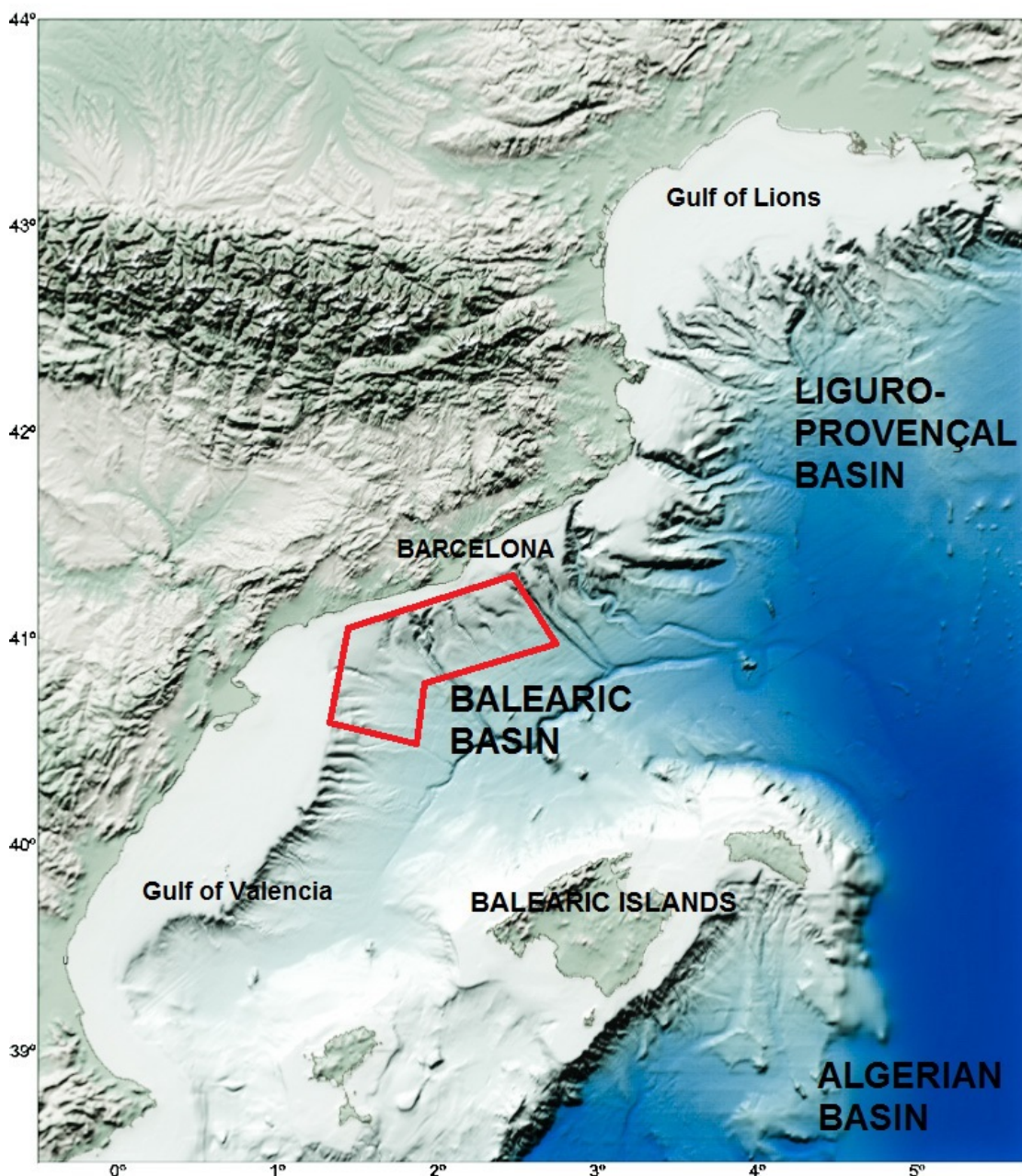


FIGURE 1.13: The Balearic basin and study area inside the red polygon.

The hydrology in the western basin is defined by three main water masses: the surface Modified Atlantic Water (MAW), the Levantine Intermediate Water (LIW) and the West Mediterranean Deep Water (WMDW). The MAW inflows through the Strait of Gibraltar subject to evaporation and mixing with the underlying waters. That increases salinity towards the east from 36.3 in the Strait of Gibraltar to 37.3 ppt in the Strait of Sicily ([Zavatarelli and Mellor, 1995](#)), while the mean value of deep Mediterranean salinity is 38.2 ppt associated to a mean temperature of about 12.8°C. LIW takes place in the Eastern sub-basin in winter and flows between 200 to 400 m in the Western basin. Deeper waters remain separate between East and West. The source of the deep western current, the WMDW, is located in the Gulf of Lions, where in winter the convective movements occur influenced by cold and dry winds, causing the sinking and mixing of cold and salty surface waters to a depth of about 1200 to 1500 m ([Zavatarelli and Mellor, 1995](#)). This water mass can outflow at Gibraltar without mixing with the LIW ([Kinder and Parrilla, 1987](#)). These currents can affect and alter the presumed homogeneity of the deep sea environment [Garcia-Ladona et al. \(1996\)](#).

At surface, in Liguro-Provençal Basin, dense waters originated in the north are associated with a permanent circulation along the continental slope: the Northern Current (NC). The Algerian Basin, in the south, is dominated by intense mesoscale eddies and the unstable Algerian Current (AC). The NC flows southward along the Iberian peninsula slope and during summer is covered by a warm surface layer spreading over the whole Catalan Sea. This warming creates the intense thermal Pyrenees Front. Near the Balearic Islands, another Front, the Balearic Front, is created by the recent Atlantic water and anticyclonic eddies from the Algerian Current and contributes to mesoscale variability ([Garcia-Ladona et al., 1996](#)).

The NW Mediterranean is classified as oligotrophic (however less than the eastern basin), as the whole Mediterranean, where chlorophyll concentration in the open areas rarely exceeds 2-3 mg m<sup>-3</sup> ([Margalef and Castellví, 1967](#)). The primary production shows a seasonal dynamic, with higher biomass in winter and lower during summer, a pattern that has been regularly observed for more than 20 years ([Marty et al., 2002](#)). Plankton blooms occur in autumn, at the beginning of the mixing period and in winter-spring: wind driven winter up-wellings are important in the Gulf of Lions, where the coastal profile is favourable ([Minas, 1968](#)). There the winter deep convection after breakdown of the thermocline enhances productivity, bringing nutrients from deep waters to the surface layers. Thus,



large bloom have been observed in the Liguro-Provençal Region (D'ortenzio and Ribera d'Alcalà, 2009). With a minor scale and intensity up-wellings occur also in the Catalano-Levantine coast of Spain (Margalef and Castellví, 1967).

Phytoplankton estimates show a Deep Chlorophyll Maximum (DCM) during a large part of the year, when there is a certain degree of stratification of the water column. The DCM occurs within the pycnocline (see Fig. 2 in Estrada, 1996), at a depth in which nutrients become available and light, although generally of the order of 1% that at surface, is still sufficient for growth. The presence of the DCM accentuates the strong vertical differentiation of the pelagic ecosystem into a light-sufficient but nutrient-limited upper layer, based mainly on recycled production, and a nutrient sufficient but light-limited lower layer, where new production takes place (Herbland and Voituriez, 1979). These vertical patterns affect the structure of the trophic links among the diverse plankton components and are accompanied by changes in the relative importance of the microbial versus the classical, zooplankton-based, food web.

The responsible hydrographic features include: 1) turbulent mixing in the Straits, which drags nutrient from deep Mediterranean waters into the euphotic zone (Minas et al., 1984); 2) up-welling in the Alboran Sea and frontal zones associated with the anticyclonic gyres caused by the inflow of Atlantic water (Lohrenz et al., 1988; Minas et al., 1984); and 3) the effects of the Atlantic current, which has a higher nutrient content than surface Mediterranean waters and presents strong dynamic activity along the Algerian coast, where meanders and eddies can produce points of enhanced phytoplankton growth (Millot et al., 1990).

The NW basin also presents a cyclonic circulation which extends from the Gulf of Genoa to the Gulf of Valencia, across the Liguro-Provençal and Balearic basins. This feature is bound by shelf/slope fronts associated with the SW-flowing northern current on the continental side, and NE currents on the Corsican, Sardinian and Balearic Islands side (Estrada and Margalef, 1988; Prieur and Tiberti, 1984). The central zone, marked by a doming of isotherms and isopycnals, has lower vertical stability than the margins and can be interpreted as a divergence. Both the shelf/slope fronts and the central dome or ridge-like structure play a key role in the primary production of this part of the Mediterranean.

Land run-off is also important in the northern zone, where rivers like the Rhône, flowing into the Ligurian Sea and to a lesser extent the Ebro in the Catalanian Sae,

are important sources of phosphorus, nitrogen and other nutrients. Temporary discharges due to storms may produce intense local enrichment (Estrada, 1996).

## 1.7 Purposes of the study

The final objective of this thesis is to explore the occurrence of trophic cascade in the bathyal ecosystem driven by the fishery of the red shrimp *Aristeus antennatus*.

The rest of the thesis is structured into three parts: PART I, where an analysis of the macrofauna in canyon and in adjacent slope is performed aiming to relate the structure and principal feeding types of the assemblages with environmental variability; PART II describes the landings per unit effort of the fleet of *A. antennatus* in relation to environmental fishing and economic variables, PART II returns an ecosystem approach of the bathyal soft bottom community where the red shrimp fishery is developed. The concrete aims for each part are:

- Aims of PART I, Chapter 2 are

1. Describe the seasonal composition of the infaunal macrobenthos in two characteristic environments of the Catalan Slope, inside the Besòs canyon and on its adjacent slope at 800 m depth;
2. Identify the main variables both in the sediment and close to the sediment-water interface (the Benthic Boundary Layer), that explain trends observed in the taxonomic composition and biomass of the infaunal macrobenthos.

- Aims of PART II, Chapters 3 and 4 are

1. Describe the most influential variables in the variability of the red shrimp LPUE.
2. Identify important variables to account for management purposes using generalized additive regression models and structured additive distributional regression models.
3. Demonstrate the usefulness of structured additive distributional regression in modelling and predict shrimp LPUE

4. Provide guidance for model choice and variable selection.

- Aims of PART III, Chapters 5 and 6 are

1. Reconstruct the soft-bottom food web of the continental slope in NW Mediterranean (bathyal domain) defining its principal characteristics through the network analysis and study the current fishing impact.
2. Explore the existence of the trophic cascade mechanism in the modelled food web considering both top-down (fishery) and bottom-up (source availability) processes as possible drivers of ecosystem changes.

Finally, the last PART IV includes a general discussion (Chapter 7) that encompasses the results of each chapter and the Conclusions 8.



---

PART I

---



## CHAPTER 2

---

A temporal analysis on the dynamics of deep-sea macrofauna:  
influence of environmental variability in the Catalan Sea  
(western Mediterranean)

---

## Abstract

A seasonal analysis of deep-sea infauna (macrobenthos) based on quantitative sampling was conducted in two stations on the continental slope: 1) within the Besòs canyon (at ~ 550–600 m) and 2) on the adjacent open slope (at 800 m). Both sites were sampled in February, April, June-July and October 2007, covering all seasons. Environmental variables were also recorded in the sediment and sediment/water interface. Dynamics of macrobenthos at the two stations showed differences in biomass/abundance patterns and trophic structures. Biomass was higher inside the Besòs canyon than on the adjacent slope. The community was mostly dominated by surface-deposit feeding polychaetes (Ampharetidae, Paraonidae, Flabelligeridae) and crustaceans (amphipods such as *Carangoliopsis spinulosa* and *Harpinia* spp.) inside the canyon. On the contrary subsurface deposit feeders (mainly the sipunculan *Onchnesoma steenstrupii*) were dominant on the adjacent slope. Inside the canyon we found a clear temporal succession of species that we related to both food availability and quality and the proliferation of opportunistic species was consistent with higher variability in food sources (*toc*, C/N,  $\delta^{13}\text{C}$ ) in comparison to adjacent slope. This was likely caused by a greater influence of terrigenous inputs from river discharges. Inside the canyon, Capitellidae, Spiroonidae and Flabelligeridae, in general considered as deposit-feeders, were more abundant in June-July (when the water column is stratified) coinciding with a clear signal of terrigenous carbon (depleted  $\delta^{13}\text{C}$ , high C/N) in the sediments. By contrast, during October and under conditions of high water turbidity and *tom* increment, (mainly) carnivorous polychaetes (Glyceridae, Onuphidae) increased. Total macrobenthos biomass found on the Catalan canyon, were higher than in the neighbouring Toulon canyon, probably because the two canyons are influenced by different river inputs, connected with distinct terrigenous sources.

**Keywords:** macrofauna, canyon, seasonal dynamics, food availability



## 2.1 Introduction

The deep sea, is composed of a variety of ecosystems distributed on hard and soft bottoms and is not as homogeneous as once believed. Continental slopes are mainly covered by soft sediments (Pérès, 1985; Thistle, 2003). However, they also constitute a variety of habitats and the canyons crossing them comprise a mosaic of patches and faunal assemblages (Curdia et al., 2004; Macquart-Moulin and Patriti, 1996; Reyss, 1971). Continental slopes and especially canyons represent zones of matter and energy transfer between the continental shelf and the abyssal domain (Gardner, 1989; Griggs et al., 1969) often providing focused sources of high quality food (Epping et al., 2002; Josselyn et al., 1983; Rowe et al., 1982).

The main energy flow probably depends on advective fluxes (Féral et al., 1990) and in submarine canyons terrestrial inputs may be the most important for their ecodynamics. Organic matter is often channelled through canyons, enhancing food supply and creating depocenters where hotspots of benthos production can be observed (Vetter and Dayton, 1999). This channelling can change seasonally, establishing varying seasonal environmental dynamics at the sea floor in and close to canyons, mostly driven by changes in food availability (Vetter, 1998). This may influence assemblage composition, life cycles of benthos and trophic relationships, including the role of benthic taxa, the main prey for deep-sea shrimps (Cartes, 1994) and fishes (Fanelli and Cartes, 2010; Madurell and Cartes, 2005) in this environments.

The distribution and diversity of deep macrobenthos have mainly been related with depth gradients at several spatial scales, and with sediment size (Stora et al., 1999; Tselepides and Eleftheriou, 1992; Tselepides et al., 2000). Small-scale changes in the sediment structure and in the distribution of food on sedimentary bottoms are associated with adaptation of fauna and with its high diversification in the deep sea (Gage and Tyler, 1991; Sanders et al., 1965). In the western Mediterranean many canyons traverse the continental slope close to mainland areas. The Balearic Basin resembles a large submarine canyon, represented by the Valencia Trough, that separates the mainland and insular slopes (the latter belonging to the Balearic Islands. The mainland slope is crossed by a system of tributary canyons (from N to S: Palamós, Blanes, Arenys/Besòs, Berenguera and Foix).

Quantitative data on benthic deep-sea macrofauna are still too scarce to describe the dynamics of margin systems. Studies on infaunal macrobenthic assemblages in

the Mediterranean Deep Sea have been performed mainly by dredging, which permits only qualitative descriptions (Carpine, 1970; Pérès and Picard, 1964; Reyss, 1971; Vamvakas, 1970), and rarely by sediment cores (Gerino et al., 1994; Stora et al., 1999; Tchukhtchin, 1964) that allow quantitative analyses. Quantitative studies, both in the deep Mediterranean and elsewhere, have lacked until now a temporal-seasonal approach, that surprisingly reveals the crucial role of infauna in food webs around submarine canyons (Cartes, 1994; Cartes, Grémare, Maynou, Villora-Moreno and Dinet, 2002; Cartes et al., 2009). Studies of ecosystem functioning on the Catalan slope have focused on megafauna, fishes and decapods crustaceans, collected by different kind of trawls (e.g. Cartes, 1994; Cartes et al., 2009) and on suprabenthic macrofauna collected with sledges (Cartes, 1998). There has also been a study of the distribution of megafaunal invertebrates, both epifauna and infauna (Cartes et al., 2009). The multidisciplinary project BIOMARE, focused on the natural variability of, and human impact on, marginal ecosystems off the Catalan coasts, included studies of the temporal dynamics of all macrofaunal compartments (the infauna for the first time) in deep environments and of the possible environmental factors influencing their distributions and biomass. The difficulty in collecting environmental and biological samples simultaneously is the most evident reason for the lack of information of environment-biota coupling in deep sea (as noted by Stora et al., 1999).

In this chapter a temporal study of deep-sea infauna (macrobenthos) is presented based on a quantitative approach. The study has been conducted simultaneously in two characteristic slope environments. The main aim was to analyse the seasonal dynamics of deep-sea macrobenthos (between 600 and 800 m) in the Mediterranean sea.

The study has been focused on:

- describing the seasonal composition of the infaunal macrobenthos in two characteristic environments of the Catalan Slope, inside the Besòs canyon and on its adjacent slope at 800 m depth;
- identifying the main variables both in the sediment and close to the sediment-water interface (the Benthic Boundary Layer), that explain trends observed in the taxonomic composition and biomass of the infaunal macrobenthos.

## 2.2 Materials and Methods

### 2.2.1 The Study area and sampling design

The sampling was performed along the mid-slope (Figure 2.1) on the mainland part of the Balearic Basin: between  $40^{\circ}48'9''$  N and  $41^{\circ}09'30''$  N -  $2^{\circ}04'00''$  E and  $2^{\circ}35'4''$  E, within the project BIOMARE (ref. CTM2006-13508-CO2-02/MAR).

Samples were collected at four stations situated within two canyons and on their adjacent slopes. At two of these stations (the Buscarró canyon, C1, a tributary of the larger Besòs canyon and on its adjacent slope, S1), four cruises were performed seasonally (B1 cruise February 2007, B2 April 2007, B3 June-July 2007, B4 October 2007). In the Berenguera canyon station (C2), and the adjacent slope station (S2), sampling was carried out only in June-July 2007. The Besòs (C1) and Berenguera (C2) canyons stations were located at depths of 550 – 600 m approx. near the southern walls of the canyons, close to the canyon heads. The adjacent slope stations were located at approximately 800 m depth in two fishing grounds known by local fishermen as Serola (S1) and Abissinia (S2), close to Besòs and Berenguera canyons respectively. Both canyons are also fishing grounds, though there was hardly any fishing activity at C1 in the last 5 years. The seasonal analyses were based only on C1 and S1 samples.

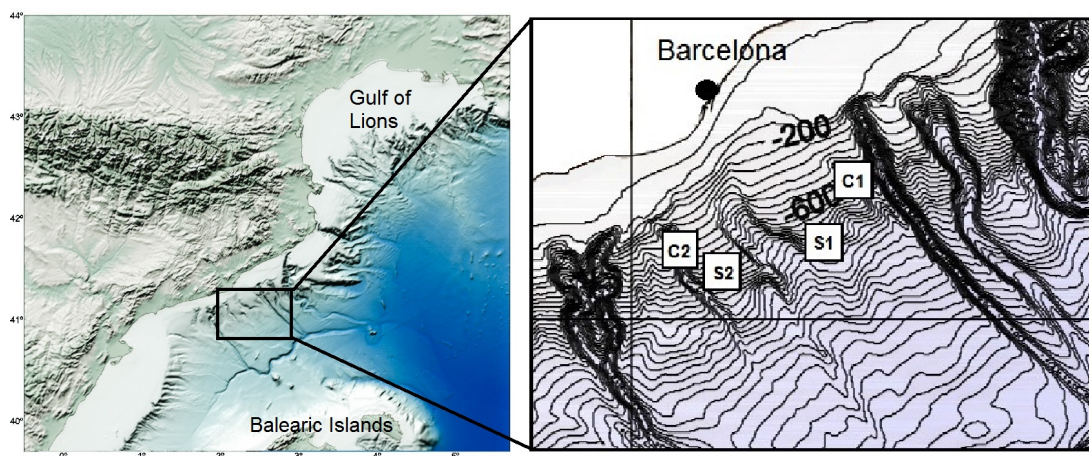


FIGURE 2.1: Map of the study area off the Catalan coast, showing the positions of samples inside canyons Besòs and Berenguera (C1, C2) and on the adjacent slopes (S1, S2) stations.

A total of 34 box-cores were collected. The replicates (cores taken very close to the same positions, i.e. < 200 m between replicates) were distributed as follows: cruise B1 (3 at C1 and 3 at S1), cruise B2 (4 at C1 and 4 at S1), cruise B3 (4 at C1 and 3 at C2; 4 at S1 and 1 at S2) and cruise B4 (4 at C1 and 4 at S1). The box-corer used was a Reineck model, with 21x31 cm box sides, sampling a surface area of 0.065 m<sup>2</sup>. The uppermost 20 cm of sediments were sieved through a 0.5 mm mesh size to retain macrofauna, as in other similar studies performed in the deep Mediterranean (see [Stora et al., 1999](#)). Infauna was sorted, classified to the lowest possible taxonomic level, counted and weighed (wet weight, WW). Some keys used for the identification are available in [Day \(1967\)](#); [Parapar et al. \(2012\)](#); [San Martín Peral \(2004\)](#); [Viéitez Martín et al. \(2004\)](#).

## 2.2.2 Environmental data collection

Biological data were analysed together with a number of environmental variables defining both the characteristics of the sediments and the near-bottom water column. During each cruise, one CTD per station was performed in parallel to the biological sampling using Seabird-25 profilers furnished with pressure, temperature, salinity, fluorescence and turbidity sensors (obtaining 24 data sets s<sup>-1</sup>). The CTD recorded data from the surface to 5 m above the bottom. Sediments were collected with a multi-corer at the same stations where box-cores were taken (three samples per multi-corer) and the first 5 cm were used for environmental analyses.

The CTD measured the following variables:

- Temperature and salinity 5 m above the sea bottom ( $T_{5mab}$ ,  $S_{5mab}$ ).
- Fluorescence ( $f_{0-200m}$ , mean value in the range 0 – 200 m) as the sum of fluorometer readings each 1 m in vertical bins from surface to 200 m depth; values were proportional to Chl a and indicative of surface phytoplankton standing stock.
- Turbidity at 5 m above the sea bottom ( $Turb_{5mab}$ ).

Multi-corer samples were used to measure the following parameters:

- Percentage of total sedimentary organic matter (*tom*), calculated as the difference between dry weight (DW: 60°C for 24 h until constant weight reached) and ash weight (500°C in a furnace for 2 h).
- Percentage of total organic carbon (*toc*), carbon-nitrogen ratios (C/N) and the stable isotope ratio ( $\delta^{13}\text{C}$ ) in sediments (for details of sample treatment and isotope analysis see [Fanelli and Cartes, 2008](#); [Fanelli et al., 2009](#)).  $\delta^{13}\text{C}$  indicates the origin of food sources (terrigenous or pelagic) arriving on the seafloor. Detailed sediment C/N and  $\delta^{13}\text{C}$  are published in [Papiol et al. \(2012\)](#).

REDOX ( $Eh$ ) was measured directly in box-corer sediments using a ThermoOrion 250A sensor. Voltage was read at the sediment surface and at 5 cm depth in the sediment.

Mean monthly flow estimates ( $\text{m}^3 \text{s}^{-1}$ ) for the main rivers discharging off the central Catalan coasts (Llobregat, see [Figure 2.1](#)) were obtained from the website <http://aca-web.gencat.cat/aca/appmanager/aca/aca/>. Phytoplankton pigment concentration (ppc,  $\text{mg Chla m}^{-3}$ ) were obtained from <http://reason.gsfc.nasa.gov/Giovanni>. Values of ppc were used as indicators of the surface primary production in the area. A monthly average reading of ppc of the positions of stations was used.

### 2.2.2.1 Diversity and biomass trends by season

All infaunal taxa were classified to the lowest possible taxonomic level. Within BIOMARE, we attempted to analyse the stable isotopic composition of macrofauna. We therefore undertook an initial sorting of fauna on board the ship, and then froze specimens, remaining bulk samples and sediment at  $-20^\circ\text{C}$  for later analysis. In the laboratory, the macrofaunal sorting was completed and the animals classified into groups in order to obtain the required minimum masses for isotope analysis. This treatment partially damaged polychaetes. As a result, some specimens could only be determined to genus or family level. Taxa were counted and weighted individually in order to obtain the wet weight (WW, grams, after eliminating water by blotting). Taxa abundance and biomass were standardized to individuals and weight per  $\text{m}^2$ , both per station (600 m and 800 m) and cruise. For comparisons with data from other benthic studies, we transformed WW to dry

weight (DW) using the factor 0.2 (source: EMPRELAT data base, Alfred Wegener Institute).

### 2.2.3 Statistical analysis

An analysis of all the box-core data was first conducted using non-metric multidimensional scaling (Clarke and Warwick, 1994, nMDS), distance-based permutational multivariate analysis of variance (PERMANOVA Anderson, 2001) and similarity percentage analysis (SIMPER, Clarke, 1993). A seasonal analysis was then carried out based on data from stations C1 and S1, where 3 – 4 replicate samples were available from all cruises. For this purpose we used as statistical analyses the principal component analysis (PCA) and canonical correspondence analysis (CCA, Ter Braak, 1986).

All multivariate analyses were performed on individual box-core replicates. The non-parametric Multidimensional Scaling procedure was performed using Spearman's Rank Correlation as a distance measure. The matrix of all taxa identified was used (removing taxa appearing less than twice). Principal factors in the hauls ordination were: *habitat* (2 levels: canyon, *can*, vs adjacent slope, *slo*), and *water\_condition* (= water column temperature conditions, with 2 levels: homogeneous, *hom*, during February and April, and stratified, *str*, during June-July and October).

The PERMANOVA was used in a 2 factors complete model design, testing the null hypothesis  $H_0$  of no significant main effects and interaction. The factors included in the model, considered as fixed and crossed, were habitat and water condition. The same matrix and distance measure were used as in the nMDSs and we applied a permutation of residuals under a reduced model (maximum number of permutations = 9999) (Anderson and Ter Braak, 2003; Anderson and Legendre, 1999). For each Pseudo- $F$  test, Monte Carlo and post-hoc tests were also obtained.

One-way SIMPER analysis was performed on the taxon matrix using Bray-Curtis distances in order to identify contributions of taxa to assemblages at the two habitats: inside the canyon and on the adjacent slope.

The PCA was performed on a correlation matrix of the environmental data, and a bi-plot was used to describe the resulting ordination patterns of samples. CCA was applied to study the association of environmental variables with taxon/species

abundances. Three CCAs were constructed. The first used the broad matrix of taxa, the other two used separate species data matrices for the canyon and the adjacent slope sites. A permutation test with 500 random permutations was used to test the null hypothesis of no linear relationship between abundances and environmental variables, with  $p$ -level = 0.05.

Generalized additive models (Equation 1.25) using penalized cubic regression splines (Wood, 2006) were implemented to point out relationships between taxon biomasses,  $B_j$  where  $j = 1, \dots, J$  referring to biomass  $j$  with observations  $b_{1,j}, \dots, b_{I,j}$ , and environmental/trophic variables,  $x_1, \dots, x_P$ . Independent models were initially constructed to identify variables with best explanatory values. Also interactions between variables were tested. The final models presented in the results, were selected according to both the Akaike information criterion (AIC: Akaike, 1973) and the percentage of explained deviance (ED).

Recalling to Equation 1.26 in the introduction, the final models here presented have the form

$$\eta_{i,j} = \beta_0 + t(x_{il}, x_{im}) \quad (2.1)$$

where  $\eta_{i,j}$  is the regression predictor linked to the expectation,  $E[b_{i,j}|x_{il}, x_{im}]$ , of taxon biomass  $b_{i,j}$  conditional on  $x_{il}$  and  $x_{im}$ , where  $l, m \in i$  and  $l \neq m$  and  $\beta_0$  is the intercept. The predictor  $\eta_{i,j}$  is linked to  $E[b_{i,j}|x_{il}, x_{im}]$  through the logarithmic function to ensure positivity of the response, hypothesized belonging to a gamma distribution. The function  $t$  is an unknown surface function estimated by tensor product (Wood, 2006). The tensor estimates both the marginal (main) and the interaction effects of covariates  $x_{il}$  and  $x_{im}$ , thus, there was no need to specify functions  $s_l$  and  $s_m$  in equation 2.1.

More specifically the biomasses  $b_j$  analysed were of: (1) total fauna, (2) polychaetes, (3) crustaceans and (4) molluscs separately. It was assumed that the underlying probability distribution of the response belongs to the gamma and the appropriate link function is the natural logarithm. Generalized Cross Validation criterion (GCV: Craven and Wahba, 1979; Golub et al., 1979) was used to select automatically smoothing parameters. Also taxon abundances were examined. Since models for abundances yielded fairly similar patterns in regression analysis, only biomass results are reported.

Also the cumulative number of species (S) and the Shannon's index (H') were calculated considering all replicate by season.

All statistical analyses were performed using PRIMER6 and PERMANOVA+ (Clarke and Gorley, 2006), XLSTAT (Addinsoft TM) for CCAs and R2.9.0 ([www.r-project.org](http://www.r-project.org)) for general analyses, GAMs (mgcv-package) and PCA analyses.

## 2.3 Results

### 2.3.1 Taxonomic composition

A total of 106 taxa (ranging from species to families) was identified, belonging to 19 higher groups from Order to Class (Tables B.1, B.2, B.3). Although not identified to the lowest taxonomic level, polychaetes included the largest number of taxa (34). Among the groups identified to species, gammaridean amphipods were the most specious (at least 15 species), followed by cumaceans and bivalves (both with 9 species).

### 2.3.2 Diversity and biomass trends by habitat and season

The cumulative number of species showed some stabilization after the analysis of 3-4 cores at 800 m. However, at the shallowest station in Besòs canyon (Station C1, 600 m) we did not find any asymptotic stabilization of the cumulative number of species after analysis of 6 cores.

The number of species (S) increased from February to October both inside the canyon and at the adjacent slope (from 39 to 44 inside the canyon; from 32 to 48 at the adjacent slope: Figure 2). S was higher inside the canyon, except in October 2007. Diversity measured as Shannon's index, H', increased from February to April both inside the canyon and on the adjacent slope, decreasing in June-July (mainly inside the canyon) and increasing later (Figure 2.2). Maximum H' was found in April inside the canyon,  $H' = 3.53$ , and in October on the adjacent slope,  $H' = 3.56$ .

Total biomass of infauna increased within Besòs canyon (C1) from February-April to June/July 2007 (Figure 2.3), while at the adjacent slope (S1) peaks of biomass



were also found in February and again in June/July. Among individual taxa, polychaetes showed maximum biomass in June/July and October inside the canyon and in June/July at the adjacent slope. Crustaceans (mainly peracarids) showed maximum biomass in April inside the canyon and in February on the adjacent slope (1-Way ANOVA at the adjacent slope:  $F_{1,13} = 16.000$ ,  $p = 0.002$ ; significant paired Tukey's comparisons: February > April,  $p = 0.004$ ; June/July > October,  $p = 0.005$ ). The remaining, rather secondary, taxa showed some irregular variations, perhaps influenced by the limited number of replicates. However, peaks of biomass were found regularly in February (for echinoderms inside the canyon and for bivalves at the adjacent slope) and in June/July (molluscs inside the canyon and sipunculans at the adjacent slope). Variance of data was high, and most temporal trends were not significant, except that of echinoderms in February (1-Way ANOVA at adjacent slope:  $F_{1,13} = 9.152$ ,  $p = 0.011$ , paired Tukey's significant comparisons: February > April,  $p = 0.001$ ; June-July > October,  $p = 0.003$ ). Total biomass and biomasses of crustaceans and echinoderms were higher inside the canyon than at the adjacent slope (t test: total biomass,  $p = 0.074$ ; crustaceans,  $p = 0.006$ ; echinoderms,  $p = 0.002$ ).

All taxa (total infauna, polychaetes, peracarids - see Figure 2.3,b - sipunculans and echinoderms) showed the highest N (ind/m<sup>2</sup>) in February 2007 inside the canyon. Bivalves represented an exception with peaks in April and June/July. Echinoderms also showed maximum N in June/July. These differences, however, were not significant. Only on the adjacent slope did we find significant seasonal changes in infauna abundance. This was true for total infauna N ( $F_{1,13} = 14.22$ ,  $p = 0.001$ , higher in February than in October: Tukey's test,  $p = 0.021$ , Figure

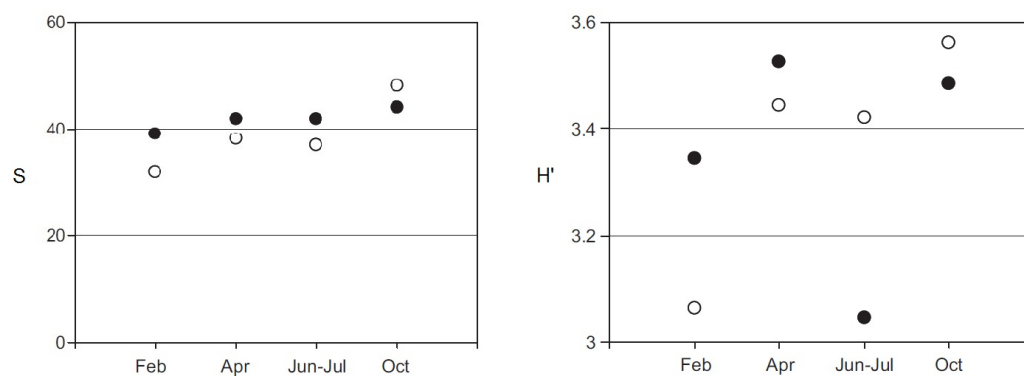


FIGURE 2.2: Diversity parameters: S represents the total number of species, H' is the Shannon index in S1 (white dots) and C1 (black dots).

2.3,b), for crustaceans ( $F_{1,13} = 20.08$ ,  $p = 6 \times 10^{-4}$ , higher N in February than in October: Tukey's test,  $p = 0.009$ , Figure 3b) and for echinoderms ( $F_{1,13} = 17.16$ ;  $p = 0.001$ , higher N in February than in the other seasons: Tukey's tests,  $p = 0.001$ ).

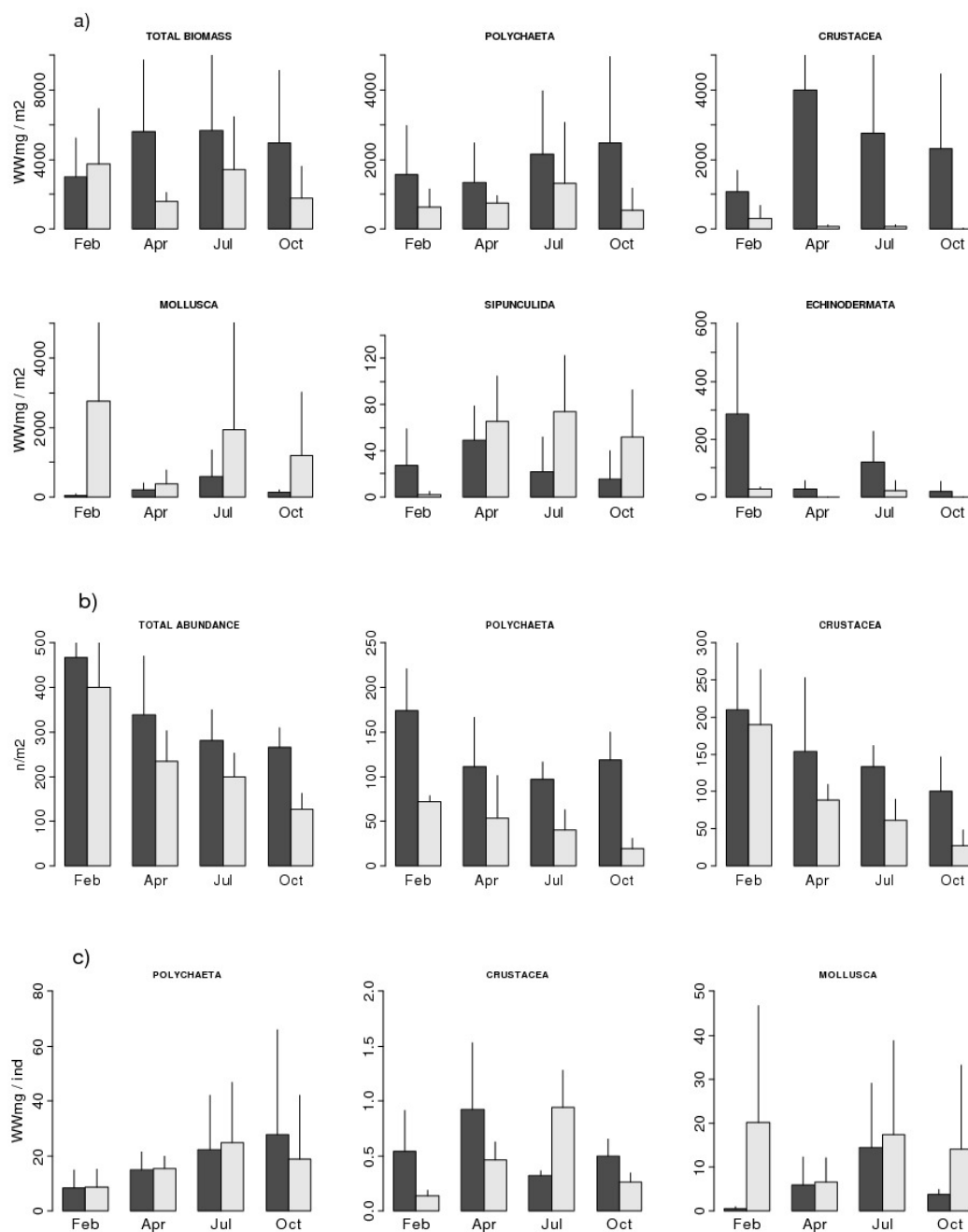


FIGURE 2.3: (a) Annual mean biomass (WWmg/m<sup>2</sup>) profiles of total infauna and major taxa, (b) Annual mean density (ind/m<sup>2</sup>) of total infauna, polychaetes and crustaceans, (c) individual mean weight (WWmg/ind) of polychaetes, crustaceans and molluscs. Dark gray bars indicate C1 samples and light gray bars indicate S1 samples.

Total N and was significantly higher inside the canyon ( $338.2 \pm 107.1$ ) than at the adjacent slope ( $240.2 \pm 71.4$ ; t tests;  $p = 0.004$ ). Major taxa inside the canyon and on the adjacent slope are shown in Table 2.1 (SIMPER analysis).

Mean weight (Figure 2.3,c) showed the lowest values in February 2007 for polychaetes both inside the canyon and on the adjacent slope sites (1-Way ANOVA at the adjacent slope:  $F_{1,13} = 5.16$ ,  $p = 0.016$ ; inside the canyon:  $F_{1,13} = 2.11$ ,  $p = 0.075$ ). Crustacean mean weight was low in October inside the canyon and on the adjacent slope (1-Way ANOVA at adjacent slope:  $F_{1,13} = 4.24$ ,  $p = 0.057$ ). Inside the canyon, the mean weight for all dominant taxa (polychaetes, crustaceans and molluscs) increased in April, a tendency that was still evident in June/July

<b>A) Canyon</b>		Av. sim.: 28.29		
<b>Code</b>	<b>Acr.</b>	<b>Taxon</b>	<b>Con. (%)</b>	<b>Cum. (%)</b>
AM	Cspi	<i>Carangoliopsis spinulosa</i>	20.14	20.14
PO	Amph	Ampharetidae	15.99	36.12
AM	Harp	<i>Harpinia</i> spp.	14.97	51.09
PO	Para	Paraonidae	5.06	56.15
AM	Pocu	<i>Paraphoxus oculatus</i>	3.65	59.8
PO	Flab	Flabelligeridae	3.31	63.12
IS	Pfre	<i>Pilosanthura fresii</i>	2.99	66.11
PO	Glyc	Glyceridae	2.98	69.09
SI	Oste	<i>Onchnesoma steenstrupii</i>	2.87	71.96
EC	Achi	<i>Amphiura chiajei</i>	2.76	74.71
PO	Spio	Spionidae	2.18	76.9
PO	Onup	Onuphidae	1.88	78.77
PO	Capi	Capitellidae	1.74	80.52
<b>B) Adj. slope</b>		Av. sim.: 22.09		
<b>Code</b>	<b>Acr.</b>	<b>Taxon</b>	<b>Con. (%)</b>	<b>Cum. (%)</b>
SI	Oste	<i>Onchnesoma steenstrupii</i>	33.93	33.93
BI	Eaeg	<i>Ennucula aegeensis</i>	13.15	47.07
AM	Cspi	<i>Carangoliopsis spinulosa</i>	7.52	54.6
CA	Proc	<i>Prochaetoderma</i> spp.	6.53	61.13
BI	Alon	<i>Abra longicallus</i>	5.55	66.68
PO	Para	Paraonidae	5.26	71.94
CA	Falc	<i>Falcidens</i> spp.	4.63	76.57
CU	Llon	<i>Leucon longirostris</i>	2.52	79.1
IS	Pfre	<i>Pilosanthura fresii</i>	2.38	81.47

TABLE 2.1: One way SIMPER analysis (factor used: habitat) based on Bray-Curtis similarity (cut-off: 80%). Percentage contribution and cumulative percentage of taxa are reported for each level of the factor, as well as the acronyms of taxa used as labels in CCAs. AM: amphipoda, PO: polychaeta, IS: isopoda, SI: sipuncala, EC: echinodermata, BI: bivalvia, CA: caudofoveata, CU: cumacea.

for polychaetes and molluscs. This same tendency was observed at the adjacent slope, excluding molluscs which had higher mean weight in February.

### 2.3.3 Assemblage structure: composition by habitat (canyon and adjacent slope)

The nMDS plot shows the hauls grouped according to both habitat (canyon or adjacent slope) and water column condition (stratified or homogenised) (Figure 2.4).

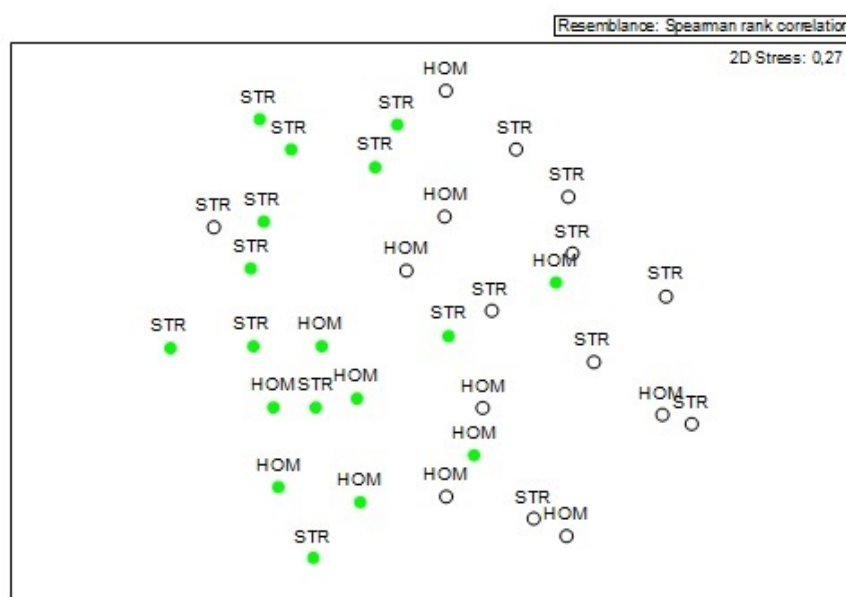


FIGURE 2.4: nMDS ordination of samples from a full year (B1, B2, B3 and B4). Labels indicated: *hom* = water column homogenization and *str* = water column stratification for the factor WATER CONDITIONS. Symbols indicate: full cycles = canyon; empty cycles = adjacent slope for the factor HABITAT.

Samples from the canyon are grouped in the left part of the graphic, while samples from the adjacent slope are grouped in the right part. In contrast samples collected during stratified water column condition occupy mainly the top, while samples collected during homogenized conditions occupy the bottom of the graphic.

The two-way PERMANOVA (Table 2.2) showed statistically significant main effects, i.e. effect of both habitat ( $p = 3 \times 10^{-4}$ ) and water column condition ( $p = 0.031$ ). The test did not showed a significant effect of the interaction between

the two factors. Pairwise tests indicated higher abundance inside the canyon than at the adjacent slope, especially under stratified water column conditions.

Finally, SIMPER analyses of abundances (Table 2.1) showed that the amphipod *Carangoliopsis spinulosa*, ampharetid polychaetes and amphipods of the genus *Harpinia* spp. were the most abundant taxa at the canyon site, representing less than 50% of total abundance. At the adjacent slope site the sipunculan *Onchnesoma steenstrupii* dominated in the assemblage, followed by the bivalve *Ennucula aegeensis* and *C. spinulosa*. These three species together represented the 54.6% of the total abundance.

<b>A) Main test</b>				
Source	df	MS	Pseudo- <i>F</i>	<i>P</i> -value
<i>habitat</i>	1	1.578	4654	$3 \times 10^{-4}$
<i>water_ccondition</i>	1	0.766	2258	0.031
<i>habitat</i> × <i>water_ccondition</i>	1	0.335	0.988	0.448
Res	30	0.339		
Total	33			

<b>B) Pairwise tests</b>
<i>can</i> > <i>slo</i>
<i>hom</i> > <i>str</i>
<i>can</i> > <i>slo</i> (within <i>str</i> )

TABLE 2.2: A) Permanova based on Sperman rank correlation distance matrix of whole dataset and B) pairwise tests (Only significant tests are reported; Monte Carlo significance within brackets if differs from permanova's). (ns: not significant; \*: < 0.05, \*\*: < 0.01, \*\*\*: < 0.001). Factors: habitat (levels: *can*, *slo*) and water column condition (levels: homogenized, *hom*, and stratified, *str*)

### 2.3.4 Environmental variables

Temperature ( $T_{5mab}$ ) varied within a narrow range through the year both inside the canyon and especially at the adjacent slope (Figure 2.5). Anyhow  $T_{5mab}$  was always lower at the adjacent slope rather than at the canyon station. Inside the canyon site,  $T_{5mab}$  increased between June/July and October. At the adjacent slope site  $T_{5mab}$  was quite constant all year round except for a slight rise in April. There was a period of water column homogeneity in February and April and of stratification in June-October. Salinity 5 m above the bottom ( $S_{5mab}$ ) ranged between 38.43 and 38.56 (Figure 2.5). The salinity,  $S_{5mab}$ , showed higher values at the canyon station, where it increased from April to October. This pattern

was not observed at the adjacent slope where  $S_{5mab}$  showed the same pattern found for  $T_{5mab}$ . Fluorescence ( $f_{0-200m}$ ) followed the same temporal pattern at both the canyon and the slope stations. As regularly happens in the study area with surface *Chl a* (satellite imagery, see below), maximum  $f_{0-200m}$  was found in January-February (winter) and minimum  $f_{0-200m}$  was observed in July-August (summer) (Figure 2.5). Water turbidity at 5 m above the seafloor ( $Turb_{5mab}$ )

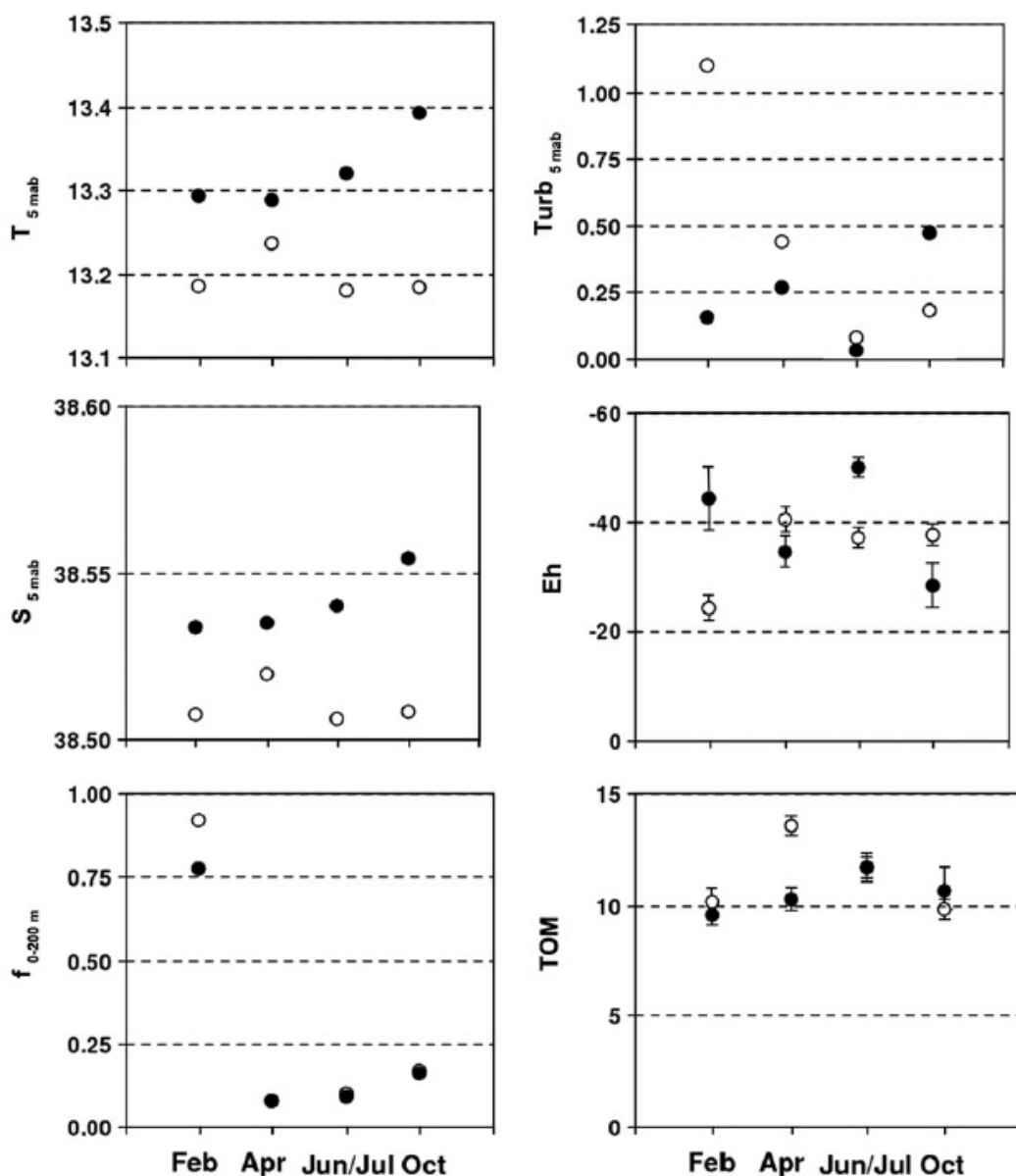


FIGURE 2.5: Environmental variables as a function of season. Temperature above the bottom ( $T_{5mab}$ ); salinity ( $S_{5mab}$ ); fluorescence ( $f_{0-500m}$ ); water turbidity close to the bottom ( $turb_{5mab}$ ); potential redox of sediments (at a depth of 1 cm:  $Eh$ );  $tom$  in sediments. (dark dots): canyon; (white dots): adjacent slope.

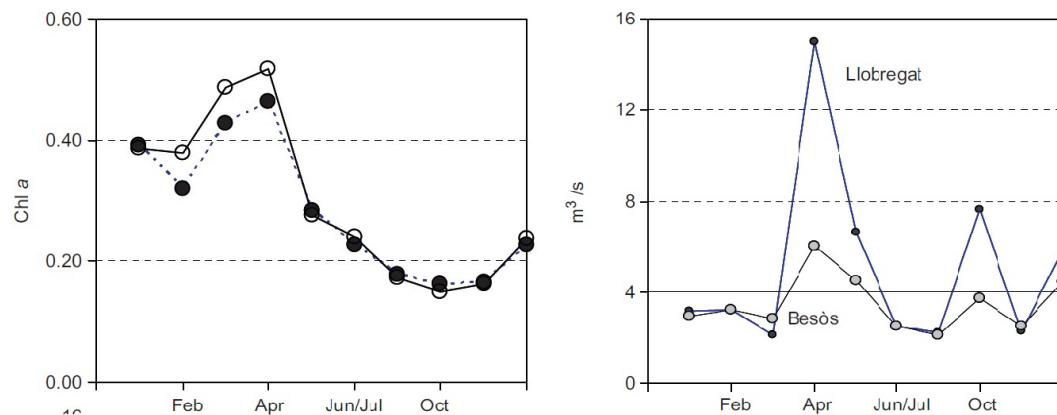


FIGURE 2.6: Environmental variables. a) *Chl a* in surface by satellite imagery (dark dots: canyon; white dots: adjacent slope); b) river flow ( $\text{m}^3 \text{s}^{-1}$ ) of the two most important rivers in central Catalan coasts.

reached maximum values in February at the adjacent slope and in April inside the canyon (Figure 2.5). At both stations  $Turb_{5mab}$  decreased in June/July, when minimum values were observed, increasing again in October. REDOX Potential ( $Eh$ : Figure 2.5) showed different trends at the canyon and the slope stations. Inside the canyon sediments were least reduced in February ( $-24.4 \text{ mV}$ ) with an abrupt drop in  $Eh$  in April-June/July-October (between  $-40.4$  and  $-37.7 \text{ mV}$ ). At the adjacent slope  $Eh$  was on average a little more reduced than at the canyon station, with lower  $Eh$  in June/July than October. Inside the canyon the total organic matter ( $tom$ ) in sediments increased from February to June/July then decreased (Figure 2.5). At the adjacent slope  $tom$  increased from February to April and decreased in June/July and October. The total organic matter,  $tom$ , was, on average, higher in samples taken at slope than inside the canyon, the difference being significant in April. Flow volume of the most important rivers in the area was maximal in April-May ( $15.5\text{-}4.5 \text{ m}^3 \text{ s}^{-1}$ ) and minimal in June-July ( $2.5 \text{ m}^3 \text{ s}^{-1}$ ), followed by some increase in August-October (Figure 2.6). *Chl a* at the surface, obtained by satellite imagery, decreased sharply from a maximum value in April to an annual minimum in July-August (Figure 2.6).

### 2.3.5 Influence of environmental variables

The first two principal components in the PCA of C1 stations (Figure 2.7, a) explained 46% and 32% of the total variance, respectively. A strong seasonality was evident in the ordination of samples, with habitat variables often associated

with specific sample stations. Thus, fluorescence was associated with February (B1), *rivDisch*, *toc* and  $\delta^{13}\text{C}$  with April (B2), C/N with July (B3) while  $T_{5mab}$ ,  $S_{5mab}$ ,  $Turb_{5mab}$  and less reduced sediments (*Eh*) were associated with October (B4).

The first two principal components in the PCA for S1 (adjacent slope: Figure 2.5, b) explained 44% and 36% of the total variance, respectively. Those samples also showed a seasonal relationship in the ordination, but it was less evident than that inside canyon. Moreover, the strength of the association with habitat variables varied across the canyon samples: February (B1) was coupled with fluorescence, but also with less reduced sediment (*Eh*) and Turbidity; April (B2) was associated with river discharge, but also with  $T_{5mab}$ ,  $S_{5mab}$ , and *tom*; July-October (B3 and B4) were related to gradients of *toc* (positively) and to  $\delta^{13}\text{C}$  in the sediment (negatively).

Canonical correspondence analyses (CCAs; Figure 2.8) produced an ordination of the most abundant taxa and their relationship with environmental variables, as a function of both habitat and season. CCA of the joint data set from C1 and S1 (Figure 2.8) explained 89.8% of the total variance. The permutational test revealed a significant linear relationship between taxa abundances and environmental variables (pseudo- $F = 0.580$ ;  $p = 0.009$ ). Clear segregation between canyon station and adjacent slope samples was observed, with an evident association between canyon samples and the abundance of polychaetes and also of crustaceans. This

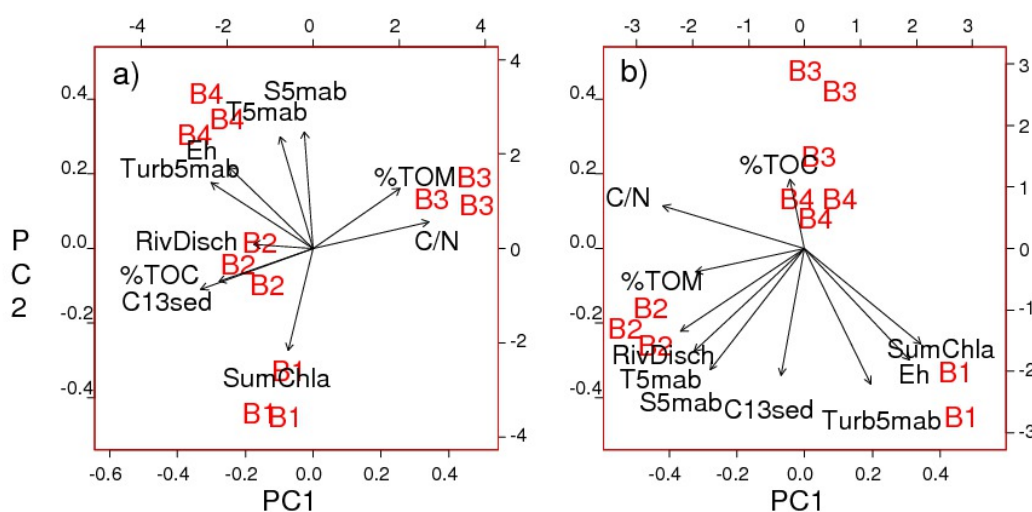


FIGURE 2.7: PCAs of environmental variables collected in (a) canyon stations and (b) adjacent slope.



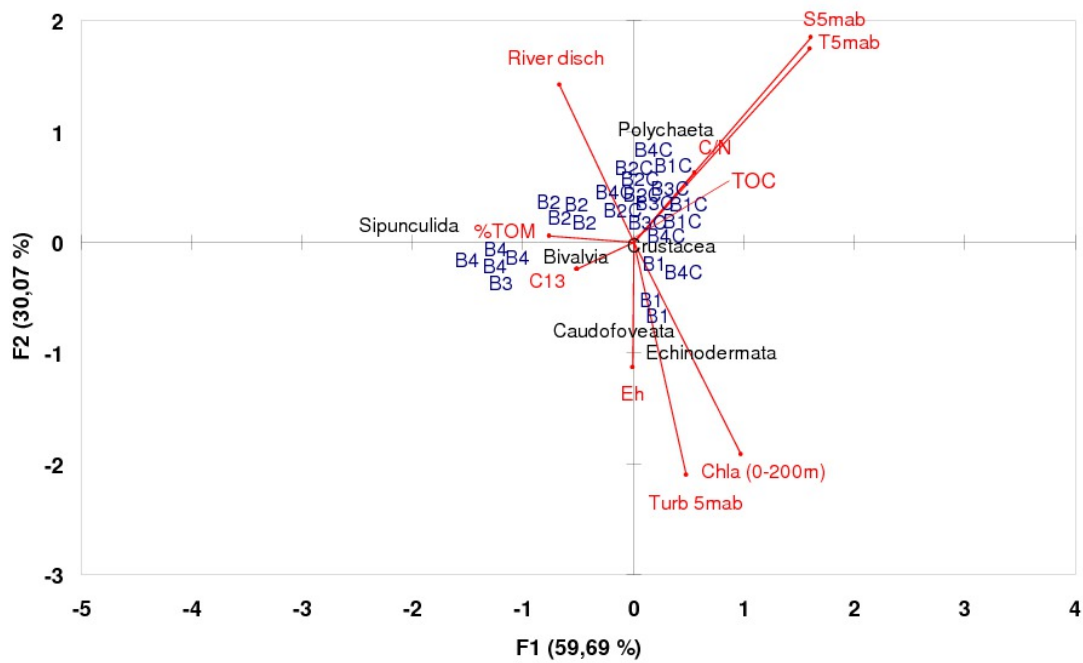


FIGURE 2.8: CCA of broad taxa, considering both canyon and adjacent slope samples, with selected environmental variables.

segregation was mainly linked to higher salinity ( $S_{5mab}$ ) and temperature ( $T_{5mab}$ ) inside the canyon. Canyon samples were also linked to higher *toc*, indicating a response to the amount of available food, and with C/N, i.e. organic matter quality. To a lesser extent canyon station samples were associated with higher river discharge, more reduced sediments and more depleted  $\delta^{13}\text{C}$ . Canyon samples were grouped in one subset. Seasonality is masked by stronger difference between habitats (Canyon versus adjacent slope), although to some extent that was related to the seasonal condition (e.g. homogeneity in B2, B1) of the water column. Adjacent slope samples showed some seasonal segregation, with different dominant taxa in each season. Caudofoveata and Echinoderms were related to *Chla* and  $Turb_{5mab}$  in February (B1) and to greater reduction of the sediments. Sipuncula and to a lesser extent Bivalvia were related to *tom* and to enriched  $\delta^{13}\text{C}$  values in July-October (B3-B4).

The two CCAs performed on dominant species (except polychaetes distinguished only to Family level) showed some ordination of species both at canyon station and on the adjacent slope (Figures 2.9 a and 2.5 b, respectively). The CCA for station C1 explained 75.1% of the total variance (Permutational test: pseudo- $F = 0.301$ ,  $p = 0.058$ ). Sample ordination showed some seasonal pattern. B1 and B2 from February-April (obtained under homogenized water mass conditions) were located

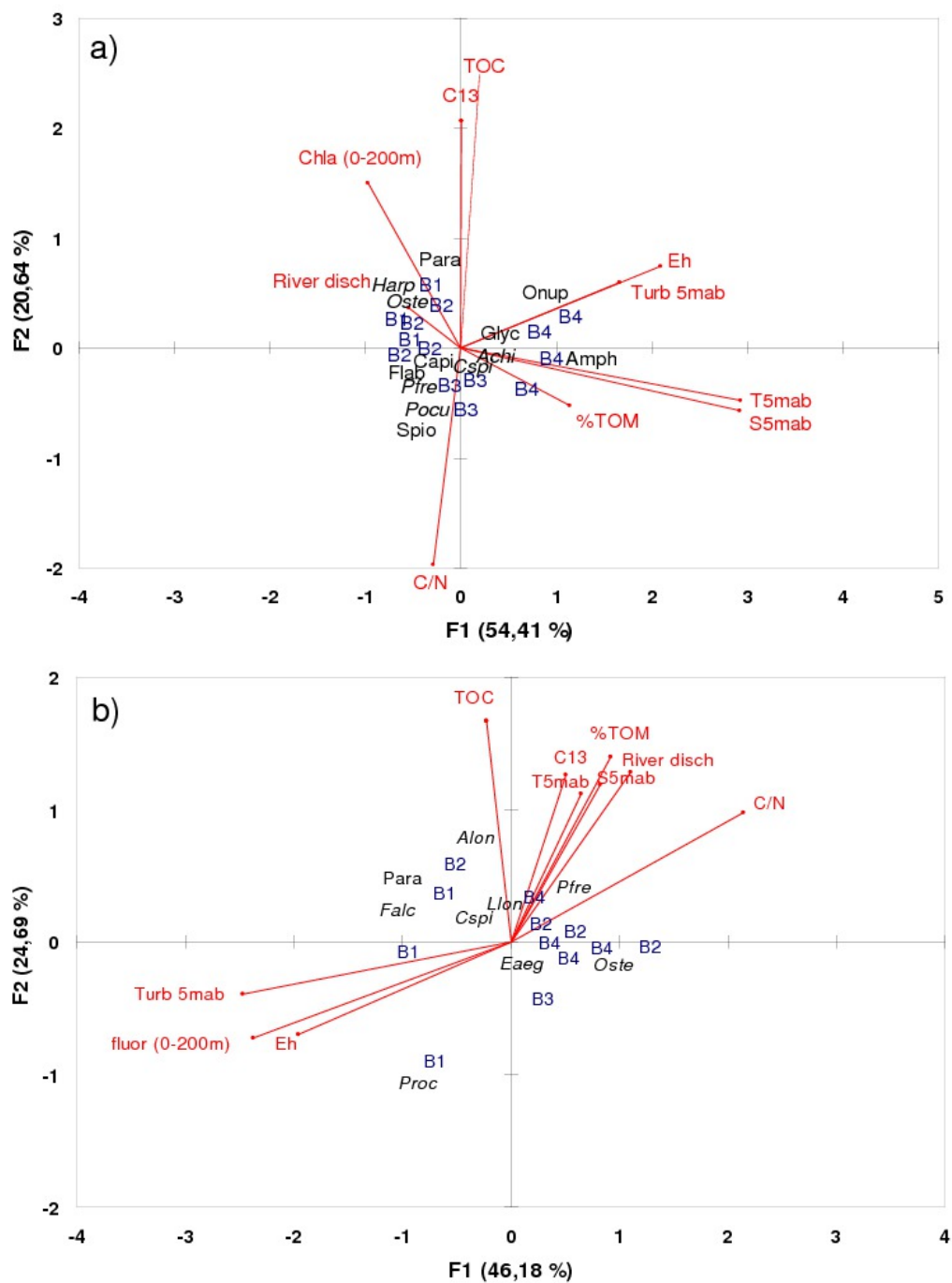


FIGURE 2.9: CCA of dominant species (a) inside the canyon and (b) on the adjacent slope and the environmental variables. For the full name of species' acronyms see Table 2.1.

together in the left-upper part of the biplot, while samples collected under stratified conditions (B3, B4 from July and October) were in the opposite corner. B1 and B2 were mainly associated with Paraonidae, *Harpinia* spp. and *O. steenstrupii*, which were positively related to *Chla*, *toc*, enriched  $\delta^{13}\text{C}$  and high river discharge. B4 (July) cores were associated with Onuphidae and Glyceridae, both opportunistic carnivorous polychaetes, and with reduced Eh in sediments. Ampharetidae and the ophiuroid *Amphiura chiajei* were related more to high  $T_{5mab}$  and  $S_{5mab}$ . A number of surface and sub-surface deposit-feeding polychaetes (Capitellidae, Spionidae, Flabelligeridae) were more abundant in B3 (July) cores and associated with high C/N. C/N is indicative of fresh OM, probably lipids, in sediments.

On the adjacent slope (S1) CCA explained 70.9% of the total variance and the permutational test was significant (pseudo- $F = 0.507$ ,  $p = 0.021$ ). Samples showed some seasonal grouping (less clear than in the Besòs canyon CCA): B1 was associated with Caudofoveata (*Falcidens* spp., *Prochaetoderma* spp.), Paraonidae and with the amphipod *C. spinulosa*. These were positively correlated in turn with  $Turb_{5mab}$ , fluorescence and reduced Eh in sediments. Caudofoveates are surface deposit feeders preying on foraminiferans (meiofauna) and Paraonidae, and they can also feed selectively on small diatoms. The bivalve *Abra longicallus* and the isopod *Paranthura fresii* seemed mainly associated with B2 in April and with a high number of variables; among the most important were *toc*, *tom*, enriched  $\delta^{13}\text{C}$  in sediments and river discharge. *O. steenstrupii* and the bivalve *E. aegensis* were more abundant in July (B3) and October (B4) under conditions of low  $Turb_{5mab}$ , and high C/N in sediments.

### 2.3.6 Regression models

Models with higher explanatory deviance are reported in Table 2.3. Total biomass, and the biomass of principal taxa, are functions of interactions among several environmental variables, including  $T_{5mab}$  (or  $S_{5mab}$ , strongly correlated with  $T_{5mab}$ ) and trophic variables, especially *toc* in the sediment, and to a lesser extent with river discharge, *Chla*, C/N,  $\delta^{13}\text{C}$  and turbidity. Total biomass, as well as polychaete and crustacean biomasses, showed higher values when high *toc* and low  $T_{5mab}$  were combined (figures not reported), while total biomass was positively related to C/N (fresh organic matter) and to  $T_{5mab}$ . Crustaceans and molluscs showed

Response	Model's right side	<i>p</i> -value	GCV	AIC	R <sup>2</sup> (adj)	DE (%)
Total	= $t(T_{5mab}, toc)$	0.006	1071	281	0.236	75.3
	= $t(T_{5mab}, C/N)$	0.013	1251	335	0.196	29.0
Polychaetes	= $t(S_{5mab}, toc)$	0.014	1194	235	0.430	72.8
Crustaceans	= $t(T_{5mab}, toc)$	0.006	5680	183	0.434	76.5
	= $t(T_{5mab}, RivDisch)$	0.013	4956	230	0.228	46.8
Molluscs	= $t(T_{5mab}, RivDisch)$	0.031	4989	190	0.089	39.1
	= $t(T_{5mab}, f_{0-200m})$	0.039	5502	192	0.046	38.8

TABLE 2.3: GAMs for A) the total biomass of the macrofauna, B) Polychaetes' biomass C) Crustaceans' biomass and D) Molluscs' biomass. For each response, the right side of the model, the significance of the effect, the GCV, the AIC, the adjusted r-squared (R2) and the deviance explained (DE) are given.

a strong positive relationship with river discharges, as did molluscs with *Chla* at medium values of  $T_{5mab}$ .

## 2.4 Discussion

Benthos is the dominant trophic resource for fish and large crustaceans inside the Catalan canyons (e.g. Carrassón and Cartes, 2002; Cartes, 1994; Cartes and Maynou, 1998; Macpherson, 1981; Maynou and Cartes, 1998), quantitative studies on macrofauna are required to establish, for instance, mass-balance models.

This is the first seasonal quantitative study performed on deep-sea macrobenthos in the NW Mediterranean Sea. Previous studies analysed patterns of biomass and assemblage distribution as e.g. a function of depth (e.g. Stora et al., 1999; Tselepides and Eleftheriou, 1992). In addition, most previous studies have been performed on large epifauna-infauna (i.e. the megafauna) (Cartes et al., 2009; Pérès, 1985; Pérès and Picard, 1964) and non-quantitative (e.g. Reyss, 1971).

The analysis of deep-sea macrofauna distribution with environmental variables returned significant effects of depth (Pérès, 1985) and of a group of factors related

with sediment characteristics (Reyss, 1971), such as the grain size (Stora et al., 1999) and the organic matter content (Tselepidis and Eleftheriou, 1992; Tselepidis et al., 2000). These explanatory variables for macrobenthos variability have been evaluated in these previous works along a wide depth range on the continental slope (200 – 1000/2000 m).

As supported by a variety of statistical analyses, changes in macrofauna assemblages and trends in biomass are related with variables associated to sediment characteristics, particularly nutritional value (*toc*, C/N,  $\delta^{13}\text{C}$ ), but also with characteristics of near-bottom water masses (T, S), typifying the overall status of the benthic boundary layer, BBL (Gage and Tyler, 1991).

The macrofauna is related mainly to the total organic carbon in sediments (*toc*), i.e. the quantity of food available to the macrofauna. This relation has also been found deeper in both the Atlantic Ocean (Sibuet et al., 1989) and the Angola Basin (Kröncke and Türkay, 2003).

Fresh organic matter inside the Besòs canyon in June-July has a terrigenous origin, as shown by the increase of C/N and depletion of  $\delta^{13}\text{C}$ . Apart from the highly depleted  $\delta^{13}\text{C}$ , the C/N ratio was very high in June-July, as expected from terrestrial POM (Thornton and McManus, 1994) and the main food input is from advective fluxes. On the adjacent slope (800 m), C/N has lower values, and the food input is more independent from advective flux. Regarding to water-mass dynamics, higher infaunal abundance was found inside Besòs when T and S were higher. This coincided with the arrival of the Levantine intermediate water (LIW) in the Balearic Basin, once the flow of winter intermediate water is interrupted in the area (López-Jurado et al., 2008). Changes in deep-water masses can influence the re-suspension of particles and inputs of POM from other areas, in our case from the most productive region of the Ligurian Sea, situated to the east of the Balearic Basin. Thus, this current produces more favourable conditions, especially a large supply of nutrients, that favours the proliferation of macrofauna.

We assumed in our study design that our sample replication would be enough to characterize infaunal communities, although species accumulation curves did not reach an asymptotic shape after analysing 3 or 4 replicates per station at the Besòs canyon site, although considering both stations was sufficient. Stora et al. (1999) tested sample replicability in muddy bottoms of the neighbouring Toulon canyon using the same 0.06 m<sup>2</sup>-box corer used here. Except for the shallowest stations

(at 250 m), they concluded that “3 replicates would have been enough to assess assemblage variation at depths between 500–2000 m”. The station C1 was inside the canyon, close to its head, where the temporal pattern of food supply was similar to that on the continental shelf at 60 m (e.g.  $\delta^{13}\text{C}$ : Authors’ unpubl. data). This higher variability probably requires more replicates to fully capture the diversity of fauna in the canyon. However, our replicates, by contrast, showed higher within cruise affinity than between cruise affinity, as demonstrated in PCAs-CCAs where replicates belonging to the same cruise were grouped together and linked to the same environmental conditions.

### 2.4.1 Comparison with other quantitative studies

There are only a few quantitative studies on benthos in the deep Mediterranean (Stora et al., 1999; Tselepides and Eleftheriou, 1992). Off the deep Catalan slope mean annual biomass ranges between 3.1 g WW/m<sup>2</sup> at 800 m and 4.8 g WW/m<sup>2</sup> inside canyon (ca. 0.62–0.96 g DW/m<sup>2</sup> respectively). Biomass was ca. two-times higher than levels recorded in or close to Toulon canyon at comparable depths (500 m: 0.32–0.54 g DW/m<sup>2</sup>: Stora et al., 1999). This could be related, among other things (e.g. seasonal variation), to the existence of a small river (mean annual flow 3.4 m<sup>3</sup>/sec in 2007) debouching to the north of Barcelona, of which the Besòs canyon is the natural extension, while the Toulon canyon is not an extension of any existing river on the continent (Stora et al., 1999). The higher diversity (S) (despite not including foraminiferans or classifying polychaetes to species level) and total abundance (338.2 ind/m<sup>2</sup>) found within Besòs in comparison to the Toulon canyon (S = 36; N = 176 ind/m<sup>2</sup>: Stora et al., 1999) confirms that food availability is higher in our small canyon. As expected, our biomass data were clearly higher than values in the South Cretan Sea (Tselepides et al., 2000), where biomass (0.05–0.09 g DW/m<sup>2</sup>) was an order of magnitude lower than at comparable depths on Catalan slopes. This is explained by the increasing oligotrophy from West to East in the Mediterranean (Azov, 1991; Salihoğlu et al., 1990) and by the particularly low food sources in the southern Aegean Sea (Tchukhtchin, 1964; Tselepides et al., 2000). On the Catalan slope, sediment redox potential (*Eh*) was clearly lower (on average –40.7 mV) than in the South Aegean Sea (Tselepides et al., 2000), indicating higher organic matter availability for benthos.

The taxonomic composition of infauna varied between stations at different depths on the Catalanian slope. Inside the Besòs canyon polychaetes (Ampharetidae, Paraonidae, Flabelligeridae), amphipods (*C. spinulosa*, *Harpinia* spp., *Paraphoxus oculatus*) and the echinoderm *A. chiajei* dominated. On the adjacent slope the sipunculan *O. steenstrupii* and bivalves (*E. aegeensis*, *A. longicallus*) were more important, together with several caudofoveates (*Falcidens* spp., *Prochaetoderma* spp.). From a trophic perspective, surface deposit feeders (e.g. Ampharetidae among polychaetes and the echinoderm *A. chiajei*) dominated in Besòs canyon, replaced by subsurface deposit feeders (e.g. sipunculans) on the adjacent slope. This is consistent with existing literature on deep-sea macrobenthos food webs (Flach and Heip, 1996; Kröncke et al., 2003): species feeding mainly at the sediment surface are linked to fresh organic matter, whereas subsurface deposit-feeders and predators are found in sediments with more refractory material. The same replacement of trophic guilds with depth was observed in the abyssal Indian Sea (Pavithran et al., 2009). Stora et al. (1999) found a similar increase of subsurface deposit feeders at 1000-1500 m in Toulon canyon. At our slope station, adjacent to Besòs canyon, we attributed the shift to higher habitat stability on deeper bottoms: temporal fluctuations of food sources (*toc*, C/N,  $\delta^{13}\text{C}$ ) are less evident on the adjacent slope than inside Besòs (Authors' unpubl. data). That reasonably explains why the Besòs canyon assemblage was dominated by surface deposit feeders throughout the year and seasonally by opportunistic trophic groups (Capitellidae, Flabelligeridae, Glyceridae), better able to adapt to rapid temporal changes in food inputs.

## 2.4.2 Dynamics of infauna assemblages

Continental shelf infaunal assemblages often show intra-annual variability, with shifting peaks of biomass and diversity during short lag times after triggering events (e.g. the change from a spring assemblage to a summer one: de Juan and Cartes, 2011). This is probably a consequence of both spatial heterogeneity and coupling with a diversified food source. Off Banyuls (western Mediterranean) both the highest growth rates of the deposit-feeding bivalve *Abra ovata* and peaks of meiofauna were found in spring, coupled with maximal pigment concentrations at the surface of the sediment (Gremare et al., 1997). Close to river mouths, the distribution of species is also related to fluctuations in hydrodynamic regime that influence substrate characteristics and particle re-suspension. Sediment discharges

of rivers can change species composition close to delta fronts (Akoumianaki and Nicolaidou, 2007; Cartes et al., 2007). Such information is not generally available for deep-sea systems.

The two stations we sampled on the Catalan slope showed of course differences in the amount of biomass (higher in the Besòs canyon), but also some important differences in seasonal dynamics. Biomass in the canyon increased progressively from February to June-July, while at adjacent slope it remained low, increasing moderately in February and/or July. Also assemblage diversity inside canyon and on adjacent slope showed different patterns through the year. While station C1 showed higher diversity during the period of water column homogeneity (February and April) with a minimum in June-July, the adjacent slope site showed higher diversity during the period of water column stratification with a minimum in February. This is probably linked to higher organic matter quantity (*toc*) and quality of sedimentary food (higher C/N) inside Besòs canyon (Authors' unpubl. data) supplied by river discharges. At Besòs canyon we found depleted  $\delta^{13}\text{C}$  values closer to those found at 60 m at a shelf station (Authors' unpubl. data). Depleted  $\delta^{13}\text{C}$  indicates terrigenous origin of organic matter by river flows.

The quality of POM deposited at the seafloor determines changes in the composition and biomass of macrofauna communities (e.g. off Banyuls: Gremare et al., 1997, in the North Sea: Dauwe et al., 1998; Wieking, 2002; Wieking and Kröncke, 2003). These changes correspond to the feeding types of the constituent taxa/species, matches being established between the available food and the feeding modes of the dominant consumers. Highly mobile predators can proliferate, consuming new production derived from abundance peaks of species belonging to lower trophic levels (Mamouridis et al., 2011).

Among infauna, we found consistent relationships between feeding types and the quantity and quality of POM arriving on Catalan slopes. At the level of broad taxa, polychaetes were more abundant under canyon environmental conditions that include: (1) high *toc* and high C/N, which are indicative of low fresh food availability because C/N is often correlated with lipid contents (Bodin et al., 2007), an important source of fresh food for benthos (Cartes, Gremare, Maynou, Villora-Moreno and Dinet, 2002; Gremare et al., 1997), (2) high river discharge, with a delay of  $\sim 2$  months, which suggests an important food source of terrigenous origin for benthos, and (3) increase of T and S indicating changes in water masses (LIW) in the study area (Hopkins, 1978). By contrast outside the canyon, caudofoveates



and echinoderms (mainly small surface feeding ophiurids) were linked to high near-bottom turbidity and pigment fluorescence in the water column, conditions found especially in February. This suggests stronger coupling with peaks of primary production at surface. Caudofoveats (e.g. *Falcidens* spp.) prey on foraminiferans (meiofauna) (Salvini-Plawen, 1981, 1988). Amphipholidae are surface deposit feeders (Buchanan, 1964), which probably benefit from turbidity increases (more suspended particles) close to the bottom. On the other hand, sipunculans are sub-surface deposit feeders (Romero-Wetzel, 1987) that were more abundant on the slope in October, when more recycled POM (enriched in  $\delta^{13}\text{C}$ ) and rather more *tom* ( $\sim 10\%$ ) were found in sediments. In general, such ecological relationships are subject to strong spatio-temporal variations, with seasonal shifts in the species occupying the dominant trophic guilds. Sipunculans, for instance, can save up fresh labile material below the sediment-water interface (Galeron et al., 2009), hence becoming surface deposit feeders. Such relationships were more difficult to establish at species level, due to the lack of detailed information on species diets. In general, dominant species in the canyon during February and April (Paraonidae and *Harpinia* spp.) were more clearly related with variables indicating inputs of pigments in the water column, probably derived from the peak of surface primary production. Paraonidae are partially surface feeders (Fauchald and Jumars, 1979) consuming diatoms, and foraminiferans, though only a single species has been studied (Röder, 1971). However, *Harpinia* spp. gave an isotopic signal corresponding to omnivory (Fanelli et al., 2009), and they may also prey on meiofauna. Most polychaetes (Capitellidae, Spionidae, Flabelligeridae) were more abundant in June-July in Besòs canyon coinciding with a decrease of *toc* in sediments, but also with a clear signal of terrigenous C (depleted  $\delta^{13}\text{C}$  and high C/N: Cartes et al., 2010; Authors' unpubl. data). These polychaetes are considered to be opportunistic and non-selective in food-particle selection (Fauchald and Jumars, 1979). Spionidae are potentially mobile and can behave as suspension-feeders (Pardo and Zacagnini Amaral, 2004), while Flabelligeridae are typically tubicolous. Inside Besòs canyon other surface deposit feeders were found in this period (e.g. the ampharetid *Melinna* sp.: Gaston, 1987, and *A. chiajei*: Buchanan, 1964). Surface deposit feeders also dominate (representing between 36% and 73% of abundance) in Toulon canyon assemblages (Stora et al., 1999) in samples mainly taken in May-July. By contrast on Catalan slopes, during October and under conditions of maximum water turbidity and increases of *tom* and *toc*, carnivorous polychaetes (Glyceridae, Onuphidae: Fauchald and Jumars, 1979) were dominant,

together with Ampharetidae, considered as surface deposit feeders. Carnivorous polychaetes were also more abundant at the two shallowest stations at Toulon canyon (Stora et al., 1999). This trophic group is more characteristic of disturbed areas (i.e. with high hydrodynamism) exposed to strong organic inputs (Pearson and Rosenberg, 1978). These conditions were likely found at the sediment-water interface rather than deeper in the sediment. This explains why carnivorous polychaetes (*Harmothoe* sp., *Nephtys* spp.) collected with the suprabenthic sledge dominated this “suprabenthic” habitat, showing their maximum abundance under higher  $Turb_{5mab}$  (Mamouridis et al., 2011).

At the slope site temporal relationships between species and environmental variables were less marked than in the Besòs canyon, as indicated by PCA and CCA results. This tendency is in agreement with higher fluctuations of food sources (*toc*, C/N,  $\delta^{13}C$ ) at the Besòs canyon (see above); conditions were more stable at the adjacent slope stations. The only consistent relationships at the adjacent slope were caudofoveates (*Falcidens* spp., *Prochaetoderma* spp.) and Paraonidae with  $Turb_{5mab}$  and fluorescence, likely because these taxa are surface deposit feeders that can eat diatoms and foraminiferans (meiofauna) (Fauchald and Jumars, 1979; Jones and Baxter, 1987). As foraminiferans respond rapidly to inputs of fresh organic matter (Gooday, 1988), it is possible that they already reach high densities in February because the maximum of primary production at the surface begins in November-December off Catalan coasts (from <http://reason.gsfc.nasa.gov/Giovanni>).

In conclusion, the dynamics of macrobenthos at the two stations sampled over Catalan slopes showed differences in biomass and abundance patterns and in their trophic structure. Biomass was higher inside the Besòs canyon than on the adjacent slope. Communities inside the canyon are mostly dominated by surface detritus polychaetes and crustaceans and on the adjacent slope by subsurface deposit feeders (mainly sipunculans). Also epibenthic-mobile assemblages of polychaetes were clearly different in composition from those of infauna, being composed of carnivorous forms associated with higher near-bottom turbidity. The proliferation of opportunistic species inside the Besòs canyon and a stronger temporal succession there of species in relation of food availability and quality were consistent with greater variability in food sources (*toc*, C/N,  $\delta^{13}C$ ) (Authors unpubl. data) and with greater influence of terrigenous inputs by river discharges. Total macrobenthos biomass found over Catalan slopes was higher than that found in the neighbouring

Toulon canyon ([Stora et al., 1999](#)), probably because the canyons are differently conditioned by their relationships with rivers and river flows.

**Acknowledgements:** The authors thank all the participants of the BIOMARE (ref. CTM2006-13508-CO2-02/MAR) surveys, especially the crew of the F/V García del Cid for their inestimable help. A number of taxonomists helped us in the determination of different taxa. Our acknowledgements to Drs C. Salas and S. Gofas (Univ. Málaga) for their help determining some bivalves and gastropods, and to Dr L. Salvini-Plawen (Univ. of Vienna) for caudofoveates.



---

PART II

---



## CHAPTER 3

---

Analysis and standardization of landings per unit effort of red shrimp from the trawl fleet of Barcelona (NW Mediterranean)

---

## Abstract

Monthly landings and effort data from the Barcelona trawl fleet (NW Mediterranean) were selected to analyse and standardize the landings per unit effort (LPUE) of the red shrimp (*Aristeus antennatus*) using generalized additive models. The dataset covers a span of 15 years (1994 – 2008) and consists of a broad spectrum of predictors: fleet-dependent (e.g. number of trips performed by vessels and their technical characteristics, such as the gross registered tonnage), temporal (inter- and intra-annual variability), environmental (North Atlantic Oscillation [NAO] index) and economic (red shrimp and fuel prices) variables. All predictors individually have an impact on LPUE, though some of them lose their predictive power when considered jointly. That is the case of the NAO index. Our results show that six variables from the whole set can be incorporated into a global model with a total explained deviance (DE) of 43%. We found that the most important variables were effort-related predictors (trips, tonnage, and groups) with a total DE of 20.58%, followed by temporal variables, with a DE of 13.12%, and finally the red shrimp price as an economic predictor with a DE of 9.30%. Taken individually, the main contributing variable was the inter-annual variability (DE = 12.40%). This high DE value suggests that many factors correlated with inter-annual variability, such as environmental factors (the NAO in specific years) and fuel price, could in turn affect LPUE variability. The standardized LPUE index with the effort variability removed was found to be similar to the fishery-independent abundance index derived from the MEDITS programme.

**Keywords:** landings per unit effort, bathyal ecosystem, red shrimp fishery, NW Mediterranean, LPUE standardization



### 3.1 Introduction

Deep-water red shrimp is one of the main resources in Mediterranean fisheries in terms of landings and economic value (Bas et al., 2003), primarily in Spain and Algeria, where catches reach more than 1000 t y<sup>-1</sup> (FAO/FISHSTAT, 2011). In the Mediterranean Sea, two red shrimp species, *Aristeus antennatus* and *Aristaeomorpha foliacea*, are caught by specialized trawl fleets operating on the upper and middle continental slope. The distribution of these two species varies geographically and in the NW Mediterranean catches are composed exclusively of *A. antennatus* (Bas et al., 2003). Cartes, Maynou and Fanelli (2011); Cartes, Maynou, Abelló, Emelianov, de Sola and Solé (2011) have suggested environmental causes to explain the extinction of *A. foliacea* in these waters.

The deep-water distribution of red shrimp stocks extends to below 2000 m depth (Cartes and Sardà, 1992) but commercial trawlers fish from 400 to 900 m depth. The red shrimp life-cycle includes seasonal, bathymetric and spatial migrations of different fractions of the population with great size and sex segregation: juveniles and small-sized males are more abundant in autumn and early winter in submarine canyons, while reproductive females concentrate on the open slope fishing grounds in late winter and spring (Sardà et al., 1997). This complex life cycle, coupled with a relatively long life span (more than 10 years according to Orsi Relini et al., 2013) differentiates this species from tropical coastal shrimp resources elsewhere (Neal and Maris, 1985).

The catches of *A. antennatus* show inter-annual fluctuations that have been related to environmental factors determining strong recruitment (Carbonell et al., 1999; Maynou, 2008). Maynou (2008) suggested that winter NAO (North Atlantic Oscillation) is positively correlated with landings of *A. antennatus* two to three years later and that enhanced trophic resources for maturing females in winter and early spring result in stronger recruitments. The NAO has been demonstrated to be a pervasive environmental driver in other marine stocks elsewhere in the Mediterranean and Atlantic (e.g. Brodziak and O'Brien, 2005; Dennard et al., 2010). However, the effect of technical and economic variables has received less attention. For instance, in the red shrimp fishery of the NW Mediterranean, Maynou et al. (2003) showed the importance of individual fisher behaviour in determining catch rates, and Sardà and Maynou (1998) discuss the effect of prices on changes of daily fishing effort targeting this species. Intra-annual variability in landings

has been linked to market-driven variations in prices, which may result in changes in the fishing effort applied to the stocks, as the trawl fleet moves to alternative resources (Sardà et al., 1997).

Despite the commercial importance of *A. antennatus* in the Mediterranean (Sardà et al., 1997), deriving standardized catches or landings per unit effort (CPUE or LPUE) is not straightforward because of the lack of reliable time series at regional or sub-regional level (Leonart and Maynou, 2003). In fact, determining the abundance of marine stocks is notoriously a widespread problem (Hilborn and Walters, 1992). Methodologies basically rely on two different data sources: fisheries-dependent or fisheries-independent data. Fisheries-dependent data tend to be the preferred source to assess the status of marine stocks (Lassen and Medley, 2000) but since the applicability of these traditional assessment methods is limited when it comes to crustaceans, fisheries-independent methods are usually preferred. However, fisheries-independent experimental trawl surveys in the western Mediterranean (Mediterranean International Trawl Surveys: MEDITS, Bertrand et al., 2002) are also problematic because they only partially cover the distribution depth range of *A. antennatus*. Thus, fisheries-dependent data are indeed used but methods that require age data are avoided and instead only regression style methods are used. For instance, in the Spanish Mediterranean sub-area 6 (ca. 1000 km long) just 4 to 12 trawl hauls are carried out annually in the 500-800 m depth stratum and none any deeper (Cardinale et al., 2012). Additionally, obtaining reliable landings including age information is problematic owing to difficulties in determining age in crustaceans (Orsi Relini et al., 2013). In these cases the information collected by a fishery is the main source of abundance data available (Maunder et al., 2006) and, when appropriately standardized, can be used to produce series of population abundance that should help fishery managers to promote the sustainable production of marine stocks.

Here, we evaluate the landings per unit effort from the daily sale slips provided by the Barcelona Fishers Association from 1994 to 2008, corresponding to all the commercial transactions involving *A. antennatus* by a total of 21 trawlers operating on continental slope fishing grounds. The landings of *A. antennatus* have varied by almost an order of magnitude in this area in the last ten years, from a historical low of 13 t y<sup>-1</sup> in 2006 to 96 t y<sup>-1</sup> in 2012. Considering that the average ex-vessel price of the species in this period was 36 e kg<sup>-1</sup> (among the highest seafood prices in Europe), these inter-annual fluctuations in landings have

important economic consequences. Fisheries in Spanish Mediterranean waters are allowed between 50 and 1000 m depth for a maximum of 12 h during daytime, except weekends. Hence, trawl skippers must decide which fishing grounds to visit taking into account that on the continental shelf they can be reached in a shorter time but will produce relatively cheap finfish, whereas deep-water fishing produces more valuable red shrimp but entails high economic costs and the risk of losing or damaging fishing gear.

The main objective of this study was to establish the factors influencing the LPUE (for terminology see e.g. Denis, 2002) of *A. antennatus* in order to evaluate their relative importance (fishery-related, economic and environmental), which can be considered to manage effort constraints and to obtain a standardized series of LPUE as a reliable relative abundance index to assess natural abundance. We used generalized additive models (GAMs: Hastie and Tibshirani, 1986) to capture the possible nonlinear dependence of LPUE on explanatory variables (Su et al., 2008, among others).

## 3.2 Materials and Methods

### 3.2.1 Data source

Trawlers from the Barcelona port operate on the continental shelf and slope fishing grounds (50 – 900 m depth) located between 1°50' and 2°50' longitude east and 40°50' and 41°30' latitude north (Sardà et al., 1997) (see also Figure 1.11 in the introduction). The fleet operates on a daily basis (with mandatory exit from port after 6 am and return to port before 6 pm) and a limited license system whereby total effort in the area has been frozen since 1986. New boats are only permitted if an existing boat is decommissioned. In addition to effort control, the only other measure of control is limiting mesh sizes (minimum 40 mm cod-end stretch mesh size) and neither in the study area nor in any other Mediterranean areas is there output control. Fish is auctioned daily at the premises of the port fish market and all transactions are recorded electronically for statistical purposes by the Barcelona Fishers Association.

We used the daily sale slips containing all transactions of red shrimp (*A. antennatus*) over the period 1994 – 2008 to calculate the total monthly landings (kg

month<sup>-1</sup>, *lands*), the effort measured as total number of trips performed monthly by each vessel (number of trips per month, *trips*), and the monthly average ex-vessel shrimp price (€kg<sup>-1</sup>, *shprice*). The same data set contained information on the engine power (horse power, *hp*) and gross registered tonnage (tons, *grt*), which we used as boat capacity indicators. As an indicator of fishing costs we used the average monthly fuel price (10<sup>-3</sup> €L<sup>-1</sup>, *fprice*) from the EUROSTAT website: <http://ec.europa.eu/energy/observatory/oil/bulletin.en.htm>. As the environmental driver we used the NAO index, taken from the website of the Climate Analysis Group of the University of Exeter (UK): <http://www1.secam.ex.ac.uk/cat/NAO>. We considered: *nao1*, *nao2* and *nao3*, corresponding to one, two and three years before the year of observed landings, using the significant time lags reported in Maynou (2008).

The response variable, the nominal LPUE with observations *lpue<sub>i</sub>*, was estimated as

$$lpue_i = \frac{lands_i}{trips_i}. \quad (3.1)$$

The adjective “nominal” refers to the variable not standardized and *lpue<sub>i</sub>* is the monthly average of landings of one vessel in each trip, corresponding to one fishing day (kg boat<sup>-1</sup> d<sup>-1</sup>), which will form the basis for providing a standardized abundance index.

To assess the individual effect of each vessel, a numeric variable *code* was assigned to each of the 21 vessels in the fleet. Each observation was attributed to a sequential *time* variable from January 1994 to December 2008 (180 months) and a *month* variable describing the month of the year. Two more variables were derived a posteriori from *code* and *month*, after checking for statistical differences among their categories in the model, and then by performing the Tukey Honest Significant Differences test (TukeyHSD). We thus derived the new variables, *group* and *period*, for *code* and *month*, respectively. The *group* variable combines the 21 trawlers into three groups of increasing *lpue* and *period* is a binary variable which classifies the months in “high effect” (*period1*: all months excluding June and November) and “low effect” (*period2*: June and November). All variables are listed in Table 3.1.

### 3.2.2 Model construction

We used generalized additive models, GAM, as described by [Hastie and Tibshirani \(1990\)](#) to model the *lpue* as a function of the covariates in [Table 3.1](#). The structure of the GAM has been described in [Section 1.5](#), The predictor of [Equation 1.28](#) adapted to the LPUE problem becomes  $\eta_i = G(E[lpue_i|z, x_p])$ , where  $G$  will be defined after the analyses on the response variable, of which the distribution must also be defined. The model building process consists of the following steps: 1) selection of the underlying distribution of the response (see [Section 2.2.2](#) for more details); 2) selection of predictors building independent models for each covariant deleting insignificant effects in the final model; 3) selection between correlated predictors through the Pearson correlation coefficient (threshold value:  $\rho = |0.6|$ )

Variable	Description (unit)
<i>lands</i>	total monthly landings per vessel (kg month <sup>-1</sup> )
<i>lpue</i>	landings per unit effort derived from <i>lands</i> and <i>trips</i> (kg boat <sup>-1</sup> day <sup>-1</sup> )
<i>code</i>	a categorical variable assigned to each boat, $c = 1, \dots, 21$
<i>time</i>	time index of months, $t = 1, \dots, 180$ , from Jan 1994 to Dec 2008
<i>trips</i>	number of trips performed by each vessel during the time $t$
<i>hp</i>	engine power of vessels
<i>grt</i>	gross registered tonnage of vessels
<i>shprice</i>	red shrimp ex-vessel price ( kg <sup>-1</sup> )
<i>fprice</i>	fuel price one month before the observed <i>lands</i> (10 <sup>-3</sup> €L <sup>-1</sup> )
<i>nao<sub>k</sub></i>	mean annual NAO index, $k = 1, \dots, 3$ years before the year of observed lands
<i>month</i>	12 categories corresponding to months from January to December
<i>period</i>	categorical variable with 2 categories of grouped months <i>period1</i> : all month excluding Jun and Nov and <i>period2</i> : Jun and Nov
<i>group</i>	3 categories corresponding to groups of vessel

TABLE 3.1: List of variables. Differences between pairs of categories of the variable *month* were checked through Tukey HSD test. Non-significantly different categories were grouped to create the new variable *period*, to which the same test was applied. The same procedure was applied for the variable *code*, to create the variable *group* (all significant tests with  $p \leq 0.001$ ).

to avoid problems of collinearity (Brauner and Shacham, 1998) using the covariant with the most explanatory potential; and 4) analysis of residuals diagnostics.

All analyses were performed in R3.0.1 (mgcv-Rpackage: Wood, 2006). The generalized cross validation (GCV: Craven and Wahba, 1979) and the outer Newton iteration procedure were used to estimate model parameters. GCV is preferable to the UBRE/AIC method in the case of unknown scale parameter for the response variable (Wood, 2006). Second order P-spline as defined by Marx and Eilers (1998) was used as a smoother for nonlinear functions.

### 3.2.3 Theoretical response probability function

LPUE is usually modelled following Gaussian or gamma distribution functions, often without formal justifications (Stefánsson, 1996). Here, we assigned a theoretical probability function to *lpue*, using the nonparametric technique described by Wasserman (2006). The density,  $p(lpue)$ , was estimated using a histogram and the Gaussian kernel. We used the nrd rule-of-thumb to select the bandwidth as described by Scott (2009).

The empirical cumulative distribution function,  $\hat{F}_n(lpue)$ , and the lower  $L(lpue)$  and upper  $U(lpue)$  confidence intervals with  $\alpha = 0.05$  (95%) were calculated according to the Dvoretzky-Kiefer-Wolfowitz (DKW) inequality (Wasserman, 2006) as follows

$$\hat{F}_n(lpue) = \frac{(lpue_n - 0.5)}{N}$$

$$L(lpue) = \max\{\hat{F}_n(lpue) - \epsilon_n, 0\}$$

$$U(lpue) = \min\{\hat{F}_n(lpue) + \epsilon_n, 1\},$$

where  $lpue_n$  is the ordered vector of observations *lpue*,  $N$  the total number of observations and  $\epsilon_n$  results from the DKW inequality as

$$\epsilon_n = \sqrt{\frac{1}{2n} \log_e \left( \frac{2}{\alpha} \right)},$$

such that the probability of  $F(lpue)$  to fall between the upper and lower bounds is

$$P(L(lpue) \leq F(lpue) \leq U(lpue) \forall n) \geq 1 - \alpha.$$

The hypothesis tested is  $H_0 : \hat{F}_n(lpue) = F_0(lpue)$  versus the alternative hypothesis  $H_1 : \hat{F}_n(lpue) \neq F_0(lpue)$ , where  $F_0(lpue) = Ga(a, b)$  with density function

$$p(lpue) \propto lpue^{(a-1)} e^{-b lpue}$$

and  $lpue > 0$ . Parameters  $a$  and  $b$  are derived from the expectation,  $E[lpue] = a/b$ , and variance  $Var[lpue] = a/b^2$ . Then, the resulting assumed distribution function and cumulative distribution function were graphically compared.

### 3.2.4 Selection criteria and explained deviance

Both AIC ([Akaike, 1973](#)) and percentage of deviance explained (DE) were used as selection criteria: the selected model presented both the lowest AIC and the highest DE and all term parameters significantly different from zero.

The DE for each variable was also calculated in order to determine their relative importance in the final model. The residual deviance of the full model and the deviances of reduced models (i.e. the model excluding variable  $x_i$ ) were calculated to derive the proportion explained by variable  $x_i$ :

$$DE_{x_i} = \frac{[D(M_r) D(M_f)]}{D(M_n)}$$

where  $M_f$ ,  $M_n$  and  $M_r$  are the full, null and reduced models and  $D(\cdot)$  represents the deviance for a given model. In the reduced model variable  $x_i$  is omitted.

### 3.2.5 LPUE standardization

The model used for standardization was built in order to avoid dependency on fleet variables, maintaining environmental variables, which are expected to be related

to the natural abundance of the species. The standardized LPUE,  $lpue_s$  is then

$$lpue_{i_s} = E[lpue_i] + (lpue_i - E[lpue_i|z, x_p]) \quad (3.2)$$

where  $lpue_i$  are observations of the “nominal” or “raw” LPUE defined in Equation 3.1,  $E[lpue_i]$  is the unconditional expectation and  $E[lpue_i|x_p]$  is the expectation conditional to covariates  $x_1, \dots, x_P$ , estimated using the appropriate standardization model. Finally we compared our standardized LPUE,  $lpue_s$  with an alternative abundance index derived from fisheries-independent data, available in the technical report SGMED–12–11 (Cardinale et al., 2012, pp. 136–150) after normalization of both variables.

## 3.3 Results

### 3.3.1 Overview of data and response distribution

Figure 3.1 provides the raw LPUE time series as reckoned in Equation 3.1 with its spline estimation (upper plot) and the annual average of the NAO index (lower plot). The  $lpue$  series, initially constant, started to decline at the end of 1998 with a sharp maximum low in the period 1999 – 2000. Then the trend changed to inter-annual variation. Conversely, the NAO index shows the lowest records in the period 1995 – 1996. The  $lpue$  begins to decrease after three years from the first year of negative NAO. In Figure 3.2 the time series of the fuel price shows an increasing trend during the observed period (upper panel). The total number of trips per month performed by the whole fleet declines during the same period (middle panel), but it declines only at the beginning of the fuel price rise, then remaining almost constant (lower panel). Low  $lpue$  in the period 2000 – 2001 is also related to the peak of  $fprice$  in the same period (compare upper plots of Figures 3.1 and 3.2).



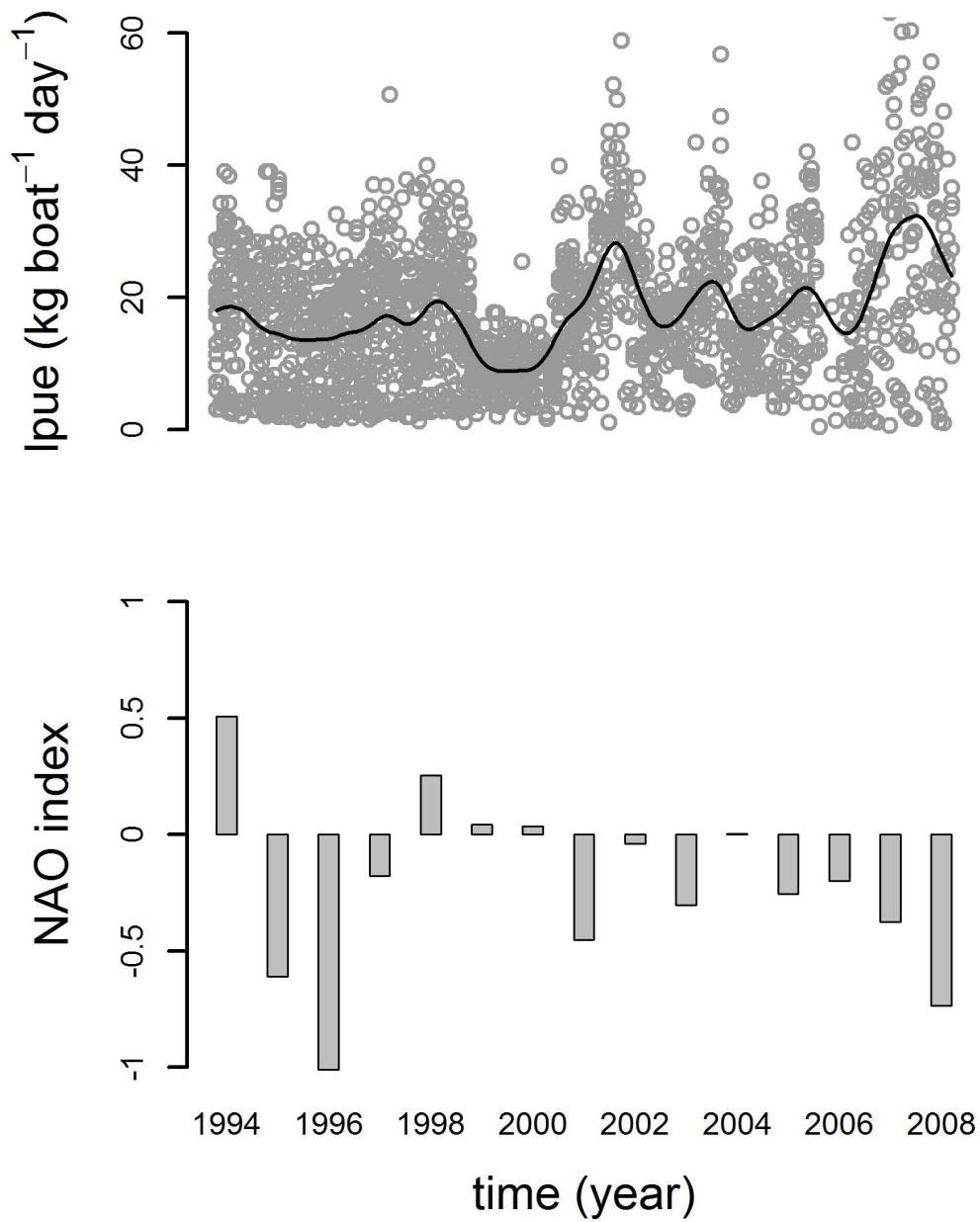


FIGURE 3.1: Time series from 1994 to 2008 of LPUE data and spline estimation (upper panel) and mean annual North Atlantic Oscillation (NAO) (lower panel).

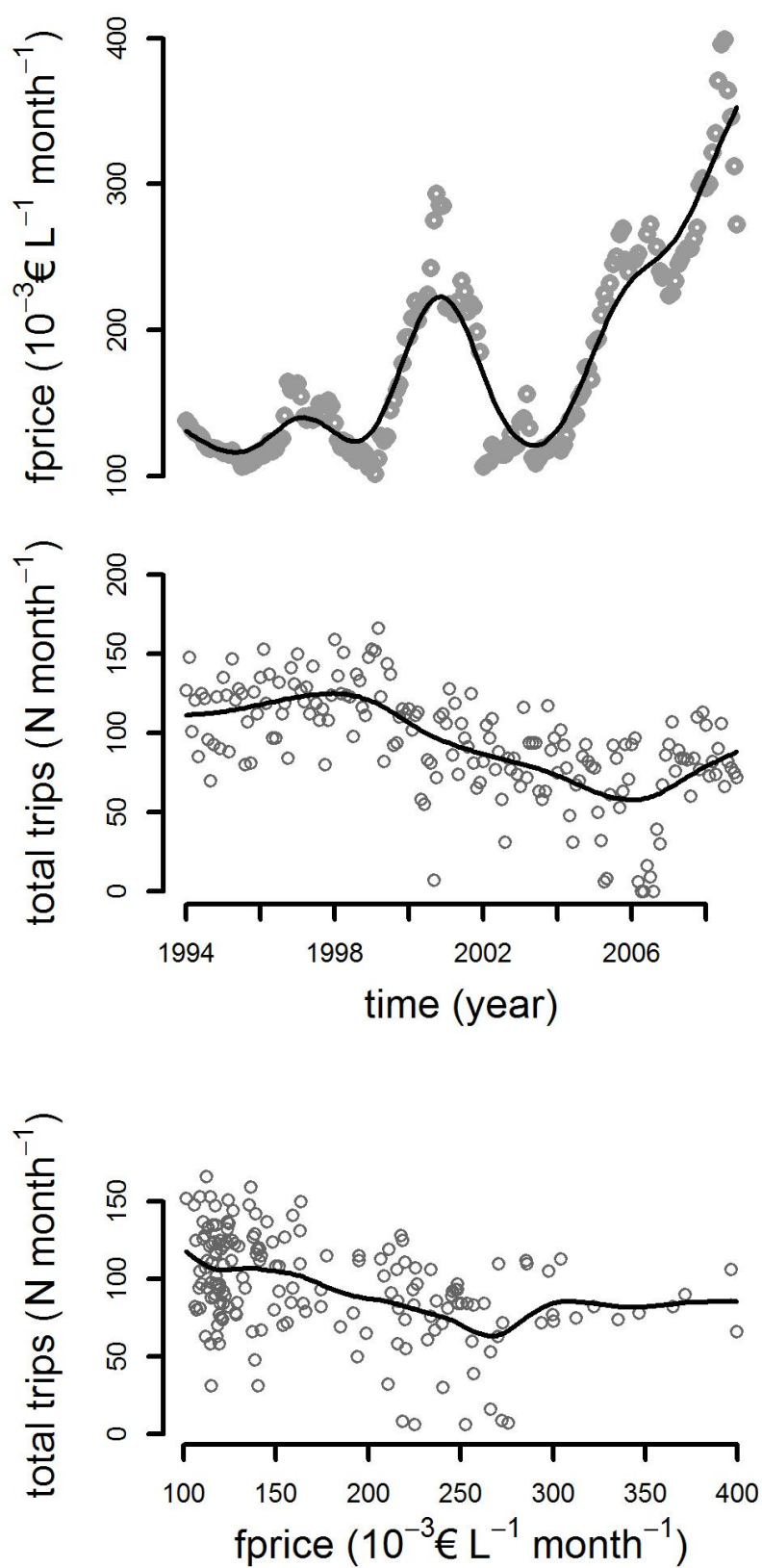


FIGURE 3.2: From top to bottom: spline estimation of the fuel price, monthly total number of trips performed by the fleet from year 1996 to 2008, and relationship between the fuel price and the total monthly number of trips.

Characteristics of *lpue* are plotted in Figure C.1, Appendix C. The probability density function (*pdf*) is positively skewed (upper panels). Data hold atypical values in the right tail (see the box-plot, left middle panel) and the distribution function of the gamma distribution lies approximately inside the 95% confidence intervals of the empirical cumulative distribution function (*ecdf*) of *lpue* (right middle panel). Finally, the QQ-plots for the gamma and the Gaussian distributions provide evidence of a better fit of data to the gamma rather than the Gaussian distribution (on the left and the right lower panels respectively).

### 3.3.2 Model building and comparison

The model building process is summarised in Table 3.2. Here is implemented the same notation used in Equation 1.28, with  $\delta_0, \dots, \delta_3$  regression parameters for the intercept, linear (*hp* and *grt*) and binary variables (*period*). However for simplicity the subindices defining the observations were eliminated and due to the high number of categories for some of the variables, additional parameters  $\gamma_{k_1}$ , with  $k_1 = 2, 3$  and  $\gamma_{k_2}$ ,  $k_2 = 2, \dots, 21$ , were introduced to explicitly define the regression coefficients for the dummy coded variables *group* and *code* respectively.

Models are sorted in ascending order of total DE, with the exception of models 11 and 12, corresponding to the GLM (generalized linear model) version of the final model 7 and the standardization model respectively. In comparison with the GLM (model 11), GAMs AIC decreases and the DE increases substantially (1.56 times), though the number of degrees of freedom increases considerably ( $df_{\text{GAM}} = 27.7$  versus  $df_{\text{GLM}} = 9$ ). Variables *grt* and *time* were selected as better predictors than *hp* and *fprice*, respectively, according to the Pearson correlation coefficients (*grt* – *hp* was  $\rho = 0.61$ ; *time* – *fprice*  $\rho = 0.69$ ) and larger ED of former variables. All other correlations were  $\rho < |0.6|$ . Table 3.2 incorporates also the  $nao_k$  terms, though their explanatory potential in the full model is too weak to be significant. Adding  $nao_k$  terms to model 7 (Table 3.2: models 8, 9 and 10) did not improve model fit in terms of DE and AIC. Nevertheless, we found significant  $nao_k$  effect in less complex models, without the inclusion of economic parameters.

### 3.3.3 The descriptive model

The final model for the LPUE is

n	model	df	RD	DE (%)	AIC
1	$\delta_0$	2	863.8	0	13544
2	$\delta_0 + \delta_1 hp^{(+)}$	3	844.4	2.2	13501
2.1	$\delta_0 + \delta_2 grt$	3	815.3	5.6	13432
3	$\delta_0 + \delta_2 grt + \sum^{k_1} \gamma_{k_1} group_{k_1}$	5	741.0	14.2	13250
4	$\delta_0 + \delta_2 grt + \sum^{k_1} \gamma_{k_1} group_{k_1} + \delta_3 period_2$	6	734.7	15	13235
5	$\delta_0 + \delta_2 grt + \sum^{k_1} \gamma_{k_1} group_{k_1} + \delta_3 period_2 + s(trips)$	8.9	627.8	27.3	12936
6	$\delta_0 + \delta_2 grt + \sum^{k_1} \gamma_{k_1} group_{k_1} + \delta_3 period_2 + s(trips) + s(fprice)^{(+)}$	12.4	614.0	28.9	12900
6.1	$\delta_0 + \delta_2 grt + \sum^{k_1} \gamma_{k_1} group_{k_1} + \delta_3 period_2 + s(trips) + s(time)$	24.8	527.0	39	12632
7	$\delta_0 + \delta_2 grt + \sum^{k_1} \gamma_{k_1} group_{k_1} + \delta_3 period_2 + s(trips) + s(time) + s(shprice)$	27.7	493.5	43.0	12512
8	$\delta_0 + \delta_2 grt + \sum^{k_1} \gamma_{k_1} group_{k_1} + \delta_3 period_2 + s(trips) + s(time) + s(shprice) + s(nao1)^{(ns)}$	28.7	493.3	43.0	12513
9	$\delta_0 + \delta_2 grt + \sum^{k_1} \gamma_{k_1} group_{k_1} + \delta_3 period_2 + s(trips) + s(time) + s(shprice) + s(nao2)^{(ns)}$	28.7	493.5	43.0	12514
10	$\delta_0 + \delta_2 grt + \sum^{k_1} \gamma_{k_1} group_{k_1} + \delta_3 period_2 + s(trips) + s(time) + s(shprice) + s(nao3)^{(ns)}$	28.7	493.4	43.0	12513
11	$\delta_0 + \delta_2 grt + \sum^{k_1} \gamma_{k_1} group_{k_1} + \delta_3 period_2 + trips + time + shprice$	9	626.4	27.5	12932
12	$\delta_0 + \delta_2 grt + \sum^{k_2} code_{k_2} + s(trips)$	24.75	608.7	29.5	12910

TABLE 3.2: Model construction. N, number associated with each model; model, models right part of the formula; df, models degree of freedom; RD, residual deviance, DE, percentage of deviance explained by each model; AIC, Akaike Information Criterion; term(ns), insignificant terms in a model; term (+), terms not incorporated in next steps (i.e. models with the incorporation of *hp* or *fprice* gave a lower DE than the incorporation of *grt* and *time*, respectively).

Model 12 is the model used for standardization.

$$\eta_i = \delta_0 + \delta_2 \text{grt}_i + \delta_3 \text{period}_i + \sum_{k=2,3} (\gamma_k \text{group}_{ik}) + s_1(\text{trip}_i) + s_2(\text{time}_i) + s_3(\text{shprice}_i), \quad (3.3)$$

where the predictor  $\eta_i$  is linked to expectation as follows

$$\eta_i = \log(E[\text{lpue}_i | \text{grt}, \text{period}, \text{group}, \text{trip}, \text{time}, \text{shprice}]). \quad (3.4)$$

Here the conditional expectation of the  $\text{lpue}$  is assumed to belong to the gamma  $Ga(a, b)$  and coefficients are defined as in previous section.

Figure C.2 in Appendix C shows the diagnostic plots for this model (corresponding to Equation 3.3 and model 7 in Table 3.2). Residual quantiles lie on the straight line of the theoretical quantiles, although slightly heavy-tailed; in the histogram, residuals are consistent with normality and the relationship between response and

(a)	$\mu$	$\sigma$	$t$	$p$	DE (%)	
$\delta_0$	1.746	0.103	16.980	$\leq 2\text{E-}16$	0	
$\delta_2$	0.010	0.001	16.205	$\leq 2\text{E-}16$	5.62	
$\delta_3$	-0.152	0.035	-4.383	1.24E-05	0.72	
$\gamma_2$	0.281	0.081	3.449	5.75E-04	3.58	
$\gamma_3$	0.637	0.086	7.404	2.02E-13		
(b)	$edf$	$\lambda$	$F$	$p$	DE (%)	
$s_1$	2.457	30.007	71.01	$\leq 2\text{E-}16$	11.38	
$s_2$	15.239	0.011	24.82	$\leq 2\text{E-}16$	12.40	
$s_3$	4.026	0.059	26.36	$\leq 2\text{E-}16$	9.30	
(c)	$df$	$scale$	$R^2(\text{adj})$	AIC	GCV	$\text{DE}_{tot}$ (%)
	27.722	0.274	0.488	12512	0.282	43.00

TABLE 3.3: Results of the final model (Equation 3.3). Results associated with (a) linear terms, (b) smooth terms and (c) global estimations.  $\mu$ : estimation of the mean;  $\sigma$ : standard deviation;  $t$ : value of  $t$ -statistic;  $F$ : the  $F$ -statistic value;  $p$ :  $p$ -value associated to the  $t$  or the  $F$  statistic; DE: deviance explained by each term in percentage;  $edf$ : effective degrees of freedom;  $\lambda$ : estimated smoothing parameter;  $df$ : total degree of freedom;  $scale$ : estimation of the scale parameter;  $R^2(\text{adj})$ : adjusted R-squared; AIC: Akaike Information Criterion; GCV, generalized cross validation;  $\text{DE}_{tot}$  (%): percentage of total deviance explained by the model.

fitted values is linear and positive. Residuals versus the linear predictor (that is, the sum of all partial effects) show a faint heteroscedasticity.

Table 3.3 shows results related to (a) the linear part, (b) the smooth functions and (c) the global parameters of the final model (Equation 3.3), with a total explained deviance of 43.00%. The predictor with the highest explanatory potential was time (DE = 12.40%), which captured the intra-annual fluctuations in red shrimp *lpue*. The second predictor in terms of explained deviance was *trips* (DE = 11.38%). Red shrimp price was the third most important predictor (DE = 9.30%). Other variables such as *grt*, *group* and *period* had less impact. The model returned all significant parameters ( $p \ll 0.001$ ).

All partial effects are reported in Figure 3.3. The partial effect for time shows a substantial difference before and after the period 1999 – 2000, when a clear drop is exhibited in the shape. Before this threshold the shape is almost constant, whereas after the abrupt decay increasing variation is observed over recent years. Predictor *trips* represents a positive and monotonic relationship, reaching a plateau for *trips* > 15; *shprice* reached its maximum value around 30 €kg<sup>-1</sup>; *lpue* was significantly lower for *period2*, representing June and November, than for the rest of the year (*period1*). There were significant differences between the three groups of vessels. Variable *grt* showed a positive linear effect, meaning that larger vessels had higher *lpue*.

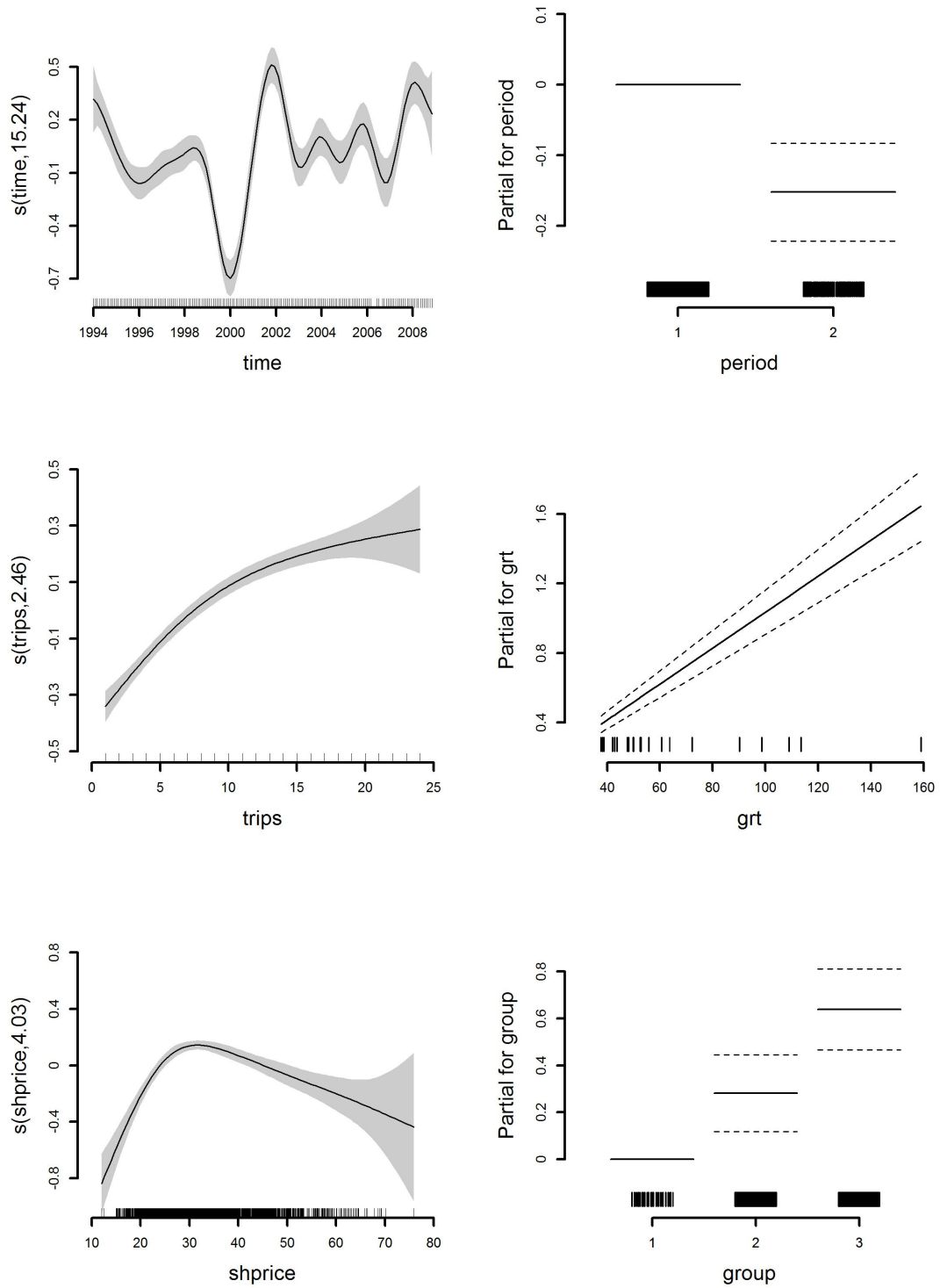


FIGURE 3.3: Partial effects of model 7. Bayesian credible intervals (95%).

### 3.3.4 LPUE standardization

The model used to standardize *A. antennatus* LPUE is

$$\eta_i = \delta_0 + \delta_1 grt_i + \sum_{k=2,21} (\gamma_{k2} code_{ik2}) + s_1(trips_i), \quad (3.5)$$

where

$$\eta_i = \log(E[lpue_i | grt, code, trip]). \quad (3.6)$$

With the aim of standardizing, this model comprises all fleet-dependent variables, whose effect must be removed from the nominal value. The diagnostic plots show reasonably good outputs (not shown).

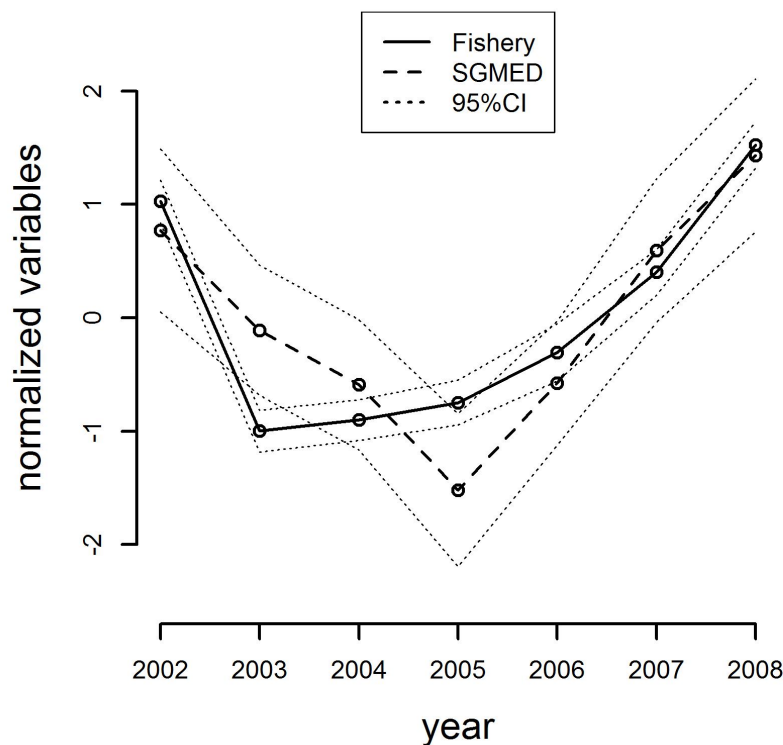


FIGURE 3.4: Comparison between the fishery-derived (standardized LPUE) and the SGMED index. Variables have been normalized for comparison.



Finally, LPUE index and the SGMED in 2002 – 2008 with their confidence intervals after normalization of variables are plotted in Figure 3.4. The normalized Barcelona fishery's LPUE, calculated using Equations 3.3 and 3.5, has narrower confidence intervals than the normalized SGMED index. Only in 2004 were the two indices statistically different and in 2005 index estimates were at the limit of the other CI. Thus, five out of seven estimates can be considered equivalent.

## 3.4 Discussion

This study presents models for relative abundance of *A. antennatus* harvested by one important Catalan fleet in the NW Mediterranean from 1994 to 2008. To our knowledge it is the first combined use of commercial fisheries data from Spain analysing environmental and economic variables with GAM techniques. Our objectives were: 1) to define the relative importance of predictors (model 7, Tables 3.2 and 3.3) and 2) to construct a standardized fishery-dependent index to compare with fishery-independent indices (Figure 3.4). The results contribute to the identification of simple roles in red shrimp fishery management.

### 3.4.1 The role of explanatory variables

We incorporated effort, temporal, economic and environmental variables into a global regression model to evaluate their relative importance. Model 7 captures LPUE variability with a total deviance of 43% explained by six predictors. In order to quantify the different sources of LPUE variability, we found that the set of fishery-related variables (*trips*, *grt* and *group*) was the most important source, with a DE of 20.58%, followed by temporal (time and period, DE = 13.12%) and finally economic variables (*shprice*, DE = 9.30%). Among the variables taken from fishery data, *trips* has provided the greatest impact to date. A low number of trips per month could be associated with generalist trawlers operating usually on the continental shelf and with less knowledge about red shrimp fishing grounds than trawlers specialized in this fishery (Maynou et al., 2003), suggesting that the higher activity of non-specialized trawlers in deep-water harbours yields lower LPUE values (see Figure 3.3: partial for *trips*). Conversely, boats performing a higher number of trips per month are expert in deep-water fishing grounds and their skippers are more likely to find high-concentration shoals through a process

of trial and error (as hypothesized by [Sardà and Maynou, 1998](#)). Boat characteristics (*grt*) also influence LPUE, as was to be expected. The greater the gross registered tonnage, the higher the LPUE that is observed. The variable *group* captures other capabilities of fishermen and technical characteristics of vessels, such as the type of engine, net shape and skipper's expertise, which have been shown to positively bias the LPUE ([Marriott et al., 2011](#); [Maynou et al., 2003](#)) and are expected to be important in many fisheries ([Maunder and Punt, 2004](#)). The importance of these predictors implies that their influence should be eliminated during standardization. Inter-annual variable (*time*) is much more important than intra-annual variable (*period*) (Table 3.3). The former is more strongly determined by a range of sources, such as environmental and economic drivers, than the latter. The same order of importance was found by [Maynou et al. \(2003\)](#). The LPUE was almost constant before 1999 – 2000, when a sharp decline was observed. We hypothesized a relationship with low NAO in the previous three years (see Figure 3.1 and the introduction) that confirms the findings of [Maynou \(2008\)](#) and a possible relationship with the increase in fuel prices beginning in 2000. The following years were characterized by high inter-annual variability, when the price of fuel increased and showed greater variations. We believe that the trend could be explained by economic factors (Figure 3.2), especially since very high fuel-related costs are incurred in the fishing of red shrimp as a result of it being performed in deep-water ([Sardà et al., 1997](#)). The partial effect of ex-vessel prices, *shprice*, shows a parabolic-like shape and significant explanatory potential (DE = 9.30%). Low selling prices do not induce fishermen to practice this deep-water fishery, because they could not offset the high associated costs, and trawlers would rather switch to continental shelf fisheries, with lower costs and lower risk. When there are profits to be made, probably owing to the low availability of the product, fishermen practice this deep-water fishery more intensely and landings per unit effort also increase. At the higher sales price bracket (i.e. more than about 30 €kg<sup>-1</sup>) decreasing landing rates mean higher sale prices. Here, an alternation of cause and effect between the two variables probably comes into play. As mentioned, *fprice* is also an important explanatory variable, although it was not inserted in the final model because of its correlation with time. Fuel price has a significant effect on LPUE and can reach approximately 1.6% of explained deviance (as can be deduced from the model building process in Table 3.2).

### 3.4.2 Implications for management

Obtaining information on deep-sea species population dynamics is notoriously difficult, but our analysis suggests that the peculiarity of red shrimp fishery makes it possible to use fishery-dependent data to accurately describe the relative abundance of this resource. There are no discards for this fishery and the by-catch fraction of commercial interest, represented for example by *Merluccius merluccius*, *Micromesistius poutassou* and *Phycis blennoides*, is small. These characteristics enable landings to be considered equivalent to catches and interchange LPUE and CPUE as indices (Denis, 2002; Hilborn and Walters, 1992).

In turn, the definition of the relative importance of explanatory variables enables their impact on LPUE to be understood and makes intervention on the relevant variables possible from a management perspective. Fishery-related variables tend to have a significant effect on LPUE (DE = 21% in our case), and management measures aiming to reduce fishing mortality in this heavily harvested stock (Cardinale et al., 2012) could be based on limiting the size of the trawlers. Furthermore, the number of trips permitted in deep-water fishing grounds in this fishery could be limited, for example, by defining a threshold when the number of trips does not significantly increase the partial effect for LPUE (see Figure 3.3). In addition, to evaluate the impact of predictors on the LPUE, the regression analysis could be the basis to provide a standardized index for assessing species stocks. Standardization of landings data allows an index of the real species abundance to be developed, assuming that the explanatory variables available remove (or explain) most of the variation in the data that is not attributable to natural changes (Maunder and Punt, 2004). We advocate the selection of effort predictors for standardization.

Trends in CPUE (and LPUE) are usually assumed to reflect changes in the abundance of marine stocks (Maunder and Punt, 2004), but the raw index is often not proportional to abundance (Maunder et al., 2006). The raw LPUE is in fact dependent on many human factors that could be avoided. Time variables have a strong relationship with the abundance and environmental factors, which in turn are related to abundance, so they cannot be used in the model during standardization (e.g. see Maunder and Punt, 2004). The economic source of variability should be considered, but shrimp price and LPUE realistically have a cause-effect relationship, so they could be not properly used. Conversely, fishery-related variables seem to be the most reliable for this purpose. During the study period, the

fleet was practically constant, making monthly trips a good indicator of fishing effort and landing ability, and remained almost constant despite potential technological creep (Marriott et al., 2011) because no significant changes in fishing technology have occurred in the area in the last 20 years. Studies of deep-water systems, where harsh conditions limit methods for evaluating sheries, often suffer from a lack of data in order to assess stock status. Although the goal of sheries managers is to promote sustainable production of sh stocks through formal stock assessment, it is often impractical to collect shery-independent data in isolated or harsh environments. In these cases the information collected by a shery is the main (or only) source of abundance data available (Maunder et al., 2006).

**Acknowledgements:** The authors would like to express their sincere thanks to the Fisheries Directorate of the Government of Catalonia for giving access to the sales data of the Barcelona Fishers Association, as well as to fishers of Barcelona. The first author is also very grateful to A. Rodríguez Casal and C. Cadarso Suárez for transmitting their knowledge in nonparametric statistics, to A. Gallen for revising the English and to M. Reyes for his suggestions on the manuscript. G. Aneiros is partly supported by Grant number MTM2011-22392 from the Ministerio de Ciencia e Innovación (Spain). Finally, this study was financed by the Spanish National Research Council (CSIC) through the JAE-predoc grant programme.

## CHAPTER 4

---

### Extended Additive Regression for Analysing LPUE Indices in Fishery Research

---

## Abstract

We analysed the landings per unit effort (LPUE) from the Barcelona trawl fleet (NW Mediterranean) of the red shrimp (*Aristeus antennatus*) using the novel Bayesian approach of additive extended regression or distributional regression, that comprises a generic framework providing various response distributions, such as the log-normal and the gamma and allows estimations for location and scale or shape (as the frequentist counterpart Generalized Additive Models for Location Scale and Shape, GAMLSS, does). The dataset covers a span of 17 years (1992-2008) in which the whole fleet has been monitored and consists of a broad spectrum of predictors: fleet-dependent (e.g. number of trips performed by vessels and their technical characteristics, such as the gross registered tonnage), temporal (inter- and intra-annual variability) and environmental (NAO index) variables. This dataset offers a unique opportunity to compare different assumptions and model specifications. So that we compared (1) log-normal versus gamma distribution assumption, (2) modelling the location parameter of the LPUE versus modelling both location and scale (or shape) of of the variable, and finally (3) fixed versus random specifications for the catching unit effects (boats). Our results favour the gamma over the log-normal and modelling of both location and shape parameters (in the case of the gamma) rather than only the location, while not noticeable differences occur in estimation when considering catching units as fixed or random, however accounting for random effects avoids problems related to time-series, such as correlations in data.

**Keywords:** landings per unit effort, red shrimp fishery, NW Mediterranean, generalized additive models for location, scale and shape; mixed models; Markov Chain Monte Carlo simulation

## 4.1 Introduction

In fishery research, the LPUE (Landings Per Unit Effort or CPUE, catches per unit effort, when it refers to the catch) is an index of abundance widely used in stock assessment to estimate the relative abundance of an exploited species (Marchal et al., 2002; Mendelsohn and Cury, 1989). The “landings” portion of the measure is the quantity of the stock brought to the port by each boat and is usually expressed as number of specimens or weight of the stock, while the “unit effort” portion refers to the unit of time spent by a unit of the gear used to catch (e.g. boat or meters of net soaked per unit of time). LPUE (or the CPUE) constitutes one of the most common pieces of information used in assessing the status of fish stocks.

Its importance should not be undervalued because it may be the only information available for a stock and could be applied also within the newer ecosystem approach to fisheries management when searching for suitable abundance parameters. When data derive from catches of the stock (e.g. from scientific surveys), the LPUE is more properly defined as CPUE.

The LPUE is reckoned in different ways depending on data availability. Its use is based on different assumptions. Usually it is taken to be proportional to the natural quantity of the target species, such that  $lpue = q \times B$  where  $B$  is the biomass landed and  $q$  a constant of proportionality called catchability. This proportionality needs strong assumptions (e.g. Maunder and Punt, 2004; Paloheimo and Dickie, 1964) that make its use questionable leaving an open debate (e.g. Bannerot and Austin, 1983; Gulland, 1964; Maunder and Punt, 2004). Another approach is to undertake regression modelling (e.g. Venables and Dichmont, 2004), in order to standardise the index removing the bias induced by influential variables (Maunder et al., 2006) related to causes other than natural (i.e. anthropogenic).

In fact, many factors can affect the index (e.g. time, seasonality, fishing area and fleet characteristics, among others). Many of them are related to the life-cycle of the species, other to environmental changes and other have an origin that is independent from natural factors, that if not considered can lead to biased interpretations of stock states. The idea of the standardization is then to detect and avoid the influence on the stock of latter variables. Therefore, although the catches and landings may strongly depend on these variables, an index of abundance “at sea” should somehow becomes independent from factors related to fishing. Also

the associated economy can be very influential, either directly or indirectly as described in Chapter 3.

The most common classes of regression models to determine the impact of available covariates  $x_1, \dots, x_p$  on the conditional expectation of the LPUE,  $E[lpue_i|x_p]$ , are generalized linear models (GLM, [McCullagh and Nelder, 1989](#)) and generalized additive models (GAM, [Hastie and Tibshirani, 1986](#)). In GLM the expectation of LPUE is modelled as a linear combination of the covariate effects as introduced in Chapter 1, Section 1.5, Equation 1.23). In GAM (Equation 1.25, same section), the possibility of nonlinear effects of some covariate is acknowledge, allowing the their flexible estimation directly by data. Both methods have been widely used in fisheries research (e.g. [Damalas et al., 2007](#); [Denis, 2002](#)).

Moreover, in most cases LPUE data are collected repeatedly for the same catching units over time leading to the necessity to account for unobserved characteristics of these units to avoid correlations in the repeated measurements. This fact leads to the use of other extensions of GLM and GAM approaches, where catching unit-specific effects are introduced to acknowledge the effect that usually multiple observations are collected for the same unit and that unobserved heterogeneity remains even when accounting for some covariate effects. Regression analysis is thus able to capture the variability among fishing vessels ([Thorson and Ward, 2014](#); [Thorson and Berkson, 2010](#)), the importance of which has been recognized when interpreting fishery data ([Beverton and Holt, 1957](#); [Garstang, 1900](#); [Wilberg et al., 2009](#)). Catching-unit specified effects can be modelled with the class of mixed models, such as generalized linear mixed models (GLMMs, [Pinheiro and Bates, 2000](#)) or generalized additive mixed models (GAMMs, [Wood, 2006](#)), defined in Equations 1.29 and 1.30 respectively (introductory chapter).

Another important aspect when modelling LPUE is the choice of the response distribution. In most cases, skewed distributions have been considered, including in particular the gamma distribution ([Maynou et al., 2003](#); [Stefánsson, 1996](#)), the log-normal distribution ([Brynjarsdóttir and Stefánsson, 2004](#); [Myers and Pepin, 1990](#)) and the delta distribution ([Gavaris, 1980](#); [Pennington, 1983](#)). The latter provides a form of zero-adjustment where zero catches are modelled separately from the nonnegative catches via a Bernoulli distribution. As a possibility to differentiate between gamma and log-normal distribution, the Kolmogorov-Smirnov test has been applied to fitted values from corresponding GLMs. Then, the distribution leading to a lower value for the test statistic can be considered to be closer



to the distribution of the data ([Brynjarsdóttir and Stefánsson, 2004](#); [Stefánsson and Palsson, 1998](#)).

In this Chapter, structured additive distributional regression models, Equation 1.33, ([Klein et al., 2013](#)) has been considered as a comprehensive, flexible class of models that encompasses all special cases discussed so far and a number of further extensions. More specifically, this class of models allows to deal with the following problems:

- Selection of the response distribution: additive distributional regression comprises a generic framework providing various response distributions and in particular the log-normal and the gamma distributions. Extensions including zero-adjustment to account for an inflation of observations with zero catch are also possible but not required in the data set considered here. Tools for effectively deciding between competing modelling alternatives will also be considered.
- Linear versus nonlinear effects: effects of continuous covariates can be estimated nonparametrically based on penalized splines approximations that allow for a data-driven amount of smoothness and therefore deviation from the linearity assumption.
- Models for location, scale and shape: instead of restricting attention to only modelling the expected LPUE, distributional regression allow to specify a further parameter of the distribution that correspond to scale or shape. This both enables for additional flexibility and a better understanding of how different covariates affect the distribution of LPUE.
- Fixed versus random effects: both fixed and random specifications for the catching unit-specific effects are supported and can be compared in terms of their ability to fit the data.
- Mode of inference: distributional regression can be formulated both from a frequentist and a Bayesian perspective and corresponding estimation schemes either rely on penalized maximum likelihood or Markov chain Monte Carlo simulations. This paper is focused on the Bayesian inference.

Structured additive distributional regression is in fact an extension of structured additive regression (STAR, [Brezger and Lang, 2006](#); [Fahrmeir et al., 2004](#)) in the

framework of generalized additive models for location, scale and shape (GAMLSS, [Rigby and Stasinopoulos, 2005](#)). The parameter specifications rely very much on STAR, a comprehensive class of regression models for the expectation of the response that comprises geoaddivitive models ([Kammann and Wand, 2003](#)), generalized additive models ([Hastie and Tibshirani, 1986](#)) and generalized additive mixed models ([Lin and Zhang, 1999](#)) as special cases.

Our analysis deals with the LPUE derived from the red shrimp (*Aristeus antennatus*) fishery. The red shrimp is the target species for the deep-water trawl fishery in the western Mediterranean ([Bas et al., 2003](#)), where catches have reached more than 1000 t/yr ([FAO/FISHSTAT, 2011](#)). This species occurs between 300 and 2000 m ([Sardà and Cartes, 1993](#); [Tudela et al., 1998](#)) and its biological and ecological characteristics have been deeply studied ([Bianchini and Ragonese, 1994](#); [Carbonell et al., 2008](#); [Demestre, 1995](#); [Demestre and Fortuño, 2013](#); [Ragonese and Bianchini, 1996](#)). Its fishery is developed in deep-waters (450-900 m) on the continental slope and near submarine canyons, where its occurrence is higher ([Sardà et al., 1997](#); [Tudela et al., 1998](#)). *A. antennatus* LPUE, as well as other related indices, has already been studied: its fluctuations have been related to changes in oceanographic conditions, e.g. at least partially triggered by changes in the North Atlantic Oscillation ([Maynou, 2008](#)) explained by seasonal availability of preys and its life cycle ([Carbonell et al., 1999](#); [Sardà et al., 1997](#)), or linked to the fishing activity in turn influenced by economic factors, such as fuel and red shrimp prices and so subjected to the market demand ([Mamouridis, Maynou and Aneiros Pérez, 2014](#)).

In our case LPUE and CPUE terms are perfectly interchangeable because all the catch of commercial trawlers is landed to the port, thus there are no discarding or other losses at sea for this lucrative species ([Mamouridis, Maynou and Aneiros Pérez, 2014](#)). However, for formal congruences we will refer to the LPUE, being this case data derived from landings.

The main objective of this study is to demonstrate the usefulness of structured additive distributional regression in modelling and predict shrimp LPUE and to provide guidance for model choice and variable selection, questions that arise in the process of developing an appropriate model for a given data set. Therefore, we will discuss tools such as quantile residuals, information criteria and predictive mean squared errors to evaluate the ability of models to describe and predict LPUE adequately.

## 4.2 Materials and Methods

### 4.2.1 Data description

Data proceed from the daily sale slips of the Barcelona trawling fleet, granted by the Barcelona Fishers' Association. This data set comprises the information for 21 trawlers, with their total monthly landings (*landings*, kg), their monthly number of trips performed (*trips*) and the Gross Registered Tonnage (*grt*, GRT). Furthermore, the monthly average value of the North Atlantic Oscillation index (NAO) was obtained from the web site of the Climatic Research Unit of the University of East Anglia (Norwich, UK): <http://www.met.rdg.ac.uk/cag/NAO/slpdata.html>. Then we computed the year average of NAO, whose relationship with landings of three years later has been detected through cross-correlation analysis in previous studies by [Maynou \(2008\)](#).

The total number of observations amounts to  $N = 2314$  using the whole data set: 21 trawlers having practised deep-fishing in the period from January 1992 to December 2008 (17 complete years). Landings of the whole fleet were monitored over time, so, they depict the entire population of the fleet in the studied area and period. Red shrimp fishery is a specific fishery, thus, all the product caught on board appears in landings, due to its high commercial value, while, when landings are not reported for a given boat is due to its inactivity, rather than to zero catches of the source.

The landings (*lands*) and number of trips (*trips*) were used to estimate *lpue*, the “nominal” LPUE index,

$$lpue_{ij} = \frac{lands_{ij}}{trips_{ij}}, \quad (4.1)$$

where  $i$  and  $j$  refer to the observation  $i$  of the vessel  $j$ . The difference with Equation 3.1 of the previous chapter is that here the subindex  $j$  makes explicit the grouping of the observations of the same boat.

Table 4.1 and the introductory part of this section provides information on all variables involved. Trips are always performed in one day, hence, the *lpue* represents the daily biomass average caught by a boat during one day ( $\text{kg d}^{-1}$ ) with a monthly resolution.

As in previous regression analysis, months associated to not significant parameters of the categorical variable *months* with categories  $month_k$ ,  $k = 1, \dots, 12$  were backward assembled into two categories of a new variable *period* (period of the year): *period1* defines all months excluding June and November and *period2* refers to June and November. All variables are summarised in Table 4.1.

Variable	Description
<i>lands</i>	the total catches landed at port by each boat in one month
<i>lpue</i>	the daily LPUE index for each boat calculated as in Eq. 4.1
<i>code</i>	a categorical variable assigned to each boat, $c = 1, \dots, 21$
<i>time</i>	a total of 204 months from January 1992 to December 2008 coded with a letter and two digits, e.g. J92 is January 1992
<i>trips</i>	the number of trips performed by each vessel during one month
<i>grt</i>	Gross Registered Tonnage of each boat
<i>nao<sub>3</sub></i>	mean annual NAO index of 3 years before the year of estimated <i>lpue</i>
<i>month</i>	categorical variable with $m = 1, \dots, 12$ from January to December
<i>period</i>	binary variable with grouped months holding the same effect <i>period1</i> = all month excluding June and November <i>period2</i> = June and November

TABLE 4.1: List of variables.

## 4.2.2 Methodology

It has become quite popular to model the expected LPUE conditional on covariates  $x_1, \dots, x_P$  as a function of linear covariates effects. The results obtained from linear mean regression are easy to interpret but depreciated by possible misspecification due to a more complex underlying covariate structure, violation of homoscedastic errors or correlations caused by clustered data. To deal with these problems we apply Bayesian distributional structured additive regression models (Klein et al., 2013) a model class originally proposed by Rigby and Stasinopoulos (2005) in a frequentist setting. The idea is to assume a parametric distribution for the conditional behaviour of the response and to describe each parameter of this distribution as a function of explanatory variables as has been described in Section 1.5. In the

following, we consider log-normal and gamma distribution since the response in this study is skewed and always greater than zero.

We consider the log-normal distribution with parameters  $\mu_{ij}$  and  $\sigma_{ij}^2$  such that

$$E[lpue_{ij}] = \exp\left(\mu_{ij} + \frac{\sigma_{ij}^2}{2}\right)$$

$$Var[lpue_{ij}] = (\exp(\sigma_{ij}^2) - 1) \exp(2\mu_{ij} + \sigma_{ij}^2).$$

Accordingly,  $\log(lpue_{ij})$  is normal distributed with

$$E[\log(lpue_{ij})] = \mu_{ij}$$

and

$$Var[\log(lpue_{ij})] = \sigma_{ij}^2.$$

As an alternative, we assume a gamma distribution with parameters  $\mu_{ij} > 0$ ,  $\sigma_{ij} > 0$  and density

$$f(lpue_{ij}|\mu_{ij}, \sigma_{ij}) = \left(\frac{\sigma_{ij}}{\mu_{ij}}\right)^{\sigma_{ij}} \frac{lpue_{ij}^{\sigma_{ij}-1}}{\Gamma(\sigma_{ij})} \exp\left(-\frac{\sigma_{ij}}{\mu_{ij}} lpue_{ij}\right).$$

Then, the expectation and variance are given by

$$E[lpue_{ij}] = \mu_{ij} \quad Var[lpue_{ij}] = \frac{\mu_{ij}^2}{\sigma_{ij}}$$

such that  $\mu_{ij}$  is the location parameter and  $\sigma_{ij}$  the shape that is inverse proportional to the variance.

All parameters involved are linked to structured additive predictors, yielding

$$\eta_{ij,\mu} = \mu_{ij} \quad \eta_{ij,\sigma^2} = \log(\sigma_{ij}^2)$$

for the log-normal distribution where the log-link is used to ensure positivity of the  $\sigma_{ij}^2$ .

For the gamma distribution, both parameters are restricted to be positive so that we obtain

$$\eta_{ij,\mu} = \log(\mu_{ij}) \quad \eta_{ij,\sigma} = \log(\sigma_{ij}).$$

For each parameter, a generic structured additive predictor is of the form

$$\eta_{ij,\theta_k} = z'_{ij}\delta + \sum_{p=1}^P s_p(x_{ijp}) + \alpha_i,$$

that recalls Equation 1.33 for a  $k$ -order parameter  $\theta$  of the distribution. Here,  $s_1, \dots, s_P$  are modelled by Bayesian P(enalized) splines (Lang and Brezger, 2004), assuming that  $s_p$  can be approximated by a linear combination of B-spline basis functions (Eilers and Marx, 1996). Hence,  $s_p$  can be written in matrix notation as  $Z_p\beta_p$ , where  $Z_p$  is the design matrix with B-spline basis functions evaluated at the observations and  $\beta_p$  is the vector of regression coefficients to be estimated. To enforce smoothness of the function estimates we use second order random walk priors for the regression coefficients such that

$$p(\beta_p|\tau_p^2) \propto (\tau_p^2)^{-0.5\text{rank}(K)} \exp\left(-\frac{1}{\tau_p^2}\beta_p'K\beta_p\right)$$

where  $K = D'D$  for a second order difference matrix  $D$  and  $\tau_p^2$  are the smoothing variances with inverse gamma hyperpriors.

The additional, boat-specific effect  $\alpha_i$  is introduced to represent any effect specific to the catching unit that is not represented in the covariate effects of  $z_{ij}, x_{ij1}, \dots, x_{ijP}$ . A standard assumption for this effect would be  $\alpha_i$  i.i.d.  $N(0, \tau^2)$ , to acknowledge the fact that the catching units represent a sample from the population of catching units. Alternatively,  $\alpha_i$  can be treated as a fixed effect resulting from dummy coding of the different catching units. There has been considerable debate in the past (Bishop et al., 2004; Cooper et al., 2004; Helser et al., 2004; Venables and Dichmont, 2004) about whether it is more appropriate to specify  $\alpha_i$  as random or fixed effects from a methodological perspective, but then random effects have been rarely considered (e.g. Marchal et al., 2007). One differentiation goes along the lines discussed above, i.e. differentiating between situations where the catching units in the data set define a (random) subsample of the population of the

catching unit (which would favour the specification as random effects) and situations where (almost) the complete fleet has been observed (which would favour the specification as fixed effects). From the Bayesian perspective, this differentiation provides an incomplete picture since the differentiation between random and fixed parameters only corresponds to a difference in prior specifications. From a practical point of view the random effects assumption can also be seen as a possibility to regularise estimation in case of large numbers of catching units and/or small individual time series where estimation of fixed effects may easily become unstable. Note also that in case of a fixed effects specification, no other time-constant covariates  $z_i$  characterising the catching units can be included since they can not be separated from the fixed effects. In our data set, this applies for the gross register tonnage which may be expected to provide important information on LPUE but which can not be included in a fixed effects analysis. This problem can be avoided for example by clustering catching units but with a probable loss of information (as the solution used in [Mamouridis, Maynou and Aneiros Pérez, 2014](#)). In the next section, we compare the performance of random and fixed effects specifications based on model fit criteria to decide which model has a better explanatory ability.

Our inferences is based on efficient Markov chain Monte Carlo (MCMC) simulation techniques (for more details see [Klein et al., 2013](#)). In principle, the approach in all models could also be performed in a frequentist setting ([Stasinopoulos and Rigby, 2007](#)) via direct optimization of the resulting penalized likelihood which is often achieved by Newton-type iterations with numerical differentiation. However, many models turned out to be numerically unstable leading to no estimation results or warnings concerning convergence. Therefore the study is restricted to the Bayesian analysis. The Bayesian approach with MCMC also reveals several additional advantages, e.g. simultaneous selection of the smoothing parameters due to the modularity of the algorithm, credibility intervals which are directly obtained as quantiles from the samples and the possibility to extend the model for instances with spatial variations. All models have been estimated in the free open source software BayesX ([Belitz et al., 2012](#)).

The performance of models is compared in terms of the Deviance Information Criterion, DIC ([Spiegelhalter et al., 2002](#)). The DIC is similar to the frequentist Akaike Information Criterion, compromising between the fit to the data and the complexity of the model. Furthermore it can easily be computed from a sample

$\theta^1, \dots, \theta^M$  of the posterior distribution  $p(y|\theta)$ ,

$$\text{DIC} = 2\overline{D(\theta)} - D(\bar{\theta}),$$

with deviance  $D(\theta) = -2 \log(p(y|\theta))$  and  $\overline{D(\theta)} = \frac{1}{M} \sum_{m=1}^M D(\theta^m)$ ,  $\bar{\theta} = \frac{1}{M} \sum_{m=1}^M \theta^m$  respectively. We also use the DIC to determine important variables and optimal predictors  $\eta_{i,\mu}$  and  $\eta_{i,\sigma^2}$  or  $\eta_{i,\sigma}$ .

To validate the distribution assumption we used normalized quantile residuals. That allowed to decide between equivalent models under different response assumptions. Normalized quantile residuals are defined as  $r_i = \Phi^{-1}(u_i)$ . Here,  $\Phi^{-1}$  is the inverse cumulative distribution function of a standard normal distribution and  $u_i$  is the cumulative distribution function of the estimated model and with plugged in estimated parameters. For consistent estimates, the residuals  $r_i$ ,  $i = 1, \dots, n$  follow approximately a standard normal distribution if the estimated distribution is the true distribution. Therefore, models can be compared graphically in terms of quantile-quantile-plots.

Finally, we performed a k-fold Cross Validation to assess the predictive accuracy of the models using the mean squared error of prediction (MSEP)

$$\text{MSEP}_k = \frac{\sum_{i=1}^N (lpue_{i,k} - \widetilde{lpue}_{i,k})^2}{N}.$$

Here  $lpue_{i,k}$  is the observation  $i$  of subset  $k$ ,  $\widetilde{lpue}_{i,k}$  is the prediction of the expected LPUE in the validation set, given parameters estimated on the  $k$ -th training set and  $N$  refers to the number of observations of the corresponding validation set. We performed a 10 fold random partition within each catching unit to ensure a minimum number of observations for each boat in both the training and the validation sets. Taking the 10% of the data to built the latter, we ensure at least 10 observations per unit in the validation set. If at least one catching unit is not represented in one of the partitions, the prediction for the missing catching unit in fixed effects models could not be computed. This clarifies the usefulness of mixed effects models when interested on predictions for unobserved units.



## 4.3 Results

### 4.3.1 Model selection, diagnostics and comparison

Variables were chosen using a stepwise forward procedure according to DIC scores. For each distribution we first modelled the predictor for location, adding variables till the best combination. Then, using the most appropriate predictor for location, also the predictor for the second parameter, scale or shape, depending on the distribution assumed, has been modelled using the same procedure. We imposed the same number of knots found in Chapter 3 using the effective degree of freedom (edf) returned by the frequentist approach (Wood, 2006).

According to the DIC scores, for log-normal assumption, the appropriate predictor structures for location  $\eta_\mu$  and scale  $\eta_{\sigma^2}$ , are

$$\begin{aligned}\eta_\mu &= \beta_{0,\mu} + \beta_{1,\mu}period_2 + s_{1,\mu}(trips) + s_{2,\mu}(time) + s_{3,\mu}(nao_3) + \sum_i \alpha_{i,\mu} \\ \eta_{\sigma^2} &= \beta_{0,\sigma^2} + s_{1,\sigma^2}(trips) + s_{2,\sigma^2}(time) + \sum_i \alpha_{i,\sigma^2}\end{aligned}\tag{4.2}$$

for both fixed and mixed effects specification. Here the  $\beta_{k,\cdot}$  are parameters associated to the intercept and linear fixed effects of the variable *period*. The  $\alpha_{i,\cdot}$  are parameters associated to the effects of *code*, specified as fixed in fixed effects models and as random in mixed effects models. Instead,  $s_{l,\cdot}$  are smooth functions associated to nonlinear effects of the variables *trips*, *time* and *nao<sub>3</sub>*. The second sub-index of all parameters identifies which predictor the parameter or function belongs,  $\eta_\mu$  or  $\eta_{\sigma^2}$  respectively.

Using fixed effects specification for *code* the inclusion of variable *grt* leads to instability, due to the reasons mentioned in Section 4.2.2, so then, the model with *grt* cannot be estimated in these cases. On the contrary, *grt* could be estimated in mixed effect models and it returned significant positive effect, however the DIC score was equal or lightly higher (although with minimum difference). Thus, for the purpose of this study it has been backward eliminated to be able to compare consistently fixed and mixed effects models with the same variables.

Under the gamma distribution assumption, the log-link function has been chosen, since the support of both parameters is the positive real domain and the final predictor structures for location and shape are

$$\begin{aligned}\eta_{\mu} &= \beta_{0,\mu} + \beta_{1,\mu}period_2 + s_{1,\mu}(trips) + s_{2,\mu}(time) + s_{3,\mu}(nao_3) + \sum_i \alpha_{i,\mu} \\ \eta_{\sigma} &= \beta_{0,\sigma} + s_{1,\mu}(trips) + s_{2,\sigma}(time) + \sum_i \alpha_{i,\sigma}\end{aligned}\tag{4.3}$$

for both fixed and mixed effects specification. The notation here is the same specified for the log-normal models however here the second parameter, the shape, is denoted with  $\sigma$ .

The Table 4.2 provides a selection of models that we used for comparison purposes and their corresponding global parameters: the deviance, the effective number of parameters and the DIC, estimated on the whole dataset, and the MSEP calculated by predictions on the validation subsets as described in the methodology. These eight models present a combination between alternatives of the following parametrisations:

- (A) The log-normal (LN) or gamma (GA) as the underlying distribution assumption;

M	A	B	C	DEV	EP	DIC	MSEP
M1	LN	LO	FI	16163.9	47.1	16258.0	98.3 ± 12.3
M2	LN	LO	MI	16164.2	46.8	16257.7	96.9 ± 12.4
M3	LN	LS	FI	15138.4	91.2	15320.8	436.2 ± 434.9
M4	LN	LS	MI	15142.7	87.2	15317.2	315.0 ± 307.4
M5	GA	LO	FI	16095.7	45.6	16187.0	77.8 ± 11.5
M6	GA	LO	MI	16096.8	43.9	16184.7	77.3 ± 11.7
M7	GA	LS	FI	15027.1	90.9	15208.9	71.5 ± 9.2
M8	GA	LS	MI	15032.4	86.9	15206.1	71.7 ± 9.4

TABLE 4.2: Global scores of selected models. M: model coding; A: the assumed distribution is log-normal (LG) or gamma (GA); B: (LO) the location varies w.r.t. explanatory variables while the second parameter is constant or (LS) both vary; C: if the unit-specific effect is considered as fixed, thus the model has only fixed effects (FI) or random and the model is a mixed effects model (MI); DEV, the residual deviance; EP: Effective total number of Parameters, DIC: Deviance Information Criterion, MSEP, mean and sd of the mean square error of predictions calculated through 10-fold validation.

- (B) Only location (LO) or both location and scale/shape (LS) parameters explicitly modelled using one or more explanatory variables;
- (C) Effects of *code* as fixed or random leading to a fixed effects model (FI) or mixed effects model (MI) respectively;

The predictors for location in models denoted as M1, M2, M5 and M6 (with B=LO) have the same structure of  $\eta_\mu$  in Equations 4.2 and 4.3, while the corresponding predictor for scale/shape is a constant. Both predictors in models M3, M4, M7 and M8 correspond to Equations 4.2 and 4.3.

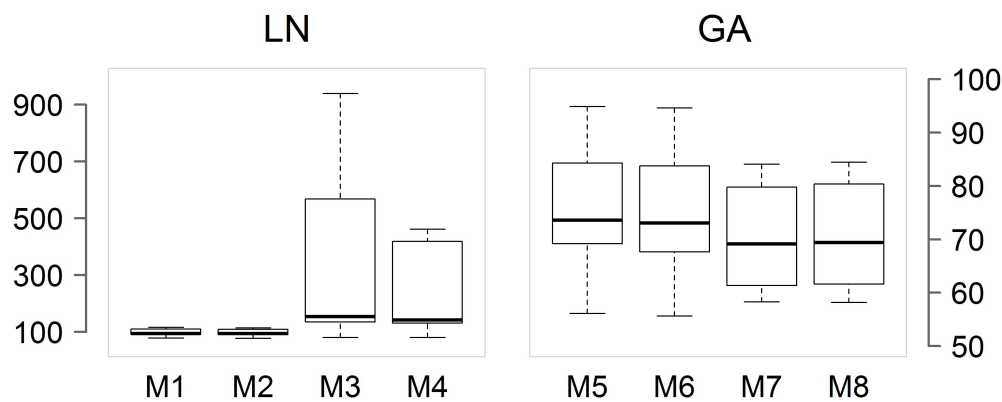


FIGURE 4.1: Boxplots for MSEP calculated for all models. See Table 4.2 and Equations in the text for model specifications.

Concerning to (A), model specifications widely favour the gamma over the log-normal distribution. In fact DIC scores are lower under the gamma assumption, with approximately 100 scores of difference between analogous models (i.e. same variables specified in the predictors). The benefit in assuming the gamma distribution is also evident comparing MSEP scores (lower scores for better predictions). Nevertheless, results of log-normal models' MSEP is not entirely satisfactory, because when accounting for both predictors MSEP should behave as in the gamma models, i.e. lower scores when considering both predictors than accounting only for  $\eta_\mu$ . Regarding to the estimation of both predictors for first and second parameters (B), models under the gamma assumption show an improvement when explicitly modelling the dependence of second parameter  $\sigma$  from explanatory variables in both DIC and MSEP scores (both decrease). Contrariwise, under the log-normal assumption, however the DIC decreases, the MSEP increases and presents higher variability, suggesting worse predictions, when the second parameter is explicitly

modelled. But as discussed few lines above,  $\eta_{\sigma^2}$  follows a strange behaviour and further research is needed.

Finally no notable leaps have been observed between fixed and random effects models (C). Whereby the best DIC and MSEP scores and QQplots lead to the final model with predictors given in (4.3).

According to the DIC (Table 4.2) the model providing better estimations is the gamma model (M8, predictors given in Equation 4.3) specifying catching units as random effects.

The boxplots of MSEPs also favour the gamma assumption (see Figure 4.1 and values in Table 4.2). The minor MSEP the better prediction, MSEP results divide models into three distinguishable groups from highest to lowest mean MSEP: 1) log-normal models considering scale modelling, 2) log-normal models considering  $\eta_{\sigma^2}$  constant (compare M1-M2 with M3-M4), and 3) all gamma models (M1, M4, M5 and M8). Within this group, modelling the shape in dependence to variables, consistently decreases MSEP estimates, e.g. in terms of median and variance of the MSEP (compare M5 and M6 with M7 and M8).

In order to validate the distribution assumptions, QQplots for residuals are reported in Figure 4.2, from which it follows that:

- the residuals in gamma models almost follow the straight line (M5 and M8 in the Figure), while in the log-normal they show upward-humped curves (M1 and M4), suggesting a definitively “better approximation” of models to the gamma distribution.
- Modelling the second parameter in gamma models improves QQplot outputs, while the opposite happens for log-normal models. Focusing only in gamma models, the outlier is “absorbed” into the straight line in the right part validating the improvement in estimations (compare M5 and M6 with M7 and M8 in Figure 4.2).

We finally assessed the normality for random effects for the model M8 corresponding to Equation 4.3. Figure 4.3 provides the QQplots of the random effects for both predictors. The majority of sample quantiles approximatively follow the normal quantiles, however they depart from it at the extremes, especially evident in the lower tails and for  $\alpha_{\mu}$  (on the left).

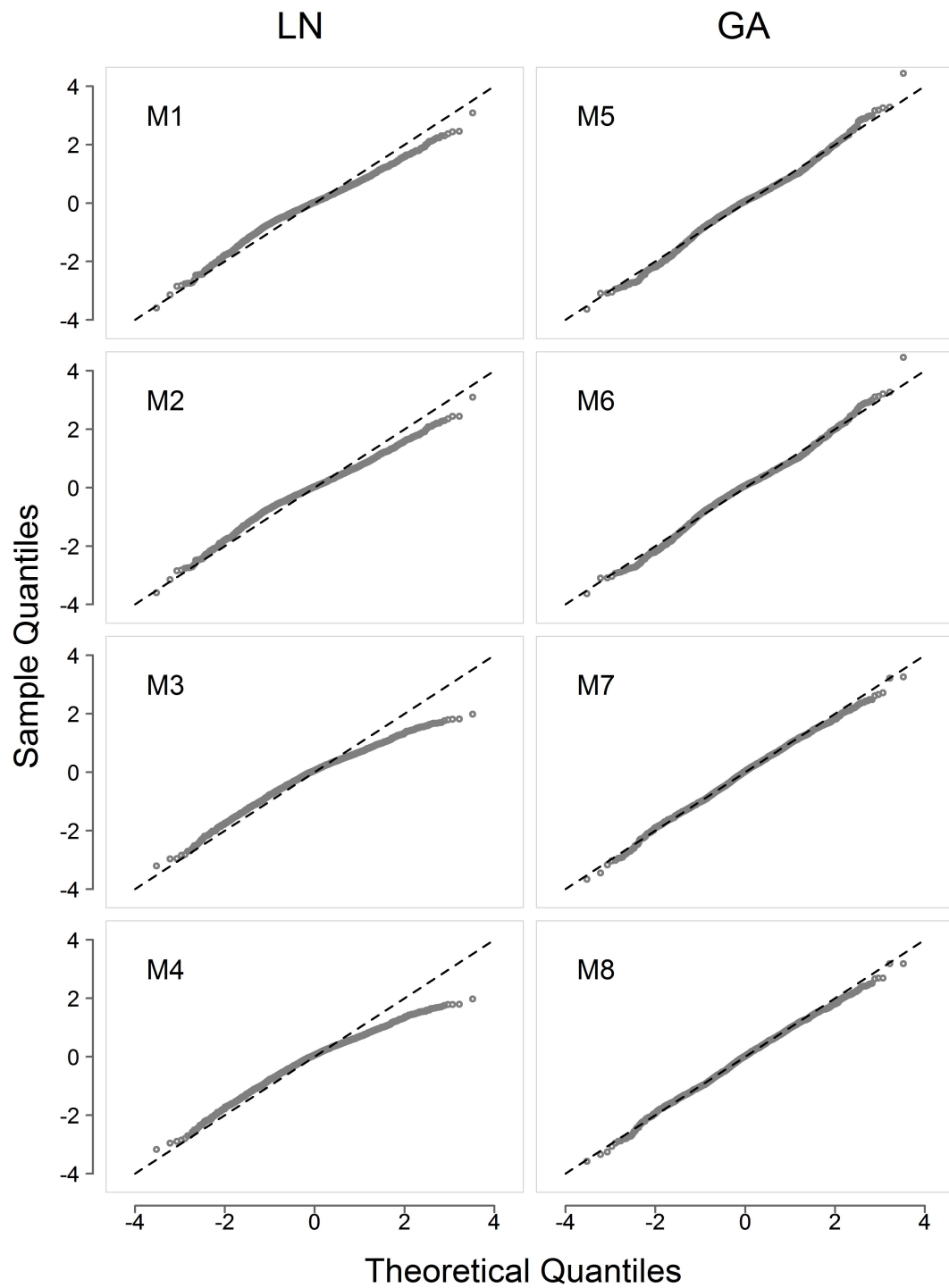


FIGURE 4.2: QQplots of the normalized residuals calculated as described in the methodology section for all models.

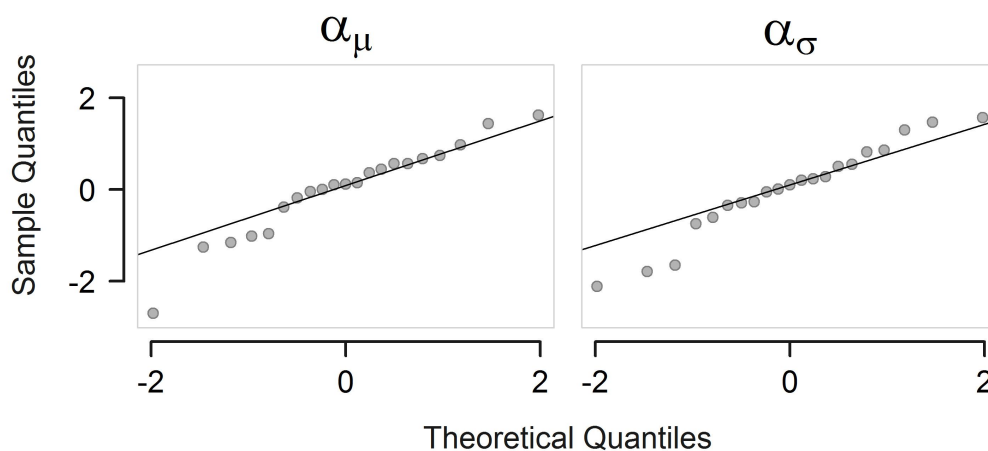


FIGURE 4.3: QQplots for normality of catching units parameters as random effects in the mixed model M8.  $\alpha_\mu$  refer to random effects in the predictor for location, while  $\alpha_\sigma$  refers to the predictor for the shape.

### 4.3.2 Description of partial effects

Estimations of linear fixed effects for A)  $\mu$  and B)  $\sigma$  predictors of final model M8, (4.3), are reported in Table 4.3 and nonparametric effects are shown in Figure 4.5.

All partial effects associated to  $\eta_\mu$  are linked to the expectation of LPUE,  $E(\text{LPUE})$ , through the exponential of  $\eta_\mu$ . When partial effects hire positive values, the expectation increases while decreases otherwise. Contrariwise the variance of LPUE is affected by both predictors being directly proportional to  $\mu$  and inverse proportional to  $\sigma$ .

	A)		B)	
	mean	sd	mean	sd
<i>const</i>	2.889	0.059	1.743	0.096
<i>period<sub>2</sub></i>	-0.154	0.023		

TABLE 4.3: Estimations of linear fixed effects for the model M8, Eq. (4.3) associated to A)  $\mu$  and B)  $\sigma$  respectively.

The variable *period* describes the intra-annual variability and shows a negative effect in *period<sub>2</sub>*, corresponding to June and November in comparison to the rest of the year. That should be related to a lower demand of this source during these months.

The variable *grt* (results not reported), referring to the gross registered tonnage of boats, returns a significant and positive slope parameter, causes a linear increment on the predictor for location. Its effect has been estimated in Chapter 3. However it has a minor impact in the considered dataset, it can be important when comparing with other fisheries where it could (or not) have a major impact on the response. *grt* is not the only variable characterising a fleet, nevertheless it is the only reliable available metric for boats of this fishery.

The second fishery-related variable is *code*, representing catching units' effect. The variable captures abilities of fishermen and technical characteristics of the fleet, appropriate technologies and strategies, e.g. the power and type of the engine, the net shape and the skipper's expertise and ability. Results (Figure 4.4) show that many trawlers have similar effects (around zero), but many of them hold positive or negative effects. The former are very specialised and powerful boats catching large amounts of the resource leading to higher values of LPUE while the latter are not specialised in deep-sea fisheries and capture lower amounts, leading to lower LPUE (see the partial effects on  $\mu$ ). At the same time catching units associated to higher effects on the predictor of  $\mu$  also present higher effects on the predictor for  $\sigma$ , while boats associated to lower effects on  $\mu$  also hold lower

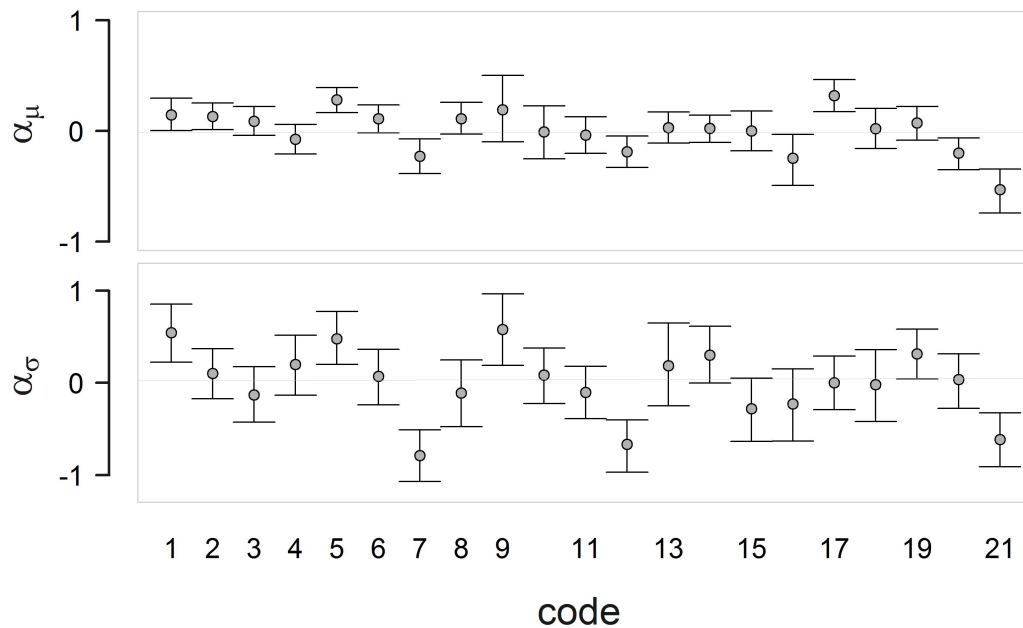


FIGURE 4.4: Interval plots of estimated random effects in the predictor for location ( $\alpha_\mu$ ) and shape ( $\alpha_\sigma$ ) on the upper and lower plots respectively. Bars indicates 95% CI.

effects on  $\sigma$ . In summary, more specialised trawlers capture more quantities and also present less variability (see the relationship between shape and variance in gamma distribution). Contrariwise not specialised trawlers catch less quantities and present more variability in landings. This fraction of the fleet more likely is represented by boats that fish on the continental shelf and occasionally displace towards deeper waters going in search of the red shrimp.

Concerning to nonparametric effects (Figure 4.5), *trips* and *time* influence both  $\eta_\mu$  and  $\eta_\sigma$ , while *nao3* showed to slightly affect only  $\eta_\mu$ .

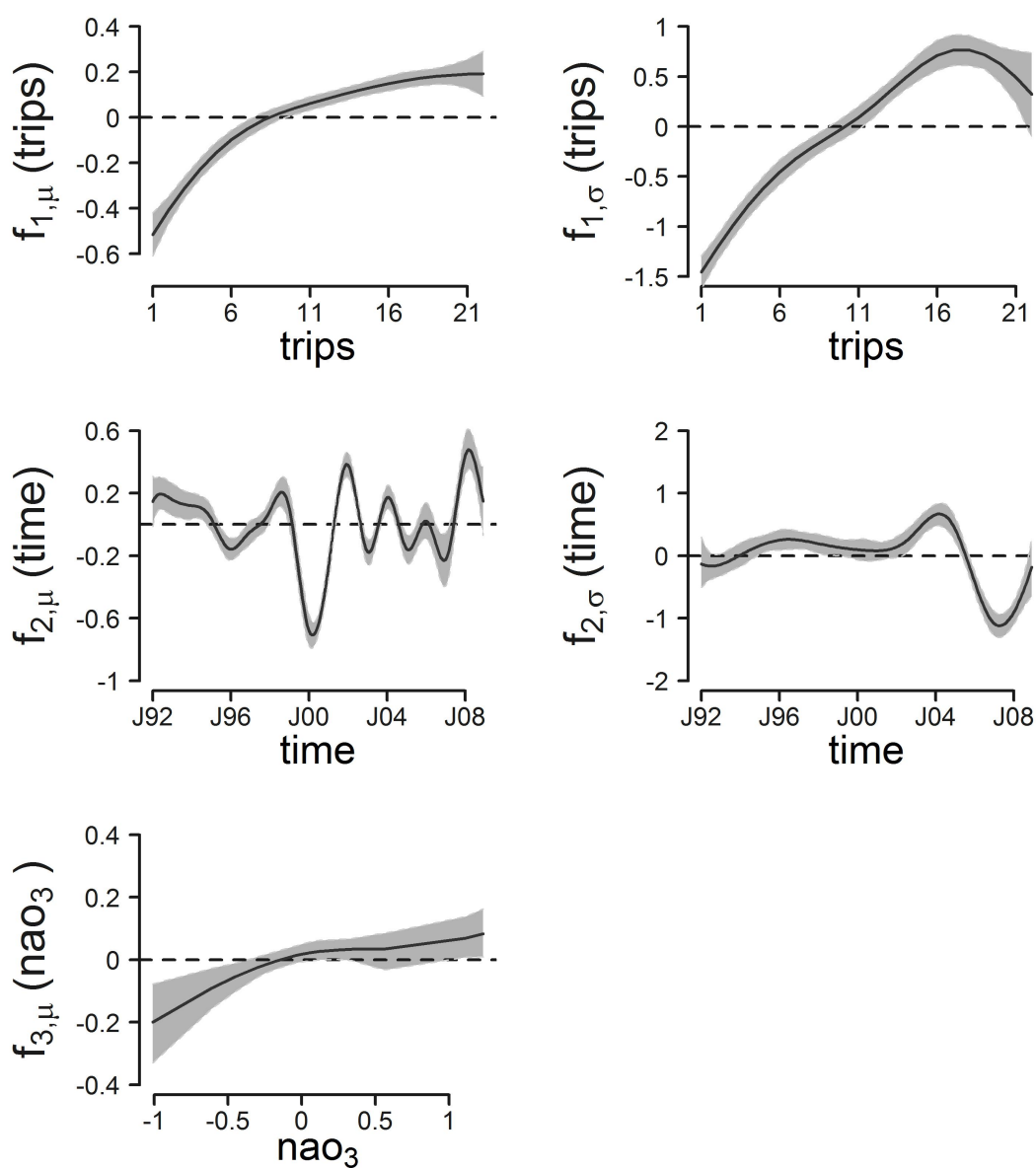


FIGURE 4.5: Nonparametric effects for the model M8. Effects on predictors for  $\mu$  (left side) and for  $\sigma$  (right side). Grey shapes represent 95% credible intervals.



Variable *trips* shows a negative effect on the predictor for  $\mu$  when  $trips \leq 8$ , while positive otherwise. The rate of the effect rises moving through the covariate interval till a plateau beginning around  $trips = 17$ . For extreme high values *trips* has an uncertain effect. Low values of its effect could be associated with the trawlers operating usually on the continental shelf and with less knowledge of red shrimp fishing grounds (Maynou et al., 2003) and/or to period of bad weather and vice versa for high values. Increasing the number of trips per month, also the probability to find high-concentration shoals inside the fishing grounds increases for a given boat in a process of trial and error as suggested by Sardà and Maynou 1998.

The effect of *time* on the predictor for  $\mu$  shows high inter-annual variability, certainly caused from multiple factors. Between 1992-1996, the effect decreases while increases in next three years. We could not find a reasonable explanation to this trend. Afterwards, between 1999-2000, it drops till a minimum low followed by a rapid increase up to a pick in 2004. We believe that the minimum is related to both negative NAO observed in previous years and to the rising of fuel price started in 2000, that in turn is related to a lower number of trips performed by trawlers (see discussion in Chapter 3. Then, for five years it presents a slightly oscillatory trend till the last year characterised by another positive pick probably related to the rise of the economic value of the resource, that offsets the increase in the fuel price.

Finally, results show that  $nao_3$  has a moderate effect for this deep-sea species, however it can lead to a significant reduction of LPUE when reaches negative values shown by the partial effect lower than zero for negative NAO values. On the contrary the positive effect on LPUE for high values of the NAO is less evident.

In the predictor for  $\sigma$ , the effect of *trips* is negative for low values of the covariate ( $trips \leq 10$ ) and positive for higher values. It also shows a high increment till a maximum corresponding to  $trips = 17$ , while decreasing again for higher values, but continuing to be positive. The effect of *time* is slightly negative before 1995 and slightly positive between 1995 and 2000. Then for two years has no effect. Then, in 2002 it switches clearly positive again till 2006, showing a high pick in 2004 and finally negative in the last years during 2006-2008, reaching an abrupt drop in late 2007. Thus, regarding to the  $Var(LPUE)$ , results that values of covariates associated to positive effects in  $\eta_\mu$  and negative effects in  $\eta_\sigma$ , in turn affect positively (increase) the variance. We can therefore deduce that *time* is

the driver in causing the heteroscedasticity in LPUE, mainly in last years when its effect on  $\eta_\mu$  is positive and its effect on  $\eta_\sigma$  is strongly negative. This high variability could be related to different factors, mainly of economic origin, such as the fuel and ex-vessel shrimp prises as discussed above.

## 4.4 Discussion

In this study we proposed distributional structured additive models (DSTAR) for the first time to model the LPUE index (or CPUE) widely used in fisheries research. Data deal with the LPUE of red shrimp (*A. antennatus*) from the Barcelona's fleet during years 1992 – 2008.

On a methodological view, we demonstrated that the gamma distribution more properly describes residuals providing better estimations as shown by results of the deviance information criterion (DIC) and the QQ-plots and also better predictions (MSEP).

In addition, distributional structured additive models, as the frequentist counterpart, the generalized additive models for location scale and shape GAMLSS, allowed to model both first and second order moments of the response, returning even better estimates, when considering the second parameter. In fact the second moment (the shape for gamma distribution or scale for log-normal) can be explained by many of the explanatory variables we used (i.e. *trips* and *time*). Thanks to this kind of models we rose a more detailed understanding of how and why LPUE changes and how it is affected by the covariates. For example the analysis performed on (almost) the same data set, a frequentist approach using GAM accounting only for the location, could not avoid the heteroscedasticity in the residuals (see Figure C.2). Here we demonstrated that both the number of trips and time strongly influence the second parameter, that in turn is (inverse) proportional to the variance (while the location is directly proportional). This meant, e.g., that during years 2007-2008 the variance is higher and is effected by both  $\mu$  and  $\sigma$ , such that the predictor for location increases, while the predictor for the shape decreases. This high variability could be related to different factors, mainly of economic origin, such as the fuel and ex-vessel shrimp prises. Thus,

regarding to the  $Var(LPUE)$ , results that values of covariates associated to positive effects in  $\eta_\mu$  and negative effects in  $\eta_\sigma$ , in turn affect positively (increase) the variance.

The LPUE also showed a seasonality probably related to the demand of this source across the months. The gross registered tonnage of boats returns a significant and positive effect the LPUE. The effects and importance of these variables have been estimated in Chapter 3. However significant they returned very low impact with respect to all other variables considered.

The NAO is a very interesting environmental variable. It has a moderate effect for this deep-sea species, however results suggest that it can lead to a significant reduction of LPUE when it reaches negative values. Numerous publications demonstrated its influence on marine populations and on different exploited stocks, including this and other fish stocks (e.g. [Báez et al., 2011](#); [Maynou, 2008](#)). These authors show that the NAO can bear important effects when either it is extremely positive or negative. Considering both results of TIME and NAO and comparing data series of both the raw LPUE and the NAO, we believe that the LPUE low starting at the end of 1999 can be related to consecutive negative NAO during the previous four years, especially during 1996, corresponding to three years before the beginning of the decline of LPUE. Negative NAO leads to paucity of resources while it enhances productivity when it is highly positive. Between  $nao_3 = 0.50$  and  $nao_3 = 1$  the effect increases however without a significant evidence. In the middle region of the variable span, there is no effect, that could represent a “buffering region” related to “normal” weather conditions for the stock. In some studies the relationship NAO-stock has been explained by the modulation of the recruitment strength (in cod: [Brodziak and O’Brien, 2005](#)) and the effect is stronger when the spawning stock biomass is low ([Brander, 2005](#)). In many cases has been found that the relationship is mediated by changes in prey composition and biomass, i.e. zooplankton (see e.g. [Fromentin and Planque, 1996](#); [Reid and Croxall, 2001](#); [Stige et al., 2006](#)). In our case, we found that NAO strongly influences the red shrimp biomass when it is low. That is in accordance with the founding by [Brander \(2005\)](#) for the cod. In fact, being landing and so the lpue as well, composed mainly by mature individuals, we can infer that NAO play a higher role when the spawning stock biomass is low. To the other hand we found a positive relationship when both NAO and stock are high. This is in agreement with ([Maynou, 2008](#)). The author suggested that positive NAO is related to low rainfall, that in turn is linked

to enhanced vertical mixing of water masses in the NW Mediterranean (Gulf of Lions: [Demirov and Pinardi, 2002](#); [Jordi and Hameed, 2009](#), because when rainfall is low, waters are saltier (and so more dense), and superficial waters tend to fall dawn. Has been postulated that when this occurs the red shrimp switch from its generalistic diet to a high-energy content diet based on zooplankton ([Cartes, Madurell, Fanelli and López-Jurado, 2008](#); [Maynou, 2008](#); [Vicente-Serrano and Trigo, 2011](#)). Increasing the resource (of high quality), the predator (red shrimp in this case) assimilates more energy and the stock is expected to increase as well.

Catching-units captures all abilities of fishermen and technical characteristics. We found that many trawlers have similar effects (or no effect). However many of them hold positive effects on mean LPUE and vice versa on variance. This portion of the fleet is composed by very specialised and powerful boats that catch large amounts of the resource. The LPUE also returns lower variability. On the contrary those holding a negative effect capture less amounts and the LPUE presents high variability. They are probably specialised in other fisheries. Also low values of TRIPS effect could be associated with not specialised trawlers operating usually on the continental shelf and with less knowledge of red shrimp fishing grounds ([Maynou et al., 2003](#)) and/or to period of bad weather and vice versa for high values. The number of trips is also associated to find high-concentration shoals improving the expertise of fishermen in a process of trial and error as suggested by [Sardà and Maynou 1998](#).

Finally we point out another methodological issue concerning to fixed versus mixed specification. In our study the fixed effects can be considered appropriate representing sampling units the whole population of the studied fleet (in accordance to the definition by [Pinheiro and Bates, 2000](#)), however mixed models are particularly suitable not only for unobserved catching units but also for correlated observations in time series analysis. In practise we clashed with estimation instability when trying to incorporate both CODE and TRB in fixed effects models. We could avoid the problem clustering catching units when modelling LPUE with generalized additive models in Chapter 3. In the present Chapter with the incorporation of random effects into a mixed effects model, we avoided this drawback.

**Acknowledgements:** Authors would like to thank the Fisheries Directorate of Catalonia's Autonomous Government to facilitate access to the sales data of the

Barcelona Fishers' Association, as well as fishers of Barcelona. Financial support from the Spanish National Council of Research (CSIC) through the JAE-predoc grant and the German Research Foundation (DFG) grant KN 922/4-1 are gratefully acknowledged.



---

PART III

---





## CHAPTER 5

---

Food web modelling in a soft-bottom continental slope  
ecosystem (NW Mediterranean)

---

## Abstract

We present a quantitative food-web analysis of the soft bottom community at the continental slope of the NW Mediterranean at 600–800 m depth. A total of 40 carbon flows among 7 internal and 6 external compartments, were reconstructed using linear inverse modelling (LIM) by merging site-specific biomass data, on-board oxygen consumption rates and published parameters to create population and physiological constraints. The total carbon flux to the community was 2.62 mmol C m<sup>-2</sup> d<sup>-1</sup> (range estimations: 0.92 – 4.16 mmol C m<sup>-2</sup> d<sup>-1</sup>), entering as vertical OM (average: 5.2E-03, range: 8.9E-04 – 2.5E-02) and advective OM (average: 2.6E-00, range: 9.2E-01 – 4.1E-00). The influx was then partitioned between the total organic matter in sediment, 87.05%) and suspension and filter feeders (12.95%), comprising zooplankton (1.08%), suprabenthos (3.07%) and macrobenthos (95.74%).

The fate of carbon deposited in sediments was its burial, its degradation by prokaryotes or the ingestion by metazoan deposit feeders. The total ingestion of C in sediments by the metazoan community (excluding the meiofauna, e.g. nematods) was 0.83 mmol C m<sup>-2</sup> d<sup>-1</sup>, corresponding to 31.68% of the total C entering the food web and to 36.34% of the C in sediments, the rest was used by the prokaryotes and nematods (1.58 mmol C m<sup>-2</sup> d<sup>-1</sup>, 69.28%) or trapped in the sediment (0.73 mmol C m<sup>-2</sup> d<sup>-1</sup>, 32.19%).

The respiration of the whole community (including the TOM) was 1.89 mmol C m<sup>-2</sup> d<sup>-1</sup> (ranging between 0.84 – 2.34): 83.75% for sediments, including prokaryotes and meiofauna, 13.34% for macrofauna, 2.86% for megafauna, including the red shrimp *Aristeus antennatus*.

**Keywords:** food web, bathyal ecosystem, NW Mediterranean, linear inverse modelling

## 5.1 Introduction

Food webs are descriptions of biological interactions between consumers and resources which help to determine the dynamics of populations, as well as the transfer of matter and energy in marine ecosystems (de Ruiter et al., 2005; Polis, 1999). Quantifying the dynamics of deep-sea trophic webs is an important step to increase our understanding of these ecosystems, which are increasingly subject to human exploitation through the extraction of mineral resources or harvesting of fisheries products (de Ruiter et al., 2005). Fishing has direct and indirect impacts on the dynamics of ecosystems, altering their structure and function (Pikitch et al., 2004). The quantitative analysis of networks and their sensitivity to disturbance (mainly changes in the fluxes due to fish harvesting) (de Ruiter et al., 2005) may be of use to fisheries assessment in the newest context of an Ecosystem Approach to Fisheries (EAF, Plagányi, 2007). In deep-sea ecosystems, where traditional data for fisheries assessment is often inadequate as there is limited scientific sampling (van Oevelen et al., 2009), is even more important to find the appropriate techniques in data-limited contexts.

Many tools are available to describe trophic interactions. The most used and popular is ECOPATH with Ecosim (EwE) (Christensen and Walters, 2004). ECOPATH is based on mass balance equations and steady state assumption for the quantitative estimations of flows. It was originally initiated by Polovina (1984) and has been development since 90's (Christensen and Pauly, 1992) into a software, allowing spatio-temporal dynamic simulations (Walters et al., 1999, 2000, 1997). The mathematics below makes use of standard matrix algebra. A generalized inverse is used if the determinant is zero or the matrix is not square (Mackay, 1981). If the set of equations is over-determined (more equations than unknowns) and the equations are not mutually consistent the generalized inverse method provides least squares estimates, which minimise discrepancies (Christensen and Pauly, 1992). ECOPATH also solves under-determined problems for missing stocks, using an iterative algorithm before setting up the set of linear equations, becoming then an even-or over-determined system, that can be solved by the generalized inverse method. It makes use of a defined energy balance within each group using an equation similar to

$$C = P + R + U$$

where  $C$  is consumption,  $P$  production,  $R$  respiration and  $U$  unassimilated food, that represents the basic energy conservation assumption for biological units (Winberg, 1956). However ECOPATH does not explicitly estimate gonadal growth and energetic assumptions cannot be changed.

Also the Linear Inverse Modelling (LIM, Soetaert and van Oevelen, 2009b) is based on mass balance equations but it also allows more flexible construction of physiological constraints giving a flexible tool to formulate energetic assumptions that better fit to available data. The LIM is a modified version of the original LIM proposed by Niquil et al. (1998); Vézina and Savenkoff (1999); Vézina and Platt (1988) and which are based on Least Distance Programming (LDP) or linear Programming (LP) techniques that estimate the flows within biologically reasonable bounds (Diffendorfer et al., 2001). In its original version, these methods selected one food web, the parsimonious (simplest) one, amongst the infinite number of foodwebs that satisfy the data. Later methods were developed to also return the uncertainty of the flows, e.g. by a monte carlo analysis Kones et al. (2006). For under-determined problems, the LIM also permits the estimation of the ranges of physiological parameters (not for stocks).

Thanks to this flexibility, the LIM is particularly suitable for quantifying deep-sea food webs, where data limitation is the normal situation (Soetaert and van Oevelen, 2009b). To date available reconstructed deep-sea food web models using LIM are given for a cold-water coral (*Lophelia pertusa*) community around 800 m depth at Rockall Bank (van Oevelen et al., 2009), in three sections (300-750 m, 2700-3500 m and 4000-5000 m) of the Nazaré canyon (van Oevelen, Soetaert, García, de Stigter, Cunha, Pusceddu and Danovaro, 2011), of a sub-arctic deep sea macrofaunal community in the Faroe-Shetland Channel at 1080 m (Gontikaki et al., 2011), at 2500 m in the deep-sea observatory HAUSGARTEN (Fram Strait, Artic Ocean) (van Oevelen, Bergmann, Soetaert, Bauerfeind, Hasemann, Klages, Schewe, Soltwedel and Budaeva, 2011) and at 4850 m in the Porcupine Abyssal Plain (northeast Atlantic) (van Oevelen et al., 2012).

Another example of food web modelling using the LIM methodology (but not in the deep-sea) is the benthic food web in the Molenplaat intertidal flat located in the saline part (salinity 2025) of the Scheldt estuary (Belgium, The Netherlands) (van Oevelen, Soetaert, Middelburg, Herman, Moodley, Hamels, Moens and Heip, 2006).

In this Chapter we aim to quantify the principal pathways through the food web of the continental slope between 600-800 m in the Catalan Sea (Balearic basin, NW Mediterranean) subjected to red shrimp, *Aristeus antennatus*, fishery (more information on this fishery is given in Chapters 3 and 4). In particular we aimed to: 1) describe the main pathways involved in the bathyal food web and their strength with particular attention on the energy input, the loss due to fishery and the role of red shrimp; 2) characterise the food web through the analysis of network indices, that condense the information contained in the trophic networks (Fath and Patten, 1999; Ulanowicz, 2004).

## 5.2 Materials and Methods

### 5.2.1 The study area

The study area is located on the continental margin of the mainland part of the Balearic basin (NW Mediterranean, Figure 5.1). Data were derived from oceanographic surveys performed along the mid-slope at 600-800 m depth between the Ebro delta and Barcelona city within the BIOMARE (ref. CTM2006-13508-CO2-02/MAR) and ANTROMARE (ref. CTM2009-12214-CO2-01-MAR) projects.

All 7 stations are fishing grounds for *A. antennatus* and are subjected to different intensities of exploitation. Detailed information of the sampled stations are reported in Table 5.1.

CODE	POS	DEPTH (m)	YEAR	HAB
S1-a	41°15N – 02°40E	600	2007	MUD
S1-b	41°15N – 02°40E	800	2007	MUD
S2-a	41°09S – 02°24E	600	2007	MUD
S2-b	41°09S – 02°24E	800	2007	MUD
S3	40°54N – 1°35E	615–648	2011	MUD
S4	40°41N – 01°26E	615–648	2011	MC
S5	40°34N – 01°26E	615–648	2011	MC

TABLE 5.1: Main information about sampling statio: CODE: code of each station; POS: the corresponding positions; DEPTH: the corresponding depths; YEAR: the years when samples were performed; HAB: specific habitat, MUD: mud habitat on the open slope, and MD: mud coral habitat (with *Isidella elongata*) on the open slope.

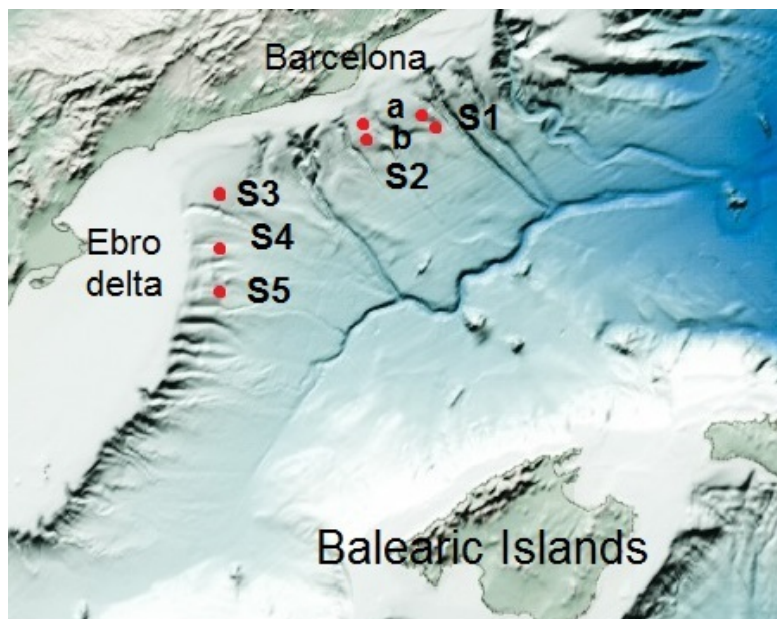


FIGURE 5.1: The food web study area comprises the soft-bottom slope in front of the Catalonia at 600-800 m.

In the NW Mediterranean, the deep sea presents unique characteristics, e.g. warm temperatures ( $13^{\circ}\text{C}$  in comparison to the deep ocean,  $2\text{--}4^{\circ}\text{C}$ ) and high salinity (38 ppt) below 150 m. The area is characterized by soft-sediments at the bottom and by late winter blooms at the surface with a deep chlorophyll maximum (DCM) in open waters during summer (Estrada, 1996). The open slope is influenced by river discharges, although inside the submarine canyons that are particularly numerous in this area, this process is more evident. Although less than in the Gulf of Lions, there is a significant vertical mixing during winter in front of the Ebro river, enhancing the circulation of water masses and the coupling between surface and deep waters (Marty et al., 2002; Salat et al., 2002). The organic matter thus reaches the deep-sea regions along two main pathways: the vertical flux of settling particles and the advective flux across the slope (Pusceddu et al., 2010; Vetter and Dayton, 1999). Advective fluxes are strongly enhanced by river discharges. In contrast, vertical settling is the result of organic matter produced in the epipelagic zone (the phytodetritus, fecal pellets and dead animals). The matter originating from advection can reach significantly higher values than that of pelagic origin (for example in the Gulf of Lions a difference of two orders of magnitudes has been calculated) (Durrieu De Madron et al., 2000).

### 5.2.2 Biomass data

Samples of fauna were collected using four types of gears for the different typologies of fauna (megafauna, macrobenthos, suprabenthos and zooplankton-micronekton, described below). We used:

1. A Reineck's box-corer (surface:  $A = 0.065 \text{ m}^2$ ) to sample the benthic macrofauna, mainly infauna (0.5–20 mm). The uppermost 20 cm of sediments were picked up and sieved through a 0.5 mm mesh size to retain specimens. This mesh size samples sometimes animals belonging to the meiofauna (size range usually inbetween 0.1–0.5 mm), such as nematodes, benthic ostracods and very small polychaetes, i.e. some paraonid species. The fraction of meiobenthic specimens did not affect the total biomass of the samples analysed. A total of 28 box-corers were collected (3–4 replicates per station depending on the supposed diversity of stations). The distance between replicates was less than 200 m in BIOMARE and less the 30 m in ANTROMARE cruises for each station. In the model the corresponding macrobenthic compartment is called MACBN.
2. A Macer-GIROQ sledge was used to sample suprabenthos, mainly crustaceans such as amphipods, cumaceans and isopods (0.5–20 mm) during daytime. The sledge was equipped with two superimposed nets with mouth openings between 10–40 cm and 50–90 cm above the bottom. Both nets where processed. The sledge nets have 0.5 mm mesh size and were trawled to a speed of 1.5 knots. The duration of sledge hauls over the bottom were 10 min. Both vessel speed with hauls duration and standard 2030 flowmeters (General Oceanics Inc.) reading (attached to sledge mouth) were used to estimate the area of samples for standardizing abundances. A total of 6 sledges were taken. In the model the corresponding compartment is called SUPBN.
3. A WP2 net was used to sample zooplankton-micronekton (meso- /macrozooplankton /micronekton). The net was equipped with 0.5 mm mesh size with mouth area of  $1 \text{ m}^2$  and a system of closure (1000DT General Oceanics Ltd) performed as closer to the bottom as possible. We used a SCANMAR sensor to estimate the closest distance per sample (range between 4 and 43 m). During tows (total duration = 10 min) the boat speed was around 1.5

knots. A standard 2030 flowmeter was attached to the mouths of nets to measure the amount of water filtered and/or the distance covered in each haul to estimate the volume. A total of 6 samples were taken, all during daytime. This WP2 allows to collect mesoplankton (species ranging from 0.2 mm to 0.5 mm, such as copepods, ostracods and some small pteropods), macroplankton (0.5–20 mm, i.e. hyperiids, euphausiids, jellyfish) and micronekton (small but actively swimming organisms ranging in size between 2 and 10 cm, i.e. mesopelagic fish and natantian decapods). However, considering the mesh size of the net (0.5 mm) it is more suitable for macrozooplankton and micronekton, but the mesoplanktonic fraction is not well sampled. 1 haul is considered enough to represent the faunistic composition of zooplankton in a concrete depth/period (see [Cartes, Fanelli, Lloris and Matallanas, 2013](#)). In the model this component is called ZPLMNK.

4. An OTSB-14 bottom trawl was used to catch the megafauna (larger than 2 cm). The OTSB-14 is a standard sampler for deep-sea megafauna ([Merrett et al., 1991](#)), it is a 1-warp trawl with 6 mm mesh size at the codend, an horizontal opening between wings of ca. 7 m and a vertical opening of ca. 1.2 m (recorded by a SCANMAR sensor in the mouth of the trawl). Towing speed was 2.5 knots. The position of the start and end of the hauls was recorded with a GPS (Global Positioning System). A total of 15 hauls were collected (three replicates per station). In the model the megafauna was divided into megaichthyofauna (called MEGAICT), megabenthos (MEGABN) and the red shrimp *Aristeus antennatus* (AANT).

All macrofauna samples were sieved through filters of 0.5 mm mesh size on board, fixed in buffered formaldehyde or frozen at  $-20^{\circ}\text{C}$  and the individuals identified at the laboratory. Animals were classified to the lowest possible level under a stereomicroscope (at  $10\times$ – $40\times$ ), counted and weighed (wet weight after eliminating blotting water, balance resolution:  $1\text{E} - 05$  g). Polychaetes were also analysed under a compound microscope (at  $10\times$ – $40\times$ ).

The difference between these three compartments relates to their habitat preference and their mobility. The macrobenthos lives mainly in or occasionally on the sediment and usually leads a sedentary lifestyle. The suprabenthos has high swimming ability and lives the most of its life in the benthic boundary layer (BBL), one to two meters above the bottom. Suprabenthos remains fairly close to the



sediment, however it can show some vertical migration. Finally zooplankton comprises both motile and not motile taxa and can be found in the open water. This component can be highly migratory and can reach almost the bottom.

### 5.2.3 Other data

Other data we collected are:

1. Total sediment Organic matter (TOM) was calculated as percentage of OM in sediment samples, taken by multi-corer and preserved at  $-20^{\circ}\text{C}$ . At the laboratory it was dried at  $60^{\circ}\text{C}$  for 24 h till reaching constant weight and then oxidised (ashed) at  $500^{\circ}\text{C}$  for 2 h in a muffle furnace and weighted before and after the oxidation. The first measure represents the weight of both organic and inorganic matter, called dry weight (DW), while the second is called ash weight and represents the inorganic matter. Thus, their difference is the portion of organic matter. The TOM is a heterogeneous compartment comprising both abiotic and biotic organic matter. In fact, it contains detritus, labile and refractory organic matter, as well as micro and meiofauna (biotic matter  $\leq 0.5$  mm). The total organic matter was included in the model as another component, called TOM. Thus the model does not distinguish the detritus pool from the micro and meiofauna.
2. Sediment oxygen consumption (SOC) estimates the “respiration of sediments” and has been measured during the ANTRMARE cruise in June 2011. Sediments and the overlying water required for the experiment derived from three box-corers (one from S3 and two from S4). Each incubator consists of a perspex chamber ( $d = 30$  cm) with a detachable lid containing a Teflon-coated magnetic stirrer. Water samples were analysed every 6 hours in triplicate for dissolved oxygen concentration with the modified Winkler method (Carpenter, 1965) (see Appendix H). Incubations lasted between 24 and 37 hours, up to find no changes between consecutive measures. All measurements were done in the absence of light by covering the chambers with black plastic. Afterwards SOC rates, expressed in  $\text{mmol O}_2 \text{ m}^{-2} \text{ d}^{-1}$ , were calculated by means of linear regression of the initial decrease in oxygen concentration during time (extended methodology in Glud (2008)). Chambers are described in Figures , Appendix H.

3. We used fishery's data of red shrimp from the temporal series available from the Catalan government. We estimated maximum and minimum of fishing rates on the *A. antennatus* (AANT → LANDS in the model) combining the information about landings, number of boats and trips per boats performed in each month during years 1996 – 2008, and the extension of the fishing ground Serola (comprising three sub-areas called by local fishermen: Serola, Abissinia and Morràs) in the depth range between 600 – 800 m (covering approximately an area of 230 km<sup>2</sup>) and considering that trawlers cover approx. 400,000 m<sup>2</sup> h<sup>-1</sup> and haul duration is around 4 h per day. So, we could standardize the flow to gm<sup>-2</sup>d<sup>-1</sup> (minimum, maximum and mean values). Contrariwise for fish (MEGAICT) and invertebrates (MEGABN) catch rates, we used the proportion found for MEGAICT and MEGABN with respect to AANT in BIOMARE surveys and multiplied the fishing rate of AANT with the proportion of MEGAICT and MEGABN for BYCATCH rate parameters (MEGAICT → BYCATCH and MEGABN → BYCATCH in the model). Fisheries data do not permit to estimate bycatch species, because a considerable portion is usually thrown back to sea by the fishermen. However, considering that the catch is sorted later, during the return to the port or (when saleable) in the same port, the bycatch portion represents a loss of biomass from the network and must be considered in the model.

All biomasses were converted from wet weight (WW g) to dry weight (DW g) and/or ash free dry weight (AFDW g), depending on the available information and then to carbon content (mmol C) using conversion factors from [Brey \(2001\)](#) and standardized to mmol C m<sup>-2</sup> (Table 5.2).

#### 5.2.4 Literature data

In addition to our measurements, a variety of data on process rates is available from the literature for the same area, from other deep-sea areas or, in lack of the previous, parameters from shallow waters were used, and to which a temperature correction was applied. All data were implemented as constraints by setting the minimum and maximum values found as lower and upper bounds respectively (Table E.3, Appendix E). Biomass-specific maintenance respiration of all faunal compartments was defined as 0.01 d<sup>-1</sup> at 20°C (see references in [van Oevelen, Soetaert, Middelburg, Herman, Moodley, Hamels, Moens and Heip, 2006](#); [van](#)

Oevelen, Bergmann, Soetaert, Bauerfeind, Hasemann, Klages, Schewe, Soltwedel and Budaeva, 2011) and temperature-corrected with a  $Q_{10}$  of 2 (correction factor  $Tlim$ ). We used the literature revised in other models (van Oevelen, Soetaert, Middelburg, Herman, Moodley, Hamels, Moens and Heip, 2006; van Oevelen, Bergmann, Soetaert, Bauerfeind, Hasemann, Klages, Schewe, Soltwedel and Budaeva, 2011) as basis for constraints of assimilation efficiencies and biomass-specific maintenance respiration.

The model did not consider some important processes in benthic food webs, such as the hydrolysis to dissolved organic carbon of detritus due to prokaryotes included in detritus pools (OM and TOM), because we did not estimate prokaryote stocks. Part of the ingested matter by the faunal compartments is not assimilated but instead expelled as faeces and this is represented by a flow directed to the TOM. Respiration by faunal compartments is defined as the sum of maintenance

	A	B	C	D	E
Internal	zooplankton-micronekton	ZPLMNK	0.047	B	6
	Macrobenthos	MACBN	23.712	B-A	28
	Suprabenthos	SUPBN	0.094	B	10
	Megabenthos*	MEGABN	5.700	B	13
	<i>A. antennatus</i>	AANT	0.076	B	13
	megaichthyofauna	MEGAICT	0.830	B	13
	Total organic matter in sediment	TOM	76157	B	4
External	Particulate organic matter from water column	OMv			
	Particulate organic matter from upper sediment strata	OMa			
	Landings	LANDS			
	Bycatch	BYCATCH			
	Dissolved inorganic carbon	DIC			
	Burial	BUR			

TABLE 5.2: Standing stocks of the food web compartments for the soft bottom slope food web. The binary structure is defined in Section 5.2.6 and quantified by data available in Section 5.2.2. A) Compartments' name, B) Abbreviation used through the text, C) Stock values (mean,  $\text{mmol C m}^{-2}$ ), D) Origin of data: A=ANTROMARE B=BIOMARE, E) Number of samples. (\*) Excluding megaichthyofauna and *A. antennatus*. (\*\*) %  $C_{org}$  in sediment (gDW).

respiration (biomass-specific respiration) and growth respiration (overhead on new biomass production).

We also set OM input from advection 500 times OM from vertical fall, to take into account the different magnitudes between the two flows. In fact in the bibliography the mean OM vertical flux is  $0.998 \text{ mmol C m}^{-2} \text{ d}^{-1}$  in the productive area of the Gulf of Lions (converted from [Durrieu De Madron et al., 2000](#)) with minima around  $0.293 \text{ mmol C m}^{-2} \text{ d}^{-1}$  in autumn and maxima around  $21.667 \text{ mmol C m}^{-2} \text{ d}^{-1}$  during winter ([Buscail et al., 1995, 1990](#)). In the Pacific ocean at 4000 m the flow is much weaker (maximum around  $1.67 \text{ mmol C m}^{-2} \text{ d}^{-1}$ , [Ruhl et al., 2008](#); [Ruhl and Smith, 2004](#)). Advective fluxes on the continental slopes are instead much higher (from 50 to  $4583.33 \text{ mmol C m}^{-2} \text{ d}^{-1}$ ) and mean value of  $291.67 \text{ mmol C m}^{-2} \text{ d}^{-1}$  in the Gulf of Lions ([Durrieu De Madron et al., 2000](#)).

### 5.2.5 Linear inverse modelling

The model developed for this food web was built using the linear inverse modelling (LIM) methodology according to [van Oevelen et al. \(2009, 2010\)](#). We used both observed and literature data to derive model parameters as described in Sections [5.2.2](#), [5.2.3](#), [5.2.4](#). The topology of the food web is determined by the number of compartments and their connections (see Section [5.2.6](#) and Figure [5.2](#)) and is represented in the model by the mass balance of each compartment (Table [E.2](#)).

All parameters are defined by ranges provided in Table [E.3](#). Representing (uncertain) parameters by ranges rather than single values, avoids undesirable overfitting. The result of this procedure is that the flow magnitudes are constrained within reasonable upper and lower boundaries (rather than one value).

The LIM consists of equalities and inequalities that are solved simultaneously to obtain quantitative values for each flow  $x$ :

$$\begin{aligned} \mathbf{Ax} &= \mathbf{b} + \epsilon \\ \mathbf{Ex} &= \mathbf{f} \\ \mathbf{Gx} &\geq \mathbf{h}. \end{aligned} \tag{5.1}$$

Here, the first equation defines both the topology of the food web and the mass balance conservation of involved compartments: the matrix  $\mathbf{A}$  represents the topology and  $\mathbf{b}$  is a vector with growth rates or rates of change for each component. For a given number of components,  $K$ , then for each component,  $S_k$ , the mass balance equation is

$$\frac{dS_k}{dt} = \sum_i f_{ki}^{in} - \sum_j f_{kj}^{out} \quad (5.2)$$

$dS_k/dt$  is the derivative of the mass of compartment  $S_k$  w.r.t. the time  $t$ ,  $f_{ki}^{in}$  and  $f_{kj}^{out}$ , with  $i = 1, \dots, I$  and  $j = 1, \dots, J$ , represent the  $I$  incoming and  $J$  outgoing flows to and from the compartment  $S_k$ . In steady-state  $dS_k/dt = 0$ . The vector  $\mathbf{x}$  represents the unknown flows, and  $\epsilon$  is the error term that is minimized. The rest of the equations contains restrictions as equalities (in the case of  $\mathbf{E}$ ) or inequalities ( $\mathbf{G}$ ) and the vectors  $\mathbf{f}$  and  $\mathbf{h}$  contain the empirical data or data from the literature. The third set of equations leads to ranges in estimated flows consistent with parameters' ranges. The model can be solved within such ranges to minimize the error  $\epsilon$ .

The solution of the model is given by the set of flows  $\mathbf{x}$ , that is consistent with the set of linear equations. These models are usually under-determined, because of a general lack of data and the large number of the unknown flows (Soetaert and van Oevelen, 2009b; Van den Meersche et al., 2009; van Oevelen et al., 2009). In the ECOPATH modelling framework (Christensen and Pauly, 1992) the under-determinacy is avoided by adding literature data and reaching the state of even-determinacy (Soetaert and van Oevelen, 2009b).

In contrast, in the LIM there are three methods to solve under-determinacy models.

One type is to find the parsimonious solution (originally proposed by Vézina and Platt, 1988). This method minimizes the objective function

$$\min \left( \sum_i x_i^2 \right),$$

where  $x_i$  represents the  $i$ -th unknown flow. Another, similar, approach, the Least Squares with Equalities and Inequalities, uses

$$\min(\|\mathbf{Ax} - \mathbf{b}\|^2).$$

In this method, if the equality constraints  $\mathbf{Ex} = \mathbf{f}$  cannot be satisfied, a generalized inverse solution residual vector is obtained and is the minimal length for  $\|\mathbf{Ex} - \mathbf{f}\|^2$ .

These two methods return however biased flows, taking extreme values of the solution space (Kones et al., 2006).

Recently two more solution methods have been proposed to take into account the uncertainty of flows: the range (Klepper and Van de Kamer, 1987) and the MCMC solution methods (Van den Meersche et al., 2009), (Kones et al., 2006). Each method can be used for different reasons.

The range estimation is used as a measure of identifiability (i.e. the quality of estimated flows). The ranges are calculated by minimizing and maximizing each flow successively using Equations 5.1. This permits to identify which additional data could be used for constraining the food web so as to reduce ranges till they attain reasonable values.

The MCMC methodology uses markov sampling to pick random food webs that comply with the equations and allows to estimate the mean and standard deviation of each unknown. It can also be used to estimate mean and standard deviation of ecosystem indices Kones et al. (2009) as we did. Technical and methodological aspects of linear inverse modelling can be found in Soetaert and van Oevelen (2009b) and van Oevelen et al. (2010).

In this study we used all methods (parsimonious, range and MCMC). For the MCMC simulation, 10,000 samples of flows have been generated. Running the model 10,000 times, the uncertainty in the empirical input data is propagated onto an uncertainty estimate of the carbon flows as indicated by its standard deviation. Previous studies on the convergence of the mean and standard deviation of the flows verified the adequacy in setting this number of solutions (van Oevelen, Soetaert, García, de Stigter, Cunha, Pusceddu and Danovaro, 2011).

To build the model we used the R-package LIM (Soetaert and van Oevelen, 2009a,b).

## 5.2.6 Food web structure

The compartments in the food web model were chosen based on three criteria:

1. size (macrofauna: 0.5–20 mm; megafauna: larger than 2 cm),
2. vertebrates versus invertebrates within megafauna (i.e. megabenthic invertebrates and megabenthic ichthyofauna) and
3. compartments spatially divided within macrofauna (i.e. the zooplankton and micronekton, which performs vertical migrations in the water column, the suprabenthos, that lives close to the bottom, and the macrobenthos, that lives in the sediment).

Hence finally six faunal compartments have been created:

1. MACBN: benthic invertebrate macrofauna, mainly represented by polychaetes, crustaceans and molluscs,
2. SUPBN: active swimming macrofauna in the benthic boundary layer (BBL), the so-called suprabenthos, mainly represented by peracarids,
3. ZPLMNK: zooplankton and micronekton close to the BBL, that occasionally occupies this transitional zone,
4. MEGAICT: megafauna (vertebrates or megaichthyofauna), which comprises species strictly related to the bottom but also migratory species,
5. MEGABN: megabenthic invertebrates, such as crustaceans, echinodermata, sipunculans and cephalopods, and that also comprises migratory and non migratory species (among crustaceans),
6. AANT: the red shrimp *Aristeus antennatus*, target species of deep-sea fishery in the area.

The structure of the food web was chosen to describe the major flows between larger groups of the whole community, while the red shrimp was left as a own compartment to be able to relate its changes with changes in all other components.

We considered that these components are very heterogeneous categories in terms of C content, whereby we separate the different (available) groups to calculate the carbon content separately.

A seventh compartment has been considered:

7. TOM: total organic matter in sediments, including detritus (POM), bacteria, viruses and meiofauna. Percentage of total sedimentary organic matter (TOM) was calculated as the difference between dry weight (DW: 60°C for 24 h until constant weight reached) and ash weight (500°C in a furnace for 2 h).

The POM in sediment derives from the POM in the water, that settles on the bottom through sedimentation. The POM near to the bottom in turn derives from upper water strata and from advective processes downward the slope. The first has pelagic origin (e.g. phyto and zooplankton) while the second is mainly of terrigenous origin (river discharges). The quantities of these entries can vary strongly. Detritus is also produced by the living fauna in the slope community through mortality and faecal production. This detritus can be then available again and recycled by the community. We modelled two external entries, the organic matter from vertical fall (OMv) and from advection (OMa). OMv and OMa enter the continental slope food web through sedimentation to the TOM, suspension and filter feeding of macrofauna compartments.

Effflows from the food web are: respiration of all compartments to the dissolved inorganic carbon (DIC), the burial of the TOM (BUR) and the efflux to humans due to fishing activity on the target species, the red shrimp (LANDS), and on the accompanying fish and invertebrates (BYCATCH). The fraction of bycatch species usually returns to the sea as discards having no commercial interest, although it is a considerable biomass removed from the ecosystem. Few species are brought to the port, such as Gadiformes species, *Phycis blennoides* and *Merluccius merluccius* and occasionally cephalopods, that are rarely fished.

The relationships among compartments described in this section (binary food web) are shown in Figure 5.2, the quantities of stocks are in Table 5.2 and the mass balance equations included in the model and describing the relationships between components are given in Table E.2 in Appendix E.



We considered our sampling (performed during one year) to be consistent with the assumption of steady-state. With the inclusion of ANTROMARE samples for the infauna, we corrected for the possible bias related to the depth of this component during BIOMARE surveys, where only samples at 800 m were available for the open slope. The mass-balance equations of the model are reported in Table E.2, parameters ranges in Table E.3 and more constraint equations in Table E.1.

### 5.2.7 Network indices

The network indices were calculated on the 10,000 MCMC samples using the R-package NetIndices (Kones et al., 2009). The notation and details on the calculation of the indices are shown in Tables E.6, E.7 and E.8 and more information can be found in e.g. Ulanowicz (2004) and Kones et al. (2009) among others. Following Kones et al. (2009), indices can be calculated if assuming  $n$  internal compartments and an undefined number of external components. Each flow is defined with  $T_{ij}$ , of which direction is from source  $j$  to destination  $i$  ( $j \rightarrow i$ ). All flows are categorised into four groups: (1) imports (2) internal (3) export of usable energy and (4) dissipation of unusable energy (see Table E.6 in Appendix E for the corresponding nomenclature).

General network indices are descriptors of general system's properties, e.g.

1. The Total System Throughput (T., Hirata and Ulanowicz, 1984) and the Total System Throughflow (TST, Latham II and Scully, 2002) measure the total exchange transpiring in the system. But Although the former is the sum of all flows the latter is the sum of all components throughflows
2. The system size,  $n$ , refers to the number of nodes or compartments.
3.  $L$  and  $L_{int}$  are the number of total links and internal links respectively.
4. The LD is the link density and is the ratio between  $L$  and  $n$  (Bersier et al., 2002).
5. The Connectance ( $C$ ) plays a key role in community ecology being fundamental for many theories of community stability (Pimm, 1984) and structure (Martinez, 1992). Different measures of connectance exist (see Warren, 1994

for details on definitions), all based on internal number of links and number of components. A widely used measure of connectance is the Directed Connectance ( $L/n^2$ ), that corresponds to the number of actual links over the number of possible links, including cannibalistic loops (Martinez, 1992). The measure used here is slightly different (see the Table).

6. Average link weight ( $\overline{T}_{ij}$ ) is the average of all components' links.
7. Average compartment throughflow ( $\overline{TST}$ ) is the average of all components' throughflows.
8. The Compartmentalization  $\overline{C}$  assesses the degree of well-connected subsystems within a network. It can only be used to compare systems with the same number of compartments and connectance. Higher values represent higher levels of compartmentalization (i.e. more or stronger subsystems).
9. Average path length  $\overline{PL}$  is the average path length of the average inflow weighted by the sizes of the inflows.

Some indices refer to the cycling behaviour of the system. They rely on how much energy is used by recycling processes and available again for the system itself (Allesina and Ulanowicz, 2004). Such indices also measure system's independence from energy inputs. They are:

1. The Total System cycled Throughflow (TSTc) represents the recycled energy by the system and the Total system non-cycled throughflow (TSTs) also called Total system straight throughflow represents the non-cyclic pathways or the portion of total system throughflow that passes straight through the system. It gives information about the net loss of energy.
2. The Finn's cycling Index (FCI), cast as the ratio between TSTc and TST, and the revised FC1b, conceptually the same of TST, are useful for among network comparisons, because they vary between 0 and 1: 0 meaning that there is no cycling at all and 1 meaning that all flow is recycled.

There are also weighted measures for networks:

1. The Effective connectivity ( $Cz$ ) is the analogous of the link density in unweighted network weighted for the size of links. It might fall between 1 and 3.25.

2. The Effective flows ( $F_z$ ) is analogous to the number of links.
3. The Effective nodes ( $N_z$ ) is the weighted mean of the normalized throughflow of each node.
4. The Effective roles ( $R_z$ ) is a measure of weighted, differentiated, distinct functions in a network (components that take input energy and pass it to other components). It might fall between 2 and 5.

Among these measures, particularly important are  $C_z$  and  $R_z$ , because the bidimensional range of  $C_z$  and  $R_z$  has been called “window of vitality” by [Zorach and Ulanowicz \(2003\)](#).

Measure of network constraint and uncertainty are:

1. The Average Mutual Information (AMI) is the measure of the average amount of constraint placed upon an arbitrary unit of flow anywhere in the network. If highly constrained a flow in the network, the system is unable to persist when perturbed.
2. The Statistical uncertainty ( $H_R$ ) is the upper bound of the AMI.
3. The Conditional uncertainty ( $D_R$ ) is the difference between  $H_R$  and AMI. In a developing system, when the AMI falls the  $D_R$  rises. The Uncertainty is a measurable quantity expressing the degree of uncertainty about what flow will be produced by a source. The more that is known about a source, the less the uncertainty there is in what flow will be produced. In communication theory the uncertainty was termed “entropy” by Shannon, but its meaning is different from the entropy in physics. In physics, entropy is disorder, while here is synonymous of uncertainty.
4. The Realized uncertainty ( $RU_R$ ) is the fraction of the total uncertainty accounted by the network. It is useful to compare the degree of constraint across systems.
5. Given a network of  $n$  compartments, any compartment may transfer material/energy to itself or to any other compartment. The total uncertainty of a system is expressed as  $H_{max}$  and specifies the uncertainty with regard to a network where every node is interacting evenly with every other node

(Latham II, 2006). It is expressed by the Shannon uncertainty equation and is the maximum possible uncertainty.  $H_{sys}$  is the uncertainty expressed by the system. MacArthur (1955) used  $H_{sys}$  as a measure of the community stability. The difference between the maximum uncertainty,  $H_{max}$ , and the actual uncertainty,  $H_{sys}$ , may be taken as the amount of uncertainty reduced by the structure of the network, the  $H_c$ .

6. The Constraint efficiency (CE) is based upon a total of the constraints that govern flow out of individual compartments. It is a scale independent ratio of the constraint. This measure depends on  $H_{max}$  and the Network constraint ( $H_c$ ).

Measures of growth and development or maturity of the system, originally developed by Ulanowicz (1986):

1. The Ascendency (A) quantifies increasing organization and size in growth and development of the system. The organization component is measured by the AMI and the size of component is measured by the T... The Ascendency can be decomposed in four quarters: 1) internal, 2) import, 3) export, and 4) dissipation.
2. The Development capacity (DC) represents the upper bound of the Ascendency.
3. The Overhead ( $\phi$ ) is the difference between the former two indices and describes how much the Ascendency can increase. In other words it is a measure of the system's strength in reserve from which it can draw to meet unexpected perturbations.
4. The Extent of development (AC) is the fraction between A and DC and is useful for comparing ascendency across networks.

All these indices can be decomposed as the Ascendency. That was proposed by Ulanowicz and Norden (1990) to study specific aspect of the network.

The ascendency as well as other properties of an ecosystem is affected by the number of groups that are included in the system description. Noteworthy is that the ascendency diminishes notably only when the system is aggregated to less than six groups Ulanowicz (1986).

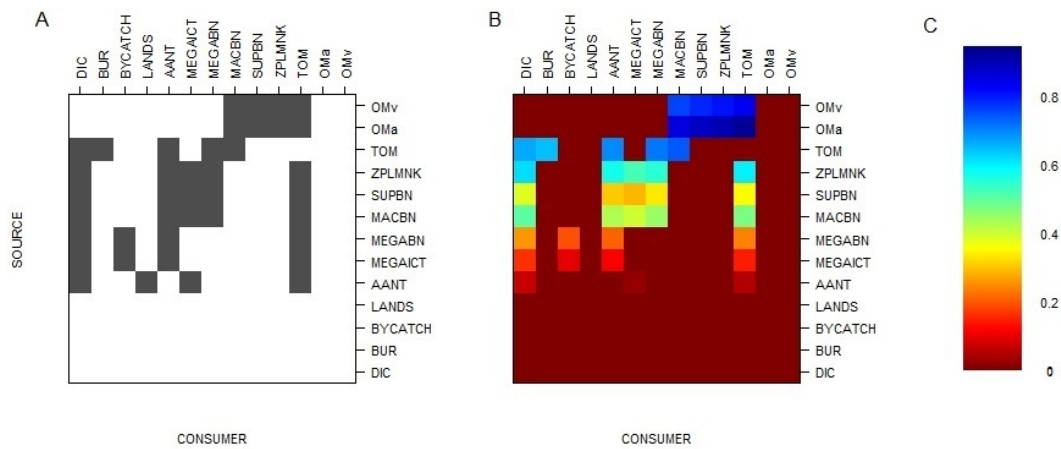


FIGURE 5.2: A) Binary food web, B) quantified food web by the model, C) legend of the flows ( $\text{mmol C m}^{-2} \text{d}^{-1}$ ).

The use of  $A$ ,  $DC$ ,  $\phi$  and  $AC$  in describing the maturity of a system derives from the correlation between  $A$  and most of Odum's properties (1969) of "mature" ecosystems (Ulanowicz and Norden, 1990).

All descriptions of symbols are given in the Appendix E, Table E.6, while equations are reported in Tables E.7 and E.8.

## 5.2.8 Software

All analysis and simulations were performed into the R environment (R3.0.2 version). The LIM (van Oevelen et al., 2010) and other required R-packages, limSolve and deSolve (Soetaert and van Oevelen, 2009a; Soetaert et al., 2010a), and its extensions (NetIndices: Kones et al., 2009) provide estimation methods that also permit a statistical analysis on the food web, network indices and dynamic simulations.

## 5.3 Results

### 5.3.1 The food web

The total number of unknowns (the flows involved in the food web) is 40, within 13 total compartments, 7 internal and 6 external. The estimations using the three

types of solutions (methods: range, parsimonious - both ldei and lsei - and MCMC) are reported in Tables E.4 and E.5 (Appendix E). In what follows, we will refer to the MCMC estimates (if mean and sd are given) or to the range estimates (min and max). Other estimations will be specified explicitly..

The food web is visualised in Figures 5.2 (the binary representation in A and flows estimations using colour gradient in B) and 5.3, representing the circular diagram of the food web, plotted with flows as net values. Flow values ranges from 0.84, estimated for TOM → DIC, to  $2.5E^{-06}$  mmol C m<sup>-2</sup> d<sup>-1</sup>, estimated for MEGABN → MEGAICT (derived from the parsimonious solution ldei). The strongest flows are the incoming flow to the community from the particulate organic matter of the upper sediment strata (OMa) to the (total) organic matter in sediment (TOM) and the efflux from the TOM to the dissolved organic carbon (DIC). The second most important component, where most of the organic matter passes after the TOM, is the macrobenthos (MACBN). Within this component,

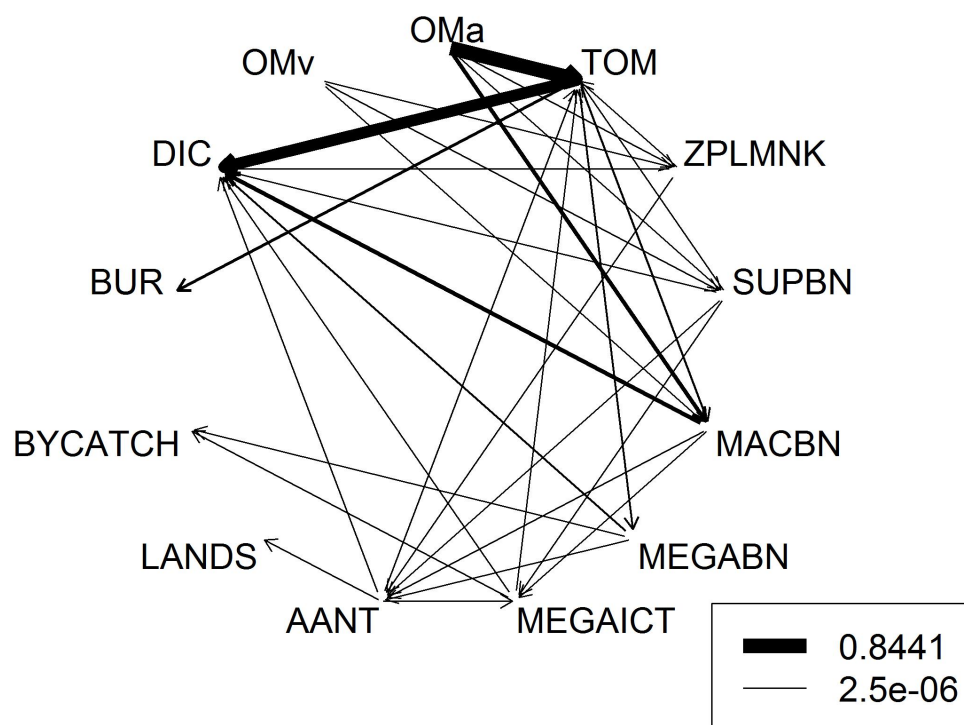


FIGURE 5.3: Food web carbon flows (mmol C m<sup>-2</sup> d<sup>-1</sup>). See Table 5.2 for abbreviations of food web compartments and Tables E.4 and E.4 for the values of the flows. The legend shows maximum and minimum flow values estimated through the parsimonium solution.

excluding few filter and suspension feeders, the majority of animals are deposit-feeders eating on the detritus in sediment (a portion is also carnivorous but not estimated).

In Figure 5.4, mean and standard deviation of flows estimated through MCMC simulations are arranged in descending order from the left to the right. Nearly all flows involving TOM and macrobenthos (MACBN) are “strong” interactions (= high values), related to their high carbon content (stocks). Other important flows in terms of strength are those involving biogeochemical processes, such as sediment respiration, advection, sedimentation and the burial process. All low-biomass compartments, suprabenthos, zooplankton and the red shrimp are involved in weak interactions (close to zero) and are potentially vulnerable.

Flows’ ranges are visualised in Figure E.1 (Appendix E) and are measures of both feasibility and uncertainty. The flows with highest uncertainty are these related to the total organic matter in sediment (TOM). The coefficient of variation, CoV (Table E.5, Appendix E), represents a better measure of the residual uncertainty than the standard deviation and better indicates the “quality” of the model solution. The CoV is a measure independent from the mean value, so the estimations of flows can be directly compared between each other: the lower CoV smaller

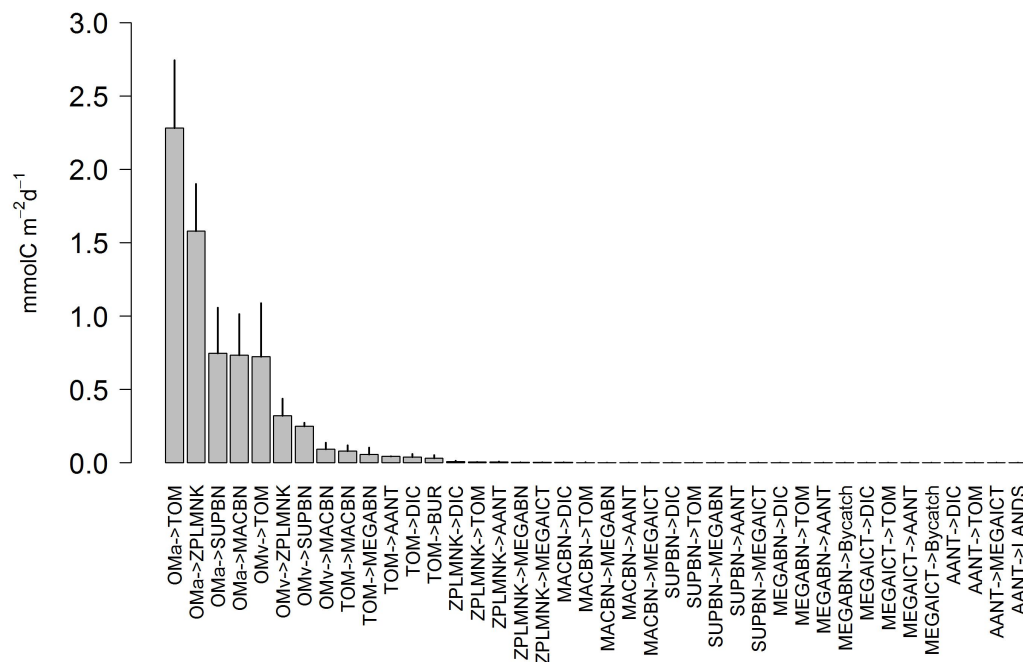


FIGURE 5.4: Barplot of the food web flows (mean  $\pm$  sd, mmol C m<sup>-2</sup> d<sup>-1</sup>) estimated using the MCMC method in descending order from the left to the right.

the uncertainty and better flow estimate. All CoVs are smaller than 1 except two flows (OMv  $\rightarrow$  TOM and OMv  $\rightarrow$  ZPLMNK); the 80% is smaller than 0.75 and the 70% of the flows is smaller than 0.50. These results suggest a good performance considering other food web models (e.g. van Oevelen et al., 2009; van Oevelen, Soetaert, García, de Stigter, Cunha, Pusceddu and Danovaro, 2011).

Using the MCMC estimations in E.5 we derived mean values of the main processes in the food web (range estimations are shown in Table 5.3).

The total carbon input to the food web has a mean value of 2.62 mmol C m<sup>-2</sup> d<sup>-1</sup> and is the sum of the suspension feeding (12.95%) and the deposition of organic matter by vertical settling or through advective processes (87.05%).

The suspension-feeding is partitioned among zooplankton (1.08%), suprabenthos (3.07%) and above all macrobenthos (95.74%). Percentages are given with respect to the total. The suspension feeding of some invertebrates belonging to the megafauna, e.g. the brachiopod *Gryphus vitreus*, has been neglected in the model, because rarely observed.

Process	value
Vertical OM input	[0.002,0.007]
Advective OM input	[1.051,3.508]
Total OM input	[1.047,3.515]
OMv Deposition	[0 0.006]
OMa Deposition	[0.843,3.419]
Total OM Deposition	[0.843,3.419]
faunal detritus production	[0.168,2.271]
C Burial Rate	[0.110,1.265]
Suspension feeding (pelagic orig)	[0.001,0.007]
Suspension feeding (terr orig)	[0.083,0.692]
Total Suspension feeding	[0.090,0.699]
Deposit-feeding	[0.316,1.913]
Total secondary production	[0.021,0.249]
Sediment Respiration	[0.603,2.002]
Total respiration	[0.941,2.247]
Total Fishery	[0.002,0.002]

TABLE 5.3: Derived global estimations, [*min,max*], (mmol C m<sup>-2</sup> d<sup>-1</sup>) of important processes in the food web.



Process	A	B	C
$F_t$ =	[2.00E-03, 2.21E-03]	[63.34, 69.99]	[0.17, 0.19]
$F_a$ =	[5.00E-04, 5.53E-04]	[15.83, 17.51]	[0.04, 0.05]
$F_i$ =	[1.50E-03, 1.66E-03]	[47.50, 52,57]	[0.13, 0.14]
$F_b$ =	[2.50E-06, 2.76E-06]	[0.08, 0.09]	[2.17E-04, 2.39E-04]

TABLE 5.4: Derived estimations of flows related to the red shrimp fishery, [ $min, max$ ]. (A) expressed in  $mmol\ C\ m^{-2}\ d^{-1}$ ; (B) expressed in  $Kg\ km^{-2}\ y^{-1}$ ; (C) expressed in  $Kg\ boat^{-1}\ d^{-1}$ , here d is “working day” and has the same units of LPUE in Chapters 3 and 4.  $F_t$  is the total fishing rate;  $F_a$  is the portion of fishing pressure on red shrimp;  $F_i$  is the portion of fishing pressure on the fish stock;  $F_b$  is the portion of fishing pressure on invertebrates.

The total ingestion of C in sediments by the metazoan community (excluding the meiofauna, e.g. nematods) was  $0.83\ mmol\ C\ m^{-2}\ d^{-1}$ , corresponding to 31.68% of the total C entering the food web. Deposit-feeders feed on the detritus incorporated in the sediments. Our model does not distinguish flows from the TOM to detritivores and to carnivores eating on prokaryotes and meiobenthos in sediments. We necessarily assumed that almost all compartments in the sediment are both detritivores or carnivores (however detritivores are definitely more abundant), comprising each of them a broad number of species.

The rest of the OC deposited was used by the prokaryotes and nematods ( $1.58\ mmol\ C\ m^{-2}\ d^{-1}$ , 69.28%) or trapped in the sediment ( $0.73\ mmol\ C\ m^{-2}\ d^{-1}$ , 32.19%).

The total respiration of the community (including the TOM) was  $1.89\ mmol\ C\ m^{-2}\ d^{-1}$  ranging between  $0.84 - 2.34$  and each component contributed in a descending order as follows: 83.75% for prokaryotes and meiofauna (TOM), 13.34% for macrofauna, 2.86% for megafauna, including the red shrimp *Aristeus antennatus*.

We also derived estimations of the loss of secondary production due to fishing activity (shown in Table 5.4) representing minimum and maximum flows estimated by area during one day (A) or one year (B). In the case of the red shrimp, if the value is multiplied for the total fishing area, it could reflect the estimation of landings per year. The estimations in (C) have the same units of the LPUE in Chapters 3 and 4. Any comparison between estimations is very difficult because a monitoring systems (e.g. satellite systems) should be used and bathymetric differences should be also considered. To estimate column C we made the following

assumptions: 1) the OTSB covers approximately  $65000 \text{ m}^2 \text{ h}^{-1}$ , while the commercial trawlers cover more than two times the OTSB area ( $\times 2.5$ ); 2) moreover the fishing boats trawls for 4–6 hours, so we considered a mean value of 5 h per each working day; 3) we considered also one month stop. Obviously this is a very rough estimate.

### 5.3.2 The network indices

All estimations of the network indices are shown in Tables E.9 and E.10 in the Appendix E. Also formulae and symbols are reported in the same Appendix (Tables E.6, E.7 and E.8).

The estimations of general indices are reported in Table E.9. Among them, the total exchange transpiring the food web (T..) is  $7.04 \pm 1.38$ , the total throughflow (TST) is  $4.42 \pm 0.97$  and average throughflow is  $0.63 \pm 0.14$ . The no-cycled throughflow is very close to the TST, such that the recycled energy is very low ( $\text{TSTc} = 0.83 \pm 0.44$ ). Also other cycling indices (FCI and FCIB) return very low values (see Table E.9, B). The estimates of trophic indices, (formulae in Table E.8), are shown in Table 5.5.

COMPONENT	LT	OI
ZPLMNK	$2.000 \pm 0.000$	$0.000 \pm 0.000$
SUPBN	$2.000 \pm 0.000$	$0.000 \pm 0.000$
MACBN	$2.000 \pm 0.000$	$0.000 \pm 0.000$
MEGABN	$2.391 \pm 0.263$	$0.168 \pm 0.073$
AANT	$3.082 \pm 0.060$	$0.051 \pm 0.043$
MEGAICT	$3.041 \pm 0.021$	$0.043 \pm 0.021$
AVERAGE	$2.419 \pm 0.531$	$0.043 \pm 0.069$

TABLE 5.5: The trophic level and omnivory index (mean  $\pm$  sd) for all living components.

The mean trophic level for each component is affected by the resolution of the food web. It should reflect the “mean” value among all species incorporated in the component. The trophic level ranges approximately between 2 and 3.08, while the omnivory index is less than 0.1.

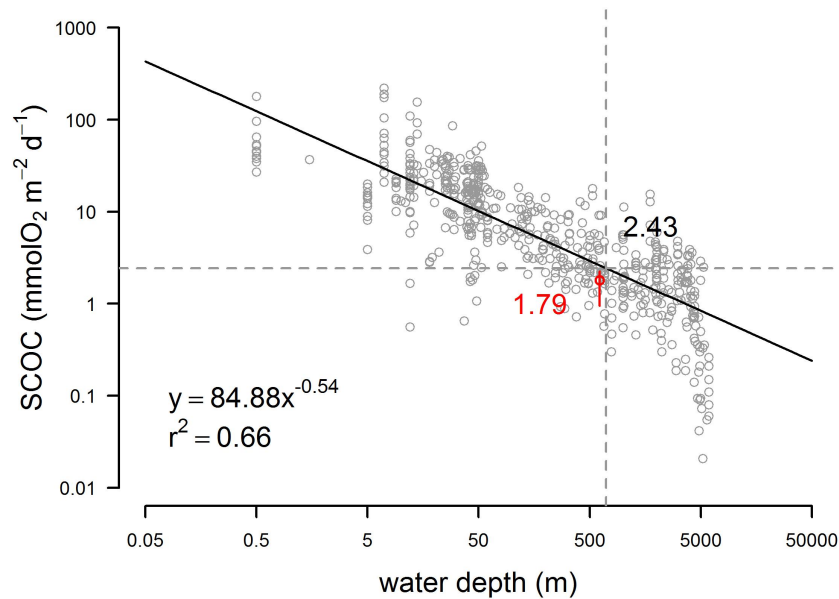


FIGURE 5.5: Sediment Community Oxygen Consumption ( $\text{mmol O}_2 \text{ m}^{-2} \text{ d}^{-1}$ ) as a function of depth (m). The grey points are observations, the continuous line represents the mean fitted value, the dashed lines corresponds to the average SCOC value (also in the Figure) at comparable depths (here we set 700 m the interpolations between 600-800 m depths, the range of our food web) and the estimation by our food web model is represented in red, the average is the red dot (with the corresponding number) and the segment represents the range. The function is the model in Equation E.2, Appendix E. Also the  $r^2$  is reported.

### 5.3.3 Oxygen consumption results

Our results from SOC experiments are in agreement with published data (Figure 5.5, available in [Andersson et al. \(2004\)](#)).

Our estimation (in red average value, lower and upper boundaries) has the same order of magnitude although lies below the SCOC estimated by the model (dark line). Details on the model are described in the Appendix E.

## 5.4 Discussion

The Catalan slope is one of the most studied bathyal ecosystems in the Mediterranean. However, as is the case for food webs in general ([Moore et al., 2004](#)), the identification of pathways within communities is difficult and even more so is its quantification.

This study is a first approximation of the principal pathways in the bathyal ecosystem of the soft-bottom continental slope (NW Mediterranean) and fishing ground for the red shrimp fishery. The main input, output and internal flows are shown in figure 5.6.

### 5.4.1 Inputs and resource partitioning

The main trophic relationships in this environment were recently studied, unravelling very diversified and unexpected components, within the lower section of the food web structure, showing specialised to omnivory behaviour (Fanelli et al., 2009; Fanelli, Cartes and Papiol, 2011; Fanelli, Papiol, Cartes, Rumolo, Brunet and Sprovieri, 2011). However the estimation of the proportion among different types of feeding behaviours is still unavailable due to the high number of species living this ecosystem and the relatively low number of species of which diet has been examined. Moreover these studies suggest a modular structure of the food web (see, e.g. Fanelli, Cartes and Papiol, 2011), such that higher modules can be considered to simplify the model and make it manageable. This fact and the necessity to build a food web model for immediate use in fishery management (FAO, 2003) requires a compromise between complexity and simplicity, so as to study the main pathways of this complicated system and could make the model useful for a rapid management of the fishery in deep sea habitats within the ecosystem approach of fisheries (EAF).

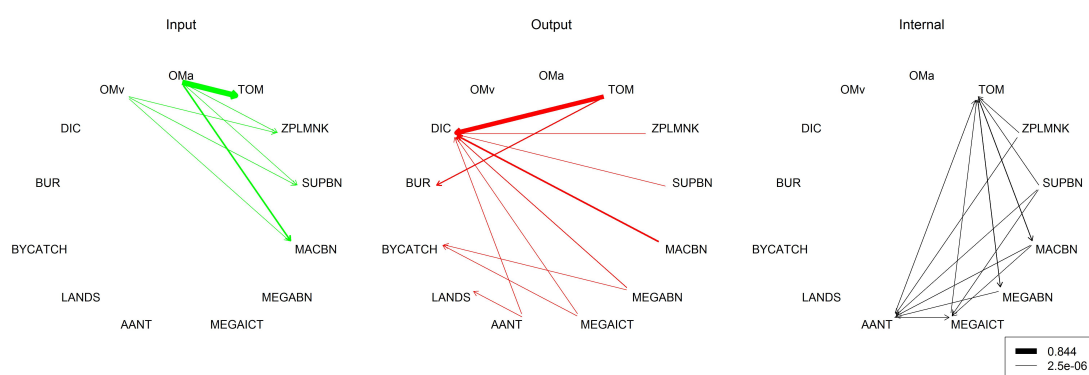


FIGURE 5.6: Food web carbon flows ( $\text{mmol C m}^{-2} \text{d}^{-1}$ ) as in Figure 5.3 but divided in A) input (green), B) output (red) and C) internal (black) flows. See Table 5.2 for abbreviations of food web compartments and Tables E.4 and E.4 for flows' estimations. The legend shows maximum and minimum flows estimated through the parsimonium solution.

With respect to other ecosystem modelling approaches, the great advantage of the LIM method is the ability to quantitatively reconstruct the food web even when the problem is under-determined (data-limited). We restricted the number of compartments, differentiating among large groups and distinguishing between two fundamental pathways in the bathyal environment that depend on external resources (vertical settling and advective processes) and recycled material.

In our area, the total biomass (only macro- and megafauna) was 30.46 mmol C m<sup>-2</sup>, very close to the bioass in the deep Faroe-Shetland Channel (30.22 mmol C m<sup>-2</sup>) (Gontikaki et al., 2011), and approximately 2/3 of that found at higher depths in the same region (45.93 mmol C m<sup>-2</sup>, converted from Tecchio et al., 2013) and also lower than at the Nazaré canyon (van Oevelen, Soetaert, García, de Stigter, Cunha, Pusceddu and Danovaro, 2011) and Rockall Bank (van Oevelen et al., 2009); the latter two are more diversified habitats and show higher secondary production. On the contrary, in our area the biomass is higher than in the Fram Strait (van Oevelen, Bergmann, Soetaert, Bauerfeind, Hasemann, Klages, Schewe, Soltwedel and Budaeva, 2011), as expected for being a food web in the Arctic Ocean and at deeper waters (2500 m). Also at the Porcupine Abyssal Plain the biomass was lower, summing the biomasses with the same size classes returned a value of 9.77 mmol C m<sup>-2</sup> (van Oevelen et al., 2012), that is 1/3 of that we found in the continental slope.

Organic matter inputs to the community from advective processes are more important than those from vertical fall (see for the magnitudes e.g. Buscail et al., 1995, 1990; Durrieu De Madron et al., 2000). This implies a higher structural role of this input. Infauna receives more OM from advective than vertical origin and then from the particulate organic matter in sediment. Between internal flows, those related to the TOM and the infauna showed higher and more uncertainty values. That is also related to their structural role in this ecosystem.

The secondary production in deep sea mainly depends on inputs of detrital matter deriving from the upper levels of the water mass and dropping down as phytodetritus, dead animals, faecal pellets, empty shells, skeletons and small organic particles of different nature. These particles falling down to the seabed have been usually called “marine snow” (Aldredge and Silver, 1988). Pelagic animals eat and also bacteria living in the water column mass degrade this source of energy during its way down, especially in the Mediterranean, where the temperature is relatively

high with respect to the open oceans (Fanelli, Cartes and Papiol, 2011). The remaining detritus is deposited on the sea floor where more bacteria deteriorate it enter in competition with metazoans which benefit of the remaining source. Deep ocean communities' carbon demand can exceed the vertical supply, being potentially supplied by lateral advection (Burd et al., 2010). That is the reason of the more structural role of advective processes in bathyal ecosystems. We found that a very low portion of this energy is recycled by the system (low Finn's index: FCI =  $0.179 \pm 0.066$ ).

The total input of C estimated by the model ranges between 0.92 and 4.16 mmol C m<sup>-2</sup> d<sup>-1</sup> (mean value: 2.62 mmol C m<sup>-2</sup> d<sup>-1</sup>), while the total secondary production (excluding prokaryotes and meiofauna) ranges between 0.02 and 0.25 mmol C m<sup>-2</sup> d<sup>-1</sup> that represents only the 2.17 – 6.01% of the organic matter that enters the community. The reason lies on biogeochemical processes and dissipation of the energy, i.e. the burial estimated to be 0.11 – 1.27 mmol C m<sup>-2</sup> d<sup>-1</sup>, equivalent to the 11.96 – 54.09% of the total organic input and the respiration, including the TOM (0.84 – 2.34 equivalent to 56.31 – 91.70% of the input).

The total input is approximately 7 times less than the input at comparable depths in the canyon of Nazaré but almost similar to the value in the lower section of the same canyon (at 4000–5000 m) (van Oevelen, Soetaert, García, de Stigter, Cunha, Pusceddu and Danovaro, 2011), this can be explained by the oligotrophic character of the Mediterranean sea, with respect to the Atlantic ocean and the habitat of canyons. Also the burial of organic carbon was lower in the Mediterranean continental slope,  $0.73 \pm 0.28$  mmol C m<sup>-2</sup> d<sup>-1</sup>, in comparison with same depths in the Nazaré canyon (van Oevelen, Soetaert, García, de Stigter, Cunha, Pusceddu and Danovaro, 2011), however the same parameters have been applied for this process. In contrast it was much higher than in the Rockall Bank's cold-water community and by van Oevelen et al. (2012) (0.03 mmol C m<sup>-2</sup> d<sup>-1</sup>) in the Porcupine Abyssal Plain, where the burial efficiency has been considered much lower than in the continental margins (van Oevelen et al., 2012).

Regarding to the feeding types, deposit and suspension feeding represent the 93.30% of the total consumption in the food web and the remaining percentage belongs to carnivores. Of this 93.30% the deposit feeding represents the 73-78%. Deposit feeders are mostly represented by the infauna (90.14% of the total deposit feeding), while the rest is consumed by megafaunal components. On the

contrary suspension feeders belongs to the zooplankton and suprabenthos. Carnivorous feeding among megafauna represents the 56.37%, such that suspension and deposit feeding are still important in these groups. Also the macrofauna comprises carnivorous species (feeding on micro- and meiofauna and on the “smaller” macrofauna). Thus carnivores are under-estimated by this model.

Has been argued that deep-sea macrobenthos (mostly detritus feeders) exhibit an expansion of trophic niches and species tend to be omnivorous to avoid competition for food (Gage and Tyler, 1991). This suggests that grouping many detritivorous in a single compartment, as in the present model, is a good compromise. Nonetheless more recent studies with isotopic methodologies found high variability in the relationship between  $\delta^{13}\text{C}$  and  $\delta^{15}\text{N}$  particularly among deposit feeders, suggesting exploitation of particulate organic matter at different stages of degradation: from fresh phytodetritus to highly refractory or recycled material (e.g. Fanelli, Papiol, Cartes, Rumolo, Brunet and Sprovieri, 2011). Also the seasonal turnover of opportunistic species is reasonable as evidenced in (Mamouridis et al., 2011). This scenario suggests a continuum in species trophic niches and the consequent difficult to compartmentalise the food web. Many examples of this repartition in food web modelling are available (van Oevelen et al., 2009; van Oevelen, Soetaert, García, de Stigter, Cunha, Pusceddu and Danovaro, 2011). When such information is not available, the compromise is to enlarge constrains in the model.

Our model gives necessarily a simplified picture of the trophic structure of the bathyal ecosystem and results represent an average within all species belonging to each modelled compartment. The TOM is considered as dead component however it comprises also living matter, but necessarily we set its TL = 1. However, micro- and meiofauna that could not be modelled present higher TL. For instance in the Nazaré canyon for nematodes the TL of deposit-feeders was estimated around 2 and omnivores and predators around 2.75 (van Oevelen, Soetaert, García, de Stigter, Cunha, Pusceddu and Danovaro, 2011). However considering that they usually have very low biomass with respect to the particulate organic matter in the sediment, is reasonable to consider that their TL do not affect to the average TL of the TOM as whole compartment. Zooplankton-micronekton (ZPLMNK), suprabenthos (SUPBN) and infauna (MACBN) have the same level (TL=2) occupying the “basis” of the bathyal food web almost eating on detritus (however of different source and quality) and as mentioned there are some carnivorous species eating on microplankton, microbenthos or meiobenthos (see also Fanelli, Cartes

and Papiol, 2011). Fish (MEGAICT) and the red shrimp (AANT) show very similar positions (close to 3), while big invertebrates (MEGABN) are in the middle between lower and upper (modelled) levels. The difficult to capture the highest trophic levels of the food web must also be considered, when discussing results, that is the case of pelagic cephalopods and bigger sharks, that could show trophic levels higher than 4. These species with pelagic behaviour can also be sustained by other sources in the water column far from the bottom.

With respect to the index of omnivory, lower trophic levels showed specialized diets, a result that in this case is an artefact of the model. Setting higher degree of compartmentalization will give higher values of omnivory, in fact many species are omnivores but can also present seasonally specialised diets. For example that happens in some polychaets, that turn their behaviour in relation to the environmental conditions from deposit to suspension feeding (e.g. species belonging to the family paraonidae) or are both deposit feeders and carnivores (e.g. caudofoveates) (Mamouridis et al., 2011). On the contrary higher trophic levels showed some degree of omnivory.

## 5.4.2 Community respiration

The total respiration with a mean value of  $1.89 \text{ mmol C m}^{-2} \text{ d}^{-1}$ , ranges between  $0.84 - 2.34 \text{ mmol C m}^{-2} \text{ d}^{-1}$  and is very low with respect to the cold-water coral community (e.g. van Oevelen et al., 2009). In our model only the sediments (without macrofauna) account for the 83.75% of the total respiration with the value of  $1.58 \pm 0.32 \text{ mmol C m}^{-2} \text{ d}^{-1}$ , while the percentages for macrofauna and megafauna are respectively 13.39% and 2.86% (sum of respirations of components of each size: 0.25 and  $0.04 \text{ mmol C m}^{-2} \text{ d}^{-1}$ ). Thus carbon processing is mainly due the living portion of the TOM (to prokaryotes and meiofauna) and only partially to metazoa (macro- and megafauna). In fact bacteria have the highest contribution within TOM compartment and for the whole community, as has been proven in other deep-sea benthic ecosystems (in the Nazaré canyon: van Oevelen, Soetaert, García, de Stigter, Cunha, Pusceddu and Danovaro, 2011 and in the Faroe-Shetland Channel: Gontikaki et al., 2011). In comparison with the CWC community at Rockall bank (van Oevelen et al., 2009), the respiration of our food web is more than 50 times lower. Despite, it is not surprising because the CWC community has characteristics of a hot spot habitat and thus respiration is higher



than all literature data available (van Oevelen et al., 2009). Respiration is instead higher than that found at higher depths in our region (Tecchio et al., 2013), where only metazoan community was modelled and respiration was estimated around  $0.64 \text{ mmol C m}^{-2} \text{ d}^{-1}$  after conversion. However we cannot say that it is statistically lower, having no estimates of the variability. Finally, however lower than the conditional mean calculated by the model E.1 (see Appendix E), our estimation falls into the range of other deep-sea soft bottoms data at comparable depths (Andersson et al., 2004) (see also Figure 5.5 in Appendix E to compare oxygen consumption data).

### 5.4.3 Network analysis

The total system throughput (T.), measuring the total food web activity has a very low value, was  $7.04 \pm 1.38$ , does not significantly differ to that found in the lower section of the Nazaré canyon at 4000–5000 m depth while is more than four times lower than at comparable and higher depths of the canyon (van Oevelen, Soetaert, García, de Stigter, Cunha, Pusceddu and Danovaro, 2011). The total system throughput (conventionally defined in Ecopath as TST, however for the definition given in Libralato et al., 2010 seems to refer to the T.) was 18.62 at higher depths (Tecchio et al., 2013). Our estimation of the TST was  $12.657 \pm 3.572$ . The network analysis suggests that almost all the energy passing through the food web is not recycled (see TST and low values of TSTc and Finn's indices). Our value of FCI was  $0.18 \pm 0.07$ , thus statistically there were no significant differences with the upper and lower sections of the Nazaré canyon in contrast with the middle section at comparable depths (van Oevelen, Soetaert, García, de Stigter, Cunha, Pusceddu and Danovaro, 2011). The Finn's index for deep sea food webs is low in comparison to other food web models in the Mediterranean considering more extended systems (Coll et al., 2007, 2006; Piroddi et al., 2010; Tsagarakis et al., 2010).

Among system development measures, the Ascendency is relatively low if compared with the development capacity of the system ( $5.75 \pm 1.12$  versus  $19.54 \pm 3.99$ ). In fact total AC is only  $0.30 \pm 0.03$ . Such indices define the maturity of the system, so, results show that the system may undergo significant changes if disturbed.

The average mutual information of the system is  $0.82 \pm 0.04$ , a very low value indicating a low trophic specialisation (Ulanowicz, 2004). However, such value

must be taken with caution, because it strongly depends on the resolution of the binary food web.

**Acknowledgements:** The authors thank all the participants of the BIOMARE (ref. CTM2006-13508-CO2-02/MAR) and ANTROMARE (ref. CTM2009-12214-C02-01-MAR) surveys. The first author would also like to thank Dorina Seitaj, PhD student at NIOZ, Yerseke (NL) for her help in SOC experiments.

## CHAPTER 6

---

Simulation of trophic cascade in the bathyal ecosystem

---

## Abstract

We present a dynamic simulation of the continental slope food web in the Catalan Sea (NW Mediterranean). After reconstruction of carbon flows among major compartments using linear inverse modelling (LIM) we performed a dynamic simulation based on a system of ordinary differential equations to predict biomasses behaviour during 5 years after perturbations induced by red shrimp fishery (top-down driver) and by the supply of food entering the web (bottom-up driver). The main purpose was the detection of indirect effects, i.e. trophic cascade, through trophic interactions encompassing three or more trophic levels.

Our simulation demonstrates that trophic cascades induced by fishery cannot occur through major interactions of the bathyal network. We only found very ephemeral indirect effects persisting less than 10 days, that we considered not enough to demonstrate the occurrence of this mechanism in the system. We found also empirical studies in which trophic cascades have not been detected, that thus support our results. Nevertheless, we investigated also interactions in couples of components and we found alternating phases that we considered as effects of the disturbances we imposed. In such cases we demonstrated which, among the perturbations, is the most relevant in altering relative biomasses. In fact, we found that organic matter inputs are stronger drivers than the fishery activity in the bathyal food web dynamics, result in agreement with the findings of other authors in different ecosystems.

The dead organic matter or detritus, a common feature of most ecosystems, is frequently overlooked. However our results emphasize the importance of detritus in benthic ecosystems sustained by allochthonous sources, helping to understand its role in structuring bathyal detritus-based food webs.

**Keywords:** dynamic food web, trophic cascades, bathyal ecosystem, red shrimp fishery, species interactions

## 6.1 Introduction

The trophic cascade consists in the removal of a predator that may result in a “release” of its prey (or competitors). This signal may proliferate throughout the food web and descend more than four trophic levels in some cases (Pinnegar et al., 2000). Such forces are defined as top-down drivers, because they directly act on the top of the network and are usually considered human induced. First descriptions of trophic cascade is given by Hairston et al. (1960) and Estes and Palmisano (1974) and the term was coined by Paine (1980). One of the most famous trophic cascade examples is the interactions between killer whale, otter, sea urchin and kelp described by Estes et al. (1998). The intensive exploitation on top predators is thus considered as one of the main factors inducing trophic cascades (Pinnegar et al., 2000) and leading to imbalances in ecosystem functioning (Jennings and Kaiser, 1998; Pinnegar et al., 2000). Many examples of profound changes in distinct ecosystems triggered by fishing have been documented: shifts in community assemblages have been reported from New Zealand and Mediterranean subtidal reefs (Guidetti and Sala, 2007; Shears and Babcock, 2002), Caribbean and African coral reefs (Hughes, 1994; McClanahan and Shafir, 1990) or from the Gulf of Maine (Steneck et al., 2004), and even more examples of trophic cascade are widely documented in literature (e.g. Estes et al., 2011; Frank et al., 2005, 2006). In the majority of cases trophic cascades have been detected in systems with alternate dominance of sea urchins and fish, while other potentially important components in trophic cascade events, such as the macrofauna (polychaetes and small crustaceans or molluscs), have not been usually investigated.

Studies on trophic cascades in the Mediterranean are almost inexistent (see also Chapter 1). The mechanism has been argued to exist in shallow hard or soft bottom communities (e.g. Pinnegar et al., 2000; Sala et al., 1998), but results are usually inferential or based on small-scale experiments, while large-scale and long-term implications remain untested (Elner and Vadas Sr, 1990; Pinnegar et al., 2000; Sala et al., 1998).

Equally, (but few) cases exist in which intense fishing has not triggered cascading effects (e.g. Cardona et al., 2007; Reid et al., 2000). For example Cardona et al. (2007) discuss as possible explanation of this results the oligotrophy of the studied area (off northern Minorca) and thus the limited production of the basal species (the genus *Cystoseira* in this case) with respect to previous studies performed on

the mainland continental shelf (in front of Catalonia, Spain). A completely lack of information there is about trophic cascades in food-limited ecosystems, such as in the deep sea

In the continental slope of the NW Mediterranean the red shrimp (*Aristeus antennatus*) fishery is the main human activity, as we described in previous chapters. Early stock assessments of this species showed that the exploitation status was close to the optimum in the 1980s and 1990s (Demestre and Leonart, 1993; García Rodríguez and Esteban, 1999), but recent stock assessments warn of excessive fishing mortality coupled to low stock abundance (Anderson et al., 2012; García Rodríguez et al., 2007). As has been demonstrated in other cases the extensive fishing can lead to trophic cascade events.

Fishing remains the most studied key driving force in ecosystem changes at the scale of decades (Coll, Libralato, Tudela, Palomera and Pranovi, 2008; Daskalov et al., 2007; Jackson et al., 2001; Jennings and Kaiser, 1998; Palkovacs et al., 2012; Pauly et al., 1998; Shackell et al., 2010; Zhou et al., 2010), recently enhanced by the general awareness that water ecosystems are undergoing high pressures by modern fisheries. There are still disputes about which analytical tool should be used to study trophic interactions in ecosystems (Walters and Martell, 2004) and how can be applied in a management perspective. But what is actually suggested by current analyses is the full exploitation of most demersal and pelagic stocks (Aldebert and Recasens, 1996; Bas et al., 2003; FAO, 2009; Papaconstantinou and Farrugio, 2000; Sardà, 1998).

Trophic cascades and any other event that results from changes in predator abundance are top-down mechanisms that are set off by exogenous drivers like fishery but also climatic changes leading for example invasive predators. To the other extreme of the food web there are potential drivers of bottom-up processes. An example of bottom-up stressor is the nutrient enrichment that can lead to significant changes in the ecosystem and can be driven by human (in most cases of eutrofication) or environmental forces (seasonal changes or occasional events) usually related with climate changes (Verity et al., 2002). All trophic levels are potentially limited by available food resources (e.g. Hunter and Price, 1992). Thus any factor influencing the source availability can “cascades up” the system and affect population dynamics of upper trophic levels.

The main source sustaining deep sea life is the allochthonous (and dead) organic matter, except for (few) chemosynthetic spots. It has been demonstrated that its input shows a seasonal pattern (Billett et al., 1983) or depend on interannual production changes (El Niño in the Pacific) (Arntz et al., 2006) and also that deep sea fauna can respond rapidly to its variations (Gooday et al., 1990). In the NW Mediterranean the vertical mixing of water masses is particularly important, mainly in winter (and specially strong in the Gulf of Lions: Marty and Chiavérini, 2010). The organic matter belongs to two main pathways: the vertical settling and the advective flux across the slope (Pusceddu et al., 2010; Vetter and Dayton, 1999). The latter is enhanced by river discharges, e.g. the Rhône in the Gulf of Lions and the Ebro in the Balearic basin. In contrast, vertical fluxes are the result of organic matter produced in the waters of the epipelagic zone (phytodetritus, faecal pellets and dead animals falling down to the bottom). Due to the high temperatures in the Mediterranean, the “marine snow” and organic matter in general is rapidly consumed by bacteria. The amount that reaches the bottom is therefore very little. The matter proceeding from advection and horizontal currents can reach significantly higher values, e.g. in the Gulf of Lions advective flows establish two order of magnitude higher than the “marine snow” Durrieu De Madron et al., 2000. Also the active vertical migration of zooplankton and micronekton Vinogradov and Tseitlin (1983), or benthopelagic megafauna (Papiol et al., 2013) provide potential energy inputs for deep-sea ecosystems.

Many studies assessed the relative importance of bottom-up and top-down processes in regulating and structuring ecosystems (e.g. Cury and Shannon, 2004; Hunter and Price, 1992; Power, 1992). It has been argued that both forces act simultaneously (Hunter and Price, 1992), and their roles could vary among biological systems depending on the biotope (Pinnegar et al., 2000).

The main aim of this Chapter was to identify possible trophic cascades in the bathyal food web induced by the fishery of the red shrimp. In turn we examined 1) the relative strength between top-down and bottom-up processes, 2) between the two major inputs of source in the web (vertical and advective) and 3) between the selective fishing on the red shrimp with respect to harvesting on the whole megafauna comprising by-catch species.

## 6.2 Materials and Methods

We used the food web model developed in Chapter 5 and shown again in (A) Figure 6.1, and in (B) all components plotted with respect to their trophic level (Table 5.5, previous Chapter).

Within all components (considering the Humans) there are few possible pathways that reflect the initial conditions for its occurrence (Figure 6.1). Other subsets were not considered because the biomasses are very similar to any of adjacent trophic levels.

1)	HUMANS	→	MTL*	⇒	LTL
2)	HUMANS	→	MTL**	⇒	MABN
3)	HUMANS	⇒	MTL***	→	ZPL/SBN

TABLE 6.1: Possible pathways of trophic cascade. MTL = mid trophic levels, AANT, ICT and MEBN, LTL = lower trophic levels, MABN, SBN and ZPL. \* Jointly. \*\* Jointly or all subsets. \*\*\* Jointly or MEBN.

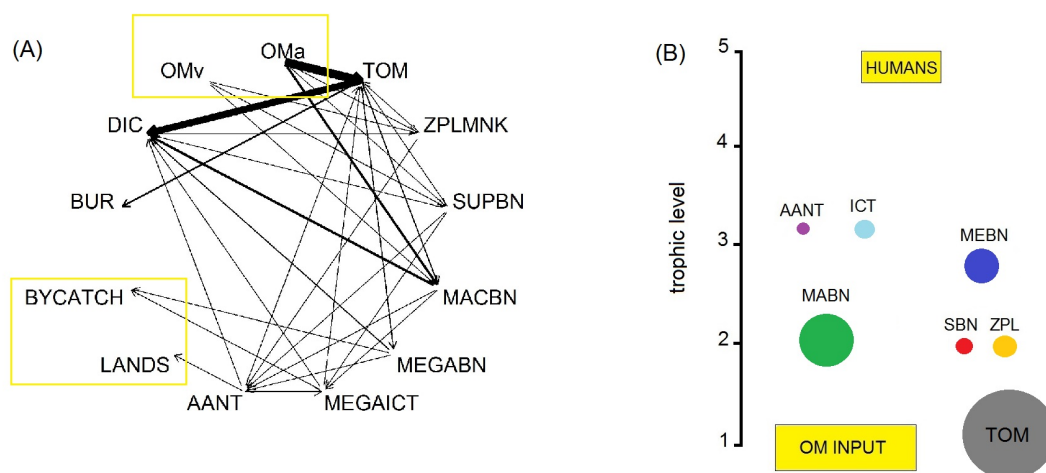


FIGURE 6.1: (A) Food web net flows and (B) trophic position of components. Colours correspond to compartments: orange = zooplankton (ZPL); red = suprabenthos (SBN); green = macrobenthos (MABN); blue = invertebrates from megafauna (MEBN); light blue = fish from megafauna (ICT); violet = red shrimp *Aristeus antennatus* (AANT).



### 6.2.1 The dynamic model

The dynamic model used to describe temporal changes in component biomasses after a disturbance (see below) is mathematically represented as an initial value problem (IVP) of ordinary differential equations (ODE, [Ascher and Petzold, 1998](#)). The ODE for the standing stock,  $s_i$ , is formally represented as

$$s_i' = f(s_i, v, , t), \quad (6.1)$$

where  $s_i'$  is the differential variable (the standing stock of a component),  $v$  a vector of parameters, and  $t$  refers to the time span during which the dynamics is simulated. Some initial conditions were required, i.e.

$$s_{it_0} = c \quad (6.2)$$

where  $c$  is constant and is the initial standing stocks of compartment at  $t_0$  [5.2](#). In addition the differential variable could obey some constraints at each time, such as to not exceed the compartment-specific growth efficiency and ensure energetic conservation assumptions.

The model relays on [Equations 1.10](#) and [1.12](#), that are here combined with the information derived from the LIM model ([Equations 5.1](#), i.e. the flowmatrix with the estimated flows rates ([Figure 5.4](#)), through the Jacobian  $\mathbf{J}$  of the system. In fact, each element,  $\alpha_{i,j}$ , of the Jacobian,

$$\alpha_{i,j} = \frac{\partial \frac{ds_i}{dt}}{\partial s_j}, \quad (6.3)$$

represents the interaction strength between two components  $s_i$  and  $s_j$ , in a manner conceptually analogous to the definition given by [May \(1972\)](#). Elements  $\alpha_{i,j}^u$  of the upper off-diagonal matrix describe the effect of  $s_j$  when it is consumed by component  $s_i$ , conversely, the elements  $\alpha_{i,j}^l$  of the lower off-diagonal matrix stand for the effect of  $s_i$  when it is the source of component  $s_i$ . Both correspond to

$$\alpha_{i,j}^u = -f(s_j) \quad \text{and} \quad \alpha_{i,j}^l = a_i p_i f(s_j). \quad (6.4)$$

Function  $f(s_j)$  is a functional response such these introduced in Equations 1.10 and 1.12 and must be defined. Many types have been described in Equations 1.13, 1.14, 1.15. According to Moore and de Ruiter (2012), for a functional response of first order, Equation 1.13, the element  $\alpha_{i,j}$  becomes

$$\alpha_{i,j}^u = -c_{ij}s_j = -\frac{x_{i,j}}{s_j}, \quad (6.5)$$

where,  $\alpha_{i,j}$  represents the effect of predator  $j$  on the prey  $i$ . Conversely,

$$\alpha_{i,j}^l = \frac{a_i p_i c_{ij}}{s_j} = a_i p_i \frac{x_{i,j}}{s_j}, \quad (6.6)$$

where, now  $\alpha_{i,j}$  represents the effect of prey  $j$  on predator  $i$ , and  $a_i$  and  $p_i$  are assimilation and production efficiencies of species  $i$ .

That leads to different functional responses for the type I and II. The first order response,  $f^1$ , between species  $s_i$  and  $s_j$ , linked with a consumption flow  $x_{j,i}$ , is

$$f^1 = \frac{x_{j,i}}{s_j}, \quad (6.7)$$

while, the second order type,  $f^2$ , is

$$f^2 = \frac{x_{j,i}}{s_j s_i}. \quad (6.8)$$

Here  $x_{j,i}$  is the flow from the source  $s_j$  to the consumer  $s_i$ .

In ODE model  $f^1$  is used for the flows from/to externals for which there are no quantitative estimates of standing stock, while  $f^2$  is used for all consumption flows from and to the component  $i$ , such that,

$$\frac{ds_i}{dt} = f^1 s_i - \sum_i (f^2 s_i s_j) + \sum_i (a_i p_i f^2 s_i s_j), \quad (6.9)$$

where here  $f^1$  is

$$f^1 = \frac{\sum x_{ext,i} - \sum x_{i,ext}}{s_i} \quad (6.10)$$

and  $x_{ext,i}$  and  $x_{i,ext}$  are flows between  $s_i$  and all externals.

Moreover, the model takes into account the conservation of the energy, such that the total flow to external can not exceed the total inflow.

## 6.2.2 Local stability of the food web

Different definitions of ecological stability have been developed centring on the capability of the system to maintain or return to its original state after perturbation (and originally supposed at equilibrium, the steady state) (McCann, 2000). Other definitions refer to the species composition or to the size of populations in a community (McCann, 2000). In this case the system must show a feasible equilibrium, i.e. all components  $s_i > 0$ . If the system is disturbed, causing a deviation,  $\Delta s_i$ , of any species from its original biomass and the system returns to its original equilibrium after a time, then the system is locally stable, otherwise it is unstable. The elements of the Jacobian of the system,  $\alpha_{ij}$  (Equation 6.3) return information about its stability (May, 1972). They represent the rate of change of the biomass in species  $s_i$  with respect to the biomass of species  $s_j$ . The stability of the system is then governed by the eigenvalues  $\lambda$  of the matrix  $\mathbf{J}$ ,

$$\lambda_{ij}(t) = \sum_{j=1}^m \alpha_{ij} s_j(t). \quad (6.11)$$

Eigenvalues can be complex numbers, such that,

$$\lambda = \chi + i\xi \quad (6.12)$$

with a real part  $\chi$  and an imaginary part  $\xi$ . The real part describes the degree of the the growth or decay while the imaginary part describes the sinusoidal oscillation of the deviation. The system is stable if the real part of all the eigenvalues is less than zero. If one or more  $\lambda$  have positive real part, than the system is unstable and will deviate from its original values. The Jacobian of the steady-state model can be used to assess the stability of the system in the time  $t_0$ .

### 6.2.3 The simulation

We set the values of the state variables, i.e. the biomasses of components (Chapter 5, Table 5.2), the flow matrix estimated through the parsimonious solution (4th column in Table E.4, Chapter 5), the model parameters (see Table E.3) and the time (5 years = 1825 days)

We controlled the following causes of perturbation:

1. Changes in the input of pelagic organic matter from vertical fall (OMv),
2. Changes in the input of terrigenous organic matter from advective processes (OMa),
3. Changes in the fishing pressure on red shrimp population,
4. Changes in the fishing pressure on bycatch components.

The first and second are both bottom-up, while the third and fourth are top-down drivers. Different components are involved in each process. The components directly effected from perturbing events are defined by the binary web (see Table E.2 in Chapter 5). Thus, changes in vertical or advective inputs directly perturb the following components: Zooplankton-Micronekton (ZPL), Suprabenthos (SBN), Macrobenthos (MABN) and the total organic matter in sediment (TOM), while changes in outflows due to fishery/bycatch perturb red shrimp (AANT), Ichthyofauna (ICT) and Megabenthos (MEBN) stocks.

The simulation is composed of three steps: 1) we first predicted the biomasses of all components for all levels of each type of disturbance, 2) we then calculated the proportion of components at each time and finally 3) we analysed the presence of shift in abundances between couples and triplets of species and so the presence of trophic cascade during the simulated time span.

Thus, we run dynamically the food web once with the steady-state solution, to ensure the stability of the model in its original built. It should remain constant, unless the food web is very unstable. Then we run the simulation for all other conditions as described below.

We built a four-nested loop to account for all types of perturbation, all calculations were made in the inner loop. We directly changed the biomasses involved in each of the processes at  $t = 1$ ,

$$s_i^{t_1} = s_i^{t_0} + (x_k \times p), \quad (6.13)$$

where  $s_i^{t_0}$  is the original biomass of component  $i$  at  $t = 0$ ,  $x_k$  is the value of the flow involved in the process, and  $p$  is a factor, indicating the magnitude of the perturbation and its direction. In practice we considered  $p \in 0, 5, 20, 50, -5, -20, -50$  for all processes. For example, let consider  $OMv \rightarrow ZPL$ . This flow goes from  $OMv$  to  $ZPL$ . When  $p = 0$ , the biomass does not change ( $s^{t_1} = s^{t_0}$ ), when  $p \in 5, 20, 50$  the flow increases with a factor of 5, 20 or 50 times, while if  $p \in -5, -20, -50$ , likewise it decreases. We used matrix calculation to change all components together. This setting allowed for one control level (0) that is, without perturbation and six more levels: three with increasing and three with decreasing disturbance. In this way the comparisons between the same magnitudes for all processes is possible as well as quantify the main effect for each one of the process and the interaction (till three factors).

The dynamic simulation returned a list of 2401 matrices ( $7^4$ , 4 factors with 7 levels each one) containing the simulated biomasses in each time,  $\mathbf{B}_{(T \times S)}$ , with  $T = 1825$  days (equivalent to 5 years) and the number of compartments,  $S = 7$ .

type rel	comb	components	
1)	PREDATION	PREY-PREDATOR	
	comb3	ZPL,MEBN	
	comb4	ZPL,ICT	
	comb5	ZPL,AANT	
	comb7	SBN,MEBN	
	comb8	SBN,ICT	
	comb9	SBN,AANT	
	comb10	MABN,MEBN	
	comb11	MABN,ICT	
	comb12	MABN,AANT	
	2)	COMPETITION	
		LOWER TL	
comb1		ZPL,SBN	
comb2		ZPL,MABN	
comb6		SBN,MABN	
UPPER TL			
comb13		MEBN,MEICT	
comb14		MEBN,AANT	
comb15	ICT,AANT		

TABLE 6.2: Relationship investigated.

### 6.2.3.1 Couples of species

We calculated the proportion of the biomasses of each compartment in the community at each time step.

Possible interactions between couples of components in the community (combinations) are

$$C(n, r) = n! / r!(n - r)! \quad (6.14)$$

where the number of components is  $n = 6$ , and interacting components are  $r = 2$ .  $C$  in our case is  $C = 15$ . However we must distinguish between combinations, because some of them are between components with the same trophic level (or competing, partially or entirely, for the same resource) or adjacent trophic levels (i.e. predator-prey interactions) as reported in Table 6.2.

We used as trade-off for the proportion the  $f = 2$ . If one component biomass (higher at the beginning) returned a proportion lower than 1/2 of another and of its original proportion and if such conditions continued for more than 10 days, then we considered enough to give evidence of a shift between the two biomasses. We also considered the opposite situation, i.e. when the biomass is more than 2 of the other component and of its initial proportion. That allowed to detect both negative and positive shifts in relative proportions.

We summarised results calculating some basic statistics shown in Table 6.3.

### 6.2.4 Software

The simulations and all statistical analyses have been performed in the R statistical programming environment (R Development Core Team, 2013).

We used R-package deSolve (Soetaert et al., 2010b) to run the dynamic model. It implements a variety of solvers and permits to specify the Jacobian and to select the solver according to the Jacobian's nature. Within the amplitude of methods we used the lsoda, because it automatically selects a stiff or nonstiff method and may switch between them during the simulation, in case the stiffness of the system

indicator	description
<i>collapse</i>	(binary) describes if one or both biomasses drop to zero during the studied period (1) or not (0)
<i>p.shift</i>	(binary) describes if component i returned higher proportion than component j during the studied period (1) or not (0)
<i>n.shift</i>	(binary) describes if component i returned lower proportion than component j during the studied period (1) or not (0)
<i>c.times</i>	returns how many times <i>collapse</i> occurs during the period
<i>p.times</i>	returns how many times <i>p.shift</i> occurs during the period
<i>n.times</i>	returns how many times <i>n.shift</i> occurs during the period
<i>c.duration</i>	returns the mean period (days) of <i>collapse</i> events
<i>p.duration</i>	returns the mean period (days) of <i>p.shift</i> events
<i>n.duration</i>	returns the mean period (days) of <i>n.shift</i> events

TABLE 6.3: List of indicators (response variables) and their description.

changes. This is the default method used in ode and specially well suited for simple problems as our food web model is.

## 6.3 Results

### 6.3.1 Interactions effected

In Table 6.4 results of variable *shift* are shown for different combinations of studied factors and each interaction between species.

In the simulation we also distinguished between selective catching of the red shrimp or of red shrimp and the accompanying fauna, i.e. all other megabenthos. But in this case as well no difference were observed.

When we checked the simultaneous existence of positive (or negative) effect on upper level and negative (or positive) on lower level, we did not find the conditions required for the existence of trophic cascades. All possible trophic cascade are shown in Table 6.1.

### 6.3.2 The total biomass

The trends of total biomass ( $\text{mmol C m}^{-2}$ ) are shown in Figures F.1, F.2 and F.3 (Appendix F) in three different scenarios (A, B, C) corresponding to the three different intensities (5, 20 and 50). In each scenario are represented the levels for factors (OM input and fishing effort). With the aim to summarise the results we show only a selection of possible interactions ( $n=21$  different plots within  $N=49$  possible interactions) and where the base-base interaction is replicated in all Figures. The base case corresponds to the unperturbed run, that, if the food web in its steady state is stable, must return a strait line (as is actually shown in A11, B11, C11 for each figure). Each row (or column) corresponds to zero (base), positive (more) or negative (less) perturbation. Different Rows correspond to different levels of energy input while columns to fishing intensity.

In all figures the difference between levels of organic matter input is evident (comparing graphics vertically), while unobservable differences exist among levels of fishing intensity. Only in the first horizontal line of all figures, corresponding to unperturbed organic matter inputs, A1·, B1·, C1·).

		(A-B-C)		
		base	more	less
(A)	base	-	-	-
	more	-	-	-
	less	ZPL-Ma	ZPL-Ma	ZPL-Ma
		ZPL-Me	ZPL-Me	ZPL-Me
		ZPL-I	ZPL-I	ZPL-I
(B)	more	ZPL-A	ZPL-A	ZPL-A
		ZPL-S	ZPL-S	ZPL-S
		S-A	S-A	S-A
	less	ZPL-A	ZPL-A	ZPL-A
		-	-	-
(C)	more	ZPL-SBN	ZPL-SBN	ZPL-SBN
		Z-Me	Z-Me	Z-Me
		S-A	S-A	S-A
		Z-A	Z-A	Z-A
	less	-	-	-

TABLE 6.4: Couples of components between which the *shift* occurs.



All lower rows in all figures and the middle row in Figure F.3 exhibit unstable dynamics that which will be analysed in depth when describing relative biomasses behaviour 6.3.3 in Section 6.3.3.

### 6.3.3 Relative biomasses

With the same logic are shown the relative biomasses of components in Figures 6.2, 6.3 and 6.4.

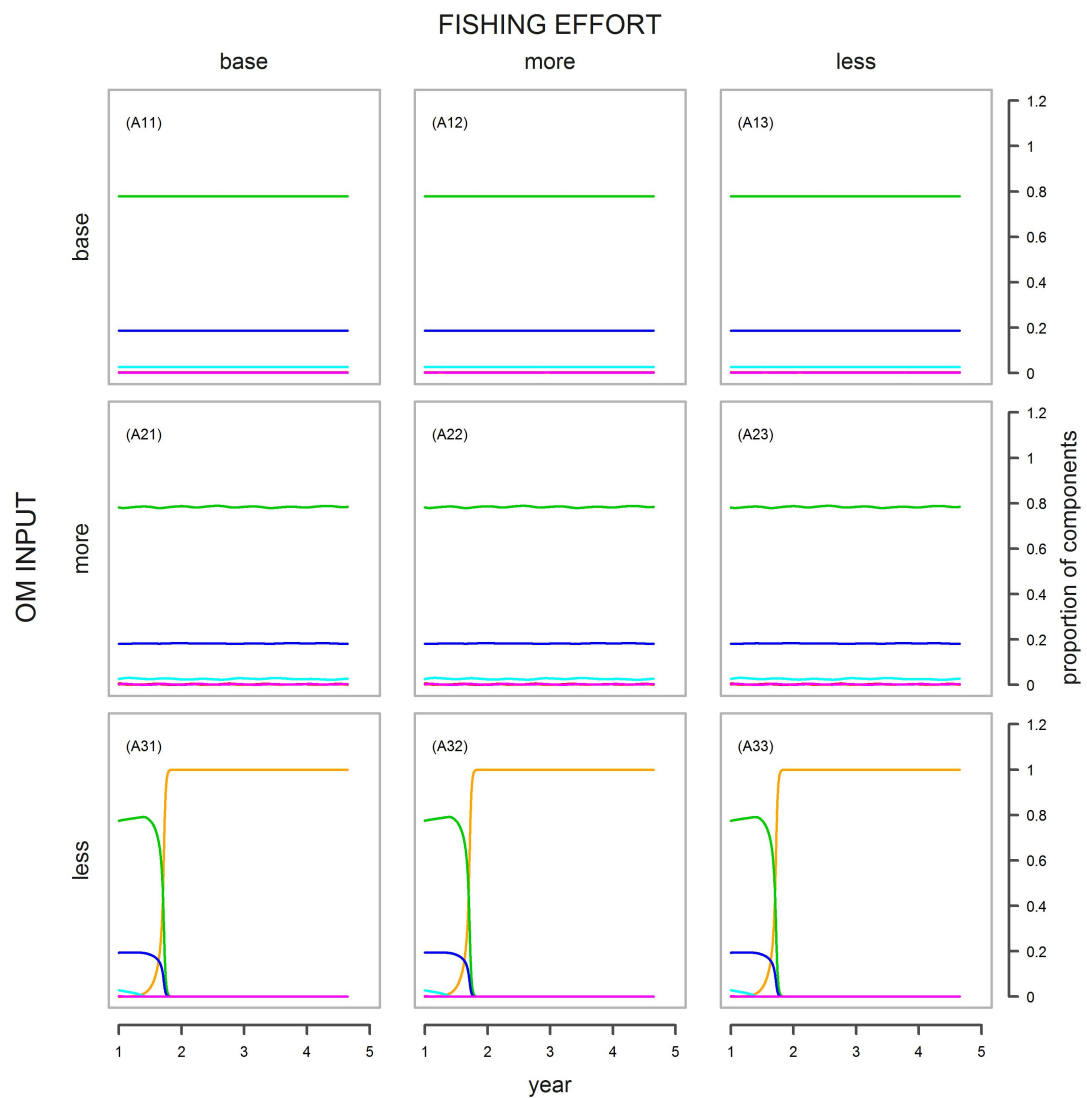


FIGURE 6.2: A) Changes of relative biomasses during the 5 years using  $p=(0,5,-5)$ .

In this case as for previous figures differences are evident among levels of organic matter input (vertical comparison), while unobservable are differences among levels of fishing effort (horizontal comparison). Notable differences can be observed in the last row (in each figure) with respect to the above rows of the same figure and between last rows of all figures (precisely between A3· and both B3· and C3·).

## 6.4 Discussion

In this study we applied dynamic simulations to the quantified food web model (fully described in Chapter 5) in order to evaluate the occurrence of trophic cascade

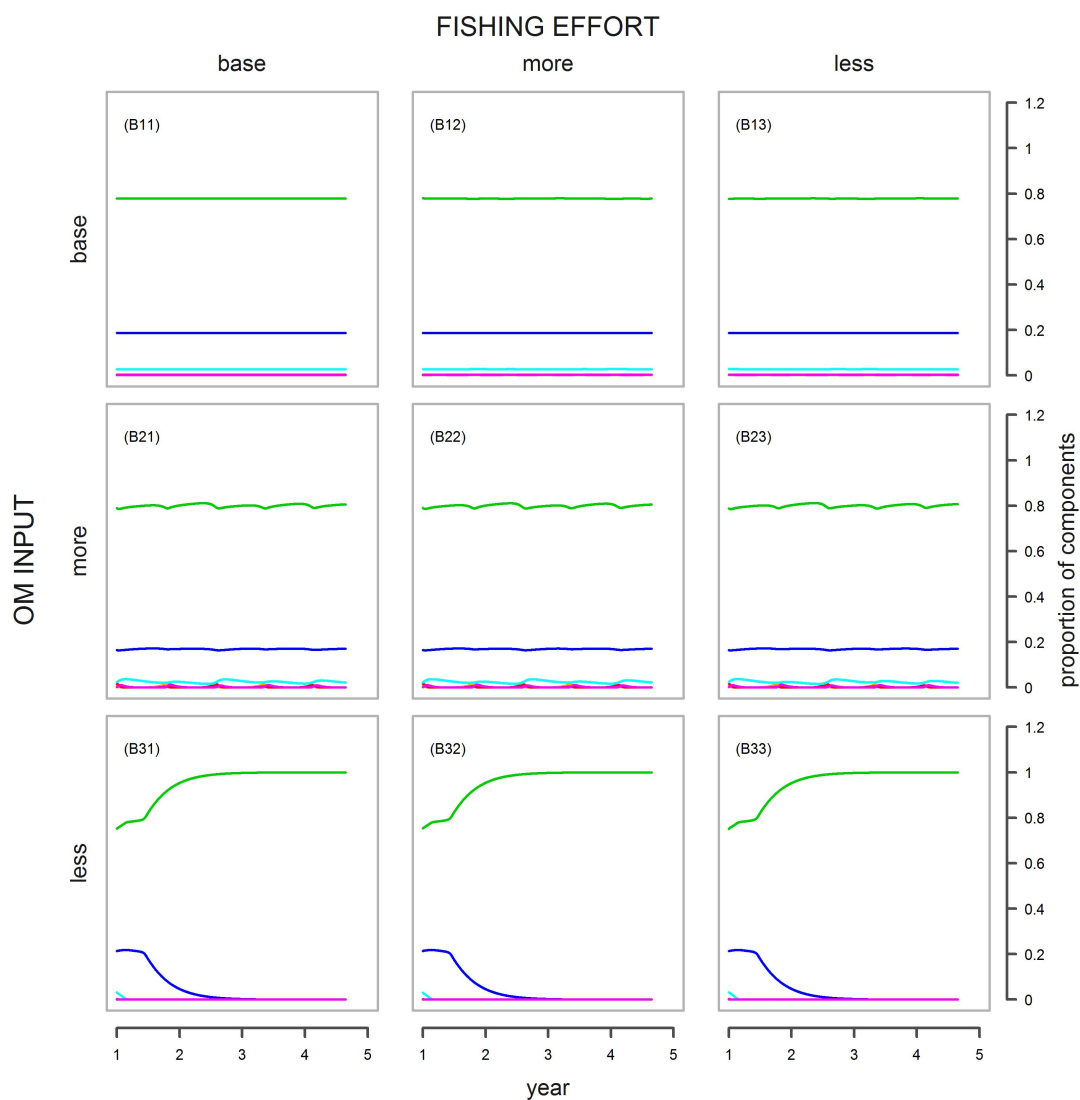


FIGURE 6.3: B) Changes of relative biomasses during the 5 years using  $p=(0,20,-20)$ .

in the bathyal ecosystem. To do so we used a system of ordinary differential equations to predict biomass trends during 5 years after perturbations induced by red shrimp fishery (top-down driver) and by food supply limitations (bottom-up driver). Then, we studied all possible pathways in the food web that might be subjected to this mechanism.

Despite the fact that many studies highlights the presence of trophic cascades in different ecosystems (e.g. [Estes et al., 2011](#); [Frank et al., 2005, 2006](#); [Guidetti and Sala, 2007](#); [Pinnegar et al., 2000](#); [Shears and Babcock, 2002](#)), in this work we have not found any evidence of trophic cascade. In fact our simulation demonstrated that trophic cascades induced by fishery cannot occur through major components

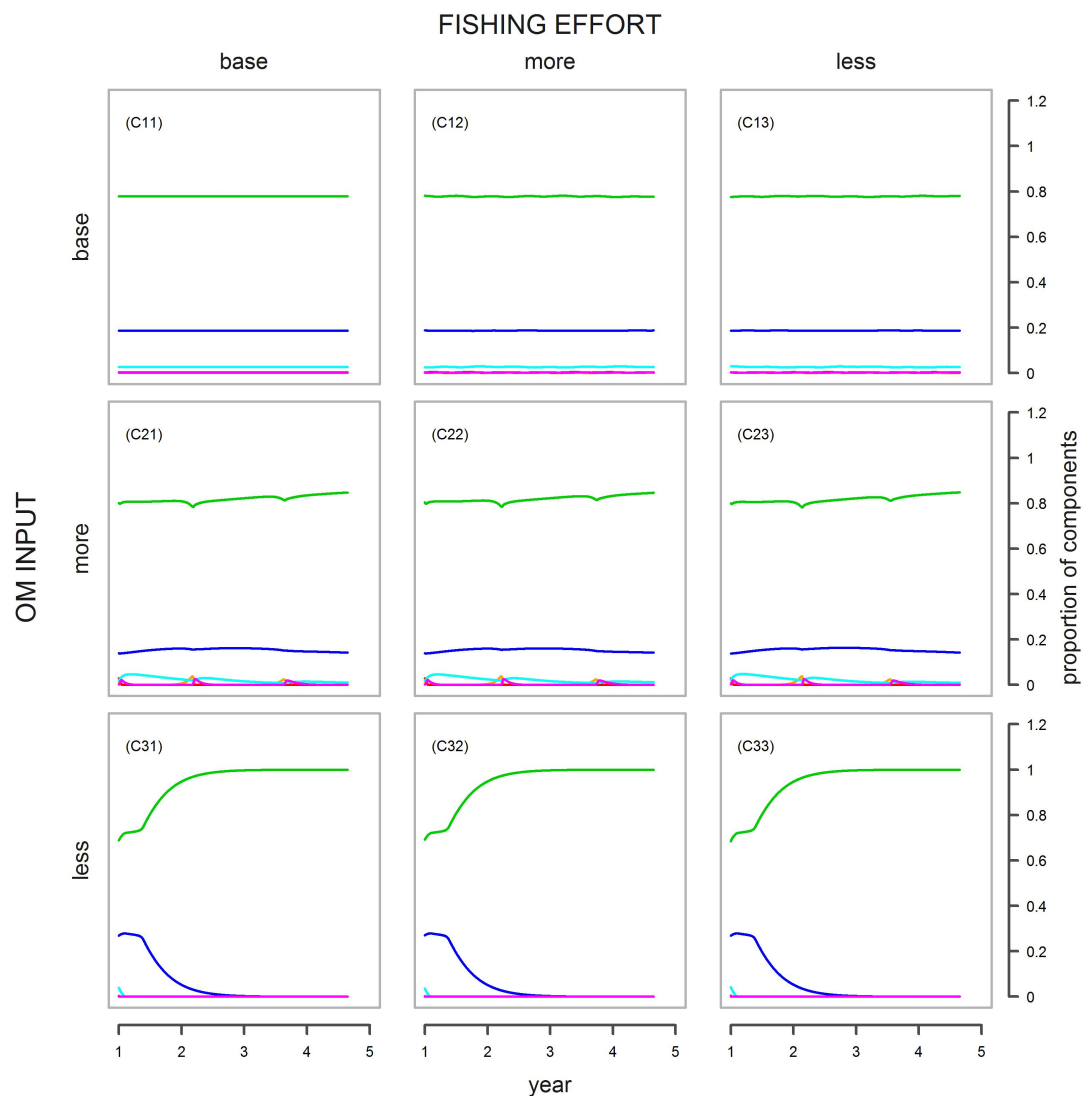


FIGURE 6.4: C) Changes of relative biomasses during the 5 years using  $p=(0,50,-50)$ .

of the bathyal food web (Table 6.1). We only found very ephemeral indirect effects persisting less than 10 days, that we considered not enough to demonstrate the occurrence of this mechanism in the system. On the contrary we found indirect effects persisting more than one month driven by source limitations. Our results are in agreement with previous studies in which trophic cascades have not been detected in benthic/detritic food webs, that have some similarities with the bathyal food web, that depends on allochthonous detritus.

Ecosystems for which trophic cascades have been shown present some common characteristics: low species diversity, simple food webs and small geographic size (Shurin et al., 2002; Strong, 1992). On the contrary Frank et al. (2005) asserted that marine continental shelf ecosystems, which generally have large spatial scales, high species diversity, and food web complexity, have not yet revealed unequivocal evidence of trophic cascades.

Other studies demonstrated the no occurrence of trophic cascade (at least Cardona et al., 2007; Reid et al., 2000) and other studies showed that detritus has a considerable implication in benthic food webs in both terrestrial and water ecosystems for example in relation to the high importance of bacteria (Hall Jr and Meyer, 1998; van Oevelen et al., 2012).

Has been argued that detritus based food webs are not controlled by predators, whereas only by the source (mainly allochthonous detritus such as in the deep sea) and have been called “donor-controlled” food webs (DeAngelis, 1980; Moore and de Ruiter, 2012). Examples considering detritus as allochthonous source have been described e.g. by Polis and Strong (1996) and Moore et al. (2004). This hypothesis (the donor control) induced e.g. Huxel and McCann (1998) to study allochthonous versus autochthonous sources in food webs finding that the food webs collapsed when the allochthonous source predominates. So, an allochthonous resource brings instability in the network. Also our simulation found high instability related to the (allochthonous) inputs. In some cases, components tended to zero (e.g. predators near to TL=3) or even very high. This is the case of the zooplankton and micronekton due to the fact that predators are scarce and that the zooplankton can directly gather from the allochthonous sources, can migrate and thus can be more competitive than other components with the same TL.

Recent studies on deep-sea food webs (e.g. Fanelli et al., 2009) showed that continental trophic webs can show complex interconnections that we not consider in

our model (Chapter 5). However, most of these complex interactions take place within the larger compartments considered, evidenced for lower trophic levels (e.g. [Fanelli et al., 2009](#)) (they represents substructures within larger structures or modules), while higher trophic levels (decapods and fish) show a continuum in their trophic niches, a continuum of benthic-pelagic sources ([Papiol et al., 2013](#)). For this reason, our low resolution food-web model is a compromise solution and do not affect to a large extent the within compartment complexities, because with its simplicity our model describes the multiplicity of interactions among larger components.

We found indirect effects due to red shrimp fishery between relative biomasses of red shrimp and the zooplankton or suprabenthic, but their biomasses remain very small with respect to the total, so we did not consider these effects as trophic cascade mechanisms.

Results also show the higher potential of resource availability in organizing the bathyal food web than the fishing effort in agreement with other studies that claimed the always important bottom-up in comparison to the top-down drivers (e.g. [Shurin et al., 2012](#)).

**Acknowledgements:** The authors thank all the participants of the BIOMARE (ref. CTM2006-13508-CO2-02/MAR) and ANTROMARE surveys, especially the crew of the F/V García del Cid for their inestimable help.



---

PART IV

---





## CHAPTER 7

---

General discussion

---



## 7.1 General discussion

In this Ph.D. thesis all topics considered aimed to understand different aspects of the bathyal ecosystem with the final intention to discuss the possibility of trophic cascade induced by fishing activity. The following sections summarise some important aspects discussed in each chapter separately but also some new features and goals, listed below.

## 7.2 PART I The infauna in the continental slope

Results from Chapter 2 show that macrofauna variability is related to physico-chemical variables in the water column and in sediments. Higher temperature and salinity, corresponding to the arrival of the Levantine intermediate water (LIW) in the Balearic Basin, and changes in water masses can influence the re-suspension of particles and inputs of the particulate organic matter (POM) from other areas, e.g. the Ligurian Sea, situated to the East of the Balearic Basin, and transferred to the studied sites from the current. These events affect to the nutritional value of sediment (not only temperature and salinity): for example TOC (quantity), C/N and  $\delta^{13}\text{C}$  (quality), with which we found significant relationship with macrofauna. The relationship between macrobenthos and TOC (the quantity of food) has been found also in other studies, e.g. in the Atlantic Ocean (Sibuet et al., 1989) and the Angola Basin (Kröncke and Türkay, 2003).

We found that the biomass in our area is higher than in nearby areas (Toulon canyon, Stora et al., 1999). Annual biomass ranges between 0.62 g DW/m<sup>2</sup> outside the canyon and 0.96 g WW/m<sup>2</sup> inside the canyon, two-times higher than in or close to Toulon canyon at comparable depths (500 m: 0.32–0.54 g DW/m<sup>2</sup>: Stora et al., 1999).

Also diversity (S) and total abundance (338.2 ind/m<sup>2</sup>) in the canyon are higher here in comparison to the Toulon canyon (S = 36; N = 176 ind/m<sup>2</sup>). We related this difference to the existence of a river in the north of Barcelona, the Besós river, while the Toulon canyon is not an extension of any river. Such different conditions are probably related to differences in food availability.

We also found differences in comparison to the eastern Mediterranean as we could expect. In our study the biomass is clearly higher (one order of magnitude) than

values in the South Cretan Sea (Tselepides et al., 2000), where biomass ranged between 0.05 – 0.09 g DW/ m<sup>2</sup> (Tchukhtchin, 1964) and that is explained by the increasing oligotrophy from West to East in the Mediterranean.

Regarding to trophodynamics, surface deposit feeders (e.g. Ampharetidae among polychaetes and the echinoderm *A. chiajei*) dominant in the canyon, are replaced by subsurface deposit feeders (e.g. sipunculans) on the adjacent slope, in agreement with existing literature (Flach and Heip, 1996; Kröncke et al., 2003): species feeding mainly at the sediment surface are more linked to fresh organic matter (lower C/N), whereas subsurface deposit-feeders and predators are found in sediments with more refractory material (higher C/N). Other studies associated this replacement of trophic guilds with the depth (Pavithran et al., 2009; Stora et al., 1999) but we believe that it depends on trophic variables changing by depth. At the adjacent slope caudofoveats (*Falcidens* spp., *Prochaetoderma* spp.) and polychaetes Paraonidae biomasses were related to turbidity and fluorescence, likely because these taxa are surface deposit feeders but also carnivorous on diatoms and foraminiferans (meiofauna) (Fauchald and Jumars, 1979; Jones and Baxter, 1987). In fact as foraminiferans respond rapidly to inputs of fresh organic matter (Goulday, 1988), it is possible that they already reach high densities becoming abundant prey for the abovementioned macrofauna. That happens in February because the maximum of primary production at the surface begins in November-December, so then there is a lag of 1-2 months.

The quality of the POM deposited at the seafloor determines changes in the composition and biomass of macrofauna communities (e.g. off Banyuls: Gremare et al., 1997, and in the North Sea: Dauwe et al., 1998; Wieking, 2002; Wieking and Kröncke, 2003). These changes correspond to the feeding types of the structural taxa/species, matches being established between the available food and the feeding modes of the dominant consumers. Fresh matter inside the canyon in June-July has a terrigenous origin. Thus, the dominant energy flux was advective. On the adjacent slope, the advective flux is lower. On the contrary, temporal fluctuations of food sources (TOC, C/N,  $\delta^{13}\text{C}$ ) are less evident on the adjacent slope (more stability). That reasonably explains why the canyon assemblage was seasonally dominated by opportunistic trophic groups (Capitellidae, Flabelligeridae, Glyceridae), better able to adapt to rapid temporal changes in food inputs (and throughout the year by the always present surface deposit feeders). The proliferation of opportunistic species inside the canyon and a stronger temporal succession

of species is related to food availability and quality (TOC, C/N,  $\delta^{13}\text{C}$ ) and with greater influence of terrigenous inputs by river discharges. That should be not surprise because advection is many order higher (roughly 1:50 or more, strongly dependent on the season) than vertical fall and higher inside canyon than on the open slope.

The biomass in the canyon undergoes major changes throughout the year, while at adjacent slope it remained low. Diversity inside canyon reached higher values during the period of water column homogeneity (February and April) while is very low during heterogeneous periods. In the adjacent slope diversity was higher during the period of water column stratification and viceversa during homogeneous periods. This is probably linked to higher organic matter quantity (TOC) and quality of sedimentary food (lower C/N) inside canyon supplied by river discharges.

Another important consideration is that also in the successive study on the in-fauna performed in a nearby area (Mamouridis, Cartes and Fanelli, 2014a,b), we found similar trends in predominant taxa and trophic behaviour diversification found in Chapter 2. In fact habitats with taxonomic diversity, with the coral *Isidella elongata* (however had been strongly reduced in last years) or inside the canyon, the heterogeneous composition reflects the coexistence of different trophic behaviours for the diversified source availability. On the contrary, the open slope is dominated (Mamouridis, Cartes and Fanelli, 2014a,b) or seasonally dominated (Chapter 2) by the genus *Prochaetoderma* spp. a carnivorous caudofoveate feeding on foraminifera followed by different (sub)surface deposit feeders species and rare suspension feeders.

We finally highlight that during this study new records of caudofoveates have been found in the study area, e.g. *Falcidens gutturosus* and *Prochaetoderma alleni* with a total of five new records (Salvini-Plawen, 2009) for this taxon.

### 7.3 PART II Landings per unit effort LPUE

In Part II we combined commercial fisheries data, environmental and economic variables to model the landings per unit effort (LPUE) index of *A. antennatus* using more conventional (Generalized additive models, GAM, Chapter 3) and novel regression techniques (the Bayesian distributional regression models, DSTAR, Chapter 4).

In the GAM model the combination of variables (six predictors) captures the 43% of the total LPUE variability. The set of fishery-related variables (*trips*, *grt* and *group*) was the most important source, with an ED of 20.58%, followed by temporal (*time* and *period*, ED = 13.12%) and finally economic variables (*shprice*, ED = 9.30%). The importance of *trips* is associated to increasing experience of fishermen, through a process of trial and error (Maynou et al., 2003; Sardà and Maynou, 1998). Boats' *grt* also influence positively LPUE. The trawlers captures other capabilities of fishermen which can bias the LPUE (Marriott et al., 2011; Maynou et al., 2003) and are expected to be important in many fisheries (Maunder and Punt, 2004). Inter-annual variable (*time*) is much more important than intra-annual variability (*period*). The former is associated to environmental changes and probably macro-economic factors. We hypothesised a relationship with low NAO in the previous three years, that confirms the findings of Maynou (2008) and a possible relationship with the increase in fuel prices beginning in 2000. The following years were characterized by high inter-annual variability, when the price of fuel increased and showed greater variations. The variable *period* is more likely associated to local economy. The ex-vessel prices, *shprice*, shows a significant explanatory potential (ED = 9.30%). Low selling prices do not induce fishermen to practice this deep-water fishery, because they could not offset the high associated costs, and trawlers would rather switch to continental shelf fisheries, with lower costs and lower risk.

Obtaining information on deep-sea species population dynamics is notoriously difficult, but our analysis suggests that the use of fishery-dependent data to accurately describe the relative abundance of this resource is possible (at least it is not very different from the available fishery-independent data).

In turn, the definition of the relative importance of explanatory variables enables to make intervention on the relevant variables possible from a management perspective. Fishery-related variables tend to have a significant effect on LPUE (ED = 21% in our case), and management measures aiming to reduce fishing mortality could be based on limiting the trawlers or the number of trips permitted in deep-water fishing grounds, by defining a threshold when the number of trips does not significantly increase the partial effect for LPUE (the profit does not exceed the cost). Also the boat size can be reduced, however the effect of the *grt* is lower, so a measure of this type becomes less effective.

Studies of deep-water systems, where harsh conditions limit methods for evaluating fisheries, often suffer from a lack of data in order to assess stock status. Although the goal of fisheries managers is to promote sustainable production of fish stocks through formal stock assessment, it is often impractical to collect fishery-independent data in isolated or harsh environments. In these cases the information collected by a fishery is the main (or only) source of abundance data available (Maunder et al., 2006). In this context it is useful the usage of random effects when data are limited or correlated as discussed below.

Concerning to the statistical methodology, in Chapter 4 we proposed distributional structured additive models, used here for the first time to model fishery index (LPUE or CPUE). DSTAR allowing to model both first and higher order moments of the response, returns lower DIC values (that is even better estimates) and a better understanding of the variability in the response, when considering the second parameter. In fact the second moment (the shape for gamma distribution or scale for log-normal, the two distributions we considered in the study) can be explained by many of the variables we used in Chapter 4 (i.e. *trips* and *time*). For example the analysis performed on (almost) the same data set, where the GAM accounts only for the location, could not avoid the heteroscedasticity in the residuals (see Figure C.2). This heteroscedasticity can be (partially) explained by modelling also the second parameter. Here we demonstrated that both the number of trips and time strongly influence the second parameter, that in turn is (inverse) proportional to the variance (while the location is directly proportional).

Finally we point out another methodological issue concerning fixed versus mixed specification. In our study the fixed effects can be considered appropriate, representing sampling units the whole population of the studied fleet. However, mixed models are particularly suitable for both unobserved catching units and correlated observations in time series. In practise we clashed with estimation instability when trying to incorporate both catching units (called *code* in Chapter 4) and *grt* in fixed effects models. In Chapter 3 we could avoid the problem with clustering catching units into three groups, however this practise can bring to a loss of information or be wearisome. Finally, if boats hold random effects, it is not more necessary to consider them for standardization, because it is not affecting parameters estimation (the expectation or both expectation and shape/scale) of the conditional distribution of the response variable, the LPUE. Another important function of using random effects is the possibility to predict for unobserved catching units,

only if the effects of observed catching units truly represent a random sample of the entire (unobservable) population.

## 7.4 PART III The bathyal food web

The Catalan slope is one of the most studied bathyal ecosystems in the Mediterranean. However, as is the case for food webs in general (Moore et al., 2004), the identification of pathways within communities is difficult and even more so is its quantification.

The main trophic relationships in this environment were recently studied, unravelling very diversified and unexpected components, within the lower section of the food web structure, showing specialised to omnivory behaviour (Fanelli et al., 2009; Fanelli, Cartes and Papiol, 2011; Fanelli, Papiol, Cartes, Rumolo, Brunet and Sprovieri, 2011). However the estimation of the proportion among different types of feeding behaviours is still unavailable due to the high number of species living this ecosystem and the relatively low number of species of which diet has been examined. Moreover these studies suggest a modular structure of the food web (see, e.g. Fanelli, Cartes and Papiol, 2011), such that higher modules can be considered to simplify the model and make it manageable. This fact and the necessity to build a food web model for immediate use in fishery management (FAO, 2003) requires a compromise between complexity and simplicity, so as to study the main pathways of this complicated system and could make the model useful for a rapid management of the fishery in deep sea habitats within the ecosystem approach of fisheries (EAF).

With respect to other ecosystem modelling approaches, the great advantage of the LIM method is the ability to quantitatively reconstruct the food web even when the problem is under-determined (data-limited). We restricted the number of compartments, differentiating among large groups and distinguishing between two fundamental pathways in the bathyal environment that depend on external resources (vertical settling and advective processes) and recycled material.

In our area, the total biomass (only macro- and megafauna) was 30.46 mmol C m<sup>-2</sup>, very close to the bioass in the deep Faroe-Shetland Channel (30.22 mmol C m<sup>-2</sup>) (Gontikaki et al., 2011), and approximately 2/3 of that found at higher depths in the same region (45.93 mmol C m<sup>-2</sup>, converted from Tecchio et al.,



2013) and also lower than at the Nazaré canyon (van Oevelen, Soetaert, García, de Stigter, Cunha, Pusceddu and Danovaro, 2011) and Rockall Bank (van Oevelen et al., 2009); the latter two are more diversified habitats and show higher secondary production. On the contrary, in our area the biomass is higher than in the Fram Strait (van Oevelen, Bergmann, Soetaert, Bauerfeind, Hasemann, Klages, Schewe, Soltwedel and Budaeva, 2011), as expected for being a food web in the Arctic Ocean and at deeper waters (2500 m). Also at the Porcupine Abyssal Plain the biomass was lower, summing the biomasses with the same size classes returned a value of  $9.77 \text{ mmol C m}^{-2}$  (van Oevelen et al., 2012), that is 1/3 of that we found in the continental slope.

Organic matter inputs to the community from advective processes are more important than those from vertical fall (see for the magnitudes e.g. Buscail et al., 1995, 1990; Durrieu De Madron et al., 2000). This implies a higher structural role of this input. Infauna receives more OM from advective than vertical origin and then from the particulate organic matter in sediment. Between internal flows, those related to the TOM and the infauna showed higher and more uncertainty values. That is also related to their structural role in this ecosystem.

The secondary production in deep sea mainly depends on inputs of detrital matter deriving from the upper levels of the water mass and dropping down as phytodetritus, dead animals, faecal pellets, empty shells, skeletons and small organic particles of different nature. These particles falling down to the seabed have been usually called “marine snow” (Aldredge and Silver, 1988). Pelagic animals eat and also bacteria living in the water column mass degrade this source of energy during its way down, especially in the Mediterranean, where the temperature is relatively high with respect to the open oceans (Fanelli, Cartes and Papiol, 2011). The remaining detritus is deposited on the sea floor where more bacteria deteriorate it enter in competition with metazoans which benefit of the remaining source. Deep ocean communities’ carbon demand can exceed the vertical supply, being potentially supplied by lateral advection (Burd et al., 2010). That is the reason of the more structural role of advective processes in bathyal ecosystems. We found that a very low portion of this energy is recycled by the system (low Finn’s index: FCI =  $0.179 \pm 0.066$ ).

The total input of C estimated by the model ranges between 0.92 and 4.16  $\text{mmol C m}^{-2} \text{ d}^{-1}$  (mean value:  $2.62 \text{ mmol C m}^{-2} \text{ d}^{-1}$ ), while the total secondary production (excluding prokaryotes and meiofauna) ranges between 0.02 and 0.25  $\text{mmol C m}^{-2}$

$\text{d}^{-1}$  that represents only the 2.17 – 6.01% of the organic matter that enters the community. The reason lies on biogeochemical processes and dissipation of the energy, i.e. the burial estimated to be  $0.11 - 1.27 \text{ mmol C m}^{-2} \text{ d}^{-1}$ , equivalent to the 11.96 – 54.09% of the total organic input and the respiration, including the TOM ( $0.84 - 2.34$  equivalent to 56.31 – 91.70% of the input).

The total input is approximately 7 times less than the input at comparable depths in the canyon of Nazaré but almost similar to the value in the lower section of the same canyon (at 4000–5000 m) (van Oevelen, Soetaert, García, de Stigter, Cunha, Pusceddu and Danovaro, 2011), this can be explained by the oligotrophic character of the Mediterranean sea, with respect to the Atlantic ocean and the habitat of canyons. Also the burial of organic carbon was lower in the Mediterranean continental slope,  $0.73 \pm 0.28 \text{ mmol C m}^{-2} \text{ d}^{-1}$ , in comparison with same depths in the Nazaré canyon (van Oevelen, Soetaert, García, de Stigter, Cunha, Pusceddu and Danovaro, 2011), however the same parameters have been applied for this process. In contrast it was higher than the values estimated estimated by van Oevelen et al. (2009) ( $0.19 \text{ mmol C m}^{-2} \text{ d}^{-1}$ ) in the Rockall Bank's cold-water community and by van Oevelen et al. (2012) ( $0.03 \text{ mmol C m}^{-2} \text{ d}^{-1}$ ) in the Porcupine Abyssal Plain, where the burial efficiency has been considered much lower than in the continental margins (van Oevelen et al., 2012).

Regarding to the feeding types, deposit and suspension feeding represent the 93.30% of the total consumption in the food web and the remaining percentage belongs to carnivores. Of this 93.30% the deposit feeding represents the 73-78%. Deposit feeders are mostly represented by the infauna (90.14% of the total deposit feeding), while the rest is consumed by megafaunal components. On the contrary suspension feeders belongs to the zooplankton and suprabenthos. Carnivorous feeding among megafauna represents the 56.37%, such that suspension and deposit feeding are still important in these groups. Also the macrofauna comprises carnivorous species (feeding on micro- and meiofauna and on the “smaller” macrofauna). Thus carnivores are under-estimated by this model.

Has been argued that deep-sea macrobenthos (mostly detritus feeders) exhibit an expansion of trophic niches and species tend to be omnivorous to avoid competition for food (Gage and Tyler, 1991). This suggests that grouping many detritivorous in a single compartment, as in the present model, is a good compromise. Nonetheless more recent studies with isotopic methodologies found high variability in the relationship between  $\delta^{13}\text{C}$  and  $\delta^{15}\text{N}$  particularly among deposit feeders, suggesting

exploitation of particulate organic matter at different stages of degradation: from fresh phytodetritus to highly refractory or recycled material (e.g. [Fanelli, Papiol, Cartes, Rumolo, Brunet and Sprovieri, 2011](#)). Also the seasonal turnover of opportunistic species is reasonable as evidenced in ([Mamouridis et al., 2011](#)). This scenario suggests a continuum in species trophic niches and the consequent difficult to compartmentalise the food web. Many examples of this repartition in food web modelling are available ([van Oevelen et al., 2009](#); [van Oevelen, Soetaert, García, de Stigter, Cunha, Pusceddu and Danovaro, 2011](#)). When such information is not available, the compromise is to enlarge constrains in the model.

Our model gives necessarily a simplified picture of the trophic structure of the bathyal ecosystem and results represent an average within all species belonging to each modelled compartment. The TOM is considered as dead component however it comprises also living matter, but necessarily we set its TL = 1. However, micro- and meiofauna that could not be modelled present higher TL. For instance in the Nazaré canyon for nematodes the TL of deposit-feeders was estimated around 2 and omnivores and predators around 2.75 ([van Oevelen, Soetaert, García, de Stigter, Cunha, Pusceddu and Danovaro, 2011](#)). However considering that they usually have very low biomass with respect to the particulate organic matter in the sediment, is reasonable to consider that their TL do not affect to the average TL of the TOM as whole compartment. Zooplankton-micronekton (ZPLMNK), suprabenthos (SUPBN) and infauna (MACBN) have the same level (TL=2) occupying the “basis” of the bathyal food web almost eating on detritus (however of different source and quality) and as mentioned there are some carnivorous species eating on microplankton, microbenthos or meiobenthos (see also [Fanelli, Cartes and Papiol, 2011](#)). Fish (MEGAICT) and the red shrimp (AANT) show very similar positions (close to 3), while big invertebrates (MEGABN) are in the middle between lower and upper (modelled) levels. The difficult to capture the highest trophic levels of the food web must also be considered, when discussing results, that is the case of pelagic cephalopods and bigger sharks, that could show trophic levels higher than 4. These species with pelagic behaviour can also be sustained by other sources in the water column far from the bottom.

With respect to the index of omnivory, lower trophic levels showed specialized diets, a result that in this case is an artefact of the model. Setting higher degree of compartmentalization will give higher values of omnivory, in fact many species are omnivores but can also present seasonally specialised diets. For example that

happens in some polychaets, that turn their behaviour in relation to the environmental conditions from deposit to suspension feeding (e.g. species belonging to the family paraonidae) or are both deposit feeders and carnivores (e.g. caudofoveates) (Mamouridis et al., 2011). On the contrary higher trophic levels showed some degree of omnivory.

The total respiration with a mean value of  $1.89 \text{ mmol C m}^{-2} \text{ d}^{-1}$ , ranges between  $0.84 - 2.34 \text{ mmol C m}^{-2} \text{ d}^{-1}$  and is very low with respect to the cold-water coral community (e.g. van Oevelen et al., 2009). In our model only the sediments (without macrofauna) account for the 83.75% of the total respiration with the value of  $1.58 \pm 0.32 \text{ mmol C m}^{-2} \text{ d}^{-1}$ , while the percentages for macrofauna and megafauna are respectively 13.39% and 2.86% (sum of respirations of components of each size: 0.25 and  $0.04 \text{ mmol C m}^{-2} \text{ d}^{-1}$ ). Thus carbon processing is mainly due the living portion of the TOM (to prokaryotes and meiofauna) and only partially to metazoa (macro- and megafauna). In fact bacteria have the highest contribution within TOM compartment and for the whole community, as has been proven in other deep-sea benthic ecosystems (in the Nazaré canyon: van Oevelen, Soetaert, García, de Stigter, Cunha, Pusceddu and Danovaro, 2011 and in the Faroe-Shetland Channel: Gontikaki et al., 2011). In comparison with the CWC community at Rockall bank (van Oevelen et al., 2009), the respiration of our food web is more than 50 times lower. Despite, it is not surprising because the CWC community has characteristics of a hot spot habitat and thus respiration is higher than all literature data available (van Oevelen et al., 2009). Respiration is instead higher than that found at higher depths in our region (Tecchio et al., 2013), where only metazoan community was modelled and respiration was estimated around  $0.64 \text{ mmol C m}^{-2} \text{ d}^{-1}$  after conversion. However we cannot say that it is statistically lower, having no estimates of the variability. Finally, however lower than the conditional mean calculated by the model E.1 (see Appendix E), our estimation falls into the range of other deep-sea soft bottoms data at comparable depths (Andersson et al., 2004) (see also Figure 5.5 in Appendix E to compare oxygen consumption data).

The total system throughput (T.), measuring the total food web activity has a very low value, was  $7.04 \pm 1.38$ , does not significantly differ to that found in the lower section of the Nazaré canyon at 4000–5000 m depth while is more than four times lower than at comparable and higher depths of the canyon (van Oevelen, Soetaert, García, de Stigter, Cunha, Pusceddu and Danovaro, 2011). The total

system throughput (conventionally defined in Ecopath as TST, however for the definition given in [Libralato et al., 2010](#) seems to refer to the T..) was 18.62 at higher depths ([Tecchio et al., 2013](#)). Our estimation of the TST was  $12.657 \pm 3.572$ . The network analysis suggests that almost all the energy passing through the food web is not recycled (see TST and low values of TSTc and Finn's indices). Our value of FCI was  $0.18 \pm 0.07$ , thus statistically there were no significant differences with the upper and lower sections of the Nazaré canyon in contrast with the middle section at comparable depths ([van Oevelen, Soetaert, García, de Stigter, Cunha, Pusceddu and Danovaro, 2011](#)). The Finn's index for deep sea food webs is low in comparison to other food web models in the Mediterranean considering more extended systems ([Coll et al., 2007, 2006](#); [Piroddi et al., 2010](#); [Tsagarakis et al., 2010](#)). Among system development measures, the Ascendency is relatively low if compared with the development capacity of the system ( $5.75 \pm 1.12$  versus  $13.79 \pm 3.03$ ). In fact total AC is only  $0.30 \pm 0.03$ . Such indices define the maturity of the system, so, results show that the system may undergo significant changes if disturbed (this will be the main topic of the next Chapter 6). Moreover if we consider the repartition of the indices in internal, import, export and dissipation, A is lower for import and dissipation rather than internal and export flows, thus related flows are more unstable and are more vulnerable to changes.

## 7.5 PART III Trophic cascades and drivers in the bathyal ecosystem.

We found changes in relative abundances of couples of components. That suggested some indirect effects of (only bottom-up) drivers on the community. In fact we did not find indirect effect for more than two levels (indicating trophic cascades). Results showed the no existence of trophic cascade, a top-down mechanism, in bathyal ecosystems. In fact the possible trophic cascades in our food web, summarised in Table 6.1, do not exist neither for increasing nor for decreasing fishing effort. At least in the resolution we used for the dynamic simulation. Other studies in benthic ecosystems came to the same conclusion (at least [Cardona et al., 2007](#)) although they gave other explanations.

However in marine environments top-down controls have been often documented as the major force (e.g. [Steele, 1998](#)), in lack of evidences of opposite drivers on an

ecosystem scale of botto-up mediation. But this mechanism is generally supported by studies on eutrofication (Reid et al., 2000). In fact both forces are likely to operate in ecosystems supported by primary producers in varying proportions (Roff et al., 1988) in different time-scale scenarios (Reid et al., 2000).

Also where trophic cascade is well documented (pelagic systems) its indirect effects are not always striking because the difference between prey-predator abundances is not surprisingly high (except for some very popular and known examples of trophic cascade, e.g. Estes and Palmisano, 1974). For example, Rudstam et al. (1994) explained the low strength of top-down drivers with the high impact of other factors (changes in the interannual productivity or nutrient inputs) that could override any effect from predation.

Switching back to the bathial food web, other studies showed that detritus has a considerable implication on the dynamics of benthic food webs in water ecosystems for example in relation to the great importance of bacteria (van Oevelen et al., 2012) as well as in terrestrial ecosystems (Hall Jr and Meyer, 1998). This is to say that food webs based on detritus have perhaps a very different behavior from other food webs. In fact has been argued that detritus based food webs are not controlled by predators, whereas only by the source (Moore and de Ruiter, 2012) (mainly allochthonous detritus such as in the deep sea) and have been called “donor-controlled” food webs (DeAngelis, 1980; Moore and de Ruiter, 2012). Examples considering detritus as allochthonous source have been described e.g. by Polis and Strong (1996) and Moore et al. (2004).

This hypothesis (the donor control) induced e.g. Huxel and McCann (1998) to study allochthonous versus autochthonous sources in food webs finding that the food webs collapsed when the allochthonous source predominates. So, an allochthonous resource brings instability in the network. Also our simulation found high instability related to the (allochthonous) inputs. In some cases, components tended to zero (e.g. predators near to TL=3) or even very high (e.g. the zooplankton due to the fact that no more predators existed and which can be more competitive than other components with the same TL).

In addition we did not find significant effect with respect to fishing pressure (and we simulated almost to the extinction of the red shrimp). The changes we detected as discussed are not evidences of trophic cascades. Even though, their existence

(that we called *shift* in Chapter 6) may have the role of indicators of direct or indirect effects of some perturbations on the ecosystem.

We then considered the occurrence of these changes as an indicator of the strength of the perturbation in order to point out the relative importance between top-down (fishery) and bottom-up drivers (resource availability). We detected an unequivocal dominance of bottom-up forces. In fact both mechanisms can affect some aspect of the fauna and their strength may be scale-dependent and vary seasonally and spatially. Thus, it is of great utility to seek evidence for where and when each mechanism is likely to have its greatest effect.

But except to the observation or not of trophic cascade the simulation was designed also in order to define the relative importance of top-down and bottom-up processes. The latter in fact returned a very important role of source availability in re-organizing the bathyal food webs much more than the fishing activity. Many studies in the past claimed the always important bottom-up in comparison to the top-down drivers (i.e. [Shurin et al., 2012](#)).





## CHAPTER 8

---

Conclusions

---

## 8.1 Conclusions

1. Our analysis showed that the infaunal assemblage changes in composition in relationship to the nutritional value of sediments, TOC, C/N,  $\delta^{13}\text{C}$ , that are different in and outside the canyon. In the canyon surface deposit feeders (e.g. Ampharetidae and *Amphiura chiajei*), linked to fresh organic matter, are always dominant and occasionally are accompanied by opportunistic groups (e.g. Capitellidae), able to adapt their feeding behaviour according to food availability and to respond rapidly to temporal changes in food inputs. At the adjacent slope, where sediments are refractory, subsurface deposit feeders (e.g. sipunculans) are abundant.
2. According to the generalized regression modelling, the variables explaining the Landing per Unit Effort variation in red shrimp fishery were of three types: fishery-related, temporal and finally economic variables and they captured the 43% of the total variability. In descending order of importance they are: time, number of trips, shrimp price, gross registered tonnage, boats and period of the year. Fishery-dependent data provided an index reasonably similar to fishery-independent indices from bottom-trawls surveys. Moreover, the detection of influential variables, such as the number of trips, can be used to define a threshold on the number of daily trips and is of practical use in fisheries management.
3. I conclude that regression models based on Bayesian inference, such as Distributional Structured additive models (DSTAR), compare favourably with the traditional regression models of GAM type. In our case, DSTAR allowed to 1) objectively define the response distribution function, 2) specify fixed and random effects in a Mixed Model setting, 3) Specify unobserved catching units (boats) and correlated observations as random effects. 4) Finally, if boats really hold random effects, then there is no need to consider them for standardization.
4. I conclude that the LIM Methodology has the ability to reconstruct quantitatively the food web even when the problem is under-determined in data-limited contexts, such as the deep sea. This method also provided a measure of the uncertainty in the estimations of flows.
5. In the dynamic simulation of the food web we found no evidence of top-down mechanism due to fishery, i.e. trophic cascades for all possible pathways.

---

On the contrary bottom-up controls occurs especially when resources are limited (scenarios of low input of organic matter). In fact, modifying the fishing effort maintaining the input constant the proportions of components do not change in time. On the contrary the proportion changes when the resource is modified. The continental slope ecosystem is based on detritus derived from the upper photic systems. We thus conclude that our detritus based food web is affected by the dynamics of the source and not by the (top)consumer, a control type called “donor control”.



---

## APPENDICES

---



## APPENDIX A

---

EAF models

---

Acronym	Name/description	Ref.
ATLANTIS	ATLANTIS	1, 2
Bioenergetic/ allometric model	Multi-species trophodynamic model using bioenergetic and allometric approach	3, 4, 5
BORMICON	BOReal MIgration and CONsumption model	6, 7
CCAMLR	models Commission for the Conservation of Antarctic Marine Living Resources	8, 9, 10, 11, 12
EPOC	Ecosystem Productivity Ocean Climate Model	13
ERSEM II	European Regional Seas Ecosystem Model	14
ESAM	Extended Single-species Assessment Model	15, 16, 17
EwE	ECOPATH with ECOSIM	18, 19, 20, 21, 22
GADGET	Globally applicivable Area Disaggregated General Ecosystem Toolbox	23, 24, 25, 26
GEEM	General Equilibrium Ecosystem Model	27, 28

TABLE A.1: Alphabetical list of models used in the ecosystem approach of fisheries (PART 1/2). Revised from (Plagányi, 2007). References are: 1. Fulton, Smith and Johnson, 2004, 2. Fulton et al., 2005, 3. Yodzis and Innes, 1992, 4. Yodzis, 1998, 5. Koen-Alonso and Yodzis, 2005, 6. Bogstad et al., 1997, 7. Stefánsson and Palsson, 1998, 8. Butterworth and Thomson, 1995, 9. Mori and Butterworth, 2004, 10. Mori and Butterworth, 2005, 11. Mori and Butterworth, 2006, 12. Thomson et al., 2000, 13. Constable, 2006, 14. Baretta-Bekker et al., 1997, 15. Livingston and Methot, 1998, 16. Hollowed et al., 2000, 17. Tjelmeland and Lindstrøm, 2005, 18. Christensen and Pauly, 1992, 19. Christensen and Walters, 2004, 20. Polovina, 1984, 21. Walters et al., 1997, 22. (Walters et al., 2000), 23. Begley and Howell, 2004, 24. Trenkel et al., 2004, 25. Taylor and Stefánsson, 2004, 26. Taylor and Taeknigardur, 2011, 27. Finnoff and Tschirhart, 2003, 28. Finnoff and Tschirhart, 2008, 29. Alonzo et al., 2003, 30. DeAngelis and Gross, 1992, 31. Purcell and Kirby, 2006, 32. Shin and Cury, 2004, 33. Fulton, Smith and Johnson, 2004, 34. Fulton, Parslow, Smith and Johnson, 2004, 35. McDonald et al., 2006, 36. Watters et al., 2005, 37. Watters et al., 2006, 38. Punt and Butterworth, 1995, 39. Jurado-Molina et al., 2005, 40. Garrison et al., 2010, 41. Sparholt, 1995, 42. Sparre, 1991, 43. Tjelmeland and Bogstad, 1998, 44. Colomb et al., 2004, 45. Shin and Cury, 2001, 46. Bertignac et al., 1998, 47. Lehodey et al., 2003, 48. Lehodey et al., 2008, 49. Tjelmeland and Lindstrøm, 2005, 50. Bax, 1985, 51. Plagányi and Butterworth, 2006, 52. Sekine et al., 1991, 53. Hamre and Hatlebakk, 1998.



Acronym	Name/description	Ref.
IBM	Individual-Based Models	29, 30, 31, 32
IGBEM	Integrated Generic Bay Ecosystem Model	33, 34
INVITRO	INVITRO	35
KPFM	Krill-Predator-Fishery Model (KPFM, KPFM2)	36, 37
MRM	Minimally Realistic Model	38
MSM	Multi-species Statistical Model	39
MSVPA/ MSFOR	Multi-species Virtual Population Analysis and Multi-species Forecasting Model	40, 41, 42
MULTSPEC	Multi-species model for the Barents Sea	6
AGGMULT	simplified version connected to an ECONMULT model describing the economies of the fishing fleet	43
MOOVES	Marine Object-Oriented Virtual Ecosystem Simulator	44
OSMOSE	Object-oriented Simulator of Marine ecOSystem Exploitation	45
SEAPODYM	Spatial Ecosystem and Population Dynamics Model (previously SEPODYM)	46, 47, 48
SEASTAR	Stock Estimation with Adjustable Survey observation model and Tag-Return data	49
SKEBUB	SKEleton Bulk Biomass ecosystem model	50
SMOM	Spatial Multi-species Operating Model	51
SSEM	Shallow Sea Ecological Model	52
SYSTMOD	System Model for the Norwegian and Barent Sea	53

TABLE A.2: Alphabetical list of models used in the ecosystem approach of fisheries (PART 2/2). Revised from (Plagányi, 2007). References in A.1.



## APPENDIX B

---

Complementary material – Chapter 2

---

TAXA	Canyon	Ad. slope
<b>Cnidaria</b>		
<i>Stephanoscyphus</i> spp. Allman, 1874	0.0	2.0
<b>Archianellida</b>		
Archianellida unid	0.0	1.0
<b>Polychaeta</b>		
<i>Ampharete</i> sp. Malmgren, 1866	0.9	0.0
Ampharetidae Malmgren, 1867	34.5	1.9
Arabellidae Hartman, 1944	0.5	0.5
<i>Aricidea</i> spp. Webster, 1879	7.6	6.4
Capitellidae Grube, 1862	6.6	1.5
<i>Diplocirrus</i> sp. Haase, 1915	5.5	1.9
Eunicidae Berthold, 1827	4.3	0.0
Flabelligeridae Joseph Saint, 1894	0.9	0.5
<i>Galathowenia</i> sp. Kirkegaard, 1959	0.5	0.0
<i>Glycera</i> sp. Savigny, 1818	0.9	0.5
Glyceridae Grube, 1850	3.2	2.9
<i>Levinsenia gracilis</i> (Tauber, 1879)	2.8	2.9
<i>Levinsenia</i> spp. Mesnil, 1897	3.6	1.5
Lumbrineridae Schmarda, 1861	1.4	1.0
<i>Lumbrineris</i> sp. Blainville, 1828	0.9	0.5
Maldanidae Malmgren, 1867	3.6	3.5
<i>Marphysa bellii</i> (Audouin & Milne Edwards, 1833)	4.8	0.5
<i>Mediomastus</i> sp. Hartman, 1944	0.0	0.5
<i>Melinna</i> sp. Grube, 1869	10.9	0.5
Nephtyidae sp. A Grube, 1850	2.4	0.5
<i>Nephtys</i> sp. Grube, 1850	0.9	0.0
<i>Notomastus</i> sp. Sars, 1851	0.5	0.5
Ophelidae Malmgren, 1867	3.7	0.0
Orbinidae Hartman, 1942	1.4	0.5
<i>Paradiopatra quadricuspis</i> (M. Sars, 1872)	6.9	7.8
<i>Paradoneis lyra</i> (Southern, 1914)	0.5	0.0
Paraonidae Cerruti, 1909	3.6	2.9
Pilargidae St. Joseph, 1899	0.9	0.0
<i>Pista</i> sp. Malmgren, 1866	0.9	0.0
<i>Prionospio</i> sp. Malmgren, 1867	0.0	0.5
Sabellidae Malmgren, 1867	0.5	0.0
Spionidae Grube, 1850	6.9	2.9
Syllidae Grube, 1850	0.5	0.0
Terebellidae Grube, 1851	0.0	0.5
Polychaeta unid <sup>D</sup>	1.4	0.5
<b>Crustacea decapoda</b>		
<i>Calocaris macandreae</i> (Bell, 1846)	2.3	1.5
<i>Ebaliacranchii</i> (Leach, 1817)	0.5	0.0

TABLE B.1: List of species (PART 1/3). Mean number of specimens (ind/m<sup>2</sup>) collected from canyon adjacent slope.

TAXA	Canyon	Ad. slope
<i>Monodaeuscouchi</i> (Couch, 1851)	1.4	0.5
<b>Copepoda</b>		
Calanoidea	0.9	9.2
<b>Amphipoda</b>		
<i>Carangoliopsis spinulosa</i> Ledoyer, 1970	82.9	12.8
<i>Eriopisa elongata</i> (Bruzelius, 1859)	0.9	0.5
<i>Idunella nana</i> (Schiecke, 1973)	0.0	0.5
<i>Harpinia crenulata</i> (Boeck, 1871)	12.8	0.0
<i>Harpinia dellawallei</i> Chevreux, 1910	5.4	3.5
<i>Harpinia</i> spp. Boeck, 1876	9.5	2.1
<i>Lilljeborgia psaltrica</i> Krapp-Schickel, 1975	0.9	0.0
<i>Maera schmidtii</i> Stephensen, 1915	3.2	0.5
<i>Metaphoxus simplex</i> (Bate, 1857)	3.7	4.0
<i>Monoculodes</i> sp. Stimpson, 1853	1.9	0.0
<i>Orchomenella nana</i> (Krøyer, 1846)	0.0	1.9
<i>Paraphoxus oculatus</i> (G. O. Sars, 1879)	6.4	0.5
Pardaliscidae Boeck, 1871	0.0	1.9
Phoxocephalidae <sup>D</sup> G.O. Sars, 1891	0.0	0.5
<i>Psammogammarus</i> sp. A. S. Karaman, 1955	0.0	1.9
<i>Sophrosyne hispana</i> Chevreux, 1887	1.4	0.5
<i>Urothoe corsica</i> (Bellan-Santini, 1965)	1.4	6.4
<b>Cumacea</b>		
<i>Diastylodes serrata</i> (G. O. Sars, 1865)	0.0	0.5
<i>Epileucon ensis</i> (Bishop, 1981)	1.9	0.0
<i>Eudorella truncatula</i> (Bate, 1856)	7.7	0.5
<i>Leucon longirostris</i> Sars, 1871	15.7	6.9
<i>Leucon macrorhinus</i> (Fage, 1951)	1.9	2.1
<i>Leucon siphonatus</i> Calman, 1905	5.8	0.0
<i>Makrokylindrus gibraltarensis</i> (Bacescu, 1961)	0.0	3.8
<i>Makrokylindrus insignis</i> (G. O. Sars, 1871)	0.0	1.0
<i>Makrokylindrus longipes</i> (G. O. Sars, 1871)	0.9	0.0
<b>Isopoda</b>		
<i>Pilosanthura fresii</i> (Wägele, 1980)	5.0	4.0
<i>Chelator chelatus</i> (Stephensen, 1915)	7.5	6.9
<i>Desmosoma linearis</i> (Linnaeus, 1767)	0.9	0.5
<i>Eugerda</i> sp. Meinert, 1890	1.9	0.0
<i>Gnathia</i> spp. <sup>L</sup> Leach, 1814	0.5	0.0
<i>Ilyarachna longicornis</i> (G. O. Sars, 1864)	1.9	0.0
<b>Tanaidacea</b>		
<i>Apseudes spinosus</i> (M. Sars, 1858)	0.5	0.0
Tanaidacea unid.	5.8	0.5
<b>Ostracoda</b>		
Cypridinidae	3.8	0.0

TABLE B.2: List of species (PART 2/3). Mean number of specimens (ind/m<sup>2</sup>) collected from canyon adjacent slope.

TAXA	Canyon	Ad. slope
Ostracoda unid	0.0	4.0
<b>Pycnogonida</b>		
Pycnogonida unid	1.9	0.0
Crustacea unid <sup>L</sup>	0.0	0.5
<b>Caudofoveata</b>		
<i>Falcidens strigisquamatus</i> Salvini-Plawen, 1977	4.3	9.2
<i>Falcidens aequabilis</i> Salvini-Plawen, 1972	1.8	1.5
<i>Falcidens guttuosus</i> (Kowalesky, 1901)	6.2	0.0
<i>Prochaetoderma alleni</i> (Scheltema & Ivanov, 2000)	0.5	0.5
<i>Prochaetoderma boucheti</i> Scheltema & Ivanov, 2000	8.1	0.0
<i>Prochaetoderma</i> spp. Thiele, 1902	5.0	11.4
<i>Scutopus ventrolineatus</i> Salvini-Plawen, 1968	1.9	0.0
<b>Scaphopoda</b>		
Scaphopoda unid	3.8	0.0
<b>Gastropoda</b>		
<i>Eulimella neoattenuata</i> (Gaglioli, 1992)	0.5	0.5
<i>Euspira fusca</i> (Blainville, 1825)	1.9	0.0
<b>Bivalvia</b>		
<i>Abra longicallus</i> (Scacchi, 1894)	8.9	9.9
<i>Axinulus croulinensis</i> (Jeffreys, 1847)	1.4	0.5
<i>Cochlodesma tenerum</i> (Fischer, 1882)	0.5	0.0
<i>Ennucula aegeensis</i> (Forbes, 1844)	4.5	14.9
<i>Kelliella miliaris</i> (Philippi, 1844)	36.0	2.1
<i>Ledella</i> cf. <i>marinostri</i> La Perna 2004	1.8	1.5
<i>Limatula bisecta</i> Allen, 2004	0.0	0.5
<i>Mendicula ferruginosa</i> (Forbes, 1844)	0.5	0.5
<i>Yoldiella messanensis</i> (Jeffreys, 187)	0.5	4.9
<b>Sipuncula</b>		
<i>Aspidosiphon muelleri</i> Diesing, 1851	1.9	1.0
<i>Nephasoma</i> cf. <i>abyssorum</i> (Koren & Danielssen, 1876)	0.0	1.9
<i>Nephasoma</i> cf. <i>diaphanes</i> (Gerould, 1913)	0.0	1.9
<i>Onchnesoma steenstrupii</i> Koren & Danielssen 1875	4.5	19.0
<b>Echiurida</b>		
<i>Echiurus abyssalis</i> Skorikov, 1906	0.0	0.5
<b>Echinodermata</b>		
<i>Amphipholis squamata</i> (Delle Chiaje, 1828)	1.9	3.6
<i>Amphiura chiajei</i> (Forbes, 1843)	18.6	0.0
<i>Amphiura filiiformis</i> (Müller, 1776)	0.9	0.0
<i>Amphiura</i> cf. <i>grandisquama</i> Lyman, 1869	1.9	0.0
Ophiuroidea unid <sup>J</sup>	1.9	1.9
<i>Brissopsis lyrifera</i> (Forbes, 1841)	0.5	0.5
<b>Nematoda</b>		
Nematoda unid	0.9	4.4

TABLE B.3: List of species (PART 3/3). Mean number of specimens (ind/m<sup>2</sup>) collected from canyon adjacent slope.

## APPENDIX C

---

Complementary material – Chapter 3

---

## C.1 Exploratory study on the response variable LPUE and diagnostic plots of the final model

In Figure C.1 are shown the characteristics of the variable *lpue*. The probability density function (*pdf*) is positively skewed (upper panels). Data hold atypical values in the right tail (see the box-plot, left middle panel) and the distribution function of the gamma distribution lies approximately inside the 95% confidence intervals of the empirical cumulative distribution function (*ecdf*) of *lpue* (right middle panel). Finally, the QQ-plots for the gamma and the Gaussian distributions provide evidence of a better fit of data to the gamma rather than the Gaussian distribution (on the left and the right lower panels respectively).

Figure C.2 shows the diagnostic plots for the selected model (corresponding to Equation 3.3 in the text and model 7 in Table 3.2, Chapter 3). Residual quantiles lie on the straight line of the theoretical quantiles, although slightly heavy-tailed; in the histogram, residuals are consistent with normality and the relationship between response and fitted values is linear and positive. Residuals versus the linear predictor (that is, the sum of all partial effects) show a faint heteroscedasticity.



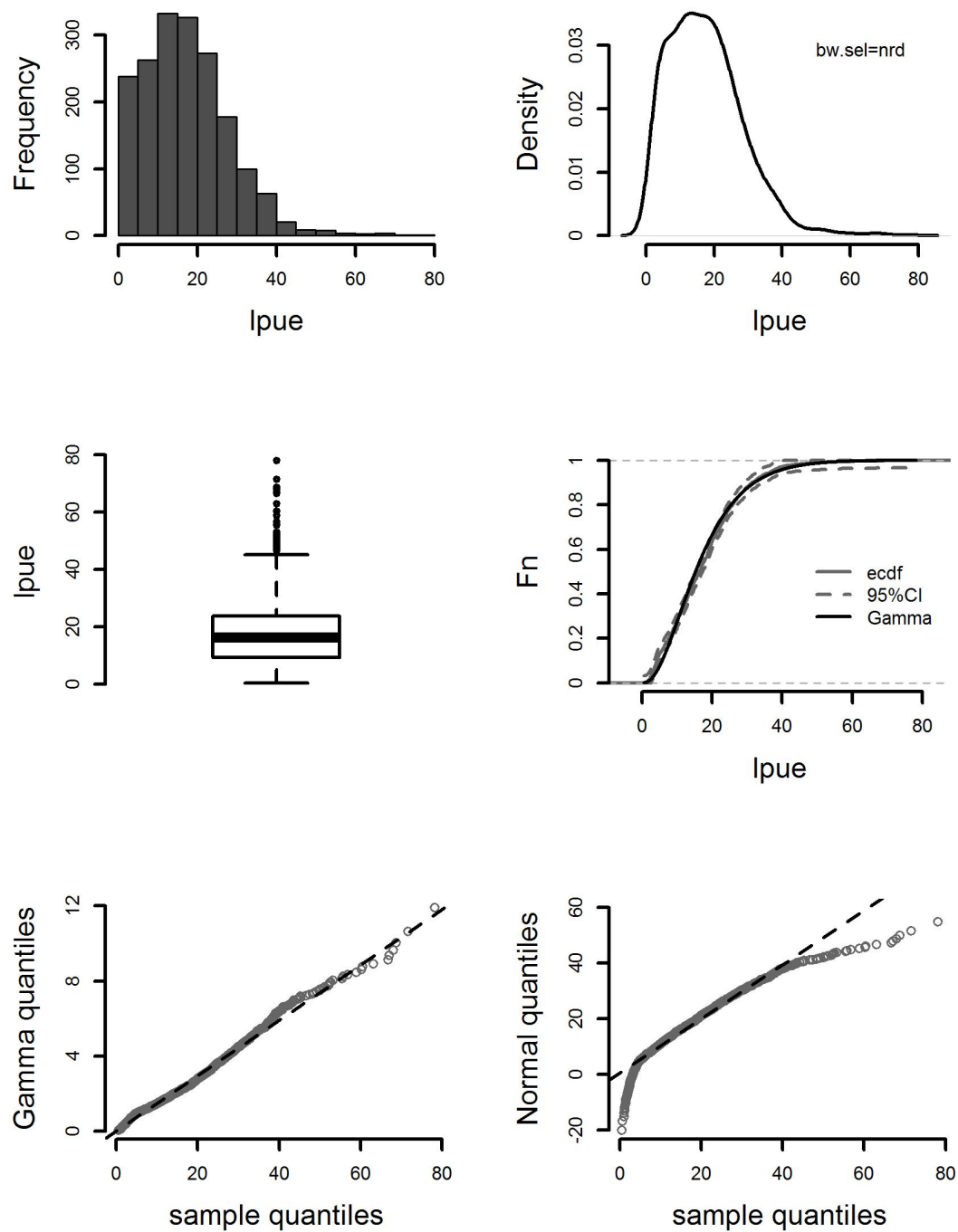


FIGURE C.1: From left to right, upper panels, histogram and kernel density estimations of  $lpue$ ; middle panels, box-plot and cumulative distribution function of data and of the gamma distribution; lower panels, QQ-plots of sample quantiles versus gamma and normal distribution quantiles.

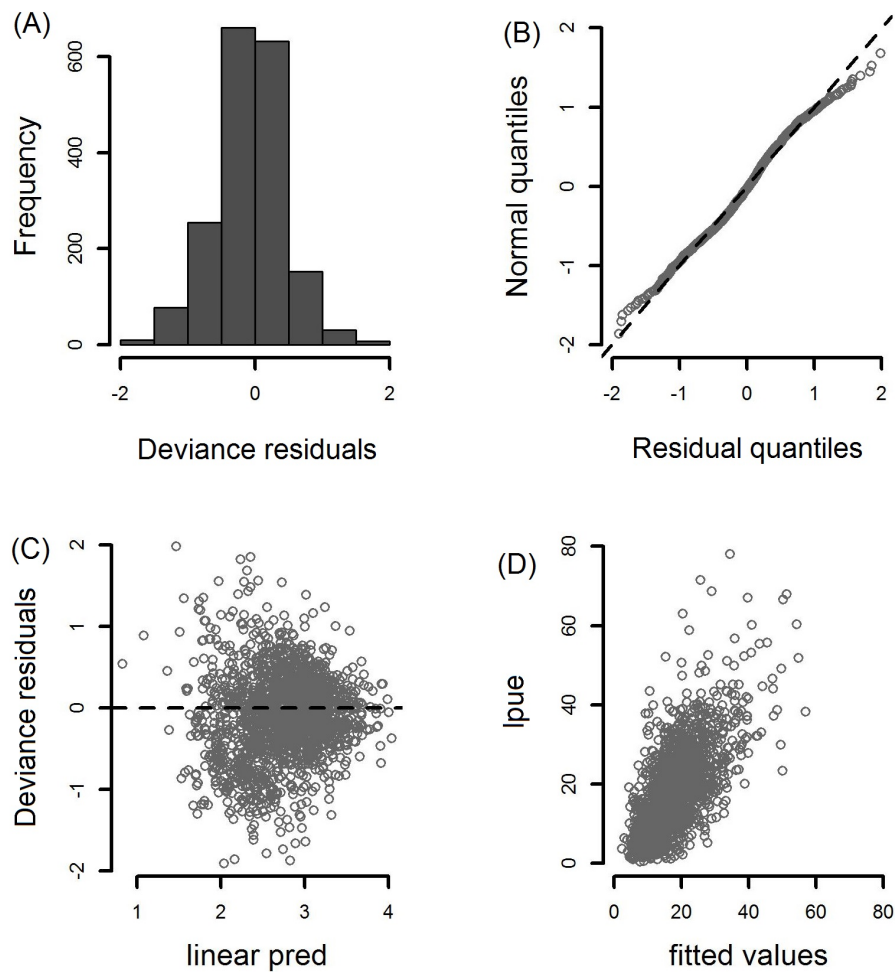


FIGURE C.2: Residual diagnostics for model 7. (A) Histogram of deviance residuals; (B) QQ-plot of deviance residuals; (C) deviance residuals against linear predictor; (D) response against fitted values.

## APPENDIX D

---

Complementary material – Chapter 4

---

## D.1 Model selection

All global results of estimated models in order to select the best final model are given in Tables D.1 (LN models) and D.2 (GA models).

	PRED	VAR	DEV	EP	DIC
		NULL	17744.4	2.06493	17748.5
1a)	$\eta_\mu$	code	17016.4	21.5726	17059.5
		code trips	16552.1	26.5423	16605.1
		code trips time	16185.7	44.6647	16275.1
		code trips time grt	NA	NA	NA
		code trips time period	16170.7	45.6919	16262.1
		<b>code-trips-time period nao</b>	<b>16163.9</b>	<b>47.0787</b>	<b>16258</b>
1b)	$\eta_\mu$	code trips-time period nao			
	$\eta_{\sigma^2}$	code	15805.5	68.1142	15941.7
		code trips	15427.2	73.2771	15573.7
		<b>code trips time</b>	<b>15138.4</b>	<b>91.1983</b>	<b>15320.8</b>
		code trips time period	15139.2	91.6031	15322.4
		code trips time nao	15139.8	92.432	15324.7
2a)	$\eta_\mu$	code	17016.9	21.5708	17060
		code trips	16553	25.463	16603.9
		code trips time	16186.5	44.0283	16274.6
		code trips time grt	16186.7	43.7525	16274.2
		code trips time period	16171.1	45.1612	16261.4
		code trips time nao	16180.6	46.1108	16272.8
		<b>code trips time period nao</b>	<b>16164.2</b>	<b>46.7896</b>	<b>16257.7</b>
2b)		code trips time period nao grt	16164.8	47.0348	16258.9
	$\eta_\mu$	code trips time period nao			
	$\eta_{\sigma^2}$	code	15808.2	66.493	15941.2
		code trips	15430	71.1313	15572.2
		<b>code trips time</b>	<b>15142.7</b>	<b>87.2506</b>	<b>15317.2</b>
		code trips time nao	15145.2	88.6634	15322.5

TABLE D.1: Global scores for LN models. 1a) fixed effects models with predictor  $\eta_\mu$ , 1b) fixed effects models with predictors  $\eta_\mu$  and  $\eta_{\sigma^2}$ , 2a) mixed effects models with predictor  $\eta_\mu$ , 2b) mixed effects models with predictors  $\eta_\mu$  and  $\eta_{\sigma^2}$ . PRED: specifies the predictor, and VAR: defines the variables in the corresponding predictor. DEV: residual deviance; EP: Effective total number of Parameters, DIC: Deviance Information Criterion. Models without global scores could not be estimated (see the corresponding Chapter).

	PRED	VAR	DEV	EP	DIC
		NULL	17302.7	2.00455	17306.7
1a)	$\eta_\mu$	code	16719.5	22.1251	16763.7
		code trips	16412.4	25.9486	16464.3
		code trips time	16127.9	42.2318	16212.3
		code trips time grt	NA	NA	NA
		code trips time nao	16118.9	44.5393	16208
		<b>code trips time nao period</b>	<b>16095.7</b>	<b>45.6132</b>	<b>16187</b>
1a)	$\eta_\mu$	code trips time nao period			
	$\eta_\sigma$	code	15700.2	66.5351	15833.3
		code trips	15282.2	71.7128	15425.6
		<b>code trips time</b>	<b>15027.1</b>	<b>90.8856</b>	<b>15208.9</b>
		code trips time nao	15033	92.5788	15218.2
		code trips time period	15026.3	91.2336	15208.8
2a)	$\eta_\mu$	code	16720.1	21.4365	16763
		code trips	16413.2	24.4744	16462.2
		code trips time	16128.5	41.309	16211.1
		code trips time nao	16119.5	43.6533	16206.8
		<b>code trips time nao period</b>	<b>16096.8</b>	<b>43.9236</b>	<b>16184.7</b>
		code trips time nao period grt	16096.7	44.2528	16185.2
2b)	$\eta_\mu$	code trips time nao period			
	$\eta_\sigma$	code	15703.1	64.5204	15832.1
		code trips	15285.7	69.3473	15424.4
		<b>code trips time</b>	<b>15032.4</b>	<b>86.8765</b>	<b>15206.1</b>
		code trips time nao	15037.5	88.4923	15214.4
		code trips time period	15031.3	88.0569	15207.4
		code trips time grt	15032.8	87.049	15206.9

TABLE D.2: Global scores for GA models. 1a) fixed effects models with predictor  $\eta_\mu$ , 1b) fixed effects models with predictors  $\eta_\mu$  and  $\eta_\sigma$ , 2a) mixed effects models with predictor  $\eta_\mu$ , 2b) mixed effects models with predictors  $\eta_\mu$  and  $\eta_\sigma$ . PRED: specifies the predictor, and VAR: defines the variables in the corresponding predictor. DEV: residual deviance; EP: Effective total number of Parameters, DIC: Deviance Information Criterion. Models without global scores could not be estimated (see text).

## D.2 Comparison of partial effects among models

Also smooth effects of all models M1-M8 are shown in Figures D.1, D.2, D.3, D.4, D.5, D.6. All models return reasonably similar results. Even so, some important differences can be observed in *time* effects. Let concentrate on the second part of the corresponding functions, after the important low in 2000 up to the end. In models accounting only for location parameter (Figures D.1 and D.4) the estimations show a second low that is not present in those models accounting for both parameters. This second low exists due to a moderate but concentrated number of low values of the response but data also hold high variability during last years, so these models tend to skip this variability, under-fitting the data and highlight the scant landing. On the contrary GA models accounting for both parameters do not model this second low in the predictor for  $\mu$ , while they better capture the oscillation of data (Figures D.5 and D.6). Finally LN models accounting for both parameters capture both negative and positive picks (Figures D.2 and D.3). So then it seems they capture the “best” shape. However none of the models correctly estimate the numerous changes that LPUE showed in last years, when four positive picks can be observed in the time series of the raw LPUE (see Figure 3.1 in Chapter 3). Note also that in the raw series the low captured by the model is not easy to detect within the cloud of observations.

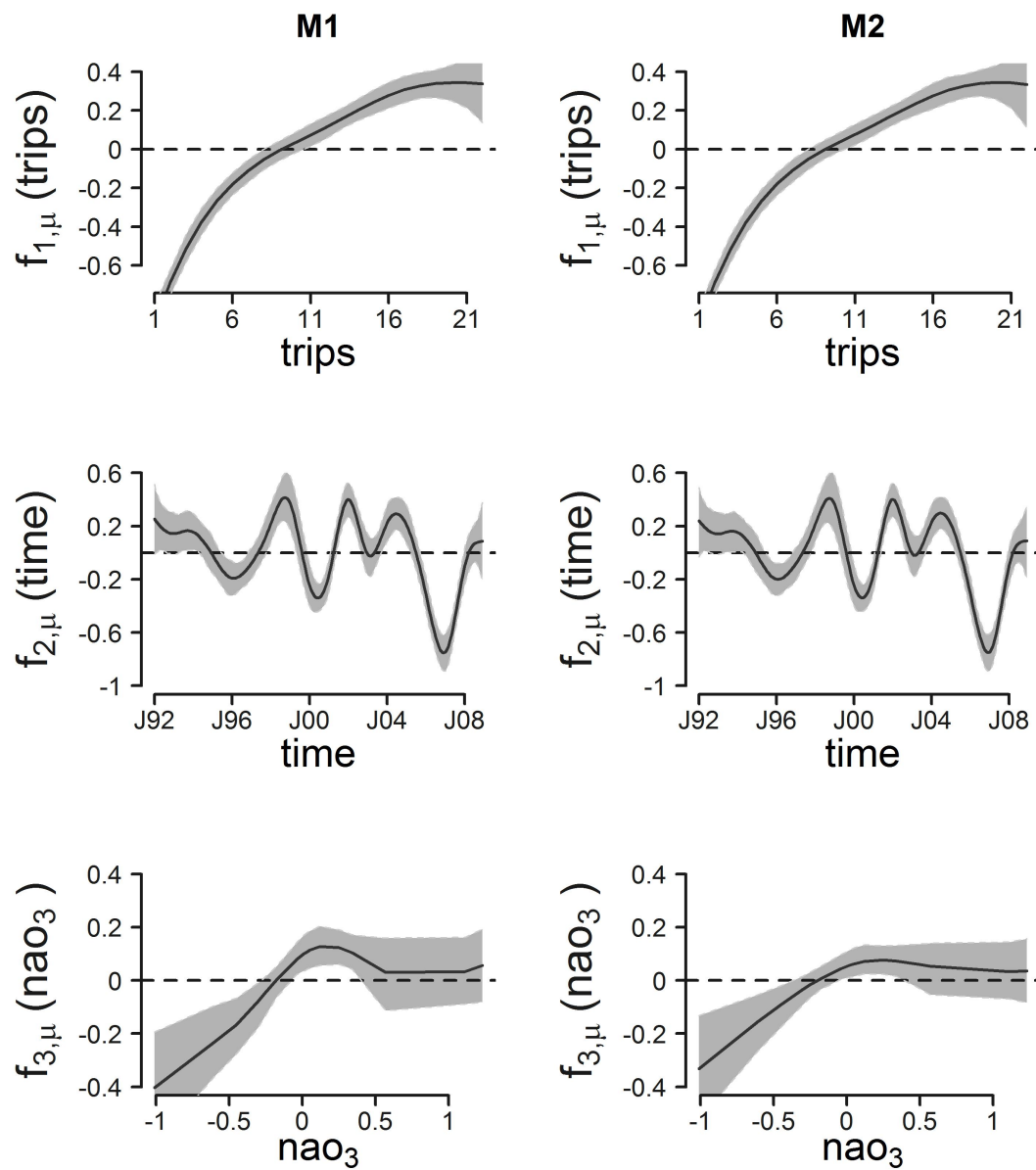


FIGURE D.1: Nonparametric effects on the predictor for  $\mu$  for the LN fixed effect model M1 and the mixed effects model M2 with best DIC score. Grey shapes represent 95% credible intervals.

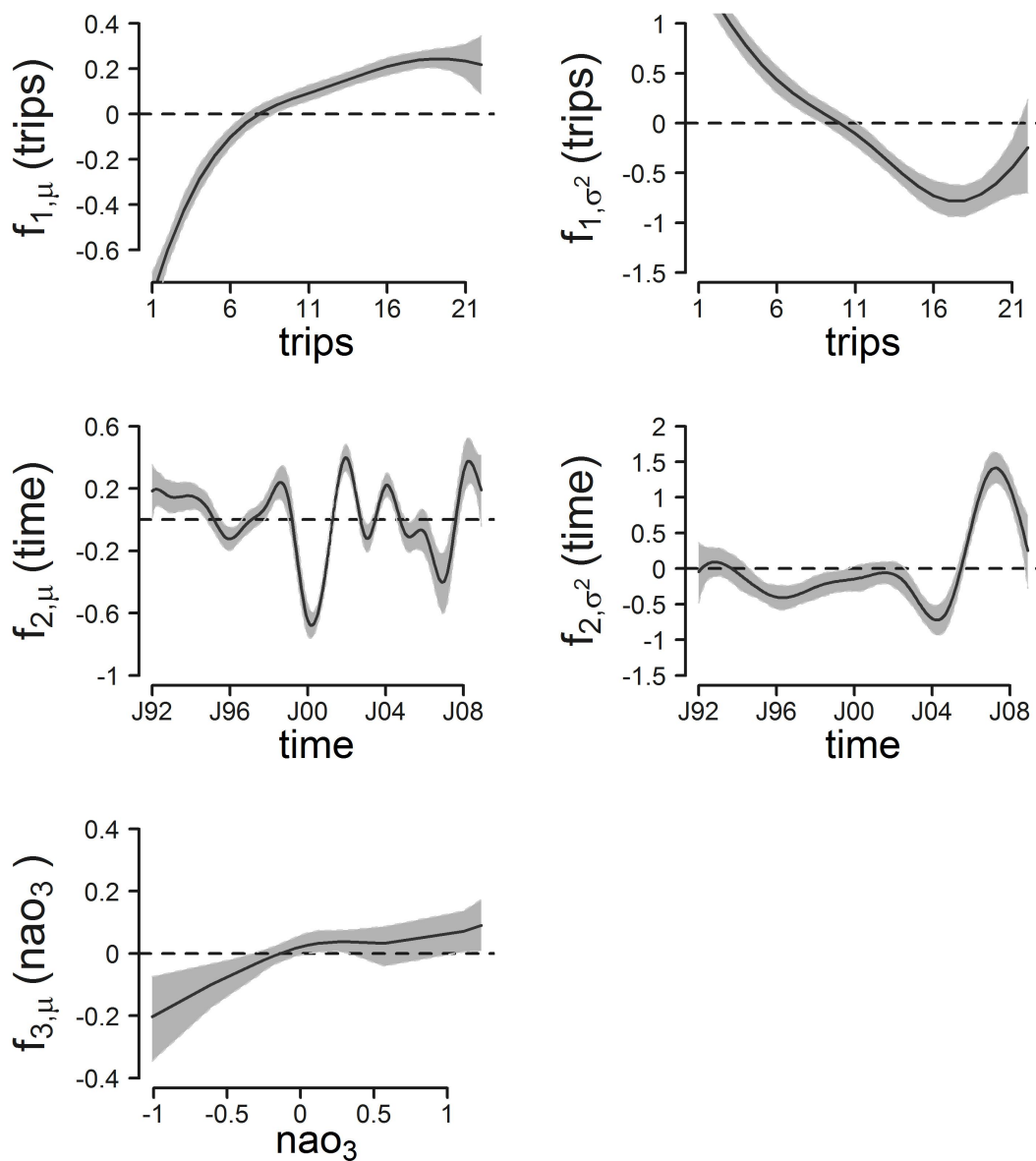


FIGURE D.2: Nonparametric effects for the LN fixed effect model M3 with best DIC score. Effects on predictor for  $\mu$  (left side) and for  $\sigma^2$  (right side). Grey shapes represent 95% credible intervals.



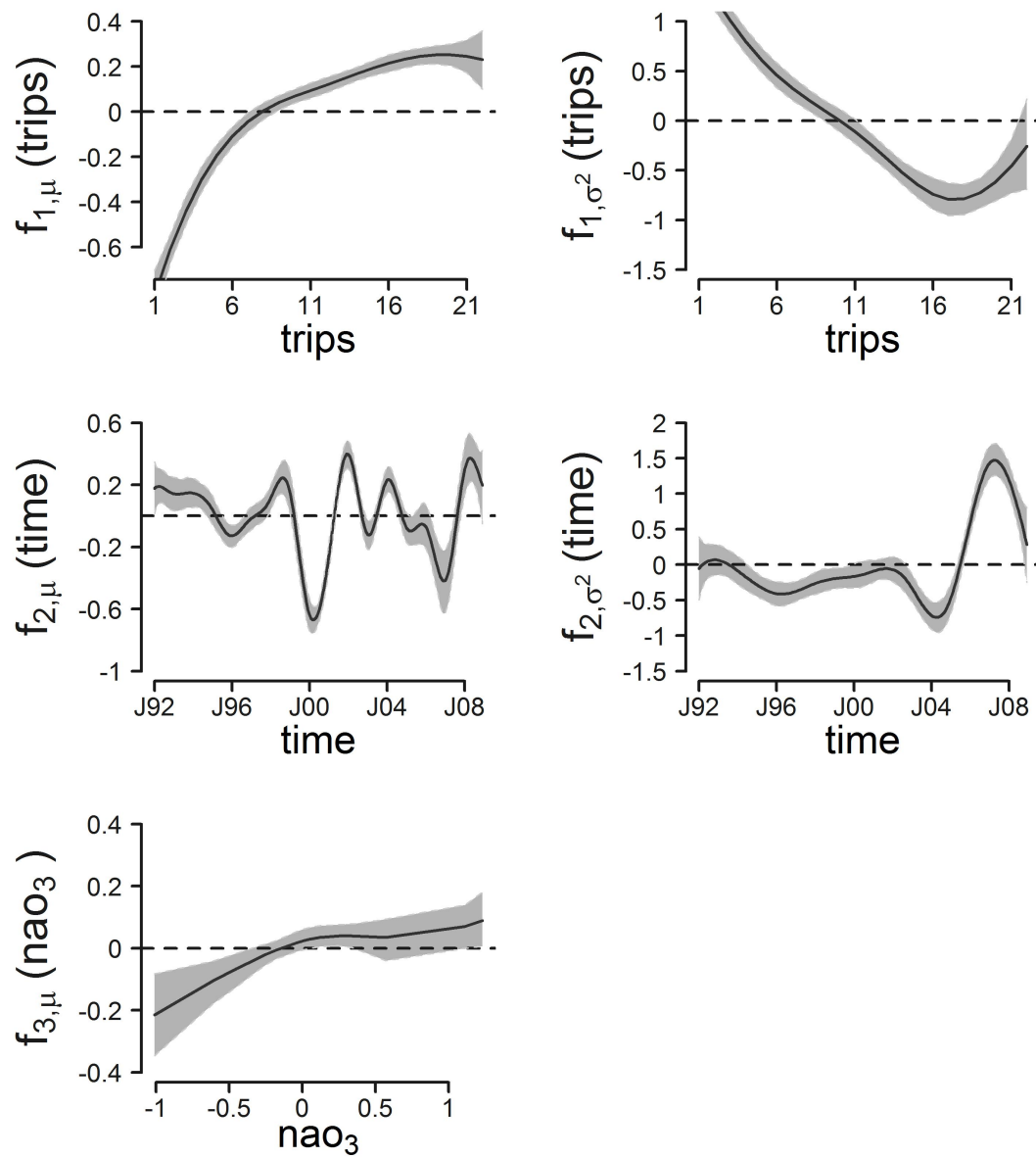


FIGURE D.3: Nonparametric effects for the LN mixed effect model M4 with best DIC score. Effects on predictor for  $\mu$  (left side) and for  $\sigma^2$  (right side). Grey shapes represent 95% credible intervals.

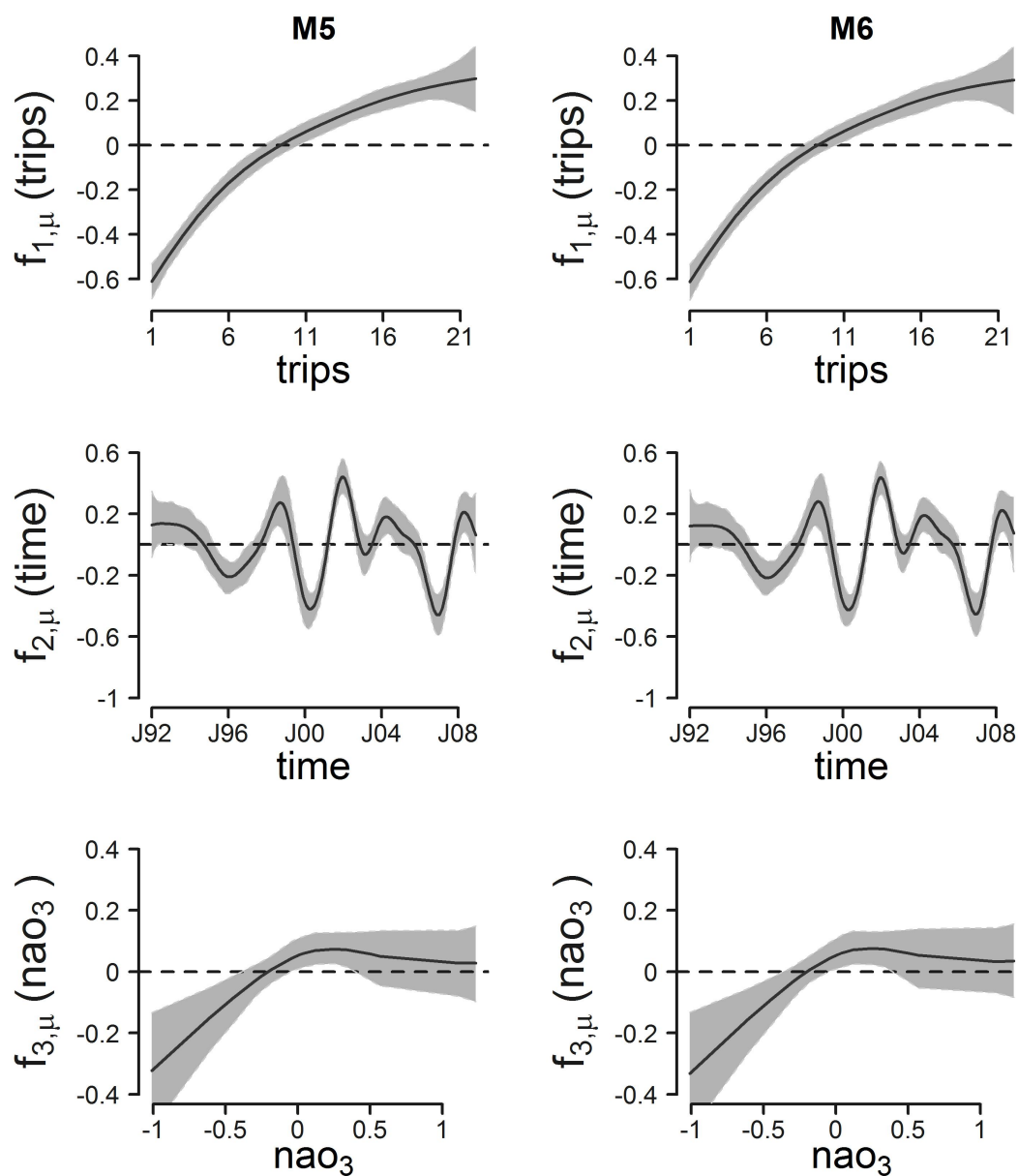


FIGURE D.4: Nonparametric effects on the predictor for  $\mu$  for the GA fixed effect model M5 and the mixed effects model M6 with best DIC score. Grey shapes represent 95% credible intervals.

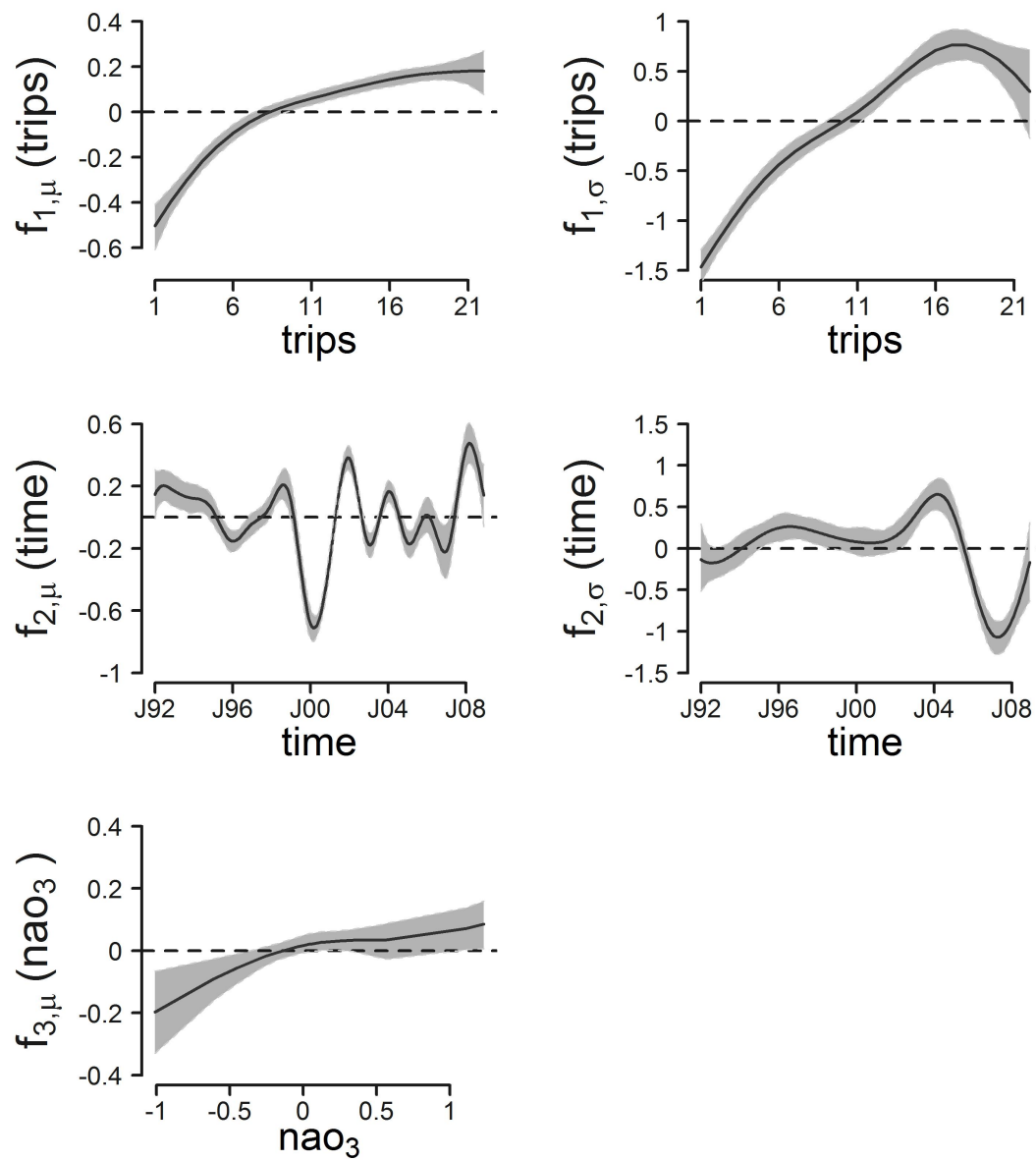


FIGURE D.5: Nonparametric effects for the GA fixed effect model M7 with best DIC score. Effects on predictor for  $\mu$  (left side) and for  $\sigma$  (right side). Grey shapes represent 95% credible intervals.

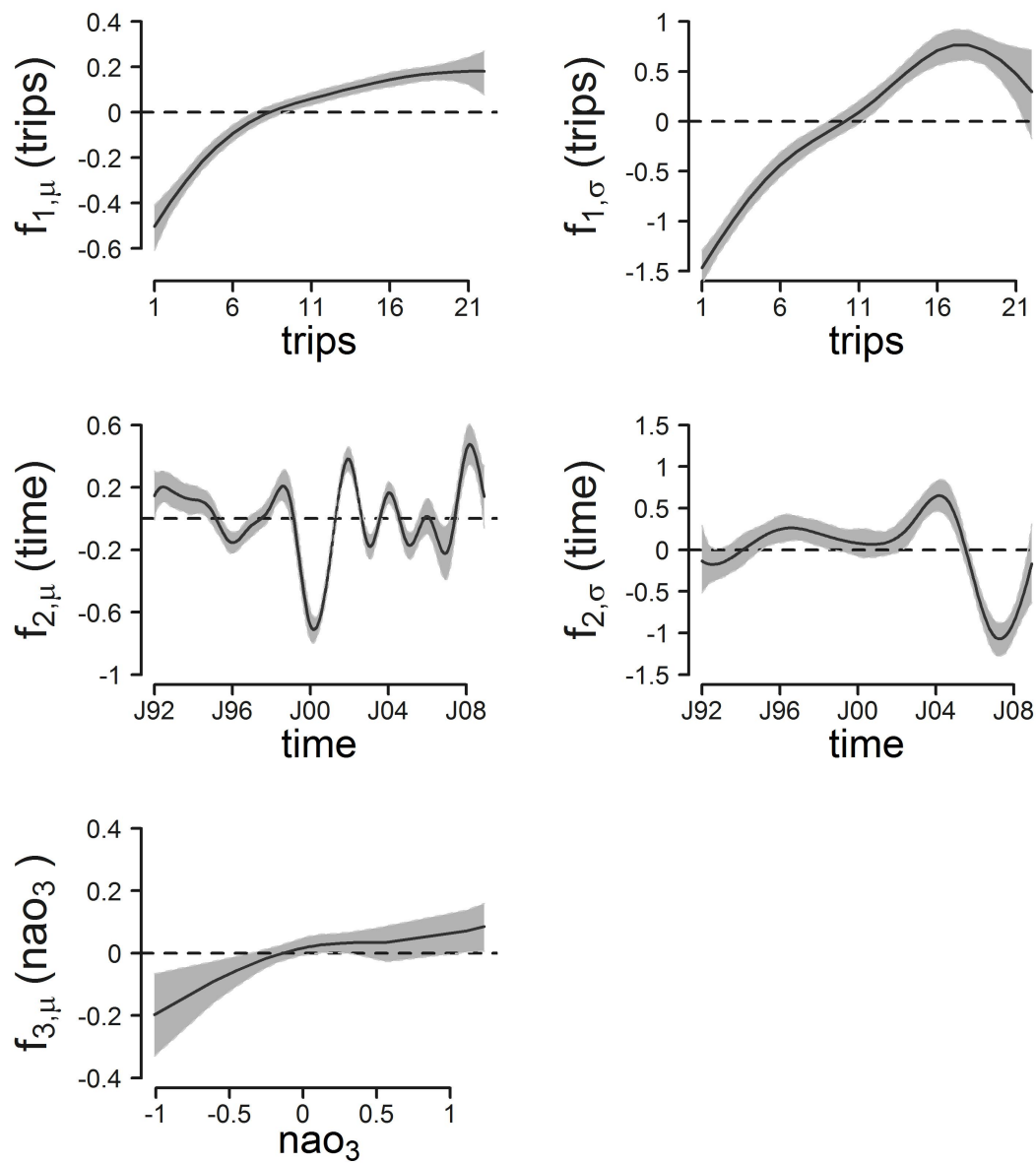


FIGURE D.6: Nonparametric effects for the GA mixed effect model M8 with best DIC score. Effects on predictor for  $\mu$  (left side) and for  $\sigma$  (right side). Grey shapes represent 95% credible intervals.

## APPENDIX E

---

Complementary material – Chapter 5

---

## E.1 Sediment Oxygen Consumption

The sediment community oxygen consumption rates in Figure 5.5, Chapter 5 with respect to the depth derive from the R-package *ecolMod* (see [Andersson et al. 2004](#)). Experiments were performed in situ incubations or via modelling of oxygen microprofiles. Here the SCOC is in  $\text{mmol O}_2 \text{ m}^{-2} \text{ d}^{-1}$  equivalent to  $\text{mmol C m}^{-2} \text{ d}^{-1}$ . The model in the Figure is derived by a log-log regression

$$\log(scoc) = \beta_0 + \beta_1 \log(depth) + \epsilon, \quad (\text{E.1})$$

where *scoc* is the response variable, *depth* the explanatory variable and  $\beta_0$  and  $\beta_1$  are the intercept and the slope respectively, while  $\epsilon$  is the error term of the regression. Thus, the model can be expressed as

$$scoc = a \times depth^b \quad (\text{E.2})$$

where the parameters are  $a = \exp(\beta_0)$  and  $b = \beta_1$ .

## E.2 LIM equations

All equations incorporated in the food web model in Chapter 5 are shown in Table E.2 and Table E.1 and all parameters used to constrain the model are shown in table E.3.

---

(A) Burial of org C = BE  $\times$  Total org C input  
 TOM R = SOC – MACBN R

(B) A = AE  $\times$  U  
 A – R + MR = NGE  $\times$  A  
 A – R + MR = PR  $\times$  stock  
 R = RR  $\times$  stock

(C)  $\text{flow}_{j \rightarrow i} = \text{PD} \times U_j$

---

TABLE E.1: Constraints imposed to the model. (A) TOM compartment, (B) Faunal compartments, (C) Diet constraint (only for the red shrimp). A: assimilation, R: respiration, U: Uptake. SOC = sediment oxygen consumption; BE = burial efficiency; RR = respiration rate; NGE = net growth efficiency; AE = assimilation efficiency; MR = maintenance respiration; PR = production rate; DP = proportion of source  $j$  in the diet of predator  $j$ .

---

$\frac{d \text{TOM}}{dt} = 0 =$	$\text{OM}_v \rightarrow \text{TOM} + \text{OM}_a \rightarrow \text{TOM} + \text{ZPLMNK} \rightarrow \text{TOM}$ $+ \text{MACBN} \rightarrow \text{TOM} + \text{SUPBN} \rightarrow \text{TOM} + \text{AANT} \rightarrow \text{TOM}$ $+ \text{MEGAICT} \rightarrow \text{TOM} + \text{MEGABN} \rightarrow \text{TOM}$ $- \text{TOM} \rightarrow \text{MACBN} - \text{TOM} \rightarrow \text{MEGABN}$ $- \text{TOM} \rightarrow \text{AANT} - \text{TOM} \rightarrow \text{BUR} - \text{TOM} \rightarrow \text{DIC}$
$\frac{d \text{ZPLMNK}}{dt} = 0 =$	$\text{OM}_v \rightarrow \text{ZPLMNK} + \text{OM}_a \rightarrow \text{ZPLMNK} - \text{ZPLMNK} \rightarrow \text{MEGABN}$ $- \text{ZPLMNK} \rightarrow \text{MEGAICT} - \text{ZPLMNK} \rightarrow \text{AANT}$ $- \text{ZPLMNK} \rightarrow \text{TOM} - \text{ZPLMNK} \rightarrow \text{DIC}$
$\frac{d \text{MACBN}}{dt} = 0 =$	$\text{OM}_v \rightarrow \text{MACBN} + \text{OM}_a \rightarrow \text{MACBN}$ $+ \text{TOM} \rightarrow \text{MACBN} - \text{MACBN} \rightarrow \text{AANT}$ $- \text{MACBN} \rightarrow \text{MEGABN} - \text{MACBN} \rightarrow \text{MEGAICT}$ $- \text{MACBN} \rightarrow \text{TOM} - \text{MACBN} \rightarrow \text{DIC}$
$\frac{d \text{SUPBN}}{dt} = 0 =$	$\text{OM}_v \rightarrow \text{SUPBN} + \text{OM}_a \rightarrow \text{SUPBN}$ $- \text{SUPBN} \rightarrow \text{AANT} - \text{SUPBN} \rightarrow \text{MEGABN}$ $- \text{SUPBN} \rightarrow \text{MEGAICT} - \text{SUPBN} \rightarrow \text{TOM} - \text{SUPBN} \rightarrow \text{DIC}$
$\frac{d \text{MEGABN}}{dt} = 0 =$	$\text{TOM} \rightarrow \text{MEGABN}$ $\text{ZPLMNK} \rightarrow \text{MEGABN} + \text{SUPBN} \rightarrow \text{MEGABN}$ $+ \text{MACBN} \rightarrow \text{MEGABN}$ $- \text{MEGABN} \rightarrow \text{AANT}$ $- \text{MEGABN} \rightarrow \text{TOM} - \text{MEGABN} \rightarrow \text{DIC}$
$\frac{d \text{MEGAICT}}{dt} = 0 =$	$\text{ZPLMNK} \rightarrow \text{MEGAICT} + \text{SUPBN} \rightarrow \text{MEGAICT}$ $+ \text{MACBN} \rightarrow \text{MEGAICT} + \text{MEGABN} \rightarrow \text{MEGAICT}$ $+ \text{AANT} \rightarrow \text{MEGAICT} - \text{MEGAICT} \rightarrow \text{BYCATCH}$ $- \text{MEGAICT} \rightarrow \text{TOM} - \text{MEGAICT} \rightarrow \text{DIC}$
$\frac{d \text{AANT}}{dt} = 0 =$	$\text{TOM} \rightarrow \text{AANT} + \text{ZPLMNK} \rightarrow \text{AANT} + \text{SUPBN} \rightarrow \text{AANT}$ $+ \text{MACBN} \rightarrow \text{AANT} + \text{MEGABN} \rightarrow \text{AANT}$ $+ \text{MEGAICT} \rightarrow \text{AANT}$ $- \text{AANT} \rightarrow \text{MEGABN} - \text{AANT} \rightarrow \text{MEGAICT}$ $- \text{AANT} \rightarrow \text{LANDINGS} - \text{AANT} \rightarrow \text{TOM} - \text{AANT} \rightarrow \text{DIC}$

---

TABLE E.2: Equations of the binary food web and steady-state assumption incorporated in the food web model.



Process	Value	units	Ref.
<i>Tlim</i>	0.54	–	1
SOC	[0.888,2.19]	mmol C m <sup>-2</sup> d <sup>-1</sup>	2
BE	[0.105,0.36]	–	3
Faunal MR	<i>Tlim</i> * 0.01 * stock	mmol C m <sup>-2</sup> d <sup>-1</sup>	4
RR of ZPLMNK and SUPBN	[0.0001,0.032]	d <sup>-1</sup>	5
RR of MACBN	[0.0055,0.012]	d <sup>-1</sup>	5
RR of MEGABN	[0.0029,0.008]	d <sup>-1</sup>	6
RR of MEGAICT	[0.00023,0.0087]	d <sup>-1</sup>	5
RR of AANT	[0.0051,0.039]	d <sup>-1</sup>	5
NGE of ZPLMNK and SUPBN	[0.7,0.9]	–	4
NGE of other Fauna	[0.5,0.7]	–	4
ZPLMNK PR	<i>Tlim</i> *[0.01,0.05]	d <sup>-1</sup>	7
SUPBN PR	[0.00487,0.06882]	d <sup>-1</sup>	8
MACBN PR	[0.0014,0.0689]	d <sup>-1</sup>	8
MEGABN PR	[0.00055,0.01373]	d <sup>-1</sup>	7,9
MEGAICT PR	<i>Tlim</i> *[0.00274,0.0137]	d <sup>-1</sup>	7
AE on OM	[0.29,0.77]	–	7
AE on fauna	[0.10,0.60]	–	4
MACBN DP on OMv	[0,0.25]	–	9,10
MACBN DP on TOM	[0.75,1]	–	9,10
AANT DP on MACBN	[0.15,0.34]	–	11
AANT DP on MEGABN	[0.1,0.25]	–	11
AANT DP on SUPBN	[0.11,0.33]	–	11
AANT DP on ZPLMNK	[0.12,0.67]	–	11
AANT FR	[0.5E-003,0.046]	mmol C m <sup>-2</sup> d <sup>-1</sup>	12
MEGAICT CR	AANT FR × 3	mmol C m <sup>-2</sup> d <sup>-1</sup>	9,12
MEGABN CR	AANT CR × 5E-003	mmol C m <sup>-2</sup> d <sup>-1</sup>	9,12

TABLE E.3: Parameters and constrains for the food web model. In brackets minimum and maximum values of parameters are reported, while single values correspond to the mean of parameters. *Tlim* = temperature limitation; SOC = sediment oxygen consumption; BE = burial efficiency; RR = respiration rate; NGE = net growth efficiency; AE = assimilation efficiency; MR = maintenance respiration; PR = production rate; DP = proportion of source *j* in the diet of predator *j*; FR = fishing rate; CR = catch rate. References: (1) [Epping et al., 2002](#), (2) Own data from ANTROMARE survey, (3) [Burdige et al., 1999](#), (4) [van Oevelen, Soetaert, Middelburg, Herman, Moodley, Hamels, Moens and Heip, 2006](#) and references therein, (5) [Mahaut et al., 1995](#), (6) [Company and Sardà, 1998](#), (7) [van Oevelen, Soetaert, García, de Stigter, Cunha, Pusceddu and Danovaro, 2011](#), (8) [Cartes, Brey, Sorbe and Maynou, 2002](#), (9) Own data from BIOMARE survey, (10) [Fauchald and Jumars, 1979](#), (11) [Cartes, Papiol and Guijarro, 2008](#), (12) From longitudinal data of the Catalan government.

### E.3 Results of the food web model

Figure E.1 shows the range estimations of the flows, a measure of both feasibility and uncertainty, however better estimator of flows' quality is represented by the Coefficient of Variation shown in Table E.5.

Tables E.4 and E.5 return all estimations of flows in  $\text{mmol C m}^{-2} \text{d}^{-1}$  derived from the existing types of solution methods: (1) range (minimum and maximum), (2) least distance, (3) least square (mean) solutions, (4) Markov Chain Monte Carlo (mean and standard deviation) and the Coefficient of Variation (CoV).

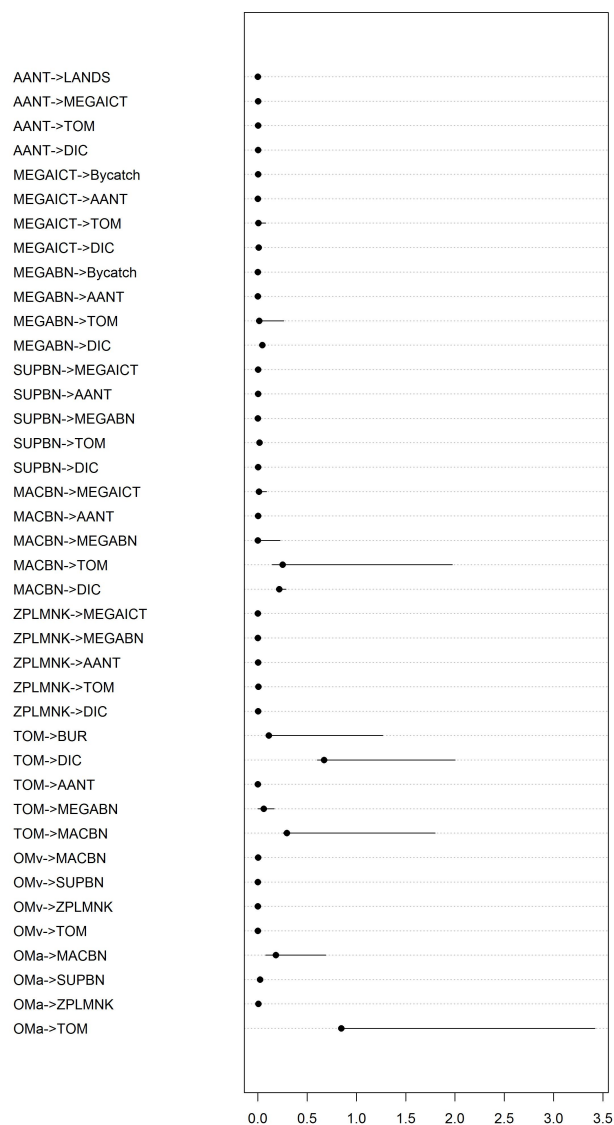


FIGURE E.1: Range estimation of food web flows. The dark point represents the parsimonious solution, the segments minimum to maximum ranges.

flow	min	max	mean <sub><i>l<sub>dei</sub></i></sub>	mean <sub><i>l<sub>sei</sub></i></sub>
OMa → TOM	8.44E-001	3.42E+000	8.44E-001	8.44E-001
OMa → ZPLMNK	1.22E-005	6.20E-003	6.20E-003	6.20E-003
OMa → SUPBN	2.07E-005	2.13E-002	2.13E-002	2.13E-002
OMa → MACBN	7.88E-002	6.90E-001	1.81E-001	1.81E-001
OMv → TOM	0.00E+000	6.08E-003	0.00E+000	0.00E+000
OMv → ZPLMNK	1.22E-005	6.10E-003	6.26E-005	6.26E-005
OMv → SUPBN	2.07E-005	6.14E-003	2.15E-004	2.15E-004
OMv → MACBN	8.58E-004	6.97E-003	1.83E-003	1.83E-003
TOM → MACBN	2.57E-001	1.80E+000	2.94E-001	2.58E-001
TOM → MEGABN	0.00E+000	1.65E-001	5.81E-002	5.81E-002
TOM → AANT	4.41E-005	7.63E-005	4.41E-005	4.41E-005
TOM → DIC	6.03E-001	2.00E+000	6.73E-001	7.00E-001
TOM → BUR	1.10E-001	1.27E+000	1.10E-001	1.10E-001
ZPLMNK → DIC	3.48E-004	7.99E-004	7.99E-004	7.99E-004
ZPLMNK → TOM	2.80E-004	4.45E-003	4.45E-003	4.45E-003
ZPLMNK → AANT	5.88E-004	1.02E-003	1.02E-003	1.02E-003
ZPLMNK → MEGABN	0.00E+000	4.29E-004	0.00E+000	0.00E+000
ZPLMNK → MEGAICT	0.00E+000	4.29E-004	0.00E+000	0.00E+000
MACBN → DIC	1.87E-001	2.85E-001	2.15E-001	1.88E-001
MACBN → TOM	1.45E-001	1.97E+000	2.50E-001	2.42E-001
MACBN → MEGABN	0.00E+000	2.27E-001	0.00E+000	0.00E+000
MACBN → AANT	9.72E-004	2.88E-003	1.67E-003	1.67E-003
MACBN → MEGAICT	8.93E-003	8.77E-002	9.62E-003	9.62E-003
SUPBN → DIC	6.70E-004	1.13E-003	1.13E-003	1.13E-003
SUPBN → TOM	4.76E-004	1.53E-002	1.53E-002	1.53E-002
SUPBN → MEGABN	0.00E+000	4.18E-003	0.00E+000	0.00E+000
SUPBN → AANT	9.23E-004	2.80E-003	1.62E-003	1.62E-003
SUPBN → MEGAICT	0.00E+000	4.18E-003	3.49E-003	3.49E-003
MEGABN → DIC	4.42E-002	4.56E-002	4.42E-002	4.42E-002
MEGABN → TOM	1.34E-002	2.64E-001	1.34E-002	1.34E-002
MEGABN → AANT	5.31E-004	2.12E-003	5.56E-004	5.56E-004
MEGABN → BYCATCH	2.50E-006	2.76E-006	2.50E-006	2.50E-006
MEGAICT → DIC	7.05E-003	7.22E-003	7.05E-003	7.05E-003
MEGAICT → TOM	5.70E-003	7.99E-002	5.70E-003	5.70E-003
MEGAICT → AANT	0.00E+000	4.24E-005	0.00E+000	0.00E+000
MEGAICT → BYCATCH	1.50E-003	1.66E-003	1.50E-003	1.50E-003
AANT → DIC	1.33E-003	2.96E-003	1.33E-003	1.33E-003
AANT → TOM	1.93E-003	5.50E-003	1.93E-003	1.93E-003
AANT → MEGAICT	1.09E-003	1.55E-003	1.14E-003	1.14E-003
AANT → LANDS	5.00E-004	5.53E-004	5.00E-004	5.00E-004

TABLE E.4: Food web flows' estimations: range (minimum and maximum), least distance and least square (mean) solutions. Flows in  $\text{mmol C m}^{-2} \text{d}^{-1}$ .

flow	mean $\pm$ sd	CoV
OMa $\rightarrow$ TOM	2.28E+000 $\pm$ 4.60E-001	2.01E-001
OMa $\rightarrow$ ZPLMNK	3.17E-003 $\pm$ 1.10E-003	3.47E-001
OMa $\rightarrow$ SUPBN	1.02E-002 $\pm$ 3.38E-003	3.31E-001
OMa $\rightarrow$ MACBN	3.21E-001 $\pm$ 1.16E-001	3.62E-001
OMv $\rightarrow$ TOM	4.64E-004 $\pm$ 5.15E-004	1.11E+000
OMv $\rightarrow$ ZPLMNK	4.91E-004 $\pm$ 4.92E-004	1.00E+000
OMv $\rightarrow$ SUPBN	5.70E-004 $\pm$ 5.16E-004	9.04E-001
OMv $\rightarrow$ MACBN	3.71E-003 $\pm$ 1.09E-003	2.94E-001
TOM $\rightarrow$ MACBN	7.47E-001 $\pm$ 3.09E-001	4.14E-001
TOM $\rightarrow$ MEGABN	8.16E-002 $\pm$ 3.82E-002	4.68E-001
TOM $\rightarrow$ AANT	5.67E-005 $\pm$ 5.36E-006	9.46E-002
TOM $\rightarrow$ DIC	1.58E+000 $\pm$ 3.19E-001	2.02E-001
TOM $\rightarrow$ BUR	7.34E-001 $\pm$ 2.79E-001	3.80E-001
ZPLMNK $\rightarrow$ DIC	5.91E-004 $\pm$ 1.12E-004	1.90E-001
ZPLMNK $\rightarrow$ TOM	2.10E-003 $\pm$ 9.81E-004	4.66E-001
ZPLMNK $\rightarrow$ AANT	8.39E-004 $\pm$ 7.41E-005	8.83E-002
ZPLMNK $\rightarrow$ MEGABN	6.19E-005 $\pm$ 5.35E-005	8.64E-001
ZPLMNK $\rightarrow$ MEGAICT	6.04E-005 $\pm$ 5.24E-005	8.67E-001
MACBN $\rightarrow$ DIC	2.51E-001 $\pm$ 2.35E-002	9.37E-002
MACBN $\rightarrow$ TOM	7.23E-001 $\pm$ 3.65E-001	5.05E-001
MACBN $\rightarrow$ MEGABN	5.64E-002 $\pm$ 4.62E-002	8.19E-001
MACBN $\rightarrow$ AANT	2.01E-003 $\pm$ 2.24E-004	1.11E-001
MACBN $\rightarrow$ MEGAICT	3.98E-002 $\pm$ 2.01E-002	5.06E-001
SUPBN $\rightarrow$ DIC	1.05E-003 $\pm$ 6.63E-005	6.31E-002
SUPBN $\rightarrow$ TOM	6.15E-003 $\pm$ 3.07E-003	4.99E-001
SUPBN $\rightarrow$ MEGABN	8.31E-004 $\pm$ 6.34E-004	7.63E-001
SUPBN $\rightarrow$ AANT	1.94E-003 $\pm$ 2.19E-004	1.13E-001
SUPBN $\rightarrow$ MEGAICT	8.34E-004 $\pm$ 6.41E-004	7.69E-001
MEGABN $\rightarrow$ DIC	4.51E-002 $\pm$ 2.93E-004	6.51E-003
MEGABN $\rightarrow$ TOM	9.24E-002 $\pm$ 4.46E-002	4.83E-001
MEGABN $\rightarrow$ AANT	1.44E-003 $\pm$ 1.78E-004	1.24E-001
MEGABN $\rightarrow$ BYCATCH	2.61E-006 $\pm$ 6.91E-008	2.65E-002
MEGAICT $\rightarrow$ DIC	7.15E-003 $\pm$ 4.13E-005	5.78E-003
MEGAICT $\rightarrow$ TOM	3.32E-002 $\pm$ 2.01E-002	6.05E-001
MEGAICT $\rightarrow$ AANT	1.54E-005 $\pm$ 9.25E-006	6.01E-001
MEGAICT $\rightarrow$ BYCATCH	1.57E-003 $\pm$ 4.14E-005	2.65E-002
AANT $\rightarrow$ DIC	1.71E-003 $\pm$ 2.71E-004	1.58E-001
AANT $\rightarrow$ TOM	2.79E-003 $\pm$ 4.51E-004	1.62E-001
AANT $\rightarrow$ MEGAICT	1.27E-003 $\pm$ 1.12E-004	8.82E-002
AANT $\rightarrow$ LANDS	5.22E-004 $\pm$ 1.38E-005	2.65E-002

TABLE E.5: MCMC (mean and standard deviation) solution and Coefficient of Variation (CoV) for the food web flows.

## E.4 Network indices equations and results

Finally Tables E.6, E.7 and E.8 show all symbols and formulae of the ecosystem indices, while the corresponding results are in Tables E.9 and E.10. Trophic indices are shown in Table 5.5, Chapter 5.

Term	Description
$n$	Number of internal compartments in the network
$j = 0$	External source
$i = n + 1$	Usable export from the network
$i = n + 2$	Unusable export from the network (respiration, dissipation)
$T_{ij}$	Flow from compartment $j$ to $i$ ; in the flow matrix $j$ are columns and $i$ the rows
$T_i$	Total inflows to compartment $i$
$T_j$	Total outflows from compartment $j$
$T_i$	Total inflows to compartment $i$ excluding inflow from external sources
$T_j$	Total outflows from compartment $j$ , excluding outflow to external sources
$(\dot{x}_i)_-$	A negative state derivative, considered as a gain of energy to the system
$(\dot{x}_i)_+$	A positive state derivative, considered as a loss of energy from the system
$z_{i0}$	Flow into compartment $i$ from outside the network
$y_{n+j}$	Flow from compartment $j$ to compartments $n + 1$ and $n + 2$
$c_{ij}$	The number of species with which both $i$ and $j$ interact divided by the number of species with which either $i$ or $j$ interact
$\mathbf{T}_{ij}^*$	Flow matrix, excluding flows to and from the external
$\mathbf{I}, \delta_{ij}$	Identity matrix and its elements
$\mathbf{G}', g_{ij}$	matrix given by $\mathbf{T}_{ij}^*/\max(T_i, T_j)$ and its elements
$\mathbf{Q}, q_{ij}$	matrix given by $(\mathbf{I} - \mathbf{G}')^{-1}$ and its elements

TABLE E.6: Nomenclature of symbols used in calculation of network index equations (Table E.7). Revised from Kones et al. (2009).

Index	Formula	Ref.
T..	$\sum_{i=1}^{n+2} \sum_{j=0}^n T_{ij}$	1
TST	$\sum_{i=1}^n \sum_{j=1}^n [T_{ij} + z_{i0}(\dot{X}_i)_-]$	2
L	$\sum_{i=1}^{n+2} \sum_{j=1}^n (T_{ij} \geq 1)$	2
LD	$\frac{\sum_{i=1}^{n+2} \sum_{j=1}^n (T_{ij} \geq 1)}{n}$	2
Lint	$\sum_{i=1}^n \sum_{j=1}^n (T_{ij} \geq 1)$	3
C	$\frac{\sum_{i=1}^n \sum_{j=1}^n (T_{ij} \geq 1)}{n(n-1)}$	2
$\bar{T}_{ij}$	$\frac{\sum_{i=1}^{n+2} \sum_{j=0}^n T_{ij}}{L}$	4
$\overline{\text{TST}}$	$\frac{\sum_{i=1}^n \sum_{j=1}^n [T_{ij} + z_{i0}(\dot{X}_i)_-]}{n}$	2
$\bar{C}$	$\frac{1}{n(n-1)} \sum_{i=1}^n \sum_{j=1}^n c_{ij}$ where $j \neq i$	4
TSTc	$\sum_{j=1}^n (1 - 1/q_{ij} T_j)$	5, 6, 7
TSTs	$\sum_{i=1}^n \sum_{j=1}^n [T_{ij} + z_{i0}(\dot{X}_i)_-] - \sum_{j=1}^n (1 - 1/q_{ij} T_j)$	5, 6, 7
FCI	$\frac{\sum_{j=1}^n (1 - 1/q_{ij} T_j)}{\sum_{i=1}^n \sum_{j=1}^n [T_{ij} + z_{i0}(\dot{X}_i)_-]}$	5, 6, 7
FCIb	$\frac{\sum_{j=1}^n (1 - 1/q_{ij} T_j)}{\sum_{i=1}^{n+2} \sum_{j=0}^n T_{ij}}$	8, 9
$\overline{\text{PL}}$	$\frac{\sum_{i=1}^n \sum_{j=1}^n [T_{ij} + z_{i0}(\dot{X}_i)_-]}{\sum z_{i0} - \sum (\dot{x}_i)_+}$	5, 6, 7
Cz	$\prod_{ij} \left[ \frac{T_{ij}^2}{T_i T_j} \right]^{-(1/2)(T_{ij} T_{..})}$	2
Fz	$\prod_{ij} \left[ \frac{T_{ij}}{T_{..}} \right]^{-(T_{ij}/T_{..})}$	2
Nz	$\prod_{ij} \left[ \frac{T_{ij}^2}{T_i T_j} \right]^{-(1/2)(T_{ij} T_{..})}$	2
Rz	$\prod_{ij} \left[ \frac{T_{ij} T_{..}}{T_i T_j} \right]^{(T_{ij}/T_{..})}$	2

TABLE E.7: Network Index formulas (PART 1/2). See Table E.6 for the definition of terms. References: (1) Hirata and Ulanowicz, 1984, (2) Latham II, 2006, (3) Kones et al., 2009, (4) Pimm and Lawton, 1980, (5) Finn, 1976, (6) Finn, 1980, (7) Patten and Higashi, 1984, (8) Allesina and Ulanowicz, 2004, (9) Ulanowicz, 1986, (10) Ulanowicz and Norden, 1990, (11) Ulanowicz, 2004, (12) Ulanowicz, 2000, (13) Christensen and Pauly, 1992, (14) Lindeman, 1942.

Revisited from ref. 3.

Index	Formula	Ref.
A	$\sum_{i=1}^{n+2} \sum_{j=0}^n T_{ij} \log_2 \frac{T_{ij} T_{..}}{T_i T_j}$	10, 11
DC	$-\sum_{i=1}^{n+2} \sum_{j=0}^n T_{ij} \log_2 \frac{T_{ij}}{T_{..}}$	10, 12
$\phi$	$\left[ -\sum_{i=1}^{n+2} \sum_{j=0}^n T_{ij} \log_2 \frac{T_{ij}}{T_{..}} \right] - \left[ \sum_{i=1}^{n+2} \sum_{j=0}^n T_{ij} \log_2 \frac{T_{ij} T_{..}}{T_i T_j} \right]$	10, 12
AC	$-\frac{\sum_{i=1}^{n+2} \sum_{j=0}^n T_{ij} \log_2 \frac{T_{ij} T_{..}}{T_i T_j}}{\sum_{i=1}^{n+2} \sum_{j=0}^n T_{ij} \log_2 \frac{T_{ij}}{T_{..}}}$	10, 12
AMI	$\sum_{i=1}^{n+2} \sum_{j=0}^n \frac{T_{ij}}{T_{..}} \log_2 \frac{T_{ij} T_{..}}{T_i T_j}$	12
H <sub>R</sub>	$-\sum_{j=0}^n \frac{T_j}{T_{..}} \log_2 \frac{T_j}{T_{..}}$	2, 10
D <sub>R</sub>	$\left[ -\sum_{j=0}^n \frac{T_j}{T_{..}} \log_2 \frac{T_j}{T_{..}} \right] - \left[ \sum_{i=1}^{n+2} \sum_{j=0}^n \frac{T_{ij}}{T_{..}} \log_2 \frac{T_{ij} T_{..}}{T_i T_j} \right]$	2, 10
RU <sub>R</sub>	$-\frac{\sum_{i=1}^{n+2} \sum_{j=0}^n \frac{T_{ij}}{T_{..}} \log_2 \frac{T_{ij} T_{..}}{T_i T_j}}{\sum_{j=0}^n \frac{T_j}{T_{..}} \log_2 \frac{T_j}{T_{..}}}$	2, 10
H <sub>max</sub>	$\sum_{i=1}^n \log_2(n+2)$	2
H <sub>c</sub>	$\sum_{i=1}^n \log_2(n+2) - \left[ -\sum_{i=1}^{n+2} \sum_{j=1}^n \frac{T_{ij}}{T_{..}} \log_2 \frac{T_{ij}}{T_{..}} \right]$	2, 10
H <sub>sys</sub>	$-\sum_{i=1}^n \sum_{j=1}^n \frac{T_{ij}}{T_{..}} \log_2 \frac{T_{ij}}{T_{..}}$	2
CE	$\frac{\sum_{i=1}^n \log_2(n+2) - \left[ -\sum_{i=1}^{n+2} \sum_{j=1}^n \frac{T_{ij}}{T_{..}} \log_2 \frac{T_{ij}}{T_{..}} \right]}{\sum_{i=1}^n \log_2(n+2)}$	2
TL <sub>j</sub>	$1 + \sum_{i=1}^n \frac{\mathbf{T}_{ij}^*}{T_j} \text{TL}_i$	13, 14
OL <sub>j</sub>	$\sum_{i=1}^n [\text{TL}_i - (\text{TL}_j - 1)]^2 \frac{\mathbf{T}_{ij}^*}{T_j}$	13

TABLE E.8: Network Index formulas (PART 2/2). See Table E.6 for the definition of terms. References: (1) Hirata and Ulanowicz, 1984, (2) Latham II, 2006, (3) Kones et al., 2009, (4) Pimm and Lawton, 1980, (5) Finn, 1976, (6) Finn, 1980, (7) Patten and Higashi, 1984, (8) Allesina and Ulanowicz, 2004, (9) Ulanowicz, 1986, (10) Ulanowicz and Norden, 1990, (11) Ulanowicz, 2004, (12) Ulanowicz, 2000, (13) Christensen and Pauly, 1992, (14) Lindeman, 1942.

Revisited from ref. 3.

Index	mean $\pm$ sd
A) Number of components ( $n$ )	7.000 $\pm$ 0.000
Number of total links (L)	39.998 $\pm$ 0.084
Number of internal links (Lint)	20.999 $\pm$ 0.070
Link density (LD)	5.714 $\pm$ 0.012
Connectance (C)	0.499 $\pm$ 0.001
Compartmentalization $\bar{C}$	0.537 $\pm$ 0.001
Average link weight ( $\bar{T}_{ij}$ )	0.175 $\pm$ 0.034
Effective Connectivity (Cz)	1.316 $\pm$ 0.044
Effective Flows (Fz)	1.974 $\pm$ 0.210
Effective Nodes (Nz)	1.496 $\pm$ 0.112
Effective Roles (Rz)	1.135 $\pm$ 0.053
Total System Throughput (T..)	7.036 $\pm$ 1.375
Total System Throughflow (TST)	4.415 $\pm$ 0.973
Total System cycled Throughflow (TSTc)	0.827 $\pm$ 0.440
Total System non-cycled Throughflow (TSTs)	3.588 $\pm$ 0.658
Finns Cycling Index (FCI)	0.179 $\pm$ 0.066
Revised Finns Cycling Index (FCIb)	0.114 $\pm$ 0.048
Average compartment throughflow ( $\overline{TST}$ )	0.630 $\pm$ 0.139
Average Path Length ( $\overline{PL}$ )	1.696 $\pm$ 0.261
B) Average mutual information (AMI)	0.817 $\pm$ 0.038
Statistical uncertainty ( $H_R$ )	1.644 $\pm$ 0.070
Conditional uncertainty ( $D_R$ )	0.827 $\pm$ 0.104
Realized uncertainty ( $RU_R$ )	0.498 $\pm$ 0.043
Hmax	24.216 $\pm$ 0.000
Network constraint (Hc)	14.330 $\pm$ 0.427
Hsys	9.885 $\pm$ 0.427
Constraint efficiency (CE)	0.591 $\pm$ 0.017
C) Network aggradation = average path length (NAG)	1.696 $\pm$ 0.261
Homogenization (HP)	1.558 $\pm$ 0.065
Synergism index (BC)	21.613 $\pm$ 6.499
Dominance indirect effect (ID)	0.753 $\pm$ 0.235
Mean of non-dimensional flow-matrix (MN)	0.313 $\pm$ 0.030
Mean of direct flow-matrix (MG)	0.096 $\pm$ 0.005
Coefficient of variation of non-dimensional flow-matrix (CVN)	1.347 $\pm$ 0.053
Coefficient of variation of direct flow-matrix (CVG)	2.097 $\pm$ 0.056

TABLE E.9: Estimations of network indices. A) Basic properties and Pathway analysis; B) Network uncertainty and constraint efficiencies; C) Environmental analysis.



Index		mean $\pm$ sd
Ascendency (A)	total	5.746 $\pm$ 1.122
	internal	1.308 $\pm$ 0.630
	import	2.154 $\pm$ 0.469
	export	2.283 $\pm$ 0.510
	dissipation	1.415 $\pm$ 0.306
Development capacity (DC)	total	19.539 $\pm$ 3.993
	internal	6.868 $\pm$ 1.868
	import	5.280 $\pm$ 1.078
	export	7.391 $\pm$ 1.348
	dissipation	5.017 $\pm$ 0.743
Overhead ( $\phi$ )	total	13.792 $\pm$ 3.027
	internal	5.559 $\pm$ 1.282
	import	3.125 $\pm$ 0.957
	export	5.107 $\pm$ 0.923
	dissipation	3.602 $\pm$ 0.574
Extent of development (AC)	total	0.295 $\pm$ 0.028
	internal	0.181 $\pm$ 0.043
	import	0.416 $\pm$ 0.091
	export	0.307 $\pm$ 0.032
	dissipation	0.281 $\pm$ 0.045

TABLE E.10: Indices of system growth and development.



## APPENDIX F

---

Complementary material – Chapter 6

---

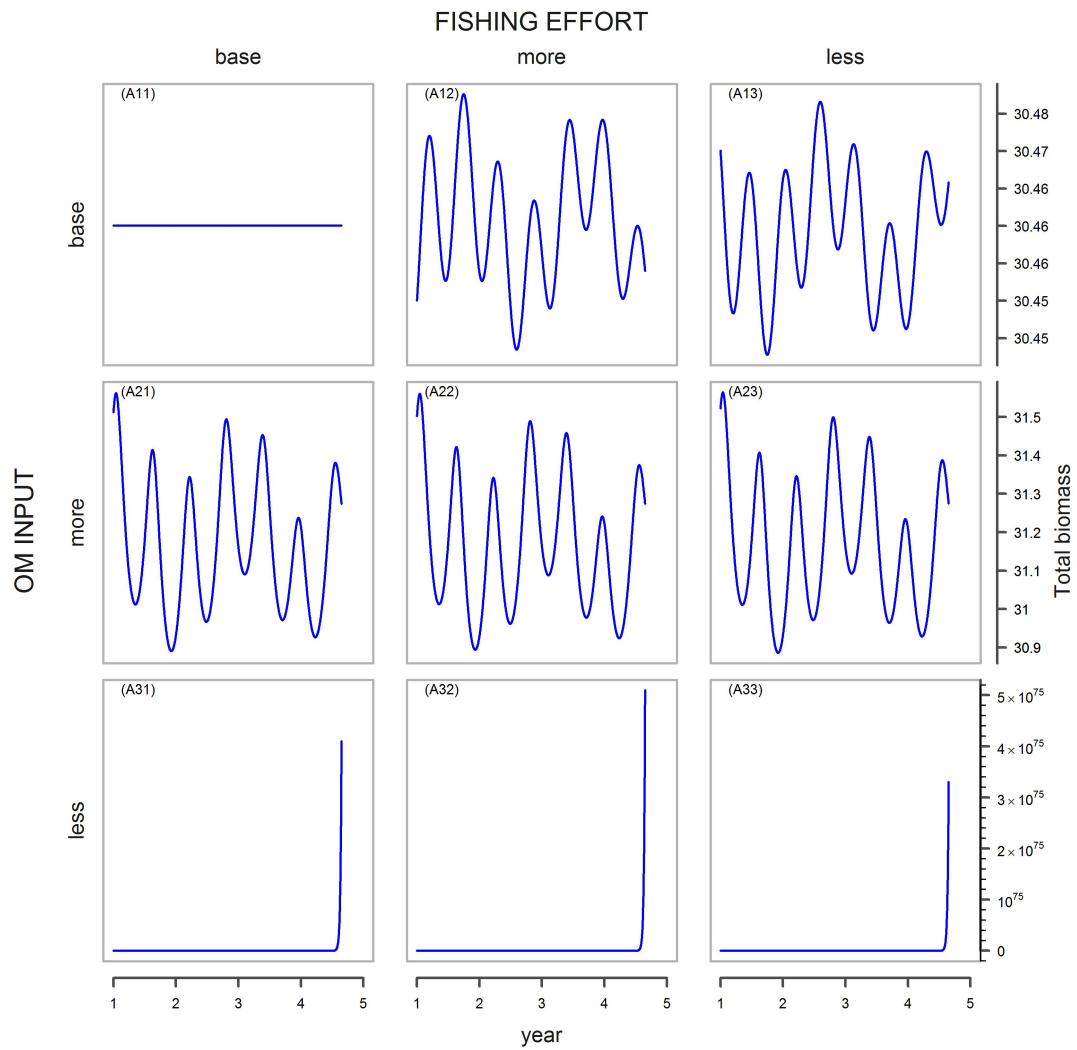


FIGURE F.1: A) Changes of total biomass during the 5 years using  $p=(0,5,-5)$ .

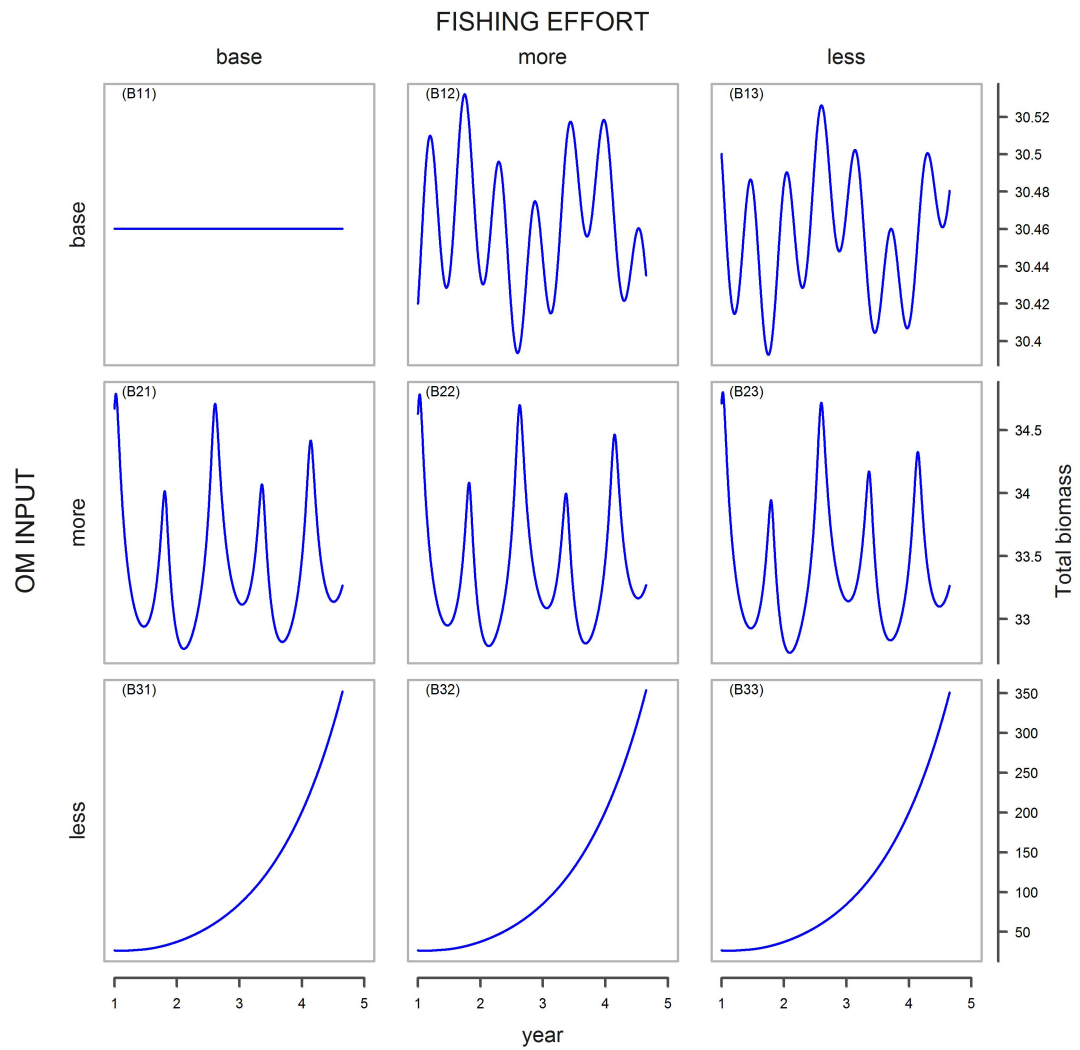


FIGURE F.2: B) Changes of total biomass during the 5 years using  $p=(0,5,-5)$ .

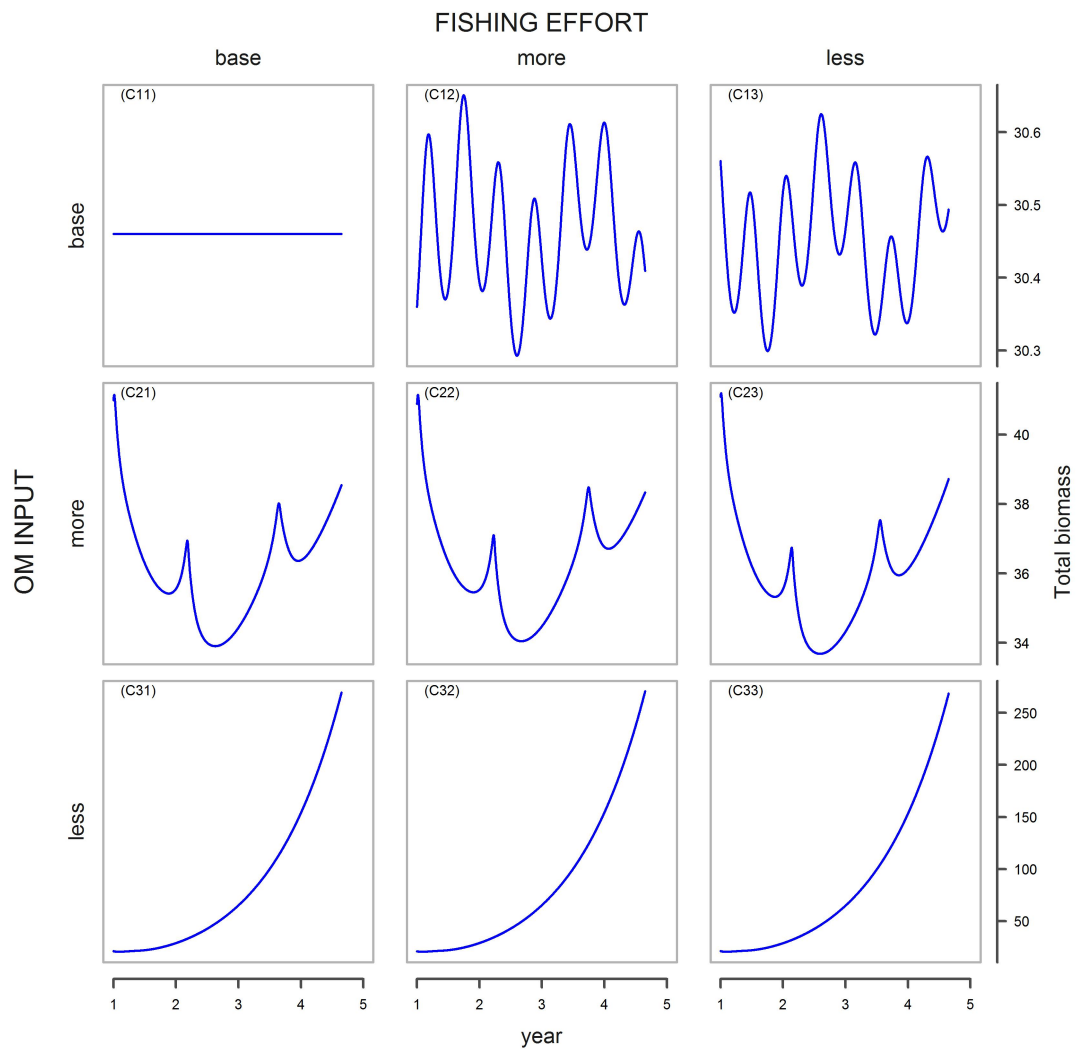


FIGURE F.3: C) Changes of total biomass during the 5 years using  $p=(0,50,-50)$ .

## APPENDIX G

---

### Species Pictures

---

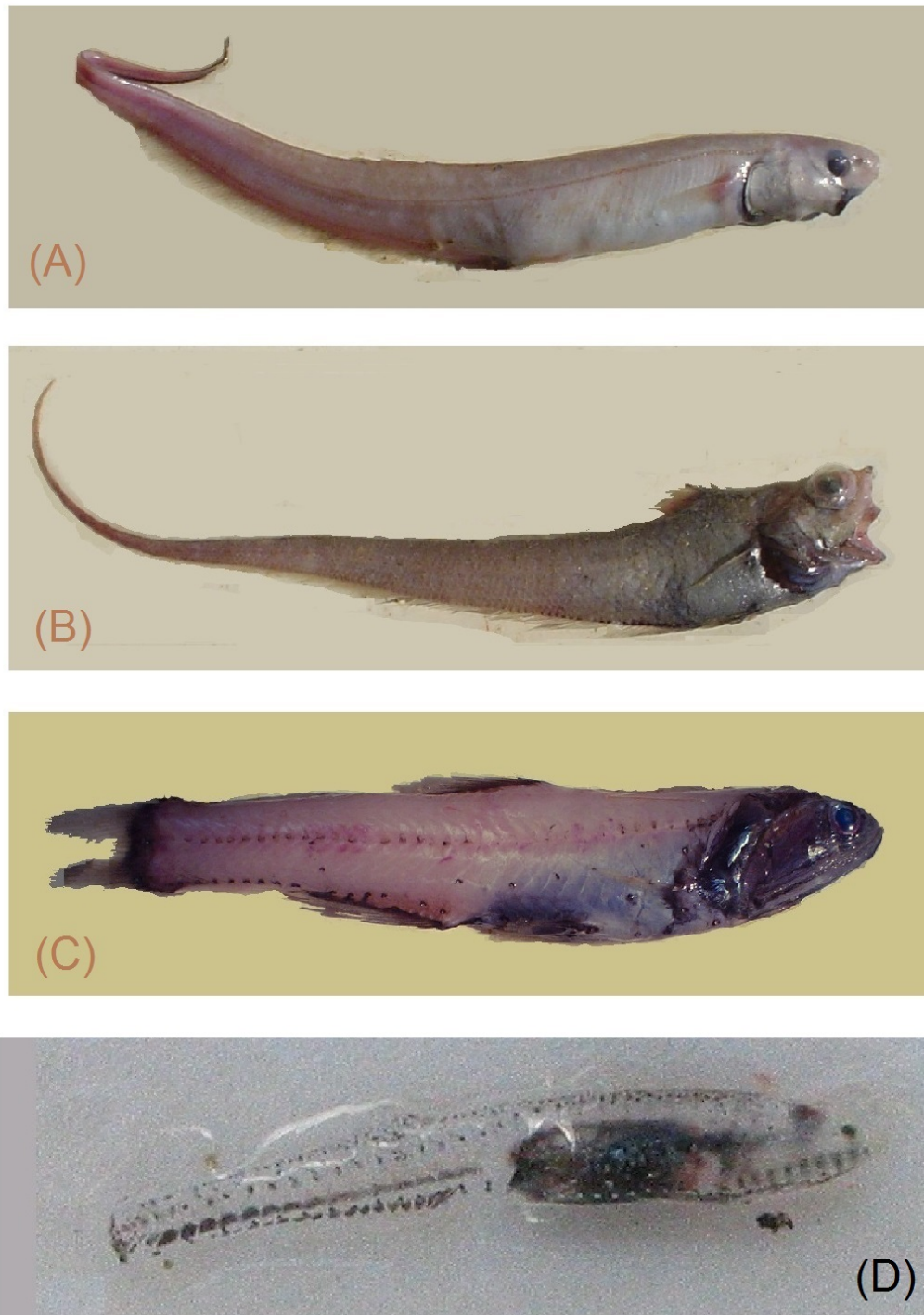


FIGURE G.1: A) The Shortfin spiny eel *Notacanthus bonaparte* Risso, 1840. Latium, MEDITS-IT, 2004; B) The macrurid Roughtip grenadier *Nezumia sclerorhynchus* (Valenciennes, 1838). Latium, MEDITS-IT, 2004; C) The Jewel lanternfish *Lampanyctus crocodilus* (Risso, 1810). Latium, MEDITS-IT, 2004; D) *Cyclothone braueri*, Jespersen & Tåning, 1926. Antromare survey, 2010.



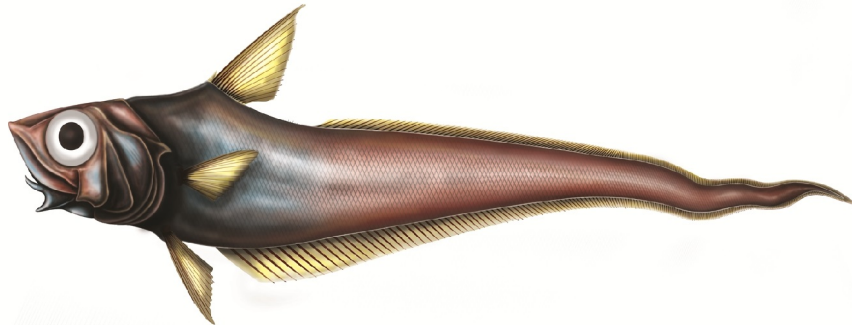


FIGURE G.2: A) The Rabbit fish *Chimaera monstrosa*, Linnaeus, 1758. Latium, MEDITS-IT, 2003; B) *Alepocephalus rostratus* Risso, 1820. Catalan Sea, Biomare 2007; C) The deep-water coral *Isidella elongata*. Catalan Sea, Antromare July 2011.

A



B



C

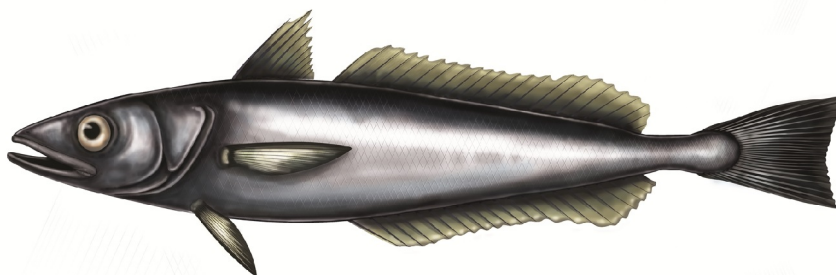
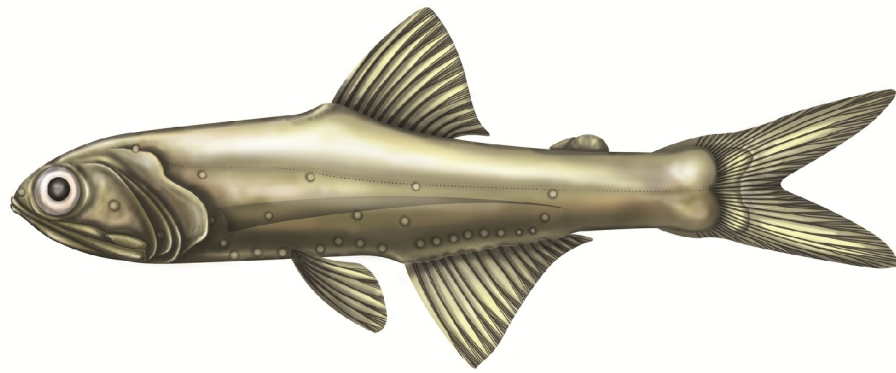


FIGURE G.3: A) The Blackmouth catshark *Galeus melastomus*, Rafinesque, 1810; B) The Common Atlantic grenadier *Nezumia aequalis* (Günther, 1878); C) The European hake *Merluccius merluccius* (Linnaeus, 1758). January 2015.

©Juan Pablo Sáez.

A



B

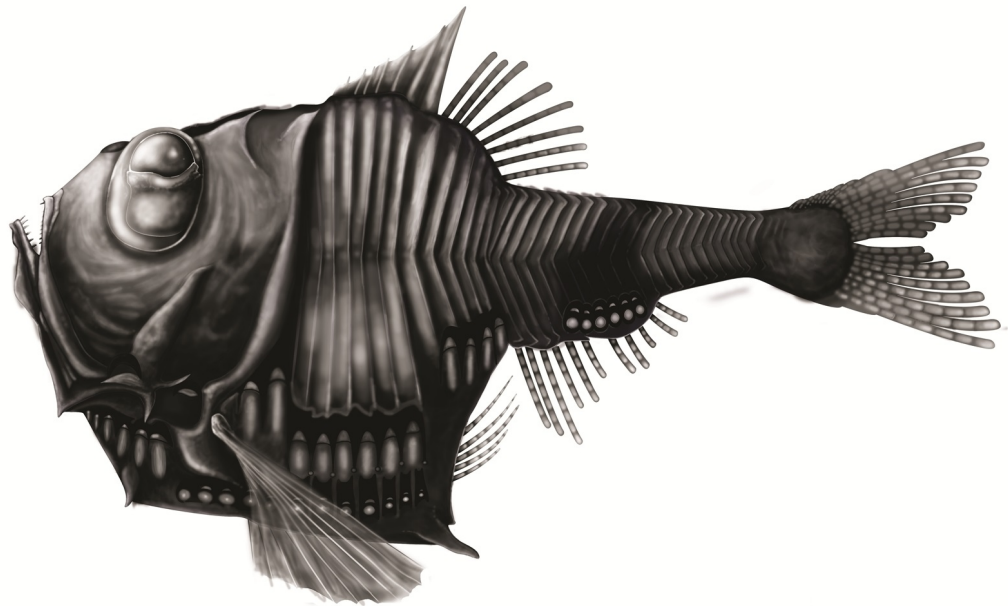


FIGURE G.4: A) The Jewel lanternfish *Lampanyctus crocodilus* (Risso, 1810); B) The half-naked hatchetfish *Argyrolepecus hemigymnus*, Cocco, 1829. January 2015. ©Juan Pablo Sáez.

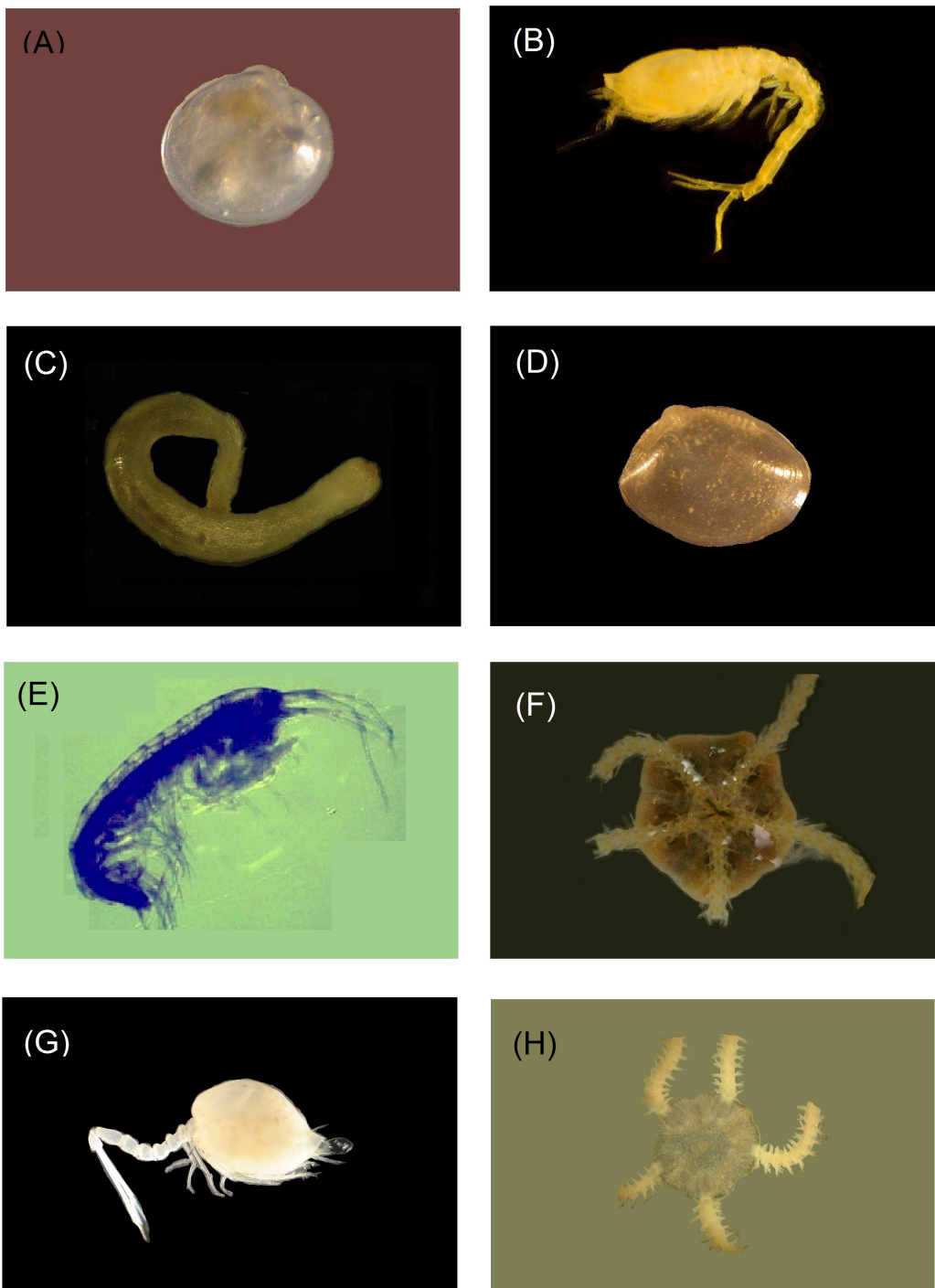


FIGURE G.5: A) The bivalve *Kelliella miliaris* (Philippi, 1844) B) The cumacean *Leucon* (*Epileucon*) *longirostris* Sars, 1871, ♂; C) A caudofoveat belonging to the genus *Falcidens* Salvini-Plawen, 1968; D) The bivalve *Ennucula aegeensis* (Forbes, 1844); E) The amphipod *Carangoliopsis spinulosa* Ledoyer, 1970; F) The ophiurid *Amphiura chiajei* Forbes, 1843 (oral view); G) *Campilaspis glabra* G. O. Sars, 1879; H) The ophiurid *Amphipholis squamata* (Delle Chiaje, 1828) (dorsal view). Specimens from boxcorer and suprabenthic sledge. Biomare 2007, Antromare 2010-2011.

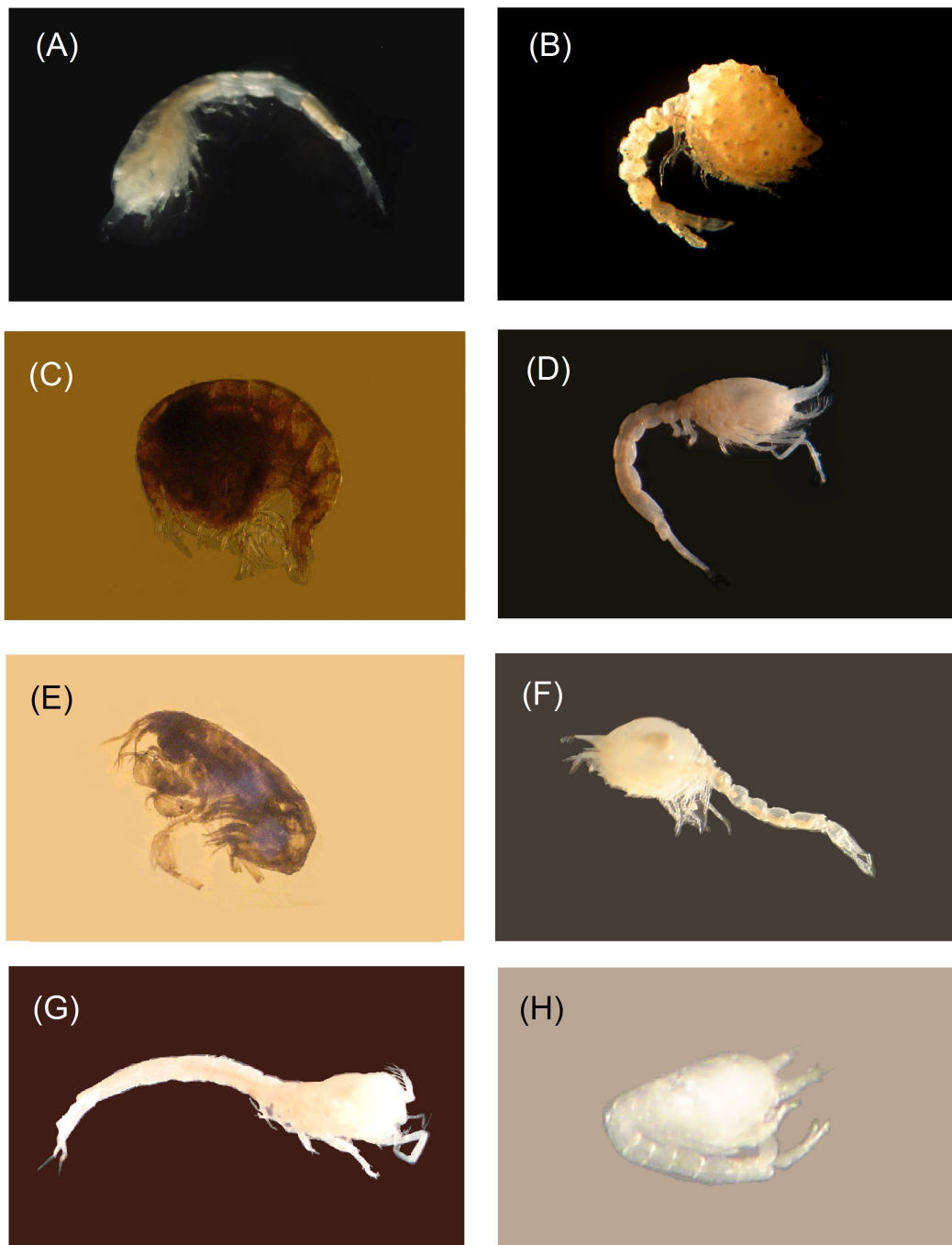


FIGURE G.6: A) *Leucon* (*Macrauloleucon*) *siphonatus* Calman, 1905; B) *Campylaspis squamifera* Fage, 1929; C) The amphipod *Stegocephalooides christianiensis* (Boeck, 1871); D) *Leucon* (*Crymoleucon*) *macrorhinus* Fage, 1951; E) The amphipod *Idunella nana* (Schiecke, 1973); F) *Diastylloides serrata* (Sars G.O., 1865); G) *Eudorella truncatula* (Bate, 1856); H) Postnauplius of a cumacean (probably *L. longirostris*). Specimens from boxcorer and suprabenthic sledge. Biomare 2007, Antromare 2010-2011.



## APPENDIX H

---

Field and Laboratory material

---



FIGURE H.1: Boxcorer. B/O García del Cid, Catalan Sea, BIOMARE October, 2007.



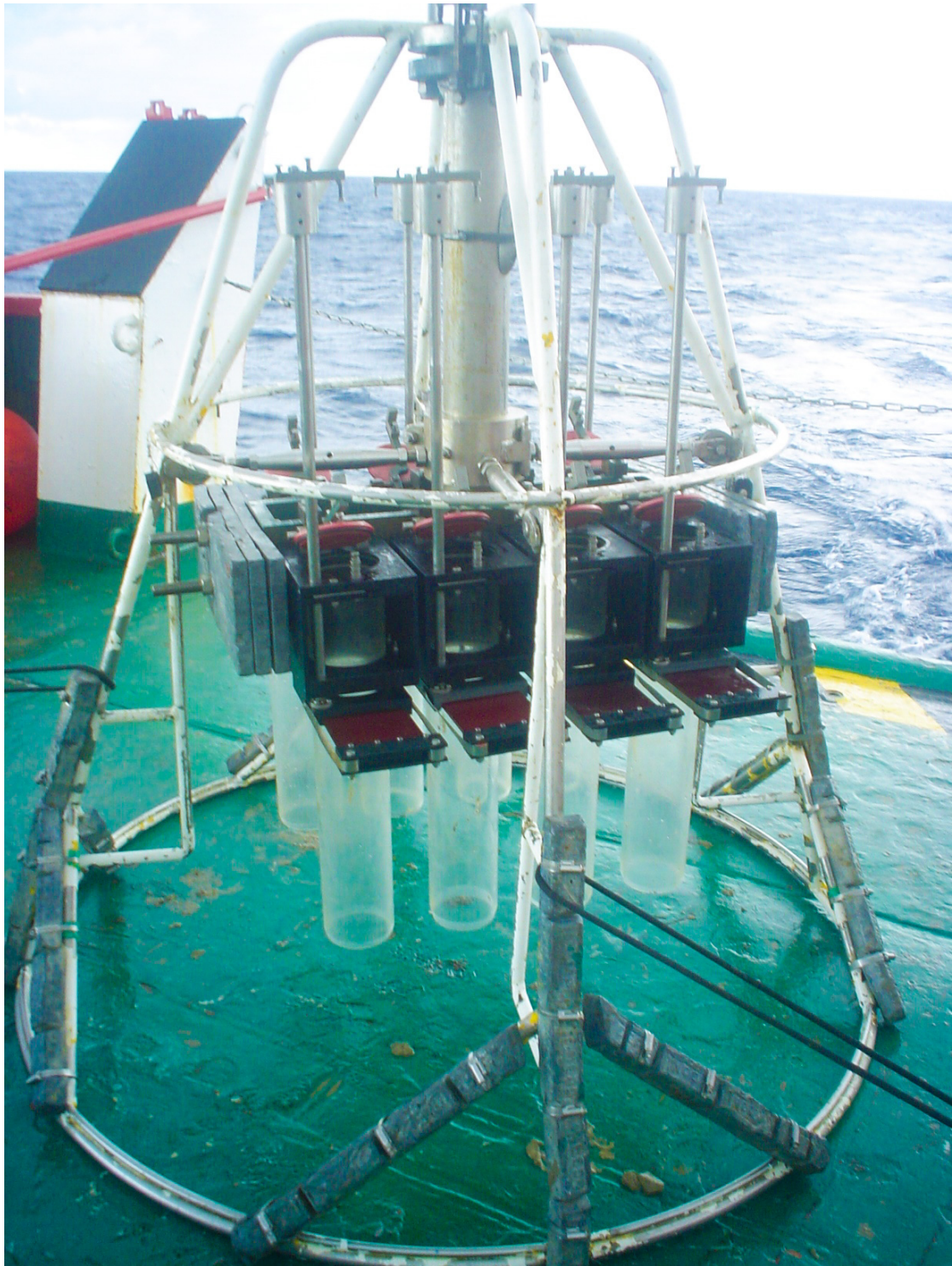


FIGURE H.2: Multicorer. B/O García del Cid, Catalan Sea, BIOMARE October, 2007.



FIGURE H.3: (A) WP2 used to sample zooplankton and micronekton. (B) Suprabenthic sledge used to sample suprabenthos. B/O García del Cid, Catalan Sea, BIOMARE October, 2007.

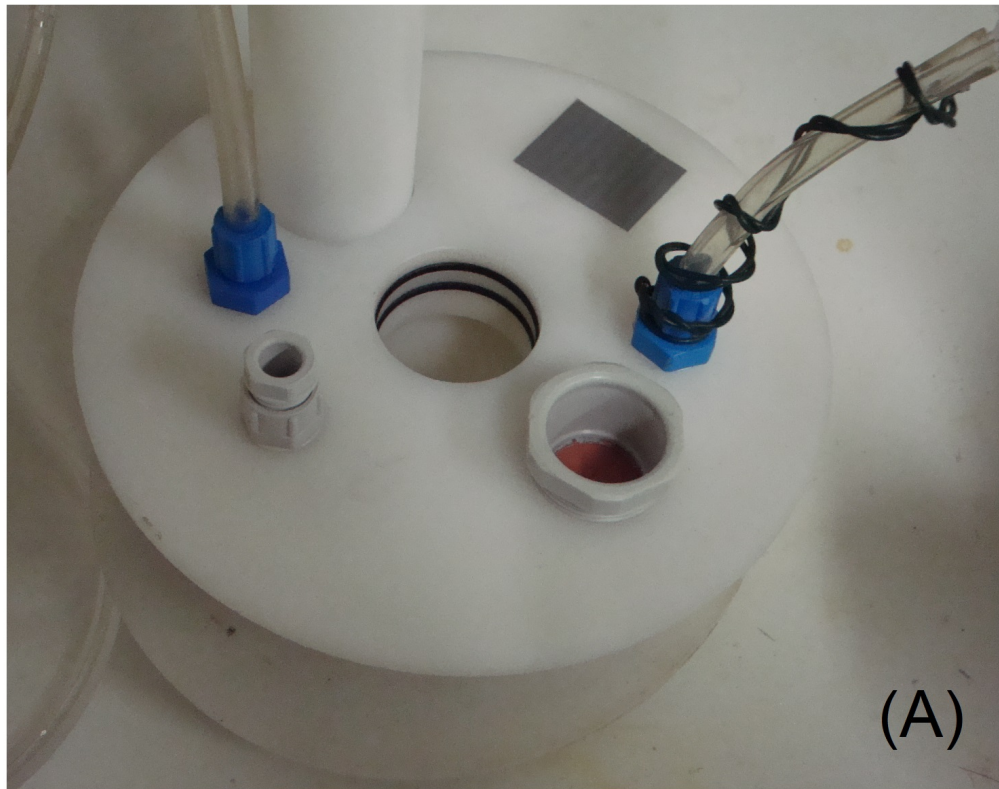


FIGURE H.4: A) A lid with different holes used to introduce the stirrer, sensors for digital records or pipettes for the Winkler titration; B) The perspex chambers ( $d = 30$  cm). All material provided by the Ecosystem studies department of the NIOZ-Yerseke.



FIGURE H.5: A lip containing a Teflon-coated magnetic stirrer. All material provided by the Ecosystem studies department of the NIOZ-Yerseke.



FIGURE H.6: An incubation with water. Preparing experiments at the NIOZ-Yerseke, 2011.

## H.1 SOC experiment and Winkler titration

Material: 9 winkler bottles (10ml), 1 pipette(50ml), 1 pipette(10ml), 1 micropipette (50 $\mu$ l), 3 needle, 1 eye-dropper, titration beaker, buret, 1 chronometer, 1 thermometer.

Reagent	ml
Sodium iodide and sodium hydroxide	0.05
Manganese (II) chloride	0.05
Sulfuric Acid	0.05
Sodium Thiosulfate Working solution	10
Starch	one drop

TABLE H.1: Reagents for one sample of water (10ml).

Procedure:

During the first part at the stern of the boat (A-D in Figure H.7) the sediments and waters of a boxcore are used to fill a chamber. If the water is not enough, supplementary water from the same depth must be available, for example from samples obtained with CDT. Recover the up water of the core (A). Collect the sediment from the by the perspex chamber (B-C). Fill the sediment by the water again (D). Don't throw the remaining water and store it in the dark.

The second part of the experiment consists in the preparation of samples in the laboratory, where the temperature must be set at the appropriate degree (the same as in natural conditions). Chambers are put into a tank filled with water at the same temperature (E). Take three first samples and add reagents (H-I), shake the sample and note the time. Then, ensure that each chamber is completely filled and without bubbles so that oxygen concentration is not altered. Tap the chambers and start the stirrer. Wait few minutes and take water from the chamber (F) to prepare three more samples (H-I) and fill the chamber with more water, always taking care not to leave bubbles inside. Each sample must be cleaned with enough water before close it. When reagent are added the sample is fixed, so the titration can be started (L) after making sure that everything else has been done and controlled (E-I).

The third step is he titration. The Erlenmeyer flask must be cleaned and fill again with the sample. Add a magnetic stir bar. Check the 10 mL buret to ensure that it is full of thiosulfate working solution. Place the erlenmeyer flask under the buret

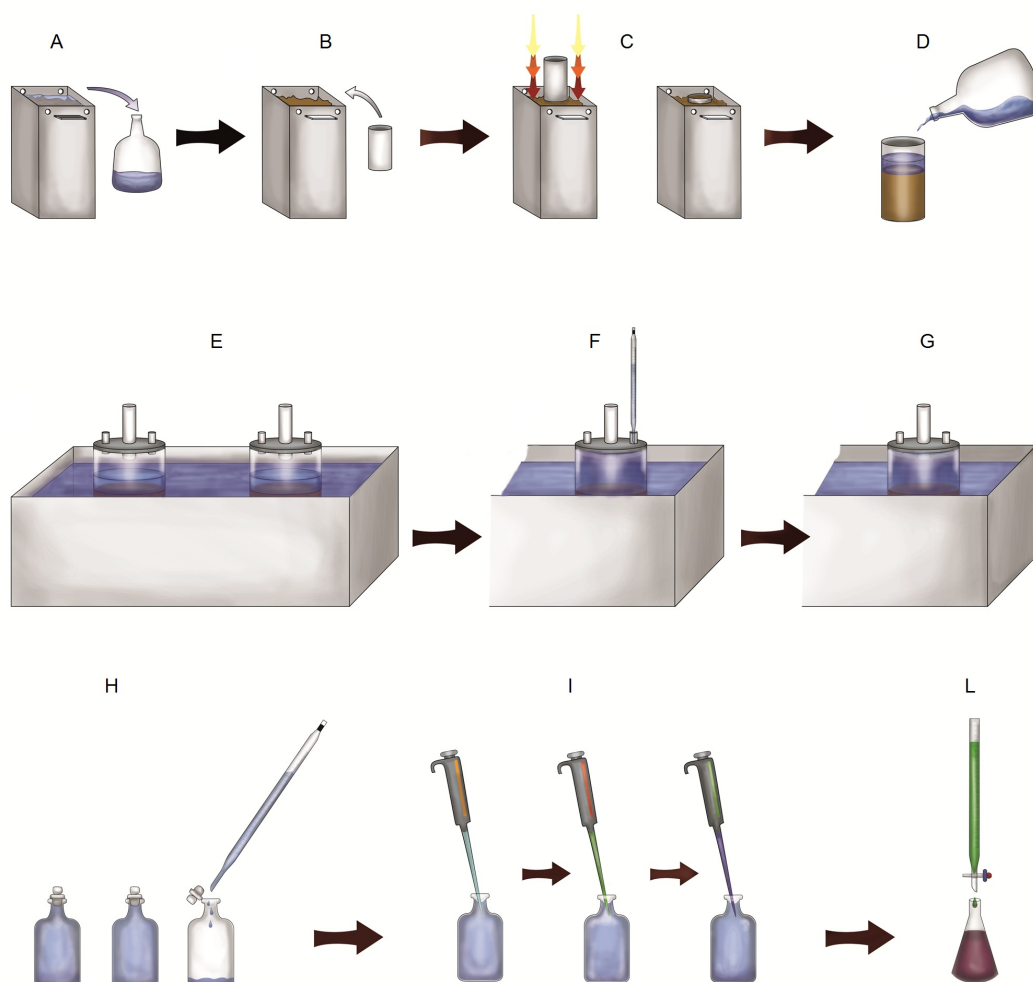


FIGURE H.7: Scheme for soc experiments and Winkler titration.

and turn on the magnetic stirrer. Keep the speed of the stir bar moderate (do not create a vortex in the solution). Then, slowly add thiosulfate to the solution until the solution turns a pale yellow colour. Stop titrating and add one drop starch solution to the flask. Continue to titrate by adding thiosulfate drop by drop just until the solution becomes colourless. Record the volume of thiosulfate added.

Repeat (F-L) every  $x$  time until there is change in the volume of thiosulfate added. In our case it has been postulated to do it every 4 hours.





## APPENDIX I

---

Offprint

---

## I.1 Publications

ATTENTION ;  
Pages 270 to 300 of the thesis are available at the editor's web

- V. Mamouridis, J.E. Cartes, S. Parra, J.I. Saiz Salinas *A temporal analysis on the dynamics of deep-sea macrofauna: Influence of environmental variability off Catalonia coasts (western Mediterranean)*. Deep Sea Research Part I: Oceanographic Research Papers Volume 58, Issue 4, April 2011, Pages 323-337  
<http://www.sciencedirect.com/science/article/pii/S0967063711000288>  
DOI <https://doi.org/10.1016/j.dsr.2011.01.005>
  
- J.E. Cartes, V. Mamouridis, E. Fanelli. *Deep-sea suprabenthos assemblages (Crustacea) off the Balearic Islands (western Mediterranean): Mesoscale variability in diversity and production*. Journal of Sea Research Volume 65, Issue 3, April 2011, Pages 340-354  
<http://www.sciencedirect.com/science/article/pii/S1385110111000074>  
DOI <https://doi.org/10.1016/j.seares.2011.02.002>



**UNIVERSIDADE DE  
SANTIAGO DE COMPOSTELA  
DEPARTAMENTO DE  
ESTADÍSTICA E INVESTIGACIÓN OPERATIVA**

**Extended Additive Regression for Analysing LPUE Indices in  
Fishery Research**

V. Mamouridis, N. Klein, T. Kneib, C. Cadarso Suárez, F. Maynou

Report 13-01

**Reports in Statistics and Operations Research**

## Extended Additive Regression for Analysing LPUE Indices in Fishery Research

Valeria Mamouridis<sup>\*1</sup>, Nadja Klein<sup>2</sup>, Thomas Kneib<sup>2</sup>, Carmen M.  
Cadarso Suárez<sup>3</sup> and Francesc Maynou<sup>1</sup>

<sup>1</sup> Institut de Ciències del Mar (CSIC), Passeig Marítim de la  
Barceloneta 37-49, 08003 Barcelona, Spain

<sup>2</sup> Georg-August University, Wilhelmplatz 1, 37073 Göttingen, Germany

<sup>3</sup> Unidade de Bioestadística, Facultade de Medicina e Odontoloxía,  
USC, Rúa de San Francisco, s/n, 15782 Santiago de Compostela, Spain

29/10/2013

### Abstract

We analysed the landings per unit effort (LPUE) from the Barcelona trawl fleet (NW Mediterranean) of the red shrimp (*Aristerus antennatus*) using the novel bayesian approach of additive extended regression or distributional regression, that comprises a generic framework providing various response distributions, such as the log-normal and the gamma and allows estimations for location and scale or shape (as the frequentist counterpart GAMLSS). The dataset covers a span of 17 years (1992-2008) during which the whole fleet has been monitored and consists of a broad spectrum of predictors: fleet-dependent (e.g. number of trips performed by vessels and their technical characteristics, such as the gross registered tonnage), temporal (inter- and intra-annual variability) and environmental (NAO index) variables. This dataset offers a unique opportunity to compare different assumptions and model specifications. So that we compared 1) log-normal versus gamma distribution assumption, 2) modelling only the expected LPUE versus modelling both expectation and scale (or shape) of LPUE, and finally 3) fixed versus random specifications for the catching unit effects (boats). Our preliminary results favour the gamma over the log-normal and modelling of both location and shape (in the case of the gamma) rather than only the location, while not noticeable differences occur in estimation when considering catching units as fixed or random.

Citation: Mamouridis, V., Klein, N., Kneib T., Cadarso Suárez, C.M., Maynou, F. 2013. Extended Additive Regression for Analysing LPUE Indices in Fishery Research. Reports in Statistics and Operations Research, Universidade de Santiago de Compostela. Departamento de Estatística e Investigacións. Vol. 28/10/2013 (2013-01), available at: <http://eio.usc.es/index.php/es/reports>.

\*mamouridis@icm.csic.es

## 1 Introduction

In fishery research, the LPUE (Landings Per Unit Effort) is an index widely used in stock assessment to estimate the relative abundance of an exploited species (Mendelsohn and Cury, 1989; Marchal et al., 2002). It constitutes one of the most common pieces of information used in assessing the status of fish stocks and is reckoned in different ways depending on data availability. The “landings” portion of the measure is the quantity of the stock brought to the port by each vessel and is usually expressed as number of individuals or weight of the whole stock, while the “unit effort” portion refers to the unit of time spent by a unit of the gear used to catch (e.g. vessel or square meters of a net). Therefore, LPUE is a relative index, which use is based on the assumption that it is proportional to the natural quantity of the species, despite their proportionality has been debated in the past (e.g. Gulland, 1964; Bannerot and Austin, 1983).

The most commonly applied analyses on LPUE is its standardisation to remove the bias induced by influential factors that do not reflect the natural variability (Maunder et al., 2006). In fact, many factors can affect the index (e.g. time, seasonality, fishing area and fleet characteristics, among others), some of which (i.e. fishery related variables) if not considered can lead to biased interpretations of stock states. Here we model the LPUE using all available explanatory variables. For some of the influential variables, a simple linear impact on LPUE as often assumed in standard statistical models may not be flexible enough and alternative, semiparametric modelling approaches may be required. Moreover, in most cases LPUE data are collected repeatedly for the same catching units over time leading to the necessity to account for unobserved characteristics of these units to avoid correlations in the repeated measurements.

The most common class of regression models to determine the impact of covariates  $x_1, \dots, x_p$  on the expectation of the LPUE are generalized linear models (GLM, McCullagh and Nelder, 1989) and generalized additive models (GAM, Hastie and Tibshirani, 1986). In GLM the expectation of LPUE is related to a linear combination of the covariate effects, i.e.

$$E(\text{LPUE}_i) = h(\beta_0 + \beta_1 x_{i1} + \dots + \beta_p x_{ip}), \quad i = 1, \dots, n$$

with a suitable transformation function  $h$  that ensures positivity of the expected LPUE and regression coefficients  $\beta_0, \beta_1, \dots, \beta_p$  (for GLM applications in LPUE analyses see (see Goffit et al., 1999; Maynou et al., 2003). Popular special cases for modelling LPUE include the gamma distribution or the normal distribution applied to log-transformed LPUE values (which is equivalent to assume a log-normal distribution). To overcome the limitation of GLMs to purely linear effects of covariates, generalized additive models, GAM have been introduced (see Damalas et al., 2007; Denis, 2002) where now the expectation is specified as

$$E(\text{LPUE}_i) = h(\beta_0 + f_1(x_{i1}) + \dots + f_p(x_{ip})).$$

The nonlinear functions  $f_1, \dots, f_p$  remain unspecified and should be estimated flexibly from the data, for example using penalized spline approaches (see Wood, 2006; Ruppert et al., 2003).

Another direction for extending the GLM approach is the inclusion of catching unit-specific effects to acknowledge the effect that usually multiple observations are

collected and that unobserved heterogeneity remains even when accounting for some covariate effects. If the individual catching units are indexed as  $i = 1, \dots, n$  and the repeated measurement for one catching unit are indexed as  $j = 1, \dots, n_i$ , the resulting model can be written as

$$E(\text{LPUE}_{ij}) = h(\beta_0 + \beta_1 x_{i1} + \dots + \beta_p x_{ip} + \alpha_i), \quad i = 1, \dots, n, j = 1, \dots, n_i.$$

The additional parameter  $\alpha_i$  is introduced to stand for any effect specific to the catching unit that is not represented in the effects of covariates  $x_1, \dots, x_p$ . Of course, similar extensions can be defined for generalized additive models. In the statistical community, the most common assumption for  $\alpha_i$  would be the specification as a random effect, i.e.  $\alpha_i$  i.i.d.  $N(0, \tau^2)$ , to acknowledge the fact that the catching units represent a sample from the population of catching units. This leads to the class of generalized linear mixed models (GLMMs, Pinheiro and Bates, 2000) or generalized additive mixed models (GAMMs, Wood, 2006). An alternative specification is to treat the  $\alpha_i$  as usual, fixed parameters that result from dummy coding of the catching units. This may be considered more appropriated if, for example, the complete fleet of catching units for a specific area has been observed. We will return to this debate later when discussing the methods in more detail, see also Bishop et al. (2004), Cooper et al. (2004) or Heiser et al. (2004) for the use of mixed models in this field.

Another important aspect when modelling LPUE is the choice of the response distribution. In most cases, skewed distributions have been considered, including in particular the gamma distribution (Maynou et al., 2003; Stefánsson, 1996), the log-normal distribution (Brynjarsdóttir and Stefánsson, 2004; Myers and Pepin, 1990) and the delta distribution (Gavarris, 1980; Pennington, 1983). The latter provides a form of zero-adjustment where zero catches are modelled separately from the nonnegative catches via a Bernoulli distribution. As a possibility to differentiate between gamma and log-normal distribution, the Kolmogorov-Smirnov test has been applied to fitted values from corresponding GLMs. Then, the distribution leading to a lower value for the test statistic can be considered to be closer to the distribution of the data (Brynjarsdóttir and Stefánsson, 2004; Stefánsson and Pálsson, 1998).

In this paper, structured additive distributional regression models (Klein et al., 2013b) has been considered as a comprehensive, flexible class of models that encompasses all special cases discussed so far and a number of further extensions. More specifically, this class of models allows to deal with the following problems:

- Selection of the response distribution: Additive distributional regression comprises a generic framework providing various response distributions and in particular the log-normal and the gamma distributions. Extensions including zero-adjustment to account for an inflation of observations with zero catch would also be possible but not required in the data set considered later. Tools for effectively deciding between competing modelling alternatives will also be considered.
- Linear versus nonlinear effects: Effects of continuous covariates can be estimated nonparametrically based on penalized splines approximations that allow for a data-driven amount of smoothness and therefore deviation from the linearity assumption.

- Fixed versus random effects: Both fixed and random specifications for the catching unit-specific effects are supported and can be compared in terms of their ability to fit the data.
- Models for location, scale and shape: Instead of restricting attention to only modelling the expected LPUE, distributional regression allow to specify a further parameter of the distribution that correspond to scale or shape. This both enables for additional flexibility and a better understanding of how different covariates affect the distribution of LPUE.
- Mode of inference: Distributional regression can be formulated both from a frequentist and a Bayesian perspective and corresponding estimation schemes either rely on penalized maximum likelihood or Markov chain Monte Carlo simulations. This paper is focused on the Bayesian inference.

Structured additive distributional regression is in fact an extension of structured additive regression (STAR, Brezger and Lang, 2006; Fahrmeir et al., 2004) in the framework of generalized additive models for location, scale and shape (GAMLSS, Rigby and Stasinopoulos, 2005). The parameter specifications rely very much on STAR, a comprehensive class of regression models for the expectation of the response that comprises geosadditive models (Kammann and Wand, 2003), generalized additive models (Hastie and Tibshirani, 1986) and generalized additive mixed models (Lin and Zhang, 1999) as special cases.

Our analysis deals with the red shrimp (*Aristeus antennatus*) LPUE. The red shrimp is the target species for the deep-water trawl fishery in the Western Mediterranean (Bas et al., 2003), where catches have reached more than 1000 t/yr (FAO/FISHSTAT, 2011). This fishery is developed in deep-waters - 450 – 900 m - on the continental slope and near submarine canyons (Sarda et al., 1997; Tudela et al., 1998). *A. antennatus* LPUE has already been studied: its fluctuations have been related to changes in oceanographic conditions, e.g. at least partially triggered by changes in the North Atlantic Oscillation (Maynou, 2008) or explained by changes in the seasonal availability of the resource, linked to its life-cycle (Carbonell et al., 1999) and source demand (Sarda et al., 1997).

The main objective of this study is to demonstrate the usefulness of structured additive distributional regression in modelling and predict shrimp LPUE and to provide guidance for model choice and variable selection, questions that arise in the process of developing an appropriate model for a given data set. Therefore, we will discuss tools such as quantile residuals, information criteria and predictive mean squared errors to evaluate the ability of models to describe and predict LPUE adequately.

The rest of the paper is structured as follows: In Section 2 a description of the data set is given to illustrate the application of structured additive distributional regression. Section 3 provides an overview of the methods dealing with the real data set, including the choice of an appropriate response distribution and variable selection. In Section 4, we perform an extensive analysis of the red shrimp data, comparing different response distributions, regression specifications and random versus fixed effects for the repeated observations. The final Section 5 concludes and comments on main results and directions of future research.

## 2 Data description

Data proceed from the daily sale slips of the Barcelona trawling fleet, granted by the Barcelona Fishers' Association. This data set comprises the information for 21 trawlers, with their total monthly landings (*landings*, kg), their monthly number of trips performed (*trips*) and the Gross Registered Tonnage (*grt*, GRT). Furthermore, the monthly average value of the North Atlantic Oscillation index (NAO) was obtained from the web site of the Climatic Research Unit of the University of East Anglia (Norwich, UK): <http://www.met.rdg.ac.uk/cag/NAO/slides.html>. Then we computed the year average of NAO, whose relationship with landings of three years later has been detected through cross-correlation analysis in previous studies by Maynou (2008).

The total number of observations,  $N$ , amounts to  $N = 2314$  using the whole fleet (21 trawlers) having practised deep-fishing in the period from January 1992 to December 2008 (17 complete years). Landings of the whole fleet were monitored over time, so, data depict the entire population of the fleet in the studied area and period. Red shrimp fishery is a specific fishery, thus, all the product caught on board appears in landings, due to its high commercial value, while, when landings are not reported for a given boat is due to its inactivity, rather than to zero catches of the source.

The landings and number of trips were used to estimate the "nominal" LPUE index,

$$lpue_{ij} = \frac{landings_{ij}}{trips_{ij}}, \quad (1)$$

where  $i$  and  $j$  refer to the observation  $i$  of the vessel  $j$ . The adjective "nominal" refers to the variable not standardized. Table 1 and the introductory part of this Section provide information on the variables in Equation 1. Trips are always performed in one day, hence, the *lpue* represents the daily biomass average caught by a boat during one day ( $\text{kg d}^{-1}$ ) with a monthly resolution.

As in previous regression analysis (see [ymamouridis2014](#)) months associated to not significant parameters of the categorical variable *months* with categories  $month_k$ ,  $k = 1, \dots, 12$  were backward assembled into two categories of a new variable *period* (period of the year): *period1* defines all months excluding June and November and *period2* refers to June and November. All variables are summarised in Table 1.

## 3 Methodology

It has become quite popular to model the expected LPUE as a function of linear covariate effects. The results obtained from linear mean regression are easy to interpret but depreciated by possible misspecification due to a more complex underlying covariate structure, violation of homoscedastic errors or correlations caused by clustered data. To deal with these problems we apply Bayesian distributional structured additive regression models (Klein et al., 2013b) a model class originally proposed by Rigby and Stasinopoulos (2005) in a frequentist setting. The idea is to assume a parametric distribution for the conditional behaviour of the response and to describe each parameter



Table 1: List of variables.

Variable	Description
<i>landings</i>	the total catches landed at port by each boat in one month
<i>lpue</i>	the daily LPUE index for each boat calculated as in Eq. 1
<i>code</i>	a categorical variable assigned to each boat, $c = 1, \dots, 21$
<i>time</i>	a total of 204 months from January 1992 to December 2008 coded with a letter and two digits, e.g. J92 is January 1992
<i>trips</i>	the number of trips performed by each vessel during one month
<i>grt</i>	Gross Registered Tonnage of each boat
<i>nao3</i>	mean annual NAO index of 3 years before the year of estimated <i>lpue</i>
<i>month</i>	categorical variable with $m = 1, \dots, 12$ from January to December
<i>period</i>	binary variable with grouped months holding the same effect
	<i>period1</i> = all month excluding June and November
	<i>period2</i> = June and November

of this distribution as a function of explanatory variables. In the following, only log-normal and gamma distribution are considered for LPUE, although also an extension to mixture distributions with point masses in zero would be possible as in Heller et al. (2006) or Klein et al. (2013a). Here they are not necessary since the response in this study is always greater than zero.

We consider the log-normal distribution with parameters  $\mu_j$  and  $\sigma_j^2$  such that

$$E(lpue_{ij}) = \exp\left(\mu_j + \frac{\sigma_j^2}{2}\right)$$

$$Var(lpue_{ij}) = (\exp(\sigma_j^2) - 1) \exp(2\mu_j + \sigma_j^2).$$

Accordingly,  $\log(lpue_{ij})$  is normal distributed with  $E(\log(lpue_{ij})) = \mu_j$  and  $Var(\log(lpue_{ij})) = \sigma_j^2$ . As an alternative, we assume a gamma distribution with parameters  $\mu_j > 0$ ,  $\alpha_j > 0$  and density

$$f(lpue_{ij}|\mu_j, \alpha_j) = \left(\frac{\alpha_j}{\mu_j}\right)^{\alpha_j} \frac{lpue_{ij}^{\alpha_j-1}}{\Gamma(\alpha_j)} \exp\left(-\frac{\alpha_j}{\mu_j} lpue_{ij}\right).$$

Then, the expectation and variance are given by

$$E(lpue_{ij}) = \mu_j$$

and

$$Var(lpue_{ij}) = \frac{\mu_j^2}{\alpha_j}$$

such that  $\mu_j$  is the location parameter and the parameter  $\alpha_j$  is inverse proportional to the variance.

All parameters involved are linked to structured additive predictors, yielding

$$\eta_{ij,\mu} = \mu_{ij} \quad \eta_{ij,\sigma^2} = \log(\sigma_{ij}^2)$$

for the log-normal distribution where the log-link is used to ensure positivity of the  $\sigma_{ij}^2$ . For the gamma distribution, both parameters are restricted to be positive so that we obtain

$$\eta_{ij,\mu} = \log(\mu_{ij}) \quad \eta_{ij,\sigma} = \log(\sigma_{ij}).$$

Dropping the parameter index, a generic structured additive predictor is of the form

$$\eta_{ij} = z_{ij}'\gamma + \sum_{p=1}^P f_p(x_{ijp}) + \alpha_i.$$

Here,  $z_{ij}$  is a vector containing binary, categorical or continuous linearly related variables and  $f_1, \dots, f_P$  are smooth functions of continuous variables  $x_{ij1}, \dots, x_{ijP}$  modelled by Bayesian P(enalized) splines (Lang and Brezger, 2004). The basic assumption is that the unknown functions  $f_p$  can be approximated by a linear combination of B-spline basis functions (Eilers and Marx, 1996). Hence,  $f_p$  can in matrix notation be written as  $Z_p \beta_p$ , where  $Z_p$  is the design matrix with B-spline basis functions evaluated at the observations and  $\beta_p$  is the vector of regression coefficients to be estimated. To enforce smoothness of the function estimates we use second order random walk priors for the regression coefficients such that

$$p(\beta_p | \tau_p^2) \propto (\tau_p^2)^{-0.5 \text{rank}(K)} \exp\left(-\frac{1}{\tau_p^2} \beta_p' K \beta_p\right)$$

where  $K = D'D$  for a second order difference matrix  $D$  and  $\tau_p^2$  are the smoothing variances with inverse gamma hyperpriors.

The additional, boat-specific effect  $\alpha_i$  is introduced to represent any effect specific to the catching unit that is not represented in the covariate effects of  $z_{ij}, x_{ij1}, \dots, x_{ijP}$ . A standard assumption for this effect would be  $\alpha_i$  i.i.d.  $N(0, \tau^2)$ , to acknowledge the fact that the catching units represent a sample from the population of catching units. Alternatively,  $\alpha_i$  can be treated as a fixed effect resulting from dummy coding of the different catching units. There has been considerable debate in the past (Bishop et al., 2004; Cooper et al., 2004; Helsler et al., 2004; Venables and Dichmont, 2004) about whether it is more appropriate to specify  $\alpha_i$  as random or fixed effects from a methodological perspective, but then random effects have been rarely considered (e.g. Marchal et al., 2007). One differentiation goes along the lines discussed above, i.e. differentiating between situations where the catching units in the data set define a (random) subsample of the population of the catching unit (which would favour the specification as random effects) and situations where (almost) the complete fleet has been observed (which would favour the specification as fixed effects). From the Bayesian perspective, this differentiation provides an incomplete picture since the differentiation between random and fixed parameters only corresponds to a difference in prior specifications. From a practical point of view the random effects assumption can also be seen as a possibility to regularise estimation in case of large numbers of catching units and/or

small individual time series where estimation of fixed effects may easily become unstable. Note also that in case of a fixed effects specification, no other time-constant covariates  $z_i$  characterising the catching units can be included since they can not be separated from the fixed effects. In our data set, this applies for the gross register tonnage which may be expected to provide important information on LPUE but which can not be included in a fixed effects analysis. This problem can be avoided for example by clustering catching units but with a probable loss of information (as the solution used in Mamouridis et al., 2014). In the next section, we compare the performance of random and fixed effects specifications based on model fit criteria to decide which model has a better explanatory ability.

Our inferences is based on efficient Markov chain Monte Carlo (MCMC) simulation techniques (for more details on distributional regression see (Klein et al., 2013b)). In principle, the approach in all models could also be performed in a frequentist setting (Stasinopoulos and Rigby, 2007) via direct optimization of the resulting penalized likelihood which is often achieved by Newton-type iterations with numerical differentiation. However, many models turned out to be numerically unstable leading to no estimation results or warnings concerning convergence. Therefore the study is restricted to the Bayesian analysis. The Bayesian approach with MCMC also reveals several additional advantages, e.g. simultaneous selection of the smoothing parameters due to the modularity of the algorithm, credibility intervals which are directly obtained as quantiles from the samples and the possibility to extend the model for instances with spatial variations. All models have been estimated in the free open source software BayesX (Belitz et al., 2012).

The performance of models is compared in terms of the Deviance Information Criterion, DIC (Spiegelhalter et al., 2002). The DIC is similar to the frequentist Akaike Information Criterion, compromising between the fit to the data and the complexity of the model. Furthermore it can easily be computed from a sample  $\theta^1, \dots, \theta^M$  of the posterior distribution  $p(y|\theta)$ ,

$$\text{DIC} = 2\overline{D(\theta)} - D(\overline{\theta}),$$

with deviance  $D(\theta) = -2\log(p(y|\theta))$  and  $\overline{D(\theta)} = \frac{1}{M} \sum_{m=1}^M D(\theta^m)$ ,  $\overline{\theta} = \frac{1}{M} \sum_{m=1}^M \theta^m$  respectively. We also use the DIC to determine important variables and optimal predictors  $\eta_{\bar{\mu}}$  and  $\eta_{\bar{\sigma}^2}$  or  $\eta_{\bar{\mu}, \bar{\sigma}}$ .

To validate the distribution assumption we used normalized quantile residuals. That allowed to decide between equivalent models under different response assumptions. Normalized quantile residuals are defined as  $r_i = \Phi^{-1}(u_i)$ . Here,  $\Phi^{-1}$  is the inverse cumulative distribution function of a standard normal distribution and  $u_i$  is the cumulative distribution function of the estimated model and with plugged in estimated parameters. For consistent estimates, the residuals  $r_i$ ,  $i = 1, \dots, n$  follow approximately a standard normal distribution if the estimated distribution is the true distribution. Therefore, models can be compared graphically in terms of quantile-quantile-plots.

Finally, to assess the predictive accuracy of the models we performed a k-fold Cross Validation using the mean squared error of prediction (MSEP)

$$\text{MSEP}_k = \frac{\sum_{i=1}^N [l_{pue_{i,k}} - \bar{E}(l_{pue_{i,k}})]^2}{N}.$$

Here  $l_{pue_{i,k}}$  is the observation  $i$  of subset  $k$ ,  $\bar{E}(l_{pue_{i,k}})$  is the expectation of the prediction in the validation set, given parameters estimated on the  $k$ -th training set and  $N$  refers to the number of observations of the corresponding test set. We performed a 10 fold stratified (within each catching unit) random partition of the whole dataset to ensure a minimum number of observations for each boat in both the training and the validation sets. Taking the 10% of the data to build the latter, we ensure at least 10 observations per unit in the validation set. If at least one catching unit is not represented in one of the partitions, the prediction for the missing catching unit in fixed effects models could not be computed. This clarifies the usefulness in using mixed effects specification when interested on predictions for unobserved catching units.

## 4 Data analysis

### 4.1 Model diagnostics and comparison

During model building variables were selected using a stepwise forward procedure according to the DIC scores and the significance of their effect. Single models have been built first for each variable, to assess its explanatory potential. For each distribution the predictor for location has been modelled, adding one variable at a time till finding the best predictor. Then, using this “best” predictor for location, also the predictor for the second parameter, the scale or shape for log-normal or gamma respectively, has been modelled using the same procedure.

For both distributions, all models with single explanatory variable returned significant effects, except some categories of *code* and *month*. So that, we decide to model *month* effect as binary (*period*), after grouping categories (see Methodology Section and Mamouridis et al. (2014)). Conversely, *code* variable has not been merged, to allow the comparison between fixed and mixed effects models.

Assuming log-normal distribution and according to the ascending DIC, variables are ordered from *code* (DIC=17059.4 as random and DIC=17060.0 as fixed effect), then *trips*, *time*, *grt*, *nao3*, to *period* (DIC=17735.7). The same ordination has been found assuming the gamma distribution with DIC scores ranged between DIC=16763.0 for *code* and DIC=17290.0 for *period*. Variables have been added in this order till the saturated model. Variables *nao3* and *grt* do not strongly improve model in terms of DIC scores (less than 20 units for each variable). However parameters are significantly different from zero and their incorporation effective to be discussed. We used the same procedure for the second predictor. According to the DIC, variables are ordered as follows: *code*, *trips*, *time*, *grt*, *nao3* and *period*. The effects of variables *nao3*, *period* and *grt* for the second parameter were not significant.

According to the DIC scores, for log-normal assumption, the appropriate predictor structures for location  $\eta_{\mu}$  and scale  $\eta_{\sigma^2}$ , are

$$\begin{aligned}\eta_{\mu} &= \beta_{0,\mu} + \beta_{1,\mu} \text{period}_2 + f_{1,\mu}(\text{trips}) + f_{2,\mu}(\text{time}) + f_{3,\mu}(\text{nao3}) + \sum_i \alpha_{i,\mu} \\ \eta_{\sigma^2} &= \beta_{0,\sigma^2} + f_{1,\sigma^2}(\text{trips}) + f_{2,\sigma^2}(\text{time}) + \sum_i \alpha_{i,\sigma^2}\end{aligned}\quad (2)$$

for both fixed and mixed effects specification. Here the  $\beta_k$  are parameters associated to the intercept and linear fixed effects of the variable *period*. The  $\alpha_i$  are parameters associated to the effects of *code*, specified as fixed in fixed effects models and as random in mixed effects models. Instead,  $f_i$  are smooth functions associated to nonlinear effects of the variables *trips*, *time* and *naos*. The second sub-index in all parameters,  $\mu$  or  $\sigma^2$ , identifies which predictor the parameter or function belongs,  $\eta_\mu$  or  $\eta_{\sigma^2}$  respectively.

Using fixed effects specification for *code* the inclusion of variable *grt* leads to instability, due to the reasons mentioned in Section 3, so then, the model with *grt* cannot be estimated in these cases. On the contrary, in mixed effects specification *grt* could be estimated but it leads to equal or tightly higher values of DIC score. Thus it has been backward eliminated, however the associated parameter was significantly different from zero and positive.

Under the gamma distribution assumption, the log-link function has been chosen, since the support of both parameters is the positive real domain and the final predictor structures for location and shape are

$$\begin{aligned}\eta_\mu &= \beta_{0,\mu} + \beta_{1,\mu} \text{period}_2 + f_{1,\mu}(\text{trips}) + f_{2,\mu}(\text{time}) + f_{3,\mu}(\text{naos}) + \sum_i \alpha_{i,\mu} \\ \eta_\sigma &= \beta_{0,\sigma} + f_{1,\sigma}(\text{trips}) + f_{2,\sigma}(\text{time}) + \sum_i \alpha_{i,\sigma}\end{aligned}\quad (3)$$

for both fixed and mixed effects specification. The notation here is the same specified for the log-normal models however here the second parameter, the shape, is denoted  $\sigma$ .

Table 2: Global scores of selected models. Columns indicate: M, refers to model coding (see specifications in the text); DEV, the residual deviance; EP: Effective total number of Parameters, DIC: Deviance Information Criterion, MSEP, mean and sd of the mean square error of predictions calculated through 10-fold validation.

M	DEV	EP	DIC	MSEP
M1	16163.9	47.1	16258.0	98.3 ± 12.3
M2	16164.2	46.8	16257.7	96.9 ± 12.4
M3	15138.4	91.2	15320.8	436.2 ± 434.9
M4	15142.7	87.2	15317.2	315.0 ± 307.4
M5	16095.7	45.6	16187.0	77.8 ± 11.5
M6	16096.8	43.9	16184.7	77.3 ± 11.7
M7	15027.1	90.9	15208.9	71.5 ± 9.2
M8	15032.4	86.9	15206.1	71.7 ± 9.4

The Table 2 provides a selection of models that we used for comparison purposes and their corresponding global parameters: the deviance, the effective number of parameters and the DIC, estimated on the whole dataset, and the MSEP calculated by predictions on the validation subsets as described in the methodology.

The eight models in table 2 present a combination between alternatives of the following assumptions:

- (A) The log-normal (LN) or gamma (GA) as the underlying distribution assumption;
- (B) Only location (LO) or both location and scale/shape (LS) parameters explicitly modelled using one or more explanatory variables;
- (C) Effects of *code* as fixed or random leading to a fixed effects model (FI) or mixed effects model (MI) respectively;

So, model M1 is specified by A=LN, B=LO and C=FI; M2 by A=LN, B=LO and C=MI; M3 by A=LN, B=LS and C=FI; M4 by A=LN, B=LS and C=MI; M5 by A=GA, B=LO and C=FI; M6 by A=GA, B=LO and C=MI; M7 by A=GA, B=LS and C=FI; and M8 by A=GA, B=LS and C=MI. The predictors for location in models denoted as M1, M2, M5 and M6 (with B=LO) have the same structure of  $\eta_{\text{loc}}$  in Equations 2 and 3, while the corresponding predictor for scale/shape is simply the constant. Both predictors in models M3, M4, M7 and M8 correspond to Equations 2 and 3.

Concerning to (A), model specifications widely favour the gamma over the log-normal distribution. In fact DIC scores are lower under the gamma assumption, with approximately 100 scores of difference between analogous models (i.e. same variables specified in the predictors). The benefit in assuming the gamma distribution is also evident comparing MSEF scores (lower scores for better predictions). Nevertheless, results of log-normal models' MSEF is not entirely satisfactory, because when accounting for both predictors MSEF should behave as in the gamma models, i.e. lower scores than accounting only for the predictor  $\eta_{\mu}$ . Regarding to the estimation of both predictors for first and second parameters (B), models under the gamma assumption show an improvement when explicitly modelling the dependence of second parameter  $\sigma$  from explanatory variables in both DIC and MSEF scores (both decrease). Contrariwise, under the log-normal assumption, however the DIC decreases, the MSEF increases and presents higher variance, suggesting worse predictions, when the second parameter is explicitly modelled. But as discussed few lines above, that is not realistic and follows a strange behaviour of  $\eta_{\sigma}$ , thus, we still working on this point. Finally no notable leaps have been observed between fixed and random effects models (C). Whereby the best DIC and MSEF scores and QQplots lead to the final model with predictors given in (3).

According to the DIC (Table 2) the model that better fits the data is the gamma model M8 whose predictors are given in Equation 3 specifying catching units as random effects.

The boxplots of MSEFs also favour the gamma assumption (see Figure 1 and values in Table 2). The minor MSEF better the prediction, MSEF results divide models into three distinguishable groups from highest to lowest mean MSEF: 1) log-normal models considering heteroscedasticity, 2) log-normal models considering constant variance (compare M1-M2 with M3-M4), and 3) all gamma models (compare M1-M4 with M5-M8). Within this group, modelling the shape in dependence to some variables, consistently decreases MSEF estimates, in terms of average and variance (compare M5-M6 with M7-M8).

In order to validate the distribution assumptions, QQplots for residuals are reported in Figure 2, from which it follows that:

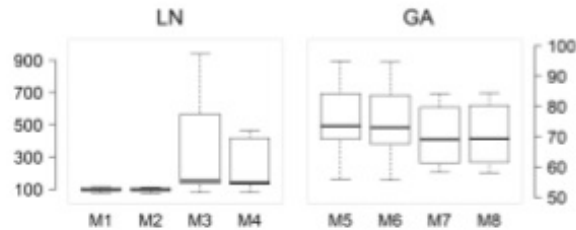


Figure 1: Boxplots for MSEP calculated for all models. See Table 2 and Equations in the text for model specifications.

- the residuals in gamma models almost follow the straight line (M5-M8 in the Figure), while in the log-normal they show upward-humped curves (M1-M4), suggesting a definitively “better approximation” of models to the gamma distribution.
- Modelling the second parameter in gamma models improves QQplot outputs, while the opposite happens for log-normal models. Focusing only in gamma models, the outlier is “absorbed” into the straight line in the right part validating the improvement in estimations (compare M5-M6 and M7-M8 in Figure 2).

We finally assess the normality for random effects for the model M8 corresponding to Equation 3. Figure 4.1 provides the QQplots of the random effects for both predictors. The majority of sample quantiles approximatively follow the normal quantiles, however they depart from it at the extremes, especially evident in the lower tails and for  $\alpha_{\mu}$  (on the left).

#### 4.2 Description of partial effects

Estimations of linear fixed effects for A)  $\mu$  and B)  $\sigma$  predictors of final model (3), to which we referred in the text as M8, are reported in table 3.

Table 3: Estimations of linear fixed effects for the final model, Eq. (3) associated to A)  $\mu$  and B)  $\sigma$  respectively.

	A)		B)	
	mean	sd	mean	sd
<i>const</i>	2.891	0.058	-1.551	0.099
<i>period<sub>2</sub></i>	-0.153	0.024		

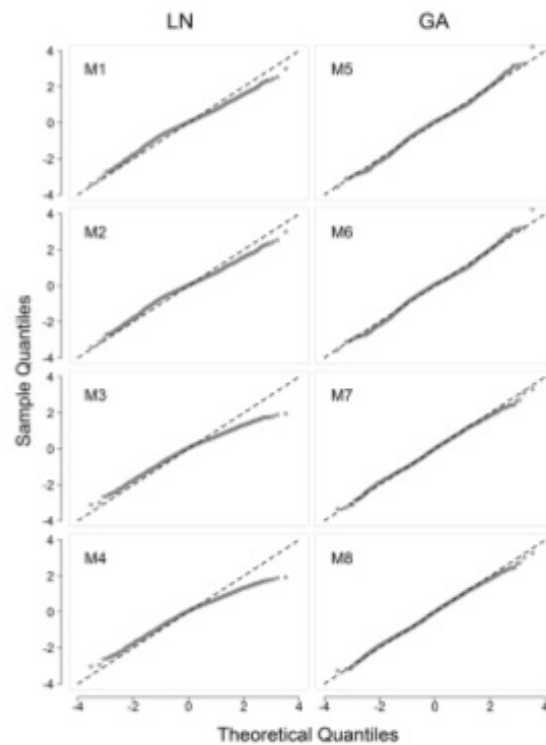


Figure 2: Q-Qplots of residuals for selected log-normal and gamma models.

The categorical variable *period* describes the intra-annual variability and shows a negative effect during *period<sub>2</sub>*, corresponding to June and November in comparison to the rest of the year. That should be related to a lower demand of this source during these months, as suggested by Sarda et al. (1997).

The variable *grt*, referring to the gross registered tonnage of boats, (not incorporated into the model because did not improve the DIC score) bears a significantly positive slope parameter ( $0.009 \pm 0.003$  when included), causes a linear increment on the predictor for location. We consider important to quantify its effect in order to compare



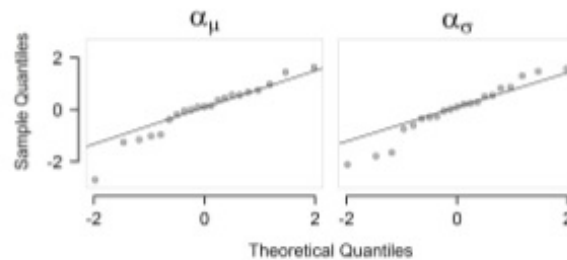


Figure 3: QQplots for normality of catching units as random effects in the mixed model MR.  $\alpha_\mu$  refer to random effects in the predictor for location, while  $\alpha_\sigma$  refers to the predictor for the shape.

it with other fisheries, where, contrarily, it could have a major effect. *grt* is not the only variable characterising a fleet, nevertheless is the only reliable for this fishery.

The second variable we can consider as fishery-related variable is represented by the catching units. Variable *code* captures all abilities of fishermen and technical characteristics of the fleet, appropriate technologies and strategies, e.g. the power and type of the engine, the net shape and the skipper's expertise and ability. Results (Figure ??) show that many trawlers have similar effects, while few of them hold or positive either negative effects. The former are very specialised and powerful boats that capture large amounts of the resource so then that leads to higher values of LPUE while the latter are not specialised trawlers that accordingly capture lower amounts, leading to lower LPUE (see the partial effects on  $\mu$ ). At the same time catching units associated to higher effects on the predictor of  $\mu$  also present higher effects on the predictor for  $\sigma$ , while boats associated to lower effects on  $\mu$  also hold lower effects on  $\sigma$ . In other words, more specialised catching units are able to capture more quantities of the resource, and they also present less variability. Contrarily landings of not specialised trawlers present more variability. This fraction of the fleet more likely is represented by boats that fish usually on the continental shelf and occasionally displace towards deeper waters going in search of the red shrimp, representing one of the most lucrative resources for the NW Mediterranean fisheries. It is likely to think that these boats have less knowledge of red shrimp fishing grounds (Maynou et al., 2003) and catch less.

Concerning to nonparametric effects (Figure 4.2), *trips* and *time* influence both  $\eta_\mu$  and  $\eta_\sigma$ , while *nao3* slightly affects only  $\eta_\mu$ .

*trips* shows a negative effect on the predictor for  $\mu$  when *trips*  $\leq$  8, while positive otherwise. The rate of the effect decreases moving through the covariate interval till rising a plateau beginning around *trips* = 17. For extreme high values this covariate has

an uncertain effect. It is plausible that increasing the number of trips per month, more likely increase the ability to find high-concentration shoals inside the fishing grounds in a process of trial and error (as suggested by Sarda and Maynou 1998).

The effect of *time* on the predictor for  $\mu$  is the most difficult to interpret, showing high inter-annual variability, certainly caused from unobservable multiple factors. Between 1992-1996, the function decreases while increases in next three years. We could not find a reasonable explanation to this trend. Afterwards, between 1999-2000, it drops till a minimum low followed by a rapid increase up to a pick in 2004. We believe that the minimum is related to both negative NAO observed in previous years and to the rising of fuel price started in 2000, that in turn is related to a lower number of trips performed by trawlers (see comments below and the discussion in Mamouridis et al., 2014). Then, for five years it presents a slightly oscillatory trend till the last year characterized by another positive pick probably related to the rise of the economic value of the resource, that offsets the increase in the fuel price.

Finally, the *nao3* has a moderate effect?? for this deep-sea species, being notoriously evident only when reaches anomalous values. Numerous studies on this and other fish stocks (e.g. Maynou, 2008; Báez et al., 2011) demonstrated that the NAO can have important effects when it reaches extreme values??, whether they are positive or negative. Our results show that *nao3* has a moderate effect?? for this deep-sea species, however they suggest that it can lead to the reduction of its biomass when reaches very negative values. Combining results of *time* and *nao3* effects and comparing data series

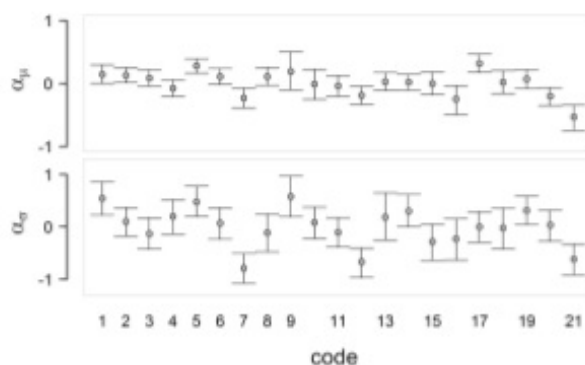


Figure 4: Interval plots of estimated random effects in the predictor for location ( $\alpha_\mu$ ) and shape ( $\alpha_\sigma$ ) of model M8 on the upper and lower plots respectively. Bars indicates 95% CI.

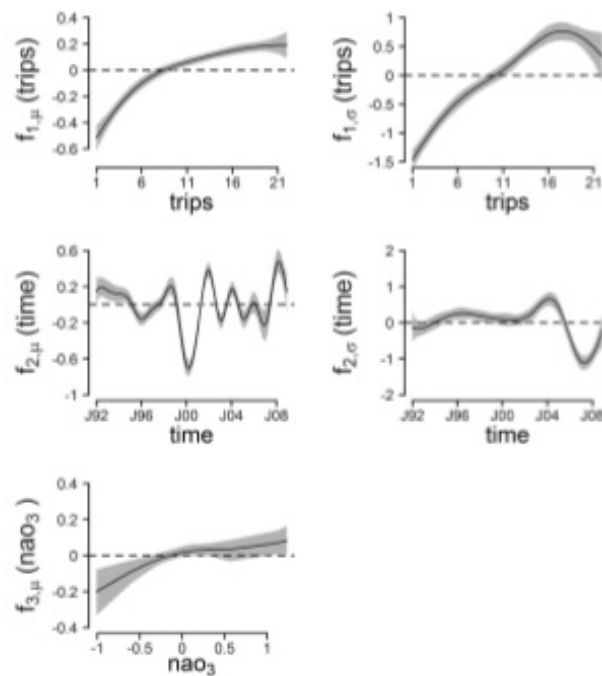


Figure 5: Nonparametric effects for the GA mixed effect of the selected gamma model (M8). Effects on predictor for  $\mu$  (left side) and for  $\sigma$  (right side). Grey shapes represent 95% credible intervals.

of both the raw (or nominal) LPUE and the NAO, we believe that the LPUE low starting at the end of 1999 can be related to consecutive negative NAO during the previous four years, especially during 1996, corresponding to three years before the beginning of the decline of LPUE ??see]] [mamouridis2014analysis. NAO leads to paucity of resources when it is low, while enhances productivity when it is high. Between  $nao_3 = 0.50$  and  $nao_3 = 1$  the effect increases however without significant evidences. In the middle region of the observed variable span, NAO shows any effect, that could represents a "buffering region" related to "normal" weather conditions for the stock.

All partial effects are linked to the expectation,  $E(LPUE)$ , through the exponential of  $\eta_{\mu}$ , such that, when partial effects of *trips*, *time* and *nao3* hire positive values,  $E(LPUE)$  is positive while negative otherwise. Regarding to the variance of LPUE, it is affected by both predictors being directly proportional to  $\mu$  and inverse proportional to  $\sigma$ .

The effect of *trips* is negative for low values of the covariate (*trips*  $\leq 10$ ) and positive for higher values. It also shows a high increment till a maximum corresponding to *trips* = 17, while decreasing again for higher values, although always positive. The effect of *time* is slightly negative before 1995 and slightly positive between 1995 and 2000. Then for two years has no effect and, in 2002, it switches clearly positive again till 2006, showing a high pick in 2004 and finally negative in the last years during 2006-2008, reaching an abrupt drop in late 2007.

Thus, regarding to the  $Var(LPUE)$ , results show that values of covariates associated to positive effects in  $\eta_{\mu}$  and negative effects in  $\eta_{\sigma}$ , in turn affect positively (increase) to the variance. We can also deduce that *time* and *trips* are drivers in causing the heteroscedasticity in LPUE, *times* mainly in last years when its effect on  $\eta_{\mu}$  is positive and its effect on  $\eta_{\sigma}$  is strongly negative. This high variability could be related to different factors, probably of economic origin, such as the fuel and ex-vessel shrimp prices.

## 5 Conclusions

In this study distributional structured additive models have been proposed for the first time to model the LPUE, index widely used in fisheries research. Data deal with the LPUE of red shrimp (*A. antennatus*) from the Barcelona's fleet during years 1992 - 2008.

Our aims were: 1) find the best distribution in relation to the response variable, comparing gamma and log-normal distributions, 2) improve estimations modelling both predictors for first and second parameter 3) compare parameter specification for catching units, fixed versus mixed effects models, and finally 4) achieve new insights in the understanding of the effect that the explanatory variables considered have on the LPUE of red shrimp.

On a methodological viewpoint, distributional structured additive models, DSTAR, as the frequentist counterpart GAMLSS, permit the estimation of both first and second order moments of the LPUE, allowing more accurate estimations and the analysis of both the expectation and the variance of the response. Results indicate that explicitly modelling the second moment in dependence to appropriate explanatory variables can lead to better estimations and predictions. We also rose a more detailed understanding of the LPUE, that bears some amount of heteroscedasticity in the time span studied. This heteroscedasticity had been observed but could not be described in previous analysis (Mamouridis et al., 2014). In fact the analysis performed on almost the same data set, a frequentist approach using GAM accounting only for the location, could not avoid the heteroscedasticity in the residuals (see Figure 4 within). Here, the modelling of the shape, in the case of the gamma assumption, permitted to infer about the variance of the

response. Here we demonstrated that both the number of trips and the time influence the second parameter leading to changes in the variance.

Concerning to fixed versus mixed specification, in our study the fixed effects can be considered appropriate representing sampling units the whole population of the studied fleet, however mixed models permit more flexibility, such as the estimation of GRT effect. Consider that mixed models also allow to get prediction for unobserved catching units and in turn to generalise predictions outside the observed fishing population.

#### Acknowledgements

Authors would like to thank the Fisheries Directorate of Catalonia's Autonomous Government to facilitate access to the sales data of the Barcelona Fishers' Association, as well as fishers of Barcelona. This study was financed by the Spanish National Council of Research (CSIC) through the IAE-produc grant program. Financial support from the German Research Foundation (DFG) grant KN 923/4-1 is gratefully acknowledged.

#### References

- J.C. Báez, J.M. Ortiz de Urbina, R. Real, and D. Macías. Cumulative effect of the north atlantic oscillation on age-class abundance of albacore (*thunnus alalunga*). *Journal of Applied Ichthyology*, 27(6):1356–1359, 2011.
- S. P. Bannerot and C. B. Austin. Using frequency distributions of catch per unit effort to measure fish-stock abundance. *Transactions of the American Fisheries Society*, 112:608–617, 1983.
- C. Bas, F. Maynou, F. Sardà, and J. Leonart. *Variacions demogràfiques a les poblacions d'espècies demersals explotades: els darrers quaranta anys a Blanes i Barcelona*. Inst. Est. Catalans. Arxiu de la Sec. Ciènc. Barcelona, 2003.
- C. Belitz, A. Brezger, T. Kneib, S. Lang, and N. Umlauf. Bayesx, 2012. - software for bayesian inference in structured additive regression models. version 2.1. available from <http://www.bayesx.org>. 2012.
- J. Bishop, W.N. Venables, and Y.-G. Wang. Analysing commercial catch and effort data from a penaeid trawl fishery: A comparison of linear models, mixed models, and generalised estimating equations approaches. *Fisheries Research*, 70(23):179 – 193, 2004. ISSN 0165-7836. doi: <http://dx.doi.org/10.1016/j.fishres.2004.08.003>. URL: <http://www.sciencedirect.com/science/article/pii/S0165783604001651>. <cc: title>Models in Fisheries Research: GLMs, {GAMS} and GLMMs</cc: title>.
- A. Brezger and S. Lang. Generalized structured additive regression based on bayesian p-splines. *Computational Statistics & Data Analysis*, 50(4):967 – 991, 2006.
- J. Brynjarsdóttir and G. Stefánsson. Analysis of cod catch data from icelandic ground-fish surveys using generalized linear models. *Fisheries Research*, 70(23):195 – 208, 2004. ISSN 0165-7836. doi: <http://dx.doi.org/10.1016/j.fishres.2004.08.004>. URL: <http://www.sciencedirect.com/science/article/pii/S0165783604001663>.

- A. Carbonell, M. Carbonell, M. Demestre, A. Grau, and S. Monserrat. The red shrimp *Aristeus antennatus* (risso, 1816) fishery and biology in the balearic islands, western mediterranean. *Fisheries Research*, 44(1):1–13, 1999.
- A. B. Cooper, A. Rosenberg, G. Stefansson, and M. Mangel. Examining the importance of consistency in multi-vessel trawl survey design based on the U.S. west coast groundfish bottom trawl survey. *Fisheries Research*, 70(2-3):239–250, December 2004. ISSN 01657836. doi: 10.1016/j.fishres.2004.08.006. URL: <http://linkinghub.elsevier.com/retrieve/pii/S0165783604001699>.
- D. Damalas, P. Megalofonou, and M. Apostolopoulou. Environmental, spatial, temporal and operational effects on swordfish (*Xiphias gladius*) catch rates of eastern Mediterranean Sea longline fisheries. *Fisheries Research*, 84(2):233–246, April 2007. ISSN 01657836. doi: 10.1016/j.fishres.2006.11.001. URL: <http://linkinghub.elsevier.com/retrieve/pii/S0165783606003846>.
- V. Denis. Spatio-temporal analysis of commercial trawler data using General Additive models: patterns of Loliginid squid abundance in the north-east Atlantic. *ICES Journal of Marine Science*, 59(3):633–648, June 2002. ISSN 10543139. doi: 10.1006/jmsc.2001.1178. URL: <http://icesjms.oxfordjournals.org/cgi/doi/10.1006/jmsc.2001.1178>.
- P. H. C. Eilers and B. D. Marx. Flexible smoothing with  $b$ -splines and penalties. *Statistical Science*, 11(2):89–102, 1996.
- L. Fahrmeir, T. Kneib, and S. Lang. Penalized structured additive regression for space-time data: a bayesian perspective. *Statistica Sinica*, 14(3):731–762, 2004.
- FAO/FISHSTAT. Fao fisheries department, fishery information, data and statistics unit. fishstatj, a tool for fishery statistical analysis, release 2.0.0, 2011.
- S. Gavaris. Use of a multiplicative model to estimate catch rate and effort from commercial data. *Canadian Journal of Fisheries and Aquatic Sciences*, 37(12):2272–2275, 1980. doi: 10.1139/f80-273. URL: <http://www.nrcresearchpress.com/doi/abs/10.1139/f80-273>.
- R. Gotti, F. Alvarez, and S. Adlerstein. Application of generalized linear modeling to catch rate analysis of western mediterranean fisheries: the castellón trawl fleet as a case study. *Fisheries Research*, 42(3):291 – 302, 1999. ISSN 0165-7836. doi: [http://dx.doi.org/10.1016/S0165-7836\(99\)00039-9](http://dx.doi.org/10.1016/S0165-7836(99)00039-9). URL: <http://www.sciencedirect.com/science/article/pii/S0165783699000399>.
- J. A. Gulland. Catch per unit effort as a measure of abundance. *Rapp. P.-V. Reun., Comm. Int. Explor. Mer Mediter.*, 155:8 – 14, 1964.
- T. Hastie and R. Tibshirani. Generalized additive models. *Statistical science*, pages 297–310, 1986.

- G. Heller, Stasinopoulos D. M., and Rigby R. A. The zero-adjusted inverse Gaussian distribution as a model for insurance data. In J. Newell J. Hinde, J. Einbeck, editor, *Proceedings of the 21th International Workshop on Statistical Modelling*, 2006.
- T. E. Helsler, A. E. Punt, and R. D. Methot. A generalized linear mixed model analysis of a multi-vessel fishery resource survey. *Fisheries Research*, 70(23):251 – 264, 2004. ISSN 0165-7836. doi: <http://dx.doi.org/10.1016/j.fishres.2004.08.007>. URL <http://www.sciencedirect.com/science/article/pii/S0165783604001705>.
- E. E. Kammann and M. P. Wand. Geostatistical models. *Journal of the Royal Statistical Society: Series C (Applied Statistics)*, 52(1):1–18, 2003.
- N. Klein, M. Denuit, T. Kneib, and S. Lang. Nonlife ratemaking and risk management with bayesian additive model for location scale and shape. Technical report, 2013a. URL <http://www.wiwi.wu.ac.at/sopec2/sopec/inn/wpaper/2013-24.pdf>.
- N. Klein, T. Kneib, and S. Lang. Bayesian structured additive distributional regression. Technical report, 2013b. URL <http://www.wiwi.wu.ac.at/sopec2/sopec/inn/wpaper/2013-23.pdf>.
- S. Lang and A. Brezger. Bayesian p-splines. *Journal of Computational and Graphical Statistics*, 13(1):183–212, 2004.
- X. Lin and D. Zhang. Inference in generalized additive mixed models by using smoothing splines. *Journal of the Royal Statistical Society: Series B (Statistical Methodology)*, 61(2):381–400, 1999. ISSN 1467-9868. doi: 10.1111/1467-9868.00183. URL <http://dx.doi.org/10.1111/1467-9868.00183>.
- V. Mamouridis, F. Maynou, and G. Anetres Pérez. Analysis and standardization of landings per unit effort of red shrimp *Aristeus antennatus* from the trawl fleet of barcelona (nw mediterranean). *Scientia Marina*, 78:INSERT, 2014. doi: 10.3989/scimar.03926.14A.
- P. Marchal, C. Ulrich, K. Korsbrekke, M. Pastoors, and B. Rackham. A comparison of three indices of fishing power on some demersal fisheries of the north sea. *ICES Journal of Marine Science: Journal du Conseil*, 59(3):604–623, 2002. doi: 10.1006/jmsc.2002.1215. URL <http://icesjms.oxfordjournals.org/content/59/3/604.abstract>.
- P. Marchal, Bo A., B. Caillart, O. Elgaard, O. Guyader, H. Hovgaard, A. Irtondo, F. Le Fur, J. Sacchi, and M. Santurtún. Impact of technological creep on fishing effort and fishing mortality, for a selection of european fleets. *ICES Journal of Marine Science: Journal du Conseil*, 64(1):192–209, 2007.
- M. N. Maunder, J. R. Sibert, A. Fonteneau, J. Hampton, P. Kleiber, and S. J. Harley. Interpreting catch per unit effort data to assess the status of individual stocks and communities. *ICES Journal of Marine Science: Journal du Conseil*, 63(8):1373–1385, 2006. doi: 10.1016/j.icesjms.2006.05.008. URL <http://icesjms.oxfordjournals.org/content/63/8/1373.abstract>.

- F. Maynou. Environmental causes of the fluctuations of red shrimp (*Aristeus antennatus*) landings in the Catalan Sea. *Journal of Marine Systems*, 71(3-4):294–302, June 2008. ISSN 09247963. doi: 10.1016/j.jmarsys.2006.09.008. URL <http://linkinghub.elsevier.com/retrieve/pii/S0924796307001935>.
- F. Maynou, M. Demestre, and P. Sanchez. Analysis of catch per unit effort by multivariate analysis and generalised linear models for deep-water crustacean fisheries off barcelona (nw mediterranean). *Fisheries Research*, 65(1-3):257–269, December 2003. ISSN 01657836. doi: 10.1016/j.fishres.2003.09.018. URL <http://linkinghub.elsevier.com/retrieve/pii/S0165783603002479>.
- P. McCullagh and J.A. Nelder. *Generalized Linear Models*. Chapman & Hall, London, 1989.
- R. Mendelssohn and P. Cury. Temporal and spatial dynamics of a coastal pelagic species, sardinella maderensis off the ivory coast. *Canadian Journal of Fisheries and Aquatic Sciences*, 46(10):1686–1697, 1989. doi: 10.1139/f89-214. URL <http://www.nrcresearchpress.com/doi/abs/10.1139/f89-214>.
- R. A. Myers and P. Pepin. The robustness of lognormal-based estimators of abundance. *Biometrics*, pages 1185–1192, 1990.
- M. Pennington. Efficient estimators of abundance, for fish and plankton surveys. *Biometrics*, 39(1):281–286, 1983.
- J. C. Pinheiro and D. M. Bates. *Mixed Effects Models in S and S-PLUS*. 2000.
- R. A. Rigby and D. M. Stasinopoulos. Generalized additive models for location, scale and shape. *Journal of the Royal Statistical Society: Series C (Applied Statistics)*, 54(3):507–554, 2005. ISSN 1467-9876. doi: 10.1111/j.1467-9876.2005.00510.x. URL <http://dx.doi.org/10.1111/j.1467-9876.2005.00510.x>.
- D. Ruppert, M. P. Wand, and R. A. Carroll. *Semiparametric regression Vol. 12*. Cambridge University Press, 2003.
- F. Sarlà and F. Maynou. Assessing perceptions: do catalan fishermen catch more shrimp on fridays? *Fisheries Research*, 36:149157, 1998.
- F. Sarlà, F. Maynou, and L. Talló. Seasonal and spatial mobility patterns of rose shrimps *Aristeus antennatus* in the western mediterranean: results of a long-term study. *Marine Ecology Progress Series*, 159:133141, 1997.
- D. J. Spiegelhalter, N. G. Best, B. P. Carlin, and A. van der Linde. Bayesian measures of model complexity and fit. *Journal of the Royal Statistical Society: Series B (Statistical Methodology)*, 64(4):583–639, 2002.
- D. M. Stasinopoulos and R. A. Rigby. Generalized additive models for location scale and shape (gamlss) in r. *Journal of Statistical Software*, 23(7):1–46, 2007.



- G. Stefánsson. Analysis of groundfish survey abundance data: combining the glm and delta approaches. *ICES Journal of Marine Science: Journal du Conseil*, 53(3):577–588, 1996. doi: 10.1006/jmsc.1996.0079. URL: <http://icesjms.oxfordjournals.org/abstract/53/3/577>.
- G. Stefánsson and O. K. Palsson. Points of view: A framework for multispecies modelling of arcto-boreal systems. *Reviews in Fish Biology and Fisheries*, 8:101–104, 1998.
- S. Tudela, F. Maynou, and M. Demestre. Influence of submarine canyons on the distribution of the deep-water shrimp, *aristeus antennatus* (risso, 1816) in the nw mediterranean. *Crustaceana*, 7(2):217225, 1998.
- W. N. Venables and C. M. Rippon. Glims, gams and glmms: an overview of theory for applications in fisheries research. *Fisheries research*, 70(2):319–337, 2004.
- S. Wood. *Generalized Additive Models: an introduction with R*. CRC Press, 2006.

ATTENTION ;  
Pages 324 to 337 of the thesis are available at the editor's  
web

- J.E. Cartes, C. Lolocono, V. Mamouridis, C. López-Pérez, P. Rodríguez.  
*Geomorphological, trophic and human influences on the bamboo coral  
Isidella elongata assemblages in the deep Mediterranean: To what extent  
does Isidella form habitat for fish and invertebrates?* Deep Sea Research Part  
I: Oceanographic Research Papers Volume 76, June 2013, Pages 52-65  
<http://www.sciencedirect.com/science/article/pii/S0967063713000265?via%3Dihub>  
DOI <https://doi.org/10.1016/j.dsr.2013.01.006>

SCIENTIA MARINA 78(1)  
March 2014, 000-000, Barcelona (Spain)  
ISSN-I: 0214-8358  
doi: <http://dx.doi.org/10.3989/scimar.03926.14A>

## Analysis and standardization of landings per unit effort of red shrimp *Aristeus antennatus* from the trawl fleet of Barcelona (NW Mediterranean)

Valeria Mamouridis<sup>1</sup>, Francesc Maynou<sup>1</sup>, Germán Aneiros Pérez<sup>2</sup>

<sup>1</sup>Institut de Ciències del Mar, CSIC, Psg. Marítim de la Barceloneta 37-49, 08003 Barcelona, Spain.  
E-mail: [mamouridis@icm.csic.es](mailto:mamouridis@icm.csic.es)

<sup>2</sup>Facultade de Informática, Campus de Elviña s/n, Universidade da Coruña, 15071 A Coruña, Spain.

**Summary:** Monthly landings and effort data from the Barcelona trawl fleet (NW Mediterranean) were selected to analyse and standardize the landings per unit effort (LPUE) of the red shrimp (*Aristeus antennatus*) using generalized additive models. The dataset covers a span of 15 years (1994-2008) and consists of a broad spectrum of predictors: fleet-dependent (e.g. number of trips performed by vessels and their technical characteristics, such as the gross registered tonnage), temporal (inter- and intra-annual variability), environmental (North Atlantic Oscillation [NAO] index) and economic (red shrimp and fuel prices) variables. All predictors individually have an impact on LPUE, though some of them lose their predictive power when considered jointly. This is the case of the NAO index. Our results show that six variables from the whole set can be incorporated into a global model with a total explained deviance (ED) of 43%. We found that the most important variables were effort-related predictors (trips, tonnage, and groups) with a total ED of 20.58%, followed by temporal variables, with an ED of 13.12%, and finally the red shrimp price as an economic predictor with an ED of 9.30%. Taken individually, the main contributing variable was the inter-annual variability (ED=12.40%). This high ED value suggests that many factors correlated with inter-annual variability, such as environmental factors (the NAO in specific years) and fuel price, could in turn affect LPUE variability. The standardized LPUE index with the effort variability removed was found to be similar to the fishery-independent abundance index derived from the MEDITS programme.

**Keywords:** LPUE; standardized LPUE; *Aristeus antennatus*; generalized additive models; NW Mediterranean; deep-water fisheries.

**Análisis y estandarización de los desembarcos por unidad de esfuerzo de la gamba roja *Aristeus antennatus* por la flota de arrastre de Barcelona (Mediterráneo noroccidental)**

**Resumen:** Se llevó a cabo un análisis del volumen de desembarcos por unidad de esfuerzo (LPUE) de la gamba roja (*Aristeus antennatus*) de la flota de arrastre en el puerto de Barcelona (Mediterráneo noroccidental) mediante modelos aditivos generalizados (GAM). El conjunto de datos cubre un periodo de 15 años (1994-2008) y consiste en un amplio espectro de predictores: variables dependientes de la flota (el número de mareas efectuadas por cada embarcación y las características técnicas de estas, como el tonelaje bruto), temporales (variabilidad inter- e intra-anual), ambientales (índice de Oscilación del Atlántico Norte [NAO]) y económicas (precio de la gamba roja y precio del combustible). Todos los predictores a nivel individual tienen impacto sobre LPUE, pero algunos de ellos pierden su poder explicativo cuando se consideran conjuntamente con otros, como en el caso del índice NAO. Nuestros resultados muestran que seis variables del conjunto pueden incorporarse en un modelo global con una desviación total explicada ED=43%. Las variables más importantes fueron aquellas relacionadas con el esfuerzo (número de mareas, tonelaje y grupos), con devianza ED=20.58%, después las variables temporales, las cuales presentaron ED=13.12%, y finalmente los predictores económicos representados por el precio de la gamba con ED=9.30%. A nivel individual, la variable con mayor contribución es la variabilidad inter-anual (ED=12.40%). Este elevado valor de devianza sugiere que muchos factores correlacionados con el tiempo pueden afectar la variabilidad de LPUE, como los factores ambientales (NAO en años particulares) y económicos, como el precio del combustible. La estandarización de LPUE con respecto al esfuerzo proporciona un índice de abundancia de la gamba roja muy parecido al índice de abundancia independiente de la pesquería obtenido mediante el programa de campañas experimentales MEDITS.

**Palabras clave:** LPUE; LPUE estandarizada; *Aristeus antennatus*; modelos aditivos generalizados; Mediterráneo noroccidental; pesquerías de profundidad.

**Citation/Como citar este artículo:** Mamouridis V., Maynou F., Aneiros Pérez G. 2014. Analysis and standardization of landings per unit effort of red shrimp *Aristeus antennatus* from the trawl fleet of Barcelona (NW Mediterranean). *Sci. Mar.* 78(1): 000-000. doi: <http://dx.doi.org/10.3989/scimar.03926.14A>

Editor: C. Frogia

Received: July 23, 2013. Accepted: December 10, 2013. Published: March 7, 2014.

Copyright: © 2014 CSIC. This is an open-access article distributed under the Creative Commons Attribution-Non Commercial License (by-nc) Spain 3.0.

2 • V. Mamouridis et al.

## INTRODUCTION

Deep-water red shrimp is one of the main resources in Mediterranean fisheries in terms of landings and economic value (Bas et al. 2003), primarily in Spain and Algeria, where catches reach more than 1000 t year<sup>-1</sup> (FAO-FISHSTAT 2011). In the Mediterranean Sea, two red shrimp species, *Aristeus antennatus* and *Aristaeomorpha foliacea*, are caught by specialized trawl fleets operating on the upper and middle continental slope. The distribution of these two species varies geographically and in the NW Mediterranean catches are composed exclusively of *A. antennatus* (Bas et al. 2003).

The deep-water distribution of stocks extends to below 2000 m depth (Cartes and Sardà 1992) but commercial trawlers fish from 400 to 900 m depth. The red shrimp life-cycle includes seasonal, bathymetric and spatial migrations of different fractions of the population with great size and sex segregation: juveniles and small-sized males are more abundant in autumn and early winter in submarine canyons, while reproductive females concentrate on the open slope fishing grounds in late winter and spring (Sardà et al. 1997). This complex life cycle, coupled with a relatively long life span (more than 10 years according to Orsi Relini 2013) differentiates this species from tropical coastal shrimp resources elsewhere (Neal and Maris 1985).

The catches of *A. antennatus* show inter-annual fluctuations that have been related to environmental factors determining strong recruitment (Carbonell et al. 1999, Maynou 2008). Maynou (2008) suggested that winter NAO (North Atlantic Oscillation) is positively correlated with landings of *A. antennatus* two to three years later and that enhanced trophic resources for maturing females in winter and early spring result in stronger recruitments. The NAO has been demonstrated to be a pervasive environmental driver in other marine stocks elsewhere in the Mediterranean and Atlantic (e.g. Brodziak and O'Brien 2005, Dennard et al. 2010). However, the effect of technical and economic variables has received less attention. For instance, in the red shrimp fishery of the NW Mediterranean, Maynou et al. (2003) showed the importance of individual fisher behaviour in determining catch rates, and Sardà and Maynou (1998) discuss the effect of prices on changes of daily fishing effort targeting this species. Intra-annual variability in landings has been linked to market-driven variations in prices, which may result in changes in the fishing effort applied to the stocks, as the trawl fleet moves to alternative resources (Sardà et al. 1997).

Despite the commercial importance of *A. antennatus* in the Mediterranean (Sardà et al. 1997), deriving standardized catches or landings per unit effort (CPUE or LPUE) is not straightforward because of the lack of reliable time series at regional or sub-regional level (Leonart and Maynou 2003). In fact, determining the abundance of marine stocks is notoriously a widespread problem (Hilborn and Walters 1992). Methodologies basically rely on two different data sources: fisheries-dependent or fisheries-

independent data. Fisheries-dependent data tend to be the preferred source to assess the status of marine stocks (Lassen and Medley 2000) but since the applicability of these traditional assessment methods is limited when it comes to crustaceans, fisheries-independent methods are usually preferred. However, fisheries-independent experimental trawl surveys in the western Mediterranean (Mediterranean International Trawl Surveys: MEDITS, Bertrand et al. 2002) are also problematic because they only partially cover the distribution depth range of *A. antennatus*. Thus, fisheries-dependent data are indeed used but methods that require age data are avoided and instead only regression style methods are used. For instance, in the Spanish Mediterranean sub-area 6 (ca. 1000 km long) just 4 to 12 trawl hauls are carried out annually in the 500-800 m depth stratum and none any deeper (Cardinale et al. 2012). Additionally, obtaining reliable landings including age information is problematic owing to difficulties in determining age in crustaceans (Orsi Relini et al. 2013). In these cases the information collected by a fishery is the main source of abundance data available (Maunder et al. 2006) and, when appropriately standardized, can be used to produce series of population abundance that should help fishery managers to promote the sustainable production of marine stocks.

Here, we evaluate the landings per unit effort from the daily sale slips provided by the Barcelona Fishers' Association from 1994 to 2008, corresponding to all the commercial transactions involving *A. antennatus* by a total of 21 trawlers operating on continental slope fishing grounds. The landings of *A. antennatus* have varied by almost an order of magnitude in this area in the last ten years, from a historical low of 13 t year<sup>-1</sup> in 2006 to 96 t year<sup>-1</sup> in 2012. Considering that the average ex-vessel price of the species in this period was 36 € kg<sup>-1</sup> (among the highest seafood prices in Europe), these inter-annual fluctuations in landings have important economic consequences. Fisheries in Spanish Mediterranean waters are allowed between 50 and 1000 m depth for a maximum of 12 hours per day during daytime, except weekends. Hence, trawl skippers must decide which fishing grounds to visit taking into account that on the continental shelf they can be reached in a shorter time but will produce relatively cheap finfish, whereas deep-water fishing produces more valuable red shrimp but entails high economic costs and the risk of losing or damaging fishing gear.

The main objective of this study was to establish the factors influencing the LPUE (see e.g. Denis et al. 2002 for terminology) of *A. antennatus* in order to evaluate their relative importance (fishery-related, economic and environmental), which can be considered to manage effort constraints and to obtain a standardized series of LPUE as a reliable relative abundance index to assess natural abundance. We used generalized additive models (GAMs: Hastie and Tibshirani 1990) to capture the possible nonlinear dependence of LPUE on explanatory variables (Su et al. 2008, among others).

## MATERIALS AND METHODS

## Data source

Trawlers from the Barcelona port operate on the continental shelf and slope fishing grounds (50-1000 m depth) located between 1°50' and 2°50' longitude east and 40°50' and 41°30' latitude north (Sardà et al. 1997). The fleet operates on a daily basis (with mandatory exit from port after 6 am and return to port before 6 pm) and a limited license system whereby total effort in the area has been frozen since 1986. New boats are only permitted if an existing boat is decommissioned. In addition to effort control, the only other measure of control is limiting mesh sizes (minimum 40 mm cod-end stretch mesh size) and neither in the study area nor in any other Mediterranean areas is there output control. Fish is auctioned daily at the premises of the port fish market and all transactions are recorded electronically for statistical purposes by the Barcelona Fishers' Association.

We used the daily sale slips containing all transactions of red shrimp (*A. antennatus*) over the period 1994-2008 to calculate the total monthly landings (kg month<sup>-1</sup>, *lands*), the effort measured as total number of trips performed monthly by each vessel (number of trips per month, *trips*), and the monthly average ex-vessel shrimp price (€ kg<sup>-1</sup>, *shprice*). The same data set contained information on the engine power (horse power, *hp*) and gross registered tonnage (tons, *grt*), which we used as boat capacity indicators. As an indicator of fishing costs we used the average monthly fuel price (10<sup>-3</sup>€ L<sup>-1</sup>, *fprice*) from the EUROSTAT website: [http://ec.europa.eu/energy/observatory/oil/bulletin\\_en.htm](http://ec.europa.eu/energy/observatory/oil/bulletin_en.htm). As the environmental driver we used the NAO index, taken from the website of the Climate Analysis Group of the University of Exeter (UK): <http://www1.secum.ex.ac.uk/cat/NAO>. We considered: *nao1*, *nao2* and *nao3*, corresponding to one, two and three years before the year of observed landings, using the significant time lags reported in Maynou (2008).

The response variable, *lpue*, was estimated as

$$lpue = \frac{lands}{trips} \quad (1)$$

hence, *lpue* is the monthly average landings of one vessel in each trip, corresponding to one fishing day (kg boat<sup>-1</sup> day<sup>-1</sup>), which will form the basis for providing a standardized abundance index.

To assess the individual effect of each vessel, a numeric variable *code* was assigned to each of the 21 vessels in the fleet. Each observation was attributed to a sequential *time* variable from January 1994 to December 2008 (180 months) and a *month* variable describing the month of the year. Two more variables were derived a posteriori from *code* and *month*, after checking for statistical differences among their categories in the model, and then by performing the Tukey Honest Significant Differences test (TukeyHSD). We thus derived the new variables, *group* and *period*, for *code* and *month*, respectively. The *group* variable combines the 21 trawlers into three groups of increasing *lpue* and *period* is a binary variable which classifies the months in "high effect" (*period1*: all months excluding June and November) and "low effect" (*period2*: June and November). All variables are shown in Table 1.

## Model construction

We used generalized additive models, GAM, as described by Hastie and Tibshirani (1990)

$$G(y) = x\beta + \sum s_j(x_j) + \varepsilon$$

where  $G(\cdot)$  is the link function,  $y$  is the response variable,  $x$  is the vector of linear predictors (explanatory variables),  $\beta$  is the corresponding vector of parameters,  $x_j$  are scalar predictors with unknown nonlinear effects represented by the functions  $s_j(\cdot)$ , and  $\varepsilon$  is the random error.

The model building process consists of the following steps: 1) selection of the underlying distribution of the response (see Section 2.2.2 for more details); 2) selection of predictors building independent models for each covariate deleting insignificant effects in the final model; 3) selection between correlated predictors through the Pearson correlation coefficient (threshold value:  $\rho=|0.6|$ ) to avoid problems of collinearity (Brauner and Shacham 1998) using the covariant with the most explanatory potential; and 4) analysis of residuals diagnostics.

Table 1. – List of variables.

Variable	description (units)
<i>lpue</i>	landings per unit effort derived from <i>lands</i> and <i>trips</i> (kg boat <sup>-1</sup> day <sup>-1</sup> )
<i>lands</i>	total monthly landings per vessel (kg month <sup>-1</sup> )
<i>time</i>	time index of months, $t=1, \dots, 180$ , from Jan 1994 to Dec 2008
<i>trips</i>	number of trips performed by each vessel during the time $t$
<i>hp</i>	engine power of vessels
<i>grt</i>	gross registered tonnage of vessels
<i>shprice</i>	red shrimp ex-vessel price (€ kg <sup>-1</sup> )
<i>fprice</i>	fuel price one month before the observed lands (10 <sup>-3</sup> € L <sup>-1</sup> )
<i>nao<sub>k</sub></i>	mean annual NAO index, $k=1, \dots, 3$ years before the year of observed lands
<i>month</i> *	12 categories corresponding to months
<i>period</i> *	2 categories: <i>period1</i> , all months excluding June and Nov; <i>period2</i> , June and Nov
<i>code</i> **	21 categories corresponding to a code assigned to each vessel
<i>group</i>	3 categories corresponding to groups of vessel

\* Differences between pairs of categories of the variable *month* were checked through Tukey HSD test. Non-significantly different categories were grouped to create the new variable *period*, to which the same test was applied.

\*\* The same procedure was applied for the variable *code*, to create the variable *group* (all significant tests with  $p<0.001$ ).

4 • V. Mamanouridis et al.

All analyses were performed in R3.0.1 (mgcv-Rpackage: Wood 2006). The generalized cross validation (GCV: Craven and Wahba 1979) and the outer Newton iteration procedure were used to estimate model parameters. GCV is preferable to the UBRH/AIC method in the case of unknown smoothing parameters  $\lambda$  (Wood 2006). Second order  $P$ -spline as defined by Marx and Eilers (1998) was used as a smoother for nonlinear functions.

#### Theoretical response probability function

Landings per unit effort are usually modelled following Gaussian or gamma distribution functions, often without formal justifications (Stefánsson 1996). Here, we assigned a theoretical probability function to the  $lpue$ , using nonparametric techniques described by Wassermann (2005). The density function,  $f(y_n)$ , was estimated using a histogram and the Gaussian kernel, where the *nrd* described by Scott 1992 was the rule-of-thumb used to select the bandwidth.

The empirical cumulative distribution function,  $F(y_n)$ , and the 95% lower,  $L(y_n)$  and upper,  $U(y_n)$ , confidence intervals were calculated as follows:

$$F(y_n) = [\text{rank}(y_n) - 0.5] / N$$

$$L(y_n) = \max\{F(y_n) - \epsilon_n, 0\}$$

$$U(y_n) = \min\{F(y_n) + \epsilon_n, 1\},$$

where  $\text{rank}(y_n)$  is the ranked vector of observations and  $\epsilon_n$  is the associated vector of errors resulting from the DKW (Dvoretzky-Kiefer-Wolfowitz) inequality

$$\epsilon_n = \sqrt{1/2n \log_e(2/\alpha)}$$

The hypothesis tested is  $H_0: F(y_n) = F_0(y_n)$  versus the alternative hypothesis  $H_1: F(y_n) \neq F_0(y_n)$ , where  $F_0(y_n)$  is a theoretical function belonging to the exponential family, especially  $F_0(y_n) = \text{Ga}(a, b)$ , the gamma distribution, whose density function is

$$p(y) \propto y^{a-1} e^{-by}$$

for  $y > 0$ . Parameters  $a$  and  $b$  are derived from the estimated expectation,  $E(y) = a/b$ , and variance  $\text{Var}(y) = a/b^2$ . Then the resulting distribution functions were graphically compared.

#### Selection criteria and explained deviance

Both AIC (Akaike 1973) and percentage of explained deviance (ED) were used as selection criteria: the selected model presented both the lowest AIC and the highest ED and all term parameters significantly different from zero.

The ED for each variable was also calculated in order to determine their relative importance in the final model. The residual deviance of the full model and the deviances of reduced models (i.e. the model excluding variable  $x_i$ ) were calculated to derive the proportion explained by variable  $x_i$ :

$$DE(x_i) = [D(\text{reduced model}) - D(\text{full model})] / D(\text{null model})$$

where  $D(\cdot)$  is the deviance for a given model and in the reduced model variable  $x_i$  is omitted.

#### LPUE standardization

The model used for standardization was built in order to avoid dependency on fleet variables, maintaining environmental variables, which are expected to be related to the natural abundance of the species. The standardized LPUE is then

$$lpue_{st} = E(lpue) + (lpue - E(lpue)_{\theta, \lambda, \dots}) \quad (2)$$

where  $lpue$  is the “nominal” or “raw” LPUE defined in Equation 1,  $E(lpue)$  is the unconditional expectation of the LPUE and  $E(lpue)_{\theta, \lambda, \dots}$  is the conditional expectation of the LPUE given the vectors of parameters  $\theta$  and  $\lambda$  estimated using the appropriate standardization model.

Finally we compared our standardized LPUE with an alternative abundance index derived from fisheries-independent data, available in the technical report SGMED-12-11 (Cardinale et al. 2012, pp. 136-150) after normalization of both variables.

## RESULTS

### Overview of data and response distribution

Figure 1 provides the raw  $lpue$  time series as reckoned in Equation 1 with its spline estimation (upper plot) and annual average of the NAO index (lower plot). The  $lpue$  series, initially constant, started to decline at the end of 1998 with a sharp maximum low in the period 1999-2000. Then the trend changed to inter-annual variation. Conversely, the NAO index shows the lowest records in the period 1995-1996. The  $lpue$  begins to decrease after three years from the first year of negative NAO. In Figure 2 the time series of the fuel price shows an increasing trend during the observed period (upper panel). The total number of trips per month performed by the whole fleet declines during the same period (middle panel), but it declines only at the beginning of the fuel price rise, then remaining almost constant (lower panel). Low  $lpue$  in the period 2000-2001 is also related to the peak of  $fprice$  in the same period (compare upper panels of Figs 1 and 2).

Characteristics of  $lpue$  are plotted in Figure 3. The probability density function (*pdf*) is positively skewed (upper panels). Data hold atypical values in the right tail (see the box-plot, left middle panel) and the distribution function of the gamma distribution lies approximately inside the 95% confidence intervals of the empirical cumulative distribution function (*ecdf*) of  $lpue$  (right middle panel). Finally, the QQ-plots for the gamma and the Gaussian distributions provide evidence of a better fit of data to the gamma rather than the Gaussian distribution (on the left and the right lower panels respectively).

## Analysis and standardization of red shrimp LPUE (NW Mediterranean) • 5

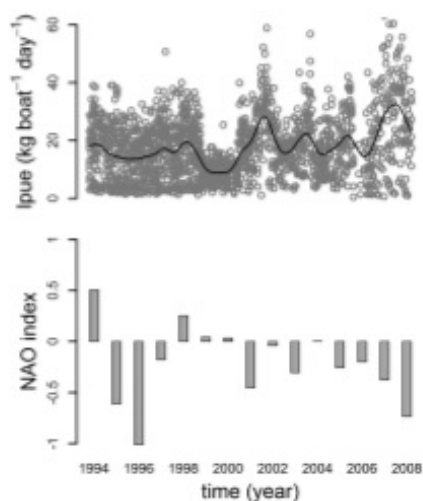


Fig. 1. – Time series from 1994 to 2008 of LPUE data and spline estimation (upper panel) and mean annual North Atlantic Oscillation (NAO) (lower panel).

#### Model building and comparison

The model building process is summarized in Table 2. All linear terms are reported before all smooth functions. Models are sorted in ascending order of total ED, with the exception of models 11 and 12, corresponding to the GLM version of the final model 7 and the standardization model respectively. In comparison with the GLM (model 11), GAM's AIC decreases and the ED increases substantially (1.56 times), though the number of degrees of freedom increases considerably ( $df_{GAM}=27.7$  versus  $df_{GLM}=9$ ). Variables *grt* and *time* were selected as better predictors than *hp* and *fprice*, respectively, according to the Pearson correlation coefficients (*grt-hp* was  $\rho=0.61$ ; *time-fprice*  $\rho=0.69$ ) and larger ED of former variables. All other correlations were  $\rho < |0.6|$ .

Table 2 incorporates the NAO terms, though their explanatory potential in the full model is too weak to be significant. Adding NAO terms to model 7 (Table 2: models 8, 9, 10) did not improve model fit in terms of ED and AIC. Nevertheless, we found significant NAO effect in less complex models.

#### The descriptive model

The final model for *A. antennatus* LPUE is

$$\log_e(lpue) = \theta + \alpha grt + \beta period2 + \sum_{k=2,3} (\gamma_k group_k) + s_1(trips) + s_2(time) + s_3(shprice) + \varepsilon \quad (3)$$

where  $lpue \sim Ga(a,b)$ ,  $\log_e$  is the link function,  $\theta$  is the intercept,  $\alpha$  is the parameter associated with the linear

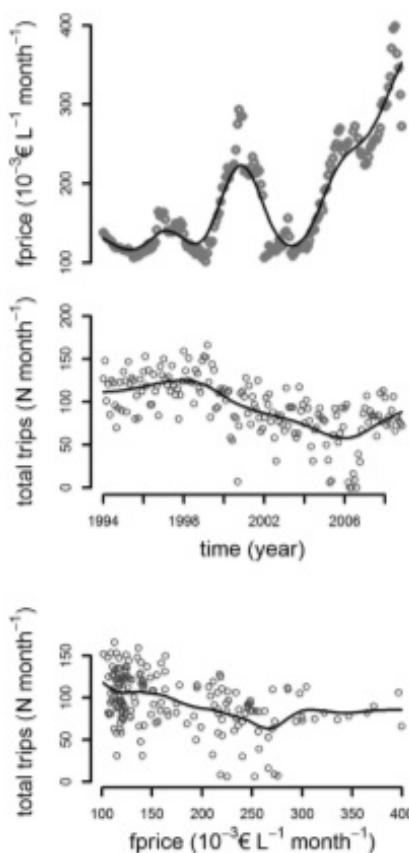


Fig. 2. – From top to bottom: spline estimation of the fuel price, monthly total number of trips performed by the fleet from year 1996 to 2008, and relationship between the fuel price and the total monthly number of trips.

effect of *grt*, and  $\beta$  and  $\gamma_k$  are the effects associated with the categorical variables *period* and *group*.  $s_j(\cdot)$  are the smooth functions associated with *trips*, *time* and *shprice*, while  $\varepsilon$  represents the random errors of the model.

Figure 4 shows the diagnostic plots for the selected model. These plots show the results for the best model (corresponding to Equation 3 in the text and model 7 in Table 2). Residual quantiles lie on the straight line of the theoretical quantiles, although slightly heavy-tailed; in the histogram, residuals are consistent with normality and the relationship between response and fitted values is linear and positive. Residuals versus the linear predictor (that is, the sum of all partial effects) show a faint heteroscedasticity.

6 • V. Mamouridis et al.

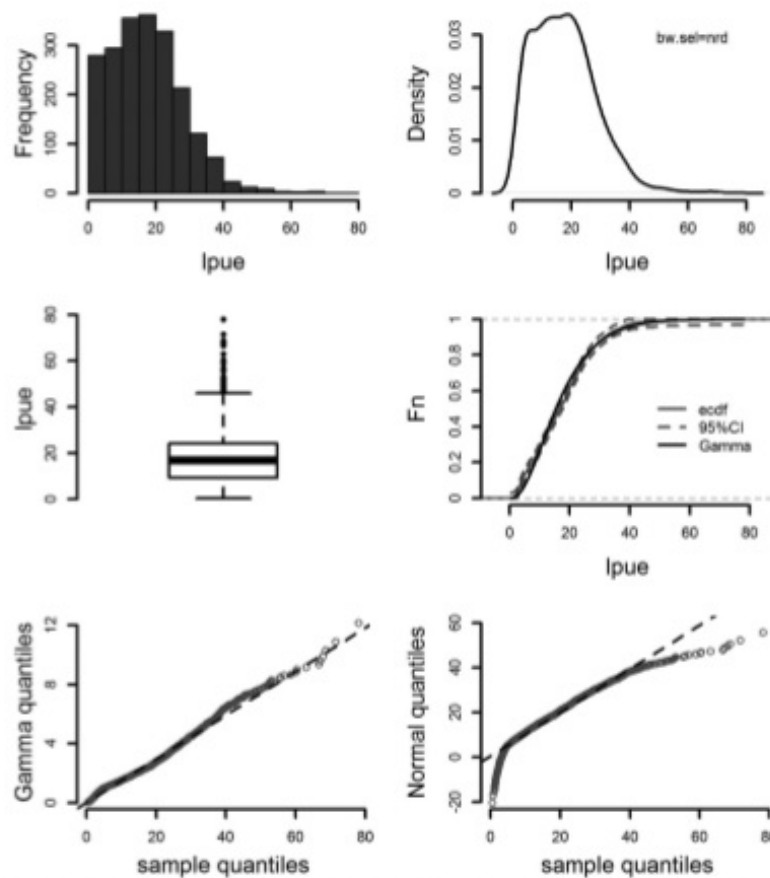


Fig 3. – From left to right, upper panels, histogram and kernel density estimations of *lpue*; middle panels, box-plot and cumulative distribution function of data and of the gamma distribution; lower panels, QQ-plots of sample quantiles versus gamma and normal distribution quantiles.

Table 2. – Model construction. *N*, number associated with each model; model, model's right part of the formula; *df*, model's degree of freedom; RD, residual deviance; ED, percentage of deviance explained by each model; AIC, Akaike Information Criterion; term<sup>ns</sup>, insignificant terms in a model; term<sup>si</sup>, terms not incorporated in next steps (i.e. models with the incorporation of *hp* or *fprice* gave a lower ED than the incorporation of *grt* and *time*, respectively). Model 12 is the model used for standardization.

<i>N</i>	model	<i>df</i>	RD	ED (%)	AIC
1	<i>Int</i>	2	863.8	0	13544
2	<i>Int+hp<sup>ns</sup></i>	3	844.4	2.2	13501
2.1	<i>Int+grt</i>	3	815.3	5.6	13432
3	<i>Int+grt+group</i>	5	741.0	14.2	13250
4	<i>Int+grt+group+period</i>	6	734.7	15	13235
5	<i>Int+grt+group+period+σ(trips)</i>	8.9	627.8	27.3	12936
6	<i>Int+grt+group+period+σ(trips)+σ(fprice)<sup>ns</sup></i>	12.4	614.0	28.9	12900
6.1	<i>Int+grt+group+period+σ(trips)+σ(time)</i>	24.8	527.0	39	12632
7	<i>Int+grt+group+period+σ(trips)+σ(time)+σ(shprice)</i>	27.7	493.5	43.0	12512
8	<i>Int+grt+group+period+σ(trips)+σ(time)+σ(shprice)+σ(nao1)<sup>ns</sup></i>	28.7	493.3	43.0	12513
9	<i>Int+grt+group+period+σ(trips)+σ(time)+σ(shprice)+σ(nao2)<sup>ns</sup></i>	28.7	493.5	43.0	12514
10	<i>Int+grt+group+period+σ(trips)+σ(time)+σ(shprice)+σ(nao3)<sup>ns</sup></i>	28.7	493.4	43.0	12513
11	<i>Int+grt+group+period+trips+time+shprice</i>	9	626.4	27.5	12932
12	<i>Int+grt+code+σ(trips)</i>	24.75	608.7	29.5	12910



Analysis and standardization of red shrimp LPUE (NW Mediterranean) • 7

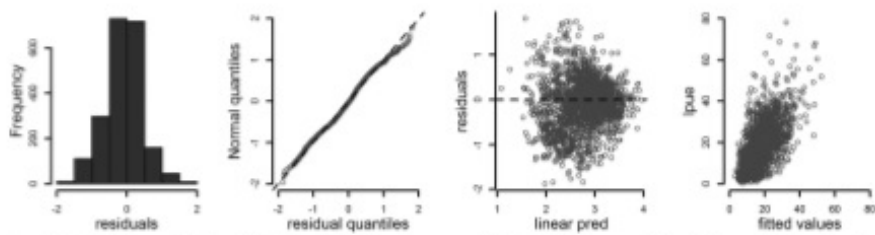


Fig. 4. – Residual diagnostics for model 7. From left to right: histogram and Q-Q plot of deviance residuals; deviance residuals against linear predictor; response against fitted values.

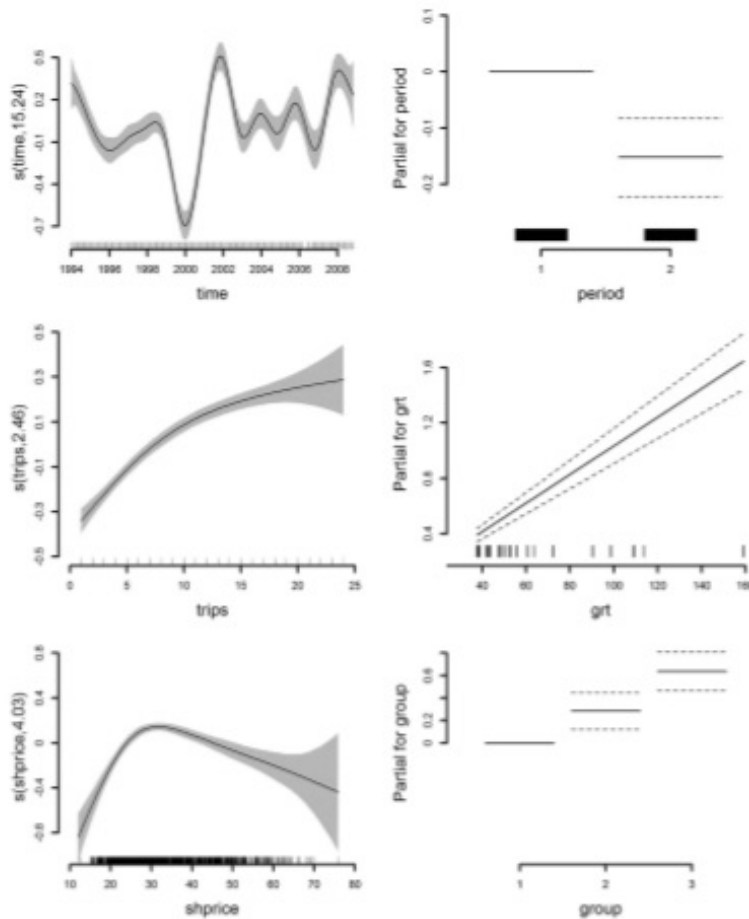


Fig. 5. – Partial effects of model 7. Bayesian credible intervals (95%).

S - V. Manouridis et al.

Table 3. Results of the final model (Eq. 3). Results associated with (a) linear terms, (b) smooth terms and (c) global estimations. Mean, estimation of the mean; *std*, standard deviation; *t*, value of *t*-statistic; *F*, the *F* statistic value; *p*, *p*-value to the *t* or the *F* statistic; ED, percentage of deviance explained by each term; *edf*, effective degrees of freedom;  $\lambda$ , estimated smoothing parameter; *df*, total degree of freedom; *sc*, the scale parameter of the regression; *R*<sup>2</sup>(adj), adjusted R-squared; AIC, Akaike Information Criterion; GCV, generalized cross validation; ED tot (%), percentage of total deviance explained by the model.

(a) Linear terms					
	mean	std	t	p	ED (%)
<i>intercept</i>	1.746	0.103	16.980	<2e-16	0
<i>period2</i>	-0.152	0.035	-4.383	1.24e-05	0.72
<i>group2</i>	0.281	0.081	3.449	5.75e-04	3.58
<i>group3</i>	0.637	0.086	7.404	2.02e-13	
<i>grt</i>	0.010	0.001	16.205	<2e-16	5.62
(b) Smooth terms					
	<i>edf</i>	$\lambda$	<i>F</i>	<i>p</i>	ED (%)
<i>s(time)</i>	15.239	0.011	24.82	<2e-16	12.40
<i>s(trips)</i>	2.457	30.007	71.01	<2e-16	11.38
<i>s(shprice)</i>	4.026	0.059	26.36	<2e-16	9.30
(c) Global					
<i>df</i>	<i>sc</i>	<i>R</i> <sup>2</sup> (adj)	AIC	GCV	ED tot (%)
27.722	0.274	0.488	12512	0.282	43.00

Table 3 shows results related to (a) the linear part, (b) the smooth functions and (c) the global parameters of the final model (Eq. 3), with a total explained deviance of 43.00%. The predictor with the highest explanatory potential was *time* (ED=12.40%), which captured the intra-annual fluctuations in red shrimp, *lpue*. The second predictor in terms of explained deviance was *trips* (ED=11.38%). Red shrimp price was the third most important predictor (ED=9.30%). Other variables such as *grt*, *group* and *period* had less impact. The model returned all significant parameters ( $p < 0.001$ ). All partial effects are reported in Figure 5. The partial effect for *time* shows a substantial difference before and after the period 1999-2000, when a clear drop is exhibited in the shape. Before this threshold the shape is almost constant, whereas after the abrupt decay increasing variation is observed over recent years. Predictor *trips* represents a positive and monotonic relationship, reaching a plateau for *trips* > 15; *shprice* reached its maximum value around 30 € kg<sup>-1</sup>; *lpue* was significantly lower for *period2*, representing June and November, than for the rest of the year (*period1*). There were significant differences between the three groups of vessels. Variable *grt* showed a positive linear effect, meaning that larger vessels had higher *lpue*.

**LPUE standardization**

The model used to standardize *A. antennatus* LPUE is

$$\log_e(lpue) = \theta + \alpha grt + \sum_{j=2,21} (\gamma_j code_j) + s(trips) + \epsilon \quad (4)$$

where *lpue* ~ *Ga*(*a, b*),  $\theta$  is the intercept,  $\alpha$  the parameter for *grt* and  $\gamma_j$  the effects associated with *code*. *s(trips)* is the smooth function for *trips* and  $\epsilon$  the random errors. With the aim of standardizing, this model comprises all fleet-dependent variables, whose effect must be removed from the nominal value. The diagnostic plots show reasonably good outputs (not shown).

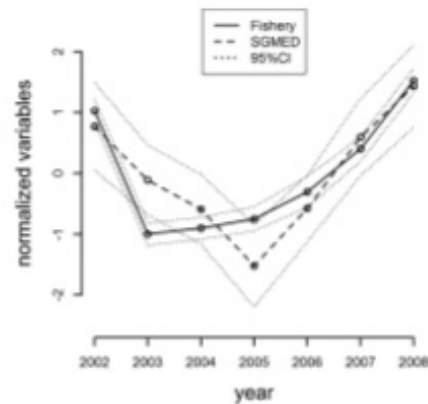


Fig. 6. Comparison between the fishery-derived index (standardized LPUE) and the SGMED index. Variables have been normalized for comparison.

Finally, LPUE index and the SGMED in 2002-2008 with their confidence intervals after normalization of variables are plotted in Figure 6. The normalized Barcelona fishery's LPUE, calculated using Equations 4 and 2, has narrower confidence intervals than the normalized SGMED index. Only in 2004 were the two indices statistically different and in 2005 index estimates were at the limit of the other CI. Thus, five out of seven estimates can be considered equivalent.

**DISCUSSION**

This study presents models for relative abundance of *A. antennatus* harvested by one important Catalan fleet in the NW Mediterranean from 1994 to 2008. To our knowledge it is the first combined use of commercial fisheries data from Spain analysing environmental and economic variables with GAM techniques. Our objectives were: 1) to define the relative importance of predictors (model 7, Tables 2 and 3) and 2) to construct a standardized fishery-dependent index to compare with fishery-independent indices (Fig. 6). The results contribute to the identification of simple roles in red shrimp fishery management.

**The role of explanatory variables**

We incorporated effort, temporal, economic and environmental variables into a global regression model to evaluate their relative importance. Model 7 captures LPUE variability with a total deviance of 43% explained by six predictors. In order to quantify the different sources of LPUE variability, we found that the set of fishery-related variables (*trips*, *grt* and *groups*) was the most important source, with an ED of 20.58%, followed by temporal (*time* and *period*, ED=13.12%) and finally economic variables (*shprice*, ED=9.30%). Among the variables taken from fishery

data, *trips* has provided the greatest impact to date. A low number of trips per month could be associated with generalist trawlers operating usually on the continental shelf and with less knowledge about red shrimp fishing grounds than trawlers specialized in this fishery (Maynou et al. 2003), suggesting that the higher activity of non-specialized trawlers in deep-water harbours yields lower LPUE values (see Fig. 5: partial effect for *trips*). Conversely, boats performing a higher number of trips per month are expert in deep-water fishing grounds and their skippers are more likely to find high-concentration shoals through a process of trial and error (as hypothesized by Sardà and Maynou 1998). Boat characteristics (*grt*) also influence LPUE, as was to be expected. The greater the gross registered tonnage, the higher the LPUE that is observed. The variable *group* captures other capabilities of fishermen and technical characteristics of vessels, such as the type of engine, net shape and skipper's expertise, which have been shown to positively bias the LPUE (Maynou et al. 2003, Marriott et al. 2011) and are expected to be important in many fisheries (Maunder and Punt 2004). The importance of these predictors implies that their influence should be eliminated during standardization.

Inter-annual variable (*time*) is much more important than intra-annual variable (*period*) (Table 3). The former is more strongly determined by a range of sources, such as environmental and economic drivers, than the latter. The same order of importance was found by Maynou et al. (2003). The LPUE was almost constant before 1999-2000, when a sharp decline was observed. We hypothesized a relationship with low NAO in the previous three years (see Fig. 1 and the introduction) that confirms the findings of Maynou (2008) and a possible relationship with the increase in fuel prices beginning in 2000. The following years were characterized by high inter-annual variability, when the price of fuel increased and showed greater variations. We believe that the trend could be explained by economic factors (Fig. 2), especially since very high fuel-related costs are incurred in the fishing of red shrimp as a result of it being performed in deep-water (Sardà et al. 1997).

The partial effect of ex-vessel prices, *shprice*, shows a parabolic-like shape and significant explanatory potential (ED=9.30%). Low selling prices do not induce fishermen to practice this deep-water fishery, because they could not offset the high associated costs, and trawlers would rather switch to continental shelf fisheries, with lower costs and lower risk. When there are profits to be made, probably owing to the low availability of the product, fishermen practice this deep-water fishery more intensely and landings per unit effort also increase. At the higher sales price bracket (i.e. more than about 30 € kg<sup>-1</sup>) decreasing landing rates mean higher sale prices. Here, an alternation of cause and effect between the two variables probably comes into play. As mentioned, *fprice* is also an important explanatory variable, although it was not inserted in the final model because of its correlation with *time*. Fuel price has a significant effect on LPUE and can reach approximately 1.6% of explained deviance (as can be deduced from the model building process in Table 2).

### Implications for management

Obtaining information on deep-sea species population dynamics is notoriously difficult, but our analysis suggests that the peculiarity of red shrimp fishery makes it possible to use fishery-dependent data to accurately describe the relative abundance of this resource. There are no discards for this fishery and the by-catch fraction, represented for example by *Merluccius merluccius* and *Micromesistius poutassou*, is small. These characteristics enable landings to be considered equivalent to catches and interchange LPUE and CPUE as indices (Hilborn and Walters 1992, Denis et al. 2002).

In turn, the definition of the relative importance of explanatory variables enables their impact on LPUE to be understood and makes intervention on the relevant variables possible from a management perspective. Fishery-related variables tend to have a significant effect on LPUE (ED=21% in our case), and management measures aiming to reduce fishing mortality in this heavily harvested stock (Cardinale et al. 2012) could be based on limiting the size of the trawlers. Furthermore, the number of trips permitted in deep-water fishing grounds in this fishery could be limited, for example, by defining a threshold when the number of trips does not significantly increase the partial effect for LPUE (see Fig. 5).

In addition, to evaluate the impact of predictors on the LPUE, the regression analysis could be the basis to provide a standardized index for assessing species stocks. Standardization of landings data allows an index of the real species abundance to be developed, assuming that the explanatory variables available remove (or explain) most of the variation in the data that is not attributable to natural changes (Maunder and Punt 2004). We advocate the selection of effort predictors for standardization.

Trends in CPUE (and LPUE) are usually assumed to reflect changes in the abundance of marine stocks (Maunder and Punt 2004), but the raw index is often not proportional to abundance (Maunder et al. 2006). The raw LPUE is in fact dependent on many human factors that could be avoided. Time variables have a strong relationship with the abundance and environmental factors, which in turn are related to abundance, so they cannot be used in the model during standardization (e.g. see Maunder and Punt 2004). The economic source of variability should be considered, but shrimp price and LPUE realistically have a cause-effect relationship, so they could be not properly used. Conversely, fishery-related variables seem to be the most reliable for this purpose.

During the study period, the fleet was practically constant, making monthly trips a good indicator of fishing effort and landing ability, and remained almost constant despite potential technological creep (Marriott et al. 2011) because no significant changes in fishing technology have occurred in the area in the last 20 years.

Studies of deep-water systems, where harsh conditions limit methods for evaluating fisheries, often suffer from a lack of data in order to assess stock status.

10 • V. Mamouridis et al.

Although the goal of fisheries managers is to promote sustainable production of fish stocks through formal stock assessment, it is often impractical to collect fishery-independent data in isolated or harsh environments. In these cases the information collected by a fishery is the main (or only) source of abundance data available (Maunder et al. 2006).

## ACKNOWLEDGEMENTS

The authors would like to express their sincere thanks to the Fisheries Directorate of the Government of Catalonia for giving access to the sales data of the Barcelona Fishers' Association, as well as to fishers of Barcelona. The first author is also very grateful to A. Rodríguez Casal and C. Cadarso Suárez for transmitting their knowledge in nonparametric statistics, to A. Gallen for revising the English and to M. Reyes for his suggestions on the manuscript. G. Aneiros is partly supported by Grant number MTM2011-22392 from the Ministerio de Ciencia e Innovación (Spain). Finally, this study was financed by the Spanish National Research Council (CSIC) through the JAE-predoc grant programme.

## REFERENCES

- Akaike H. 1973. Information theory as an extension of the maximum likelihood principle. In: Petrov B.N., Csaki F. (eds), Proc. 2nd Int. Symp. Information Theory, Akadémiai Kiadó, Budapest, pp. 267-281.
- Bas C., Maynou F., Sardà F., Leonart J. 2003. Variacions demogràfiques a les poblacions d'espècies demersals explotades: els barrers quaranta anys a Blanes i Barcelona. Inst. Est. Catalans. Arxiv de la Sec. Ciències, Barcelona.
- Bertrand J.A., de Sola L.G., Papaconstantinou C., Refini G., Souplet A. 2002. The general specifications of the MEDITS surveys. *Sci. Mar.* 66: 9-17.
- Brauner N., Shacham M. 1998. Role of range and precision of the independent variable in regression of data. *Am. Inst. Chem. Eng. J.* 44: 603-611. <http://dx.doi.org/10.1002/aic.690440311>
- Brodziak J., O'Brien L. 2005. Do environmental factors affect recruits per spawner anomalies of New England groundfish? *ICES J. Mar. Sci.* 62: 1394-1407. <http://dx.doi.org/10.1016/j.icjms.2005.04.019>
- Carbonell A., Carbonell M.S., Demestre M., Grau A., Montserrat S. 1999. The red shrimp *Arctostea antennatus* (Risso, 1816) fishery and biology in the Balearic Islands, western Mediterranean. *Fish. Res.* 44: 1-13. [http://dx.doi.org/10.1016/S0165-7836\(99\)00079-X](http://dx.doi.org/10.1016/S0165-7836(99)00079-X)
- Cardinale M., Osio G.C., Charef A. (eds). 2012. Report of the Scientific, Technical and Economic Committee for Fisheries on Assessment of Mediterranean Sea stocks – part I. JRC Scientific and Policy Reports. European Commission.
- Cartes J.E., Sardà F. 1992. Abundance and diversity of decapod crustaceans in the deep-Catalan sea (western Mediterranean). *J. Nat. Hist.* 26: 1305-1323. <http://dx.doi.org/10.1080/00222939200770741>
- Craven P., Wahba G. 1979. Smoothing noisy data with spline functions: estimating the correct degree of smoothing by the method of generalized cross-validation. *Numer. Mat.* 31: 377-403. <http://dx.doi.org/10.1007/BF01404567>
- Denis V., Lejeune J., Robin J.P. 2002. Spatio-temporal analysis of commercial trawler data using General Additive models: patterns of Loliginid squid abundance in the north-east Atlantic. *ICES J. Mar. Sci.* 59: 633-648. <http://dx.doi.org/10.1006/jmsc.2001.1178>
- Dennard S.T., MacNeil M.A., Treble M.A., Campana S., Fisk A.T. 2010. Hierarchical analysis of a remote, Arctic, artisanal longline fishery. *ICES J. Mar. Sci.* 67: 41-51. <http://dx.doi.org/10.1003/jmsc.2009.0220>
- FAO-FISHSTAT. 2011. FAO Fisheries Department, Fishery information, Data and Statistics Unit. Fishstat, a tool for fishery statistical analysis, release 2.0.0. FAO, Rome.
- Hastie T., Tibshirani R. 1990. Generalized additive models. Chapman Hall, London.
- Hilborn R., Walters C.J. 1992. Quantitative Fisheries Stock Assessment. Chapman & Hall, New York. <http://dx.doi.org/10.1007/978-1-4615-3598-0>
- Lassen H., Medley P. 2000. Virtual population analysis. A practical manual for stock assessment. FAO Fisheries Technical Paper. No. 400. FAO, Rome. 129 p.
- Leonart J., Maynou F. 2003. Fish stock assessments in the Mediterranean: state of the art. *Sci. Mar.* 67: 37-49.
- Marriott R.J., Wise B., St John J. 2011. Historical changes in fishing efficiency in the west coast demersal scalefish fishery, Western Australia: implications for assessment and management. *ICES J. Mar. Sci.* 68: 76-86. <http://dx.doi.org/10.1003/jmsc.2009.0220>
- Marx B.D., Eilers P.H.C. 1998. Direct generalized additive modeling with penalized likelihood. *Comput. Statist. Data Anal.* 28: 193-209. [http://dx.doi.org/10.1016/S0167-9473\(98\)00033-4](http://dx.doi.org/10.1016/S0167-9473(98)00033-4)
- Maunder M. N., Punt A. E. 2004. Standardizing catch and effort data: a review of recent approaches. *Fish. Res.* 70: 141-159. <http://dx.doi.org/10.1016/j.fishres.2004.08.002>
- Maunder M. N., Sibert J. R., Fonteneau A., Hampton J., Kleiber P., Harley S.J. 2006. Interpreting catch per unit effort data to assess the status of individual stocks and communities. *ICES J. Mar. Sci.* 63: 1373-1385. <http://dx.doi.org/10.1016/j.icjms.2006.05.008>
- Maynou F. 2008. Environmental causes of the fluctuations of red shrimp (*Arctostea antennatus*) landings in the Catalan Sea. *J. Mar. Sys.* 71: 294-302. <http://dx.doi.org/10.1016/j.jmarsys.2006.09.008>
- Maynou F., Demestre M., Sánchez P. 2003. Analysis of catch per unit effort by multivariate analysis and generalized linear models for deepwater crustacean fisheries off Barcelona (NW Mediterranean). *Fish. Res.* 64: 257-269. <http://dx.doi.org/10.1016/j.fishres.2003.09.018>
- Neal R.A., Maris R.C. 1985. Fishing biology of shrimps and shrimplike animals. In: Provenzano A.J. (ed.) *The Biology of Crustacea Vol 10: Economic aspects: fisheries and culture*. Academic Press Inc.
- Orsi Refini L., Mannini A., Refini G. 2013. Updating knowledge on growth, population dynamics, and ecology of the blue and red shrimp, *Arctostea antennatus* (Risso, 1816), on the basis of the study of its instars. *Mar. Ecol.* 34: 90-102. <http://dx.doi.org/10.1111/j.1439-0485.2012.00528.x>
- Sardà F., Maynou F. 1998. Assessing perceptions: do Catalan fishermen catch more shrimp on Fridays? *Fish. Res.* 36: 149-157. [http://dx.doi.org/10.1016/S0165-7836\(98\)00102-7](http://dx.doi.org/10.1016/S0165-7836(98)00102-7)
- Sardà F., Maynou F., Talló L. 1997. Seasonal and spatial mobility patterns of rose shrimps *Arctostea antennatus* in the Western Mediterranean: results of a long-term study. *Mar. Ecol. Prog. Ser.* 159: 133-141. <http://dx.doi.org/10.3354/meps159133>
- Scott D.W. 1992. *Multivariate Density Estimation: Theory, Practice, and Visualization*. Wiley, New York. <http://dx.doi.org/10.1002/9780470316849>
- Steffansson G. 1996. Analysis of groundfish survey abundance data: combining the GLM and delta approaches. *ICES J. Mar. Sci.* 53: 577-588. <http://dx.doi.org/10.1006/jmsc.1996.0079>
- Su N.J., Yeh S.Z., Sun C.L., Punt A.E., Chen Y., Wang S.P. 2008. Standardizing catch and effort data of the Taiwanese distant-water longline fishery in the western and central Pacific Ocean for bigeye tuna, *Thunnus obesus*. *Fish. Res.* 90: 235-246. <http://dx.doi.org/10.1016/j.fishres.2007.10.024>
- Wasserman L. 2005. *All of Nonparametric Statistics*. Springer, New York.
- Wood S. N. 2006. *Generalized Additive Models: An Introduction with R*. CRC/Chapman Hall, Boca Raton, Florida.

**ATTENTION ;**

Pages 348 to 352 of the thesis are available at the editor's web

- J.J. Saiz, J.E. Cartes, V. Mamouridis, A. Mecho and M.A. Pancucci-Papadopoulou  
*New records of Phascolosoma turnerae (Sipuncula: Phascolosomatidae) from the Balearic Basin*, Mediterranean Sea Marine Biodiversity Records, page 1 of 5  
<https://www.cambridge.org/core/journals/marine-biodiversity-records/article/new-records-of-phascolosoma-turnerae-sipuncula-phascolosomatidae-from-the-balearic-basin-mediterranean-sea/CA8115F9B952330F99010E346DF34518>  
doi:10.1017/S1755267214000153; Vol. 7; e16; 2014

## I.2 Congress proceedings



### Frequentist or Bayesian Additive Mixed Models? A comparison of perspectives to provide better estimates of CPUE

Valeria Mamouridis<sup>\*1</sup>, Germán Aneiros Pérez<sup>2</sup>, Carmen Cadarso Suarez<sup>3</sup>,  
Francesc Maynou<sup>1</sup>



#### Purposes

The CPUE (Catch per Unit Effort) is an index of relative species abundance used in fisheries research.

1. Improve red shrimp (*Aristeus antennatus*) CPUE modelling [1], by the incorporation in a joint model of: (a) additional (environmental and effort) predictors, (b) **random effects** for fishing vessels [2], (c) smooth functions.

2. Compare available methods to achieve aim 1: (a) Frequentist REstricted Maximum Likelihood, REML (**FR**), (b) Empirical Bayesian version of REML (**EB**), (c) Full Bayesian Markov Chain Monte Carlo, MCMC, simulation (**FB**).

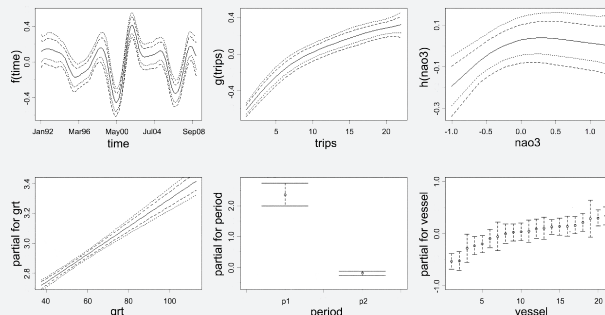
#### The model

The final model, whose three estimations were compared, belongs to the class of GAMMs, Generalized Additive Mixed Models, and is

$$\ln(cpue) = \alpha + \beta grt + f(time) + g(trips) + h(nao3) + \gamma p2 + \sum_{j=1}^J b_j vessel + \epsilon \quad (1)$$

where  $cpue \in Gamma(a, b)$ ,  $\alpha$ ,  $\beta$  and  $\gamma$  are the linear fixed parameters,  $f(\cdot)$ ,  $g(\cdot)$  and  $h(\cdot)$  represent the smooth functions,  $b_j$ 's are random effects of vessels and  $\epsilon$  the regression residuals.

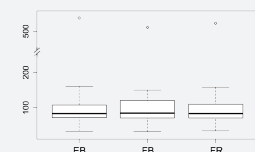
#### Partial effects - EB method



Percentage of Deviance Explained (DE%) by fixed effects.

	$g(trips)$	$grt$	$period$	$f(time)$	$h(nao3)$	model (1)	linear model
DE%	14.73	4.73	3.67	2.92	2.54	28.60	18.42

#### Comparing methods by MSEP



Percentage of the lowest MSEP between FR, EB and FB for the  $J$  subsets:

$$\{EB_j < FB_j\} \cap \{EB_j < FR_j\} = 48\%$$

$$\{FR_j < FB_j\} \cap \{FR_j < EB_j\} = 28\%$$

$$\{FB_j < EB_j\} \cap \{FB_j < FR_j\} = 24\%$$

#### Contacts

\* E-mail: mamouridis@icm.csic.es.

1 Institut de Ciències del Mar, CSIC, Psg Marítim de la Barceloneta 37-49, 08003 Barcelona, Spain, 2 Facultat de Informàtica, Campus de Elviña s/n, 15071, A Coruña, Spain, 3 Facultat de Medicina e Odontologia, R/ de San Francisco, s/n, 15782 Santiago de Compostela, Spain.

#### Goals

1. What is new in red shrimp CPUE model: (a.i) Effort predictor ( $trips$ ) is the most important sources of variability. (a.ii) The NAO (North Atlantic Oscillation) index is to date the only environmental predictor available for deep sea fisheries. (b) Random effects allow to predict for unknown vessels. (c) Smooth functions increase the explanatory power of the model.

2. There is no difference in predictions between methods, however the EB gives lowest MSE in almost the 50% of subsets.

#### Variables

##### Response

$cpue$  monthly CPUE for each vessel, =  $landing / \#trips$  ( $kg day^{-1}$ )<sup>a</sup>,  $i = 1, \dots, 2314$

##### Predictors

$time$  months from 01-1992 to 12-2008  
 $t = 1, \dots, 204$

$vessel$  a numeric code assigned to each vessel,  
 $j = 1, \dots, 21$

$trips$  number of trips performed by vessel  $j$  during month  $t$

$grt$  Gross Registered Tonnage of vessels

$nao3$  mean annual NAO index of 3 years before the year of observed  $landing$

$period$  categorical with 2 levels,  $p2$ : June and November;  $p1$ : otherwise

<sup>a</sup>Catches are landed daily and 1  $day = 1 trip$

#### Methodology

The frequentist REML was used to obtain the final model (1) with the highest deviance explained, after checking model assumptions (the R-package mgcv [3] was implemented). Predictors were selected by a stepwise forward procedure and 2-nd order P-spline was used as smoother.

Afterwards, model (1) was fitted through the two Bayesian inferences using *BayesX* software [4].  $J = 21$  subsets, excluding  $vessel j$ , were used to estimate model (1) by each method. The mean square error of predictions, MSEP, was calculated on predictions from subset  $-j$  on subset  $j$  and used as comparative criterion.

#### References

- [1] Maynou, F., Demestre, M., Sánchez, P., 2004. *Fish. Res.* 65: 257-269.
- [2] Cooper, A.B., Rosenberg, A.A., Stefánsson, G., Mangel, M., 2004. *Fish. Res.* 70: 239-250.
- [3] Wood, S.N., 2011 *J. Roy. Stat. Soc. B*, 73: 1, 3-36.
- [4] Brezger, A., Kneib, T., Lang, S., 2005. *J. Stat. Software*, 14 (11): 1-22.

#### Acknowledgments

Authors thank Dr. T. Kneib for his hints on BayesX usage.

## Frequentist or Bayesian Mixed Models? A comparison to provide better estimates of CPUE

### Student oral presentation

Valeria Mamouridis<sup>1</sup>, Carmen Cadarso Suarez<sup>2</sup>, Germán Aneiros Pérez<sup>3</sup>, Francesc Maynou<sup>1</sup>

<sup>1</sup> Institut de Ciències del Mar, CSIC, Pg Marítim de la Barceloneta 37-49, 08003 Barcelona, Spain. E-mail: mamouridis@icm.csic.es

<sup>2</sup> Facultade de Medicina e Odontoloxía, R/ de San Francisco, s/n, 15782 Santiago de Compostela, Spain.

<sup>3</sup> Facultade de Informática, Campus de Elviña s/n, 15071, A Coruña, Spain.

**Abstract:** Generalized Additive Mixed Models were used to make up a regression analysis applied to red shrimp CPUE. Mixed Models are required when units are not repeatable, such as the case of fishing boats. We also compared the methodologies actually in use: the frequentist REML, the full Bayesian by MCMC techniques and the empirical Bayesian methods.

**Keywords:** GAMM; Fisheries; CPUE; REML; MCMC.

### 1 Introduction

In fisheries research, regression models are often used to analyze CPUE (Catch per Unit Effort), an index of relative abundance of an exploited species. To date CPUE has been mainly analyzed through Generalized Linear Models (GLM), e.g. Goñi et al. (1999), and rarely Generalized Additive Models (GAM) e.g. Damalas et al. (2007). Instead, fishery data usually hold a random nature, being associated to fishing vessels, that are in fact unrepeatable units. That is not contemplated in such kind of models. In very few occasions random effects has been considered, e.g. using Generalized Linear Mixed Models (GLMM), e.g. Cooper et al. (2004).

On the other side, recent advancements in regression methodologies provide many estimators of random effects in a Generalized Additive Mixed model (GAMM) framework using frequentist (Lin and Zhang, 1999) or Bayesian (Fahrmeir and Lang, 2001) inference.

In this work we present a regression analysis of red shrimp (*Aristeus antennatus*) CPUE from the port of Barcelona (Spain). The last update of red shrimp CPUE modeling in the NW Mediterranean Sea was through GLM (Maynou et al. 2003).

## 2 Frequentist or Bayesian Mixed Models?

## 2 Methodology

WE can devide the methodology in two steps:

1. The frequentist REML was used, implementing the R-package *mgev* (Wood, 2006), to obtain the final model, that is, after checking assumptions, the one with the highest deviance explained (DE%). Predictors were selected by a stepwise forward procedure and 2-nd order P-spline was used as smoother.
2. Afterwards, the final model was fitted using the two Bayesian inferences as well, with the implementation of *BayesX* software (Brezger et al., 2005).  $J - 21$  subsets, excluding vessel  $j$ , were used to estimate the model by each method. Then they were compared using the mean square error of predictions, MSE<sub>P</sub>, calculated on predictions from subset  $\{J - j\}$  on subset  $\{j\}$ .

Variables implemented in the model are reported in Table 1.

TABLE 1. Variables used in the study.

Name	Description
$y$	monthly CPUE for each vessel, $i = 1, \dots, 2314$
$time$	months from 01-1992 to 12-2008, $t = 1, \dots, 204$
$ves$	a numeric code assigned to each vessel, $j = 1, \dots, 21$
$trips$	number of trips performed monthly by each vessel, $j$ during month $t$
$grt$	Gross Registered Tonnage of vessels
$nao3$	NAO index of 3 years before the observed $cpue$
$period$	season variable with 2 levels, $p2$ : Jun and Nov; $p1$ : otherwise

## 3 Results

The selected final model belongs to the class of GAMMs:

$$\ln(y) = \alpha \beta \text{ grt} + f(\text{time}) + g(\text{trips}) + h(\text{nao3}) + \gamma p2 + \sum_{j=1}^J b_j \text{ves} + \epsilon \quad (1)$$

where  $\epsilon \in \text{Gamma}(a, b)$ .

The partial effects of model 1 are visualized in Figure 1. Effort predictor ( $trips$ ) is the most important sources of variability. The NAO (North Atlantic Oscillation) index is to date the only environmental predictor available for deep sea fisheries. Random effects allow to predict for unknown boat effects. Smooth functions increase the explanatory power of the model.



Mamouridis et al. 2012 3

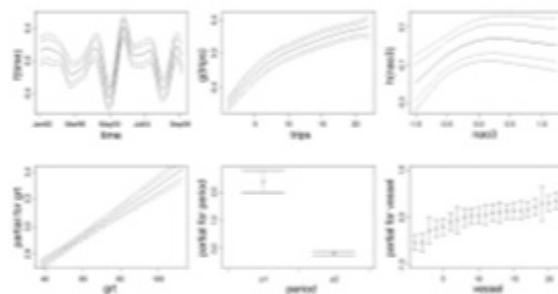


FIGURE 1. Partial effects of model 1 estimated through EB method.

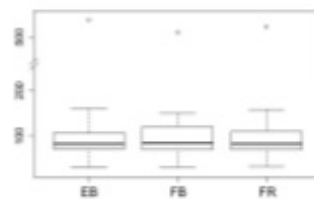


FIGURE 2. Box plot of MSEP estimated for the different methods.

Figure 2 shows that there is no difference in predictions between methods, however the EB gives lowest MSEP in almost the 50% of subsets.

#### 4 Conclusion

That study updates the red shrimp CPUE modeling through the implementation of effort and environmental predictors, of smooth functions and random effects. It also demonstrate that there is no difference in predictions between methods. The use of mixed models permits to infer on the entire population however when units, boats in this case, are not repeatable.

## 4 Frequentist or Bayesian Mixed Models?

**Acknowledgments:** Authors thank Dr. T. Kneib for his hints on BayesX usage.

**References**

- Brezger, A., Kneib, T., Lang, S. (2005). BayesX : Analyzing Bayesian Structured Additive Regression Models. *Journal of Statistical Software*, 14 (11), 1-22.
- Cooper, A.B., Rosenberg, A.A., Stefánsson, G., Mangel, M. (2004). Examining the importance of consistency in multi-vessel trawl survey design based on the U.S. west coast groundfish bottom trawl survey. *Fisheries Research*, 70: 239-250.
- Damalas, D., Megalofonou, P. and Apostolopoulou, M. (2007). Environmental, spatial, temporal and operational effects on swordfish (*Xiphias gladius*) catch rates of eastern Mediterranean Sea longline fisheries. *Fisheries Research*, 84, 233-246.
- Fahrmeir, L. and Lang, S. (2001). Bayesian inference for generalized additive mixed models based on Markov random field priors. *Journal of the Royal Statistical Society C*, 50, 201-220.
- Goñi, R., Alvarez, F. and Adlerstein, S. (1999). Application of generalized linear modeling to catch rate analysis of Western Mediterranean fisheries: the Castellón trawl fleet as a case study. *Fisheries Research*, 42, 291-302.
- Lin, X. and Zhang, D. (1999). Inference in generalized additive mixed models using smoothing splines. *Journal of the Royal Statistical Society, Series B*, 61, 381-400.
- Maynou, F., Demestre, M. and Sánchez, P. (2004). Analysis of catch per unit effort by multivariate analysis and generalised linear models for deep-water crustacean fisheries off Barcelona (NW Mediterranean). *Fisheries Research*, 65, 257-269.
- Wood, S.N. (2006). *Generalized Additive Models: An Introduction with R*. CRC Chapman & Hall, Boca Raton, Florida.

## Dynamic simulations of food webs with R Student oral presentation

Valeria Mamouridis<sup>1</sup>, Laurine Burdorf<sup>2</sup>, Karline Soetaert<sup>2</sup>

<sup>1</sup> Institut de Ciències del Mar, CSIC, Pg Marítim de la Barceloneta 37-49, 08003 Barcelona, Spain. E-mail: mamouridis@icm.csic.es

<sup>2</sup> NIOZ (Royal Netherlands Institute for Sea Research) Yerseke, Koningeweg 7, P.O. Box 140, 4400 AC Yerseke, The Netherlands.

**Abstract:** We present a methodology to create and dynamically simulate food webs in the open source software R. This is done in three steps. First a plausible binary food web is generated with a preset number of species ( $S$ ) and links ( $L$ ). Then a quantified steady-state foodweb is generated using linear inverse modeling (LIM) techniques. Thirdly, the food web flows are converted into dynamic formulations. The flexibility of this methodology allows to study the stability of these webs and how they react when perturbed.

**Keywords:** food webs; linear inverse models; dynamic models.

### 1 Introduction

Food webs describe who eats whom in an ecosystem. For a given number of species  $S$ , and links  $L$ , a food web can be represented by an  $S \times S$  matrix  $S$ , where if the species  $i$  is a prey of species  $j$  then element  $s_{i,j} = 1$  while  $s_{i,j} = 0$  otherwise. This is a "binary food web". However, species interactions are only feasible if enough energy is transferred to the predator. To assess the energetic feasibility, a foodweb needs to be quantified. This generates a  $S \times S$  flow matrix  $X$ , whose elements  $x$  are estimates of the magnitude of each feeding flow. This is a "quantified food web".

Theoretical ecologists have suggested simple models to generate binary food webs, based on the assumption that  $L \in U(0, 1)$  (i.e. random and cascade models: Cohen and Newman, 1985) or  $L \in B(\alpha\beta)$ , (i.e. niche model: Williams and Martinez, 2000; and nested-hierarchy model: Cattin et al. 2004). The two latter models describe more realistic food webs.

On the other hand, applied ecologists have used Linear Inverse Modeling (LIM) to quantify the flows of real food webs (see van Oevelen et al., 2010), given an incomplete data set. The LIM methodology consists in solving the following linear problem for the unknown flows  $x$ :

$$Ex = F \quad (1)$$

$$Ax \approx B \quad (2)$$

## 2 Dynamic simulations of food webs with R

$$\mathbf{Gx} > \mathbf{H} \quad (3)$$

Here the first and/or second set of equations typically contain the component's mass balance equations and observed data, while the third set of equations holds physiological information and positivity constraints (i.e. the flows have a direction).

A LIM returns a "steady-state" snapshot of a food web, although the behavior of food webs under changing conditions is often of interest. This implies that the food web should be written as a dynamic model and solved by numerical integration.

Recently the R software has been made suitable for solving LIMs and for dynamic simulation thanks to two add-on packages (the R-package `limSolve` (Soetaert et al., 2009), and `deSolve` (Soetaert et al., 2010).

## 2 Methodology

We present how these three approaches can be combined in R:

1. We first generate binary food webs according to a theoretical model. Three functions generate the random, the cascade and the niche binary webs.
2. We then check the (energetic) feasibility, using the LIM methodology and quantify the flows. To do this, we convert the binary matrices into a LIM (1) assuming a minimal "growth efficiency" when consuming a species. If the LIM can be solved, then the problem is feasible and allows to estimate the flows.
3. The stability and long-term behavior of the quantified food web is then studied in dynamic simulations. To generate the dynamic system the species biomasses are needed, to convert the total ingestion and respiration rates into mass-specific rates and second order rates. We assumed allometric scaling of rates according to the trophic level of each species. The Jacobian matrix of the dynamic system allows to check the model's stability properties.

## 3 Examples

Figure 1 gives an illustration of the three types of simulated food webs. The random model was not feasible and could not be solved given the energetic constraints, so its flows are not represented. The cascade and niche model were feasible and the flows could be quantified. Figure 2 represents the dynamic simulation made for the niche food web. The output represents a stable unperturbed foodweb (black line), and an increasingly instable foodweb when perturbed (the red and green lines).

Mamouridis et al. 3

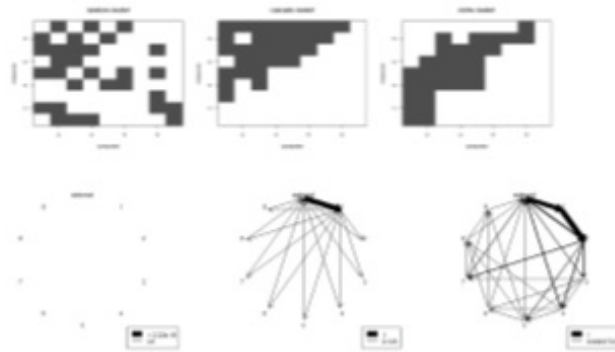


FIGURE 1. The binary food web and the quantitative food web for the three theoretical models.

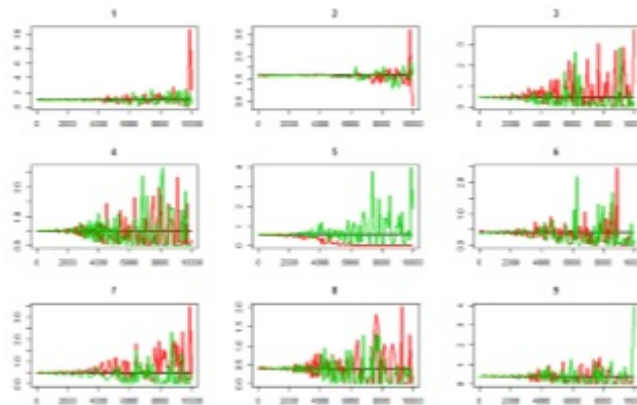


FIGURE 2. Output of the dynamic simulation for a niche food web.

#### 4 Conclusion

The functions implemented in the open source framework R will allow to study the effect of human and environmental perturbations on artificially

## 4 Dynamic simulations of food webs with R

generated food webs.

**Acknowledgments:** The first author thanks to the CSIC grant program JAE-predoc, that made possible this study.

**References**

- Cattin, M-F., Bersier, L-F., Banasek-Richter, C. et al. (2004). Phylogenetic constraints and adaptation explain food-web structure. *Nature*, **427**, 835-837.
- Cohen, J.E. and Newman, C. M. (1985) A stochastic theory of community food webs I. Models and aggregated data. *Proceeding of the Royal Society of London, B*, **224**, 449-461.
- Soetaert, K., Van den Meersche, K., van Oevelen, D. (2009) limSolve: Solving Linear Inverse Models. R-package version 1.5.1.
- Soetaert, K., Petzoldt, T. and Setzer R.W. (2010). Solving Differential Equations in R: Package deSolve. *Journal of Statistical Software*, **33** (9), 1-25.
- van Oevelen, D., Van den Meersche, K., Meysman, F.J.R., et al. (2010). Quantifying Food Web Flows Using Linear Inverse Models. *Ecosystems*, **13**, 32-45.
- Williams, R.J. and Martinez, N.D. (2000). Simple rules yield complex food webs. *Nature*, **404**, 180-183.

## Structured Additive Distributional Regression in Fishery Research

Valeria Mamouridis  
Institut de Ciències del Mar (ICM-CSIC)  
mamouridis@icm.csic.es

The quantification of abundance or biomass of an exploited species is extremely important in fishery research, so that indices of relative abundance are widely used to assess the status of the stock and manage the fishing activity. Indices of relative abundance are widely used for these purposes. They are influenced by many factors, some of which if not considered could lead to biased interpretations of stock states. Those indices are influenced by many factors, some of which, if not considered, could lead to biased interpretations of stock states. Regression analysis has become common in this field in order to define the different sources of variability (e.g. time, seasonality and fleet characteristics, among others) and eliminate those that deviate the index from the natural abundance of the species in a process named standardization (Maunder and Punt, 2004). In standard statistical models, it is often assumed that some of the influential variables have a simple linear impact, which may be not flexible enough. An alternative could be the use of semi-parametric models. Another important aspect is the choice of the response distribution. In most cases skewed distributions have been considered, including the gamma, the log-normal and delta distributions (e.g. Maynou et al., 2003; Brynjarsdóttir and Stefánsson, 2004; Gavaris, 1980). Furthermore, data are collected for a limited ensemble of catching units, e.g. the trawling boats. This implies to acknowledge the fact that the catching units represent a sample from the population and leads to the use of random effects. Finally, explanatory variables could influence the expectation but also higher moments of the response distribution, such as scale or shape.

The complexity of data in fishery research can be captured only partially by classical models such as generalised additive models (GAM, Hastie and Tibshirani, 1986) or the more recent generalised additive mixed models (GAMMs, Wood, 2006). A wider approach is given by the class of generalised additive models for location, scale and shape (GAMLSS, Rigby and Stasinopoulos, 2005), which Bayesian equivalent is represented by structured additive distributional regression (DSTAR: Klein et al., 2013). DSTAR models provide efficient approximations using Markov Chain Monte Carlo inference to deal with a variety of aims related to this applied field: 1) the possibility to estimate both linear and smooth effects, 2) the selection within different distribution function, 3) the incorporation of fixed and random effects and 4) the estimation of further parameters of the distribution than the location.

The talk aims to demonstrate the flexibility of DSTAR in modelling abundance indices and to provide a guidance for the model choice and variable selection, questions that arise in the process of developing an appropriate model for a given data set.

### References

- Brynjarsdóttir, J., Stefánsson, G., 2004. Analysis of cod catch data from Icelandic groundfish surveys using generalized linear models. *Fisheries Research* 70.2: 195-208.
- Hastie, T. J., Tibshirani, R. J., 1990. *Generalized Additive Models*. No. 43. CRC Press.
- Gavaris, S., 1980. Use of a multiplicative model to estimate catch rate and effort from commercial data. *Canadian Journal of Fisheries and Aquatic Sciences* 37.12: 2272-2275.
- Klein, N., Kneib, T., Lang, S., 2013. *Bayesian Generalized Additive Models for Location, Scale and Shape for Zero-Inflated and Overdispersed Count Data*. Technical Report.
- Maunder, M. N., Punt, A. E., 2004. Standardizing catch and effort data: a review of recent approaches. *Fisheries Research* 70.2: 141-159.
- Maynou, F., Demestre, M., Sánchez, P., 2003. Analysis of catch per unit effort by multivariate analysis and generalised linear models for deep-water crustacean fisheries off Barcelona (NW Mediterranean). *Fisheries Research* 65.1: 257-269.
- Rigby, R. A., Stasinopoulos, D. M., 2005. Generalized additive models for location, scale and shape. *Journal of the Royal Statistical Society: Series C (Applied Statistics)* 54.3: 507-554.
- Wood, S., 2006. *Generalized additive models: an introduction with R*. CRC Press.

## The macrofauna associated to the deep-sea coral *Isidella elongata*: human impact and natural variability

V Mamouridis<sup>1\*</sup>, JE Cartes<sup>1</sup> & E Fanelli<sup>2</sup>

1. Institut de Ciències del Mar (CSIC), Passeig Marítim de la Barceloneta 37-49, 08003 Barcelona, Spain.

2. Marine Environment Research Center - ENEA Santa Teresa, Pozzuolo di Lerici 19032 (SP) Italy.

\* mamouridis@icm.csic.es



### Introduction

Deep-sea habitats associated to cold water corals (CWC) show unique complexity and species diversity, acting as potential areas of foraging, refuge and breeding for many deep-sea species enhancing their ecological niche dimensions. An example is the bamboo coral *Isidella elongata* that formed pristine forests on soft sediments off the Ebro river mouth (NW Mediterranean) till 1996, when *Isidella* habitat began to be subjected to fishing activity [1].

### Main Objectives

1. Analyse the infauna associated to two different habitats: (a) mud habitat, and (b) mud coral habitat.
2. Define the differences in biomass, abundance and taxonomic diversity between both habitats.
3. Investigate possible mesoscale gradients related to environmental variability.

### Materials and Methods

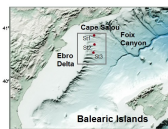


Figure 1: The study area.

The study area is located on the slope of the Catalan Sea, NW Mediterranean (Figure 1): we sampled three stations at 613-619 m depth in June 2011. S1 (a) is in a mud habitat without the *Isidella elongata* and a fishing ground since 50's; S2 and S3 (b) are mud coral habitat, subjected to rather low fishing activity since mid 90's, with 2-3 boats sporadically operating in the area [2]. Here coral density has reduced from 255 to 0.9 colonies/ha [2].

We collected (macro)infauna using a Reyneck box-corer, with a surface of 0.065 m<sup>2</sup> cm and then sieved samples through 0.5 mm mesh size

(4 replicates per station, N=12). We collected also environmental variables: temperature (T5mab), salinity (S5mab), turbidity (Turb5mab) and oxygen concentration (O5mab) in the near-bottom water and total organic matter (tom) and redox potential in sediments at 1 and 5 cm from surface (mv1cm, mv5cm). All statistical analysis were performed using the R-package Vegan v2.0-10.

### Results

A total of 81 taxa has been identified. For the five major groups were counted in ascending order 35 taxa of polychaets, 25 crustaceans, 8 mollusca, 5 sipunculans and 2 echinoderms. The overall abundance and biomass were 392.30±138.30 n/m<sup>2</sup> and 3.42±4.68 g/m<sup>2</sup> respectively and specifically, in mud habitat were 407.69±164.98 n/m<sup>2</sup> and 0.97±0.98 g/m<sup>2</sup> and in mud coral habitat 384.61±134.87 n/m<sup>2</sup> and 4.64±5.38 g/m<sup>2</sup>.

factor	R	F	δ
habitat	0.11**	1.73**	0.90**
station	0.25*	1.53**	0.91*

Table 1: ANOSIM (R), PERMANOVA (F) and MRPP (δ) tests. Response: biomass, explanatory factors: habitat and station.

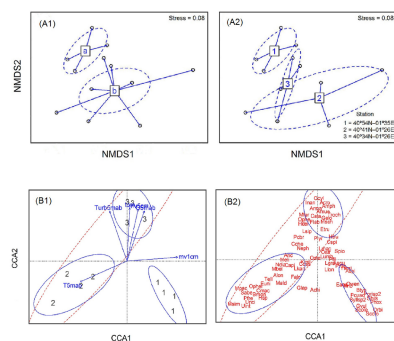


Figure 2: (A) nMDS on biomass matrix. Points represent boucoons. In (A1) ellipses define 95% confidence areas from centroids according the habitat, (a = mud, b = mud coral) and in (A2) according to stations (S1, S2, S3). Replicates of same levels are combined with the corresponding centroid. (B) CCA constrained with factors habitat and position (coordinates) on the biomass matrix. (B1) the sites ordination (numbers) with environmental variables (vectors), that all returned significant relationship with two first dimensions ( $\leq 0.05$ ). (B2) the corresponding species ordination. Ellipses depict 0.95 confidence regions of factor station (continuous lines) and habitat (dashed line).

Taxa	ab	rel	cum	Taxa	ab	rel	cum
(a) <i>Prochaetoderma</i> spp.	50.00	11.81	11.81	(b) <i>Leucon longirostris</i>	26.92	6.54	6.54
<i>Leucon longirostris</i>	34.61	8.18	20.00	<i>Chelator chelatus</i>	17.30	4.20	10.74
<i>Ennucula aegeensis</i>	30.76	7.27	27.27	<i>Prochaetoderma</i> spp.	17.30	4.20	14.95
<i>Amphipolis squamata</i>	30.76	7.27	34.54	<i>Kelliella miliaris</i>	15.38	3.73	18.69
<i>Carangotopsis spinulosa</i>	26.92	6.36	40.90	<i>Aricidea</i> sp.	13.46	3.27	21.96
<i>Prionospio</i> spp.	15.38	3.63	44.54	Maldanidae	13.46	3.27	25.23
<i>Scolelepis</i> sp.	15.38	3.63	48.18	<i>Harpinia dellavallei</i>	13.46	3.27	28.50
Owentidae	11.53	2.72	50.90	<i>Harpinia truncata</i>	13.46	3.27	31.77
				Nematoda	13.46	3.27	35.04
				<i>Carangotopsis spinulosa</i>	11.53	2.80	37.85
				<i>Leviniseta gracilis</i>	9.61	2.33	40.18
				<i>Prionospio</i> sp.	9.61	2.33	42.52
				<i>Syllidae</i> sp.	9.61	2.33	44.85
				<i>Pseudogorda fulipes</i>	9.61	2.33	47.19
				Ostracoda	9.61	2.33	49.53
				<i>Amphipolis squamata</i>	9.61	2.33	51.86

Table 2: Mean taxa abundance (ab, n/m<sup>2</sup>) calculated for (a) mud and (b) mud coral habitats. rel: relative, and cum: cumulative percentages up to 50% of the total.

### Conclusions

- Habitat (nMDS A1) and stations (nMDS A2) were the main factors in sample segregation when considering biomasses, that are significantly higher in mud coral habitat (b), while abundances are higher in mud habitat (a).
- Mud coral habitat showed also high variability and heterogeneity in biomasses with respect to mud habitat (ANOSIM).
- Also species composition was heterogeneous in mud coral habitat with the coexistence of different types of detritivorous species, while mud habitat was co-dominated by both detritivores and carnivores (mainly the caudofoveates *Prochaetoderma* spp.).
- The community structure was also related to environmental conditions (CCA); the wider spectrum of different detritivores in mud coral habitat could be a consequence of the higher availability (higher tom) and variability in source quality (labile and refractory detritus, higher turbidity, lower mv1cm, higher oxygen concentration) and other favourable conditions, such that different types of basal consumers were observed, on the contrary in mud habitat where the source is limited and less heterogeneous the community is composed by less number of species and carnivores (on meiofauna) show higher relative abundance.
- Some similar findings concerning the abundances and the different trophic organizations of infaunal communities have been also observed comparing other deep-sea habitats, e.g. canyons [3, 4] and in the same mud coral habitat for the megafauna [2].
- The lower functional diversity in the mud habitat can also be related with the higher trawling activity compared to mud coral stations.

### References

- [1] Maynou, F and Cartes, JE, 2012. Effects of trawling on fish and invertebrates from deep-sea coral facies of *Isidella elongata* in the western Mediterranean. *Journal of the Marine Biological Association of the United Kingdom*, 92(7): 1501-1507.
- [2] Cartes, JE and Llocacono, C and Mamouridis, V and López-Pérez, C and Rodríguez, P, 2013. Geomorphological, trophic and human influences on the bamboo coral *Isidella elongata* assemblages in the deep Mediterranean: To what extent does *Isidella* form habitat for fish and invertebrates? *Deep Sea Research Part I: Oceanographic Research Papers*, 76: 52-65.
- [3] Mamouridis, V and Cartes, JE and Parra, S and Fanelli, E and Saiz Salinas, JI, 2011. A temporal analysis on the dynamics of deep-sea macrofauna: influence of environmental variability of Catalonia coasts (western Mediterranean). *Deep Sea Research Part I: Oceanographic Research Papers*, 58(4): 323-337.
- [4] Stora, G and Bourcier, M and Arroux, A and Gerino, M and Campion, J Le and Gilbert, F and Durbec, P, 1999. The deep-sea macrobenthos on the continental slopes of the northwestern Mediterranean Sea: a quantitative approach. *Deep Sea Research Part I: Oceanographic Research Papers*, 46(8): 1339-1368.

### Acknowledgements

Authors thank all participants to the project ANTRIMARE (CTM2009-12214-C02-01).



Figure 3: (A) *Isidella elongata* (Esper, 1788), ROV image from the CORALG survey, (B) *Leucon longirostris* Sars, 1871, (C) Caudofoveata.



## Trophodynamics in a bathyal food web (NW Mediterranean) controlled by food limitations and fishing activity

V Mamouridis<sup>1\*</sup>, D van Oevelen<sup>2</sup>, K Soetaert<sup>2</sup>,  
F Maynou<sup>1</sup>, E Fanelli<sup>3</sup>, JE Cartes<sup>1</sup>

1. Institut de Ciències del Mar (CSIC), Passeig Marítim de la Barceloneta 37-49, 08003 Barcelona, Spain.

2. NIOZ, Korrिंगaweg 7, 4401 NT Yerseke, Netherlands

3. Marine Environment Research Center - ENEA Santa Teresa, Pozzuolo di Lerici 19032 (SP) Italy.

\* mamouridis@icm.csic.es



### Introduction

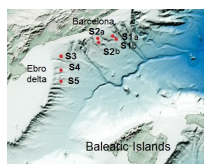


Figure 1: The study area.

We present a dynamic simulation of a bathyal food web quantified using site-specific data from the continental slope (600-800 m depth, years 2007 and 2011), Catalan Sea (Figure 1).

Many works have been performed assessing the importance of resource limitation (bottom-up control) or predation (top-down control) in regulating and structuring ecosystems, e.g. [1, 2, 3].

The continental slope is dominated by detritivores feeding on different types of detritus but also by species with benthic or benthic-pelagic behaviours and a wider range of their trophic niche feeding partially on detritus and on other metazoa (see e.g. [4]).

### Aims

1. Investigate the response of the bathyal food web under two types of perturbation: bottom-up (induced by resource limitation) and top-down (induced by fishing activity).
2. Detect the existence of trophic cascades including the humans as top predator, that fish the red shrimp (*Aristeus antennatus*), or competition for food.

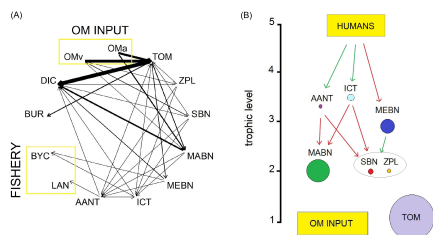


Figure 2: (A) Food web net flows and (B) trophic position of components with examples of possible hypotheses of trophic cascades. Arrows colour indicate positive effect of upper on lower levels (green) and negative effect (red). Colours associated to compartments: orange = zooplankton (ZPL); red = suprabenthos (SRN); green = macrobenthos (MABN); blue = invertebrates from megafauna (MEBN); light blue = fish from megafauna (ICT); violet = red shrimp *Aristeus antennatus* (AANT).

### The simulation

After quantifying the food web in steady-state using linear inverse modelling (LIM, ctevanoevelen2010), we run it dynamically through 5 years under perturbations induced by resource limitation and by fishing activity, both for three cases:

1. unchanged biomass (base), used to estimate all original flows,
2. add to the biomass the value corresponding to  $p$  times the original flow, input of organic carbon or output due to fishery (more), and
3. decreasing the biomass to the value corresponding to  $p$  times the original flow (less).

We repeated the simulations for different magnitudes of  $p$ ,  $p = 5, 10, 20$ , returning a total of 25 different scenarios. The dynamic model is basically

$$\frac{dx}{dt} = \sum f(x, p^1, t) - \sum f(y, p^2, t) \quad (1)$$

where the flows are functions  $f(\cdot)$  of e.g. the state variable ( $x$ ), parameters ( $p^1$ ) and time ( $t$ ). We then calculated relative biomasses of faunal components for each time and the presence/absence of change in relative biomasses between each possible interaction ( $I = 15$ ).

We also imposed a trade-off of 2 for both the proportion between the original biomass of each component (used to estimate the flows) and its biomass at time  $t \neq t_0$  and the proportion between biomasses of couples of components to ensure that at least one biomass is doubled with respect to the other to give evidence of a significant change.

We used the R-packages LIM [5] and deSolve [6].

### Results

We found shift of relative biomasses for some components as shown in Table 1 and the most representative outputs among all scenarios are shown in Figure 3.

	(A) $p = 5$			(B) $p = 10$			(C) $p = 20$		
	base	more	less	base	more	less	base	more	less
base	ZA	ZA	ZA	ZA	ZA	ZA	ZA	ZA	ZA
more	ZA	ZA	ZA	SA	SA	SA	SA	SA	SA
less	ZA	ZA	ZA	SZ	SZ	SZ	SZ	SZ	SZ
	ZMa	ZMa	ZMa	ZMe	ZMe	ZMe	ZI	ZI	ZI

Table 1: Affected relationships for each scenario. ZA=ZPL-AANT, SA=SRN-AANT, SZ=SRN-ZPL, ZMa=ZPL-MABN, ZMe=ZPL-MEBN, ZI=ZPL-ICT. In rows are the levels of OM INPUT while in columns are the levels of FISHING EFFORT.

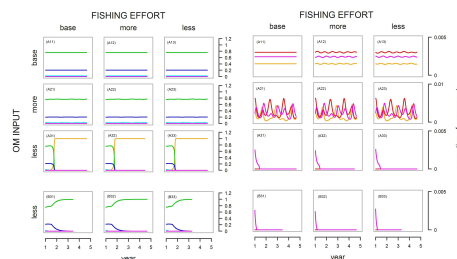


Figure 3: On the left: simulation output for all components; on the right: simulation output showing only less abundant components.

### Conclusions

- There is no impact due to fishery neither evidences of any top-down mechanism, i.e. trophic cascades for all scenarios. On the contrary bottom-up controls can occur especially when resources are limited. In fact modifying the fishing effort maintaining the input constant the proportions of components do not change in time. On the contrary the proportion changes when the resource is modified.
- When the resource input is higher there are alternative states of no-dominant components (zooplankton, suprabenthos and the red shrimp), but their proportion remains low during the simulated period.
- When the resource is limited but still high the unique component that grows is the zooplankton, that feeds directly on allochthonous resource and does not depend on the organic matter in sediments. When the resource is strongly limited all components show changes in their relative biomass but any shift occurs and the (macro)infauna is the component that predominates in the food web.
- The continental slope ecosystem is based on detritus derived from the aboveground photic systems. We thus suggest that a detritus food web is affected by the dynamics of the source and not by the consumer, a control type called "donor control" [7].

### References

- [1] Worm, B and Myers, RA, 2003. Meta-analysis of cod-shrimp interactions reveals top-down control in oceanic food webs. *Ecology*, 84(1): 162-173.
- [2] Sala, E and Boudouresque, CF and Harmelin-Vivien, M, 1998. Fishing, trophic cascades, and the structure of algal assemblages: evaluation of an old but untested paradigm. *Oikos*, 82: 425-439.
- [3] Hunter, MD and Price, PW, 1992. Playing chutes and ladders: heterogeneity and the relative roles of bottom-up and top-down forces in natural communities. *Ecology*, 73(3): 723-732.
- [4] Papiol, V and Cartes, JE and Fanelli, E and Rumolo, F, 2013. Food web structure and seasonality of slope megafauna in the NW Mediterranean elucidated by stable isotopes: Relationship with available food sources. *Journal of Sea Research*, 77: 53-69.
- [5] van Oevelen, D and Van den Meersche, K and Meysman, FJR and Soetaert, K and Middelburg, JJ and Vézina, AF, 2010. Quantifying food web flows using linear inverse models. *Ecosystems*, 13(1): 32-45.
- [6] Soetaert, K and Petzoldt, T and Setzer, RV, 2010. Solving differential equations in R: Package deSolve. *Journal of Statistical Software*, 33(9): 1-25.
- [7] DeAngelis, DL, 1980. Energy flow, nutrient cycling, and ecosystem resilience. *Ecology*: 764-771.

### Acknowledgements

Authors thank all participants of the projects BIOMARE (CTM2006-13508-CO2-02/MAR) and ANTRMARE (CTM2009-12214-CO2-01).





---

## References

---

- Abelló, P and FJ Valladares (1988), ‘Bathyal decapod crustaceans of the Catalan Sea (northwestern Mediterranean)’, *Mésogée* **48**, 97–102.
- Akaike, H (1973), Information theory and an extension of the maximum likelihood principle, in C. F. Petrov BN, ed., ‘Second international symposium on information theory’, Akademinai Kiado, Budapest, pp. 267–281.
- Akoumianaki, I and A Nicolaidou (2007), ‘Spatial variability and dynamics of macrobenthos in a Mediterranean delta front area: the role of physical processes’, *Journal of Sea Research* **57**(1), 47–64.
- Aldebert, Y and L Recasens (1996), ‘Comparison of methods for stock assessment of European hake *Merluccius merluccius* in the Gulf of Lions (Northwestern Mediterranean)’, *Aquatic Living Resources* **9**(01), 13–22.
- Allredge, AL and MW Silver (1988), ‘Characteristics, dynamics and significance of marine snow’, *Progress in oceanography* **20**(1), 41–82.
- Allesina, S and RE Ulanowicz (2004), ‘Cycling in ecological networks: Finn’s index revisited’, *Computational biology and chemistry* **28**(3), 227–233.
- Alonzo, SH, PV Switzer and M Mangel (2003), ‘An ecosystem-based approach to management: using individual behaviour to predict the indirect effects of Antarctic krill fisheries on penguin foraging’, *Journal of Applied Ecology* **40**(4), 692–702.

- Anderson, J, N Carvalho, F Contini and J Virtanen (2012), 'The 2012 Annual Economic Report on the EU Fishing Fleet (STECF-12-10)', *Technical report. Scientific, Technical and Economic Committee for Fisheries European Commissions. Luksemburg* .
- Anderson, MJ (2001), 'A new method for non-parametric multivariate analysis of variance', *Austral Ecology* **26**(1), 32–46.
- Anderson, MJ and C Ter Braak (2003), 'Permutation tests for multi-factorial analysis of variance', *Journal of Statistical Computation and Simulation* **73**(2), 85–113.
- Anderson, MJ and P Legendre (1999), 'An empirical comparison of permutation methods for tests of partial regression coefficients in a linear model', *Journal of Statistical Computation and Simulation* **62**(3), 271–303.
- Andersson, JH, JWM Wijsman, PMJ Herman, JJ Middelburg, K Soetaert and C Heip (2004), 'Respiration patterns in the deep ocean', *Geophysical Research Letters* **31**(3).
- Angelini, R and AA Agostinho (2005), 'Parameter estimates for fishes of the upper Paraná River floodplain and Itaipu reservoir (Brazil)', *Naga, Worldfish Center Quarterly* **28**(1–2), 53–57.
- Arntz, WE, VA Gallardo, D Gutiérrez, E Isla, LA Levin, J Mendo, C Neira, GT Rowe, J Tarazona and M Wolff (2006), 'El Niño and similar perturbation effects on the benthos of the Humboldt, California, and Benguela Current upwelling ecosystems', *Advances in Geosciences* **6**, 243–265.
- Aronson, RB (1989), 'Brittlestar beds: low-predation anachronisms in the British Isles', *Ecology* **70**(4), 856–865.
- Aronson, RB (1990), 'Onshore-offshore patterns of human fishing activity', *Palaios* **5**(1), 88–93.
- Aronson, RB (1992), 'Biology of a scale-independent predator-prey interaction', *Marine Ecology Progress Series* **89**(1), 1–13.
- Ascher, UM and LR Petzold (1998), *Computer methods for ordinary differential equations and differential-algebraic equations*, Vol. 61, Society for Industrial and Applied Mathematics, Philadelphia.
- Azov, Y (1991), 'Eastern Mediterranean - a marine desert?', *Marine Pollution Bulletin* **23**, 225–232.
- Báez, JC, JM Ortiz de Urbina, R Real and D Macías (2011), 'Cumulative effect of the North Atlantic Oscillation on age-class abundance of albacore (*Thunnus alalunga*)', *Journal of Applied Ichthyology* **27**(6), 1356–1359.

- Baldwin, RJ, RC Glatts and KL Smith Jr (1998), 'Particulate matter fluxes into the benthic boundary layer at a long time-series station in the abyssal NE Pacific: composition and fluxes', *Deep Sea Research Part II: Topical Studies in Oceanography* **45**(4–5), 643–665.
- Bannerot, SP and CB Austin (1983), 'Using Frequency Distributions of Catch per Unit Effort to Measure Fish-Stock Abundance', *Transactions of the American Fisheries Society* **112**, 608–617.
- Baretta-Bekker, JG, JW Baretta and W Ebenhöh (1997), 'Microbial dynamics in the marine ecosystem model ERSEM II with decoupled carbon assimilation and nutrient uptake', *Journal of Sea Research* **38**(3), 195–211.
- Bas, C, F Maynou, F Sardà and J Lleonart (2003), *Variacions demogràfiques a les poblacions d'espècies demersals explotades: els darrers quaranta anys a Blanes i Barcelona*, Vol. 135, Institut d'Estudis Catalans. Arxiu de la Secció de Ciències, Barcelona.
- Bax, NJ (1985), 'Application of multi- and univariate techniques of sensitivity analysis to SKEBUB, a biomass-based fisheries ecosystem model, parameterized to Georges Bank', *Ecological Modelling* **29**(1), 353–382.
- Begley, J and D Howell (2004), 'An overview of Gadget, the Globally applicable Area-Disaggregated General Ecosystem Toolbox ICES CM 2004/FF: 13'.  
**URL:** <http://www.hafro.is/gadget>
- Belitz, C, A Brezger, T Kneib, S Lang and N Umlauf (2012), 'Bayesx, 2012. - Software for Bayesian inference in structured additive regression models. Version 2.1'.  
**URL:** <http://www.bayesx.org>
- Bell, JD (1983), 'Effects of depth and marine reserve fishing restrictions on the structure of a rocky reef fish assemblage in the north-western Mediterranean Sea', *Journal of Applied Ecology* pp. 357–369.
- Bellan-Santini, D (1990), 'Mediterranean deep-sea amphipods: composition, structure and affinities of the fauna', *Progress in Oceanography* **24**(1), 275–287.
- Bersier, LF, C Banasek-Richter and MF Cattin (2002), 'Quantitative descriptors of food-web matrices', *Ecology* **83**(9), 2394–2407.
- Bertignac, M, P Lehodey and J Hampton (1998), 'A spatial population dynamics simulation model of tropical tunas using a habitat index based on environmental parameters', *Fisheries Oceanography* **7**(3–4), 326–334.

- Bertrand, JA, LG de Sola, C Papaconstantinou, G Relini and A Souplet (2002), 'The general specifications of the MEDITS surveys', *Scientia Marina* **66**, 9 – 17.
- Beverton, RJH and SJ Holt (1957), *On the dynamics of exploited fish populations*, Chapman & Hall, London.
- Bianchini, ML and S Ragonese (1994), Life cycles and fisheries of the deep-water red shrimps *Aristaeomorpha foliacea* and *Aristeus antennatus*, in 'Proceedings of the International workshop held in the Istituto di Tecnologia della Pesca e del Pescato, Mazara del Vallo. NTR-ITPP Special Publication', Vol. 3, pp. 1–87.
- Billett, DSM, RS Lampitt, AL Rice and RFC Mantoura (1983), 'Seasonal sedimentation of phytoplankton to the deep-sea benthos', *Nature* **302**(5908), 520 – 522.
- Bishop, J, WN Venables and Y-G Wang (2004), 'Analysing commercial catch and effort data from a Penaeid trawl fishery: A comparison of linear models, mixed models, and generalised estimating equations approaches', *Fisheries Research* **70**(2–3), 179 – 193.
- Bodin, N, F Le Loc'h and C Hily (2007), 'Effect of lipid removal on carbon and nitrogen stable isotope ratios in crustacean tissues', *Journal of Experimental Marine Biology and Ecology* **341**(2), 168–175.
- Bogstad, B, KH Hauge and Ø Ulltang (1997), 'MULTSPEC—a multi-species model for fish and marine mammals in the Barents Sea', *Journal of Northwest Atlantic Fishery Science* **22**, 317–341.
- Botsford, LW, JC Castilla and CH Peterson (1997), 'The management of fisheries and marine ecosystems', *Science* **277**(5325), 509–515.
- Brander, KM (2005), 'Cod recruitment is strongly affected by climate when stock biomass is low', *ICES Journal of Marine Science* **62**(3), 339–343.
- Brauner, N and M Shacham (1998), 'Role of range and precision of the independent variable in regression of data', *AIChE journal* **44**(3), 603–611.
- Brey, T (2001), 'Population dynamics in benthic invertebrates. A virtual handbook. Version 01.2.'.   
**URL:** <http://www.thomas-brey.de/science/virtualhandbook/navlog/index.html>
- Brezger, A and S Lang (2006), 'Generalized structured additive regression based on Bayesian P-splines', *Computational Statistics & Data Analysis* **50**(4), 967 – 991.
- Brodziak, J and L O'Brien (2005), 'Do environmental factors affect recruits per spawner anomalies of New England groundfish?', *ICES Journal of Marine Science: Journal du Conseil* **62**(7), 1394–1407.

- Broecker, WS (1991), 'The great ocean conveyor', *Oceanography* **4**(2), 79–89.
- Brown, JH and JF Gillooly (2003), 'Ecological food webs: high-quality data facilitate theoretical unification', *Proceedings of the National Academy of Sciences* **100**(4), 1467–1468.
- Brynjarsdóttir, J and G Stefánsson (2004), 'Analysis of cod catch data from Icelandic groundfish surveys using generalized linear models', *Fisheries Research* **70**(2–3), 195–208.
- Buchanan, JB (1964), 'A comparative study of some features of the biology of *Amphiura filiformis* and *Amphiura chiajei* (Ophiuroidea) considered in relation to their distribution', *Journal of the Marine Biological Association of the UK* **44**, 565–576.
- Buesseler, KO, CH Lamborg, PW Boyd, PJ Lam, TW Trull, RR Bidigare, JKB Bishop, KL Casciotti, F Dehairs, M Elskens, M Honda, DM Karl, DA Siegel, MW Silver, DK Steinberg, J Valdes, B Van Mooy and S Wilson (2007), 'Revisiting carbon flux through the ocean's twilight zone', *Science* **316**(5824), 567–570.
- Buhl-Mortensen, L, A Vanreusel, AJ Gooday, LA Levin, IG Priede, P Buhl-Mortensen, H Gheerardyn, NJ King and M Raes (2010), 'Biological structures as a source of habitat heterogeneity and biodiversity on the deep ocean margins', *Marine Ecology* **31**(1), 21–50.
- Burd, AB, DA Hansell, DK Steinberg, TR Anderson, J Arístegui, F Baltar, SR Beupre, KO Buesseler, F DeHairs, GA Jackson, DC Kadko, R Koppelman, Lampitt RS, T Nagata, T Reinthaler, C Robinson, BC Robison, C Tamburini and T Tanaka (2010), 'Assessing the apparent imbalance between geochemical and biochemical indicators of meso- and bathypelagic biological activity: What the \$#! is wrong with present calculations of carbon budgets?', *Deep Sea Research Part II: Topical Studies in Oceanography* **57**(16), 1557–1571.
- Burdige, DJ, WM Berelson, KH Coale, J McManus and KS Johnson (1999), 'Fluxes of dissolved organic carbon from California continental margin sediments', *Geochimica et Cosmochimica Acta* **63**(10), 1507–1515.
- Buscail, R, R Pocklington and C Germain (1995), 'Seasonal variability of the organic matter in a sedimentary coastal environment: sources, degradation and accumulation (continental shelf of the Gulf of Lions/northwestern Mediterranean Sea)', *Continental Shelf Research* **15**(7), 843–869.



- Buscail, R, R Pocklington, R Daumas and L Guidi (1990), 'Fluxes and budget of organic matter in the benthic boundary layer over the northwestern Mediterranean margin', *Continental Shelf Research* **10**(9), 1089–1122.
- Butterworth, DS and RB Thomson (1995), 'Possible effects of different levels of krill fishing on predators—some initial modelling attempts', *Commission for the Conservation of Antarctic Marine Living Resources Science* **2**, 79–97.
- Caddy, JF (1983), 'The cephalopods: factors relevant to their population dynamics and to the assessment and management of stocks', *Advances in assessment of world cephalopod resources. FAO Fisheries Technical Paper* **231**, 416–449.
- Canals, M, R Danovaro, S Heussner, V Lykousis, P Puig, F Trincardi, A Calafat, X Durrieu de Madron, A Palanques and A Sánchez-Vidal (2009), 'Cascades in Mediterranean submarine grand canyons', *Oceanography* **22**(1), 26–43.
- Carbonell, A, J Lloret and M Demestre (2008), 'Relationship between condition and recruitment success of red shrimp (*Aristeus antennatus*) in the Balearic Sea (Northwestern Mediterranean)', *Journal of Marine Systems* **71**(3), 403–412.
- Carbonell, A, M Carbonell, M Demestre, A Grau and S Monserrat (1999), 'The red shrimp *Aristeus antennatus* (Risso, 1816) fishery and biology in the Balearic Islands, Western Mediterranean', *Fisheries Research* **44**(1), 1–13.
- Cardinale, M, GC Osio and A (eds) Charef (2012), 'Report of the Scientific, Technical and Economic Committee for Fisheries on Assessment of Mediterranean Sea stocks part 1.', *JRC Scientific and Policy Reports. European Commission* .
- Cardona, L, M Sales and D López (2007), 'Changes in fish abundance do not cascade to sea urchins and erect algae in one of the most oligotrophic parts of the Mediterranean', *Estuarine Coastal and Shelf Science* **72**(1), 273–282.
- Carpenter, JH (1965), 'The Chesapeake Bay Institute technique for the Winkler dissolved oxygen method', *Limnology and Oceanography* **10**(1), 141–143.
- Carpenter, SR and JF Kitchell (1988), 'Consumer control of lake productivity', *BioScience* pp. 764–769.
- Carpenter, SR, JF Kitchell and JR Hodgson (1985), 'Cascading trophic interactions and lake productivity', *BioScience* **35**(10), 634–639.
- Carpenter, SR, JJ Cole, JR Hodgson, JF Kitchell, ML Pace, D Bade, KL Cottingham, TE Essington, JN Houser and DE Schindler (2001), 'Trophic cascades, nutrients, and lake productivity: whole-lake experiments', *Ecological Monographs* **71**(2), 163–186.

- Carpine, C (1970), 'Écologie de l'étage bathyal dans la Méditerranée occidentale', *Mémoires de l'Institut Océanographique de Monaco* **2**, 1–146.
- Carrassón, M and JE Cartes (2002), 'Trophic relationships in a Mediterranean deep-sea fish community: partition of food resources, dietary overlap and connections within the benthic boundary layer', *Marine Ecology Progress Series* **241**, 41–55.
- Cartes, JE (1994), 'Influence of depth and season on the diet of the deep-water aristeid *Aristeus antennatus* along the continental slope (400 to 2300 m) in the Catalan Sea (western Mediterranean)', *Marine Biology* **120**(4), 639–648.
- Cartes, JE (1998), 'Dynamics of the bathyal Benthic Boundary Layer in the north-western Mediterranean: depth and temporal variations in macrofaunal–megafaunal communities and their possible connections within deep-sea trophic webs', *Progress in Oceanography* **41**(1), 111–139.
- Cartes, JE, A Grémare, F Maynou, S Villora-Moreno and A Dinet (2002), 'Bathymetric changes in the distributions of particulate organic matter and associated fauna along a deep-sea transect down the Catalan sea slope (Northwestern Mediterranean)', *Progress in Oceanography* **53**(1), 29–56.
- Cartes, JE, C LoIacono, V Mamouridis, C López-Pérez and P Rodríguez (2013), 'Geomorphological, trophic and human influences on the bamboo coral *Isidella elongata* assemblages in the deep Mediterranean: To what extent does *Isidella* form habitat for fish and invertebrates?', *Deep Sea Research Part I: Oceanographic Research Papers* **76**, 52–65.
- Cartes, JE, D Jaume and T Madurell (2003), 'Local changes in the composition and community structure of suprabenthic peracarid crustaceans on the bathyal Mediterranean: influence of environmental factors', *Marine Biology* **143**(4), 745–758.
- Cartes, JE, E Fanelli, D Lloris and J Matallanas (2013), 'Effect of environmental variations on sharks and other top predators in the deep Mediterranean Sea over the last 60 years', *Climate Research* **55**(3), 239–251.
- Cartes, JE, E Fanelli, V Papiol and F Maynou (2010), 'Trophic relationships at intrannual spatial and temporal scales of macro and megafauna around a submarine canyon off the Catalanian coast (western Mediterranean)', *Journal of Sea Research* **63**(3), 180–190.
- Cartes, JE and F Maynou (1998), 'Food consumption by bathyal decapod crustacean assemblages in the western Mediterranean: predatory impact of megafauna and the

- food consumption-food supply balance in a deep-water food web', *Marine Ecology Progress Series* **171**, 233–246.
- Cartes, JE, F Maynou and E Fanelli (2011), 'Nile damming as plausible cause of extinction and drop in abundance of deep-sea shrimp in the western Mediterranean over broad spatial scales', *Progress in Oceanography* **91**(3), 286–294.
- Cartes, JE, F Maynou, E Fanelli, C Romano, V Mamouridis and V Papiol (2009), 'The distribution of megabenthic, invertebrate epifauna in the Balearic Basin (western Mediterranean) between 400 and 2300 m: Environmental gradients influencing assemblages composition and biomass trends', *Journal of Sea Research* **61**(4), 244–257.
- Cartes, JE, F Maynou, F Sardà, JB Company, D. Lloris and S Tudela (2004), *The Mediterranean deep-sea ecosystems: an overview of their diversity, structure, functioning and anthropogenic impacts, with a proposal for conservation*, Málaga, IUCN and Rome, WWF, chapter Part I. The Mediterranean deep-sea ecosystems: an overview of their diversity, structure, functioning and anthropogenic impacts, pp. 9–38.
- Cartes, JE, F Maynou, P Abelló, M Emelianov, LG de Sola and M Solé (2011), 'Long-term changes in the abundance and deepening of the deep-sea shrimp *Aristaeomorpha foliacea* in the Balearic Basin: Relationships with hydrographic changes at the Levantine Intermediate Water', *Journal of Marine Systems* **88**(4), 516–525.
- Cartes, JE and F Sardà (1992), 'Abundance and diversity of decapod crustaceans in the deep-Catalan sea (western Mediterranean)', *Journal of Natural History* **26**, 1305–1323.
- Cartes, JE and F Sardà (1993), 'Zonation of deep-sea decapod fauna in the Catalan Sea (Western Mediterranean)', *Marine Ecology Progress Series* **94**, 27–27.
- Cartes, JE and JC Sorbe (1996), 'Temporal population structure of deep-water cumaceans from the western Mediterranean slope', *Deep Sea Research Part I: Oceanographic Research Papers* **43**(9), 1423–1438.
- Cartes, JE and JC Sorbe (1999), 'Deep-water amphipods from the Catalan Sea slope (western Mediterranean): Bathymetric distribution, assemblage composition and biological characteristics', *Journal of Natural History* **33**(8), 1133–1158.
- Cartes, JE, T Brey, JC Sorbe and F Maynou (2002), 'Comparing production biomass ratios of benthos and suprabenthos in macrofaunal marine crustaceans', *Canadian journal of fisheries and aquatic sciences* **59**(10), 1616–1625.

- Cartes, JE, T Madurell, E Fanelli and JL López-Jurado (2008), 'Dynamics of suprabenthos-zooplankton communities around the Balearic Islands (western Mediterranean): Influence of environmental variables and effects on the biological cycle of *Aristeus antennatus*', *Journal of Marine Systems* **71**(3), 316–335.
- Cartes, JE, V Mamouridis and E Fanelli (2011), 'Deep-sea suprabenthos assemblages (Crustacea) off the Balearic Islands (western Mediterranean): Mesoscale variability in diversity and production', *Journal of Sea Research* **65**(3), 340–354.
- Cartes, JE, V Papiol, A Palanques, J Guillén and M Demestre (2007), 'Dynamics of suprabenthos off the Ebro Delta (Catalan Sea: western Mediterranean): Spatial and temporal patterns and relationships with environmental factors', *Estuarine, Coastal and Shelf Science* **75**(4), 501–515.
- Cartes, JE, V Papiol and B Guijarro (2008), 'The feeding and diet of the deep-sea shrimp *Aristeus antennatus* off the Balearic Islands (Western Mediterranean): Influence of environmental factors and relationship with the biological cycle', *Progress in Oceanography* **79**(1), 37–54.
- Casini, M, J Lövgren, J Hjelm, M Cardinale, J-C Molinero and G Kornilovs (2008), 'Multi-level trophic cascades in a heavily exploited open marine ecosystem', *Proceedings of the Royal Society B: Biological Sciences* **275**(1644), 1793–1801.
- Cattin, MF, LF Bersier, C Banašek-Richter, R Baltensperger and JP Gabriel (2004), 'Phylogenetic constraints and adaptation explain food-web structure', *Nature* **427**(6977), 835–839.
- Christensen, V (1998), 'Fishery-induced changes in a marine ecosystem: insight from models of the Gulf of Thailand', *Journal of Fish Biology* **53**(sA), 128–142.
- Christensen, V and CJ Walters (2004), 'Ecopath with Ecosim: methods, capabilities and limitations', *Ecological Modelling* **172**(2), 109–139.
- Christensen, V and D Pauly (1992), 'ECOPATH IIa software for balancing steady-state ecosystem models and calculating network characteristics', *Ecological Modelling* **61**(3), 169–185.
- Christensen, V, S Guenette, JJ Heymans, CJ Walters, R Watson, D Zeller and D Pauly (2003), 'Hundred-year decline of North Atlantic predatory fishes', *Fish and Fisheries* **4**(1), 1–24.
- Clarke, KR (1993), 'Non-parametric multivariate analyses of changes in community structure', *Australian Journal of Ecology* **18**(1), 117–143.

- Clarke, KR and RM Warwick (1994), *Change in marine communities: an approach to statistical analysis and interpretation*, Natural Environment Research Council Plymouth.
- Clarke, KR and RN Gorley (2006), 'PRIMER V6: user manual/tutorial', *Primer-E Ltd. Plymouth*.
- Coelho, R and K Erzini (2008), 'Life history of a wide-ranging deepwater lantern shark in the north-east Atlantic, *Etmopterus spinax* (Chondrichthyes: Etmopteridae), with implications for conservation', *Journal of Fish Biology* **73**(6), 1419–1443.
- Cohen, JE and CM Newman (1985), 'A stochastic theory of community food webs: I. Models and aggregated data', *Proceedings of the Royal society of London. Series B. Biological sciences* **224**(1237), 421–448.
- Coll, M, A Santojanni, I Palomera, S Tudela and E Arneri (2007), 'An ecological model of the Northern and Central Adriatic Sea: analysis of ecosystem structure and fishing impacts', *Journal of Marine Systems* **67**(1), 119–154.
- Coll, M, H K Lotze and TN Romanuk (2008), 'Structural degradation in Mediterranean Sea food webs: testing ecological hypotheses using stochastic and mass-balance modelling', *Ecosystems* **11**(6), 939–960.
- Coll, M, I Palomera, S Tudela and F Sardà (2006), 'Trophic flows, ecosystem structure and fishing impacts in the South Catalan Sea, Northwestern Mediterranean', *Journal of Marine Systems* **59**(1), 63–96.
- Coll, M and S Libralato (2012), 'Contributions of food web modelling to the ecosystem approach to marine resource management in the Mediterranean Sea', *Fish and Fisheries* **13**(1), 60–88.
- Coll, M, S Libralato, S Tudela, I Palomera and F Pranovi (2008), 'Ecosystem overfishing in the ocean', *PLoS one* **3**(12), e3881.
- Colloca, F, M Cardinale, A Belluscio and G Ardizzone (2003), 'Pattern of distribution and diversity of demersal assemblages in the central Mediterranean sea', *Estuarine, Coastal and Shelf Science* **56**(3), 469–480.
- Colomb, A, J Le Fur and D Gascuel (2004), MOOVES: an individual-based model to study the functioning of a tropical ecosystem and its reaction to fishing pressure, in 'The Fourth European Conference on Ecological Modelling ECEM 2004', pp. 37–38.

- Company, JB and F Sardà (1998), 'Metabolic rates and energy content of deep-sea benthic decapod crustaceans in the western Mediterranean Sea', *Deep-Sea Research Part I* **45**(11), 1861–1880.
- Constable, AJ (2006), Using the EPOC modelling framework to assess management procedures for Antarctic krill in Statistical Area 48: evaluating spatial differences in productivity of Antarctic krill, in 'Workshop document presented to WG-EMM subgroup of CCAMLR. Commission for the Conservation of Antarctic Marine Living Resources. WG-EMM-06/38'.
- Cooper, AB, A Rosenberg, G Stefansson and M Mangel (2004), 'Examining the importance of consistency in multi-vessel trawl survey design based on the U.S. west coast groundfish bottom trawl survey', *Fisheries Research* **70**(2-3), 239–250.
- Corliss, BH (1979), 'Size variation in the deep-sea benthonic foraminifer *Globocassidulina subglobosa* (Brady) in the southeast Indian Ocean', *The Journal of Foraminiferal Research* **9**(1), 50–60.
- Craven, P and G Wahba (1979), 'Smoothing noisy data with spline functions: estimating the correct degree of smoothing by the method of generalised cross-validation', *Numerische Mathematik* **31**(4), 377–403.
- Curdia, J, S Carvalho, A Ravara, JD Gage, AM Rodrigues and V Quintino (2004), 'Deep macrobenthic communities from Nazaré submarine canyon (NW Portugal)', *Scientia Marina* **68**(1), 171–180.
- Cury, P, A Bakun, RJM Crawford, A Jarre, RA Quiñones, LJ Shannon and HM Verheye (2000), 'Small pelagics in upwelling systems: patterns of interaction and structural changes in "wasp-waist" ecosystems', *ICES Journal of Marine Science: Journal du Conseil* **57**(3), 603–618.
- Cury, P and L Shannon (2004), 'Regime shifts in upwelling ecosystems: observed changes and possible mechanisms in the northern and southern Benguela', *Progress in Oceanography* **60**(2), 223–243.
- Cury, P, L Shannon and YJ Shin (2003), *Responsible fisheries in the marine ecosystem*, CABI, chapter The Functioning of Marine Ecosystems: a Fisheries Perspective, pp. 103–123.
- Damalas, D, P Megalofonou and M Apostolopoulou (2007), 'Environmental, spatial, temporal and operational effects on swordfish (*Xiphias gladius*) catch rates of eastern Mediterranean Sea longline fisheries', *Fisheries Research* **84**(2), 233–246.

- Danovaro, R, A Dinet, G Duineveld and A Tselepides (1999), 'Benthic response to particulate fluxes in different trophic environments: a comparison between the Gulf of Lions–Catalan Sea (western-Mediterranean) and the Cretan Sea (eastern-Mediterranean)', *Progress in Oceanography* **44**(1), 287–312.
- Danovaro, R and M Serresi (2000), 'Viral density and virus-to-bacterium ratio in deep-sea sediments of the Eastern Mediterranean', *Applied and environmental microbiology* **66**(5), 1857–1861.
- Danovaro, R, N Della Croce, A Eleftheriou, M Fabiano, N Papadopoulou, C Smith and A Tselepides (1995), 'Meiofauna of the deep Eastern Mediterranean Sea: distribution and abundance in relation to bacterial biomass, organic matter composition and other environmental factors', *Progress in oceanography* **36**(4), 329–341.
- Daskalov, Georgi M, Alexander N Grishin, Sergei Rodionov and Vesselina Mihneva (2007), 'Trophic cascades triggered by overfishing reveal possible mechanisms of ecosystem regime shifts', *Proceedings of the National Academy of Sciences* **104**(25), 10518–10523.
- Dauwe, B, PMJ Herman, CHR Heip et al. (1998), 'Community structure and bioturbation potential of macrofauna at four North Sea stations with contrasting food supply', *Marine Ecology Progress Series* **173**, 67–83.
- Day, JH (1967), *A monograph on the Polychaeta of southern Africa*, British Museum (Natural History), London.
- de Forges, BR, JA Koslow and GCB Poore (2000), 'Diversity and endemism of the benthic seamount fauna in the southwest Pacific', *Nature* **405**(6789), 944–947.
- de Juan, S and JE Cartes (2011), 'Influence of environmental factors on the dynamics of macrobenthic crustaceans on soft-bottoms of the Ebro Delta continental shelf (northwestern Mediterranean)'.
- de Ruiter, PC, V Wolters and JC Moore (2005), *Dynamic food webs: multispecies assemblages, ecosystem development and environmental change*, Vol. 3, Academic Press.
- DeAngelis, DL (1980), 'Energy flow, nutrient cycling, and ecosystem resilience', *Ecology* pp. 764–771.
- DeAngelis, DL and LJ Gross (1992), *Individual-based models and approaches in ecology: populations, communities and ecosystems.*, Chapman & Hall.
- Demestre, M (1995), '*Aristeus antennatus* (Decapoda: Dendrobranchiata)', *Marine Ecology Progress Series* **127**, 57–64.

- Demestre, M and J Lleonart (1993), 'Population dynamics of *Aristeus antennatus* (Decapoda: Dendrobranchiata) in the northwestern Mediterranean', *Scientia Marina* **57**(2–3), 183–189.
- Demestre, M and JM Fortuño (2013), 'Reproduction of the deepwater shrimp *Aristeus antennatus* (Decapoda: Dendrobranchiata)', *Marine Ecology Progress Series* **84**, 41–51.
- Demirov, E and N Pinardi (2002), 'Simulation of the Mediterranean Sea circulation from 1979 to 1993: Part I. The interannual variability', *Journal of Marine Systems* **33**, 23–50.
- Denis, V (2002), 'Spatio-temporal analysis of commercial trawler data using General Additive models: patterns of Loliginid squid abundance in the north-east Atlantic', *ICES Journal of Marine Science* **59**(3), 633–648.
- Dennard, ST, MA MacNeil, MA Treble, S Campana and AT Fisk (2010), 'Hierarchical analysis of a remote, Arctic, artisanal longline fishery', *ICES Journal of Marine Science: Journal du Conseil* **67**(1), 41–51.
- Deuser, WG, EH Ross and RF Anderson (1981), 'Seasonality in the supply of sediment to the deep Sargasso Sea and implications for the rapid transfer of matter to the deep ocean', *Deep Sea Research Part A. Oceanographic Research Papers* **28**(5), 495–505.
- Devine, JA, KD Baker and RL Haedrich (2006), 'Fisheries: deep-sea fishes qualify as endangered', *Nature* **439**(7072), 29–29.
- Diffendorfer, JE, PM Richards, GH Dalrymple and DL DeAngelis (2001), 'Applying Linear Programming to estimate fluxes in ecosystems or food webs: an example from the herpetological assemblage of the freshwater Everglades', *Ecological Modelling* **144**(2), 99–120.
- D'Onghia, G, P Maiorano, L Sion, A Giove, F Capezzuto, R Carlucci and A Tursi (2010), 'Effects of deep-water coral banks on the abundance and size structure of the megafauna in the Mediterranean Sea', *Deep Sea Research Part II: Topical Studies in Oceanography* **57**(5), 397–411.
- D'ortenzio, F and M Ribera d'Alcalà (2009), 'On the trophic regimes of the Mediterranean Sea: a satellite analysis', *Biogeosciences* **6**(2), 139–148.
- Duda, AM and K Sherman (2002), 'A new imperative for improving management of large marine ecosystems', *Ocean & Coastal Management* **45**(11), 797–833.



- Duffy, JE (2003), 'Biodiversity loss, trophic skew and ecosystem functioning', *Ecology Letters* **6**(8), 680–687.
- Dulvy, NK, Y Sadovy and JD Reynolds (2003), 'Extinction vulnerability in marine populations', *Fish and Fisheries* **4**(1), 25–64.
- Durrieu De Madron, X, A Abassi, S Heussner, A Monaco, JC Aloisi, O Radakovitch, P Giresse, R Buscail and P Kerherve (2000), 'Particulate matter and organic carbon budgets for the Gulf of Lions (NW Mediterranean)', *Oceanologica Acta* **23**(6), 717–730.
- Eilers, PHC and BD Marx (1996), 'Flexible Smoothing with *B*-splines and Penalties', *Statistical Science* **11**(2), 89–102.
- Elnor, RW and RL Vadas Sr (1990), 'Inference in ecology: the sea urchin phenomenon in the northwestern Atlantic', *American Naturalist* pp. 108–125.
- Epping, E, C van der Zee, K Soetaert and W Helder (2002), 'On the oxidation and burial of organic carbon in sediments of the Iberian margin and Nazaré Canyon (NE Atlantic)', *Progress in Oceanography* **52**(2), 399–431.
- Estes, JA, J Terborgh, JS Brashares, ME Power, J Berger, WJ Bond, SR Carpenter, TE Essington, RD Holt and JBC Jackson (2011), 'Trophic downgrading of planet earth', *Science* **333**(6040), 301–306.
- Estes, JA and JF Palmisano (1974), 'Sea otters: their role in structuring nearshore communities', *Science* **185**(4156), 1058–1060.
- Estes, JA, MT Tinker, TM Williams and DF Doak (1998), 'Killer whale predation on sea otters linking oceanic and nearshore ecosystems', *Science* **282**(5388), 473–476.
- Estrada, M (1996), 'Primary production in the northwestern Mediterranean', *Scientia Marina* **60**, 55–64.
- Estrada, M and R Margalef (1988), 'Supply of nutrients to the Mediterranean photic zone along a persistent front', *Oceanologica Acta* **9**, 133–142.
- Fahrmeir, L, T Kneib and S Lang (2004), 'Penalized structured additive regression for space-time data: a Bayesian perspective', *Statistica Sinica* **14**(3), 731–762.
- Fanelli, E and JE Cartes (2008), 'Spatio-temporal changes in gut contents and stable isotopes in two deep Mediterranean pandalids: influence on the reproductive cycle', *Marine Ecology Progress Series* **355**, 219–233.

- Fanelli, E and JE Cartes (2010), 'Temporal variations in the feeding habits and trophic levels of three deep-sea demersal fishes from the western Mediterranean Sea, based on stomach contents and stable isotope analyses', *Marine Ecology Progress Series* **402**, 213–232.
- Fanelli, E, JE Cartes, P Rumolo and M Sprovieri (2009), 'Food-web structure and trophodynamics of mesopelagic–suprabenthic bathyal macrofauna of the Algerian Basin based on stable isotopes of carbon and nitrogen', *Deep Sea Research Part I: Oceanographic Research Papers* **56**(9), 1504–1520.
- Fanelli, E, JE Cartes and V Papiol (2011), 'Food web structure of deep-sea macrozooplankton and micronekton off the Catalan slope: insight from stable isotopes', *Journal of Marine Systems* **87**(1), 79–89.
- Fanelli, E, V Papiol, JE Cartes, P Rumolo, C Brunet and M Sprovieri (2011), 'Food web structure of the epibenthic and infaunal invertebrates on the Catalan slope (NW Mediterranean): Evidence from  $\delta^{13}\text{C}$  and  $\delta^{15}\text{N}$  analysis', *Deep Sea Research Part I: Oceanographic Research Papers* **58**(1), 98–109.
- FAO (2003), *Fisheries management 2: The ecosystem approach to fisheries. FAO Technical Guidelines for Responsible Fisheries*, Vol. 4, FAO, Rome, Italy.
- FAO (2009), *Rapport de la trente-troisième session de la Commission générale des pêches pour la Méditerranée (CGPM)*, FAO, Rome, Italy.
- FAO/FISHSTAT (2011), 'FAO Fisheries Department, Fishery information, Data and Statistics Unit. FishstatJ, a tool for fishery statistical analysis, release 2.0.0'.
- Fath, BD and BC Patten (1999), 'Review of the foundations of network environ analysis', *Ecosystems* **2**(2), 167–179.
- Fauchald, K and PA Jumars (1979), *The diet of worms: a study of polychaete feeding guilds*, Aberdeen University Press, Aberdeen.
- Felleman, FL, JR Heimlich-Boran and RW Osborne (1991), 'The feeding ecology of killer whales (*Orcinus orca*) in the Pacific Northwest', *Dolphin societies: discoveries and puzzles* pp. 113–147.
- Féral, J-P, J-G Ferrand and A Guille (1990), 'Macrobenthic physiological responses to environmental fluctuations: the reproductive cycle and enzymatic polymorphism of a eurybathic sea-urchin on the northwestern Mediterranean continental shelf and slope', *Continental Shelf Research* **10**(9), 1147–1155.

- Fernandez-Arcaya, U, E Ramirez-Llodra, G Rotllant, L Recasens, H Murua, I Quaggio-Grassiotto and JB Company (2013), 'Reproductive biology of two macrourid fish, *Nezumia aequalis* and *Coelorinchus mediterraneus*, inhabiting the NW Mediterranean continental margin (400–2000m)', *Deep Sea Research Part II: Topical Studies in Oceanography* **92**, 63–72.
- Ferretti, F, RA Myers, F Serena and HK Lotze (2008), 'Loss of large predatory sharks from the Mediterranean Sea', *Conservation Biology* **22**(4), 952–964.
- Finn, JT (1976), 'Measures of ecosystem structure and function derived from analysis of flows', *Journal of theoretical Biology* **56**(2), 363–380.
- Finn, JT (1980), 'Flow analysis of models of the Hubbard Brook ecosystem', *Ecology* **61**(3), 562–571.
- Finnoff, D and J Tschirhart (2003), 'Protecting an endangered species while harvesting its prey in a general equilibrium ecosystem model', *Land Economics* **79**(2), 160–180.
- Finnoff, D and J Tschirhart (2008), 'Linking dynamic economic and ecological general equilibrium models', *Resource and Energy Economics* **30**(2), 91–114.
- Fiorentino, F (2009), 'La situazione delle risorse ittiche nelle aree di pesca siciliane ed il contributo delle scienze della pesca per un nuovo sviluppo sostenibile. Rapporto Annuale sulla Pesca e sull'Acquacoltura in Sicilia 2009', *Osservatorio della Pesca del Mediterraneo* pp. 77–109.
- Flach, E and C Heip (1996), 'Vertical distribution of macrozoobenthos within the sediment on the continental slope of the Goban Spur area (NE Atlantic)', *Marine Ecology Progress Series* **141**(1), 55–66.
- Frank, KT, B Petrie, JS Choi and WC Leggett (2005), 'Trophic cascades in a formerly cod-dominated ecosystem', *Science* **308**(5728), 1621–1623.
- Frank, KT, B Petrie and NL Shackell (2007), 'The ups and downs of trophic control in continental shelf ecosystems', *Trends in Ecology & Evolution* **22**(5), 236–242.
- Frank, KT, B Petrie, NL Shackell and JS Choi (2006), 'Reconciling differences in trophic control in mid-latitude marine ecosystems', *Ecology Letters* **9**(10), 1096–1105.
- Fredj, G and L Laubier (1985), *Mediterranean Marine Ecosystems*, Plenum Press, New York, chapter The deep Mediterranean benthos, pp. 109–146.
- Fretwell, SD (1987), 'Food chain dynamics: the central theory of ecology?', *Oikos* pp. 291–301.

- Fromentin, JM and B Planque (1996), ‘*Calanus* and environment in the eastern North Atlantic. 2. Role of the North Atlantic Oscillation on *Calanus finmarchicus* and *C. helgolandicus*’, *Marine Ecology Progress Series* **134**, 11–118.
- Fulton, EA, ADM Smith and AE Punt (2005), ‘Which ecological indicators can robustly detect effects of fishing?’, *ICES Journal of Marine Science: Journal du Conseil* **62**(3), 540–551.
- Fulton, EA, ADM Smith and CR Johnson (2004), ‘Biogeochemical marine ecosystem models I: IGBEM-a model of marine bay ecosystems’, *Ecological Modelling* **174**(3), 267–307.
- Fulton, EA, JS Parslow, ADM Smith and CR Johnson (2004), ‘Biogeochemical marine ecosystem models II: the effect of physiological detail on model performance’, *Ecological Modelling* **173**(4), 371–406.
- Gage, JD and PA Tyler (1991), *Deep-sea biology: a natural history of organisms at the deep-sea floor*, Cambridge University Press.
- Galeron, J, L Menot, N Renaud, P Crassous, A Khripounoff, C Treignier and M Sibuet (2009), ‘Spatial and temporal patterns of benthic macrofaunal communities on the deep continental margin in the Gulf of Guinea’, *Deep Sea Research Part II: Topical Studies in Oceanography* **56**(23), 2299–2312.
- Garcia-Ladona, E, A Castellon, J Font and J Tintore (1996), ‘The Balearic current and volume transports in the Balearic basin’, *Oceanologica Acta* **19**(5), 489–497.
- García Rodríguez, M and A Esteban (1999), ‘On the biology and fishery of *Aristeus antennatus* (Risso, 1816),(Decapoda, Dendrobranchiata) in the Ibiza channel (Balearic Islands, Spain)’, *Scientia Marina* **63**(1), 27–37.
- García Rodríguez, M, JL Pérez Gil, A Esteban, N Carrasco and A Carbonell (2007), Stock assessment of red shrimp (*Aristeus antennatus*) exploited by the Spanish trawl fishery (1996–2006) in the Geographical Sub-Area 06 (Northern Spain), in ‘Scientific Advisory Committee of the GFCM 9th Meeting of the Sub-Committee on Stock Assessment (SCSA) Working Group on Demersals Document n° 2’, 10-12 September, Athens Greece.
- Garcia, S (1986), ‘Seasonal trawling bans can be very successful in heavily overfished areas: the “cyprus effect”’, *The WorldFish Center Working Papers* .
- Gardner, WD (1989), ‘Baltimore Canyon as a modern conduit of sediment to the deep sea’, *Deep Sea Research Part A. Oceanographic Research Papers* **36**(3), 323–358.

- Garrison, LP, JS Link, DP Kilduff, MD Cieri, B Muffley, DS Vaughan, A Sharov, B Mahmoudi and RJ Latour (2010), 'An expansion of the MSVPA approach for quantifying predator-prey interactions in exploited fish communities', *ICES Journal of Marine Science: Journal du Conseil* **67**(5), 856–870.
- Garstang, W (1900), 'The impoverishment of the sea. A critical summary of the experimental and statistical evidence bearing upon the alleged depletion of the trawling grounds', *Journal of the Marine Biological Association of the United Kingdom (New Series)* **6**(01), 1–69.
- Gaston, GR (1987), 'Benthic polychaeta of the Middle Atlantic Bight: feeding and distribution', *Marine Ecology Progress Series* **36**(3), 251–262.
- Gavaris, S (1980), 'Use of a Multiplicative Model to Estimate Catch Rate and Effort from Commercial Data', *Canadian Journal of Fisheries and Aquatic Sciences* **37**(12), 2272–2275.
- Gerino, M, G Stora and JP Durbec (1994), 'Quantitative estimation of biodiffusive and bioadvective sediment mixing-in-situ experimental approach', *Oceanologica acta* **17**(5), 547–554.
- Gili, JM, F Pages, J Bouillon, A Palanques, P Puig, S Heussner, A Calafat, M Canals and A Monaco (2000), 'A multidisciplinary approach to the understanding of hydromedusan populations inhabiting Mediterranean submarine canyons', *Deep Sea Research Part I: Oceanographic Research Papers* **47**(8), 1513–1533.
- Gili, JM, J Bouillon, A Palanques and P Puig (1999), 'Submarine canyons as habitats of prolific plankton populations: three new deep-sea Hydroidomedusae in the western Mediterranean', *Zoological Journal of the Linnean Society* **125**(3), 313–329.
- Glover, AG and CR Smith (2003), 'The deep-sea floor ecosystem: current status and prospects of anthropogenic change by the year 2025', *Environmental Conservation* **30**(3), 219–241.
- Glud, RN (2008), 'Oxygen dynamics of marine sediments', *Marine Biology Research* **4**(4), 243–289.
- Golub, GH, M Heath and G Wahba (1979), 'Generalized cross-validation as a method for choosing a good ridge parameter', *Technometrics* **21**(2), 215–223.
- Gontikaki, E, D van Oevelen, K Soetaert and U Witte (2011), 'Food web flows through a sub-arctic deep-sea benthic community', *Progress in Oceanography* **91**(3), 245–259.

- Gooday, AJ (1988), 'A response by benthic Foraminifera to the deposition of phytodetritus in the deep sea', *Nature* **332**(6159), 70 – 73.
- Gooday, AJ, CM Turley and JA Allen (1990), 'Responses by Benthic Organisms to Inputs of Organic Material to the Ocean Floor: A Review', *Philosophical Transactions of the Royal Society of London. Series A, Mathematical and Physical Sciences* **331**(1616), 119–138.
- Gordon, JDM (2001), 'Deep-water fisheries at the Atlantic Frontier', *Continental Shelf Research* **21**(8), 987–1003.
- Gori, A, C Orejas, T Madurell, L Bramanti, M Martins, E Quintanilla, P Marti-Puig, C Lo Iacono, P Puig and S Requena (2013), 'Bathymetrical distribution and size structure of cold-water coral populations in the Cap de Creus and Lacaze-Duthiers canyons (northwestern Mediterranean)', *Biogeosciences* **10**(3).
- Goutx, M, SG Wakeham, C Lee, M Duflos, C Guigue, Z Liu, B Moriceau, R Sempéré, M Tedetti and J Xue (2007), 'Composition and degradation of marine pArticles with different settling velocities in the northwestern Mediterranean Sea', *Limnology and oceanography* **52**(4), 1645.
- Grassle, FJ and HL Sanders (1973), 'Life histories and the role of disturbance', *Deep Sea Research and Oceanographic Abstracts* **20**(7), 643–659.
- Gremare, A, JM Amouroux and F Charles (1997), 'Temporal changes in the biochemical composition and nutritional value of the particulate organic matter available to surface deposit-feeders: a two year study', *Oceanographic Literature Review* **44**(9), 934–935.
- Griggs, GB, AG Carey Jr and LD Kulm (1969), 'Deep-sea sedimentation and sediment-fauna interaction in Cascadia Channel and on Cascadia Abyssal Plain', *Deep Sea Research and Oceanographic Abstracts* **16**(2), 157–170.
- Guidetti, P and E Sala (2007), 'Community-wide effects of marine reserves in the Mediterranean Sea', *Marine Ecology Progress Series* **335**, 43–56.
- Gulland, JA (1964), Catch per unit effort as a measure of abundance, in 'Rapport et PV de la Commission internationale pour l'Exploration Scientifique de la Mer Méditerranéer', Vol. 155, pp. 8–14.
- Haedrich, RL, NR Merrett and NR O'Dea (2001), 'Can ecological knowledge catch up with deep-water fishing? A North Atlantic perspective', *Fisheries Research* **51**(2), 113–122.

- Hairston, N, F Smith and L Slobodkin (1960), 'Community structure, population control and competition', *American Naturalist* **94**, 421–425.
- Hall Jr, RO and JL Meyer (1998), 'The trophic significance of bacteria in a detritus-based stream food web', *Ecology* **79**(6), 1995–2012.
- Hamre, J and E Hatlebakk (1998), System model (systmod) for the norwegian sea and the barents sea, in 'Models for multispecies management', Springer, pp. 93–115.
- Harris, PT and T Whiteway (2011), 'Global distribution of large submarine canyons: Geomorphic differences between active and passive continental margins', *Marine Geology* **285**(1), 69–86.
- Hastie, T and R Tibshirani (1986), 'Generalized additive models', *Statistical science* pp. 297–310.
- Hastie, TJ and RJ Tibshirani (1990), *Generalized additive models*, Chapman & Hall.
- Hecker, B (1990), 'Photographic evidence for the rapid flux of pArticles to the sea floor and their transport down the continental slope', *Deep Sea Research Part A. Oceanographic Research Papers* **37**(12), 1773–1782.
- Heleno, R, C Garcia, P Jordano, A Traveset, JM Gómez, N Blüthgen, J Memmott, M Moora, J Cerdeira, S Rodríguez-Echeverría, H Freitas and JM Olesen (2014), 'Ecological networks: delving into the architecture of biodiversity', *Biology letters* **10**(1), 20131000.
- Helser, TE, AE Punt and RD Methot (2004), 'A generalized linear mixed model analysis of a multi-vessel fishery resource survey', *Fisheries Research* **70**(2–3), 251 – 264.
- Herbland, A and B Voituriez (1979), 'Hydrological structure analysis for estimating the primary production in the tropical Atlantic Ocean', *Journal of Marine Research* **37**(1), 87–101.
- Hilborn, R and CJ Walters (1992), *Quantitative Fisheries Stock Assessment*, Chapman & Hall.
- Hirata, H and RE Ulanowicz (1984), 'Information theoretical analysis of ecological networks', *International journal of systems science* **15**(3), 261–270.
- Holling, CS (1959), 'The components of predation as revealed by a study of small-mammal predation of the European pine sawfly', *The Canadian Entomologist* **91**(05), 293–320.

- Hollowed, AB, N Bax, R Beamish, J Collie, M Fogarty, P Livingston, J Pope and JC Rice (2000), 'Are multispecies models an improvement on single-species models for measuring fishing impacts on marine ecosystems?', *ICES Journal of Marine Science: Journal du Conseil* **57**(3), 707–719.
- Holme, NA (1984), 'Fluctuations of *Ophiothrix fragilis* in the western English Channel', *Journal of the Marine Biological Association of the United Kingdom* **64**(02), 351–378.
- Hopkins, TS (1978), 'Physical processes in the Mediterranean basins', *Estuarine transport processes* pp. 269–310.
- Hughes, TP (1994), 'Catastrophes, phase shifts, and large-scale degradation of a Caribbean coral reef', *SCIENCE-NEW YORK THEN WASHINGTON* pp. 1547–1547.
- Hunter, MD and PW Price (1992), 'Playing chutes and ladders: heterogeneity and the relative roles of bottom-up and top-down forces in natural communities.', *Ecology* **73**(3), 723–732.
- Huvenne, VAI, PA Tyler, DG Masson, EH Fisher, C Hauton, V Hühnerbach, TP Le Bas and GA Wolff (2011), 'A picture on the wall: innovative mapping reveals cold-water coral refuge in submarine canyon', *PloS one* **6**(12), e28755.
- Huxel, GR and K McCann (1998), 'Food web stability: the influence of trophic flows across habitats.', *American Naturalist* **152**, 460–469.
- Jackson, JBC, MX Kirby, WH Berger, KA Bjorndal, LW Botsford, BJ Bourque, RH Bradbury, R Cooke, J Erlandson, JA Estes, TP Hughes, S Kidwell, CB Lange, HS Lenihan, JM Pandolfi, CH Peterson, RS Steneck, MJ Tegner and RR Warner (2001), 'Historical overfishing and the recent collapse of coastal ecosystems', *Science* **293**(5530), 629–637.
- Jennings, S and MJ Kaiser (1998), 'The effects of fishing on marine ecosystems', *Advances in marine biology* **34**, 201–352.
- Jones, AM and JM Baxter (1987), *Molluscs: Caudofoveata, Solenogastres, Polyplacophora and Scaphopoda: Keyes and Notes for the Identification of Species*, number 37 in 'xii', Brill Archive.
- Jordi, A and S Hameed (2009), 'Influence of the Icelandic low on the variability of surface air temperature in the Gulf of Lion: implications for intermediate water formation', *Journal of Physical Oceanography* **39**(12), 3228–3232.



- Josselyn, MN, GM Cailliet, TM Niesen, R Cowen, AC Hurley, J Connor and S Hawes (1983), 'Composition, export and faunal utilization of drift vegetation in the Salt River submarine canyon', *Estuarine Coastal and Shelf Science* **17**(4), 447–465.
- Jurado-Molina, J, PA Livingston and JN Ianelli (2005), 'Incorporating predation interactions in a statistical catch-at-age model for a predator-prey system in the eastern Bering Sea', *Canadian Journal of Fisheries and Aquatic Sciences* **62**(8), 1865–1873.
- Kaiser, MJ and BE Spencer (1996), 'The effects of beam-trawl disturbance on infaunal communities in different habitats', *Journal of Animal Ecology* pp. 348–358.
- Kammann, EE and MP Wand (2003), 'Geoaddivitive models', *Journal of the Royal Statistical Society: Series C (Applied Statistics)* **52**(1), 1–18.
- Kenyon, KW (1969), 'The sea otter in the eastern Pacific Ocean', *North American Fauna* pp. 1–352.
- Kinder, TH and G Parrilla (1987), 'Yes, some of the Mediterranean outflow does come from great depth', *Journal of Geophysical Research* **92**(C3), 2901–2906.
- Klein, N, T Kneib and S Lang (2013), Bayesian Structured Additive Distributional Regression, Technical report, University of Innsbruck.  
**URL:** <http://eeecon.uibk.ac.at/wopec2/repec/inn/wpaper/2013-23.pdf>
- Klepper, O and JPG Van de Kamer (1987), 'The use of mass balances to test and improve the estimates of carbon fluxes in an ecosystem', *Mathematical Biosciences* **85**(1), 37–49.
- Koen-Alonso, M and P Yodzis (2005), 'Multispecies modelling of some components of the marine community of northern and central Patagonia, Argentina', *Canadian Journal of Fisheries and Aquatic Sciences* **62**(7), 1490–1512.
- Kones, JK, K Soetaert, D van Oevelen and JO Owino (2009), 'Are network indices robust indicators of food web functioning? a monte carlo approach', *Ecological Modelling* **220**(3), 370–382.
- Kones, JK, K Soetaert, D van Oevelen, JO Owino and K Mavuti (2006), 'Gaining insight into food webs reconstructed by the inverse method', *Journal of Marine Systems* **60**(1), 153–166.
- Koslow, JA, GW Boehlert, JDM Gordon, RL Haedrich, P Lorange and N Parin (2000), 'Continental slope and deep-sea fisheries: implications for a fragile ecosystem', *ICES Journal of Marine Science: Journal du Conseil* **57**(3), 548–557.

- Kröncke, I and M Türkay (2003), ‘Structural and functional aspects of the benthic communities in the deep Angola Basin’, *Marine Ecology Progress Series* **260**, 43–53.
- Kröncke, I, M Türkay and D Fiege (2003), ‘Macrofauna communities in the Eastern Mediterranean deep sea’, *Marine Ecology* **24**(3), 193–216.
- Lang, S and A Brezger (2004), ‘Bayesian P-Splines’, *Journal of Computational and Graphical Statistics* **13**(1), 183–212.
- Lassen, H and P Medley (2000), Virtual population analysis. A practical manual for stock assessment. FAO Fisheries, Technical Report No. 400, FAO, Rome.
- Latham II, LG (2006), ‘Network flow analysis algorithms’, *Ecological Modelling* **192**(3), 586–600.
- Latham II, LG and EP Scully (2002), ‘Quantifying constraint to assess development in ecological networks’, *Ecological Modelling* **154**(1), 25–44.
- Lehodey, P, F Chai and J Hampton (2003), ‘Modelling climate-related variability of tuna populations from a coupled ocean–biogeochemical–populations dynamics model’, *Fisheries Oceanography* **12**(4–5), 483–494.
- Lehodey, P, I Senina and R Murtugudde (2008), ‘A spatial ecosystem and populations dynamics model (SEAPODYM)–Modeling of tuna and tuna-like populations’, *Progress in Oceanography* **78**(4), 304–318.
- Levin, LA and M Sibuet (2012), ‘Understanding continental margin biodiversity: a new imperative’, *Annual Review of Marine Science* **4**, 79–112.
- Libralato, S, M Coll, M Tempesta, A Santojanni, M Spoto, I Palomera, E Arneri and C Solidoro (2010), ‘Food-web traits of protected and exploited areas of the Adriatic Sea’, *Biological Conservation* **143**(9), 2182–2194.
- Lin, X and D Zhang (1999), ‘Inference in generalized additive mixed models by using smoothing splines’, *Journal of the Royal Statistical Society: Series B (Statistical Methodology)* **61**(2), 381–400.
- Lindeman, RL (1942), ‘The trophic-dynamic aspect of ecology’, *Ecology* **23**(4), 399–417.
- Livingston, PA and RD Methot (1998), ‘Incorporation of predation into a population assessment model of eastern Bering Sea walleye pollock’, *Fishery stock assessment models* pp. 663–678.
- Leonart, J and F Maynou (2003), ‘Fish stock assessments in the Mediterranean: state of the art’, *Scientia Marina* **67**, 37–49.

- Lohrenz, SE, RA Arnone, DA Wiesenburg and IP DePalma (1988), Satellite detection of transient enhanced primary production in the western Mediterranean Sea, Technical report, DTIC Document.
- López-Jurado, JL, M Marcos and S Monserrat (2008), ‘Hydrographic conditions affecting two fishing grounds of Mallorca island (Western Mediterranean): during the IDEA Project (2003–2004)’, *Journal of Marine Systems* **71**(3), 303–315.
- MacArthur, R (1955), ‘Fluctuations of animal populations and a measure of community stability’, *ecology* **36**(3), 533–536.
- Mackay, A (1981), ‘The generalized inverse’, *Practical Computing* **Sep.**, 108–110.
- Macpherson, E (1981), ‘Resource partitioning in a Mediterranean fish community’, *Marine Ecology Progress Series* **4**, 183–193.
- Macquart-Moulin, C and G Patriti (1996), ‘Accumulation of migratory micronekton crustaceans over the upper slope and submarine canyons of the northwestern Mediterranean’, *Deep Sea Research Part I: Oceanographic Research Papers* **43**(5), 579–601.
- Madurell, T and JE Cartes (2005), ‘Trophodynamics of a deep-sea demersal fish assemblage from the bathyal eastern Ionian Sea (Mediterranean Sea)’, *Deep Sea Research Part I: Oceanographic Research Papers* **52**(11), 2049–2064.
- Mahaut, ML, M Sibuet and Y Shirayama (1995), ‘Weight-dependent respiration rates in deep-sea organisms’, *Deep Sea Research Part I: Oceanographic Research Papers* **42**(9), 1575–1582.
- Mamouridis, V, F Maynou and G Aneiros Pérez (2014), ‘Analysis and standardization of landings per unit effort of red shrimp *Aristeus antennatus* from the trawl fleet of Barcelona (NW Mediterranean)’, *Scientia Marina* **78**, 7–16.
- Mamouridis, V, JE Cartes and E Fanelli (2014a), Multivariate techniques in ecology: The infauna associated to a CWC habitat (facies of *Isidella elongata*), influences of fishing activity and natural variability, in ‘Conf. Proc. Workshop: Young Researchers in Biostatistics’.
- Mamouridis, V, JE Cartes and E Fanelli (2014b), The macrofauna associated to the deep-sea coral *Isidella elongata*: human impact and natural variability, in ‘Conf. Proc.: International Oceanographic research Conference’.
- Mamouridis, V, JE Cartes, S Parra, E Fanelli and JI Saiz Salinas (2011), ‘A temporal analysis on the dynamics of deep-sea macrofauna: influence of environmental

- variability off Catalonia coasts (western Mediterranean)', *Deep Sea Research Part I: Oceanographic Research Papers* **58**(4), 323–337.
- Marchal, P, B Andersen, B Caillart, O Eigaard, O Guyader, H Hovgaard, A Iriondo, F Le Fur, J Sacchi and M Santurtún (2007), 'Impact of technological creep on fishing effort and fishing mortality, for a selection of European fleets', *ICES Journal of Marine Science: Journal du Conseil* **64**(1), 192–209.
- Marchal, P, C Ulrich, K Korsbrekke, M Pastoors and B Rackham (2002), 'A comparison of three indices of fishing power on some demersal fisheries of the North Sea', *ICES Journal of Marine Science: Journal du Conseil* **59**(3), 604–623.
- Margalef, R and J Castellví (1967), 'Fitoplancton y producción primaria de la costa catalana, de julio de 1966 a julio de 1967', *Investigación Pesquera* **31**(3), 491–502.
- Marriott, RJ, B Wise and J St John (2011), 'Historical changes in fishing efficiency in the west coast demersal scalefish fishery, Western Australia: implications for assessment and management', *ICES Journal of Marine Science: Journal du Conseil* **68**(1), 76–86.
- Martinez, ND (1992), 'Constant connectance in community food webs', *American Naturalist* pp. 1208–1218.
- Marty, JC and J Chiavérini (2010), 'Hydrological changes in the Ligurian Sea (NW Mediterranean, DYFAMED site) during 1995–2007 and biogeochemical consequences', *Biogeosciences Discussions* **7**(1), 1377–1406.
- Marty, JC, J Chiavérini, MD Pizay and B Avril (2002), 'Seasonal and interannual dynamics of nutrients and phytoplankton pigments in the western Mediterranean Sea at the DYFAMED time-series station (1991–1999)', *Deep Sea Research Part II: Topical Studies in Oceanography* **49**(11), 1965–1985.
- Marx, BD and PHC Eilers (1998), 'Direct generalized additive modeling with penalized likelihood', *Computational Statistics & Data Analysis* **28**(2), 193–209.
- Maunder, MN and AE Punt (2004), 'Standardizing catch and effort data: a review of recent approaches', *Fisheries Research* **70**(2), 141–159.
- Maunder, MN, JR Sibert, A Fonteneau, J Hampton, P Kleiber and SJ Harley (2006), 'Interpreting catch per unit effort data to assess the status of individual stocks and communities', *ICES Journal of Marine Science: Journal du Conseil* **63**(8), 1373–1385.
- May, RM (1972), 'Will a large complex system be stable?', *Nature* **238**, 413–414.

- Maynou, F (2008), 'Environmental causes of the fluctuations of red shrimp (*Aristeus antennatus*) landings in the Catalan Sea', *Journal of Marine Systems* **71**(3–4), 294–302.
- Maynou, F and JE Cartes (1998), 'Daily ration estimates and comparative study of food consumption in nine species of deep-water decapod crustaceans of the NW Mediterranean', *Marine Ecology Progress Series* **171**, 221–231.
- Maynou, F, M Demestre and P Sanchez (2003), 'Analysis of catch per unit effort by multivariate analysis and generalised linear models for deep-water crustacean fisheries off Barcelona (NW Mediterranean)', *Fisheries Research* **65**(1–3), 257–269.
- Maynou, F, M Sbrana, P Sartor, C Maravelias, S Kavadas, D Damalas, JE Cartes and G Osio (2011), 'Estimating trends of population decline in long-lived marine species in the Mediterranean Sea based on fishers' perceptions', *PloS one* **6**(7), e21818.
- McCann, KS (2000), 'The diversity–stability debate', *Nature* **405**(6783), 228–233.
- McClanahan, TR and E Sala (1997), 'A Mediterranean rocky-bottom ecosystem fisheries model', *Ecological Modelling* **104**(2), 145–164.
- McClanahan, TR and SH Shafir (1990), 'Causes and consequences of sea urchin abundance and diversity in Kenyan coral reef lagoons', *Oecologia* **83**(3), 362–370.
- McCullagh, P and JA Nelder (1989), *Generalized Linear Models*, Chapman & Hall, London.
- McDonald, AD, E Fulton, LR Little, R Gray, KJ Sainsbury and VD Lyne (2006), *Complex Science for a Complex World: Exploring Human Ecosystems with Agents*, ANU E Press, chapter Multiple use management strategy evaluation for coastal marine ecosystems using InVitro, pp. 265–279.
- Mendelsohn, R and P Cury (1989), 'Temporal and Spatial Dynamics of a Coastal Pelagic Species, *Sardinella maderensis* off the Ivory Coast', *Canadian Journal of Fisheries and Aquatic Sciences* **46**(10), 1686–1697.
- Menge, BA (1995), 'Indirect effects in marine rocky intertidal interaction webs: patterns and importance', *Ecological monographs* **65**(1), 21–74.
- Merino, G, C Karlou-Riga, I Anastopoulou, F Maynou and J Lleonart (2007), 'Bio-economic simulation analysis of hake and red mullet fishery in the Gulf of Saronikos (Greece)', *Scientia Marina* **71**(3), 525–535.

- Merrett, NR, RL Haedrich, JDM Gordon and M Stehmann (1991), 'Deep demersal fish assemblage structure in the Porcupine Seabight (eastern North Atlantic): results of single warp trawling at lower slope to abyssal soundings', *Journal of the Marine Biological Association of the United Kingdom* **71**(02), 359–373.
- Millot, C, I Taupier-Letage and M Benzohra (1990), 'The Algerian eddies', *Earth-Science Reviews* **27**(3), 203–219.
- Minas, HJ (1968), 'A propos d'une remontee d'eau "profonde" dans les parages du Golfe de Marseille (octobre 1964): Consequences biologiques', *Cahier Oceanographique* **20**, 641–674.
- Minas, HJ, B Coste and M Minas (1984), 'Oceanographie du detroit de Gibraltar et des parages annexes', *Le Courrier du CNRS* **57**, 10–17.
- Miquel, JC, SW Fowler, J La Rosa and P Buat-Menard (1994), 'Dynamics of the downward flux of pArticles and carbon in the open northwestern Mediterranean Sea', *Deep Sea Research Part I: Oceanographic Research Papers* **41**(2), 243–261.
- Moksnes, PO, M Gullström, K Tryman and S Baden (2008), 'Trophic cascades in a temperate seagrass community', *Oikos* **117**(5), 763–777.
- Möllmann, C, B Müller-Karulis, G Kornilovs and MA St John (2008), 'Effects of climate and overfishing on zooplankton dynamics and ecosystem structure: regime shifts, trophic cascade, and feedback loops in a simple ecosystem', *ICES Journal of Marine Science: Journal du Conseil* **65**(3), 302–310.
- Möllmann, C, M Lindegren, T Blenckner, L Bergström, M Casini, R Diekmann, J Flinkman, B Müller-Karulis, S Neuenfeldt, JO Schmidt, M Tomczak, R. Voss and A Gårdmark (2013), 'Implementing ecosystem-based fisheries management: from single-species to integrated ecosystem assessment and advice for Baltic Sea fish stocks', *ICES Journal of Marine Science: Journal du Conseil* **71**(5), 1187–1197.
- Moore, JC, EL Berlow, DC Coleman, PC de Ruiter, Q Dong, A Hastings, N Collins Johnson, KS McCann, K Melville, PJ Morin, K Nadelhoffer, AD Rosemond, DM Post, JL Sabo, KM Scow, MJ Vanni and DH Wall (2004), 'Detritus, trophic dynamics and biodiversity', *Ecology letters* **7**(7), 584–600.
- Moore, JC and PC de Ruiter (2012), *Energetic food webs: an analysis of real and model ecosystems*, Oxford University Press, Oxford UK.
- Moore, JC, PC De Ruiter and HW Hunt (1993), 'Influence of productivity on the stability of real and model ecosystems', *Science* **261**, 906–908.

- Moranta, J, C Stefanescu, E Massutí, B Morales-Nin and D Lloris (1998), 'Fish community structure and depth-related trends on the continental slope of the Balearic Islands (Algerian basin, western Mediterranean)', *Marine Ecology Progress Series* **171**, 247–259.
- Moranta, J, E Massutí and B Morales-Nin (2000), 'Fish catch composition of the deep-sea decapod crustacean fisheries in the Balearic Islands (western Mediterranean)', *Fisheries Research* **45**(3), 253–264.
- Morato, T, R Watson, TJ Pitcher and D Pauly (2006), 'Fishing down the deep', *Fish and Fisheries* **7**(1), 24–34.
- Mori, M and DS Butterworth (2004), 'Consideration of multispecies interactions in the Antarctic: a preliminary model of the minke whale–blue whale–krill interaction', *African Journal of Marine Science* **26**(1), 245–259.
- Mori, M and DS Butterworth (2005), 'Modelling the predator-prey interactions of krill, baleen whales and seals in the Antarctic', *IWC Scientific committee paper SC/57 O* **21**.
- Mori, M and DS Butterworth (2006), 'A first step towards modelling the krill-predator dynamics of the Antarctic ecosystem', *CCAMLR Science* **13**, 217–277.
- Myers, RA and B Worm (2005), 'Extinction, survival or recovery of large predatory fishes', *Philosophical Transactions of the Royal Society B: Biological Sciences* **360**(1453), 13–20.
- Myers, RA and P Pepin (1990), 'The robustness of lognormal-based estimators of abundance', *Biometrics* **1**, 1185–1192.
- Neal, RA and RC Maris (1985), *The Biology of Crustacea Vol 10: Economic aspects: fisheries and culture*, Academic Press Inc., chapter Fisheries biology of shrimps and shrimplike animals.
- Nédélec, H (1982), 'Ethologie alimentaire de *Paracentrotus lividus* dans la baie Galeria (Corse) et son impact sur les peuplements phytobenthiques', PhD thesis, Université Pierre et Marie Curie and Université Aix-Marseille II, Marseille.
- Niquil, N, GA Jackson, L Legendre and B Delesalle (1998), 'Inverse model analysis of the planktonic food web of Takapoto Atoll (French Polynesia)', *Marine Ecology Progress Series* **165**, 17–29.
- Nittrover, CA and LD Wright (1994), 'Transport of particles across continental shelves', *Reviews of Geophysics* **32**(1), 85–113.

- Odum, EP (1969), 'The strategy of ecosystem development', *Science* **164**, 262–270.
- Odum, HT (1957), 'Trophic structure and productivity of Silver Springs, Florida', *Ecological Monographs* **27**(1), 55–112.
- Oksanen, T (1990), 'Exploitation ecosystems in heterogeneous habitat complexes', *Evolutionary Ecology* **4**(3), 220–234.
- Oliver, P (1993), 'Analysis of fluctuations observed in the trawl fleet landings of the Balearic Islands', *Scientia Marina* **57**, 219–227.
- O'Neill, RV (1969), 'Indirect estimation of energy fluxes in animal food webs', *Journal of Theoretical Biology* **22**(2), 284–290.
- Orsi Relini, L, A Mannini and G Relini (2013), 'Updating knowledge on growth, population dynamics, and ecology of the blue and red shrimp, *Aristeus antennatus* (Risso, 1816), on the basis of the study of its instars', *Marine Ecology* **34**, 90–102.
- Paine, RT (1980), 'Food webs: linkage, interaction strength and community infrastructure', *Journal of Animal Ecology* **49**(3), 667–685.
- Palanques, A, X Durrieu de Madron, P Puig, J Fabres, J Guillén, A Calafat, M Canals, S Heussner and J Bonnin (2006), 'Suspended sediment fluxes and transport processes in the Gulf of Lions submarine canyons. The role of storms and dense water cascading', *Marine Geology* **234**(1), 43–61.
- Palkovacs, EP, MT Kinnison, C Correa, CM Dalton and AP Hendry (2012), 'Fates beyond traits: ecological consequences of human-induced trait change', *Evolutionary Applications* **5**(2), 183–191.
- Paloheimo, JE and LM Dickie (1964), 'Abundance and fishing success', *Rapports et Proces-Verbaux des Réunions du Conseil International pour l'Exploration de la Mer* **155**.
- Papaconstantinou, C and H Farrugio (2000), 'Fisheries in the Mediterranean', *Mediterranean Marine Science* **1**(1), 5–18.
- Papiol, V, JE Cartes, E Fanelli and F Maynou (2012), 'Influence of environmental variables on the spatio-temporal dynamics of benthic-pelagic assemblages in the middle slope of the Balearic Basin (NW Mediterranean)', *Deep Sea Research Part I: Oceanographic Research Papers* **61**(0), 84–99.
- Papiol, V, JE Cartes, E Fanelli and P Rumolo (2013), 'Food web structure and seasonality of slope megafauna in the NW Mediterranean elucidated by stable isotopes: Relationship with available food sources', *Journal of Sea Research* **77**(0), 53–69.



- Parapar, J, C Alós, J Núñez, J Moreira, E López, F Aguirrezabalaga, C Besteiro and A Martínez (2012), *Fauna Iberica 36: Annelida Polychaeta III*, Museo Nacional de Ciencias Naturales, CSIC, Madrid.
- Pardo, EV and AC Zacagnini Amaral (2004), 'Feeding behavior of *Scolecopsis* sp.(Polychaeta: Spionidae)', *Brazilian Journal of Oceanography* **52**(1), 74–79.
- Patten, BC and M Higashi (1984), 'Modified cycling index for ecological applications', *Ecological Modelling* **25**(1), 69–83.
- Pauly, D (1982), 'A method to estimate the stock-recruitment relationship of shrimps', *Transactions of the American Fisheries Society* **111**(1), 13–20.
- Pauly, D (1985), 'Population dynamics of short-lived species, with emphasis on squids', *NAFO Scientific Council Studies* **9**, 143–154.
- Pauly, D, V Christensen and C Walters (2000), 'Ecopath, Ecosim, and Ecospace as tools for evaluating ecosystem impact of fisheries', *ICES Journal of Marine Science: Journal du Conseil* **57**(3), 697–706.
- Pauly, D, V Christensen, J Dalsgaard, R Froese and F Torres (1998), 'Fishing down marine food webs', *Science* **279**(5352), 860–863.
- Pavithran, S, BS Ingole, M Nanajkar, C Raghukumar, BN Nath and AB Valsangkar (2009), 'Composition of macrobenthos from the central Indian Ocean Basin', *Journal of Earth System Science* **118**(6), 689–700.
- Pearson, TH and R Rosenberg (1978), *Oceanography and marine biology: an annual review*, Vol. 16, CRC Press Taylor & Francis Group, chapter Macrobenthic succession in relation to organic enrichment and pollution of the marine environment.
- Pennington, M (1983), 'Efficient Estimators of Abundance, for Fish and Plankton Surveys', *Biometrics* **39**(1), 281–286.
- Pérès, JM (1985), *History of the Mediterranean biota and the colonization of the depths*, Vol. 7, Pergamon Press Oxford.
- Pérès, JM and J Picard (1964), 'Nouveau manuel de bionomie benthique de la Mer Méditerranée', *Recueil des Travaux de la Station Marine d'Endoume* **31**(47), 1–137.
- Pikitch, EK, C Santora, EA Babcock, A Bakun, R Bonfil, DO Conover, P Dayton, P Doukakis, D Fluharty, B Heneman, ED Houde, J Link, PA Livingston, M Mangel, MK McAllister, J Pope and KJ Sainsbury (2004), 'Ecosystem-Based Fishery Management', *Science* **305**(5682), 346–347.

- Pimm, SL (1984), 'The complexity and stability of ecosystems', *Nature* **307**(5949), 321–326.
- Pimm, SL and JH Lawton (1980), 'Are food webs divided into compartments?', *The Journal of Animal Ecology* pp. 879–898.
- Pinheiro, JC and DM Bates (2000), *Mixed Effects Models in S and S-PLUS*, Springer-Verlag, New York.
- Pinnegar, JK, NVC Polunin, P Francour, F Badalamenti, R Chemello, ML Harmelin-Vivien, B Hereu, M Milazzo, M Zabala, G d'Anna and C Pipitone (2000), 'Trophic cascades in benthic marine ecosystems: lessons for fisheries and protected-area management', *Environmental Conservation* **27**(02), 179–200.
- Pipitone, C, F Badalamenti, G D'Anna and B Patti (2000), 'Fish biomass increase after a four-year trawl ban in the Gulf of Castellammare (NW Sicily, Mediterranean Sea)', *Fisheries Research* **48**(1), 23–30.
- Piroddi, C, G Bearzi and V Christensen (2010), 'Effects of local fisheries and ocean productivity on the northeastern Ionian Sea ecosystem', *Ecological Modelling* **221**(11), 1526–1544.
- Plagányi, ÉE (2007), *Models for an ecosystem approach to fisheries*, Vol. 477, FAO, Rome.
- Plagányi, ÉE and D Butterworth (2006), A spatial multi-species operating model (SMOM) of krill–predator interactions in small-scale management units in the Scotia Sea, in 'Workshop document presented to WG–EMM subgroup of CCAMLR (Commission for the Conservation of Antarctic Marine Living Resources), WG–EMM–06/12', p. 28.
- Polis, GA (1999), 'Why are parts of the world green? Multiple factors control productivity and the distribution of biomass', *Oikos* **86**, 3–15.
- Polis, GA and DR Strong (1996), 'Food web complexity and community dynamics', *American Naturalist* **147**(5), 813–846.
- Politou, C, S Kavadas, Ch Mytilineou, A Tursi, R Carlucci and G Lembo (2003), 'Fisheries resources in the deep waters of the Eastern Mediterranean (Greek Ionian Sea)', *Journal of Northwest Atlantic Fishery Science* **31**, 35.
- Polovina, JJ (1984), 'Model of a coral reef ecosystem', *Coral reefs* **3**(1), 1–11.
- Power, ME (1992), 'Top-down and bottom-up forces in food webs: do plants have primacy', *Ecology* **73**(3), 733–746.

- Prena, J, P Schwinghamer, TW Rowell, DC Gordon, KD Gilkinson, WP Vass and DL McKeown (1999), 'Experimental otter trawling on a sandy bottom ecosystem of the Grand Banks of Newfoundland: analysis of trawl bycatch and effects on epifauna', *Marine Ecology Progress Series* **181**, 107–124.
- Prieur, L and M Tiberti (1984), 'Identification et échelles des processus près du front de la mer Ligure', *Rapport Committee internationale Mer Méditerranée* **29**, 35–36.
- Puig, P, A Palanques, DL Orange, G Lastras and M Canals (2008), 'Dense shelf water cascades and sedimentary furrow formation in the Cap de Creus Canyon, northwestern Mediterranean Sea', *Continental Shelf Research* **28**(15), 2017–2030.
- Puig, P, AS Ogston, BL Mullenbach, CA Nittrouer and RW Sternberg (2003), 'Shelf-to-canyon sediment-transport processes on the Eel continental margin (northern California)', *Marine Geology* **193**(1), 129–149.
- Punt, AE and DS Butterworth (1995), 'The effects of future consumption by the Cape fur seal on catches and catch rates of the Cape hakes. 4. Modelling the biological interaction between Cape fur seals *Arctocephalus pusillus pusillus* and the Cape hakes *Merluccius capensis* and *M. paradoxus*', *South African Journal of Marine Science* **16**(1), 255–285.
- Purcell, SW and DS Kirby (2006), 'Restocking the sea cucumber *Holothuria scabra*: Sizing no-take zones through individual-based movement modelling', *Fisheries Research* **80**(1), 53–61.
- Pusceddu, A, S Bianchelli, M Canals, A Sanchez-Vidal, X Durrieu De Madron, S Heussner, V Lykousis, H de Stigter, F Trincardi and R Danovaro (2010), 'Organic matter in sediments of canyons and open slopes of the Portuguese, Catalan, Southern Adriatic and Cretan Sea margins', *Deep Sea Research Part I: Oceanographic Research Papers* **57**(3), 441–457.
- Ragonese, S and ML Bianchini (1996), 'Growth, mortality and yield-per-recruit of the deep-water shrimp *Aristeus antennatus* (Crustacea-Aristeidae) of the Strait of Sicily (Mediterranean Sea)', *Fisheries Research* **26**(1), 125–137.
- Real, LA (1977), 'The kinetics of functional response', *American Naturalist* **111**(978), 289–300.
- Reid, K and JP Croxall (2001), 'Environmental response of upper trophic-level predators reveals a system change in an Antarctic marine ecosystem', *Proceedings of the Royal Society of London. Series B: Biological Sciences* **268**(1465), 377–384.

- Reid, PC, EJV Battle, SD Batten and KM Brander (2000), 'Impacts of fisheries on plankton community structure', *ICES Journal of Marine Science: Journal du Conseil* **57**(3), 495–502.
- Reyss, D (1971), 'Les canyons sous-marins de la mer Catalane: le rech du Cap et le rech Lacaze-Duthiers. III. Les peuplements de macrofaune benthique', *Vie Milieu* **22**(3B), 529–613.
- Rigby, RA and DM Stasinopoulos (2005), 'Generalized additive models for location, scale and shape', *Journal of the Royal Statistical Society: Series C (Applied Statistics)* **54**(3), 507–554.
- Righini, P and A Abella (1994), 'Life cycle of *Aristeus antennatus* and *Aristaeomorpha foliacea* in the Northern Tyrrhenian Sea', *NTRITPP Special Publication* **3**, 29–30.
- Roberts, J Murray, Andrew J Wheeler and André Freiwald (2006), 'Reefs of the deep: the biology and geology of cold-water coral ecosystems', *Science* **312**(5773), 543–547.
- Röder, H (1971), 'Gangsysteme von *Paraonis fulgens* Levinsen 1883 (Polychaeta) in ökologischer, ethologischer und aktuopaläontologischer Sicht', *Senckenbergiana maritima* **3**, 3–51.
- Roff, JC, K Middlebrook and F Evans (1988), 'Long-term variability in North Sea zooplankton off the Northumberland coast: productivity of small copepods and analysis of trophic interactions', *Journal of the Marine Biological Association of the United Kingdom* **68**(01), 143–164.
- Romero-Wetzel, MB (1987), 'Sipunculans as inhabitants of very deep, narrow burrows in deep-sea sediments', *Marine Biology* **96**(1), 87–91.
- Ross, SW and AM Quattrini (2007), 'The fish fauna associated with deep coral banks off the southeastern United States', *Deep Sea Research Part I: Oceanographic Research Papers* **54**(6), 975–1007.
- Rotterman, LM and TS Jackson (1988), *Sea otter, *Enhydra lutris**, Marine Mammal Commission.
- Rowe, GT, PT Polloni and RL Haedrich (1982), 'The deep-sea macrobenthos on the continental margin of the northwest Atlantic Ocean', *Deep Sea Research Part A. Oceanographic Research Papers* **29**(2), 257–278.
- Rudstam, LG, G Aneer and M Hildén (1994), 'Top-down control in the pelagic Baltic ecosystem', *Dana* **10**, 105–129.

- Ruhl, HA, JA Ellena and KL Smith (2008), 'Connections between climate, food limitation, and carbon cycling in abyssal sediment communities', *Proceedings of the National Academy of Sciences* **105**(44), 17006–17011.
- Ruhl, HA and KL Smith (2004), 'Shifts in deep-sea community structure linked to climate and food supply', *Science* **305**(5683), 513–515.
- Ruppert, D, MP Wand and RaJ Carroll (2003), *Semiparametric regression Vol. 12*, Cambridge University Press, Cambridge.
- Sala, E (1997a), 'Fish predators and scavengers of the sea urchin *Paracentrotus lividus* in protected areas of the north-west Mediterranean Sea', *Marine Biology* **129**(3), 531–539.
- Sala, E (1997b), 'The role of fishes in the organization of a Mediterranean sublittoral community: II: Epifaunal communities', *Journal of Experimental Marine Biology and Ecology* **212**(1), 45–60.
- Sala, E, CF Boudouresque and M Harmelin-Vivien (1998), 'Fishing, trophic cascades, and the structure of algal assemblages: evaluation of an old but untested paradigm', *Oikos* **82**, 425–439.
- Sala, E and M Zabala (1996), 'Fish predation and the structure of the sea urchin *Paracentrotus lividus* populations in the NW Mediterranean', *Marine Ecology Progress Series* **140**(1), 71–81.
- Salat, J, MA Garcia, A Cruzado, A Palanques, L Arín, D Gomis, J Guillén, A de León, J Puigdefàbregas, J Sospedra and Z Velásquez (2002), 'Seasonal changes of water mass structure and shelf slope exchanges at the Ebro Shelf (NW Mediterranean)', *Continental Shelf Research* **22**(2), 327–348.
- Salihoğlu, İ, C Saydam, Ö Baştürk, K Yılmaz, D Göçmen, E Hatipoğlu and A Yılmaz (1990), 'Transport and distribution of nutrients and chlorophyll-*a* by mesoscale eddies in the northeastern Mediterranean', *Marine chemistry* **29**, 375–390.
- Salvini-Plawen, Lv (1981), 'The molluscan digestive system in evolution', *Malacologia* **21**(37), 1–40.
- Salvini-Plawen, Lv (1988), 'The structure and function of molluscan digestive systems', *The Mollusca* **11**, 301–379.
- Salvini-Plawen, Lv (2009), 'Geographical notes on iberian caudofoveata (mollusca)', *Iberus* **27**, 107–112.

- San Martín Peral, G (2004), *Fauna ibérica. Vol. 21. Annelida polychaeta II*, Museo Nacional de Ciencias Naturales, CSIC, Madrid.
- Sanders, HL (1968), 'Marine benthic diversity: a comparative study', *American Naturalist* **102**(925), 243–282.
- Sanders, HL, RR Hessler and GR Hampson (1965), 'An introduction to the study of deep-sea benthic faunal assemblages along the Gay Head-Bermuda transect', *Deep Sea Research and Oceanographic Abstracts* **12**(6), 845–867.
- Sardà, F (1998), 'Symptoms of overexploitation in the stock of the Norway lobster (*Nephrops norvegicus*) on the "Serola Bank" (western Mediterranean Sea off Barcelona)', *Scientia Marina* **62**(3), 295–299.
- Sardà, F and F Maynou (1998), 'Assessing perceptions: do Catalan fishermen catch more shrimp on Fridays?', *Fisheries Research* **36**, 149–157.
- Sardà, F, F Maynou and L Talló (1997), 'Seasonal and spatial mobility patterns of rose shrimps *Aristeus antennatus* in the Western Mediterranean: results of a long-term study', *Marine Ecology Progress Series* **159**, 133–141.
- Sardà, F and JE Cartes (1993), 'Relationship between size and depth in decapod crustacean populations on the deep slope in the Western Mediterranean', *Deep Sea Research Part I: Oceanographic Research Papers* **40**(11), 2389–2400.
- Sardà, F, JE Cartes and W Norbis (1994), 'Spatio-temporal structure of the deep-water shrimp *Aristeus antennatus* (Decapoda:Aristeidae) population in the western Mediterranean', *Fishery Bulletin (US)* **92**, 599–607.
- Scheffer, M, S Carpenter, JA Foley, C Folke and B Walker (2001), 'Catastrophic shifts in ecosystems', *Nature* **413**(6856), 591–596.
- Scheffer, M, SH Hopper, ML Meijer, B Moss and E Jeppesen (1993), 'Alternative equilibria in shallow lakes', *Trends in Ecology & Evolution* **8**(8), 275–279.
- Schindler, DW (2006), 'Recent advances in the understanding and management of eutrophication', *Limnology and Oceanography* **51**(1), 356–363.
- Scott, DW (2009), *Multivariate density estimation: theory, practice, and visualization*, Vol. 383, John Wiley & Sons Inc.
- Sekine, M, H Nakanishi, M Ukita and S Murakami (1991), 'A shallow-sea ecological model using an object-oriented programming language', *Ecological Modelling* **57**(3), 221–236.

- Shackell, NL, KT Frank, JAD Fisher, B Petrie and WC Leggett (2010), ‘Decline in top predator body size and changing climate alter trophic structure in an oceanic ecosystem’, *Proceedings of the Royal Society B: Biological Sciences* **277**(1686), 1353–1360.
- Shears, NT and RC Babcock (2002), ‘Marine reserves demonstrate top-down control of community structure on temperate reefs’, *Oecologia* **132**(1), 131–142.
- Shin, Y-J and P Cury (2001), ‘Exploring fish community dynamics through size-dependent trophic interactions using a spatialized individual-based model’, *Aquatic Living Resources* **14**(2), 65–80.
- Shin, Y-J and P Cury (2004), ‘Using an individual-based model of fish assemblages to study the response of size spectra to changes in fishing’, *Canadian Journal of Fisheries and Aquatic Sciences* **61**(3), 414–431.
- Shiomoto, A, K Tadokoro, K Nagasawa and Y Ishida (1997), ‘Trophic relations in the subarctic North Pacific ecosystem: possible feeding effect from pink salmon’, *Marine Ecology Progress Series* **150**(1), 75–85.
- Shurin, JB, ET Borer, EW Seabloom, K Anderson, CA Blanchette, B Broitman, SD Cooper and BS Halpern (2002), ‘A cross-ecosystem comparison of the strength of trophic cascades’, *Ecology letters* **5**(6), 785–791.
- Shurin, JB, JL Clasen, HS Greig, P Kratina and PL Thompson (2012), ‘Warming shifts top-down and bottom-up control of pond food web structure and function’, *Philosophical Transactions of the Royal Society B: Biological Sciences* **367**(1605), 3008–3017.
- Sibuet, M, CE Lambert, R Chesselet and L Laubier (1989), ‘Density of the major size groups of benthic fauna and trophic input in deep basins of the Atlantic Ocean’, *Journal of Marine Research* **47**(4), 851–867.
- Smith, KL, HA Ruhl, BJ Bett, DSM Billett, RS Lampitt and RS Kaufmann (2009), ‘Climate, carbon cycling, and deep-ocean ecosystems’, *Proceedings of the National Academy of Sciences* **106**(46), 19211–19218.
- Soetaert, K and D van Oevelen (2009a), ‘LIM: Linear Inverse Model examples and solution methods’, *R package version 1*.
- Soetaert, K and D van Oevelen (2009b), ‘Modeling food web interactions in benthic deep-sea ecosystems. A practical guide’, *Oceanography* **22**.
- Soetaert, K and T Petzoldt (2010), ‘Inverse modelling, sensitivity and monte carlo analysis in R using package FME’, *Journal of Statistical Software* **33**(3), 1–28.

- Soetaert, K, T Petzoldt and RW Setzer (2010a), ‘Solving differential equations in R’, *The R Journal* **2**.
- Soetaert, K, T Petzoldt and RW Setzer (2010b), ‘Solving differential equations in R: Package deSolve’, *Journal of Statistical Software* **33**(9), 1–25.
- Sparholt, H (1995), ‘Using the MSVPA/MSFOR model to estimate the right-hand side of the Ricker curve for Baltic cod’, **52**(5), 819–826.
- Sparre, P (1991), ‘Introduction to multispecies virtual population analysis’, *ICES Journal of Marine Science: Journal du Conseil* **193**, 12–21.
- Spiegelhalter, DJ, NG Best, BP Carlin and A van der Linde (2002), ‘Bayesian Measures of Model Complexity and Fit’, *Journal of the Royal Statistical Society. Series B (Statistical Methodology)* **64**(4), 583–639.
- Spiller, DA and TW Schoener (1994), ‘Effects of top and intermediate predators in a terrestrial food web’, *Ecology* **75**(1), 182–196.
- Stasinopoulos, DM and RA Rigby (2007), ‘Generalized Additive Models for Location Scale and Shape (GAMLSS) in R’, *Journal of Statistical Software* **23**(7), 1–46.
- Steele, JH (1998), ‘Regime shifts in marine ecosystems’, *Ecological Applications* **8**(sp1), S33–S36.
- Stefanescu, C, B Morales-Nin and E Massutí (1994), ‘Fish assemblages on the slope in the Catalan Sea (Western Mediterranean): influence of a submarine canyon’, *JMBA-Journal of the Marine Biological Association of the United Kingdom* **74**(3), 499–512.
- Stefánsson, G (1996), ‘Analysis of groundfish survey abundance data: combining the GLM and delta approaches’, *ICES Journal of Marine Science: Journal du Conseil* **53**(3), 577–588.
- Stefánsson, G and OK Palsson (1998), ‘Points of view: A framework for multispecies modelling of Arcto-boreal systems’, *Reviews in Fish Biology and Fisheries* **8**, 101–104.
- Steneck, RS, J Vavrinec and AV Leland (2004), ‘Accelerating trophic-level dysfunction in kelp forest ecosystems of the western north atlantic’, *Ecosystems* **7**(4), 323–332.
- Stige, LC, G Ottersen, K Brander, K-S Chan and NC Stenseth (2006), ‘Cod and climate: effect of the North Atlantic Oscillation on recruitment in the North Atlantic’, *Marine Ecology Progress Series* **325**, 227–241.



- Stora, G, M Bourcier, A Arnoux, M Gerino, J Le Campion, F Gilbert and JP Durbec (1999), 'The deep-sea macrobenthos on the continental slope of the northwestern Mediterranean Sea: a quantitative approach', *Deep Sea Research Part I: Oceanographic Research Papers* **46**(8), 1339–1368.
- Strauss, SY (1991), 'Indirect effects in community ecology: their definition, study and importance', *Trends in Ecology & Evolution* **6**(7), 206–210.
- Strong, DR (1992), 'Are trophic cascades all wet? Differentiation and donor-control in speciose ecosystems', *Ecology* **73**(3), 747–754.
- Su, N-J, S-Z Yeh, C-L Sun, AE Punt, Y Chen and S-P Wang (2008), 'Standardizing catch and effort data of the Taiwanese distant-water longline fishery in the western and central Pacific Ocean for bigeye tuna, *Thunnus obesus*', *Fisheries Research* **90**(1), 235–246.
- Taylor, L and G Stefánsson (2004), Gadget models of cod-capelin-shrimp interactions in Icelandic waters, Technical report, ICES Document CM.
- Taylor, LA and D Taeknigardur (2011), Gadget models of cod–shrimp interactions in icelandic waters, Technical report, RH-03-2011. Science Institute, University of Iceland.
- Tchukhtchin, VD (1964), 'Quantitative data on benthos of the Tyrrhenian Sea', *Trudy Sevastopol Biological Station* **17**, 48–50.
- Tecchio, S, M Coll, V Christensen, JB Company, E Ramírez-Llodra and F Sarda (2013), 'Food web structure and vulnerability of a deep-sea ecosystem in the NW Mediterranean Sea', *Deep Sea Research Part I: Oceanographic Research Papers* **75**, 1–15.
- Ter Braak, CJF (1986), 'Canonical correspondence analysis: a new eigenvector technique for multivariate direct gradient analysis', *Ecology* **67**(5), 1167–1179.
- Thistle, D (2003), 'On the utility of metazoan meiofauna for studying the soft-bottom deep sea', *Vie et Milieu* **53**(2–3), 97–102.
- Thomson, RB, DS Butterworth, IL Boyd and JP Croxall (2000), 'Modeling the consequences of Antarctic krill harvesting on Antarctic fur seals', *Ecological Applications* **10**(6), 1806–1819.
- Thornton, SF and J McManus (1994), 'Application of organic carbon and nitrogen stable isotope and C/N ratios as source indicators of organic matter provenance in estuarine systems: evidence from the Tay Estuary, Scotland', *Estuarine, Coastal and Shelf Science* **38**(3), 219–233.

- Thorson, JT and EJ Ward (2014), 'Accounting for vessel effects when standardizing catch rates from cooperative surveys', *Fisheries Research* **155**, 168–176.
- Thorson, JT and J Berkson (2010), 'Evaluating single-and multi-species procedures to estimate time-varying catchability functional parameters', *Fisheries Research* **101**(1), 38–49.
- Thurstan, RH, S Brockington and CM Roberts (2010), 'The effects of 118 years of industrial fishing on UK bottom trawl fisheries', *Nature Communications* **1**(15), 1–6.
- Tjelmeland, S and B Bogstad (1998), 'MULTSPEC—a review of a multispecies modelling project for the Barents Sea', *Fisheries Research* **37**(1), 127–142.
- Tjelmeland, S and U Lindstrøm (2005), 'An ecosystem element added to the assessment of Norwegian spring-spawning herring: implementing predation by minke whales', *ICES Journal of Marine Science: Journal du Conseil* **62**(2), 285–294.
- Trenkel, VM, JK Pinnegar, JL Blanchard and AN Tidd (2004), Can multispecies models be expected to provide better assessments for Celtic Sea groundfish stocks, in 'ICES Annual Science Conference, Vigo, ICES CM'.
- Tsagarakis, K, M Coll, M Giannoulaki, S Somarakis, Costas Papaconstantinou and A Machias (2010), 'Food-web traits of the North Aegean Sea ecosystem (Eastern Mediterranean) and comparison with other Mediterranean ecosystems', *Estuarine, Coastal and Shelf Science* **88**(2), 233–248.
- Tselepides, A and A Eleftheriou (1992), South Aegean (Eastern Mediterranean) Continental Slope Benthos: Macroinfaunal-Environmental Relationships, in 'Deep-sea food chains and the global carbon cycle', Springer, pp. 139–156.
- Tselepides, A, K-N Papadopoulou, D Podaras, W Plaiti and D Koutsoubas (2000), 'Macro-benthic community structure over the continental margin of Crete (South Aegean Sea, NE Mediterranean)', *Progress in Oceanography* **46**(2), 401–428.
- Tudela, S, F Maynou and M Demestre (1998), 'Influence of Submarine Canyons on the Distribution of The Deep-Water Shrimp, *Aristeus antennatus* (risso, 1816) In The NW Mediterranean', *Crustaceana* **7**(2), 217–225.
- Ulanowicz, RE (1986), *Growth and development: ecosystems phenomenology*, Springer-Verlag New York.
- Ulanowicz, RE (2000), *Ecological integrity: Integrating Environment, Conservation, and Health*. Island Press, Washington, DC, Island Press, chapter Toward the measurement of ecological integrity, pp. 99–113.

- Ulanowicz, RE (2004), 'Quantitative methods for ecological network analysis', *Computational Biology and Chemistry* **28**(5), 321–339.
- Ulanowicz, RE and JS Norden (1990), 'Symmetrical overhead in flow networks', *International Journal of Systems Science* **21**(2), 429–437.
- Valiela, I (1995), *Marine ecological processes*, Springer.
- Vamvakas, C (1970), 'Peuplements benthiques des substrats meubles du sud de la Mer Egée', *Tethys* **2**(1), 89–130.
- Van den Meersche, K, K Soetaert and D Van Oevelen (2009), 'xsample(): An R function for sampling linear inverse problems', *Journal of Statistical Software* **30**(1), 1–15.
- Van Dover, CL (1995), 'Ecology of mid-Atlantic ridge hydrothermal vents', *Geological Society, London, Special Publications* **87**(1), 257–294.
- Van Dover, CL, CR German, KG Speer, LM Parson and RC Vrijenhoek (2002), 'Evolution and biogeography of deep-sea vent and seep invertebrates', *Science* **295**(5558), 1253–1257.
- van Oevelen, D, G Duineveld, M Lavaleye, F Mienis, K Soetaert and CHR Heip (2009), 'The cold-water coral community as a hot spot for carbon cycling on continental margins: A food-web analysis from Rockall Bank (northeast Atlantic)', *Limnology and Oceanography* **54**(6), 1829.
- van Oevelen, D, K Soetaert and C Heip (2012), 'Carbon flows in the benthic food web of the Porcupine Abyssal Plain: The (un) importance of labile detritus in supporting microbial and faunal carbon demands', *Limnology and Oceanography* **57**(2), 645–664.
- van Oevelen, D, K Soetaert, JJ Middelburg, PMJ Herman, L Moodley, I Hamels, T Moens and CHR Heip (2006), 'Carbon flows through a benthic food web: Integrating biomass, isotope and tracer data', *Journal of Marine Research* **64**(3), 453–482.
- van Oevelen, D, K Soetaert, R García, H C de Stigter, M R Cunha, A Pusceddu and R Danovaro (2011), 'Canyon conditions impact carbon flows in food webs of three sections of the Nazaré canyon', *Deep Sea Research Part II: Topical Studies in Oceanography* **58**(23), 2461–2476.
- van Oevelen, D, K Van den Meersche, FJR Meysman, K Soetaert, JJ Middelburg and AF Vézina (2010), 'Quantifying food web flows using linear inverse models', *Ecosystems* **13**(1), 32–45.

- van Oevelen, D, M Bergmann, K Soetaert, E Bauerfeind, C Hasemann, M Klages, I Schewe, T Soltwedel and NE Budaeva (2011), 'Carbon flows in the benthic food web at the deep-sea observatory HAUSGARTEN (Fram Strait)', *Deep Sea Research Part I: Oceanographic Research Papers* **58**(11), 1069–1083.
- van Oevelen, Dick, Jack J Middelburg, Karline Soetaert and Leon Moodley (2006), 'The fate of bacterial carbon in an intertidal sediment: Modeling an in situ isotope tracer experiment', *Limnology and Oceanography* **51**(3), 1302–1314.
- Venables, WN and CM Dichmont (2004), 'GLMs, GAMs and GLMMs: an overview of theory for applications in fisheries research', *Fisheries Research* **70**(2), 319–337.
- Verity, PG, V Smetacek and TJ Smayda (2002), 'Status, trends and the future of the marine pelagic ecosystem', *Environmental Conservation* **29**(02), 207–237.
- Vetter, EW (1998), 'Population dynamics of a dense assemblage of marine detritivores', *Journal of Experimental Marine Biology and Ecology* **226**(1), 131–161.
- Vetter, EW and PK Dayton (1998), 'Macrofaunal communities within and adjacent to a detritus-rich submarine canyon system', *Deep-Sea Research Part II: Topical Studies in Oceanography* **45**(1–3), 25–54.
- Vetter, EW and PK Dayton (1999), 'Organic enrichment by macrophyte detritus, and abundance patterns of megafaunal populations in submarine canyons', *Marine Ecology Progress Series* **186**, 137–148.
- Vézina, AF and C Savenkoff (1999), 'Inverse modeling of carbon and nitrogen flows in the pelagic food web of the northeast subarctic Pacific', *Deep Sea Research Part II: Topical Studies in Oceanography* **46**(11), 2909–2939.
- Vézina, AF and T Platt (1988), 'Food web dynamics in the ocean. 1. Best-estimates of flow networks using inverse methods', *Marine Ecology Progress Series* **42**(3), 269–287.
- Vicente-Serrano, SM and RM Trigo (2011), *Hydrological, Socioeconomic and Ecological Impacts of the North Atlantic Oscillation in the Mediterranean Region*, Vol. 46, Springer, London and New York.
- Viéitez Martín, JM, G San Martín Peral and C Alos Calvo (2004), *Fauna ibérica. Annelida polychaeta I*, Vol. 25, Museo Nacional de Ciencias Naturales, CSIC, Madrid.
- Vinogradov, ME and VB Tseitlin (1983), *The Sea, Volume 8: Deep-Sea Biology*, Vol. 8, Harvard University Press, chapter Deep-sea pelagic domain (aspects of bioenergetics), pp. 123–165.

- Virnstein, RW (1977), 'The importance of predation by crabs and fishes on benthic infauna in Chesapeake Bay', *Ecology* **58**(6), 1200–1217.
- Walsh, JJ (1991), 'Importance of continental margins in the marine biogeochemical cycling of carbon and nitrogen', *Nature* **350**(6313), 53–55.
- Walters, C, D Pauly and V Christensen (1999), 'Ecospace: prediction of mesoscale spatial patterns in trophic relationships of exploited ecosystems, with emphasis on the impacts of marine protected areas', *Ecosystems* **2**(6), 539–554.
- Walters, C, D Pauly, V Christensen and JF Kitchell (2000), 'Representing density dependent consequences of life history strategies in aquatic ecosystems: EcoSim II', *Ecosystems* **3**(1), 70–83.
- Walters, C, V Christensen and D Pauly (1997), 'Structuring dynamic models of exploited ecosystems from trophic mass-balance assessments', *Reviews in fish biology and fisheries* **7**(2), 139–172.
- Walters, CJ and SJD Martell (2004), *Fisheries ecology and management*, Princeton University Press.
- Warren, PH (1994), 'Making connections in food webs', *Trends in Ecology & Evolution* **9**(4), 136–141.
- Wasserman, L (2006), *All of nonparametric statistics*, Springer New York.
- Watters, GM, JT Hinke, K Reid and S Hill (2005), A krill–predator–fishery model for evaluating candidate management procedures, in 'Convention on the Conservation of Antarctic Marine Living Resources (CCAMLR) Working Group on Ecosystem Monitoring and Management Working Paper WG-EMM', Vol. 5, pp. 14–15.
- Watters, GM, JT Hinke, K Reid and S Hill (2006), 'KPFM2, be careful what you ask for—you just might get it', *CCAMLR document WG-EMM-06/22*.
- Wieking, G (2002), The macrofauna at the Dogger Bank: food supply in relation to hydroclimate, PhD thesis, University of Oldenburg.
- Wieking, G and I Kröncke (2003), 'Macrofauna communities of the Dogger Bank (central North Sea) in the late 1990s: spatial distribution, species composition and trophic structure', *Helgoland Marine Research* **57**(1), 34–46.
- Wilberg, MJ, JT Thorson, BC Linton and J Berkson (2009), 'Incorporating time-varying catchability into population dynamic stock assessment models', *Reviews in Fisheries Science* **18**(1), 7–24.

- Williams, RJ and ND Martinez (2000), 'Simple rules yield complex food webs', *Nature* **404**(6774), 180–183.
- Winberg, GG (1956), 'Rate of metabolism and food requirements of fishes', *Fisheries Research Board of Canada. Translation Series* **194**, 1–202.
- Wood, S (2006), *Generalized additive models: an introduction with R*, CRC press.
- Woodward, G, DC Speirs and AG Hildrew (2005), 'Quantification and resolution of a complex, size-structured food web', *Advances in ecological research* **36**, 85–135.
- Worm, B, EB Barbier, N Beaumont, JE Duffy, C Folke, BS Halpern, JBC Jackson, HK Lotze, F Micheli and SR Palumbi (2006), 'Impacts of biodiversity loss on ocean ecosystem services', *Science* **314**(5800), 787–790.
- Worm, B, R Hilborn, JK Baum, TA Branch, JS Collie, C Costello, MJ Fogarty, EA Fulton, JA Hutchings, S Jennings, OP Jensen, HK Lotze, PM Mace, TR McClanahan, C Minto, SR Palumbi, AM Parma, D Ricard, AA Rosenberg, R Watson and D Zeller (2009), 'Rebuilding global fisheries', *Science* **325**(5940), 578–585.
- Worm, B and RA Myers (2003), 'Meta-analysis of cod-shrimp interactions reveals top-down control in oceanic food webs', *Ecology* **84**(1), 162–173.
- WWF/IUCN (2004), *The Mediterranean deep-sea ecosystems: an overview of their diversity, structure, functioning and anthropogenic impacts, with a proposal for conservation*, IUCN, Málaga and WWF, Rome.
- Yodzis, P (1998), 'Local trophodynamics and the interaction of marine mammals and fisheries in the Benguela ecosystem', *Journal of Animal Ecology* **67**(4), 635–658.
- Yodzis, P and S Innes (1992), 'Body size and consumer-resource dynamics', *American Naturalist* **139**(6), 1151–1175.
- Zavatarelli, M and GL Mellor (1995), 'A numerical study of the Mediterranean Sea circulation', *Journal of Physical Oceanography* **25**(6), 1384–1414.
- Zhou, S, ADM Smith, AE Punt, AJ Richardson, M Gibbs, EA Fulton, S Pascoe, C Bulman, P Bayliss and K Sainsbury (2010), 'Ecosystem-based fisheries management requires a change to the selective fishing philosophy', *Proceedings of the National Academy of Sciences* **107**(21), 9485–9489.
- Zorach, AC and RE Ulanowicz (2003), 'Quantifying the complexity of flow networks: how many roles are there?', *Complexity* **8**(3), 68–76.



## GALILEO AND THE LITTLE MONK

the social responsibility of scientists

[...] THE LITTLE MONK *Don't you think the truth will prevail, even without us, if it is the truth?*

GALILEO *No, no, no. Truth prevails only when we make it prevail. The triumph of reason can only be the triumph of reasoning men. You describe your peasants in the Campagna as if they were moss on their huts. How can anyone imagine that the sum of the angles of a triangle runs counter to their needs! But if they don't rouse themselves and learn how to think, the best irrigation systems in the world won't do them any good. Damn it, I see the divine patience of your people, but where is their divine wrath?*

THE LITTLE MONK *They're tired.*

GALILEO (throws a bundle of manuscripts in front of him) *Are you a physicist, my son? Here you'll find the reasons for the ocean's tides. But don't read it, do you hear. Ah, reading already? I see you're a physicist. (The little monk has immersed himself in the papers)*

GALILEO *An apple from the tree of knowledge. He gobbles it up. He'll be damned for all eternity, but he's got to bolt it down, the hapless glutton. Sometimes I think I'd gladly be locked up in a dungeon ten fathoms below ground, if in return I could find out one thing: What is light? And the worst of it is: What I know I must tell others. Like a lover, a drunkard, a traitor. It's a vice, I know, and leads to ruin. But how long can I go on shouting into empty air - that is the question.*

THE LITTLE MONK (points at a passage in the papers) *I don't understand this sentence.*

GALILEO *I'll explain it to you, I'll explain it to you.*

from *Life of Galileo*  
by Bertold Brecht





